CONTENTS

CONTENTS (con't)

CONTENTS (con't)

CONTENTS (con't)

CONTENTS (con't)

CONTENTS (con't)

Foreword

Currently, the weather is high variation around the world. This can be seen from the severe disaster such as storm, extreme weather (very high and low temperature) including to drought and flood. Theireffects are to damage agriculture, industry and fisheries etc. One of natural resources that shows clearly variation both quantity and distribution is precipitation. The climate change is currently a hot issue. It is mentioned as a cause of above. A simple question about climate change is a complication for solution.

The arrangement of the international conference on “Climate Change and Water & Environment Management in Monsoon Asia” aims to provide a platform to share new knowledge among researchers in disaster, irrigation and water management.

On behalf of Thai Hydrologist Association, it is our impression to welcome for joining this conference. We hope that this conference will fulfill its objectives and that the knowledge we are gaining will be applied and build-upon to develop our ability for climate change adaptation.

Dr.Subin Pinkayan

President of Thai Hydrologist Association

Preface

The international conference on climate change and water & environment management in monsoon area provides an opportunity for researchers and scientists to share and discuss their finding and knowledge regarding climate change. There are four main topics on the issues: climate change and uncertainty in hydrology and meteorology, participatory management for water and irrigation project, emerging technologies in water and environment management, and water related disaster management. These topics have covered from the projection and effect of climate change to the reduction and mitigation through new technologies and better management. In addition climate change adaptation at various levels especially field and community which are extremely important is also another issue for the conference.

There are 66 papers submitted and 48 papers are selected for presentation including 11 invited papers. The organizing committee would like to send our gratitude to the reviewers for their time and effort in reviewing the papers. The quality of the papers is a tribute to the authors and also to the reviewers who have guided any necessary improvement.

This conference cannot be accomplished with assistant from many member and friends of the Thai Hydrologist Association for their contribution and afford since last year. Thanks must also be expressed to royal irrigation department, department of water resources, faculty of engineering at Kamphaengsaen, Kasetsart University and faculty of engineering, Chulalongkorn University for their strong support and sponsorship. The THA2015 conference and proceedings are a credit to a large group of people and everyone should be proud of the outcome.

Assoc.Dr.Bancha Kwanyuen

Editor of Proceedings THA2015

Organizing Committee

Advisory Committees :

Prof. Dr. Pirom Kamol-ratanakul, M.D.	Chulalongkorn University
Assoc. Vudtechai Kapilakanchana	Kasetsart University
Prof. Dr. Worsak Kanok-Nukulchai	Asian Institute of Technology
Mr. Lertviroj Kowattana	Director General of Royal Irrigation Department
Mr. Jatuporn Buruspat	Director General of Department of Water Resources
Dr. Suthipun Jitpimolmard, M.D.	Director General of Thailand Research Fund
Prof. Kuniyoshi Takeuhi	ICHARM, Japan
Prof. Makoto KIMURA	Kyoto University, Japan
Prof. Wei-Fuu Yang	President of PAWEES, Japan
Dr. Ramasamy Jayakumar	UNESCO-IHE

Organizing Chair :

Dr. Subin Pinkayan	President of Thai Hydrologist Association

Organizing Co-Chair :

Prof. Dr. Bundhit Eua-arporn	Chulalongkorn University
Assoc.Prof.Dr. Bancha Kwanyuen	Kasetsart University
Dr. Thongplew Kongjun	Royal Irrigation Department
Mr. Chaiporn Siripornpibul	Ministry of Natural Resources and Environment
Asst. Prof. Dr. Chanatip Pharino	Thailand Research Fund

International Scientific Committees :

Assoc. Prof. Dr. Bancha Kwanyuen	Kasetsart Uuniversity
Dr. Yutaka Matsuno	PAWEES, Kinki University, Japan
Prof. Dr. SAYAMA Takahiro	ICHARM, Public Works Research Institute, Japan
Prof. Dr. Yasuto TACHIKAWA	Kyoto University, Japan
Dr. Ailikun	Chinese Academy of Sciences,China
Prof. LIONG Shie-Yui	National University of Singapore, Singapore
Prof. Ke-Sheng Cheng	National Taiwan University, Taiwan
Prof.Jiaguo Qi	Zhejinag University China, China
Prof.Tissa Illangasekare	Colorado School of Mines, USA
Dr.Fi John Chang	National Taiwan University, Taiwan
Dr. Byung Man Choi	K-water Institute, Korea

Dr. Ole Mark	DHI, Denmark
Assoc. Prof. Dr. Sucharit Koontanakulvong	Chulalongkorn University
Asst. Prof. Dr. Aksara Putthividhya	Chulalongkorn University
Dr. Anurak Sriariyawat	Chulalongkorn University
Dr. Piyatida Hoisungwan	Chulalongkorn University
Dr. Pongsak Suttinon	Chulalongkorn University
Dr. Sutat Weesakul	Asian Institute of Technology
Dr. Sangam Shrestha	Asian Institute of Technology
Dr. Somchai Chonwattana	Asian Institute of Technology
Assoc. Prof. Amnat Chidthaisong	King Mongkut's University of Technology Thonburi, TRF
Dr. Yutthana Talaluxmana	Kasetsart University
Dr. Jeerasorn Santisirisomboon	Ramkhamhaeng University

Working Committees :

Assoc.Prof.Dr. Sucharit Koontanakulvong	Chulalongkorn University
Dr. Yutthana Talaluxmana	Kasetsart University
Dr. Sutat Weesakul	Asian Institute of Technology
Mr. Thada Sukhapunnaphan	Royal Irrigation Department
Mr. Adisorn Champathong	Royal Irrigation Department
Mrs. Wasna Proiamphaeng	Department of Water Resources
Mrs. Orathai Ongrattana	Department of Water Resources
Ms. Kanokwan Yoowong	Department of Water Resources
Assoc. Prof. Amnat Chidthaisong	King Mongkut's University of Technology Thonburi, TRF

Website and Information System :

Miss Mada Iaumsupanimit	Chulalongkorn University
Miss Marayart Petcharat	Thai Hydrologist Association

Co-organizers :

1. Thai Hydrologist Association (**THA**)
2. Faculty of Engineering, Chulalongkorn University (**CU**)
3. Faculty of Engineering at Kamphaengsaen, Kasetsart University (**KU**)
4. Royal Irrigation Department (**RID**)
5. Department of Water Resources (**DWR**)
6. Thailand Research Fund (**TRF**)
7. Asian Institute of Technology (**AIT**)

Aims and Scope

The objective is to provide a platform for researchers, scientists, practitioners, and policy makers to share and present new advances, research findings, perspectives, and experiences in Disaster Irrigation and Water Management. Special attentions will be given to developing certain skills or competence, or general upgrading of performance ability for climate change adaptation, participatory water management disaster and environmental management, and sustainable development in irrigation and drainage in the monsoon Asia. The conference will bring together leading researchers, engineers, scientists, and officials in the domain of interest from around the world.

Program of THA 2015 International Conference on "Climate Change and Water & Environment Management in Monsoon Asia"

<table>
<tr><th>TIME</th><th colspan="4">WEDNESDAY- 28 JANUARY 2015</th></tr>
<tr><td>08.00- 09.00</td><td colspan="4">Registration at Le Concorde Ballroom, 2nd floor, Swissôtel Le Concorde</td></tr>
<tr><td colspan="5">Venue: Le Concorde Ballroom, Level 2</td></tr>
<tr><td>09.00-09.10</td><td colspan="4">Opening Ceremony</td></tr>
<tr><td>09.10-09.20</td><td colspan="2">Conference Report</td><td colspan="2">Dr. Subin Pinkayan
President of Thai Hydrologist Association</td></tr>
<tr><td>09.20-09.30</td><td colspan="2">Opening Remarks
and Group Photo</td><td colspan="2">His Excellency Mr. Ampol Senanarong
Privy Councillor</td></tr>
<tr><td>09.30-10.15</td><td colspan="4">Exhibition Tour/Press Conference</td></tr>
<tr><td>10.15-10.30</td><td colspan="4">Coffee Break</td></tr>
<tr><td>10.30-11.00</td><td colspan="2">Keynote Speaker I
Water related disasters due to changing climate</td><td colspan="2">Dr. Gwang-Jo Kim
Director, UNESCO Asia and Pacific Regional Bureau for Education (UNESCO Bangkok)</td></tr>
<tr><td>11.00-11.30</td><td colspan="2">Keynote Speaker II</td><td colspan="2">Mr. Miguel Musngi
Senior Officer of DMHA Division, ASEAN Secretariat</td></tr>
<tr><td>11.30-12.00</td><td colspan="2">Keynote Speaker III
Water related Project Planning under Climate Change
Thailand NESDB representative</td><td colspan="2">Mr. Arkhom Termpittayapaisith
Secretary-General, Office of the National Economic and Social Development Board (NESDB), Thailand</td></tr>
<tr><td>12.00-13.00</td><td colspan="4">Lunch Break</td></tr>
<tr><td>Room</td><td>Venue: Salon A
Plenary session presentation</td><td>Venue: Jamjuree
Plenary session presentation</td><td>Venue: Krisana
Plenary session presentation</td><td rowspan="3">Venue: Salon B
Workshop on "ASEAN Academic Networking in Water& Disaster Management and Climate Change"</td></tr>
<tr><td>Chair</td><td>Dr. Dusadee Sukawat</td><td>Asst. Prof. Dr.Ekasit Kositsakulchai</td><td>Dr. Pongsak Suttinon</td></tr>
<tr><td>Briefing</td><td>Dr. Saisunee Budhakooncharoen</td><td>Dr. Sarawut Jansuwan</td><td>Dr. Sompong Boonprasert</td></tr>
<tr><td>13.00</td><td>Invited paper A01
Introduction to Monsoon Asia Integrated Regional Study and possible involvement of Thailand in the regional initiative
Dr. Ailikun
Chinese Academy of Sciences, China</td><td>Invited paper B01
Can regional climate models provide proxies for sustainable water resources management over data sparse regions?
Prof. LIONG, Shie- Yui
National University of Singapore,Singapore</td><td>Invited paper D01
Analyses and Strategies for handling climate change impacts on flooding
Dr. Ole Mark
DHI, Denmark</td><td>Session 1: Planning presentation
Opening speech and introduction to the session by Dr. Ramasamy Jayakumar, Programme Specialist and Chief Natural Sciences, UNESCO Office in Bangkok, Thailand</td></tr>
</table>

Update 26/01/2015

TIME	WEDNESDAY- 28 JANUARY 2015			
Room	**Venue: Salon A** **Plenary session presentation**	**Venue: Jamjuree** **Plenary session presentation**	**Venue: Krisana** **Plenary session presentation**	**Venue: Salon B** **Workshop on "ASEAN Academic Networking in Water& Disaster Management and Climate Change"** (ASEAN Workshop)
13.30	**Paper TA 01:** **Uncertainty in climate change projection and its impact on hydrology of the Nam Ou River Basin** (Manisha Maharjan[1, a *], Mukand S. Babel [1, b] and Shreedhar Maskey [3, c] ,Thailand)	**Invited paper B02** **Climate Change Mitigation: Water and Energy Nexus in Urban Environments** **Dr. Tamim Younos** The Cabell Brand Center for Global Poverty and Resource Sustainability Studies, USA.	**Paper TD 01:** **Development of operational flood optimization within the flood forecasting system to determine the optimal release for Ubonrat reservoir for flood mitigation** (Sathit Chantip[1, a *], Piyamarn Sisomphon[2,b] Surajate Boonya-aroonnet[3,c] ,Thailand)	**Session 1: Planning presentation (Cont.)** - **Dr. Thongplew Kongjun** The Office of Water Management and Hydrology, Royal Irrigation Department, Thailand - **Flood Risk Management in the Delta Areas of Myanmar** **Dr. Hrin Nei Thiam**, Director-General of the Department of Meteorology and Hydrology, Ministry of Transportation, Myanmar - **Report on Water Disaster Management in Lao PDR** **Mr. Maykong Phonephommavong**, Director-General of the Department of Irrigation, Ministry of Agriculture and Forestry of Laos - **Prof. Duong Hong Son**, Deputy Director General of Vietnam Institute of Meteorology, Hydrology and Environment of Vietnam - **Ir Mohd Zaki Mat Amin**, Director of Research Centre for Water Resources, National Hydraulic Research Institute of Malaysia (NAHRIM)
13.50	**Paper TA 05:** **Impact of climate change on groundwater recharge in Ho Chi Minh City area** (Ha Quang Khai[1, a *], Sucharit Kooltanakulvong [2,b] ,Thailand)	**Paper TB 02:** **Assessment of Water Requirement of Chulsa Rice by using CROPWAT model** (Mrs. Men Nareth, Cambodia)	**Paper TD 03:** **Assessment of River Bank Erosion and Vulnerability of Embankment to Breaching: A RS and GIS Based Study in Subansiri River in Assam** (BIPUL TALUKDAR[1,a*], RANJIT DAS[2,b] , India)	
14.10	**Paper TA 07:** **Introduction to TCCIP: dynamic and statistical downscaling and its applications** (Lee-Yaw Lin [1,a*] , Yung- Ming Chen[1, b] , Jung-Lien Chu[1,c] , Chao-Tzuen Cheng [1,d] , Jun-Jih Liou [1,e] , Yun-Ju Chen [1,f] and, Yuan-Fong Su [1,g] , Taiwan)	**Paper TB 05:** **Analysis of Hydrologic Variables Changes related to Large Scale Reservoir Operation by Using Mann-Kendall Statistical Tests in Thailand** (MANEE Donpapob[1, a *], TACHIKAWA Yasuto[2, b] and YOROZU Kazuaki[3, c] , Japan)	**Paper TD 07:** **Technology Assisted Flood Management** (Surajate Boonya-aroonnet[1, a], Peraya Tantianuparp.[1,b] Sutat Weesakul[1,2,c*] and Royol Chitradon[1,d] , Thailand)	
14.30	**Paper TA 08:** **Urban-induced Rainfall in Chiang Mai, Thailand** (KLONGVESSA Pawee[1, a *] and LU Minjiao[1,b], Japan)	**Paper TB 06:** **Effect of AWDI Practices on GHG Emission in a Small Scale Lysimeter** (Mr. Ishwar Pun, Japan)	**Paper TD 10:** **Impact of Climate Change on Urban Flood Management: A Case Study in Mae Sot Municipality in Tak Province** (Assoc.Prof. Sombat CHUENCHOOKLIN, Thailand)	

Update 26/01/2015

TIME	WEDNESDAY- 28 JANUARY 2015			
14.50	**Coffee Break**			
Room	**Venue: Salon A** **Plenary session presentation**	**Venue: Jamjuree** **Plenary session presentation**	**Venue: Krisana** **Plenary session presentation**	**Venue: Salon B** **Workshop on "ASEAN Academic Networking in Water& Disaster Management and Climate Change"** (ASEAN Workshop)
Chair	Dr. Shrestha Sangam	Assoc. Prof. Suwatana Chittaladakorn	Asst. Prof. Dr. Aksara Putthividhya	
Briefing	Dr. Saisunee Budhakooncharoen	Dr. Sarawut Jansuwan	Dr. Sompong Boonprasert	
15.10	**Paper TA 12:** **Application of a Land Surface Model for Bias Correction of Runoff Generation Data from MRI- AGCM3.2S Dataset** (DUONG Duc Toan[1, a *], TACHIKAWA Yasuto[1, b] and YOROZU Kazuaki[1, c], Japan)	**Invited paper B03** **Integrated study of the water-ecosystem-economy in the Heihe River Basin and its implication for water resource management in world's inland river basins** **Prof. Xin Li,** Academy of Sciences (CAS),China	**Invited paper D02** **Mitigating Water Insecurity through Disaster Preparedness in Korea** **Dr. CHOI Byungman** Executive Director of K-water Institute and Co-chair of the Regional Process Commission of the7th World Water Forum, Korea	**Session 1: Planning presentation (Cont.)** - **Ir. Mudjiadi, M.SC.**, Director-General of Water Resources, Ministry of Republic Work, Government of Indonesia - **Enhancing Resiliency through Community Participatory Flood Observation System for the Laguna Lake Basin** **Mrs. Adelina C. Santos-Borja**, Division Chief III, International Linkages & Research Development Unit, Laguna Lake Authority, Philippines - **Flood and drought management under climate change** **Mr. Nirut Koonphol**, Director, Bureau of Water Resources Policy and Planning, Department of Water Resources, Thailand **16.15-17.15 PM** **Session 2: Discussion issues on Water & Disaster Management and Climate Change**
15.40	**Paper TA 16:** **Evaluation of Precipitation over Northern Thailand in CMIP5 MRI-CGCM3 Simulations** (Parichat Wetchayont [1, 3, a *] and Srilert Chotpantarat [1, 2, b],Thailand)	**Paper TB 01:** **Participatory Approach on Management of Communal Irrigation Systems in Upland Areas: *Case Studies of Water Governance in Three Provinces of Northern Luzon*** (Agnes M. Ramos[1,a,], Orlando F. Balderama[2,b,*] , Philippines)	**Paper TD 02:** **Hydrodynamics Simulation of An Overland Flow Over Low Lying Flat Land:** **A Case Study of The 2011 Severe Flood in Sam-Khok and Khlong Luang Districts** (SAIFHON Tomkratoke[a*] and SIROD sirisup[b] ,Thailand)	
16.00	**Invited paper C01** **Assessment of climate change impact on large scale flooding – a case study in the Chao Phraya River Basin via new modeling technology** **Dr. Takahiro Sayama** ICHARM, Public Works Research Institute, Japan	**Paper TB 07:** **Irrigation Demand and the Flood Retention Potential by Changing of Cropping Calendar of the In-season Rice and Off-season Rice in Chao Phraya River Basin Area**. (Songsak Puttrawutichai[1, a *], Buncha Kwanyeun [2, b] and Thongplew Kongjun [3, c] , Thailand	**Paper TD 04:** **Development of Technology for Monitoring, Evaluation and Prediction of Global and Local Water Related Disaster using Various Observation System** (Dr. LEE Eulrae ,Korea)	

Update 26/01/2015

TIME	WEDNESDAY- 28 JANUARY 2015			
Room	**Venue: Salon A** **Plenary session presentation**	**Venue: Jamjuree** **Plenary session presentation**	**Venue: Krisana** **Plenary session presentation**	**Venue: Salon B** **Workshop on "ASEAN Academic Networking in Water& Disaster Management and Climate Change"** (ASEAN Workshop)
16.20	**Paper TC 03:** **Applying satellite communication for weather data to improve the efficiency of telemetry system in the upstream area.** (Wasukree Sae-tia[1, a *], Thakolpat Khampuengson[2,b], Piyamarn Sisomphon [3,c] and Surajate Boonya-aroonnet [4,d], Thailand)	**Paper TB 10:** **Benchmarking for Performance Assessment of Irrigation Schemes: Comparison of National Irrigation Systems(NIS) and Communal Irrigation System(CIS) in Cagayan River Basin** (Prof. Dr. Orlando Balderama , Philippines)	**Paper TD 06:** **Quasi-real-time satellite monitoring for assessing agronomic flood damage** (Akihiko KOTERA[1, a *], Youtaro UENO[1] and Takanori NAGANO[1] ,Japan)	**17.15-17.30 PM** **Session 3: Discussion on support to collaborative academic network**
16.40	**Paper TC 07:** **Development of a User-Friendly Web-based Rainfall Runoff Model** (Khin Htay Kyi[1,a *], Minjiao Lu[2,3,b] and Xiao Li[4,c], Japan)	**Paper TB 11:** **Effect of depth and spacing of subsurface drains on salinity of drainage water from rice paddy fields** (Mehdi Jafari-Talukolaee[1, a,*], Ali Shahnazari[2,b], Abdullah Darzi-Naftchali[2,c] ,Iran)	**Paper TD 08:** **Derivation Of Optimal Rule Curves For Flood Control Study Of Ubolratana Reservoir, Thailand** (Pich Hirun[1, a *] and Areeya Rittima[1,b] , Thailand)	
17.00	**Paper TC 20:** **Zn removal from synthetic wastewater using zeolite modified with oxidizing agent** (SALWA Mohd Zaini Makhtar[1, a *], ISMAIL Abustan[1,b], MAHYUN Ab Wahab[1,c] , NOR AMIRAH Abu Seman[1,d] , NUR ATIQAH Ahmad Awalluddin[1])			
18.00	**Reception Dinner** (For registration participant) Venue: Le Lotus 1			

TIME	THURSDAY- 29 JANUARY 2015		
Room	**Venue: Salon A** **Plenary session presentation**	**Venue: Salon B** **Plenary session presentation**	**Venue: Krisana** **Workshop on "ASEAN Academic Networking in Water& Disaster Management and Climate Change"** (ASEAN Workshop)
Chair	Dr. Shrestha Sangam	Asst. Prof. Dr. Sanit Wongsa	
Briefing	Dr. Suppattana Wichakul	Dr. Siriluk Chumchean	**Session 4: Technical presentation** To present recent findings or on-going research related to Water & Disaster Management and Climate Change Speakers from ASEAN countries - **Research Issues on Water Disaster Management and Climate Change in Western Part of Java Island, Indonesia** **Prof. Dr. M. Syahril B. Kusuma** Faculty of Civil And Environmental Engineering of Institut Teknologi Bandung, Indonesia - **Assessment of water resources for improved water governance under climate change: case study in Stung Chrey Bak Catchment of Tonle Sap Great Lake Basin in Cambodia** **Dr. Ly Sarann**, Head of Department of Rural Engineering of Institute of Technology of Cambodia - **A new technology in purification of sea-water and produced-water** **Dr. Pham Van Sang,** School of Transportation Engineering, Hanoi University of Science and Technology, Vietnam - **Vulnerability of Vietnamese coasts to coastal disasters and climate change** **Dr. Nguen Danh Thao** Director, External Relations Office, HCMC University of Technology , Vietnam - **Prof. Dr. Ismail Bin Abustan** School of Civil Engineering, University of Sains Malaya, Malaysia
09.00	**Invited paper C02** **Artificial intelligence technologies for urban flood control** **Prof. Fi-John Chang** National Taiwan University, Taiwan	**Invited paper A02** **"Improving Understanding of Atmospheric Loading of Greenhouse Gases Driving Climate Change: Filling Knowledge Gaps to Develop Strategies for Mitigation"** **Prof. Tissa Illangasekare** Colorado School of Mines, USA	
09.30	**Paper TC 09:** **Fluctuation and its change during rainfall events in water temperature at the upstream tropical forested watershed; study case: Kracak reservoir catchment - Indonesia** (Luki Subehi and Kwansue Jung, South Korea)	**Paper TA 06:** **Comparative evaluation of storm characteristics derived from observed rainfalls and GCM precipitation outputs** (Yuan-Fong Su[1,a*] , Jun-Jih Liou[1,b] and Ke-Sheng Cheng[2, c] , Taiwan)	
09.50	**Paper TC 12:** **Estimation of Evapotranspiration in Lam Ta Kong Basin using Surface Energy Balance Algorithm for Land (SEBAL) Model** (Miss. Haruetai maskong , Thailand)	**Paper TA 09:** **Bias correction test of simulted rainfall from PRECIS using adjustment factors based on distribution mapping** (Kowit Boonrawd[1, a]Chatchai Jothityangkoon[1, b] ,Thailand)	
10.10	**Paper TC 15:** **Sensitivity of Snow Covered Area of Brahmaputra River Basin to Temperature** (Swapnali Barman[1,a*], R.K. Bhattacharjya[2,b] , India)	**Paper TA 15:** **Designed Intensity-duration-frequency (IDF) curves under climate change condition in urban area** (Ashish Shrestha [1, a *], Sutat Weesakul[1,b], Mukand Singh Babel[1,c] and Zoran Vojinovic [2,d] ,Thailand)	

10.30	**Coffee Break**		
TIME	**THURSDAY- 29 JANUARY 2015**		
Room	**Venue: Salon A** **Plenary session presentation**	**Venue: Salon B** **Plenary session presentation**	**Venue: Krisana** **Workshop on "ASEAN Academic Networking in Water& Disaster Management and Climate Change"** (ASEAN Workshop)
Chair	Dr. Shreshta Sangam	Dr. Chaiwat Ekkawatpanit	
Briefing	Dr. Suppattana Wichakul	Dr. Siriluk Chumchean and Dr. Sompong Boonprasert	
10.50	**Paper TC 23:** **The Study of Relationship between Deciles and VCI in the Northern Part of Thailand** (Aphantree Yuttaphan [1, 2, a *], Sombat Chuenchooklin [2,b] and Somchai Baimoung [3,c] ,Thailand)	**Paper TA 19:** **Rainfall-Runoff-Inundation Simulation with Bias-corrected Satellite Based Rainfall: Case Study Yom River Basin** (Teerawat Ram-Indra [1, a], Anurak Sriariyawat [1,b *] and Piyatida Hosisungwan [1,c], Thailand)	**Session 4: Technical presentation (Cont.)** - **Climate Change in Myanmar and the Dry Zone** **Dr. Win Naing Tun** Myanmar Environment Institute, Myanmar - **Climate of Yangon city** **Dr. Khin Kay Khaing**, Lecturer, Department of Geography, University of Yangon, Myanmar - **Assessment of groundwater vulnerability in Yangon City, Myanmar** **Dr. Wint Wint Htun**, Department of Geology, Yangon University, Myanmar - **Application of community-based arsenic removal unit (SARSAC) for provision of safe water in affected provinces of Laos** **Dr. Keoduangchai Keokhamphui,** Lecturer, Faculty of Water Resources Engineering, National University of Laos (NUOL), Laos - **Status of climate change research in Thailand** **Assoc. Prof. Dr. Sucharit Koontanakulvong** Head of Dept.Water Resources Engineering, Faculty of Engineering Chulalongkorn University, Thailand
11.10	**Paper TC 24:** **Effect of Particle Size Distribution to Remove Colour and *Escherichia coli* in Groundwater** (Nur Aziemah Abd Rashid [1,a*], Ismail Abustan [2,b], Mohd Nordin Adlan [3,c] , Malaysia)	**Paper TA 02:** **Climate Change Scenario on Surface Water Resource in Bangnampriao District, Chachernsao Province** (Dr. Charuvan Kasemsap ,Thailand)	
11.30	**Paper TC 01:** **Aerobic Rice Technology(ART) in the Philippines and Southeast Asia: *Improving Productivity and Enhancing Technology Adaption towards Rice Sufficiency and Climate Change Resiliency*** (Orlando F. Balderama [1,a,*], Philippines)	**Paper TA 03:** **Uncertainty of rainfall from CMIP3 and CMIP5 climate models downscaling for Bangkok** (Seree Supratid [1, a] and Thannob Aribarg [1,2,b*] ,Thailand)	
11.50	**Paper TC 02:** **Autonomous Surface Vehicle for Bathymetric and Environmental Survey: Implementation and Result** (Pasan Kulvanit *, Thailand)	**Paper TA 11:** **Uncertainty of stream flow under climate change scenarios using statistical downscaling data** (Yun-Ju Chen [1], Yuan-Fong Su [1], Jun-Jih Liou [1] and Yung-Ming Chen [1] , Taiwan)	
12.10	**Lunch Break**		

Update 26/01/2015

TIME	THURSDAY- 29 JANUARY 2015			
Room	**Venue: Salon A** **Plenary session presentation**	**Venue: Salon B** **Plenary session presentation**	**Venue: Krisana** **ASEAN Workshop**	**Venue: Jamjuree** **Technical training**
Chair	Dr. Sutat Weesakul	Dr. Pariwate Varnakovida	**Session 5: Preparation for collaborative academic network setup for water, disaster management and climate change among ASEAN countries** **13.00-13.15 PM** Summary of presentations from Technical presentation session in the morning **13.15-13.30 PM** - Introduction to preparation for collaborative academic network setup by **Dr. Ramasamy Jayakumar** and **Assoc. Prof. Dr. Sucharit Koontanakulvong** **13.00- 14.30 PM** - **Dr. Ailikun** Director, International Program Office of Monsoon Asia Integrated Regional Study (MAIRS), Institute of Atmospheric Physics, Chinese Academy of Sciences, China - **Prof. Dr. Kaoru Takara** Chair, Japanese National Committee for UNESCO-IHP - **Prof. Dr. Takahiro Sayama** Senior researcher, International Centre for Water Hazard and Risk Management (ICHARM), Public Works Research Institute (PWRI), Japan	**Technical training by University of California - Irvine with UNESCO's International Hydrological Programme (IHP) "Satellite-based Rainfall (PERSIANN) for Planning and Management for Natural Disasters in Monsoon Asia"** **(For who reserved a seat)**
Briefing	Dr. Duangruedi Khosit kittiwong	Dr. Sompong Boonprasert		
13.00	**Invited paper C03** **IWRM for Climate Change Adaptation in the Mekong River Basin** **Dr. Kittiwet Kuntiyawichai,** Department of Civil Engineering, Faculty of Engineering, Khon Kaen University.	**Invited paper A03** **Adapting to Climate Change through Effective Risk Assessment and Management in East Asia - An Initiative for International Collaboration** **Prof. Jiaguo Qi, Zhejinag** University China, China		
13.30	**Paper TC 08:** **Strategy to Automatically Calibrate Parameters of a Hydrological Model: A Multi-step Optimization Scheme and its Application to Xinanjinag Model** (Minjiao Lu[1, 2,a*] and Xiao Li[3,b], Japan)	**Paper TA 13:** **River Discharge Assessment under a Changing Climate in the Chao Phraya River, Thailand by using MRI-AGCM3.2S** (Supattana WICHAKUL[1, a *], Yasuto TACHIKAWA[1, b], Michiharu SHIIBA[1, c] and Kazuaki YOROZU [1,d], Japan)		
13.50	**Paper TC 10:** **Detection of paddy fields in sub-state level by combined use of MODIS and Landsat imagery** (Assoc. Prof. Dr. Takanori Nagano , Japan)	**Paper TA 17:** **Climate Change impact on Groundwater Recharge in Plaichumpol Irrigation Project** (Mr. Chokchai suthidhummajit, Thailand)		
14.10	**Paper TC 13:** **Deep Groundwater and Possible Signals for Human and Climatic Effects** (UMA Seeboonruang[*], Thailand)	**Paper TA 18:** **Possibility to achieve 1 % rh uncertainty in meteorological application: Temperature effect of commercial thermo-hygrometers** (T. Sinhaneti[*], P. Phuauntharo, and T. Keawprasert , Thailand)		
14.30	**Coffee Break**			

Update 26/01/2015

TIME	THURSDAY- 29 JANUARY 2015			
Room	**Venue: Salon A** **Plenary session presentation**	**Venue: Salon B** **Plenary session presentation**	**Venue: Krisana** **ASEAN Workshop**	**Venue: Jamjuree** **Technical training**
Chair	Dr. Sutat Weesakul	Assoc. Prof. Dr. Tuantan Kitpaisalsakul	**Session 5: Preparation for collaborative academic network setup for water, disaster management and climate change among ASEAN countries (Cont.)** - **Prof. Dr. Kwansue Jung** Director, International Water Resources Research Institute, Chungnam National University, Korea - **Dr. Ole Mark** Head of Research and Development, Danish Hydraulic Institute (DHI), Denmark - **Prof. Dr. Fi-John Chang** Department of Bioenvironmental Systems Engineering, National Taiwan University, Taiwan - **Asst. Prof. Dr. Chanathip Pharino** TRF, Thailand - **Mr. Miguel Musngi**, Senior Officer of DMHA Division, ASEAN Secretariat - 15.45-16.00 pm Discussion and confirmation of the statement of setting up an academic network on water, disaster management and climate change among ASEAN countries	Technical training by University of California - Irvine with UNESCO's International Hydrological Programme (IHP) "Satellite-based Rainfall (PERSIANN) for Planning and Management for Natural Disasters in Monsoon Asia" (For who reserved a seat)
Briefing	Dr. Sompong Boonprasert	Dr. Duangruedi Khosit kittiwong		
14.50	**Paper TC 14:** **Improvement of a Kinemative Wave-based Distributed Hydrologic Model to Predict Flow Regimes in Arid Areas** (Tomohiro Tanaka, Japan)	**Invited paper D03** **Impact assessment of climate change on water-related disasters for building up an adaptation strategy** **Prof. Yasuto TACHIKAWA** Graduate School of Engineering, Kyoto University, Japan		
15.10	**Paper TC 16:** **Estimation of urban asset value for natural disaster risk assessment at the macro scale** (Tiratas Suwathep[1, a *], Wee Ho Lim[1,b *], Yoshihiko Iseri[1,c] and Shinjiro Kanae[1,d], Japan)	**Paper TD 09:** **The basin-wide flooding loss assessments under extreme climate scenario** (Hsin-Chi Li[1] , Hsiao-Ping Wei[1] ,Tingyeh Wu[1], Hung-Ju Shih[1] ,Wei-Bo Chen[1], Yuan-Fong Su[1] and Yung-Ming Chen[1] , Taiwan)		
15.30	**Paper TC 21:** **Study on the Sustainable Sand Removal Capacity on Sand Mining Activities.** (Syamsul Azlan Saleh[1, a]*, Ismail Abustan[2,b], and Mohd Remy Rozainy Mohd Arif Zainol[3,c] , Malaysia)	**Paper TD 11:** **Drought Monitoring using the Normalized Difference Infrared Index (NDII) for the Upper Ping River Basin** (Assoc.Prof. Dr. Nutchanart Sriwongsitanon , Thailand)		
15.50	**Paper TC19:** **Water quality and hydraulic performances of the HMGDS Drainage Module.** (Nor Amirah A.S[1]., Abustan, I[2]., Remy Rozainy M. A. Z[3]., Salwa M. Z. M[4]., Mahyun A.W[4], Malaysia)	**Paper TD 12:** **Mainstreaming Disaster Risk Management in the Governance of Cagayan River Basin: Institutional Design and Stakeholder Participation towards Development of Integrated River Basin Masterplan** (Prof. Dr. Orlando Balderama, Philippines)		

TIME	THURSDAY- 29 JANUARY 2015	
Venue: Le Concorde Ballroom, Level 2		
16.10	**Summary Plenary session presentation**	**Assoc. Prof. Dr. Bancha Kwanyuen** Dean of Faculty of Engineering, Kasetsart Universit, Kampaengsaen Campus
16.15	**Meeting on collaborative academic network setup for water, disaster management and climate change among ASEAN countries**	**Prof. Dr. Bundhit Eua-arporn** Dean of Faculty of Engineering, Chulalongkorn University
16.30	**THA Summary Meeting** **- Closing Remarks**	**Dr. Subin Pinkayan** President of Thai Hydrologist Association
18.00	**Farewell Party Dinner** (For registration participant) Venue: Le Lotus 1	

(The programs are subject to change without notice.)

Remark:

TA: Topic A Climate Change and Uncertainty in Hydrology and Meteorology

TB: Topic B Participatory Management for Water and Irrigation Project

TC: Topic C Emerging Technologies in Water and Environment Management

TD: Topic D Water Related Disaster Management

Update 26/01/2015

SCALE 1:500

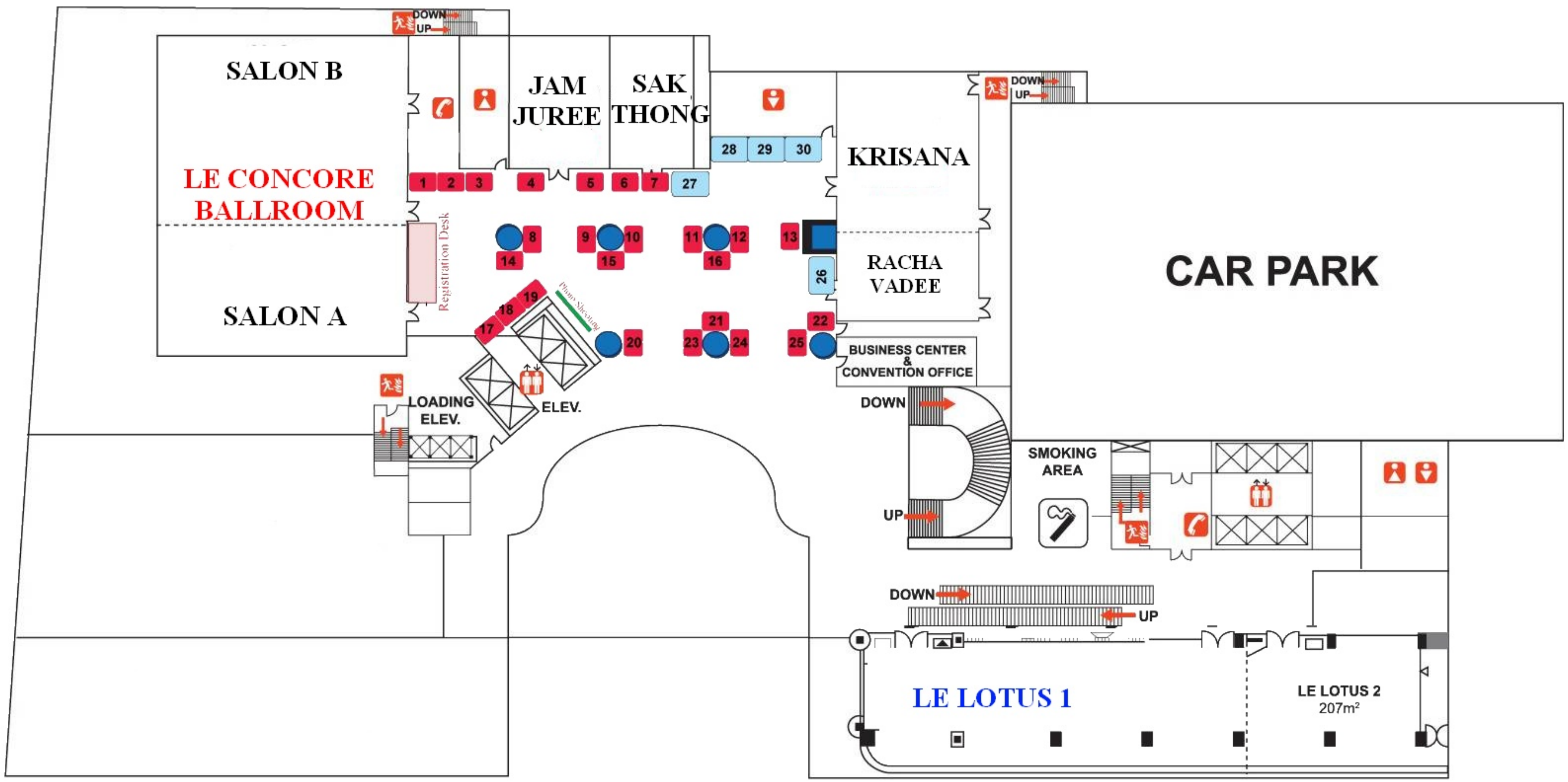

Conference Venue Plan
THA2015

28-29 January 2015

2nd floor, Swissotel Le Concorde, Bangkok

Key of Symbols
Elevator
Fire Exit
Telephone
Men Toilet
Women Toilet

Update 26/01/2015

Keynote Speakers

Session A Climate Change and Uncertainty in Hydrology and Meteorology

"Improving Understanding of Atmospheric Loading of Greenhouse Gases Driving Climate Change: Filling Knowledge Gaps to Develop Strategies for Mitigation"

Prof. Tissa Illangasekare is the AMAX Distinguished Chair and Professor of Civil and Environmental Engineering at the Colorado School of Mines and the Director of *Center for Experimental Study of Subsurface Environmental Processes* (CESEP). He received M.Eng degree in Water Resources Development from the Asian Institute if Technology, a PhD in Civil Engineering from Colorado State University and an Honorary Doctorate from the Uppsala University, Sweden. He is a Fellow of American Geophysical Union (AGU), Fellow of American Association for Advancement of Science (AAAS) and Fellow of American Society of Civil Engineers (ASCE). He is a registered Professional Engineer and a Professional Hydrologist, Board Certified Environmental Engineer by American Academy of Environmental Engineers and Diplomate of American Academy of Water Resources Engineers and recipient of 2012 Darcy Medal from European Geosciences Union (EGU) for outstanding scientific contributions in water resources research and engineering. He was a Shimuzu Visiting Fellow in the Department of Civil and Environmental Engineering at Stanford University in 2012. He was the past editor of *Water Resources Research*, past editor of *Earth Science Review* and past co-editor of *Vadose Zone Journal*. His research experience and expertise are in mathematical and numerical modeling of flow and transport in porous and fractured media, unsaturated and saturated zone processes, surface-subsurface interaction, snow hydrology, land-atmospheric interaction, multiphase flow, carbon storage, aquifer remediation, physical modeling of flow and transport in laboratory test systems and sensor technologies for environmental and hazard monitoring. He headed up a team of US and European scientists sponsored by the US National Science Foundation who visited Sri Lanka to assess the effects of South Asian 2004 tsunami on the coastal aquifer systems.

"Introduction to Monsoon Asia Integrated Regional Study and possible involvement of Thailand in the regional initiative"

Dr. Ailikun is the director of International Program Office of Monsoon Asia Integrated Regional Study (MAIRS), Institute of Atmospheric Physics, Chinese Academy of Sciences. She got PhD in geosciences from Tsukuba University of Japan, her scientific background is climatology with the research field in the Asian monsoon climate change and relationship with natural and human systems. Dr. Ailikun has been served for MAIRS program since 2006, her duty in MAIRS IPO is to help developing international/national cross-cutting global change research, establishing related international projects, and coordination of international collaborations across Asian and Pacific region.

"Adapting to Climate Change through Effective Risk Assessment and Management in East Asia - An Initiative for International Collaboration"

Professor Jiaguo Qi has a broad research interest in global change. He is at the forefront of international engagement and results-driven research using advanced spatial technologies and models. At the moment, he is implementing several projects focusing on sustainable intensification, food systems development and institutional and human capacity building as ways to mitigating and adapting to long-term climate change and short-term climate variability. With more than 25 years of experience in several technical areas critical to global change science, Dr. Qi is dedicated to generate information and knowledge from a variety of data sources ranging from satellite imagery to household surveys to help communities to build resilience, particularly in developing countries in Asia (Central, Southeast and East Asia), Africa (East and West), and South America. Dr. Qi's long-term goal is to make information and knowledge useful for users worldwide and integrate human, technology and environment to understand the interacting nature of system complexity at local, regional and global scales for sustainable development.

Session B Participatory Management for Water and Irrigation Project

"Mitigation Climate Change in Urban Environments: The water and Energy Nexus

Dr. Tamim Younos serves as President & CEO of the Cabell Brand Center for Global Poverty and Resource Sustainability Studies, a non-profit organization in Virginia (USA). Previously, Dr. Younos was a research professor of water resources at Virginia Tech. Dr. Younos earned a doctoral degree in urban and environmental engineering from the University of Tokyo. His research and educational interests include watershed assessment and sustainable management of water resources, water and energy nexus, and climate change mitigation. Dr. Younos has served as a principal investigator for over 40 research/technical projects, and authored/co-authored more than 150 publications. Dr. Younos has edited five books, most recently "Potable Water: Emerging Global Problems and Solutions (Springer, 2014) and "Climate Change and Water Resources" (Springer, 2013).

"Drought Analysis and Projections at some SE Asia's Agriculture Fields"

Dr. Liong, Shie-Yui has been with Tropical Marine Science Institute of National University of Singapore (NUS) since 2004 after spending about 20 years with the Department of Civil and Environmental Engineering of NUS. He received his Dipl.-Ing. and Ph.D degrees from University of Karlsruhe (Germany) and Iowa Institute of Hydraulics Research of University of Iowa (USA) respectively.

Dr. Liong's most recent research focus is on climate downscaling for Southeast Asia domain and deriving valuable information from the downscaled climate to evaluate the impacts of climate change on water resources, flooding, saltwater intrusion, crop yields, etc. He is also leading a team of researchers of different disciplines to develop an Eco-Hydraulics model for NeeSoon Swamp Forest.

He is currently an associate editor of Journal of Environmental Science and Policy (2011–present) and was an associate editor of Journal of Hydroinformatics (2004-2011). He was the President of Hydrological Science Section of AOGS (2008-2010), and Chairman of Joint IAHR-IWA-IAHS Hydroinfomatics Committee (2009-2012).

Dr. Liong is a 3-time recipient of the Best Paper Award of IAHR-APD Congress (1994, 2002 and 2012). In 2007 he was awarded by the President of Federal Republic of Germany the Order of Merit ("Bundesverdienstkreuz"). In June 2013 he presented the Plenary Talk at the 11th International Conference on Hydroinformatics (2014) in New York City; and the Distinguished Lecture at the 10th Asia-Oceania Geosciences Society (AOGS; 2013) meeting in Brisbane.

"Integrated study of the water-ecosystem-economy in the Heihe River Basin and its implication for water resource management in world's inland river basins"

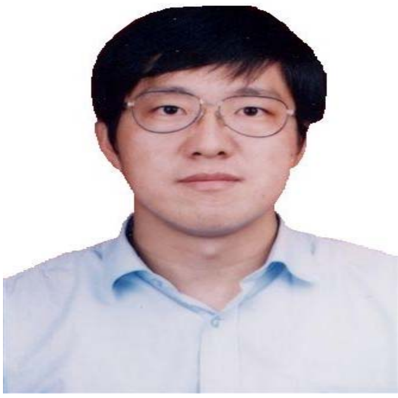

Dr. Xin Li is a professor at Cold and Arid Regions Environmental and Engineering Research Institute (CAREERI), Chinese Academy of Sciences (CAS) and the Director of Laboratory of Remote Sensing and Geospatial Science at CAREERI/CAS. His primary research interests include land data assimilation, application of remote sensing and GIS in hydrology and cryosphere science, and integrated watershed study. He is currently also a member of WCRP GEWEX scientific steering committee, co-chair of the Chinese Committee for WCRP/GEWEX, and the chair of the working group on remote sensing and data of Chinese Committee for WCRP/CliC and IUGG/IACS.

He has published over 230 journal articles (SCI > 90), and authored or coauthored six books. Total citations to these publications are more than 5000. He has been a recipient of the Outstanding Science and Technology Achievement Prize of the Chinese Academy of Sciences in 2005, NSFC China National Funds for Distinguished Young Scientists in 2009, first class Science and Technology Progress Prize of Gansu Province.

He and his group have developed the Chinese Cryosphere Information System. One of his recent achievements is the development of the Chinese Land Data Assimilation System. He is the lead scientist of WATER (Watershed Allied Telemetry Experimental Research, 2007-2010) and HiWATER (Heihe Watershed Allied Telemetry Experimental Research, 2012-2015), which is a comprehensive remote sensing experiment conducted in recent years in China, with more than 400 participants. HiWATER was highlighted on the BAMS cover as "Comprehensive Watershed Science in China".

Session C Emerging Technologies in Water and Environment Management

"IWRM for Mekong River Basin"

Professor Stefan Uhlenbrook (born in 1969) works with UNESCO-IHE since January 2005 as Professor of Hydrology and was appointed as Director for Academic Affairs (August 2010-2012). Since January 2013, he is the Vice-Rector for Academic and Student Affairs.

Prof. Uhlenbrook obtained his PhD and Habilitation at the University of Freiburg, Germany, in 1999 and 2003, respectively. After working as assistant and associate professor in Germany, he became Professor of Hydrology at UNESCO-IHE (Delft, The Netherlands; 2005) and at the Vrije Universiteit Amsterdam (2005-2010). Since 2009, he is also Professor of Experimental Hydrology at Delft University of Technology, The Netherlands.

His main expertise as a hydrologist is in the area of hydrological processes research and river basin modeling at various scales (from headwater to river basin scale). He is an expert in using experimental techniques (e.g. tracer methods) to explore flow pathways and residence times of water, and he has (co-) developed a distributed hydrological model that was applied in catchments in various hydro-climatic regions. Many of his research projects study the impact of global changes on water cycle dynamics in different areas in Africa and Asia.

Prof. Uhlenbrook is a well-established scientist. He received several awards, is frequently invited to give keynote presentations at international conferences, has been member of several editorial boards of top journals in the field of water and environment, and he has published over 120 peer-reviewed papers in ISI-listed journals. Furthermore, he has been involved in steering committees of a number of international initiatives and programmes (e.g. UNESCO-IHP, IAHS-PUB, HELP etc.).

Prof. Uhlenbrook is a dedicated and well appreciated educator; he has been lecturing and supervising students in many university programmes worldwide. Since he became Director of Academic Affairs, he carries substantive responsibilities for the education and research programmes of UNESCO-IHE and several partner institutes that are involved in joint education and research programmes. He is taking on this challenge and wants to upscale the impact of these programmes further to contribute effectively to sustainable management of water and environmental resources through education, research and capacity development.

Prof. Uhlenbrook is recently appointed Officer-in-Charge of the Institute by UNESCO. He will take up this position until a new Rector is appointed.

"Assessment of climate change impact on large scale flooding – a case study in the Chao Phraya River Basin via new modeling technology"

Dr. Takahiro Sayama is a senior researcher at International Centre for Water Hazard and Risk Management (ICHARM), Public Works Research Institute (PWRI), Japan. He is also adjunct associate professor at National Graduate Institute for Policy Studies (GRIPS) in Tokyo. He graduated from Kyoto University and received the doctorate degree in January 2007. From 2007 to 2009 he was a visiting scientist at Oregon State University on JSPS research fellowship. The field of his study is hydrology and flood disasters, in particular he has been developing a Rainfall-Runoff-Inundation (RRI) model, which led for the award of 2013 Young Scientists' Prize from Minister of Education (MEXT) in Japan.

"Artificial intelligence technologies for urban flood control"

Prof. Fi-John Chang, For the past twenty years, Professor Fi-John Chang has endeavored with great interest to conduct researches in technology revolution and the modernization of computer-based modelling and simulation, particularly in the fields of intelligent controlling theories (including artificial neural network, fuzzy theory, genetic algorithm) and the interdisciplines of engineering, hydroinformatics and ecosystems. His developed novel technology/techniques/solutions have been applied with success to governmental projects in various fields comprising climate change, hydro-meteorology, integrated water resources management, eco-hydrosystems, water quantity/quality, etc. More than 170 papers have been published in peer-review journals. Besides, He is also actively engaged in international affairs: coordinating international collaboration projects with partners in European and USA; serving as the Associate Editor for the *Journal of Hydrology* since 2009; jointly publishing research results in SCI journals with authors from Europe, USA and Asia; organizing PAWEES 2011 & 2014 International Conferences; and attending international academic activities. He is the Funding President of "Taiwan Hydro-Informatics Society", which aims to develop hydroinformatics sciences and technology-oriented researches. His achievements have been recognized though his receipt of "Outstanding Research Award" from Taiwan's Ministry of Science and Technology, "Award of Outstanding Contribution to Water Industry" from Taiwan's Ministry of Economic Affairs in 2010 and "International Award" from PAWEES in 2014; and being appointed as Distinguished Professor by National Taiwan University since 2011.

Session D Disaster Management

"Analyses and Strategies for handling climate change impacts on flooding"

Dr. Ole Mark is a specialist in urban water systems, in particular sewerage, drainage and surface water in cities. His work is highly focused on research and practical problem solving within the hydrological cycle in cities, including urban flooding and urban water impacts on receiving waters.

Ole Mark has worked on research projects throughout his career. He has written 95+ publications for scientific journals and conferences – reporting and disseminating the findings of his research activities. His research projects have always aimed at providing better insight and understanding of processes in the urban water cycle. The research results have later, to the greatest possible extent, been transferred into methods applicable for practical problem solving.

Today Ole is Head of Research and Development at DHI and e.g. responsible for DHI's research strategy and proposals within urban water. Ole spent three years as Associate Professor and Programme Coordinator at the Asian Institute of Technology, Thailand. During his career he has been the main advisor for 25+ master's students and two PhD students and he has been co-advisor for many more students.

"Impact assessment of climate change on water-related disasters for building up an adaptation strategy"

Prof.Yasuto TACHIKAWA, Department of Civil and Earth Resources Engineering,Graduate School of Engineering, Kyoto University, Japan. Research interests include rainfall-runoff modeling, rainfall-runoff analysis, real-time flood forecasting, hydrologic projection under a changing climate, hydrologic predictions in ungauged basins, and uncertainty analysis in hydrologic prediction.

"Mitigating Water Insecurity through Disaster Preparedness in Korea"

Dr. CHOI Byungman,
Executive Director of K-water Institute and Co-chair of the Regional Process Commission of the7th World Water Forum, Korea

Session A

Climate Change and Uncertainty in Hydrology and Meteorology

Introduction of MAIRS and Possible Involvement of Thailand in Regional Initiative

Ailikun

MAIRS IPO, Institute of Atmospheric Physics, Chinese Academy of Sciences, aili@mail.iap.ac.cn

ABSTRACT : Asia is a special region of the world, particularly when considering future pathways towards sustainability. The Asian monsoon and the Himalayas – Tibetan Plateau drive a unique climate with global impacts and which, through traditional cultures and practices, have supported a range of sustainable natural ecosystems and human societies for millennia. However, Asia is now in transition. As the development of global change research in monsoon Asian region, the traditional monsoon study is requested to meet the needs from various fields such as agriculture, hydrology and water management, land use and urban design, risk management., Monsoon Asia Integrated Regional Study (MAIRS) has been worked hard to deal with the question on "How to let the current monsoon study transform to support the sustainability research in monsoon Asia region". In this talk, we will mainly introduce some thinking, experiences and case studies on integrated studies under the framework of MAIRS in last several years. In specific, we will focus on monsoon simulation, future projection of Asian monsoon and how to provide support to water and land management for policy making of urban-land design in this region.

KEYWORDS : *Asian Monsoon, Integrated Study, Sustainability Research*

THA 2015 International Conference on
"Climate Change and Water & Environment Management in Monsoon Asia"
28-30 January 2015, Bangkok, Thailand.

Improving Understanding of Atmospheric Loading of Greenhouse Gases Driving Climate Change: Filling Knowledge Gaps to Develop Strategies for Mitigation

Tissa H. Illangasekare [1], Kathleen Smits[1], Elif Agertan[1], Luca Trevisan[1], Michel Plampin[1], Andrew Trautz[1], Ariel Esposito[1], Ben Wallen[1], and Paul Shulte[1].

Abstract Potential long-term impacts of climate change on both local and global water resources and the environment have been recognized. The local and regional impacts will have major implications on the sustainability of water as a resource for a rapidly growing world population facing with the issues of reliable and clean supply of potable water, water for irrigation tied to food security, water for energy development tied to industrial and economic growth, and the quality of the environmental that affects both ecological and human health. Numerical models simulating systems ranging from basin to global scales are needed for these impact predictions and risk analysis. For prediction reliability, these models need to accurately capture water flow, energy and mass transfer processes occurring in the subsurface, on the land surface and in the atmosphere. Many scientific and technological challenges still remain to accurately capture and simulate these processes at all relevant scales. Addressing these challenges require filling scientific knowledge gaps in processes understanding and their parameterization, parameter up-scaling to move across hierarchy of scales, coupling of land and atmospheric systems, among others. This presentation will discuss some of these challenges and identify critical research needs. Examples from ongoing research on green house gas loading that contributes to global warming, and mitigation through carbon storage are presented.

Keywords *Climate change, Global Climate Models, Carbon Capture and Storage, Methane Loading, Soil Moisture and evaporation.*

[1]Center for Experimental Study of Subsurface Environmental Processes (CESEP)
Colorado School of Mines
Golden, Colorado, USA
tissa@mines.edu

Introduction

Primary drivers that have contributed to global warming are loading of green house gases to the atmosphere and the water vapor. Two of the primary greenhouse gases are carbon dioxide (CO_2) and methane (CH_4). Both natural and anthropogenic activities provide sources to these gases. Water vapor in the atmosphere is also a contributor to global warming. Studies have shown that water vapor feedback roughly doubles the amount of warming caused by CO_2. Atmospheric water vapor is a critical component of the global hydrologic cycle controlled by the heat and mass flux across the terrestrial/ atmospheric interface manifested through the processes of evaporation and evapotranspiration. The soil moisture in the shallow subsurface plays critical role in modeling evaporation modeling at all relevant scales from local to the global climate modeling (General Circulation Models or GCMs) scales. Both the predication of loading of greenhouse gases and the mitigation to reduce climate change impacts require the understanding of the fundamental processes of how these gases are transported through the terrestrial systems. This understanding allows for improved detection and measurements, modeling for predication and developing strategies for mitigation. Many knowledge gaps exists in the fundamental understanding of these processes at all relevant scales to develop and validate numerical models that are used for long term predications of impacts and developing effective mitigation strategies.

Atmospheric loading and mitigation of CO_2

The primary factor that contributed to anthropogenic emission of CO_2 since the beginning of the industrial revolution is the combustion of fossil fuels. The concentrations CO_2 in the atmosphere have grown exponentially (Figure 1). These concentrations that are linearly related to radiative forcing (IPCC, 2007) have increased from a pre-industrial value of about 280 ppm to the 400 ppm reached in May 2013. Recent estimates of CO_2 loading are about 30 Gt/year (10^{12} kg) world wide (Boden et al., 2010).

IPCC (2005) proposed three strategies for stabilization and eventual reduction of atmospheric loading of CO_2: (1) reduction of global energy usage, 2) expanded use of renewable resources, and 3) capture and storage of CO_2 in geologic repositories. The first two requires long-term planning and development of strategies that factor in balancing demands with availability energy resources and economic options that vary from country to country. The third that is referred to as Carbon Capture and Storage (CCS) has the potential to achieve the desired goals in relatively short time scales is undergoing extensive research and is at the stage of field implementation.

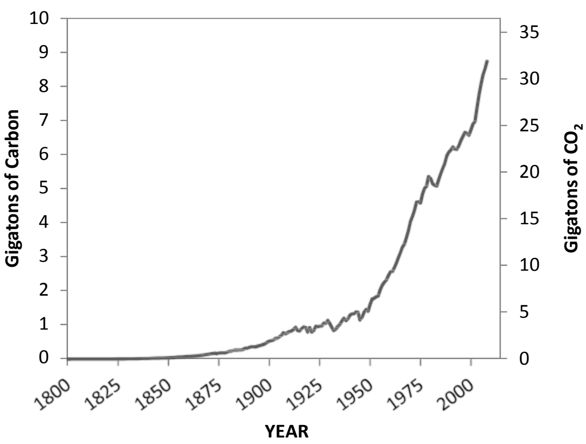

Fig. 1 Total carbon and CO_2 emissions from combustion of fossil fuels (Keating et al., 2009).

Three possible candidate formations have been identified for CCS. These include, depleted oil and gas reservoirs, un-minable coal beds due to their greater depths, and saline aquifers. Underground deep brine-bearing formations have received increased attention due to their potential for greatest storage and extensive geographic distribution around the globe. The global storage capacity estimates have been found to be highly variable in the order of 100 to 10,000 GT (Bradshow et al., 2007). This uncertainty of estimates is attributed to the poor characterization of the geology that contributes to reliability of the fate of CO_2 in the formation after its injection.

Four main trapping mechanisms that immobilize the injected supercritical CO_2 ($scCO_2$) include structural, capillary, dissolution and mineralization (Fig 2). Achieving storage permanence requires stable trapping and minimizing leakage. The fundamental processes that contribute to trapping and gas leakage involve transport and fate of multiphase fluids in porous media. Mathematical models that can be used to design injection schemes and assess storage permanence and leakage risk need to capture these processes. A number of modeling codes based on traditional reservoir engineering numerical algorithms have been developed and used in CCS investigations (e.g. DOE's TOUGH based codes). However, their ability to accurately capture the fundamental processes as controlled by the ubiquitous heterogeneities at all scales from pore to larger simulation scales are not well understood. Filling these knowledge gaps is critical to improve numerical modeling tools used in CCS.

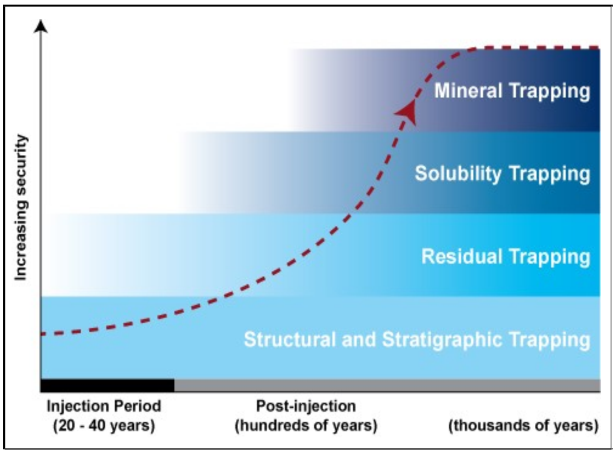

Fig. 2 Mechanisms contributing to storage security of CO2 (modified from IPCC, 2005)

Estimating atmospheric loading of CH_4

CH_4 leakage occurs during the production, processing, storage, transmission, and distribution of natural gas. Another leakage source is the trapped CH_4 in coal deposits and in the adjacent strata that can be released during both underground and surface mining operations. The world's energy picture is changing drastically as the United States is undergoing a major transition to unconventional oil and gas extraction, particularly very clean light oil and gas from shale reservoirs. Extraction of shale gas through hydraulic fracturing represents another leakage source for CH_4. In this case, the leakage can occur through wells as well as seepage through the ground. As a greenhouse gas, CH_4, is more than 20 times as potent as CO_2 over a 100 year period. CH_4 emission from natural gas development is estimated to be around 221.2 million metric tons of CO_2 equivalent in 2009. To evaluate the benefits of transitioning from burning oil and coal to natural gas in the context of reduction of greenhouse gas loading, it is necessary to get better estimates of the total CH_4 loading from unconventional energy development. To meet this demand for accurate CH_4 emission inventories, multiple researchers have looked at the most appropriate means to estimate CH_4 emissions. The methods to estimate emissions can be divided into the "bottom-up" approach and the "top-down" approach. The "bottom-up" approach uses estimated emissions factors, such as CH_4

emitted per fuel consumed. Using these emissions factors with activity data, such as how much fuel is consumed per person and what is the population of the area, they can provide an estimate of emissions for that particular area (Hsu et al. 2010). This method is convenient for statewide or nationwide estimates, because it does not require any direct measurement of atmospheric concentrations near specific sources. On the other hand, "top-down" methods have been developed where actual CH_4 concentrations in the atmosphere and around CH_4 sources such as a rice paddy field or oil and gas wells have been measured. When using the "top-down" approach for greenhouse gas inventories in Southern California, both Wunch et al. (2009) and Hsu et al. (2010) found that the "bottom-up" inventories used by the California Air Resources Board underestimated CH_4 emissions. More recently, two reports clearly show the discrepancy between "top-down" and "bottom-up" emission estimates. The first is from Karion et al. (2013) that took measurements from an airplane that traversed over the gas wells in Uintah County, Utah. They estimated the emission to be between 6.2% to 11.7% of the hourly natural gas production of the field. The second paper addressing leakage using the bottom up approach is by Allen et al. (2013). Their research used sampling from 150 production sites across the US to estimate emissions for specific processes involved in natural gas production. For these discrete activities they estimated 0.53% of the gross CH_4 produced was leaking. These findings suggest the need to reconcile the discrepancies between "top-down" and "bottom-up" estimates.

Many complex factors contribute to the migration of CH_4 in the subsurface that eventually has to be measured at the ground surface to get better estimates of atmospheric loading. Under partially saturated conditions in the soils the CH_4 leakage source will be below the water table. The CH_4 will dissolve until it reaches the solubility limit. This dissolution will act to attenuate the gas signal in the initial time period before steady state is reached. After this point both aqueous phase and gaseous phase CH_4 will be present in the saturated zone. Atmospheric conditions can also influence the gas transport in the unsaturated zone. For example, fluctuations in surface pressure caused by barometric pressure changes or wind gustiness will create a pressure pumping effect and can increase the influence of dispersion on gas flux from the soil to the atmosphere. Also under more turbulent conditions, the gas concentration in the atmosphere could fluctuate significantly based on turbulent eddy generation, leading to unsteady concentration gradients between the soil and the atmosphere at discrete locations.

Improvement to the "bottom-up" approach will depend on the ability to accurately detect and measure the gas fluxes across the land surface. The location and the flux measurements depend on the subsurface conditions as well as the dynamic interaction of the shallow subsurface and the atmospheric boundary layer. Knowledge gaps exist on how gas pathways develop from the locations of leakage to the land surface as affected by subsurface heterogeneities and feed backs between the subsurface and the atmosphere.

Soil moisture and evaporation

Soil moisture in the subsurface controls key physical processes in climate modeling, weather prediction, agricultural crop growth modeling and flood forecasting. In general circulation models (GCMs), soil moisture (defined as the total volume of water divided by the volume of a grid cell containing soil grains, water and gas phases in the numerical model) determines the distribution of the energy budget between latent and sensible heat fluxes at the land surface (Entekhabi et al., 1996), the amount of runoff generation in flood forecasting (Goodrich et al., 1994), and although not addressed here, the carbon and nitrogen biogeochemistry critical to climate feedback analyses. Despite the importance of these predictions, most models have limited capabilities to predict water fluxes, flow pathways and spatial distribution of water in soil and over the land surface. Even common practices such as understanding evaporation dynamics from homogeneous soils or water distribution after a heavy rainfall has proven to be difficult (e.g., Wang et al., 2003; Lehmann and Or, 2009; Smits et al., 2011, 2012). Practical and theoretical limitations associated with modeling are often magnified at the land-atmosphere interface, where water and energy fluxes are highly dynamic and dramatically influenced by changes in thermal and moisture gradients and direction of flows (Lehmann et al., 2012). Flow conditions at and below the soil surface are affected by atmospheric conditions (e.g., humidity, temperature, wind velocity, solar radiation) and soil thermal and hydraulic properties (e.g., thermal and hydraulic conductivity, porosity), all of which are strongly coupled (Figure 1). However, for most conventional land surface models (LSMs) these mechanisms are crudely parameterized and inconsistent with current physical understanding due to the complexity of the problem in field scenarios and the scarcity of field or laboratory data capable of testing and refining energy and mass transfer theories.

Multi-scale testing approach

Research has been undertaken to fill the knowledge gaps to improve the fundamental understanding of the processes that are of central importance in greenhouse gas loading and mitigation. Studying these at a fundamental level is not feasible in field settings because fully characterizing the geologic variability at all relevant scales and making observations on the spatial and temporal distribution of migration rates and pathways are not practical. Models that incorporate this new knowledge have to be validated. Such validation is not feasible in field settings because of high costs involved in subsurface characterization and control of boundary conditions. In our past and ongoing research, we have used a testing approach that involves experiments that are conducted at multiple scales staring from small columns and test cells to intermediate scale. It has been suggested that 2-D and 3-D aquifer experiments are an important *intermediary* between column studies and field trials (Oostrom et al, 2006, Lenhard et al, 1995). The primary advantage of intermediate-scale experiments (generally accepted as maximum length scales up to 10 m that is intermediary between lab column lengths and field size) field-scale processes can be mimicked under highly controlled conditions (Sakaki et al., 2009; Barth et al., 2001). Figure 3 schematically shows the multi-scale testing and modeling approach we currently use in a study involving CCS field-scale processes can be mimicked under highly controlled conditions.

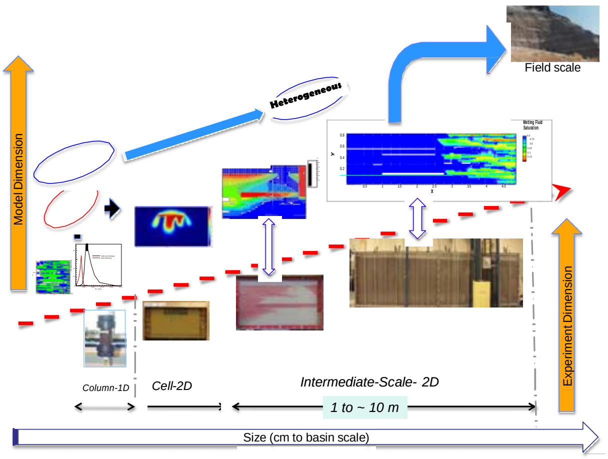

Fig. 3 Multi-scale testing and modeling approach

Results and Discussion

Sample results from intermediate scale experiments for CCS, subsurface methane migration and evaporation are presented.

a. Capillary trapping of supercritical CO2.

A key knowledge gap in the understanding of capillary trapping that has implications on assessment of trapping efficiency is associated with how the geologic heterogeneity effects trapping efficiency. The goal of the experiments is to study the effects of subsurface heterogeneity on capillary trapping. Laboratory investigations of CO_2 injection and migration are challenging, due to difficulties in recreating the high pressures that exist in deep formations. The laboratory investigations of liquid CO_2 migration without high pressure were conducted using analogous fluids having similar densities and viscosities as CO_2 –brine/water phases under sequestration conditions. A non-wetting phase (NWP) consisted of Soltrol 220 (Phillips 66), a low-toxicity, isoparaffinic solvent was used as a surrogate for $scCO_2$ and an aqueous solution of glycerol (80% w/w) was chosen to represent the wetting phase. When the formation is assumed to be homogeneous, the final trapping saturation is estimated using the immobile residual saturation as measured in the capillary pressure versus saturation curve. However, it has been demonstrated in subsurface contamination studies that in heterogeneous systems, the capillary barrier effects at the texture transitions, create saturations that are higher than the residuals (Illangasekare et al., 1995).

A series of experiments were conducted in a 8 ft. (244 cm) × 4 ft (123 cm) intermediate scale test tank. Both homogeneous and heterogeneous packing configurations were created using well-characterized laboratory test sands. After injecting the NWP, the wetting fluid saturation distribution in the tanks was monitored using an x-ray attenuation system. Figure 4 shows the experimental data from the homogeneous experiment.

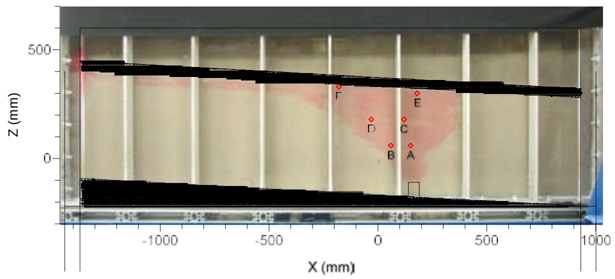

Fig. 4 $scCO_2$ surrogate fluid trapping in a homogeneous formation (Trevisan, 2014).

The heterogeneous spatially correlated packing configuration used six Granusil sands #16, #20, #30, #50, #70, and #110 with the permeability varying between 5.64×10^{-10} m^2 to 5.18×10^{-12} m^2. Figure 5 shows the final trapping configuration of the NWP.

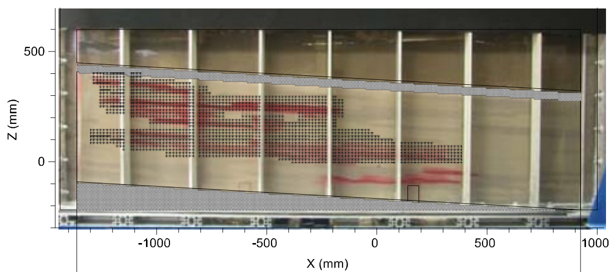

Fig. 5 scCO2 surrogate fluid trapping in a heterogeneous formation (Trevisan, 2014).

A comparison of the two final trapping configurations clearly shows the significant effect of heterogeneity on capillary trapping. The saturation measurements using the x-ray system showed that in the homogeneous packing, the final trapping saturation was close to the residual trapping of # 50 sand in the range 0.16-0.2. Whereas, in the heterogeneous case, because of the capillary barrier effects, the macro-scale trapping saturations varied from residual values up to about 95%. These findings suggest that the heterogeneity of the formation can be used to increase capillary trapping. More detailed analysis of the experimental results can be find in Trevisan et al., 2014 and Trevisan, 2014.

b. Trapping of dissolved CO2

The knowledge gap that is identified is related to the question how the formation heterogeneity affects mixing that contributes to dissolution trapping. When the trapped $scCO_2$ dissolved in formation brine, it produces a solution that is denser than brine, which leads to the generation of density-driven fingers that produce convective mixing. This mixing process contributes to trapping through the dissolved mass remaining in formation brine and in the long-term mineralization depending on the geochemical potential of the rock. To study the impact of geologic heterogeneity on dissolution trapping, a set of experiments were conducted in small test cells and intermediate scale test tanks. Sample set of results from the small tank experiments is presented. More details can be found in Agertan et al., 2014.

In the experiments reported here, as in the case of capillary trapping investigations, surrogate fluids to simulate the dissolution trapping were used. Pure food dyed water and pure Propylene glycol (PG) as surrogates of $scCO_2$ and brine, respectively were selected. The test domain had dimensions of 10 in (25.4 cm) x 6 in (15.2 cm). Figure 6 shows the development of convective fingers in # 30/40 homogeneous pack. The mixing zone profiles that variy with time are shown.

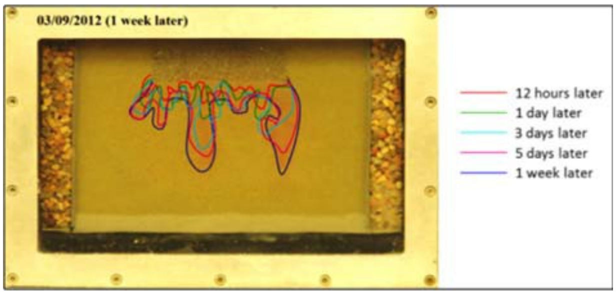

Fig 6 Convective mixing in assumed homogeneous formations (Agertan et al, 2014).

Mixing in affected by heterogeneity was investigated for number of packing configurations. Figure 7 shows how heterogeneity consisting of alternating layers of low and high permeability affects mixing.

A comparison of the results on Figures 6 and 7 highlight the variability of mixing processes at the transition from high to low permeability zones and the impacts on overall trapping. Fingers that produced convective mixing in high permeable layers merged in the diffusion controlled low permeability zones. This suggests the importance of factoring heterogeneity in analyzing the trapping potential in deep geologic formations and in modeling.

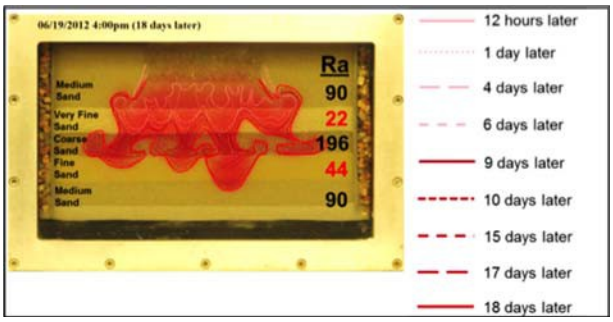

Fig 7 Convective mixing in affected by layering in the formation (Ageratn et al. 2014).

c. Potential leakage of geologically stored CO2

Another critical problem related to CCS is the need to assess the possible leakage of geologically sequestrated CO2. Leakage of CO_2 from underground formations poses risk to the DOE's storage permanence goal of 99% of injected CO_2 remaining sequestered from the atmosphere, which is needed to mitigate potential global climate change. Additionally, leaked CO_2 that invades overlying shallow aquifers may cause deleterious changes to groundwater (Apps et al., 2010) that pose risks to environmental and human health. A set of multi-scale experiments was conducted in test systems consisting of columns to large 2-D intermediate scale tanks. The goal was to understand the mechanisms of gas exsolution and attenuation when formation brine containing dissolved CO2 leaks into the shallow aquifers through defective wells, faults and fractures. The focus was on how the natural geologic heterogeneity affects exsolution and assess the attenuation capacity of the formation as a result of gas trapping and dissolution. Sample results from a set of column studies are presented. More details can be found in Plampin et al. 2014a and 2014b.

Sample results from a column experiment are presented to demonstrate how texture transition in the porous medium triggers gas exsolution. A vertical column was packed with two layers of different sands to create a geologic facies transition. Different sand combinations were used to define different permeability contrasts across the interface. Figure 8 shows a plot of the difference in saturation measured across the texture interface (ΔS_w) versus the difference in the entry pressures (ΔP_e) of the two sands. This data shows the importance of texture transitions in triggering gas exsolution. In cases where a low-permeability soil overlies a more permeable soil, CO_2 gas accumulation at the interface is controlled by the entry pressure difference. Whereas, in the case when the high-permeability soil is above a less permeable soil, the upper soil seems to control the gas accumulation. This has implications on how the gas exsolves and attenuates in heterogeneous formations.

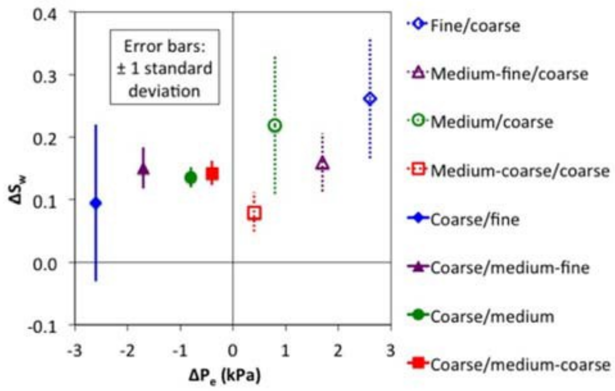

Fig 8 Leaked CO2 gas accumulation at facies transitions (Plampin et al. 2014b)

d. Methane migration is soils

The basic process that is of importance in assessing the atmospheric loading of CH_4 from subsurface sources to the atmosphere is the process of gas migration through soil. The knowledge gap that is addressed is how the mass flux crossing the land/atmospheric interface is affected by the subsurface flow dynamics and the subsurface conditions. A set of experiments was conducted in a newly developed intermediate test facility that couples a soil tank to a climate controlled low-velocity wind tunnel. A sample of these results is presented to demonstrate how the heterogeneity of the formation in combination with the conditions in the boundary layer affects CH_4 flux observed at the land surface.

Figure 9 shows the results from an experiment where the CH4 concentration was measure above the soil surface when a slug of gas was introduced at a point below the soil surface in a homogeneously packed soil tank. The concentrations were measured at different boundary layer velocities.

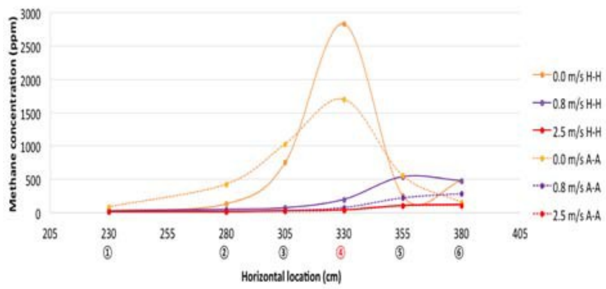

Fig. 9 Methane concentrations measured 1 cm above the soil surface at different boundary layer velocities.

The results show clearly the need to factor in climate conditions when gas saturation measurements are made and interpreted to make atmospheric loading estimates using "bottom-up" approaches.

Figure 10 gives the results from a set of experiments where the gas concentrations were measured for six simulations that allowed for the estimation and compare leakage rates for homogenous and heterogeneous subsurface conditions. In the homogenous case, the tank was filled with #30/40 sand and in the heterogeneous case single layer of finer #50/70 sand was embedded in a #30/40 coarser formation. Three injection rates of 25 mL/min, 50 mL/min and 125 mL/min, respectively were simulated. The plot shows the detected flux at the soil surface as a percentage of the injected rate.

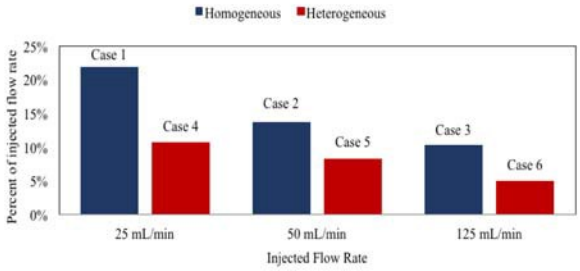

Fig 10 The percentage of the injected flow rate estimated to be leaking into the free stream

The results show clearly the gas flux reduction in the heterogeneous cases suggesting that the variability in soil conditions attenuates the gas signal. This finding directs towards the need to further study of the accumulation capacity of the subsurface when assessing CH_4 loading to atmosphere. More details can be found in Esposito et al, 2014.

e. Evaporation from bare soil

Bare soil evaporation accounts for a significant fraction of average global evapotranspiration from land surfaces on Earth and is on the order of 0.5 m/yr as 25% of the of the land surface is classified as bare soil or agricultural [*Latham et al.*, 2014]. Evaporation from bare soil is a complex non-isothermal, multiphase process that occurs in the unsaturated zone of the shallow subsurface below the land surface. The rate of evaporation is strongly coupled with atmospheric demand controlled by air temperature, relative humidity, fetch, radiation, turbulent air flow, subsurface water and vapor transport (e.g. capillary and film flow, phase change, vapor diffusion) and physical, thermal and hydraulic properties of the soil. Despite the obvious importance evaporation in all aspects of the hydrologic cycle both at local and global scales, this process remains one of the least understood and no physically based standard approach for the modeling or measurement of evaporation exits. With the goal of filling the knowledge gaps on how these strongly coupled shallow subsurface and boundary layer processes occur and effects evaporation, a research program using multi-scale testing and modeling approach (Fig. 3) is in progress. The same coupled porous media and climate controlled wind tunnel facility will be used in the up-scaling experiments.

A sample result from this ongoing study is presented. Evaporation measurements were made in a 55 cm tall, 25 cm long and 9 cm wide soil tank interfaced with a miniature open-ended wind tunnel that allows the temperature and wind velocity to be controlled. Two regions, containing loose and tight packed Accusand #30/40 was created. The tank and wind tunnel were instrumented with an array of sensors to measure wind velocity, soil and air temperature, soil moisture, relative humidity, and the total weight of the tanks to estimate the evaporation. A numerical model based on COMSOL Multiphysics code was developed using the land-atmospheric coupling algorithms presented by *Davarzani et al.* [2014]. Figure 10 compares the experimental data with the developed model and a surface energy balance (SEB) model. This comparison shows that the evaporation rates determined using both modeling methods are in good agreement. However, SEB approaches require knowledge of a large number of inputs which can quickly become cumbersome.

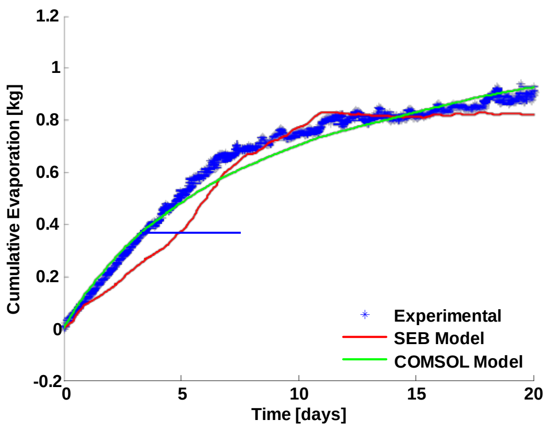

Fig10 Comparison of experimental data to model predictions.

Summary and Conclusions

Estimation of atmospheric loading of greenhouse gases is critical in the prediction of expected global warming and hence, climate change. The focus of the research presented in this paper is to identify knowledge gaps in understanding of how these gases migrate in the subsurface to develop better detection methods and strategies for mitigation. We make the argument that it is not possible to study these fundamental processes at all relevant scales in the field because of the inability to fully characterize the subsurface and lack of control of the boundary conditions and stresses. To overcome this difficulty, a multi-scale testing and modeling approach was proposed. Preliminary results from experiments to improve the understanding of trapping and leakage of CO_2 in geologic carbon sequestration, methane migration and bare soil evaporation were presented. It is our expectation that this research will lead to better conceptual and numerical models that can be used in predication, assessment and mitigation of greenhouse gas loading and thus contributing to climate change predictions.

Acknowledgement

The research reported in this paper is funded by the National Science Foundation (EAR-1045282), US Department of Energy through the National Energy Technology Laboratory (NTEL grant DE-FE0004630), National Security Science and Engineering Fellowship (NSSEFF) Supported by the National Defense Education Program (NDEP) and Unconventional Natural Gas and Oil Institute (UNGI) at the Colorado School of Mines.

References

Agartan, E., A. Cihan, L. Trevisan, J. Birkholzer, Q. Zhou and T. Illangasekare, 2014 The Analyses on Convective Mixing of Dissolved CO_2 in Layered Heterogeneous Geologic Formations with Low Permeability Zones, In revision, Water Resources Research.

Allen, D. T., Torres, V. M., Thomas, J., Sullivan, D. W., Harrison, M., Hendler, A., ... & Seinfeld, J. H. (2013). Measurements of methane emissions at natural gas production sites in the United States. Proceedings of the National Academy of Sciences, 110(44), 17768-17773.

Apps, J. A., Zheng, L., Zhang, Y., Xu, T. F., and Birkholzer, J. T., 2010, Evaluation of potential changes in groundwater quality in response to CO_2 leakage from deep geological storage: *Transport in Porous media*, v. 82, no. 215-246.

Barh, G.R., M.C. Hill, T.H. Illangasekare and H. Rajaram, 2001, Predictive modeling of flow and transport in a two-dimensional intermediate-scale, heterogeneous porous medium. *Water Resources Research*, 37(10), 2503-2512.

Boden, T.A., Marland, G., Andres, R.J., 2010. Global, Regional, and National Fossil-Fuel CO_2 Emissions. Carbon Dioxide Information Analysis Center, Oak Ridge National Laboratory, U.S. Department of Energy, Oak Ridge, Tenn., U.S.A

Bradshaw, J., Bachu, S., Bonijoly, D., Burruss, R., Holloway, S., Christensen, N.P., Mathiassen, O.M., 2007. CO_2 storage capacity estimation: Issues and development of standards. *International Journal of Greenhouse Gas Control* 1, 62-68.

Davarzani, H., K. Smits, R.M. Tolene, and T. Illangasekare (2014), Sutdy of the effect of wind speed on evaporation from soil through integrated modeling of the atmospheric boundary layer and shallow subsurface, *Water Resour. Res.*, *50*, doi:10:10.1002/2013WR013952.

Entekhabi, Dara, Ignacio Rodriguez-Iturbe, and Fabio Castelli. "Mutual interaction of soil moisture state and atmospheric processes." Journal of Hydrology 184.1 (1996): 3-17.

Esposito, E., T. Illangasekare, K. Smits, E. E. Wong, and P. Schulte, 2014, Migration of Natural Gas Through Heterogeneous Sandy Soils Affected by Atmospheric Boundary Conditions, URTeC: 1937753, Unconventional Resources Technology Conference held in Denver, Colorado, USA, 25-27 August 2014.

Goodrich, D. C., T. J. Schmugge, T. J. Jackson, C. L. Unkrich, T. O. Keefer, R. Parry, L. B. Bach, and S. A. Am (1994), Runoff simulation sensitivity to remotely sensed initial soil water content, *Water Resour.Res*.,30(5),1393–1405,doi:10.1029/93WR03083.

Hsu, Y. K., VanCuren, T., Park, S., Jakober, C., Herner, J., FitzGibbon, M., and Parrish, D. D. 2010. Methane emissions inventory verification in southern California. *Atmospheric Environment, 44(1), 1-7.*

Illangasekare, T.H., Ramsey, J.L., Jensen, K.H., Butts, M.B., 1995. Experimental-Study of Movement and Distribution of Dense Organic Contaminants in Heterogeneous Aquifers. *J Contam Hydrol* 20, 1-25.

IPCC (Intergovernmental Panel on Climate Change) special report on Carbon dioxide capture and storage, (2005), Edited by B. Metrz, O. Davidson, H. de Coninck, M. Loos, L. Meyer, Cambridge University Press, New York, USA.

IPCC Working Group I (2007) Climate Change 2007: The Physical Science Basis. Contribution of Working Group I to the Fourth Assessment Report. of the IPCC. Cambridge University Press, Cambridge, United Kingdom.

Karion, A., Sweeney, C., Pétron, G., Frost, G., Michael Hardesty, R., Kofler, J., ... & Conley, S. 2013. Methane emissions estimate from airborne measurements over a western United States natural gas field. *Geophysical Research Letters*, *40*(16), 4393-4397.

Keating, E.H., Fessenden, J., Kanjorski, N., Koning, D.J., Pawar, R., 2009. The impact of CO2 on shallow groundwater chemistry: observations at a natural analog site and implications for carbon sequestration. *Environ. Earth Sci.* 60, 521 – 536

Latham, J., R. Cumani, I. Rosati, and M. Bloise (2014), Global land cover SHARE (GLC-SHARE) database beta-release version 1.0-2014, Food and Agriculture Organization of the United Nations (FAO).

Lehmann, P., and D. Or. 2009. Evaporation and capillary coupling across vertical textural contrasts in porous media. *Phys. Rev. E Stat. Nonlin. Soft Matter Phys*., doi:10.1103/PhysRevE.80.046318.

Lehmann, P., I. Neuweiler, J. Vanderborght, and H. J. Vogel. 2012. Dynamics of Fluid Interfaces and Flow and Transport across Material Interfaces in Porous Media—Modeling and Observations. *Vadose Zone J.*, doi:10.2136/vzj2012.0105

Lenhard, R.J.; Oostrom, M.; Simmons, C.S.; White, M.D. (1995) Investigation of density-dependent gas advection of trichloroethylene: experiment and a model validation exercise. *Journal of Contaminant. Hydrology*. 19:47–67.

Oostrom, M.; Dane, J. H. and Wietsma; T. W. (2006) A review of multidimensional, multifluid intermediate-scale experiments: nonaqueous phase liquid dissolution and enhanced remediation. *Vadose Zone Journal*, Vol. 5, p.570–598.

Plampin, M., T. Illangasekare, T. Sakaki, and R. Pawar 2014a, Experimental study of gas evolution in heterogeneous shallow subsurface formations during leakage of stored CO2, *Int. J. Greenhouse Gas Control*, 22, 47–62.

Plampin, M.R., R. N. Lassen, T. Sakaki, M. L. Porter, R. J. Pawar, K. H. Jensen and T. H. Illangasekare, 2014b,Heterogeneity-enhanced gas phase formation in shallow aquifers during leakage of CO_2-saturated water from geologic sequestration sites, *Water Res. Resh*, DOI: 10.1002/2014WR015715

Sakaki, T., C. C. Frippiat, M. Komatsu, and T. H. Illangasekare (2009), On the value of lithofacies data for improving groundwater flow model accuracy in a three-dimensional laboratory-scale synthetic aquifer. *Water Resources Research*, 45, W11404, doi:10.1029/2008WR007229.

Smits, K.M., V. Ngo, A. Cihan, T. Sakaki, and T.H. Illangasekare. 2012. An evaluation of models of bare soil evaporation formulated with different land surface boundary conditions and assumptions. *Water Resour. Res*., 10.1029/2012WR012113.

Smits, K. M., A. Cihan, T. Sakaki, and T. H. Illangasekare, 2011. Evaporation from soils under thermal boundary conditions: Experimental and modeling investigation to compare equilibrium- and nonequilibrium-based approaches, *Water Resour. Res.*, 47, W05540, doi:10.1029/2010WR009533.

Trevisan, T., A. Cihan, F. Fagerlund, E. Agartan, Hiroko Mori, J.s T. Birkholzer, Q. Zhou, . H. Illangasekare, 2014. Investigation of mechanisms of supercritical CO_2 trapping in deep saline reservoirs using surrogate fluids at ambient laboratory conditions, International *J. of Greenhouse Gas Control*, Vol. 29, Pages 35–49.

Trevisan, T, 2014. A Fundamental Study Of Effects Of Heterogeneity On The Dissolution Trapping Of Supercritical Co2 In Deep Geologic Formations Through Intermediate Scale Testing And Numerical Modeling, PhD Dissertation, Dept. of Civil an

Environmental Engineering, Colorado School of Mines, Fall 2014.

Wang, Z., A. Tuli, and W.A. Jury. 2003. Unstable flow during redistribution in homogeneous soil. Vadose Zone J., 2:52–60.

Wunch, D., P. O. Wennberg, G. C. Toon, G. Keppel-Aleks and Y. G. Yavin, 2009. Emissions of greenhouse gases from a North American megacity, *Geophysical Research Letter*, 36(15), DOI: 10.1029/2009GL039825

ADAPTING TO CLIMATE CHANGE THROUGH EFFECTIVE RISK ASSESSMENT AND MANAGEMENT IN EAST ASIA - AN INITIATIVE FOR COLLABORATION

Jiaguo Qi[1,2], Guanqiong Ye[1], and Xuchao Yang[1]
1. Zhejiang University, Hangzhou, China
2. Michigan State University, East Lansing, Michigan, USA
Email: qi@msu.edu

ABSTRACT

Increases in frequency, intensity, duration, and geographic scope of extreme climate events such as floods, droughts, storm surges, and typhoons in East Asia are imposing significant threats to the nations in the region including food security, infectious disease outbreaks, landslides, infrastructure damages and human capital losses. Therefore, there is an urgent need to develop effective risk assessment and management strategies in order to adapt to the regional climate change, which requires a multidisciplinary collaboration and an integration of science, technology and stakeholders. In this study, risks are categorized and subsequently assessed based on their potential long-, mid-, and short-term impacts and related causes. Strategies to mitigate these risks through better information management, dissemination, broad scale training, and improved forecasting capabilities are discussed for developing a general framework of risk assessment and management. Using case studies in China, challenges, information and knowledge gaps are identified and analyzed, which lead to a comprehensive theoretical framework for disaster prevention, mitigation, and recovery.

Keywords: Climate Change, Adaptation, Risk Assessment

INTRODUCTION

There is significantclimate variability in the monsoon Asia, characterized by strong frequent extreme climate anomalies such as floods and droughts. The intensity and frequency of these climate extremes continue increasing (IPCC, 2012). In addition to these frequent extreme climate events, there is also a steady rise in sea level in the region that imposes significant implications to the coastal ecosystems. Rapid economic development in the coastal zones dramatically altered the pathways of hydrological systems and made the coastal communities more prone to floods and environmental risks. The interactions between all these climatic episodes and landscape alterations impose significant implications of the short-term disasters and long-term sustainability of communities in region. Shown in the report by Anshory & Herminia (2009), the Southeast Asia is at significant risk imposed

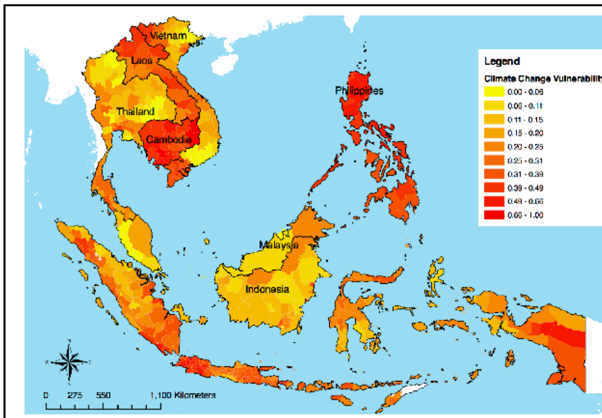

Figure 1. Climate change vulnerability in the Southeast Asia (Anshory & Herminia, 2009)

by regional climate change, sea level rise and human development (Fig. 1).

Given the fact that the climate change is to continue, even with a significant reduction in human-induced emissions of greenhouse gases (GHG), and the demand for further economic development, nations in the region must develop adaptive strategies to mitigate these risks imposed by the increasing extreme climate events (IPCC, 2013). While long-term solutions to climate change, through international treaties in a global effort to reduce GHG emissions, are still challenging, a viable approach to minimizing the negative impacts of climate change and sea level rise is to develop effective risk management options.

Adapting to climate change through effective risk management requires a holistic assessment of environmental risks, their spatial and temporal characteristics, as well as natural and human capitals in a framework that synergistically mainstream management options into decision-making processes (Cardona, 2004; Jaafari, 2001). The purpose of this paper is to demonstrate how such a framework can be established using an example of Elephant Bay ecosystem in the east coast of Zhejiang Province, China.

UNDERSTANDING RISK EXPOSURES

At the interface between water and land are coastal ecosystems, representing a complex system under multiple pressures and disturbances imposed by both human and natural variability of climate. For example, the Elephant Bay in the east coast of Zhejiang Province, China (Fig. 2) is a typical coastal ecosystem subjecting multiple pressures.

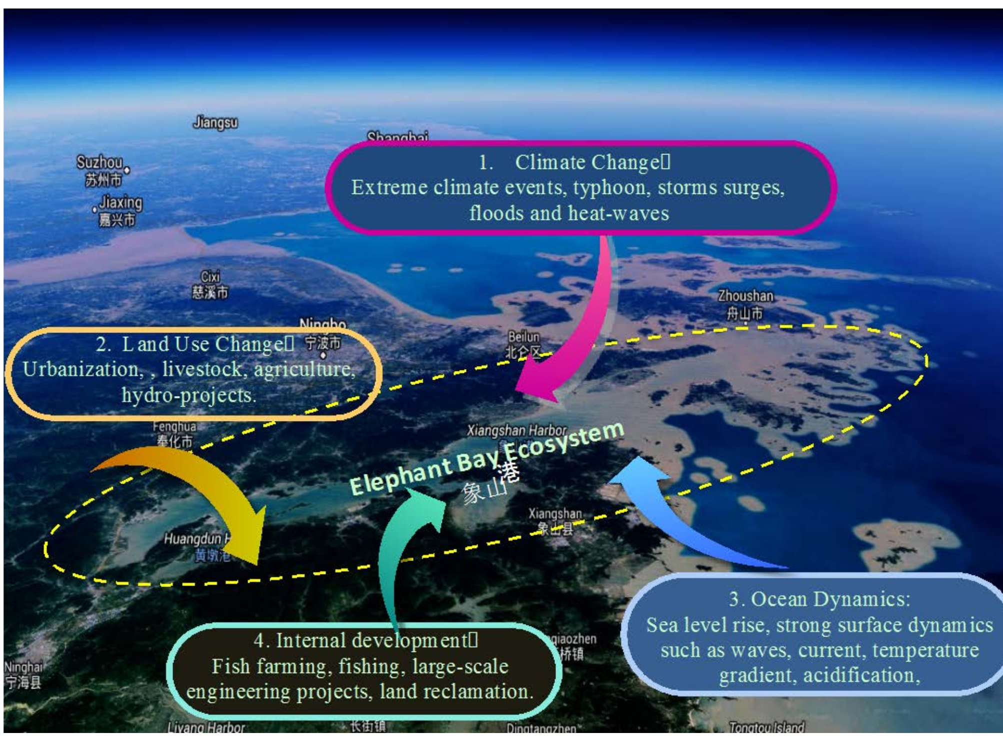

Figure 2. The Elephant Bay representing a typical coastal ecosystem subjected to multiple pressures ranging from 1) climate change, 2) human disturbance through land use change, 3) ocean dynamics changes, and 4) internal development pressures.

1. Climate Change Pressure: This mounting pressure is a result of increases

frequency, intensity, duration and spatial extent of extreme climate events, such as typhoons, heat-waves, wind-speed, floods and droughts. There is evidence that these extreme events have had significant impacts on the property damage, fish production, human health, and biodiversity of the bay ecosystems.

2. Land Use Change Pressures: Significant land use change has occurred over the past three decades in the associated watersheds that, to large extent, impacted hydrological processes, nutrient and pollutants discharges, soil erosions, and flood vulnerability. These changes include urbanizations at multi-levels ranging from small towns and villages to large metropolitans, agricultural intensification through applications of chemicals and irrigations, construction of dams and destruction of wetlands, and channelization of rivers and streams.
3. Ocean Dynamic Change Pressures: Continued sea level rise, accompanied by strong extreme climate events such as typhoons, resulted in stronger storms and wind to damage properties and human safety. At the same time, it is expected to produce more active exchanges in energy, nutrients, sediments, temperature, and other materials between bay and deep oceans that would have significant implications on the ecology of the bay system including fisheries and water quality.
4. Internal Development Pressures: Land reclamation along shorelines not only reduced the wetland buffer zones important to many coastal species but also shortened the physical distances between human settlement and water fronts. This has significant implications on the direct discharges of nutrient and pollution to the bay system as well as has imposed human to risky typhoons and other related extreme climate events. Installment of power plants and construction of bridges have resulted in large-scale modification of the thermal dynamics of water and ocean impacting the ecological environment niche for many species. Construction and intensification of fish farms has changed the micro-environment of the bay system that can lead to macro-environmental degradations and jeopardizing many aquatic species.

These pressures interact together to mount an overall exposure of the Elephant Bay system to both short-and long-term risk and sustainability. Pressures related to human activities might be reduced through management options and policy means. However, the challenges are how to balance among economic development, short-term risks and long-term sustainability. Regarding the pressures from climate change, it is yet still unmanageable through human interventions. The only viable means is adaption via effective risk management. Even then, there is still a need to balance between short-term and long-term risks that yet to be clearly defined and articulated. Here we define the risks at four levels regardless of the causes:

1) Immediate risks - those imposed by e.g., typhoons and storms that cause immediate damages to natural and human capitals;
2) Foreseeable risks – risks resulting from, for example, nutrient and pollution enrichment in the aquatic systems that are known to cause ecological degradation in a foreseeable future;
3) Long-term risks – risks associated with, for example, sea level rise and global warming that will impose challenges to ecological functions and services but

their rate of change is slow and progressive in nature;

4) Unexpected risks – risks of unknown nature that we have little knowledge at the moment but may have significant consequences to ecosystems and society, including for example, outbreaks of infectious disease such as SARS and Ebola.

A CLIMATE ADAPTATION FRAMEWORK AND RISK MANAGEMENT

To adapt climate change and its related risks, a framework is proposed (Fig. 3) that takes a system approach to link drivers and exposures (E) to impacts and vulnerability (V) of both ecosystems and social systems, then to adaptive capacity (A) of the both society and ecosystems, and finally to the policy intervention and management options (M) that are targeted at reducing the exposures and adjustment of drivers to eventually enable a sustainable evolution of socio-ecological systems (Fig. 3).

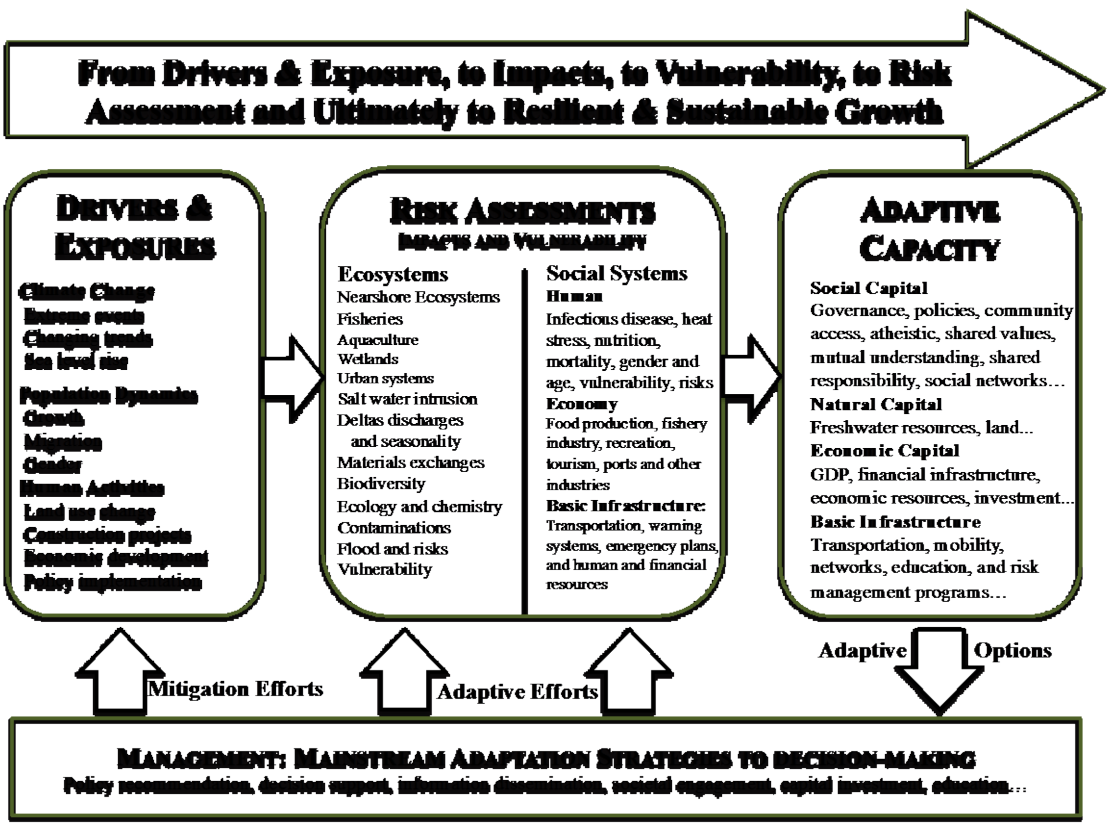

Figure 3. A general framework to adapt climate change through effective risk management

The proposed framework is a system where all components are interconnected and therefore should be considered all together when a decision is made for adaptation. In reality, all components are in motion simultaneously and a small change in one component can have significant impacts on others or be magnified, and at the same time it may also be insensitive to other components and thus having little impacts on other components. There have been substantial work dedicated to climate change adaptation and risk assessment, so the challenge is how to quantitatively link all components in a framework that couple climate change, ecosystem processes, socioeconomics, human activities, and policy interventions.

Drivers and Exposures: This component includes any changes in either climate or human system or both that can impact ecosystems and societies. Examples are weather pattern deviation from normal ranges (or climate extremes such as extended droughts and floods) and human modification of landscapes such as land use change that significantly alter the biogeochemical cycles and hydrology of earth systems. These changes can either be caused by humans or by natural processes. However, often these two are connected and act together to impact ecosystem functions and services. For risk assessments, characterization and quantification of these changes need to be analyzed to have a good measure of the human exposures to these changes.

Risk Assessment (Impacts and Vulnerability): Once we understand the exposures they need to be quantitatively linked to impacts they impose on ecosystems and society. This includes risks imposed to ecosystem services loss, basic infrastructures damage,economicloss, human health complications and loss of lives. Risk assessment and management has been researched extensively often with regard to a specific type of risk. However, effective risk assessment and management must be thorough and quantitative (Fig. 4).

One of the key issues is to determine the socio-ecological systems' assimilative capacity. This is where the ecosystem functions and communities are minimally affected by the drivers and exposures. This leads to the determination of the tipping points where increase in exposures can cause a rapid rise in risk level. If exposures and drivers are to continue mounting, the risk level may rise to the thresholds of risk zone that can cause detrimental damage to the socio-ecological systems. Knowing the characteristics of the risks under given exposures and drivers, effective risk reduction effort should focus on the "management effort zone" where rapid rise in risk occurs when exposures are elevated, with a goal to lower the risk level while allowing some uncontrollable exposures to exist or even limited increases.

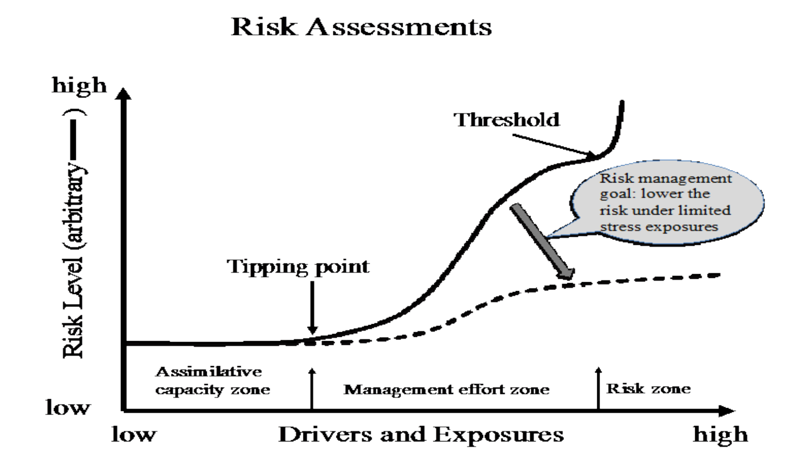

Figure 4. Risk characteristics and assessments of socio-ecological systems for effective management options

Adaptive Capacity: Once the risk levels are understood, there is a need to assess the capitals of socio-ecological systems, including social capital, natural capital, economic capital, as well as basic infrastructures that allow the development of adaptive options.

Integrating the knowledge of risk characteristics and risk levels, adaptive options should be prioritized to focus on risk reduction efficiency, feasibility, and specific types of risks that the socio-ecological system is facing. It is should be noted that the adaptive capacity assessment may not be limited to any geographic boundary, or communities or nations, due to tele-coupling nature of many acting agents, exposures, economy, social migration resulting from globalization processes (Brondízio & Chowdhury, 2013; Brown et al., 2013).

Human Interventions: Once priority adaptive options are identified, management options will be implemented through the implementation of policy recommendation, enhanced decision support tools, public education and societal engagement. It is also required to have an effort to monitor and assess the effectiveness of management option implementations, allowing an adaptive and iterative process to continue the risk level dynamics.

FUTURE PLAN AND CALL FOR COLLABORATION IN MONSOON ASIA

Monsoon Asia is characterized by dramatic demographic change and rapid economic growth and urbanization, great disparities of wealth both within and between countries, and social and ecological vulnerability to the potential impacts of climate change (Varis et al., 2012). Human activity is significantly transforming terrestrial and aquatic ecosystems through increased industrial pollution, land-use change and greenhouse gas emissions in the region that may in turn further impact monsoon climate patterns to further harm social and economic development in the region.This region is also a huge hot-spot region for air and water pollutions (Rock, 2002; Randel et al., 2010), which are affecting the health of more than 60% of the global population.

Monsoon Asia has extraordinary long coastal lines vulnerable to impacts of climate change, particularly sea level rise, and human induced pollutions (Dasgupta et al., 2007; Watson et al., 1998). Coastal water pollutions, escalated by enhanced pollution discharges, fish farming, ocean reclamation, construction of bridges and diversion and obstruction of waterways have significant negative impacts on ecosystems and human populations at local, regional and continental scales. Asian delta systems are often densely populated, intensively used and highly vulnerable to shifts or shocks originating upstream or in neighboring seas and oceans.

Monsoon Asia should collaborate to improve its capacity for risk management of both natural and human-caused disasters, since the region exhibits high human vulnerability to extreme hydro-climatological and tectonic events (e.g. typhoons, heavy rains, floods and droughts, landslides, earthquakes and tsunamis). Disasters expose different dimensions of social-ecological vulnerability and therefore disaster risk reduction is an important field of sustainability research and action. In the event of disaster, it is crucial to address immediate recovery needs as well as to develop learning systems that will improve social-ecological resilience to potential future disasters and build sustainability in the long term.

REFERENCE

Brondízio, E. S., & Chowdhury, R. R. (2013). Human-Environment Research: Past

Trends, Current Challenges, and Future Directions. In Human-Environment Interactions (pp. 391-400). Springer Netherlands.

Brown, D. G., Verburg, P. H., Pontius Jr, R. G., & Lange, M. D. (2013). Opportunities to improve impact, integration, and evaluation of land change models. Current Opinion in Environmental Sustainability, 5(5), 452-457.

Cardona, O. D. (2004). The need for rethinking the concepts of vulnerability and risk from a holistic perspective: a necessary review and criticism for effective risk management. Mapping vulnerability: Disasters, development and people, 37-51.

Dasgupta, S., Laplante, B., Meisner, C., Wheeler, D., & Jianping Yan, D. (2007). The impact of sea level rise on developing countries: a comparative analysis. World Bank policy research working paper, (4136).

Jaafari, A. (2001). Management of risks, uncertainties and opportunities on projects: time for a fundamental shift. International journal of project management, 19(2), 89-101.

IPCC (Intergovernmental-Panel-on-Climate-Change) (2012): Summary for policymakers. In: Managing the Risks of Extreme Events and Disasters to Advance Climate Change Adaptation (eds Field, C.B., Barros, V., Stocker, T.F., Qin, D., Dokken, D.J., Ebi, K.L., Mastrandrea, M.D., Mach, K. J., Plattner, G.-K., Allen, S.K., Tignor, M. & Midgley, P.M.). A Special Report of Working Groups I and II of the Intergovernmental Panel on Climate Change. Cambridge University Press, Cambridge, UK, and New York, NY, USA, pp. 1–19.

IPCC (Intergovernmental-Panel-on-Climate-Change). (2013). Climate change 2013: The physical science basis. Contribution of Working Group I to the Fourth Assessment Report to the Intergovernmental Panel on Climate Change. Cambridge University Press.

Randel, W. J., Park, M., Emmons, L., Kinnison, D., Bernath, P., Walker, K. A., ... & Pumphrey, H. (2010). Asian monsoon transport of pollution to the stratosphere. Science, 328(5978), 611-613.

Rock, M. T. (2002). Pollution control in East Asia: lessons from the newly industrializing economies. Resources for the Future.

Varis, O., Kummu, M., & Salmivaara, A. (2012). Ten major rivers in monsoon Asia-Pacific: An assessment of vulnerability. Applied Geography, 32(2), 441-454.

Yusuf A. A. &Herminia F., 2009. "Climate Change Vulnerability Mapping for Southeast Asia," EEPSEA Special and Technical Paper, Economy and Environment Program for Southeast Asia (EEPSEA), Singapore.

Watson, R. T., Zinyowera, M. C., & Moss, R. H. (Eds.). (1998). The regional impacts of climate change: an assessment of vulnerability. Cambridge University Press.

Yusuf, A. A., & Francisco, H. (2009). Climate change vulnerability mapping for Southeast Asia. Economy and Environment Program for Southeast Asia (EEPSEA), Singapore, 10-15.

Uncertainty in climate change projection and its impact on hydrology of the Nam Ou River Basin

Manisha Maharjan[1, a *], Mukand S. Babel[2,b] and Shreedhar Maskey[3,c]

Abstract Climate change is likely to increase mean temperature affecting every aspect of hydrological cycle. More frequent and severe droughts and floods are already apparent, and their impact increases as a growing population becomes more dependent upon a set of atmospheric and hydrological circulations. The variation in temperature leads to change in evapotranspiration, rainfall pattern and flow quantity. Besides, there is always an uncertainty in projection of future climate and hydrological variables. This uncertainty is attributed to use of different General Circulation Models (GCMs), greenhouse gas emission scenarios, downscaling techniques and hydrological models. This research focuses on the uncertainty in future climate projection and its impact on hydrology of the Nam Ou River Basin under different GCMs and emission scenarios. Long Ashton Research Station - Weather Generator (LARS-WG) was used to downscale future climate for 2046-2065 and 2080-2099 periods under various GCMs and two scenarios A1B and A2. The impact of uncertainty in future climate on discharge was studied using Soil and Water Assessment Tool (SWAT). Probability density functions (PDFs) were constructed to analyze uncertainty in future climate and flow of the basin. The result shows increase in maximum and minimum temperature in the future periods. Precipitation is observed to change in both positive and negative direction from the baseline, depending on the GCMs and emission scenarios used. Wide variation in temperature and precipitation is depicted during 2080-2099 compared to 2046-2065 under GCMs. Increase in inter-model variability and variance of the future projections were depicted towards the end of century.

Keywords Climate Change, Discharge, GCMs, LARS-WG, Soil and Water Assessment Tool, uncertainty

Manisha Maharjan
Water Engineering and Management
Asian Institute of Technology
Pathumthani, Thailand
maneesha064@gmail.com

Mukand Singh Babel
Water Engineering and Management
Asian Institute of Technology (AIT)
Pathumthani, Thailand
msbabel@ait.asia

Shreedhar Maskey
Department of Water Science and Engineering,
UNESCO-IHE Institute for Water Education
Delft, The Netherlands
s.maskey@unesco-ihe.org

Introduction

The Mekong River Basin is vulnerable to climate change and climate variability as the functionality of the basin is disturbed by changing hydrology and land use. The temperature is expected to increase in between 1.0 to 4.5^{o}C by the end of century (IPCC, 2007). Increase in temperature is linked with increasing evapotranspiration which might change in precipitation and hydrology of the river basin. The changes in climate will have direct and indirect impact of the hydrologic flow regime and ecology of the river basins. Different research pointed out the multi-directional change in precipitation in the future periods under different greenhouse gas emission scenarios. Spatial variation of precipitation and change in its pattern causes the variability of runoff and sediment yield. Consequently, it will be difficult to quantify the changes with robustness. Climate change does have impact on water availability and water scarcity which is one of the main concerns of climate change. Other natural disasters such as flood and drought are likely to happen with the time periods. There are different Global Climate Models (GCMs) and Regional Climate Models (RCMs) which helps in the climate change impact assessment on the water resource systems. However, the use of the GCMs and RCMs also does not provide robust result due to various kinds of uncertainties associated with climate change projections. The factors which play significant role in climate uncertainty are the use of coarser GCMs, physical derivations behind GCMs and RCMs, downscaling techniques used, greenhouse gas emission scenarios and model parameterization.

Different downscaling techniques are used to assess the impact of climate change such as statistical downscaling (Chen et al. 2011), stochastic weather generator approach (Semenov and Barrow 1997; Hashmi et al., 2009) and other. In this research, a stochastic weather generator, Long Ashton Research Station Weather Generator (LARS-WG) is used for future climate projection. LARS-WG has been tested in diverse climates and is found to be suitable in climate change projections (Semenov and Stratonovitch 2010;

Zhang et al. (2011); Khan et al. 2006). The LARS-WG has incorporated 15 GCMs used in IPCC-AR4 for future climate predictions.

The main focus of this paper is to quantify the uncertainties in climate change projections associated with various GCMs and Green House Gas Emission Scenarios (GHGES) and assess the impact of the uncertainty in future climate on the discharge of the Nam Ou River Basin.

Study area and data

The Nam Ou River Basin is one of the important sub-basins of the Mekong River Basin. It extends from latitudes 21°17'17" N to 22°30'40" N and longitudes 101°45'47" E to 103°11'57" E. (Figure. 1) with drainage area of 26000 Km^2. The average annual basin rainfall is approximately about 1700mm. The elevation varies from 263 to 2035 m above mean se level. The climate of Nam Ou River Basin is divided into two distinct seasons: wet season (May to October) and dry season (November to April). The main land use is woodland and shrubland which covers 62% of total landuse. Daily observed rainfall data for period 1980-2003 are obtained from the Secretariat of Mekong River Commsion Phnom Penh (MRC) from 11 stations and daily meteorological data such as minimum temperature, maximum temperature, solar radiation, wind speed and humidity from 3 stations for period 1992-2003. The daily maximum and minimum temperature for 1980 - 1991 were derived by using statistical relationship between observed data and 0.5 degree gridded global daily temperature data from the Santa Clara University (SCU) (http://www.engr.scu.edu/~emaurer/global_data/) for 1992-1999.

A Digital Elevation Model (DEM), soil map and land use map are collected from MRC. The daily discharge for period 1992-2003 was obtained from Muong Ngoy station.

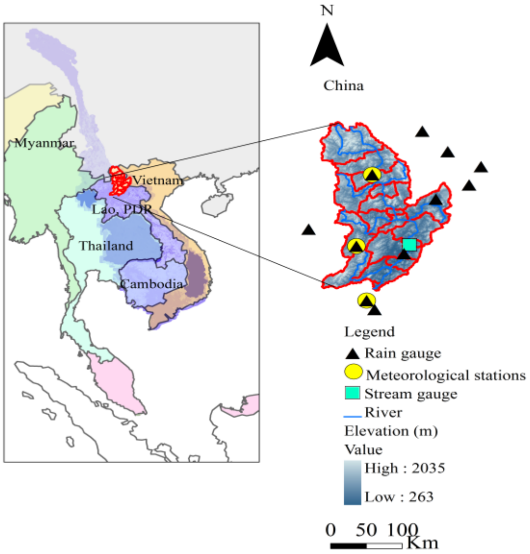

Figure 1: Study Area: Nam Ou River Basin

Methodology

Future Climate Projection

Five GCMs are selected in order to study the uncertainty of climate projection and its impact on the hydrology of the Nam Ou River Basins. These 5 GCMs namely, IPCM4, MPEH5, NCCCSM, MIHR and HADCM3 are incorporated in Long Ashton Research Station - Weather Generator (LARS-WG) and are projected under two greenhouse gas emission scenarios A1B and A2 and two future periods 2046-2055 and 2080-2099.

The resolution of selected GCMs varies from $1.4^{o} \times 1.4^{o}$ to $2.5^{o} \times 3.75^{o}$. LARS-WG is a stochastic weather generator model developed by Mikhail Semenov to predict the future climate i.e., precipitation and temperature. It follows three basic steps: first is the analysis of the observed weather parameters such as rainfall, temperature and solar radiation, and second is to perform Q-test, followed by generation of synthetic daily weather data utilizing the weather parameters obtained (Semenov and Stratonovitch, 2010). The observed baseline period is 1981-2000.

The observed precipitation, maximum and minimum temperature are used to determine the statistical parameters in the baseline period which is to generate the synthetic weather representing the baseline. The uncertainty analysis of future climate projections under various GCMs is done by constructing probability density functions (PDFs).

Hydrological Model Simulation

Soil and Water Assessment Tool (SWAT) is used to simulate the discharge in the Nam Ou River Basin. SWAT is a semi-distributed hydrological model which is capable to evaluate small or large basins by discretizing into different sub basins (Neitsch et al. 2009). The sub-basins are classified into Hydrological Response Units (HRUs) which constitutes homogeneous landuse, soil and slope. Hydrology is simulated at each HRUs is determined by using water balance equation, including rainfall, runoff, evapotranspiration, percolation and return flow components. The surface runoff in SWAT can be calculated by two different methods: SCS-Curve number method (SCS 1972) and, Green and Ampt Infiltration Method (1911). In this study, surface runoff is estimated for each HRU using SCS-Curve number method (SCS 1972) given by:

$$Q_{surface} = \frac{(R_{day} - I_a)^2}{(R_{day} - I_a + S)} \qquad (1)$$

where, $Q_{surface}$ = accumulated runoff (mm)
R_{day} = rainfall depth for the day (mm)
I_a = initial abstraction (mm) = 0.2S
S = retention parameter (mm)

The retention number is given by:

$$S = 25.4\left(\frac{1000}{CN} - 10\right) \qquad (2)$$

where, CN = curve number (function of permeability of soil)

The evapotranspiration is estimated using Penman-Monteith method (Monteith 1965) in this study. The variable storage routing method facilitated the flow routing in the channel reach.

The input datasets using in SWAT model are DEM, land use map, soil map, slope classification and climate data. The calibration of SWAT model for discharge is conducted for the period 1992-1999 and validated for 2000-2003. Two years period is considered as warm up period to maintain the initial state variables.

Three goodness-of-fit indicators (GOFIs) are used to evaluate the performance of the SWAT model during calibration and validation. These GOFIs are Nash-Sutcliffe efficiency (NSE), Pearson's correlation coefficient (R^2) and Percent Bias (PBIAS).

The Nash-Sutcliffe efficiency, NSE determines relative magnitude of the variance of the simulated compared to the observed variance given by equation 1 as follows:

$$\mathrm{NSE} = 1 - \left[\frac{\sum_{i=1}^{n}(Q_i^{obs} - Q_i^{sim})^2}{\sum_{i=1}^{n}(Q_i^{obs} - Q_i^{mean})^2}\right] \qquad (3)$$

Where, Q_i^{obs} and Q_i^{sim} are observed and simulated discharge in m^3/s and Q_i^{mean} is the mean discharge in m^3/s. NSE lies within ∞ to 1, but NSE equals to 1 fits perfectly.

Similarly, Pearson's correlation coefficient (R^2) ranges from 0 to 1; $R^2 = 1$ shows the perfect fit between observed and simulated values.

The Percent Bias (PBIAS) is used to measure the average tendency of simulated discharge being larger or smaller than observed data given by equation (2):

$$\mathrm{PBIAS} = \left[\frac{\sum_{i=1}^{n}(Q_i^{obs} - Q_i^{sim}) \text{ x } 100}{\sum_{i=1}^{n}(Q_i^{obs})}\right] \qquad (4)$$

The optimal value of PBIAS is 0 and the positive value shows underestimation and negative value shows overestimation bias of the model.

The performance of the model is considered to be satisfactory when NSE and $R^2 > 0.6$ (Santhi et al. 2001; Setegn et al. 2010) and PBIAS < 15% (Santhi et al. 2001; Van Liew et al. 2007).

Results and discussion

Projection of rainfall and temperature in the future periods

The projection of future climate is compared with the climatic conditions in the baseline period 1981-2000. From Table 1, increase in maximum and minimum temperature is obvious in future periods 2046-2065 and 2080-2099. In contrast, the precipitation is expected to increase with all GCMs except due to IPCM4.The IPCM4 is the only GCM which projected decrease in precipitation by significant amount under A1B and A2. The highest amount of annual rainfall i.e. 420mm is projected by HADCM3 during 2090s under A2.

Table 1. Changes in maximum and minimum temperature and rainfall in future periods 2046-2065 and 2080-2099 under 5 GCMs and 2 GHGES

		Change with respect to Baseline (1981-2000)		
GCMs	GHGES	Tmin (°C)	Tmax (°C)	Rainfall (mm)
		2046- 2065		
HADCM3	A1B	1.98	1.98	192.68
	A2	1.84	1.84	150.33
IPCM4	A1B	2.21	2.21	-4.87
	A2	2.16	2.16	-113.93
MIHR	A1B	2.17	2.01	55.05
	A2	N/A	N/A	N/A
MPEH5	A1B	1.46	1.47	220.07
	A2	1.77	1.77	-85.05
NCCCSM	A1B	1.68	1.67	237.74
	A2	1.69	1.69	105.17
		2080-2099		
HADCM3	A1B	3.33	3.34	289.40
	A2	3.89	3.89	420.33
IPCM4	A1B	3.82	3.83	-179.57
	A2	4.20	4.21	-130.31
MIHR	A1B	3.49	3.64	25.76
	A2	N/A	N/A	N/A
MPEH5	A1B	3.46	3.47	164.12
	A2	3.60	3.60	169.27
NCCCSM	A1B	2.40	2.40	234.53

SWAT model calibration and validation

The hydrologic model calibration and validation is based on daily observed and simulated discharge at Muong Ngoy staion. The most sensitive parameters in simulating discharge base flow alpha factor (ALPHA_BF), recharge to deep aquifer (RCHRG_DP), curve number (CN2), hydraulic conductivity of the channel (CH_K2), manning n –value of the main channel (CH_N2), Soil evaporation compensation (ESCO), Available water capacity (mm/ mm soil), Sol_AWC. Figure 2 and 3 showed the comparison of daily observed and simulate discharge for calibration and validation respectively. The simulated discharge fits the observed during calibration with NSE = 0.64, R^2 = 0.64, and PBIAS = 5.12%. Similarly, the model validation was satisfactory with NSE = 0.72, R^2 = 0.74, and PBIAS = -14.25%. These results showed that the total runoff volumes are matched with the simulated values, which shows that the discharge will be well predicted with the calibrated model.

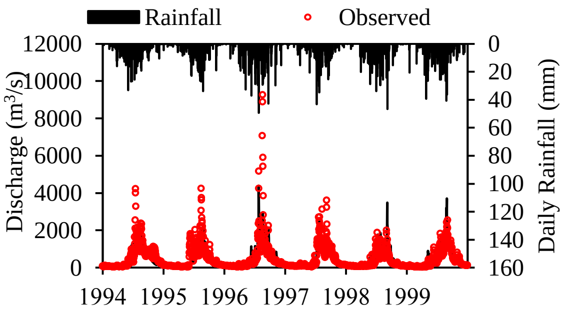

Figure 2: Comparison of observed and simulated discharge during calibration period 1994-1999.

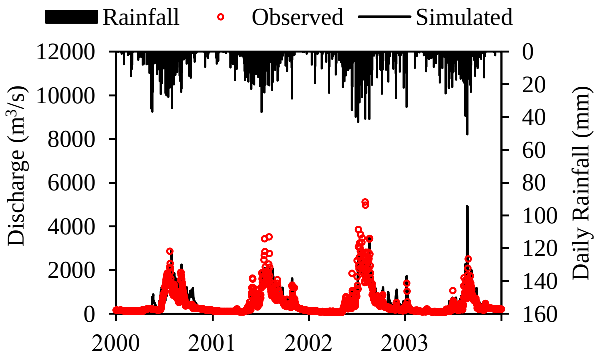

Figure 3: Comparison of observed and simulated discharge during validation period 2000-2003.eriod 1994-1999.

Uncertainties in climate change projection

The climate projection under different GCMs and GHGES resulted in the uncertainties in the projection of future climates. The probability density functions are constructed in order to quantify the amount of uncertainties. Figure 4, 5 and 6 shows the probability density functions of rainfall, maximum and minimum temperature. With the help of PDFs, the range of uncertainties between the mean of future climate as well change in climate extremes are observed. The projection of annual mean precipitation under A1B depicted the higher range of uncertainties in 2090s than in 2055s. But this uncertainties range change in both the periods under A2 scenarios as shown in figure 4c and 4d. The median value of annual rainfall is approximately about 1600mm in the baseline period. The median value of rainfall increased for each GCM under A1B in 2055s period. A GCM, IPCM4 projected decrease in median of annual mean precipitation to 1450 mm. This is the variability of rainfall in the end of the century under A1B. The study showed that the direction of change in rainfall is in both towards increment and decrement when the precipitation is projected under A2. This points out that the rainfall variation under A2 in future periods is significantly larger under different GCMs. The projection of annual mean precipitation also explains that the wet days in the baseline period are expected to be wetter in future under A1B whereas, A2 scenario demonstrated that the wetter days in the baseline period are getting drier due to IPCM4 and MPEH5. The highest range of change in mean annual precipitation varies from 1450mm to 1900 mm under A1B scenario during 2090s. This range varies from 1450 to 2050 mm under A2 during the same future period.

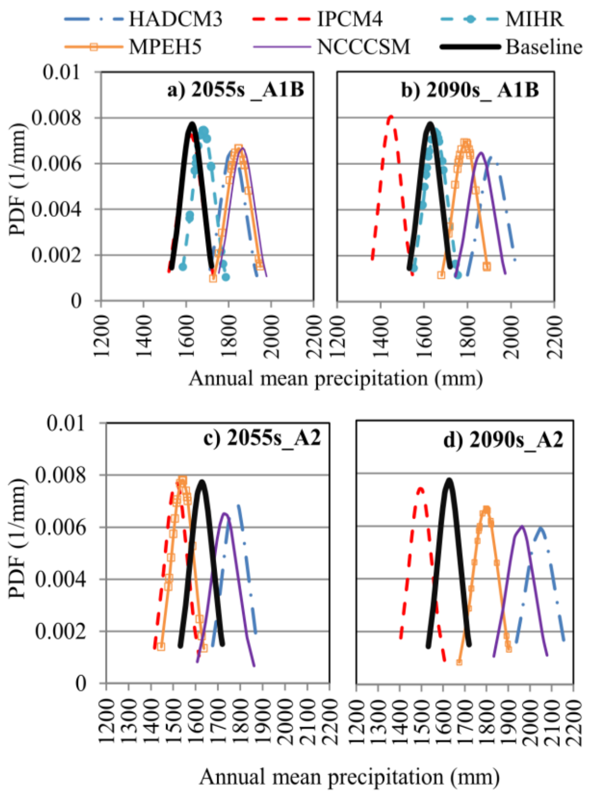

Figure 4: PDFs of the annual mean precipitation for baseline period (1981-2000) and future periods (2055s and 2090s) under A1B and A2 scenario

In case of maximum and minimum temperatures, all GCMs projected the increase in temperature irrespective of GHGES and future periods. The magnitude of increasing temperature however varies from one GCM to another in future periods. During 2055s, the median value of Tmax varies between 29.5 and 30°C under A1B, between 29.9 and 30.11°C under A2. At the same time, the ranges of median Tmax vary from 30.3 to 31.8°C under A1B and from 31 to 32.3°C under A2 during 2090s. In most of the scenarios, NCCCSM predicted lower increase in maximum temperature and IPCM4 predicted higher increase in maximum temperature.

In case of minimum temperature, the variation among the projection of GCMs during 2055s under A1B and A2 is not too much (Figure 6). The A2 scenario projected increase in minimum temperature remarkably during 2090s. The result points that the days in the future periods are getting hotter in hot and cold season. It can be concluded that the temperature is predicted to increase to higher extent in 2090s period, followed by 2055s period.

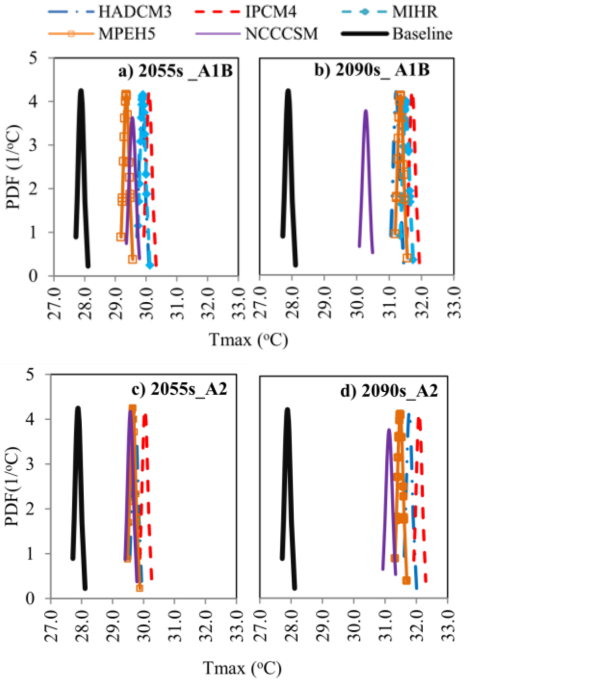

Figure 5: PDFs of the annual maximum temperature for baseline period (1981-2000) and future periods (2055s and 2090s) under A1B and A2

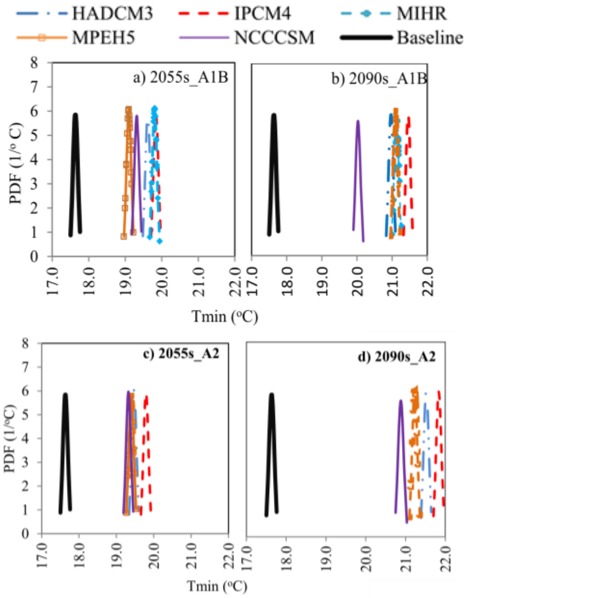

Figure 6: PDFs of the annual minium temperature for baseline period (1981-2000) and future periods (2055s and 2090s) under A1B and A2

Impact of uncertainty in climate projection on discharge of Nam Ou River Basin

The uncertainty in climate change projection i.e. precipitation and temperature has an influence on the discharge of the Nam Ou River basin. The increase in annual discharge by 5.7% during 2055s period and 3.13% during 2090s periods is observed under A1B and by 9.23% in 2090s under A2 (Figure 7). The variation of discharge is since both magnitude and direction when all GCMs are considered with two GHGES. The uncertainty in the prediction of discharge due to different GCMs and GHGES is found to be increasing with time. The analysis showed that the wetter months are going to be wetter comparatively higher than dry months.

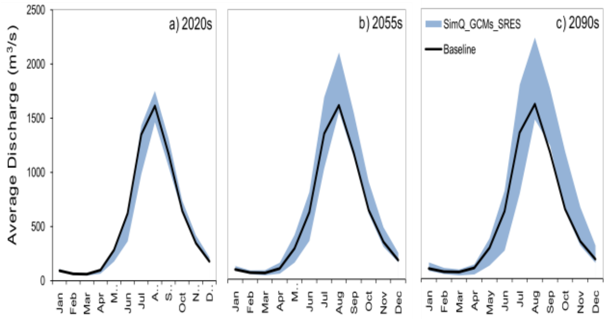

Figure 7: Envelopes of simulated discharge under different GCMs and GHGES for three future periods with the plot of simulated discharge for the baseline period 1981-2000 for comparison. (Note: SimQ_GCMS_SRES represents the result of simulated discharge under all GCMs and GHGES considered)

Summary and conclusions

The study highlighted the uncertainty in future projections of precipitation and temperature due to 5 GCMs and two GHGES and its impact on the discharge of the Nam Ou River Basin. LARS-WG was used to project future climate in two future periods 2046-2065 and 2080-2099. The study revealed that the temperature is expected to increase under both GHGES and all GCMs; whereas the precipitation is expected to change in both direction and magnitude. The uncertainty in climate data increases with time, which makes it more difficult to predict the future climate with robustness. SWAT model calculated the discharge of the basin which was then assessed to quantify the probable impact on the runoff the basin in the future climatic condition. The change in precipitation and temperature correspond to change in discharge. In addition, the results indicated quite clearly that the choice of GCMs and GHGES is very important for any climate change impact study on hydrology. This give emphasis to the necessity of better understanding about uncertainties in future projections and developing efficient techniques to reduce them

Acknowledgement

The author would like to acknowledge the support from the Government of Japan to conduct this research at the Asian Institute of Technology. This paper is developed as a part of PRoACC (Post-doctoral Programme on Climate Change Adaptation in the Mekong River basin) programme funded by the Netherlands Ministry of Development Cooperation (DGIS) through the UNESCO-IHE Partnership Research Fund. This research cannot be concluded without the data from the Mekong River Commission (MRC) and therefore would like to extend appreciation to MRC for the support. This research has not been subjected to peer and/or policy review by DGIS or UNESCO-IHE, and, therefore, does not necessarily reflect the views of these institutions.

References

Chen, J., Brissette, F.P. and Leconte, R. (2011). Uncertainty of downscaling method in quantifying the impact of climate change on hydrology. Journal of Hydrology, 401, 190-202.

Green, W.H. and Ampt, G.A. (1911). Studies on soil physics, 1. The flow of air and water through soils. Journal of Agricultural Sciences, 4, 11-24.

Hashmi, M.Z., Shamseldin, A.Y. and Melville, B.W. (2009). Downscaling of future rainfall extreme events: a weather generator based approach. 18th World IMACS/MODSIM Congress. Cairns, Australia 13-17 July 2009.

Nash, J. E. and Sutcliffe, J. V. (1970). River flow forecasting through conceptual models. Part I – a discussion of principles. Journal of Hydrology, 10, 282–290.

Neitsch, S.L., Arnold, J.G., Kiniry, J.R. and Williams, J.R. (2009). Soil & Water Assessment Tool Theoretical Documentation Version 2009.

Santhi, C., Arnold, J.G., Williams, J.R., Dugas, W.A., Srinivasan, R. and Hauck, L.M. (2001). Validation of the SWAT model on a large river basin with point and nonpoint sources. Journal of the American Water Resources Association, 37 (5), 1169-1188.

Semenov, M.A. and Barrow, E.M. (1997). Use of stochastic weather generator in the development of climate change scenarios. Climate Change, 35, 397-414.

IPCC. (2007). Climate Change 2007: The Physical Science Basis. Contribution of Working Group I to the Fourth Assessment Report of the Intergovernmental Panel on Climate Change. (S. Solomon, D. Qin, M. Manning, M. Marquis, K. Averyt, M. M. Tignor, et al., Eds.) Cambridge University Press, Cambridge, United Kingdom and New York, NY, USA.Hamlet, A.F., Snover, A. and Lettenmaier, D.P. (2003). Climate Change scenarios for Pacific Northwest Water Planning

Monteith, J.L. (1965). Evaporation and the environment: in the state and movement of water in living organisms. In: XIXth Symposium Soc. for Exp. Biol. Cam-bridge University Press, Swansea, 205–234.

Setegn, S.G., Dargahi, B., Srinivasan, R.and Melesse, A.M. (2010). Modeling of sediment yield from Anjeni-Gauged watershed, Ethiopia using SWAT model. Journal of the American Water Resources Association, 46 (3), 514-526.

Soil Conservation Service. (1972). Section 4: Hydrology In National Engineering Handbook. SCS.

Van liew, M.W., Veith, T.L., Bosch, D.D. and Arnold, J.G. (2007). Suitability of SWAT for the conservation effects assessment project: A comparison on the USDA-ARS experimental watersheds. Journal of Hydrological Engineering, 12 (2), 173-189.

Zhang, H., Huang, G.H., Wang, D. and Zhang, X. (2011).Uncertainty assessment of climate change impacts on the hydrology of small prairie wetlands. Journal of Hydrology, 396, 94–103.

Semenov, M.A. and Stratonovitch, P. (2010). The use of multi-model ensembles from global climate models for impact assessments of climate change. Clim. Res., 41, 1-14.

Khan, M.S., Coulibaly, P. and Dibike, Y. (2006). Uncertainty analysis of statistical downscaling methods. Journal of Hydrology 319, 357–382.

Climate Change Scenario on Surface Water Resource in Bangnampriao District, Chachernsao Province

Charuvan Kasemsap [1, a *] and Suppakorn Chinvanno [2,b]

Abstract. Agriculture including paddy field, fruit farm and aquaculture, in Bangnampriao District, Chachernsao Province, are affected from drought, saline intrusion during January to May and also flood during October to November. The climate change scenario was forecasted by Global Circulation Model (GCM) as ECHAM4 under A2 greenhouse gas scenario and was downscaled using PRECIS regional climate model as base year of 1990 – 2009 and future year of 2040 – 2059. It was estimated that the average minimum temperature at nighttime has trend to increase from 25.14 to 25.6 degree Celsius whereas the average maximum temperature at daytime tends to increase from 34.88 to 35.37 degree Celsius during 2040 – 2059. Mean monthly minimum and maximum temperatures have possibly to increase in the range of 0.35 – 1.83 Degree Celsius. The simulation was indicated that the annual rainfall of the lower Chao Phraya River basin and Pasak basin as the watershed of this area have inclination to rise from 1,374 millimeter to 1,439 millimeter or approximately 5 percent. However, the rainfall during wet season (May – October) contributes to step up whereas that of dry season (November – April) leads to decline. In addition, the sea level rise along inner Thailand gulf, affected saline intrusion in this area through Bangpakong River, was likely to intensify. The increasing of annual sea level are 9.41 and 20.02 centimeter during 2010 – 2029 and 2030 – 2049, respectively. Climate change scenarios are necessary to apply appropriate adaptation strategies to minimize the impact of climate change.

Keywords: Climate Change, Scenario, Surface Water Resource, Bangnampriao District

Charuvan Kasemsap
Faculty of Graduate School, Kasem Bundit University, Bangkok, Thailand.
charuvan.kas@gmail.com
Suppakorn Chinvanno
Southeast Asia START Regional Center, Chulalongkorn University, Bangkok, Thailand.
Suppakorn.ccadaptation@gmail.com

Impact of Climate Change on groundwater recharge in Ho Chi Minh City Area, Vietnam

Ha Quang Khai[1, a *], Sucharit Koontanakulvong[2,b]

Abstract. Ho Chi Minh is the biggest City in Vietnam, where is expected to be strongly influenced by climate change. Besides, Groundwater is also very important since it provides 34 % of water supply and thus groundwater level is also decreasing dramatically in recent years. At the same time, groundwater in Ho Chi Minh are directly impacted by climate factors such as precipitation, evapotranspiration river water table. However, the area have not been studied on the impact of climate change to groundwater even groundwater recharge. The study presented the application of groundwater model (MODFLOW) and Global Climate model (GCM) to study impact of climate change to groundwater recharge in the area. Global Climate Model (GCM) named MRI-AGCM3.2s (Mizuta et al., 2012) is used to project precipitation and temperature for the area in two future timeframes, which near future (2015-2039) and far future (2075-2099). Bias-correction method exhibits ability of reducing biases from the frequency and amount when compared with observed and computed values at grid nodes; based on spatially interpolated observed rainfall data. Finally, groundwater model (MODFLOW) is applied to estimate historical recharge (2010-2012) as well as simulation groundwater flow under the impacts of climate change. Based on result of groundwater model, the impact on groundwater recharge had been investigated.

Keywords: *Climate change, Global Climate Models, bias correction, Ho Chi Minh City, MODFLOW, Groundwater recharge.*

Ha Quang Khai
Department of Water Resources Engineering
Faculty of Engineering, Chulalongkorn University
Bangkok, Thailand
Email: quangkhai02@gmail.com

Sucharit Koontanakulvong
Department of Water Resources Engineering,
Faculty of Engineering, Chulalongkorn University.
Bangkok, Thailand
Email: sucharit.k@chula.ac.th

Introduction

Groundwater is a very important part of life. It provides water for the lives of more than two billion people in the world. In many places, groundwater is also an important source of water supply for industrial development and protection of crops in the dry season. According to the International Groundwater Resources Assessment Centre (IGRAC) data, some countries use groundwater resources as major sources to usage such as Bolivia, Jamaica and Barbados accounted 96% water use, or 26 to 35% water usage in the South Asia came from groundwater. Climate change will increase pressure to groundwater due to increase of water demand and change of groundwater recharge. (Döll, 2009) projected climate change impacts on groundwater resources using two climate models (ECHAM4/OPYC3 and HadCM3) under the A2 and B2 scenarios and found that by 2050, more than 10% of the renewable groundwater resources could be decreased for approximately one fifth of the global land area, which would affect approximately 2.4 billion people.

Ho Chi Minh City area is important area in Vietnam where GDP as 20% of total National. Here groundwater is important because of 34% water supply come from groundwater. This area is recognized as an area which will be most impacted by climate change in the world. In 2012, Ministry of Natural Resources and Environmental of Vietnam declared the latest climate change scenarios for Vietnam and according to the publication, during last 50 years temperature increased around 1^0C and will increase more in future, and increase 2°C at the end of century. Precipitation will change in the future. Meanwhile, According to (Vuong, 2010) in Ho Chi Minh City, there are 6 aquifers , among of them, there are four aquifers are impacted by climate factors as rainfall and recharge from rainfall in Saigon river basin varies between 0-17% (Chan.N.D, 2011). So, it seem that groundwater recharge in the area will be affected by climate. However, In Ho Chi Minh City area, there has not been studied regarding climate effect on groundwater recharge.

Numerical modelling is a useful approach to assess past and future groundwater resources in response to climate change (Koontanakulvong, Chaowiwat, & Miyazato, 2013). In additional, groundwater model (MODFLOW) can simulate groundwater flow (Koontanakulvong & Suthidhummajit, 2000) and even estimate water recharge through calibrate/simulation process (Healy, 2010).

In order to combine groundwater model with Global Climate Model, we need some methods. Due to the mismatch between relatively coarse resolutions of Global Climate Models (GCMs) and fine resolution of hydrologic models is the major drawback in climate change impact assessment on water resources at basin level. Despite being important tools to project the expected scenarios of climate parameters, GCMs contain biases when compared to observed data because of parameterized systems and larger (Taylor, Stouffer, & Meehl, 2012) than hundred kilometers-plus grid sizes or even with AGCM 3.2s is supper resolution with 20x20 km^2 (Mizuta et al., 2012). Bias correction method can largely eliminate this kind of problems with added emphasis on statistical characteristics of historical climate data. Generally, bias correction can be divided to two types, namely, rescaling and quantile-based methods. Rescaling is the simplest bias correction method that aims to improve the systematic error in the mean precipitation amount. A quantile-based bias correction is useful to statistically transform rainfall simulated by GCMs to bias-corrected data and to make it applicable to impact assessment model (Sharma, Das Gupta, & Babel, 2007)). (Ines & Hansen, 2006) applied empirical-gamma transformation and multiplicative shift methods to correct the frequency and intensity distribution of daily GCM rainfall for a particular station and then applied it for crop yield simulation. All of these techniques improved the results of maize yield simulation and also indicated the significance of bias correction.

The focus of the present paper is to investigate groundwater recharge in the past, formularize and project future recharge by applying MODFLOW. To acquire future climate conditions for impact on recharge, the paper adopted the Gamma-gamma transformation method to bias correction for statistically downscaling GCM named MRI-ACGM3.2s to project climate change in Ho Chi Minh City area. The groundwater recharge impact through future climate was also investigated.

Study area

Study area stretches from latitude 10.320 E to 11.201 E and from longitude 106.215 N to 107.024 N with an area of 8,659 km^2. It covers all area of Ho Chi Minh City and some districts of Dong Nai, Binh Duong, Long An and Tay Ninh Province. The area has a tropical climate, specifically a tropical wet and dry climate, with an average humidity of 75%. The year is divided into two distinct seasons. Mean annual rainfall is at 1,612 mm and mean annual temperature is at 27ºC. Terraced plain mainly characterize the topography of the area with elevation vary from 0 to 108m. In the area, there are 3 Major River as Sai Gon River, Vam Co Dong, River, and Dong Nai River. Regarding Hydrogeology, there are 6 aquifers distributing from top to bottom respectively as follows: upper-Pleistocene (qp_3), Upper-Middle Pleistocene (qp_{2-3}), Lower Pleistocene (qp_1), Middle Pliocene (n_2^2), Lower Pliocene (n_2^1) and upper-Miocene (n_1^3). Groundwater level in all of aquifers are decreasing and the annual rate of decline from 0.04m of upper Pleistocene aquifers to 0.9m of lower Pleistocene aquifer. Groundwater level in the area are close related with climate factors as rainfall and surface water. At the same time, Groundwater is major water supply sources for domestic and industrial and it provide 34% of total water supply in Ho Chi Minh City. Total groundwater abstraction is around 926.121m^3/day.

Daily observed precipitation, temperature, river water level data are collected at Southern Regional Hydrometeorology Center, groundwater monitoring and Hydrogeology data area collected at Division for Water Resources Planning and Investigation for the South of Vietnam (DWRPIS) and Groundwater abstraction and water use are collected at Department of Resources and Environmental.

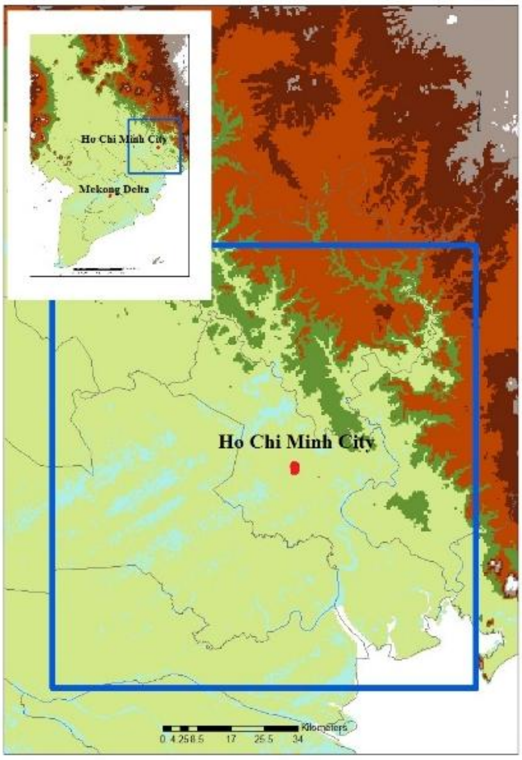

Fig. 1 The study area.

Methodology

In order to assess the impact of climate change to groundwater recharge, 3 steps were applied in this study as follows.

For the climate projection, a bias correction technique named Gamma – Gamma (GG) transformation (Ines and Hansen 2006) was applied to correct the bias of the GCMs outputs named MRI AGCM3.2s for rainfall, air temperature during the period 1980–2007, 2015–2034 and 2075–2099. Groundwater recharge flux during the period 2010 – 2012 is formulated from the calibrated value using groundwater model (MODFLOW) (Healy, 2010). A linear regression method was applied to develop relationship between recharge flux and value of monthly precipitation minus evaporation. After that groundwater model (MODFLOW) was applied again to project future groundwater recharge under new climate conditions.

Equation used

Bias-Correction

1. Establish the empirical distributions, F(x), by first classifying long-term daily rainfall for each month, based on positions of the ordered datasets. The empirical distribution function F(x) can be selected from a variety of available standard probability plotting methods. However, in present study, Weibull procedure is used as given in Eq. (1):

$$F(x) = \frac{n}{m+1} \tag{1}$$

Where n is the position of x in the ordered array, and m is the total number of data in the array. This should be followed by calculation of threshold value ($x_{GCM}^{\%}$), derived from the empirical distribution of daily historical rainfall data, to truncate the empirical distribution of the raw daily GCM rainfall for that particular month. Basically, F (x_{his}=0) is determined and then mapped to the daily GCMs rainfall distribution.

2. GG transformation method is selected for rainfall amount correction. For GG transformation, the truncated daily GCM rainfall and historical data are fitted into two-parameter gamma distribution (Eq. 2) and then the cumulative distribution (Eq. 3) of the truncated daily GCM rainfall is mapped into cumulative distribution function of the truncated historical data (Eq.4). The shape and scale parameters (α and β) for each Gamma distribution are determined using Maximum Likelihood Estimation.

$$f(x;\alpha,\beta) = \frac{1}{\beta^{\alpha}\Gamma(\alpha)} x^{\alpha-1} \exp(-\frac{x}{\beta});$$

$$x \geq x_{Trunc} \tag{2}$$

$$F(x;\alpha,\beta) = \int_{x_{Trunc}}^{x} f(t)dt \tag{3}$$

$$F(x_{GCM};\alpha,\beta|_{GCM} \Rightarrow F(x_{His};\alpha,\beta|_{His}) \tag{4}$$

The corrected GCM rainfall amount for that particular day can be computed by taking the inverse of Eq. (4) such that:

$$x_{GCM}^{'} = F^{-1}\{F(x_{His};a,\beta|_{His})\} \tag{5}$$

The bias corrected rainfall method is applied to MRI – AGCM 3.2S, relative to spatially interpolated rainfall at GCM grid node. Inverse Distance Weighted (IDW) method is used to estimate the spatial average rainfall at grid node from observed daily rainfall (Shepard, 1967). Correlation coefficient (R), Root Mean Square Error (RMSE) and Standard Deviation (SD) are determined to assess the overall ability of the bias-correction method.

$$F(x_i) = \sum_{i=1}^{n} \lambda_i f(x_i) \tag{7}$$

$$\lambda_i = \frac{h_i^{-p}}{\sum_{i=1}^{n} h_i^{-p}} \tag{8}$$

Eq. (7) and (8) are describing IDW methods, where n is the number of scatter point in the sets, $f(x_i)$ is prescribed function value at the scatter points, λ_i is Weighting functions at assigned to each scatter points, h_i is the distance from known value point to the interpolated point, and p is power parameter (generally equals to 2).

Groundwater model

Groundwater-flow models are used to simulate aquifer response, in terms of head (ground water level) and fluxes into and out of an aquifer, to natural and human-induced stresses; they are important tools for resource and environmental management, and they provide groundwater velocities needed for simulation of subsurface contaminant transport.

Partial Differential equation which represents three dimensional movement of ground water is

$$\frac{\partial}{\partial x}\left[K_{xx}\frac{\partial h}{\partial x}\right] + \frac{\partial}{\partial y}\left[K_{yy}\frac{\partial h}{\partial y}\right] + \frac{\partial}{\partial z}\left[K_{zz}\frac{\partial h}{\partial z}\right] + W = S_s\frac{\partial h}{\partial t} \tag{9}$$

where

K_{xx}, K_{yy} and K_{zz} are the values of hydraulic conductivity along the x, y, and z coordinate axes and h is the potentiometric head (hydraulic head)

W is a volumetric flux per unit volume representing sources and/or sinks of water, where negative values are water extractions, and positive values are injections/recharge. It is a function of space and time (i.e. W = W(x, y, z, t)). S_s is the specific storage of the porous material and may be function of space.

t is time.

Recharge equation

The recharge can be approximated as a function of precipitation (P) and evapotranspiration (E) using flowing equation (Krüger, Ulbrich, & Speth, 2001):

$$R = P-E-Q_0 \tag{10}$$

Equation (10) can be written again as follow:

$$R=a*(P-E)+b \tag{11}$$

Here, a and b are constant and can be found by using goodness fit test. P is precipitation, and E is evapotranspiration and can be calculated by equation of temperature (T) (Singh, 1992):

$$E = c*T+d \tag{12}$$

Where c and d are constants and can be found by using goodness fit test.

Results and discussion

Projected climate data

The Gamma-Gamma transformation method is applied to MRI – AGCM 3.2S, precipitation and temperature scenario to reduce the biases from frequency and intensity when compared with the computed frequency and amount at reference grid nodes based on spatially interpolated rainfall data (Fig 2).

Statistical parameters, which indicating the correspondence of raw GCM and bias-corrected GCM with R^2 are greater than 0.9 (Fig. 3). This result show that GG method could be applied to bias correct MRI AGCM 3.2s for the area.

Future precipitation (Fig. 5) show that precipitation tend to be decrease in the period of near future (2015-2039) and increase during the period of far future. From Fig. 4, temperature will gradually increase.

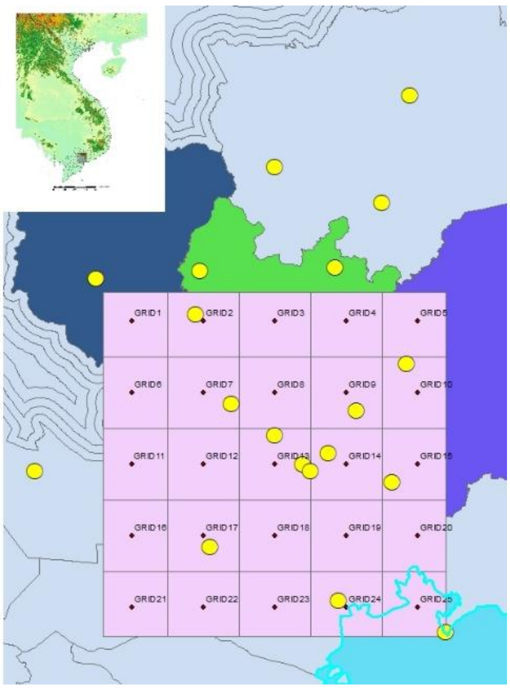

Fig. 2 The Study area and raingauge stations used in this study

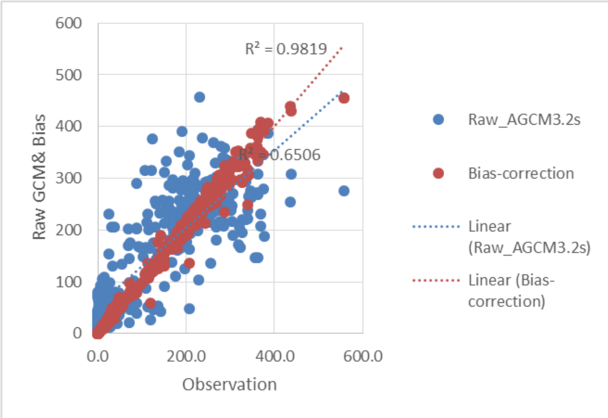

Fig.3 Correlation among precipitation observations and raw GCM and bias corrected data at Grid 13.

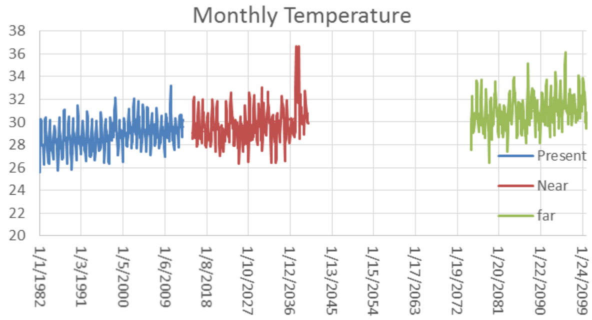

Fig.4 Mothly temperature in present (1980-2007), near future (2015-2039), and far future (2075-2099) periods

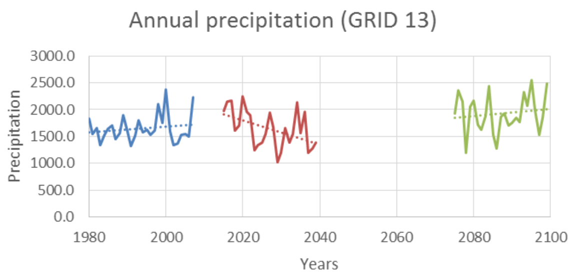

Fig.5 Annual rainfall in present (1980-2007), near future (2015-2039), and far future (2075-2099) periods

Evapotranspriration

Evapotranspiration during the period 1982-2007 was collected from the Project on "Integrated Management and Water Resources Reasonable Usage on Dong Nai River system" (Lanh Do T, 2010). A comparison of evapotranspiration and temperature show that two variables have relation as linear function with R2 =0.53 in rainy season and 0.68 in dry season (Table 2).

Table 2: Coefficients of linear function expressed relation between evapotranspiration and temperature.

River Basin	Rainy season			Dry season		
	a	b	R^2	a	b	R^2
Sai Gon	12.1	-239.5	0.54	12.7	-257.5	0.68
Vam Co Dong	12.2	-244.8	0.53	13.1	-268.4	0.68

River Basin	Rainy season			Dry season		
	a	b	R^2	a	b	R^2
Dong Nai	12.8	-260.7	0.52	13.6	-290.2	0.70

Calibrated model

Groundwater flow model (MODFLOW) was used to simulate groundwater flow conditions in the area during the period 2010 – 2012. Input data included river water level, observation groundwater level, and well abstraction as well as an assumption amount of recharge flux at different zone (Fig 6). After that, the model was calibrated until match with observation data. Result of calibration model show that computation values were close relation with observation data and expressed by average RMSE = 0.37m and Max = 0.42m, Min 0.34m detail in table 1.

Table 1*: RMSE value of aquifers in comparison with observation data.*

Aquifer	Average	Max	Min
qp3	0.34	0.70	0.15
qp23	0.35	0.81	0.02
qp1	0.35	0.77	0.08
n22	0.39	0.66	0.13
n21	0.42	0.88	0.20
Average	**0.37**		

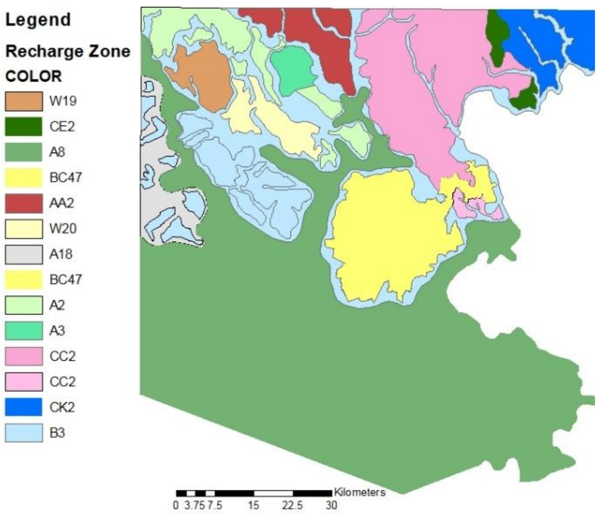

Fig 6. Distribution of recharge flux in each zone

Recharge function

Groundwater recharge fluxes in the step above were used to develop formulation between recharge and amount of monthly precipitation minus monthly evapotranspiration for each recharge zone (soil type). Results demonstrated a good relationship between groundwater recharge fluxes with amount of monthly precipitation minus monthly evapotranspiration in each recharge zone (Table 3).

Table 3*: Coefficients of linear function expressed relation between P-E and R.*

No	Zone	a	b	R^2
1	W19	0.019	1.00E-05	0.74
2	W20	0.009	-1.00E-06	0.91
3	A2	0.0072	7.00E-05	0.89
4	CK2	0.0034	-2.00E-07	0.95
5	CE2	0.0024	6.00E-08	0.93
6	AA2	0.0093	-8.00E-07	0.98
7	A2	0.0074	5.00E-06	0.91
8	BC47	0.001	-4.00E-07	0.99
9	CC2	0.0027	3.00E-08	0.98
10	B3	0.0029	8.00E-10	0.94
11	A8	0.0024	-1.00E-07	0.99
12	A18	0.0046	-5.00E-08	0.94

Projected groundwater recharge

Future groundwater recharge fluxes derived were input to groundwater model to project groundwater simulation for each aquifers (varied only recharge function and fixed for other boundary conditions). The results in the Fig. 8 show that recharge will decrease in the near future and increase in the far future periods.

A comparison of future recharge, climate variables in Fig. 9 demonstrated that climate factors were strongly impact on groundwater recharge. In near future period, rainfall will decrease 7% and evapotranspiration will increase 16% affected to groundwater recharge rate and leading recharge rate reduced amount 29% in compared with the present period. However, in the far future period, groundwater recharge rate will increase again by 23% at the end of century, due to rainfall strongly increase.

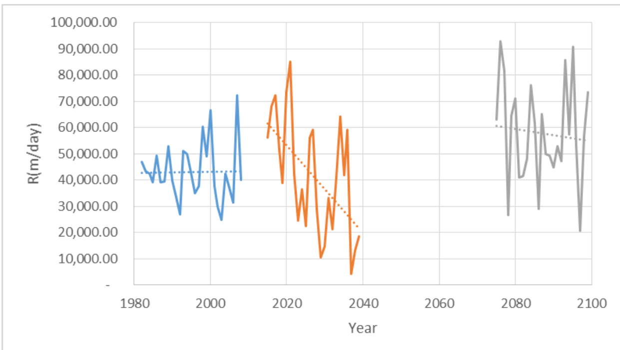

Fig. 8. Projected groundwater recharge rate

Fig. 9 Differences of future climate variables (temperature, evaporation, precipitation), recharge compared with present period

Summary and conclusions

This study is the first development of recharge function as well as impact assessment of climate change on groundwater recharge in Ho Chi Minh City area. Recharge flux in the area was divided into zones based on hydrogeology map, soil map, topography map and the study found that there were good relationship between recharge flux and value of rainfall minus evapotranspiration.

Projected precipitation for future showed that during the near future rainfall will decrease at 7% in 2030s and after that increase again in the far future, especially, in 2090s will increase amount 23%. At the same time, temperature will also gradually increase and in the end of this century will increase to 3.5^{0}C. Temperature increased and it thus lead evapotranspiration to be increased also. Evapotranspiration are expected to increase at 16% in 2090s.

Projected recharge showed that recharge will decrease 29% in 2030s and increase again in the far future. A significance rise of recharge in 2070s at 51% after that reduced to 23% in 2090s. .

This study focused on the impact on groundwater recharge, though climate change will impact on groundwater resources on both direct through recharge rate and indirect through runoff. Hence, further research on runoff change under climate change, affected to groundwater resources, is needed to investigate a comprehensive impact of climate on groundwater.

Acknowledgement

The study cannot be concluded without raw precipitation scenarios provided from government agencies, e.g., Meteorological Research Institute (MRI, Japan). We also grateful to staffs of Division of Water Resources Planning and Investigation for the South of Vietnam (DWRPIS), Ho Chi Minh Department of Natural Resources and Environmental (DONRE) for observed historical data as well. The research also done under the Department of Water Resources Engineering, Faculty of Engineering, Chulalongkorn University.

References

Chan.N.D, K. N. V. H. D. T. (2011). Generating sources of exploitable groundwater reserves in Saigon river basin area. *Vietnam National University - Ho Chi Minh City, Doctorate dissertation*(ID: 62.85.15.01).

Döll, P. (2009). Vulnerability to the impact of climate change on renewable groundwater resources: a global-scale assessment. *Environmental Research Letters, 4*(3), 035006.

Healy, R. W. (2010). *Estimating groundwater recharge*: Cambridge University Press.

Ines, A. V., & Hansen, J. W. (2006). Bias correction of daily GCM rainfall for crop simulation studies. *Agricultural and forest meteorology, 138*(1), 44-53.

Koontanakulvong, S., Chaowiwat, W., & Miyazato, T. (2013). Climate change's impact on irrigation system and farmers' response: a case study of the Plaichumpol Irrigation Project, Phitsanulok Province, Thailand. *Paddy and Water Environment*, 1-14.

Koontanakulvong, S., & Suthidhummajit, C. (2000). Groundwater Recharge Study and Simulation—Kamphaeng Phet Case Study— *Groundwater Updates* (pp. 301-306): Springer.

Krüger, A., Ulbrich, U., & Speth, P. (2001). Groundwater recharge in Northrhine-Westfalia predicted by a statistical model for greenhouse gas scenarios. *Physics and Chemistry of the Earth, Part B: Hydrology, Oceans and Atmosphere, 26*(11), 853-861.

Mizuta, R., Yoshimura, H., Murakami, H., Matsueda, M., Endo, H., Ose, T., . . . Yukimoto, S. (2012). Climate simulations using MRI-AGCM3. 2 with 20-km grid. *気象集誌 第 2 輯, 90*(0), 233-258.

Sharma, D., Das Gupta, A., & Babel, M. (2007). Spatial disaggregation of bias-corrected GCM precipitation for improved hydrologic simulation: Ping River Basin, Thailand. *Hydrology and Earth System Sciences, 11*(4), 1373-1390.

Singh, V. P. (1992). *Elementary hydrology*: Pearson College Division.

Taylor, K. E., Stouffer, R. J., & Meehl, G. A. (2012). An overview of CMIP5 and the experiment design. *Bulletin of the American Meteorological Society, 93*(4), 485-498.

Vuong. (2010). Reconstruction of Geology map, Hydrogeology map, and Geotechnical map with scale 1:50.000. *Division for Water Resources Planning and Investigation for the South of Vietnam., Report 2010*.

Comparative evaluation of storm characteristics derived from observed rainfalls and GCM precipitation outputs

Yuan-Fong Su [1, a *], Jun-Jih Liou [2,b] and Ke-Sheng Cheng [3,c]

Abstract Storm characteristics are critical for many hydrologic analyses, such as channel design and water resource management. With the increasing availability of dynamic downscaled rainfall dataset, it is possible to evaluate the future changes of typhoon rainfall characteristics, in spatial and temporal. Taiwan Climate Change Projection and Information Platform (TCCIP) project produced a set of dynamic downscaling data which has 5-km and hourly resolutions. This dataset was bias-corrected using observed data and then used to evaluate the storm characteristics. We compared the typhoon rainfall characteristics including number of events, duration, total rainfall, and inter-event time, derived from observations and dynamic downscaling data sets. Finally, with this comparative evaluation it is possible to learn the changes of storm characteristics in spatial and temporal in the future.

Keywords *Storm characteristics, dynamic downscaling, statistical downscaling*

Yuan-Fong Su
National Science and Technology Center for Disaster Reduction
New Taipei City, Taiwan.
yuanfongsu@ncdr.nat.gov.tw
Jun-Jih Liou
National Science and Technology Center for Disaster Reduction
New Taipei City, Taiwan.
jjliou@ncdr.nat.gov.tw
Ke-Sheng Cheng
Dept. of Bioenvironmental Systems Engineering
National Taiwan University
Taipei, Taiwan
rslab@ntu.edu.tw

Introduction

Many extreme weather events occurred in the world in recent years. A common course on the Earth is that the climate is changing. One of the most significant changes is that the rainfall pattern is changing in spatial and temporal dimensions. This is a general idea that most of scientists agreed. However, how the changes distributed in space and how the changes occurred in time are remain unclear. In previous studies, a lot of related studies using monthly data and focused on the annual, seasonal or monthly change of precipitation pattern in a larger spatial domain. These researches may not satisfy the demand of hydrologist for many hydrological practices such as frequency analysis and hydraulic designs. For these hydrological and hydraulic applications, hourly rainfall data is needed. Take real-time reservoir operation for flood control purpose as an example, hourly data is a very important input for real-time operation. The monthly changes from GCM outputs cannot be used in these related hydrological practices.

Dynamic downscaling data can be a proper solution for the abovementioned problem as it is an hourly rainfall data set with fine (less than 5 km) spatial resolution. The TCCIP (Taiwan Climate Change Projection and Information Platform) received the MRI-AGCM 3.2S (Oouchi et al. 2006; Mizuta et al. 2006; Kitoh et al. 2008; Mizuta et. al., 2012) from Meteorological Research Institute and further downscaled by WRF (Weather Research and Forecasting model system) to 5-km spatial resolution and hourly rainfall data. With this dataset it is possible to evaluate the storm characteristics. In Taiwan, the most serve storm comes with typhoon. In this paper, we will focus on the storm characteristics of typhoon rainfall and compare the changing in spatial and temporal using observation and GCM projection of MRI-AGCM 3.2S.

Materials

In TCCIP project, the MRI-AGCM 3.2S dataset was used as boundary and initial condition of WRF model and further downscaled to 5-km and hourly rainfall dataset which is denoted by MRI-WRF hereafter. The base period is defined as 1979-2003 and the projection periods are near future (2015-2039) and end-of-century (2075-2099), respectively. The observed rainfall data during 1979-2003 were also collected at 84 ground stations around Taiwan in which the spatial distribution of the ground stations is shown in Fig. 1.

Storm Characteristics

Before we evaluate the storm characteristics it is crucial to define a storm event. Usually a threshold approach is utilized to rainfall time series to determine storm events.

As illustrated in Fig. 2, there are two thresholds including the rainfall amount need to larger than 2.5mm/hr (refer to the definition of small rainfall of WMO) and the duration of event need to longer than 8 hours.

In this paper, we defined four storm characteristics including number of events, duration, total rainfall of events, and inter-event time. Both datasets will be compared in terms of the changes in these characteristics. To compare the change between future and base period, a change rate is defined as following:

$$\text{change rate}(\%) = \frac{Future - Base}{\text{Future}} \times 100\%$$

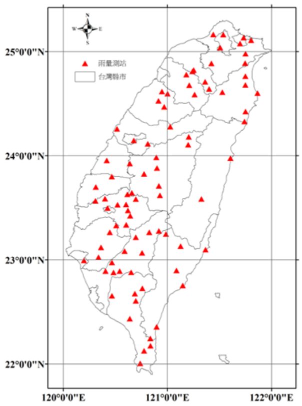

Fig. 1 Spatial distribution of ground stations.

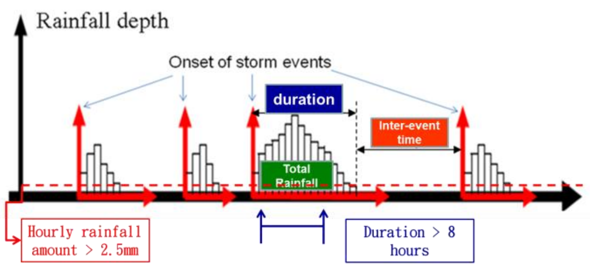

Fig. 2 Illustration of storm characteristics.

Bias correction

CDF matching method is widely used for bias correction (BC) in many studies (Piani et al. 2010a; Piani et al. 2010b; Haerter et al., 2011; Teutschbein and Seibert, 2012). An ECDF matching method is used for bias correction. This method aims to adjust the projection data to have the same feature of observation dataset in a statistical sense. An illustration of the bias correction procedure was shown in Fig. 3. The data used for BC comprising the hourly rainfall of typhoon events in the base period (1979-2003). For each percentile of the ECDF, a correction factor can be derived as a ratio between observed and projected typhoon rainfall. This correction factor of each percentile was applied to future projection dataset and yielded the bias-corrected typhoon rainfall in the near future and end-of-century.

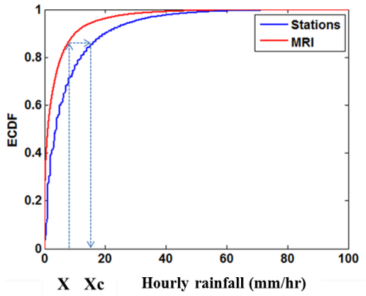

Fig. 3. Illustration of ECDF matching.

Results and discussion

The storm characteristics derived from observed typhoon rainfall revealed that the northeast of Taiwan had most storm events around Yang-Ming Mountain and in the southern part of Taiwan. The hotspot of event duration were located at central mountain area such Ali and Shei Mountain while similar spatial pattern could be observed in the results of total rainfall. As for the inter-event time, the results shown that west-central part of Taiwan had less change for the visit of storm rainfall (Fig. 4). Notably, the contours in Fig. 4-6 were all based on the 84 stations or the 84 5-km grids covering the stations.

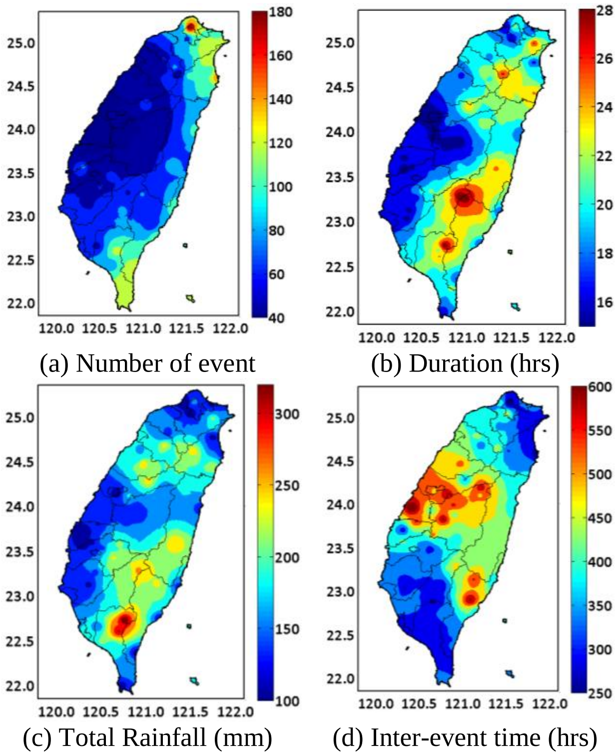

Fig. 4 Storm characteristics of observed typhoon events during base period.

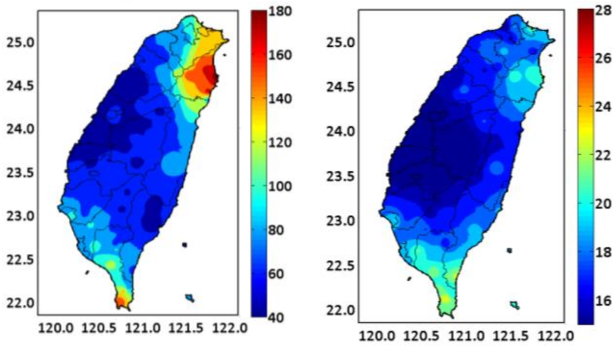

(a) Number of event (b) Duration (hrs)

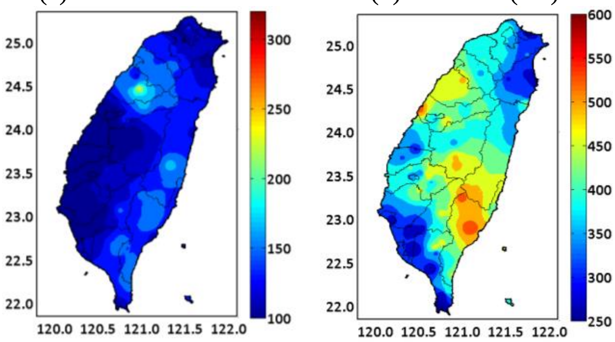

(c) Total Rainfall (mm) (d) Inter-event time (hrs)

Fig. 5 Storm characteristics of typhoon events in MRI-WRF (before BC) dataset during base period.

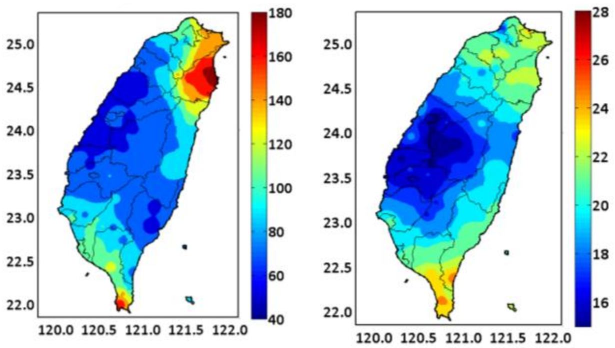

(a) Number of event (b) Duration (hrs)

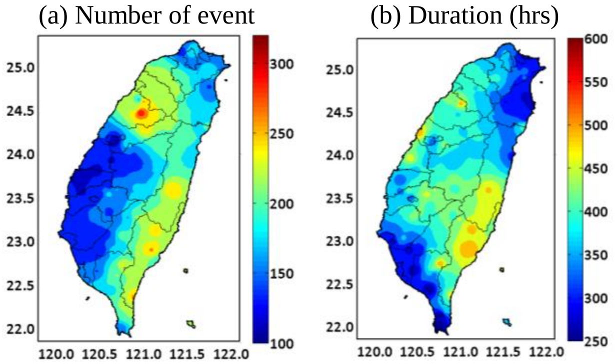

(c) Total Rainfall (mm) (d) Inter-event time (hrs)

Fig. 6 Storm characteristics of typhoon events in MRI-WRF (after BC) dataset during base period.

Before BC, the storm characteristics derived from MRI-WRF dataset revealed that the total rainfall of storms and its duration were obviously underestimated (**Fig. 5.**). It is clear from Fig. 5 that the number of event of MRI-WRF was similar to that of observed dataset while the hotspot slightly shifted to I-Lan area from Yang-Ming Mountain.

After BC, although the spatial pattern did not change but the problem of underestimation was reduced (Fig. 6). Take total rainfall as an example, comparison between Fig. 4c, 5c, and 6c, it was apparently the hotspots were located at northwest part and southeast part of Taiwan (Fig. 6c) which was similar to observed one (Fig. 4c). Compared the total rainfall and duration using scatter plots, the problem of underestimation was greatly reduced.

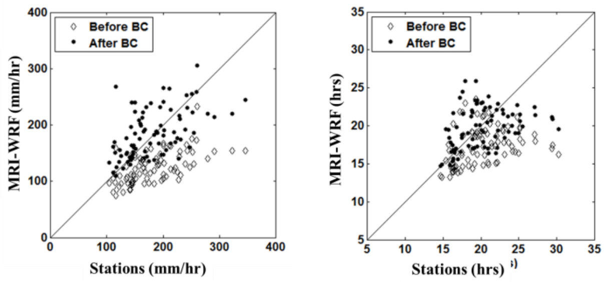

(a) Total rainfall (mm/hr) (b) Duration (hrs)

Fig. 7 Scatter plots of total rainfall and duration between MRI-WRF and observations.

Storm characteristics changes in Future

The results of BC was further applied to the 1566 MRI-WRF girds covering whole Taiwan for the future periods and the change of storm characteristics in the near future and end of century were evaluated in Fig. 8. It was apparent that storm duration was slightly increased (~5%) in central-west part of Taiwan while slightly decreased in the north and east parts in the end of century. Obviously, the total rainfall was significantly increased (~30%-50%) in central and southern parts in the end of century; however, the total rainfall in the north and east parts were decreased (~10%-15%). These results were dominated by the tracks of typhoons projected by MRI-AGCM-3.2S. Thus, if another dynamic downscaling data in different scenario were available, the change pattern could be totally different since the track of typhoon is the key factor on the rainfall pattern.

Conclusions

This study compared the storm characteristics derived from observed and projected dynamic downscaled data by MRI-AGCM-3.2S and WRF models. A bias correction procedure was also applied to the MRI-WRF dataset. Some conclusions are summarized as:

1. An ECDF matching method for bias correction reduced the underestimation problem of the total rainfall of MRI-WRF dataset.
2. After bias correction, the changes of storm characteristics in spatial and time could be evaluated. The results shown that the total rainfall of typhoon events will increase significantly in the central and southern parts of Taiwan in the end of century.
3. Although these results were dominated by the track of typhoon projected by MRI the signal from these results warned us that the rainfall fall pattern could change dramatically in the end of century.

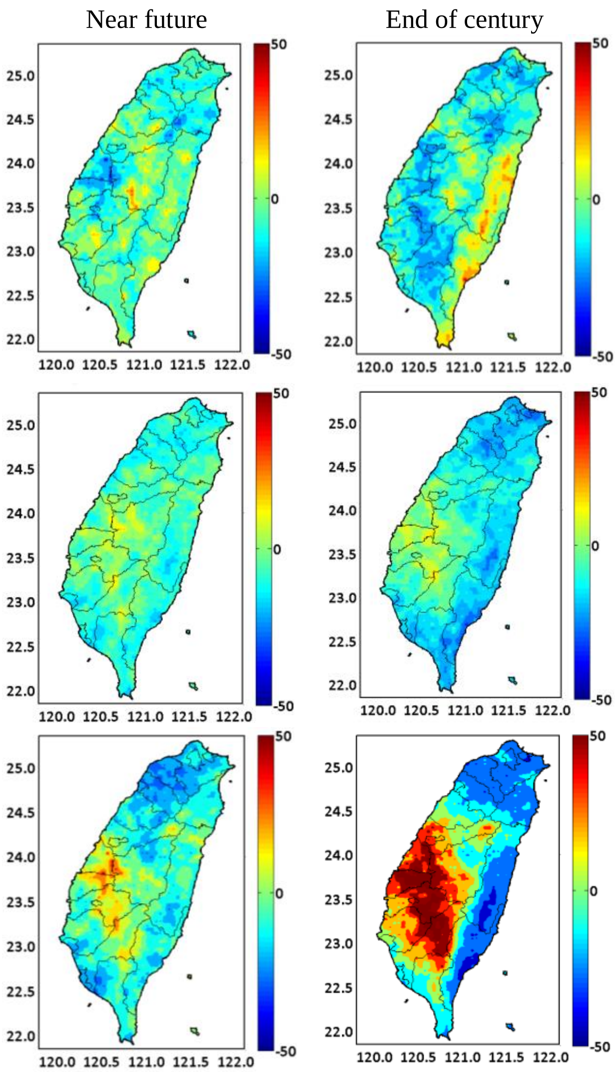

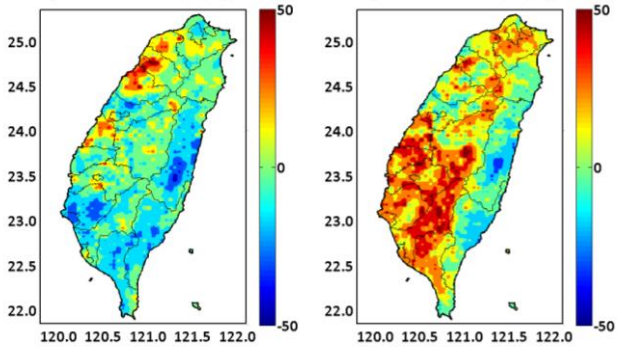

Fig. 8 The change rate (%) of near future (left column) and end of century (right column). The storm characteristics of each row from up to bottom were the number of events, duration, total rainfall, and inter-event time.

References

Haerter, J. O., Hagemann, S., Moseley, C., Piani, C., "Climate model bias correction and the role of timescales," Hydrol. Earth Syst. Sci., Vol. 15, pp. 1065-1079, 2011.

Kitoh, A., Yatagai, A., and Alpert, P., " First super-high-resolution model projection that the ancient "Fertile Crescent" will disappear in this century," Hydrol. Res. Lett., Vol. 2, pp. 1-4, 2008.

Mizuta, R., K. Oouchi, H. Yoshimura, A. Noda, K. Katayama, S. Yukimoto, M. Hosaka, S. Kusunoki, H. Kawai, and M. Nakawaga, "20-km-mesh global climate simulations using JMA-GSM model-mean climate states" J. Meteorol. Soc. Japan., Vol. 84, pp. 165-185, 2006.

Mizuta, R., H. Yoshimura, H. Murakami, M. Matsueda, H. Endo, T. Ose, K. Kamiguchi, M. Hosaka, M. Sugi, S. Yukimoto, S. Kusunoki and A. Kitoh, "Climate simulations using MRI-AGCM3.2 with 20-km grid," J. Meteor. Soc. Japan, Vol. 90A, pp. 233-258. 2012

Oouchi, K., J. Yoshimura, H. Yoshimura, R. Mizuta, S. Kusunoki, and A. Noda, "Tropical Cyclone Climatology in a Global-Warming Climate as Simulated in a 20 km-Mesh Global Atmospheric Model: Frequency and Wind Intensity Analyses," J. Meteorol. Soc. Jpn., Vol. 84, No. 2, pp.259-276, 2006.

Piani, C., Haerter, J. O., Coppola, E., "Statistical bias correction for daily precipitation in regional climate models over Europe, "Theor. Appl. Climatol. Vol. 99, pp. 187-192, 2010.

Piani, C., Weedon, G. P., Best, M., Gomes, S.M., Viterbo, P., Hagemann, S., Haerter, J. O., "Statistical bias correction of global simulated daily precipitation and temperature for the application of hydrological models," Journal of Hydrology, Vol. 395, pp. 199-215, 2010.

Teutschbein, C., and Seibert, J., "Bias correction of region climate model simulations for hydrological climate-change impact studies: Review and evalution of different methods," Journal of Hydrology, Vol. 456-457, pp. 12-29, 2012.

Introduction to TCCIP: dynamic and statistical downscaling and its applications

Lee-Yaw Lin [1,a*] , Yung-Ming Chen[1, b] , Jung-Lien Chu[1,c] , Chao-Tzuen Cheng [1,d] , Jun-Jih Liou [1,e] , Yun-Ju Chen [1,f] and, Yuan-Fong Su [1,g]

Abstract The Taiwan Climate Change Projection and Information Platform Project (TCCIP) is one of the three national major projects on climate change in Taiwan since 2010. Since TCCIP phase 1 (2010-2012) has produced substantial results such as producing digitalized, homogenized, and gridded meteorological data sets and high spatial-temporal resolution data sets by statistical downscaling and dynamic downscaling; applying climate change data to the studies of disaster reduction and water resources management, publishing "Climate Change in Taiwan: Scientific Report 2011", and constructing TCCIP web service. The TCCIP also supports government agencies to develop climate change projects such as "Climate Change Impacts and Adaptation on Water Environment" project in Water Resource Agency (WRA), and the "National Adaptation Policy Frameworks for Climate Change" and "Adaptation Programmes of Action for Climate Change" approved by National Development Council (NDC) in 2012. Last year (2013) the TCCIP (phase 2 during 2013-2015) continues to play the major role in national climate change-related researches. This paper introduced some applications of dynamic data such as water-related disasters from a perspective of Intergraded Catchment Management and climate change risk maps of flooding, drought, coastal and slopeland disasters.

Keywords *Climate change, Dynamic downscaling data, Water-related disasters*

Lee-Yaw Lin
National Science and Technology Center for Disaster Reduction
New Taipei City, Taiwan.
yaw@ncdr.nat.gov.tw
Yung-Ming Chen
ymchen@ncdr.nat.gov.tw
Jung-Lien Chu
jlchu@ncdr.nat.gov.tw
Chao-Tzuen Cheng
ctcheng@ncdr.nat.gov.tw
Jun-Jih Liou
jjliou@ncdr.nat.gov.tw
Yun-Ju Chen
yjchen@ncdr.nat.gov.tw
Yuan-Fong Su
yuanfongsu@ncdr.nat.gov.tw

Introduction

The Ministry of Science and Technology in Taiwan lunched three national major projects on climate change in 2010. One is the CCliCs project focused on developing high resolution GCM model of our own in Taiwan. Secondly, the most important project, the TCCIP plays a critical role for producing of dynamic and statistical downscaling data according newest data from IPCC. In the meantime, TCCIP also conducts impact assessment of climate change by using the produced datasets. Furthermore, TCCIP also serves for many related projects from government by providing projection data and consulting for their need in impact assessment. In TCCIP phase I (2010-2012), we had produced substantial results such as producing digitalized, homogenized, and gridded meteorological data sets and high spatial-temporal resolution data sets by statistical downscaling and dynamic downscaling; applying climate change data to the studies of disaster reduction and water resources management, publishing "Climate Change in Taiwan: Scientific Report 2011", and constructing TCCIP web service. The TCCIP also supports government agencies to develop climate change projects such as "Climate Change Impacts and Adaptation on Water Environment" project in Water Resource Agency (WRA), and the "National Adaptation Policy Frameworks for Climate Change" and "Adaptation Programmes of Action for Climate Change" approved by National Development Council (NDC) in 2012. The TCCIP (phase II during 2013-2015) continues to play the major role in national climate change-related researches. In TCCIP phase II, the applications of climate change dataset were extended to agricultural and public health related disasters. In the same time, we also extended the water related disaster to a comprehensive catchment scale in which multi-model assessing the slopeland, water level in channel, flooding in urban area and storm surge were combined. Notably, in TCCIP phase II, a focus is data service in which we reinforced communication with data user and requested many feedbacks from users. All these feedbacks were used to improve our data and the way for better data service.

There are 4 working teams within TCCIP. Team 1 focuses on constructing well-calibrated observed datasets, gridded datasets and model data analyses. Team 2 aims to produce statistical (CMIP 5) and dynamic downscaling (including 3 AGCM). Team 3 assesses the climate change data for impact studies and develops data application techniques. Team 4 is newly added in phase II and focuses on data services.

Statistical downscaling data

In the early this year the statistical downscaled CMIP5 data were produced by BCSD (Bias Correction and Spatial Disaggregation; Wood et al., 2002, 2004, Maurer, 2007) and some fundamental analyses were also conducted. In Fig. 2, the seasonal changes of medium precipitation between end of century (2081-2100) and base period (1986-2005) were compared between 4 scenarios (RCP2.6, RCP4.5, RCP6.0, RCP8.5). It was shown that the variation of seasonal precipitation generally increased from RCP2.6 to RCP8.5. This also indicated the strength of extreme rainfall may also increase in the end of century. Fig. 3 shown the projected changes for end of century in medium temperature of CMIP5 dataset and it was apparent that the temperature was increased in all seasons. For RCP8.5, the temperature could increase ~3℃ in the end of century.

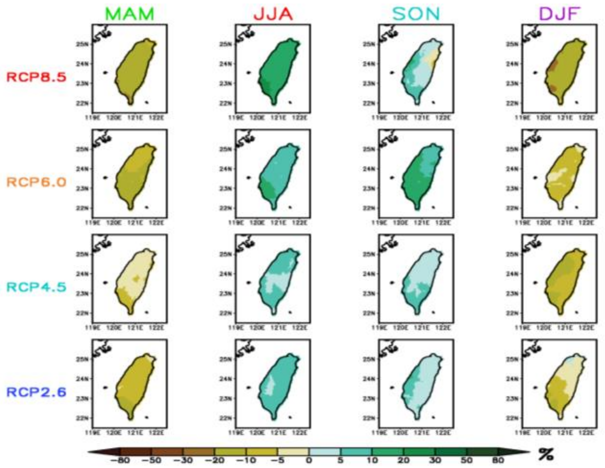

Fig. 2 Projected change (%) for end of century in medium precipitation of CMIP5 dataset.

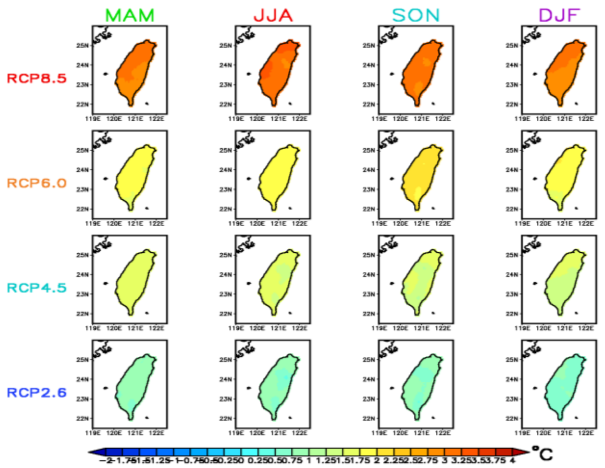

Fig. 3 Projected changes (degree) for end of century in medium temperature of CMIP5 dataset.

Dynamic downscaling data

Since TCCIP phase I, we keep cooperating with JAPAN's leading climate change project (Program for Risk Information on Climate Change (SOUSEI), 2012-2016). In the cooperation, we received MRI-AGCM 3.2S (20-km resolution, hereafter denoted as MRI) and further downscaled to 5-km resolution and hourly data set by WRF model (hereafter denoted as MRI-WRF). The domain of the WRF model was shown in Fig. 4. The seasonal precipitations of projected data were compared with observed dataset in Fig. 5. It indicated that the MRI-WRF revealed that detail spatial variation than MRI and the distribution pattern was similar, except Mei-yu, to that of observed. The projected MRI-WRF dataset was further bias-corrected using ECDF matching method (Piani et al. 2010a; Piani et al. 2010b).

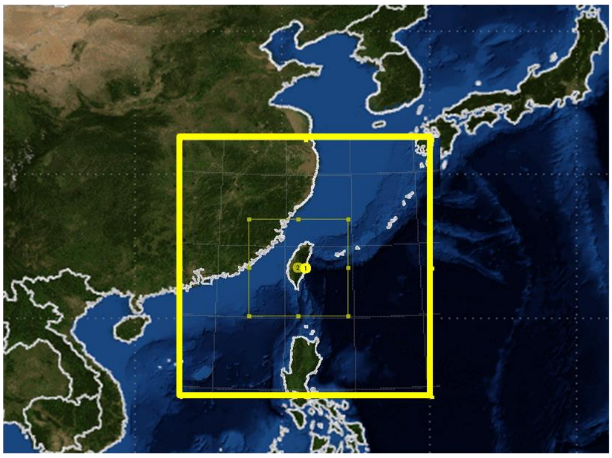

Fig. 4 Simulation model of WRF.

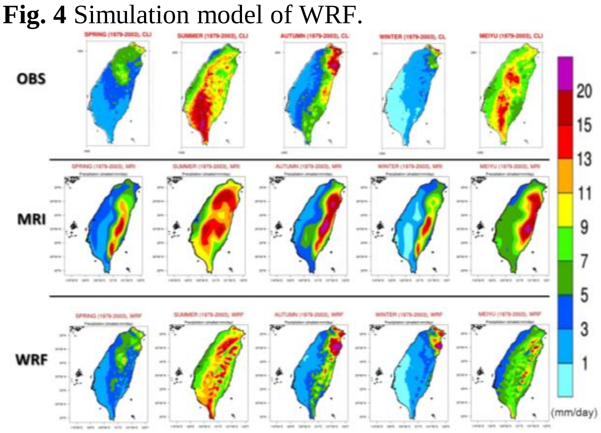

Fig. 5 Seasonal precipitation of observed, MRI, and MRI-WRF. From left to right: Spring, Summer, Autumn, Winter, and Mei-yu (May and June in Taiwan).

Application example 1: Intergraded Catchment Management using dynamic downscaling dataset

A intergraded catchment management (ICM), using Tsen-Wen catchment as an example, combined multiple models to assess the landslide/debris flow, water level of river, flooding in urban area, and storm surge and inundation area. A conceptual illustration of the ICM was shown in Fig. 6. Finally, losses assessment was also conducted. In this study, the bias-corrected Top 1 typhoon event in the end of century was used for the impact assessment. The sediments resulted from landslide and debris flow were simulated by TRIGRS and Flow-2D, respectively. The result of TRIGRS was shown in Fig. 7 and it was shown that more and more area in the danger of landslide. The debris flow simulation was conducted for 17 high risk rivers in the catchment. An example was shown in Fig. 8. The total amount of sediment results from landslide and debris flow was about 89 million m^3 which is similar to the sediment volume produced by the typhoon Morakot in 2009 (91 million m^3).

The urban flood simulation was conducted by SOBEK model in which the storm surge data simulated by FVCOM was used as boundary condition. The flooding simulation result was shown in Fig. 9. The main reasons of the flood inundation are overbank and overland flow. The urban area in the downstream had the major flooding impact. The loss assessments please refer to Li et al., (2015) in this proceeding.

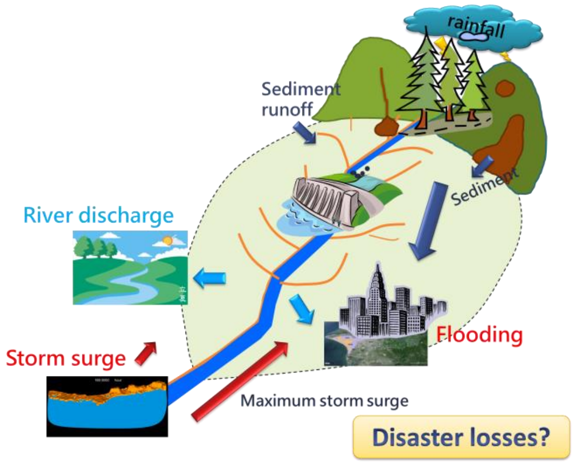

Fig. 6 Conceptual illustration of CBA.

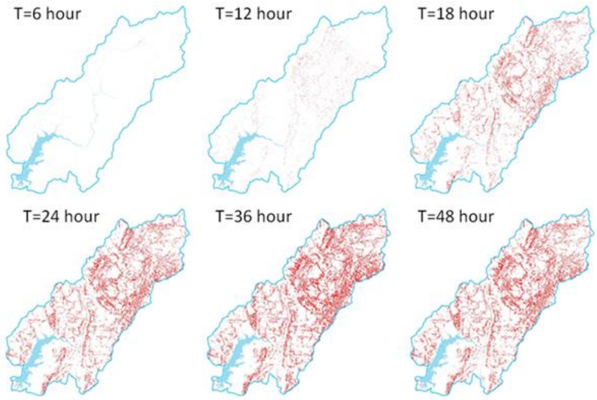

Fig. 7 TRIGRS results at different time.

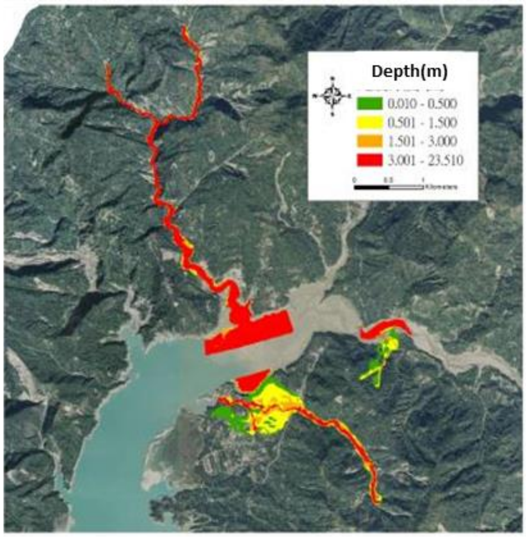

Fig. 8 An example of simulation result of Flow-2D near the Tsen-wen reservoir.

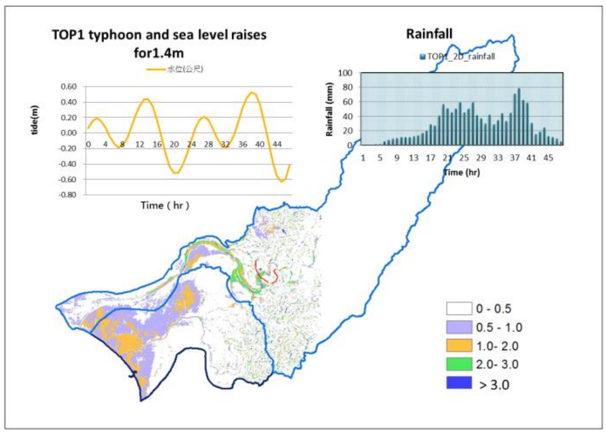

Fig. 9 2D Flood simulation of downstream of Tsen-Wen River by SOBEK

Application example 2: Climate change risk maps

To realize the potential risk of water-related disasters, the dynamic downscaling data were used to produce the risk maps of flooding, slopeland disaster, drought, and coastal inundation. The risk is defined as:

$$\text{Risk} = \text{H} \times V_{Env.} \times V_{Soc.}$$

where H stands for hazard, $V_{Env.}$ is environmental vulnerability and $V_{Soc.}$ is social vulnerability. For different kind of disaster, the calculations of H, $V_{Env.}$and $V_{Soc.}$ were different. Using flooding disaster as an example, the H was the probability of the rainfall events with the total rainfall exceeded 600mm within 24 hours. The $V_{Env.}$ took land subsidence depth into account. The $V_{Soc.}$ considered health (mortality rate), education level, and economy etc. Finally, the flooding risk maps for three periods were shown in Fig. 10. It was apparent that the high risk areas were located in central part of Taiwan and the risk extended to southern part in the end of century.

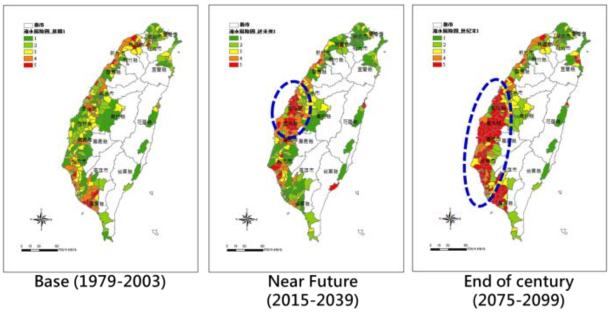

Fig. 10 Flooding risk maps of three periods.

For the slopeland risk, the H was the probability of the rainfall events with the total rainfall exceeded 350mm within 24 hours. The $V_{Env.}$ took historical disaster records, rate of landslide, slope, geology, road density etc.. The $V_{Soc.}$ combined the population density and development index. The resultant slopeland risk maps of three periods were shown in Fig. 11. The results indicated that the slopeland risk increased at the central and east parts of Taiwan.

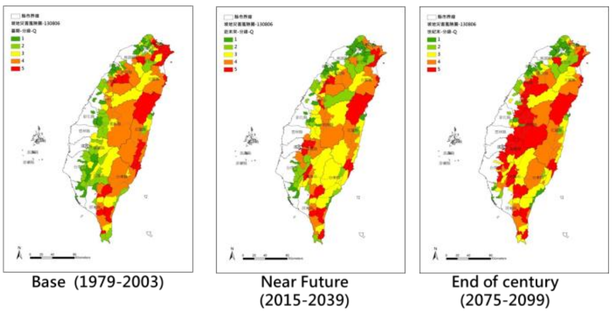

Fig. 11 Slopeland risk maps of three periods.

For the coastal risk, the H was the maximum storm surge heights simulated by FVCOM model. The $V_{Env.}$ considered annual tidal difference and coastal slope. The $V_{Soc.}$ combined the population density and development index and the resultant slopeland risk maps of three periods were shown in Fig. 12. This result revealed that the coastal risk at west part will increased in the end of century.

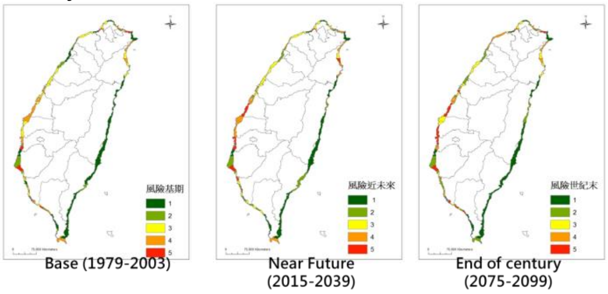

For the drought risk, two kinds of drought were evaluated including drought of public water and agricultural drought. The drought was identified by standardized precipitation index (SPI; Mckee, 1993). The H was the average SPI3, which is the average 3-monthes SPI during dry season (Nov. to April). The $V_{Env.}$ was the water shortage simulated by a mass balance model in which river flow and reservoir water level were taken into account for both public water and agricultural droughts. The $V_{Soc.}$ combined population density and industry production for public water drought; while the agricultural production was used as $V_{Soc.}$ for agricultural drought. The resultant risk maps were shown in the Fig. 13 and Fig. 14. It was clear that the risk of public water drought increased in the west part while the agricultural drought increased in both west and east part of Taiwan in the end of century.

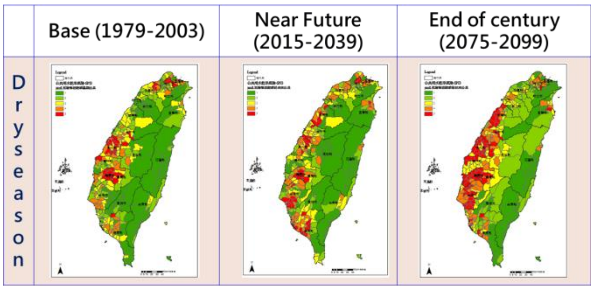

Fig. 13 Risk map of public water drought.

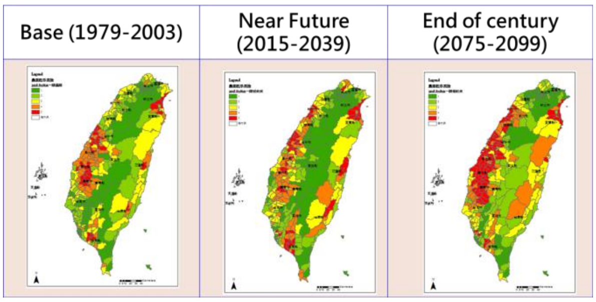

Fig. 14 Risk map of agricultural drought.

Conclusions

This paper introduced the major role and tasks of TCCIP and provided some application examples of dynamic statistical downscaling dataset produced by TCCIP. There are many other applications were not shown here such as the application of statistical downscaling dataset please refer to the Chen et al., (2015) in this proceeding. More applications in agricultural and public health in the TCCIP phase II were undergoing. For detail about TCCIP and data applications, please visit http:// http://tccip.ncdr.nat.gov.tw.

References

Mckee, T.B., Doesken, N. J., Kleist, J., 1993, The relationship of drought frequency and duration to time scales, Eighth Conference on Applied Climatology, 17-22 Jan., Anaheim, California.

Maurer, E. P., 2007. Uncertainty in hydrologic impacts of climate change in the Sierra Nevada, California under two emissions scenarios, Climatic Change, 82, 10.1007/s10584-006-9180-9.

Piani, C., Haerter, J. O., Coppola, E., "Statistical bias correction for daily precipitation in regional climate models over Europe, "Theor. Appl. Climatol. Vol. 99, pp. 187-192, 2010.

Piani, C., Weedon, G. P., Best, M., Gomes, S.M., Viterbo, P., Hagemann, S., Haerter, J. O., "Statistical bias correction of global simulated daily precipitation and temperature for the application of hydrological models," Journal of Hydrology, Vol. 395, pp. 199-215, 2010.

Wood, A.W., E. P. Maurer, A. Kumar, and D. P. Lettenmaier, 2002. Long-range experimental hydrologic forecasting for the eastern United States. J. Geophysical Research-Atmospheres 107(D20), 4429

Wood, A.W., L.R. Leung, V. Sridhar, and D.P. Lettenmaier, 2004. Hydrologic implications of dynamical and statistical approaches to downscaling climate model outputs. Clim. Change, 62, 189-216.

Urban-induced Rainfall in Chiang Mai, Thailand

Pawee Klongvessa[1, a*] and Minjiao Lu[1, b]

Abstract Urban-induced rainfall has been found in many cities all over the world. This research shows some trace of urban-induced rainfall in Chiang Mai, the largest city in the northern part of Thailand. The spatial distribution of total rainfall in Ping Basin, where Chiang Mai is located, is studied in each of pre-monsoon, southwest monsoon and northeast monsoon periods from November 2009 to October 2013. The result shows that Chiang Mai has higher rainfall amount than the surrounding area during all southwest monsoon periods of these 4 years, while during most of the pre-monsoon and northeast monsoon periods, the rainfall amount in Chiang Mai is not clearly different from that in the surrounding area. However, the data of 850 hPa level wind, sea level pressure, and specific humidity suggest that the rainfall amount in Chiang Mai can be higher than that in the surrounding area during pre-monsoon and northeast monsoon periods when the additional humidity from the ocean is brought into the area.

Keywords *Urban-induced Rainfall, Chiang Mai, Thailand, Ping Basin, Monsoon*

Introduction

Urbanization can induce the rainfall or change its pattern through the complicate mechanism (Burian and Shepherd, 2005) such as urban heat island effect from the heat released, the increasing of pollution which can be the condensation nuclei, and the occurrence of air-mass turbulence due to the urban surface (Chandler, 1965). The rainfall induced by urbanization is called urban-induced rainfall and has been found in many cities all over the world (Buishand, 1979; Shafir and Alpert, 1990; Çiçek and Turkoglu, 2005; Kishtawal et al., 2010; Kun and Ahn, 2013; Feng et al., 2014) as well as in Bangkok, Thailand (Klongvessa and Chotpantarat, 2014). Apart from the urban area, the effect of the urban-induced rainfall is sometimes found in the downwind area (Lin et al., 2007). These urban induced rainfalls can lead to flood or hydrograph modification (Reynolds et al., 2008; Changnon, 2010; Huong and Pathirana, 2013).

In this paper, the urban induced rainfall in Chiang Mai was investigated by the spatial distribution of rainfall data from November 2009 to October 2013 in each season and discussed with climatological data. The boundary of the study area is Ping Basin, which is the location of Chiang Mai, and Wang Basin, which is the upstream basin of the Ping Basin.

Study area

Ping and Wang basins are in the northern Thailand and cover the area of 45 thousand square kilometers. The area consists of the mountainous area with some plains along Ping and Wang rivers in the north and plain area in the south. Most of the urban areas are on the plain. The population data from Department of Provincial Administration in 2012 reveals that most people live outside the municipal area. However, considering the population in the municipal area, Chiang Mai is the largest urban and built-up land with the population of more than 600 thousand people in the municipal area. The second largest one is Lampang with almost 300 thousand people in the municipal area. Others are considered small with the population of at most approximately 200 thousand people in the municipal area.

In this area, the climate is controlled by monsoon. Between May and October, the monsoon is southwesterly. The air from the southern tropical ocean is bought to this area. Hence, the weather is warm and wet. According to the data during 1961-2010, the temperature is 21.7-36.6°C and the yearly average total rainfall is 975.7 mm in this period (Reda et al., 2013). Between November and mid-February, the monsoon is northeasterly. The air from the upper continental area is bought to the study area. Hence, the weather is cold and dry. According to the data during 1961-2010, the temperature is 14.6-32.5°C and the yearly average total rainfall is 57.8 mm in this period (Reda et al., 2013). Between mid-February and April, the wind is calm and the weather is warm and dry because of the high insolation. However, the cold air mass from the upper continental area sometimes intrudes the study area. This intrusion can cause the thunderstorm. This period is called pre-monsoon period. According to the data during 1961-2010, the temperature is 17.1-38.7°C and the yearly average total rainfall is 89.6 mm in this period

[1]Pawee Klongvessa and Minjiao Lu
Department of Civil and Environmental Engineering, Nagaoka University of Technology
Nagaoka, Japan
[a]nineboon@hotmail.com
[b]lu@nagaokaut.ac.jp

(Reda et al., 2013). In this study, the southwest monsoon period is defined as from May to October, the northeast monsoon period is defined as from November to January, and the pre-monsoon period is defined as from February to April.

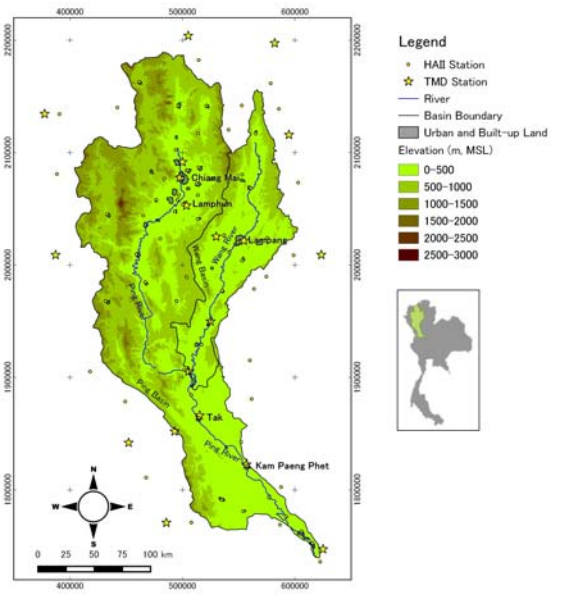

Fig. 1 Study area. HAII and TMD refer to the section of methodology. Elevation data is from GMTED10 derived by United States Geological Surveys. Urban and Built-up land data is from Present Land Use Monitoring of LDD surveyed during 2009-2013.

Methodology

In order to derive the good rainfall spatial distribution data, the good coverage of rain gauges network is required. In this study, data from 2 mm tipping bucket of Hydro and Agro Informatics Institute (HAII) which has a good coverage was used to derive the spatial data and the data from syphon rain gauge of Thai Meteorological Department (TMD) which has a good reliability was used for the spatial consistency check (Nie et al., 2012) as the quality control. The location of HAII and TMD rain gauges are shown in Fig. 1. The spatial consistency check in this paper was the comparison between the daily rainfall recorded at each HAII rain gauge and that interpolated from the recorded at the nearest 4 TMD stations by the inverse distance weighted (IDW) method. When the difference between these 2 daily rainfall data was out of 95% confidence of the normal distribution, the HAII data was excluded. The spatial consistency check was done twice. The first check was done to exclude data which was recorded as 0 when there was the rainfall. This situation possibly occurred when HAII rain gauges network was out of work. The second check was done to exclude some remaining errors due to others factor such as the effect of wind which caused the bucket to tip even though there was no rainfall. After the error data was excluded, the missing data was filled by IDW method from the nearest HAII rain gauges. If there was no data at the 4 nearest HAII rain gauges, the data from TMD rain gauges was used instead. The distribution of seasonal rainfall from November 2009 to October 2013 was determined by IDW interpolation from the quality controlled data.

Some climatological data was also used to discuss the appearance of the urban-induced rainfall in Chiang Mai. These data included daily 850 hPa level wind and 6-hour sea level pressure from the weather maps of TMD, and specific humidity calculated from daily temperature and relative humidity recorded at the TMD rain gauge in the city of Chiang Mai.

Results and discussion

The spatial rainfall distribution data obviously reveals a higher rainfall amount in the city of Chiang Mai than the surrounding areas during the southwest monsoon period as shown in Fig. 2. However, that higher rainfall amount does not appear during most of the northeast monsoon and pre-monsoon periods as shown in Fig. 3 and 4, respectively. Moreover, the rainfall data of TMD during 1981-2010 also support our finding since it reveals an increasing trend of rainfall in the city of Chaing Mai with the higher rate than the surrounding areas only during the southwest monsoon period.

Some studies have suggested that the urbanization can trigger the rainfall in the warm condition rather than in the cold condition (Kun and Ahn, 2013; Feng et al., 2014) and in the high humidity condition rather than in the limited humidity condition (Anglo and Pielke, 1993). However, since in most of the warm pre-monsoon periods, the higher amount of rainfall in the city of Chaing Mai did not appear, the suggestion that the urban area can trigger the rainfall well in the warm condition seems to have less importance in our study area. In fact, Kun and Ahn (2013) and Feng et al. (2014) conducted studies in the mid-latitude area with winter colder than the northeast monsoon period in Chiang Mai. Feng et al. (2014) suggested the reason why the urban area cannot trigger the rainfall in winter as the low temperature which is not enough to trigger the convective activity. That reason may not be applicable to the warmer tropical region in where Chiang Mai is located. Nevertheless, the study of Kun and Ahn (2013) which suggest the effect of humidity on the occurrence of the urban-induced rainfall is possibly applicable to our study since that study was conducted in the tropical region same as our study.

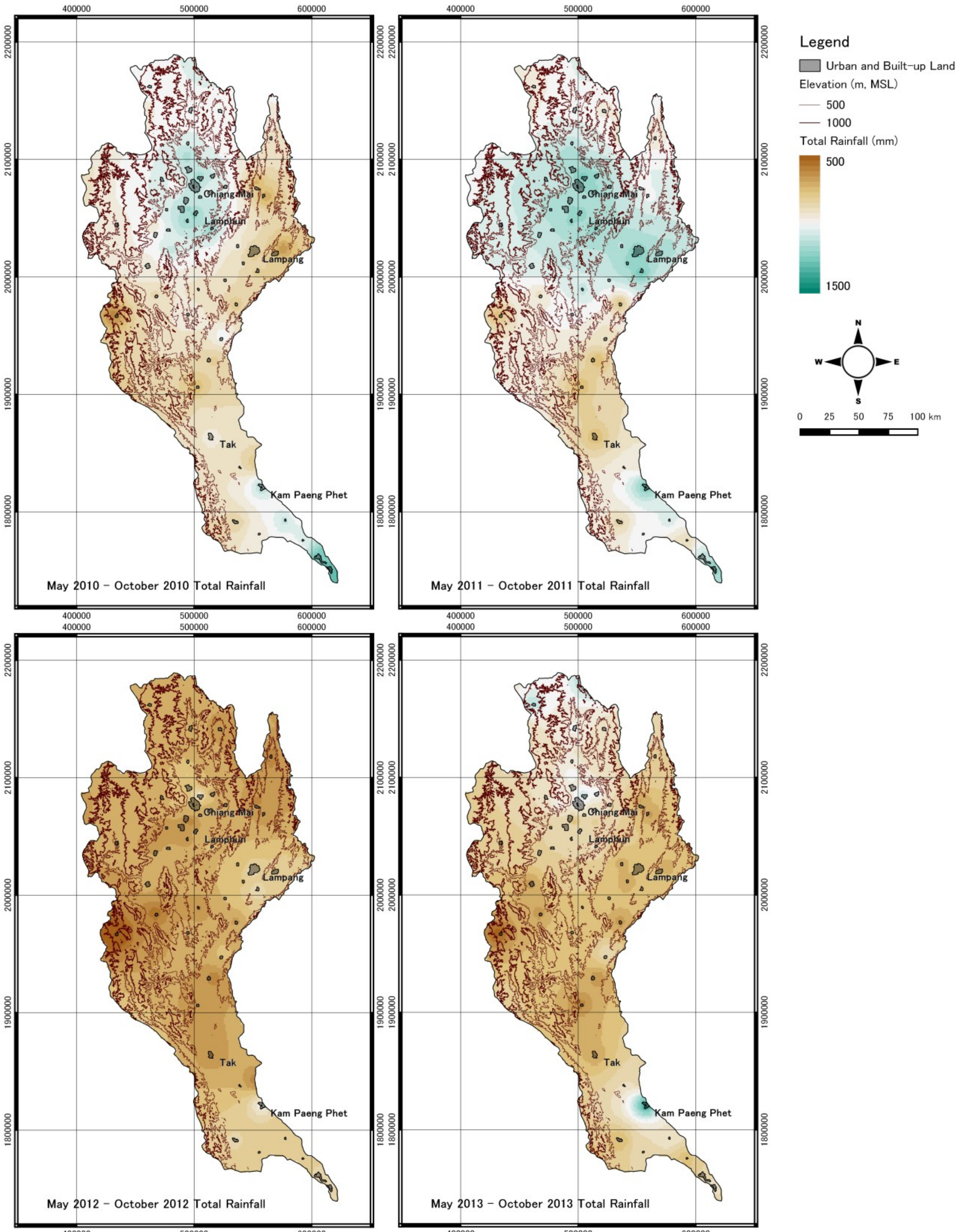

Fig. 2 Spatial distribution of rainfall amount in southwest monsoon periods.

In order to investigate if the humidity play the role on the appearance of the urban-induced rainfall in Chiang Mai, data of specific humidity at the TMD station in the city of Chiang Mai was calculated. It shows a high value during the southwest monsoon period and low value from northeast period to pre-monsoon period. The exceptions were in November 2012, April 2011 and from March to April 2012. During these 3 periods, the humidity was higher than usual as shown in Fig. 5. In November 2012, the sea level pressure data revealed many intrusions of high pressure air mass from the upper continent to the South China Sea which led to the flow of the moist air from the South China Sea to the study area and caused the increasing of humidity. In fact, Fig. 3 also shows some trace of high rainfall in the city of Chiang Mai during November 2012 - January 2013. In April 2011 and from March to April 2012, 850 hPa level wind data revealed many periods of southwest wind which brought the moist air mass from the ocean to the study area and cause the increasing of humidity as well. Fig.2 also reveals a high rainfall in the city of Chiang Mai in the pre-monsoon period of 2012. However, that high rainfall amount did not appear in the pre-monsoon period of 2013 even though the humidity is relatively high. The reason why it did not appear may be the intrusion of the cold air mass from the upper continent which caused the rainfall in the regional scale that can dominate the urbanization effect.

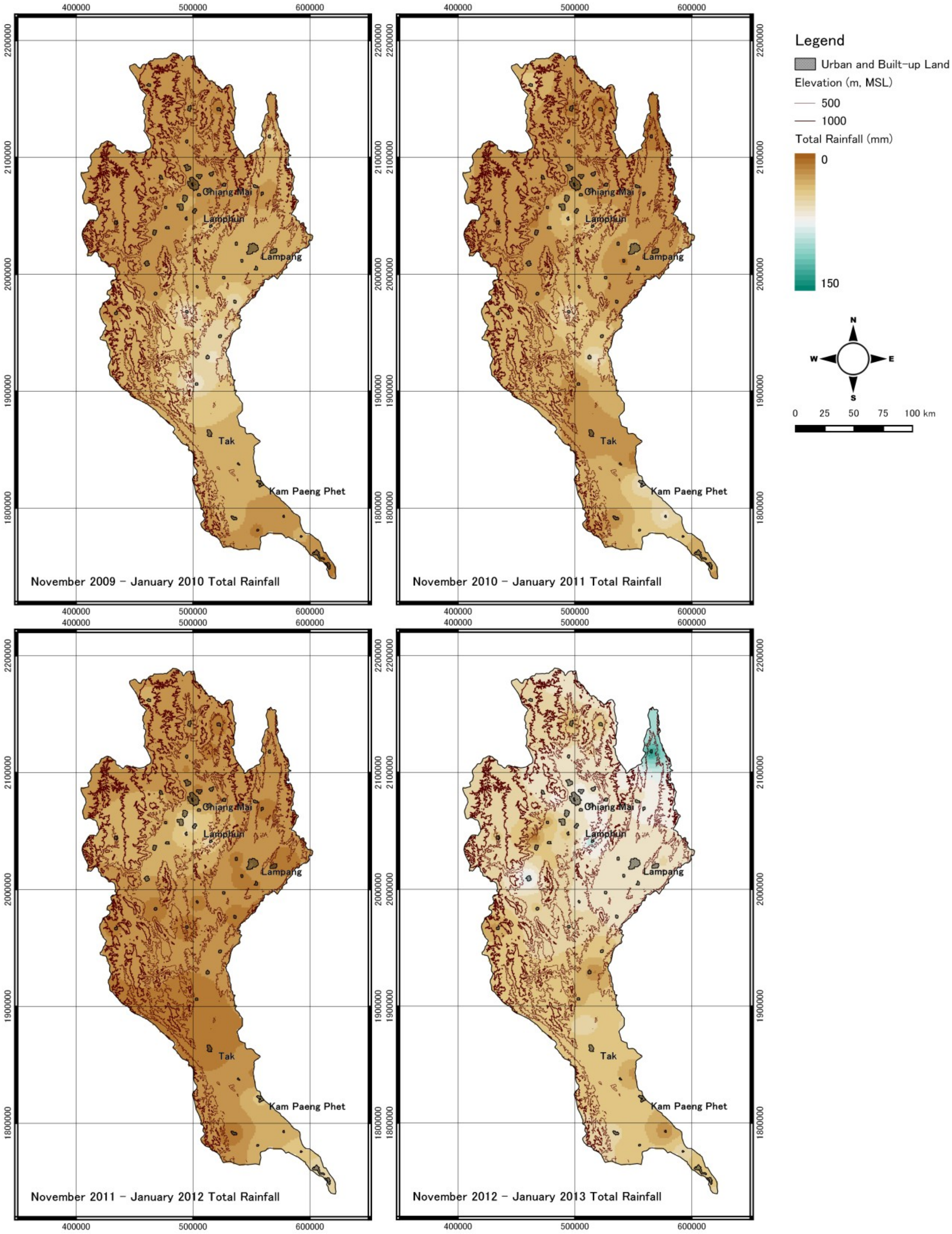

Fig. 3 Spatial distribution of rainfall amount in northeast monsoon periods.

Overall, our findings reveal the appearance of the urban-induced rainfall in the city of Chiang Mai during the period of high humidity. As a result, it is suggested that humidity plays an important role on the urban-induced rainfall in the city of Chiang Mai.

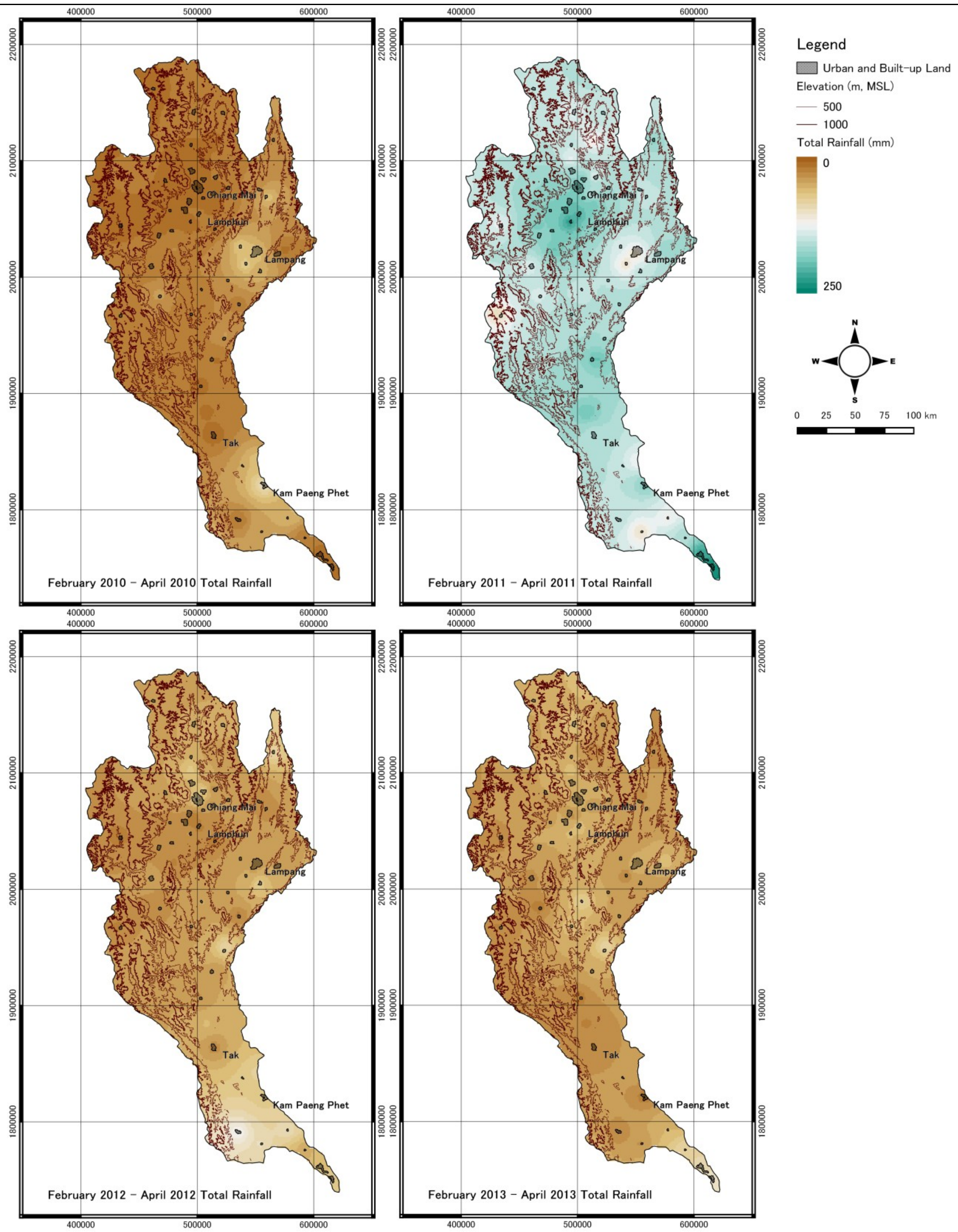

Fig. 4 Spatial distribution of rainfall amount in pre-monsoon periods.

Summary and conclusions

The urbanization effect on rainfall occurs in Chiang Mai as well as many cities. From November 2009 to October 2013, the rainfall spatial distribution data reveals a higher rainfall amount in the city of Chiang Mai during the southwest monsoon period. However, during the most of the northeast monsoon and pre-monsoon periods, this higher rainfall amount does not appear. Our finding is supported by TMD data which reveals the increasing trend of rainfall in the city of Chiang Mai during the southwest monsoon period. The factors which play the role behind the appearance of the urban induced rainfall are suspected to be temperature and humidity. However, the temperature seems to play less role in Chiang Mai because the urban-induced rainfall rarely appear in the warm pre-monsoon period. Since the climatological data reveals a high specific humidity during most of the periods the urban-induced rainfall appears in northeast monsoon and pre-monsoon periods, the humidity is suspected to play the role on the occurrence of the urban-induced rainfall in Chiang Mai. This effect of urbanization should be recognized since some researches addressed the effect of urban-induced rainfall on flood and hydrograph shape.

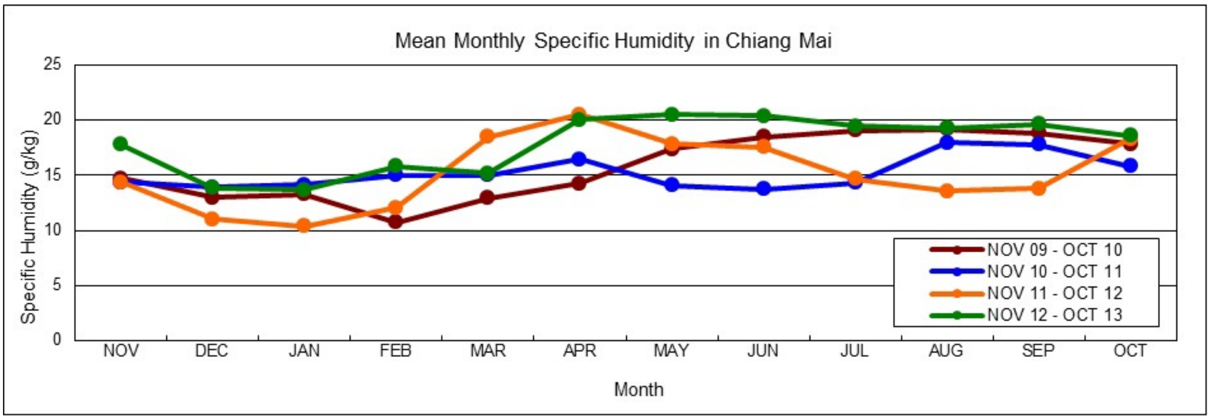

Fig. 5 Mean monthly specific humidity in Chiang Mai during November 2009 - October 2013.

Acknowledgement

The authors are thankful to Thai Meteorological Department and Hydro and Agro Informatics Institute for providing the data, and also thankful to Assistant Professor Dr. Srilert Chotpantarat from Chulalongkorn University, Thailand, for being the coordinator between the authors and these institutes.

References

Anglo, E.G., and Pielke, R.A. 1993. A numerical study of the impact of land use modification on local rainfall over Manila. Department of Atmospheric Science, Colorado State University.

Buishand, T.A. 1979. Urbanization and changes in precipitation, a statistical approach. J. Hydrol. 40 (3-4), 365-375.

Burian, S.J., and Shepherd, J.M. 2005. Effect of urbanization on the diurnal rainfall pattern in Houston. Hydrol. Process. 19, 1089-1103.

Chandler, T.J. 1965. The Climate of London, Hutchinson.

Changnon, S.A. 2010. Stormwater management for a record rainstorm at Chicago. J. Contemp. Water Resour. Res. Educ. 146 (1), 103-109.

Changnon, S.A., Semonin, R.G., and Huff, F.A. 1976. A hypothesis for urban rainfall anomalies. J. Appl. Meteorol. 15, 544-560.

Çiçek, I., and Turkoglu, N. 2005. Urban effects on precipitation in Ankara. Atmósfera 18(3), 173-187.

Feng, J., Wang, J., and Yan, Z. 2014. Impact of anthropogenic heat release on regional climate in three vast urban agglomerations in China. Adv. Atmos. Sci. 31, 363-373.

Huong, H.T.L. and Pathirana, A. 2013. Urbanization and climate change impacts on future urban flooding in Can Tho city, Vietnam. Hydrol. Earth Syst. Sci. 17, 379-394.

Jianting, C., Jun, X., Chongyu, X., Lu, L., and Zhonggen, W. 2010. Spatial and temporal variability of daily precipitation in Haihe River basin, 1958–2007. J. Geogr. Sci. 20 (2), 248-260.

Kishtawal, C.M., Niyogi, D., Tewari, M., Pielke, R.A., and Shepherd, J.M. 2010. Urbanization signature in the observed heavy rainfall climatology over India. Int. J. Climatol. 30 (13), 1908-1916.

Klongvessa, P., and Chotpantarat, C. 2014. Statistical analysis of rainfall variations in the Bangkok urban area, Thailand. Arab. J. Geosci. (in press)

Kug, J., and Ahn, M. 2013. Impact of urbanization on recent temperature and precipitation trends in the Korean peninsula. Asia-Pacific J. Atmos. Sci. 49 (2), 151-159.

Lin, C.Y., Chen, W.C., Liu S.C., Liou Y.A., Liu, G.R., and Lin, T.H. 2007. Numerical study of the impact of urbanization on the precipitation over Taiwan. Atmos. Environ. 42 (13), 2934-2947.

Nie, S., Luo, Y., Li, W., Wu, T., Shi, X., and Wang ,Z. 2012. Quality control and analysis of global gauge-based daily precipitation dataset from 1980 to 2009. Adv. Clim. Change Res. 3 (1), 45-53.

Reda, A.G., Tripathi, N.K., Soni, P.,Tipdecho, T., and Phalke, A. 2013. Temporal climate trend of Ping Basin of Thailand and implications for Maekong Region. J. Earth Sci. Clim. Change 4 (4).

Reynolds, S.K., Burian, S.J., Shepherd, M., and Manyin, M. 2008. Urban induced rainfall modifications on urban hydrologic response. W. James, Editor in Chief, Co-edited by Irvine, K.N., McBean, E.A., Pitt, R.E., and Wright, S.J. In Reliable modeling of urban water systems, Computational Hydraulics International, Guelph, Ontario, Canada, pp. 99-122.

Shafir, H., and Alpert, P. 1990. On the urban orographic rainfall anomaly in Jerusalem – a numerical study. Atmos. Environ. 24B (3), 365-375.

Bias correction test of simulated rainfall from PRECIS using adjustment factors based on distribution mapping.

KOWIT BOONRAWD[1, a] CHATCHAI JOTHITYANGKOON[1, b]

Abstract To reduce uncertainty and risk of projection bias of regional climate model (RCM) simulation in climate change studies, many bias correction approaches have been developed to manage these biases. The simple one is distribution mapping based on derived adjustment factors (AF), which is the ratio between observed and simulated rainfall for a given frequency of occurrence. Five methods are used to estimate the distribution between adjustment factors and exceedance probability. Method 1, AFs are derived from all daily rainfall data and used to shift distribution of daily rainfall intensity. Method 2, temporal scaling of input rainfall data is changed from daily to monthly. Method 3 is similar to Method 2, the difference is AFs are used to adjust distribution of daily rainfall. For Method 4, seasonal AFs are derived from monthly rainfall data for each month of all years and used to shift distribution of monthly rainfall of each month. Method 5 is the combination of Method 4 for the first step and Method 1 for the second step. These methods are tested to correct simulated rainfall from Providing Regional Climates for Impacts Studies (PRECIS) and ECHAM4 climate models with resolution 0.2 x 0.2 degree (grid size 20x20 km) daily time step, baseline period from year 1982-2005. The performance of all methods is evaluated by using the plot of inter-annual variability, intra-annual variability and daily intensity distribution against exceedance probability. The best improvement of simulated rainfall is achieved with Method 5.

Keywords *RCMs, Climate change, frequency of occurrence, exceedance probability*

Kowit Boonrawd
School of Civil Engineering.
Suranaree University of Technology.
Muang District NakhonRatchasima.
kowit_b@hotmail.com

Chatchai Jothityangkoon School of Civil Engineering. Suranaree University of Technology. Muang District NakhonRatchasima.
cjothit@sut.ac.th

Introduction

Hydrological modeling of climate change impact studies, large-scale climate variables for current and future conditions are generally provided by global climate models (GCMs). To resolve processes and features relevant to hydrology at the catchment scale, regional climate models (RCMs) are commonly used to transfer coarse-resolution GCM data to a higher resolution.
Downscaling is a technique commonly used in hydrology when investigating the impact of climate change. It is a way of bridging the gap between low spatial resolution global climate models (GCMs) and the catchment- or regional-scale hydrological models (Fowler et al., 2007). Hydrological simulations driven with the higher-skill bias corrected RCM data performed generally better than corresponding simulations driven with lower-skill bias-corrected RCM data.
The higher-skill bias corrected RCM data or distribution mapping based on derived adjustment factors (AF), which is the ratio between observed and simulated rainfall for a given frequency of occurrence. It corrects most of the statistical characteristics and has the narrowest variability ranges, combined with the best fit of the ensemble median.

Study area

The Study area covers Upper Ping River basin, Thailand is located in the northern region of Thailand. The main stream of the river flows through Chiang Mai, one of the most popular tourist destination of the northern Thailand. It flows to Bhumibol Dam on the south of the basin. The catchment area upstream of Bhumibol Dam is 26,386 km^2. Observed precipitation dataset extends over Upper Ping River basin and covers the period 1982–2005, selected a 24 years sequence of daily rainfall time series were used in this study. Projected rainfall from grid points shown in Fig.1a. Are compared to observed data from selected 42 rain gauges.

RCM data

These methods are tested to correct simulated and projected rainfall from Providing Regional Climates for Impacts Studies (PRECIS) which receives input data from ECHAM4 climate models with resolution 0.2 x 0.2

degree (grid size 20x20 km) daily time step, baseline period from year 1982-2005. (Chinvanno et.al.,2009) The simulation covers the Intergovernmental Panel on Climate Change (IPCC) emission scenarios A2 and B2.

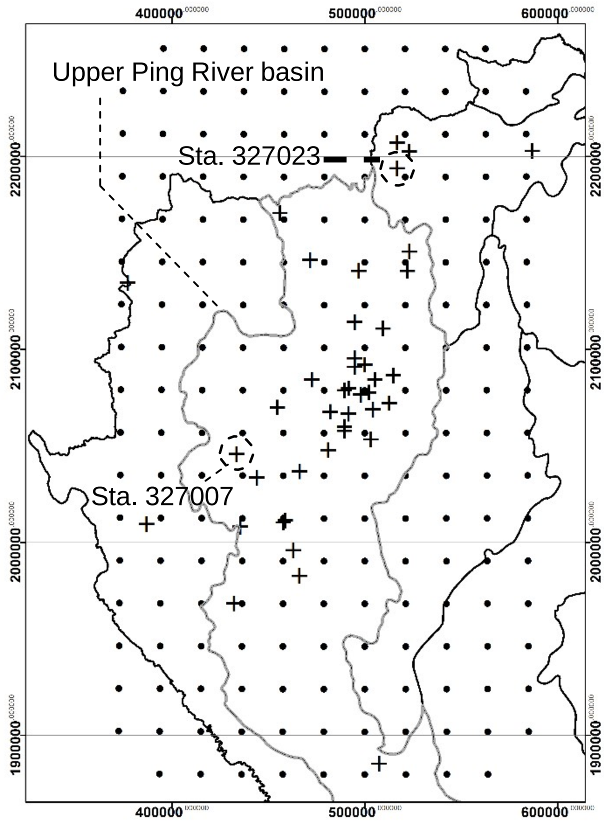

Figure 1 Study area covers Upper Ping River basin and present location of rain gauges (+) and grid points of projected rainfall (•).

Methodology

Bias correction method

A solution to the problem of RCM misrepresentation of precipitation is to pre-process the RCM output through bias correction a number of bias correction methods to adjust RCM simulations were utilized (1) linear scaling, (2) local intensity scaling, (3) power transformation, (4) variance scaling, (5) distribution mapping and (6) delta-change approach. Bias correction approaches is given in Table 1. (Gudmundsson et al.2012)

When using the linear scaling method, RCM daily rainfall amounts, P are transformed into $P*$ such that

$$�^{*} = a� \qquad (1)$$

Using an adjustment factor ��, $a = \frac{�'}{�'}$ (2)

Where $�'$ and $�'$ are Observed and RCM simulated daily or monthly rainfall data with the same frequency from 20x20 km grid size, respectively. Here, the daily, monthly adjustment factors and combination of them are applied to each uncorrected daily observation of that month, generating the corrected daily time series. The linear correction method belongs to the same family as the factor of change or delta change method. This method has the advantage of simplicity and modest data requirements.

Table 1. Overview of methods used to correct RCM-simulated precipitation (P) and/or temperature (T) data.

Methods		Short Description
linear scaling	P,T	·adjusts RCM time series with correction values based on the relationship between long-term monthly mean observed and RCM control run values ·precipitation is typically corrected with a factor and temperature with an additive term
local intensity scaling	P	·combines a precipitation threshold with linear scaling (both described above)
power transformation	P	·is a non-linear correction in an exponential form (a*Pb) that combines the correction of the coefficient of variation (CV) with linear scaling
variance scaling	T	·combines standard linear scaling with a scaling based on standard deviations
distribution mapping	P,T	·matches the distribution functions of observations and RCM-simulated climate values. ·a precipitation threshold can be introduced to avoid substantial distortion of the distribution caused by too many drizzle days (i.e., very low but non-zero precipitation) ·also known as quartile - quartile mapping, probability mapping, statistical downscaling or histogram equalization.
delta-change approach	P,T	·RCM-simulated future change signals (anomalies) are superimposed upon observational time series ·usually done with a multiplicative correction for precipitation and an additive correction for temperature

When using the distribution mapping method, to describe the probability distribution of a random variable X, we use a cumulative distribution function. The value of this function F_X (��) is simply the probability P of the event that the random variable takes on value equal to or less than the argument such that

$$F_X(��) = �[X \leq ��] \qquad (3)$$

However, correcting only the monthly mean precipitation can distort the relative variability of the inter-monthly precipitation distribution, and may adversely affect other moments of the probability distribution of daily precipitations. For bias correction test in this study, the complexity of derived AFs is added in 5 steps (5 methods)
Method 1, AFs are derived from all daily rainfall data and used to shift distribution of daily rainfall intensity.

Method 2, temporal scaling of input rainfall data is changed from daily to monthly.
Method 3 is similar to Method 2, the difference is AFs are used to adjust distribution of daily rainfall.
Method 4, seasonal AFs are derived from monthly rainfall data for each month of all years and used to shift distribution of monthly rainfall of each month.
Method 5 is the combination of Method 4 for the first step and Method 1 for the second step.
The comparison of observed, projected and adjusted rainfall station using frequency analysis of its distribution based on exceedance probability.

Results and Discussion

For Method 1, AFs is applied to projected daily rainfall with the same frequency (Fig. 2 (a)). Distribution of adjusted daily rainfall is shifted to give a perfect fit to distribution of observed rainfall (Fig. 2(b)).
After these adjusted rainfalls are accumulated to annual and monthly rainfall. The distribution of annual and monthly rainfall present a little improvement. Under-estimate annual rainfall for wet years and over-estimate annual rainfall for dry years are still exist (Fig. 2 (c)). Seasonal pattern of average monthly rainfall is far different from the pattern of observed rainfall (Fig. 2(d)).

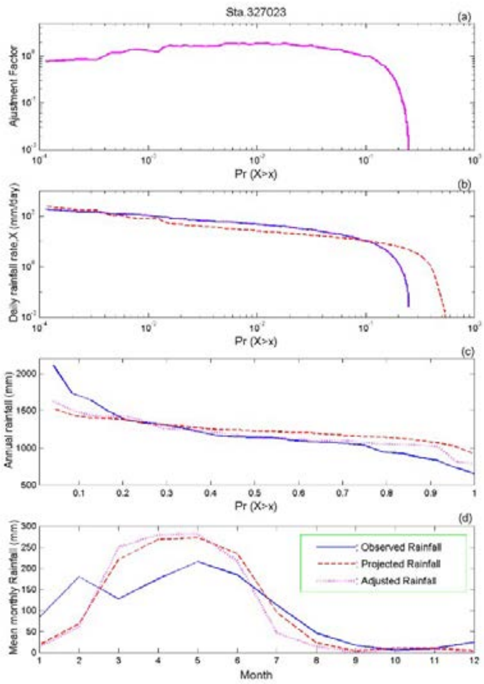

Figure 2 Method 1, Comparison of observed, projected and adjusted rainfall at Sta. 327023 using adjustment factors from daily rainfall for 24 years (1982-2005) to adjust the time series of daily rainfall (a) exceedance probability of adjustment factor, (b) exceedance probability of daily rainfall, (c) exceedance probability of annual rainfall, (d) mean monthly rainfall.

Second trial for Method 2, AFs are estimated for projected monthly rainfall with the same frequency (Fig. 3(a)). Although, distribution of adjusted monthly rainfall is shifted to give a perfect fit to the distribution of observed monthly rainfall, discrepancy between adjusted annual and monthly rainfall and observed rainfall is found. Compare to Method 1, better results of seasonal patterns of average monthly rainfall are presented.

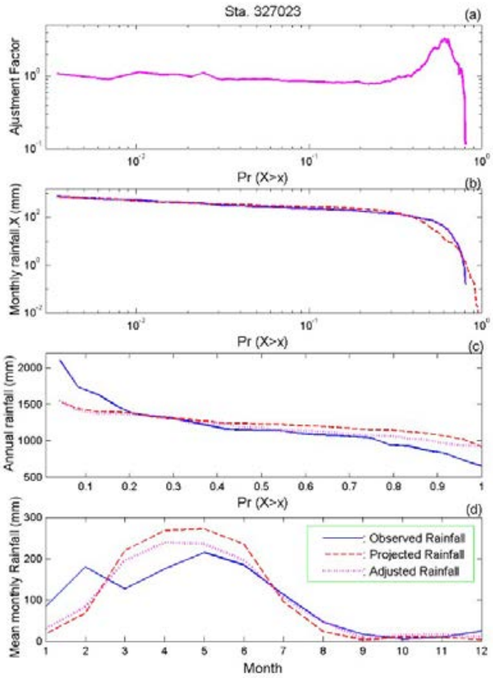

Figure 3 Method 2, Comparison of observed, projected and adjusted rainfall at Sta. 327023 using adjustment factors from monthly rainfall for 24 years (1982-2005) to adjust the time series of monthly rainfall (a) exceedance probability of adjustment factor, (b) exceedance probability of monthly rainfall, (c) exceedance probability of annual rainfall, (d) mean monthly rainfall.

Third trial for Method 3, AFs are estimated similar to Method 2 but applied for projected daily rainfall with the same frequency. Shitted distribution of adjusted daily rainfall show a good agreement with distribution of observed daily rainfall (Fig. 3(b)). However, the difference between adjusted annual and monthly rainfall and observed rainfall is not resolved fitting. Results are the same as the previous results from Method 2.

Fourth trial for Method 4, Seasonal AFs are estimated from monthly rainfall for each month of the year and applied for projected monthly rainfall. AFs for July in Fig. 5(a), can shift the distribution of adjusted July rainfall and give a perfect fit to observed July rainfall (Fig. 5(b)). However, when this method is used for every months of the year, annual adjusted rainfall show under-estimated results for the whole annual series. Seasonal pattern of adjusted monthly rainfall is shifted close to observed monthly pattern (Fig. 5(d)).

Final trial for Method 5, two steps of AFs estimation from Method 1 and Method 4 are combined. Distribution of adjusted daily, monthly and annual rainfall are shifted to give a better fit to distribution of observed rainfall, compare to the other method (Fig. 6 (b)-(d)).

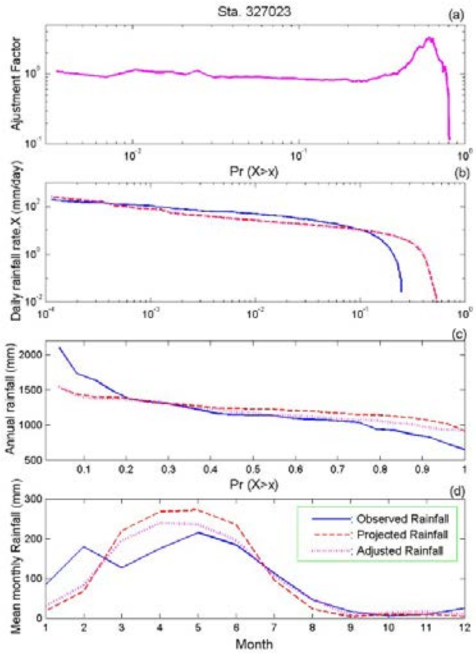

Figure 4 Method 3, Comparison of observed, projected and adjusted rainfall at Sta. 327023 using adjustment factors from monthly rainfall for 24 years (1982-2005) to adjust the time series of daily rainfall (a) exceedance probability of adjustment factor, (b) exceedance probability of daily rainfall, (c) exceedance probability of annual rainfall, (d) mean monthly rainfall.

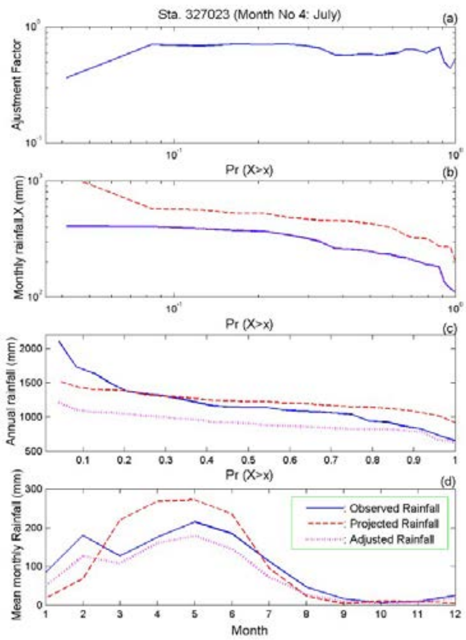

Figure 5 Method 4, Comparison of observed, projected and adjusted rainfall at Sta. 327023 using seasonal adjustment factors from monthly rainfall for each month to adjust the time series of monthly rainfall (a) exceedance probability of adjustment factor for Month No 4: July, (b) exceedance probability of July rainfall, (c) exceedance probability of annual rainfall, (d) mean monthly rainfall.

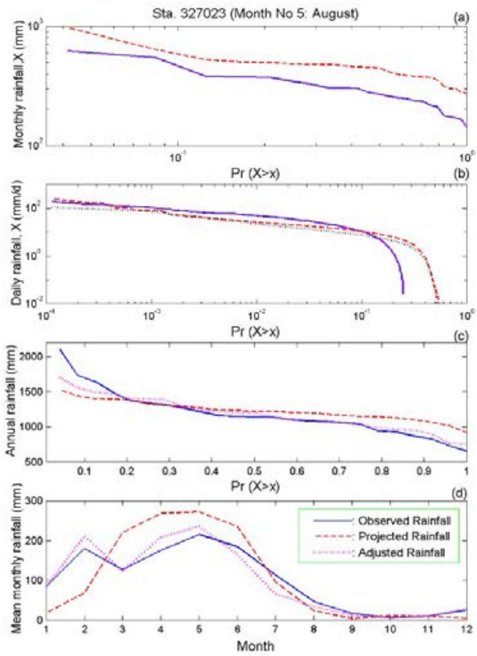

Figure 6 Method 5, Comparison of observed, projected and adjusted rainfall at Sta. 327023 using the first step: adjustment factors from monthly rainfall for each month to adjust the time series of daily rainfall and the second step: adjustment factors from previous daily rainfall to adjust the time series of daily rainfall (a) exceedance probability of adjustment factor for Month No 5: August, (b) exceedance probability of daily rainfall, (c) exceedance probability of annual rainfall, (d) mean monthly rainfall.

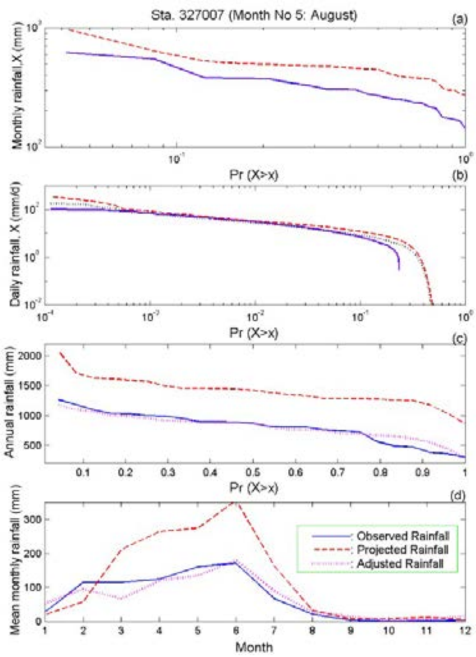

Figure 7 Method 5, Comparison of observed, projected and adjusted rainfall at Sta. 327007 using the first step:

adjustment factors from monthly rainfall for each month to adjust the time series of daily rainfall and the second step: adjustment factors from previous daily rainfall to adjust the time series of daily rainfall (a) exceedance probability of adjustment factor for Month No 5: August, (b) exceedance probability of daily rainfall, (c) exceedance probability of annual rainfall, (d) mean monthly rainfall.

To confirm the accuracy of Method 5, this bias correction test is applied to many locations of available observed rainfall. Fig. 6 and 7 present an example of this test. Projected rainfall data from 2 grid points close to rain gauge station sta. 327023 and 327007 can be shifted its distribution close to observed rainfall data with satisfied results.

Conclusion

The performance of all methods is evaluated by using the plot of inter-annual variability, intra-annual variability and daily intensity distribution against exceedance probability. The best improvement of projected rainfall using AFs is achieved with Method 5. AFs in the first step are applied to correct seasonal pattern of monthly rainfall within a year and applied to correct daily rainfall intensity in the second step.

Results further show that whereas bias correction does not seem to affect the change signals in rainfall means, it can introduce extra uncertainty to the change signals in high and low rainfall amounts, and consequently, in runoff. Future climate change impact studies need to take this into account when deciding whether to use raw or bias corrected RCM results. Nevertheless, the bias in RCM simulations will continue to reduce as RCM accuracy is improved and RCMs will become increasingly useful for hydrological studies.

Acknowledgement

This study was partly funded by the Institute of Research and Development, Suranaree University of Technology for the first author.

References

Chinvanno S., Laung-Aram V., Sangmanee C., Thanakitmetavut J., Future Climate Projection for Thailand and Mainland Southeast Asia Using PRECIS and ECHAM4 Climate Models., Southeast Asia START Regional Center Technical Report No. 18, 2009.

Fowler, H. J., Blenkinsop, S., and Tebaldi, C.: Linking climate change modelling to impacts studies: recent advances in downscaling techniques for hydrological modelling, Int. J. Climatol., 27, 1547–1578, doi:10.1002/joc.1556, 2007.

Gudmundsson, L., J. B. Bremnes, J. E. Haugen, and T. Engen-Skaugen (2012), Technical Note: Downscaling RCM precipitation to the station scale using statistical transformations - a comparison of methods, Hydrol Earth Syst Sci, 16(9), 3383–3390, doi:10.5194/hess-16-3383-2012.

Uncertainty of stream flow under climate change scenarios using statistical downscaling data

Yun-Ju Chen [1], Yuan-Fong Su[1], Jun-Jih Liou[1] and Yung-Ming Chen[1]

Abstract Based on recent studies of climate change, trend assessment of future climate, under global or continental scale, could be carried out confidently. However, the results may have inevitable uncertainty which should not be neglected for impact studies of climate change. The uncertainty analyzed climatic projections include uncertainty in future emissions of greenhouse gases, in modeling global climate and downscaling resolutions (25km2 and 5km2), while the naturel variable is assessed through data resampling. Statistic downscaling method and weather generator are applied in this study, in order to olve the problem which users need higher resolution and daily sequence data to assess impact under climate change. After downscaling and weather generation, we can get precipitation and temperature monthly change of GCM at 25 km scale and precipitation and temperature daily data in a station in Taiwan. A lump and physical mechanisms hydrological model- GWLF model is applied to assess streamflow impacts under climate change. There are four main catchments, including Dansuie River, Dajia River and Ts ngwen River and Kaoping River, to assess the likely impacts for two future time periods; the 2020~2039, and 2080~2099. This study also discussed the characteristic of precipitation and the change of streamflow of near future and end of 21st century under different emission CO2 scenarios from the result of 24 GCMs. We also choice of suitable GCMs for the users based on characteristic of rainfall change rate in wet and dry spell and performance of East Asia monsoon by GCM simulation result.

Keywords *streamflow, resolution, scenario, GWLF*

Yun-Ju Chen
1National Science and Technology Center for Disaster Reduction, New Taipei City, Taiwan.
yjchen@ncdr.nat.gov.tw
Yuan-Fong Su
yuanfongsu@ncdr.nat.gov.tw
Jun-Jih Liou
jjliou@ncdr.nat.gov.tw
Yung-Ming Chen
ymchen@ncdr.nat.gov.tw

Introduction

In Taiwan, distribution of precipitation in time and space is uneven, moreover, precipitation ratio of wet to dry season and annual precipitation is more pronounced different. About 80% of the rainfall is concentrated in the wet period from May to October. For example, the average ratio of wet to dry spell in Taiwan southern regions is 9:1 and annual precipitation reaches 3500mm in wet years but in dry years only 1600mm. Because of special geographical conditions, 3/4 of runoff flows directly into ocean and water resources cannot storage easily. These characteristic cause the lack of water resource in Taiwan.

Climate change may increase the frequency and intensity of extreme weather/climate events, leading to larger impacts of weather-related natural hazard. The patterns of rainfall tend more extremes in wet and dry spell to cause water supply seriously impacts. Tung and Li (2005) analyze impacts of streamflow under climate change in nine basins in Taiwan. The result showed streamflow decreased in winter and spring season and increased in summer season, but it is insignificant variation in autumn. Loukas et al. (2002) applied CGCMA1model to simulate tend of temperature and precipitation in future in watershed scale. The results are shown that the average amount and frequency of flooding increased trend in Campell basins in Canada, but it is opposite trend in Illecillewaet basin.

In this study, statistical downscaling is used to get climate data of higher resolution. With three climate scenarios (A1B, B1and A2), general circulation models (GCM) are statistical downscaled and provide the precipitation ratios and the differences in temperature in the future scenarios. In addition, weather generation model is applied to generate daily weather data for input of a hydrology odel. Generated daily rainfall and temperature is applied to simulate change ratio of streamflow under climate change impacts. Moreover, we also assess the variance as uncertainty of streamflow. The results provide decision-makers references which they adopt adaptation to deal with impacts of climate change on water resources.

Study area

In this study, we selected four main basins which are important for water resource management in Taiwan, including Dansuie River, Dajia River and Tsengwen

River and Kaoping River from north to south. The locations of basins are shown in Fig.1.

Fig. 1 Study area

Methodology

The spatial resolution of GCMs is order of hundreds to thousands of kilometers from IPCC (Intergovernmental Panel on Climate Change) website. Those data are too coarse to assess issues of water resource in watersheds. In this study, we use bias correction o statistical downscaling method (SDSM) to downscale spatial scale to 25km and 5km grid data of AR4 GCMs, including A1B, A2 and B1 scenarios. The change ratio for monthly rainfall and absolute change of monthly temperature are produced by SDSM. And then the weather generator model (WG) is applied to simulate daily rainfall and temperature for inputs of a hydrology model in the future periods. Finally, the uncertainty of flow change rate is analyzed. The flowchart of climate change impact on water resource is shown as Fig. 2.

First, we use bias correction o statistical downscaling method (SDSM) to downscale spatial scale to 25km from to

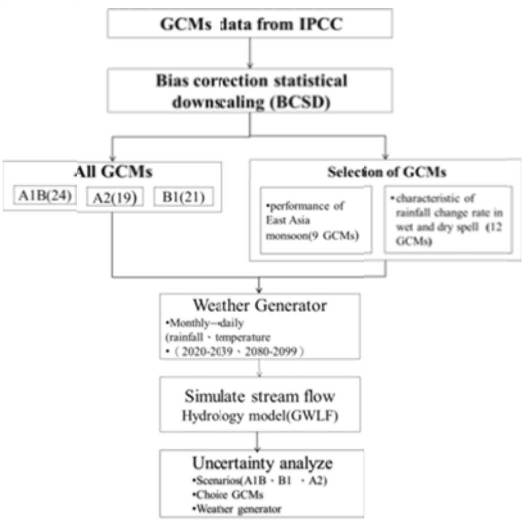

Fig. 2 flowchart of climate change impact on streamflow assessment

Statistical downscaling

The statistical downscaling data were provided by Aphrodite (Asian precipitation – Highly–Resolved Observational Data Integration Towards Evaluation) with a spatial resolution of 0.25°. This data set has been bias corrected. Bias corrected statistical downscaling is applied in this study (Chen et al. 2014).In total, 24 GCM models provided by IPCC were collected in this study. Downscaling process is developed to project GCMs' predictions to basin scale to setup climate scenarios.

Weather generation

Most of the GCMs have the monthly weather data with different scenarios, but these data cannot be used in the assessment of water resources impacts directly. Therefore, the WG is often used to generator daily weather variables. The WG is based on the statistic characteristics of weather variables (Richardson & Wright 1984, Wilks &Wilby 1999). After verified the parameters of a weather station, the WG can be applied in generating long time series with different weather variables, for agr culture and hydrological risk analysis (Mavromatis &H nsen 2001). In this study, the WG and downscale processes are proposed by Tung and Haith (1995). The weather variables, temperature and precipitation, are input of this model and the monthly change of temperature and precipitation by climate change in the resolution of 25km*25km. This study assumed that the probability of wet day and the probability of wet day after a wet day/ dry day are not change under climate change. The future climate scenarios setup based on GCMs' projections in different climate scenarios. The mean monthly temperature and precipitation are modified as follows:

$$\lambda_m \Rightarrow \lambda'_m = \lambda_m \times \frac{\lambda_{2\times CO_2}}{\lambda_{1\times CO_2}} \qquad (1)$$

$$\mu_{Tm} \Rightarrow \mu'_{Tm} = \mu_{Tm} + \left(\mu_{Tm_{2\times CO_2}} - \mu_{Tm1\times CO_2}\right) \qquad (2)$$

In Eq.(1), λ_m is the mean precipitation from observed data in the month *m*; λ'_m is the mean precipitation after climate change; $\lambda_{1\times CO_2}$ and $\lambda_{2\times CO_2}$ are the mean precipitation in current and in climate change, respectively. In Eq.(2), μ_{Tm} is the mean temperature from observed data in the month *m*; μ'_{Tm} is the mean temperature after climate change; $\mu_{Tm1\times CO_2}$ and $\mu_{Tm_{2\times CO_2}}$ are mean temperature in current and in climate change, respectively.

Temperature generation

The daily temperature in future is generated from a monthly average temperature through a first-order Markov chain(Pickering et al, 1988；Tung, 1995). The equation is as following:

$$T_i = \mu_{Tm} + \rho(T_{i-1} - \mu_{Tm}) + V_i \sigma_T \sqrt{1-\rho^2} \quad (3)$$

In Eq. (3), T_i is the temperature of the day i; μ_T is the monthly average temperature and relative to the corresponded month; ρ is the first order serial correlation coefficient of T_i and T_{i-1} . V_i is belong to N(0,1) (Normal Sampling Deviate); σ_T is the standard deviation standard.

Rainfall amount generation

The daily rainfall amounts are used Cumulative Distribution Function (CDF) and a random number to produce. Hong (1996) suggested using Exponential Distribution to simulate daily rainfall. The equation is as following:

$$F_{Rm}(R = r) = P(R \le r) = 1 - Exp[-(\frac{1.191r}{\lambda_m})^{0.75}] \quad (4)$$

In Eq. (4), P is daily rainfall (cm) . λ_m is wet day mean precipitation in month m. r is the random number$\in$Uniform[0, 1].

Hydrology Model

The GWLF (Generalized Watershed Loading Functions; Haith and Shoemaker, 1987) is used in this study, because the parameters in this model are based on the physical properties of the watershed. Uncertainty of this model is less than other complex models, so it can be used to assess impact of climate change. The water balance of this model is shown as Fig. 3. Refer to Tung (1992, 2007) for further details on this model.

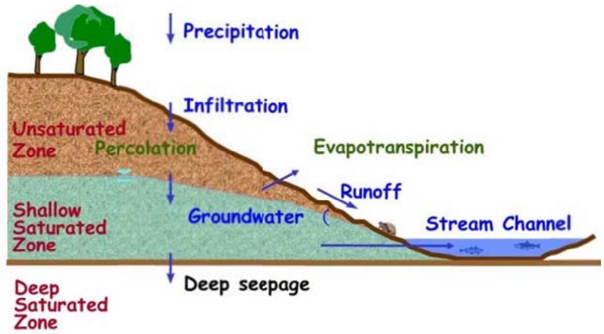

Fig. 3 Streamflow component of the GWLF model（Tung,2007）

Selection of GCMs

Method I: Selection by performance of East Asia monsoon

Based on rainfall pattern and monsoon characteristic of GCMs in East Asia area, we select the good performance GCMs which have high correlation coefficient with historical climate properties. Selection GCMs are shown as Table1.

Method II: Selection by characteristic of precipitation in wet and dry spell 式(4)

Precipitation trend in wet and dry spell is significate for water resource management under climate change impacts. An index that characteristic of precipitation in wet and dry spell is applied to classify GCMs. There are four types GCMs, (i) annual rainfall increase, and (ii) annual rainfall decrease, (iii) rainfall decrease in wet spell but increase in dry spell, and (iv) rainfall increased in wet spell but decreased in dry spell, respectively. The type (iv) has large impacts on water resource management. There are 9 GCMs that belong to type (iv) in this study area. Selected GCMs are shown as Table 1.

Table.1 Selection GCM model List based on different method

No.	GCM model name（Method I ）	GCM model name（Method II）
1	csiro_mk3_0	bccr_bcm2_0
2	csiro_mk3_5	cccma_cgcm3_1
3	gfdl_cm2_0	csiro_mk3_5
4	gfdl_cm2_1	inmcm3_0
5	ingv_echam4	ipsl_cm4
6	miroc3_2_hires	miroc3_2_hires
7	miroc3_2_medres	mri_cgcm2_3_2a
8	mpi_echam5	ncar_pcm1
9	mri_cgcm2_3_2a	ukmo_hadgem1

Uncertainty assessment

In assessing the impacts of climate change on water resources, there are a lot of models and transformations in different processes. Such as the downscaling from a global model to a regional model or an output from a grid data to a weather station exits uncertainty. The uncertainty of downscaling in selecting of grids, the estimation of different periods in future, different scenarios, different GCMs, different distribution of daily precipitation and observed precipitation are all involved in this study. The effects of these uncertainties are shown from the change of streamflow and the cases in evaluation are sh wn as Fig. 4. The variation of change ration of streamflow is applied to represent uncertainty of combinations of various variables.

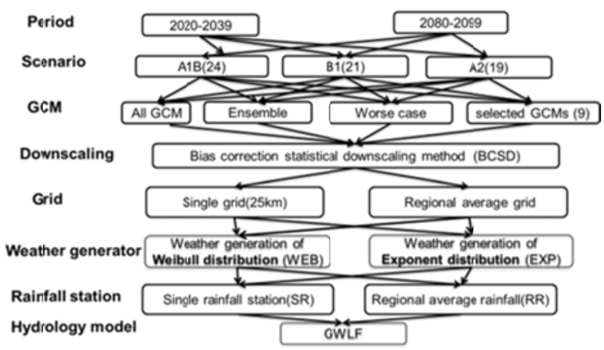

Fig. 4 The combinations of various variables in uncertainty process.

Results and discussion

Impacts of streamflow in wet and dry spell

The impacts of streamflow were simulated from three kinds of the CO2 emission scenarios and all GCMs. Fig. 5 and Fig. 6 show the Empirical cumulative distributed frequency (ECDF) of change ratio of streamflow in wet seasons and dry seasons during 2020~2023 years(near future, NF) in four basins. The variability is about -20%~+20% among all basins in a wet season, and there have no obvious different between the south basin and north basin. The results are shown that the change ratio of streamflow is from -40%~+40% in dry seasons. There is the less variability in the scenario of A2 emission. The larger change ratio of steamflow is estimated in KoPing Basin (Southern Taiwan) and the less change ratio is estimated in Dajia Basin (Central Taiwan). From the cumulative distributed frequency of streamflows, the results show the streamflow will increase in wet seasons about 60% probability and the maximum increase is about 20% in near future. In addition, the results also show the decrease in dry season about 80% probability and the maximum decrease is about 40%.

Variation of selected GCMs

Two methods to choose GCMs are used in this study. The results are compared with the results of all GCM. Fig. 7 showed the ECDF of change ratio of streamflow in dry seasons and the Box-and-whisker plot of streamflow change ratio in different months. Fig. 7 (a), Fig. 7 (b) and Fig. 7 (c) showed the ECDF of all GCM' results, the GCMs from choosing the properties of East Asia monsoon, and the GCMs from choosing the properties of precipitation in dry and wet seasons. The comparison between Fig. 7 (a) and Fig. 7 (b) is similar from range of ECDF. But the comparison between Fig.7 (a) and Fig. 7 (c), the range of ECDF is smaller and less variation for dry spell in in Fig. 7 (c). Fig.7 (e) ~ Fig. (g) are respective with the cases of Fig.7 (a) ~ Fig. 7(c), but they show the change ration of monthly stereamflow by Box-and-whisker plot. Four values are maximum, minimum, the first quartile and the th rd quartile in Box. The outliers are shown out of the Box. The most outliers are shown in Fig. 7(e). If the principle of choosing GCMs from the variations of the Box, the variations of Fig. 7(e) and Fig.7(f) are close and the less variation is shown in Fig.7(g). Therefore, the variation can be made smaller in GCMs' prediction by the choosing GCM from the properties of the dry and wet seasons.

Variation of two kinds of spatial resolution

Fig. 8 showed the change ratio of monthly streamflow in three kinds of scenarios (A1B, B1 and B1) and two resolution 25km^{2}X 25km^2 and 5km^{2}X 5km^2. The results showed that there is higher variation and more outliers in 5km^{2}X 5km^2, especially in May to October and the streamflow among GCMs are also insignificant differences. The results in February showed high variation of simulation in both resolutions.

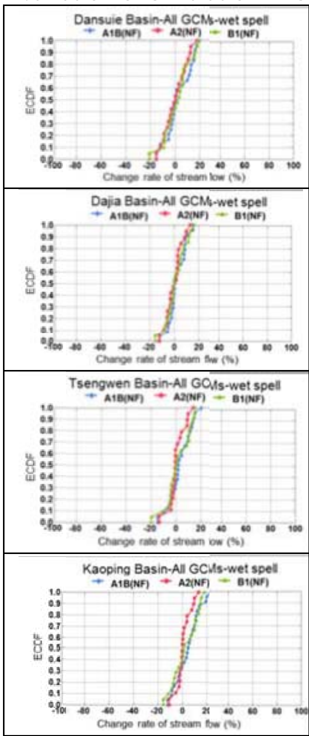

Fig. 5 Cumulative distribution function of streamflow change ratio in wet spell in near future

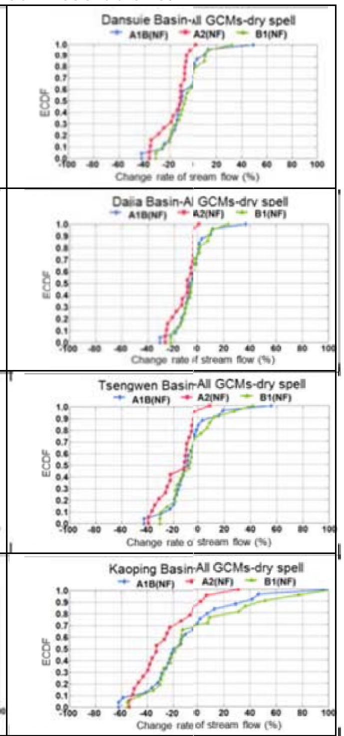

Fig. 6 Cumulative distribution function of streamflow change ratio in dry spell in near future

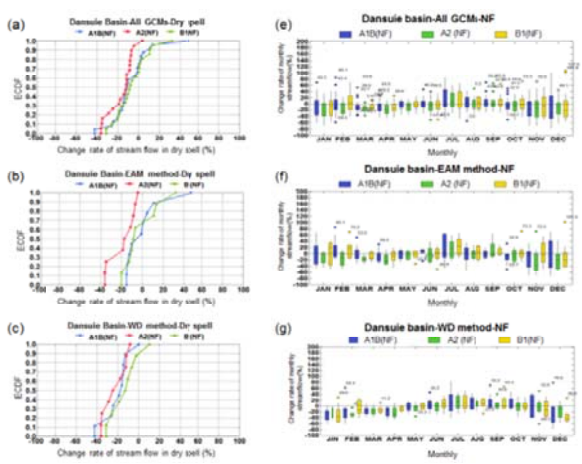

Fig. 7 Compare of change ration of streamflow in selection GCMs

The resolution 5km^{2}X 5km^2 will be not suggested, because of higher uncertainty exits in this resolution. The ECDF of change ratio of streamflow in the Kaoping Basin is shown in Fig. 8. The variations of both resolutions are small in a wet season, but the variation is higher in dry season in the resolution of 5km^{2}X 5km^2. The range of ECDF, from maximum to minimum, is large in the resolution of 5km^{2}X 5km^2. Most of GCMs showed the decrease of streamflow in future. So in the impacts of climate change on water resources, the uncertainty of resolution in assessm nt the different in wet and dry seasons is not sensitive. The results showed more streamflow in a wet season and less streamflow in a dry season. Only when a dry season in the resolution of 5km^{2}X 5km^2, the variation increase.

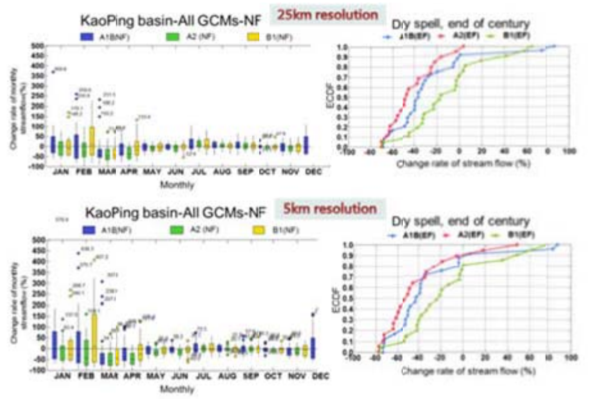

Fig. 8 The variation of change ratio of streamflow in different spatial resolution

Variation of selected girds and rainfall stations

Fig. 9 showed the uncertainty from different grid data and different observed weather stations. In the case of B1 emission scenario, the change ratio of streamflow in different seasons (dry and wet) is similar among four cases in all GCMs’ output. The four cases are NRS (near future regional average grid single rainfall station), NRR (near future regional average grid_ regional average rainfall), NSS (near future single grid single rainfall station), and NSR (near future_ single grid _regional average rainfall). The results showed the uncertainties of choosing a single weather station or regional average rainfall and single grid or regional average grid are small and did not affect the CDF of the change of streamflow.

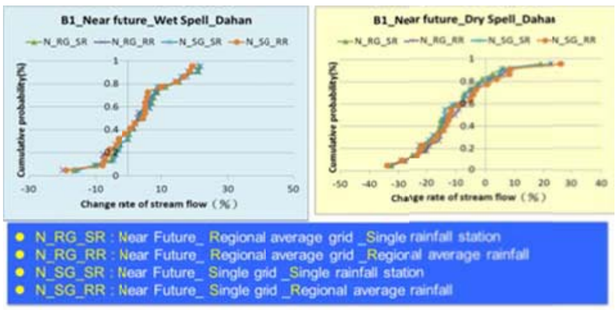

Fig. 9 ECDF of selected different girds and rainfall stations

Uncertainty of weather generator of different distribution

The uncertainty of different precipitation distribution in WG, the results are shown in Fig. 10. Both of Webuil and Exponent distribution in precipitation can fit the historical characteristics. But there is higher precipitation variation s in Webuil distribution, especially in June to August; the Exponent distribution is suggested to apply in assessment of water resource impacts.

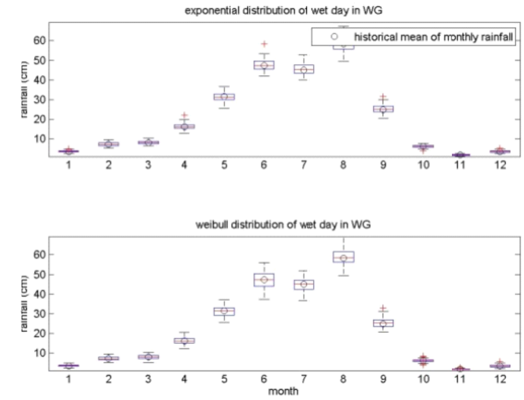

Fig. 10 The variation of using different precipitation distribution in WG

Comparison between natural variability and GCMs uncertainty

Comparing natural variations and scenarios in different GCMs, the Boot-strapping method is used to identify the natural variations. The results are shown in Fig. 11 and the natural variation is shown as Box-and-whisker plot. The precipitation variations of GCMs’ output are larger than the natural variation, especially in winter in the near future. At the end of this century, the increase of precipitation in wet seasons and the decrease in dry seasons are as predicted before.

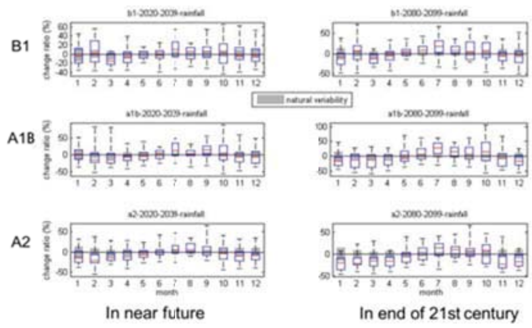

Fig. 11 The uncertain of change ratio of rainfall between natural variability and GCMs in different climate change scenario.

Summary and conclusion

Analyzing of all emission scenarios of all GCM, about 60% probability showed a 20% increase of streamflow in wet seasons and about 80% probability showed a 40% decrease of streamflow in dry seasons. The uncertainty of resolution of GCMs’ output is small when only comparing the dry/wet seasonal streamflow. The trends are all the same. So it is suggested that the resolution of 25km2X 25km2 can be taken in analysis in future for comparing the the dry/wet seasonal streamflow.

The comparison of two methods in selecting suitable GCMs, the streamflow in wet seasons has less uncertainty while 9 GCMs' outputs of are used based on characteristic of rainfall change rate in wet and dry spell. On the contrary, the streamflow in dry seasons has much uncertainty. Considering regional average of precipitation and regional average of grid data have less uncertainty than considering single weather station or single grid data.

Based on the analysis, the uncertainty from different GCMs' output is highest and choosing GCMs can reduce the uncertainty and variation. Downscaling of different resolution and choosing single/regional precipitation affect insignificantly in streamflow. There are more impacts challenges on water resources in the south of Taiwan under climate change.

The AR5 has been released by IPCC and different emission scenarios can be used to analysis the impact on water resources in future. The results of AR5 will be discussed and compared with that in this study.

References

Chen, J., Brissette, F. B., Leconte, R., 2011. Uncertainty of downscaling method in quantifying the impact of climate change on hydrology. Journal of Hydrology, 401: 190-202.

Cheng-Ta Chen, Chu, Jung-Lien, Huang-Hsiung Hsu, Mong-Ming Lu, Chung-Hsiung Sui, Chia Chou, Shu-Ping Weng, Jau-Ming Chen, Chuan-Yao Lin, Chao-Tzuen Cheng, Yi-Chao Wu, Yin-Min Cho, Jonq-Gong Chen, Ya-Ju Chang, Shi-Yao Lin, Shiou-Li Lin, Yu-Shiang Tung, Cheng-Dao Yang, 2014, Projection of climate change over Taiwan using statistical downscaling scheme, Atmospheric Sciences, 42.(In Chinese)

Haith, D.A. , and L.L. Shoemaker, 1987. Generalized Watershed Loading Functions for Stream Flow Nutrients. Water Resources Bulletin, 23(3), pp. 471-478.

Hong,Nien-ming, 1995. The Impacts of Climate Change on the Management of Water Resources in the Ta-An River. National Taiwan University, Master's Thesis (In Chinese).

Loukas, A., L. Vasiliades, and N.R. Dalezios (2002). Potential climate change impacts on flood producing mechanisms in Southern British Columbia, Canada using the CGCMa1 simulation results. Journal of Hydrology, Vol. 259(1-4), 163-188.

Prudhomme, C. , and Davies, H., 2009. Assessing uncertainties in climate change impact analyses on the river flow regimes in the UK.Part 1: baseline climate. Climatic Change, 93: 177-195.

Richardson, C.W. , and Wright, D.A., 1984. WGEN: A model for generating daily weather variables. US Department of Agriculture, Agricultural Research Service, ARS-8, USDA, Washington, DC.

Tung, C. P. , and Haith, D. A. 1995. Global Warming Effects on New York Streamflows Journal of Water Resources Planning and Management 121(2): 216-225. SCI.

Tung, C. P. and Li, M. H.,2005. The Climate Change Impacts on Hydrology and Water Resources Management and Adaptation Strategies, National Science council project (in Chinese)

Tung, Ching-Pin, 2007. Climate Change and Environmental Ecology lecture, National Taiwan University.

Wilby, R. L., and Harris, I., 2006. A framework for assessing uncertainties in climate change impacts: Low-flow scenarios for the River Thames, UK.Water Resources Research, 42, W02419.

Application of a Land Surface Model for Bias Correction of Runoff Generation Data from MRI-AGCM3.2S Dataset

DUONG Duc Toan [1, a *], TACHIKAWA Yasuto[1,b] and YOROZU Kazuaki[1,c]

Abstract In climate change researches, general circulation models or global climate models (GCMs) have been the most promising tools to project future changes and associated impacts in the hydrological cycle. However, there are biases in GCM outputs due to the coarse spatial resolution, simplified physics processes, numerical schemes, etc. Those biases should be corrected before using GCM data in climate change impact studies.

In this study, runoff generation data from the MRI-AGCM3.2S dataset were fed into distributed flow routing model 1K-FRM to project river discharge under a changing climate. Flow routing model 1K-FRM was developed in the Hydrology and Water Resources Research Laboratory, Kyoto University. The MRI-AGCM3.2S is the latest version of super-high-resolution atmospheric general circulation model which was jointly developed by Japan Meteorological Agency (JMA) and Meteorological Research Institute (MRI). Two river basins located in Kyushu (Japan) were selected as study areas, the Chikugo river basin and the Oyodo river basin.

Since the observed runoff generation data is not available, the land surface model Simple Biosphere including Urban Canopy (SiBUC) was applied to reproduce runoff generation data to use in bias correction of the MRI-AGCM3.2S's output. SiBUC model was developed in the Disaster Prevention Research Insitute, Kyoto University. Corrected runoff generation data were used to project river discharge and examine the changes in river discharge in those two basins under a changing climate.

Keywords
Land surface model, SiBUC, flow routing model, 1K-FRM, bias correction, MRI-AGCM3.2S

[1]Graduate School of Engineering, Kyoto University, Kyoto, Japan
[a]duong@hywr.kuciv.kyoto-u.ac.jp
[b]tachikawa@hywr.kuciv.kyoto-u.ac.jp
[c]yorozu@hywr.kuciv.kyoto-u.ac.jp

Introduction

Climate change is now widely accepted as a scientific fact. It is projected to have significant impacts on hydrology and water resources. The most common approach to assess the hydrological impacts of global climate change is to force hydrological models (HMs) or land surface models (LSMs) with output from general circulation models (GCMs). Therefore, the quality of hydrological impact investigations largely depends on the accuracy of GCMs in simulating climate data (Hagemann et al., 2011).

Although there are considerable improvements in the performance of GCMs in recent years, outputs of GCMs still suffer from systematic errors, or biases, which can be due to incomplete knowledge of climate system processes, numerical schemes, parameterizations of small scale (sub-grid scale) processes, and coarse spatial resolution.

Removing these biases in GCM outputs is therefore essential for improving the reliability of climate projections and hydrological simulations forced by climate model data. Several bias correction methods have been developed and received much attention in climate change impacts studies (e.g. Themeßl et al., 2011; Hagemann et al., 2011; Teutschbein and Seibert, 2012).

In this work, river discharge in two river basins in Kyushu area (Japan), Chikugo River basin and Oyodo River basin, were projected by feeding the MRI-AGCM3.2S runoff generation data into flow routing model 1K-FRM. To improve the projection of river discharge using 1K-FRM, bias correction is considered to apply to MRI-AGCM3.2S runoff generation data. Due to the unavailability of observed runoff generation data, an advanced land surface process model called Simple Biosphere including Urban Canopy (SiBUC; Tanaka, 2005) was applied to reproduce runoff generation data based on meteorological and phenological records. Output of SiBUC model was used as reference data for bias correction of MRI-AGCM3.2S runoff generation data. Biases in GCM runoff generation data were corrected using quantile-quantile mapping bias correction method (Leimer et al., 2011).

Projected river discharge in Chikugo River basin and Oyodo River basin from 1K-FRM using MRI-AGCM3.2S runoff generation data, SiBUC runoff generation data, and bias-corrected runoff generation data were compared to examine the performance of land surface process model and bias correction method in river discharge projection.

Study area

The analysis in this study was performed for two river basins in Kyushu area, Japan – Chikugo River basin and Oyodo River basin. Fig. 1 shows the location of these two river basins.

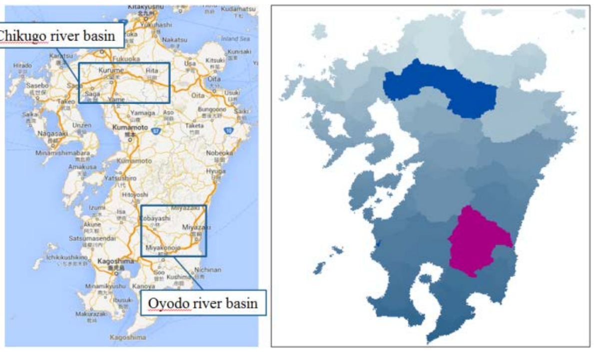

Fig. 1 Location of Chikugo River basin (blue) and Oyodo River basin (red) in Kyushu area, Japan

Chikugo River flows through Oita, Fukuoka, Kumamoto, and Saga prefectures in Kyushu area. With a total length of about 143 km, it is the longest river on Kyushu Island. The total basin area of Chikugo River is about 2,800 km^2.
Oyodo River runs through Kagoshima prefecture and Miyazaki prefectures with the basin area of about 2,230 km^2. The length of Oyodo River basin is about 107 km.

Flow routing model 1K-FRM

1K-FRM is a distributed flow routing model based on kinematic wave theory (Hunukumbura et al. 2012). It was developed by Hydrology and Water Resources Research Laboratory of Kyoto University. The kinematic wave model is applied to all slope units and runoff is routed according to the flow direction information. The basic form of the kinematic wave flow equation is:

$$\frac{\partial A}{\partial t}+\frac{\partial Q}{\partial x}=q_L(x,t) \qquad (1)$$

$$Q=\alpha A^m,\ \alpha=\frac{\sqrt{i_0}}{n}\left(\frac{1}{B}\right)^{m-1},\ m=\frac{5}{3} \qquad (2)$$

where, A(x, t) is the flow cross-sectional area, Q(x, t) is the flow discharge, $q_L(x, t)$ is the lateral inflow per unit length, i_0 is the slope, n is the Manning roughness coefficient, and B is the width of the flow.
Eq. (1) is the continuity equation. It is derived from the principle of mass conservation within a control volume. Eq. (2) is derived from Manning's laws which are flow resistance laws of open channel uniform flow.

Land surface model SiBUC

The land surface process model Simple Biosphere including Urban Canopy (SiBUC) was presented by Tanaka (2005) in Disaster Prevention Research Institute, Kyoto University. SiBUC model uses mosaic approach, which couples independently each land-use patch of the grid element to the atmosphere, to incorporate all kind of land-use to land surface scheme.
In SiBUC model, the surface of each grid cell is divided into three land-use categories including green area (vegetation canopy and ground), urban area (urban canopy and urban ground), and water body. Fig. 2 shows the schematic image of surface elements in SiBUC model.

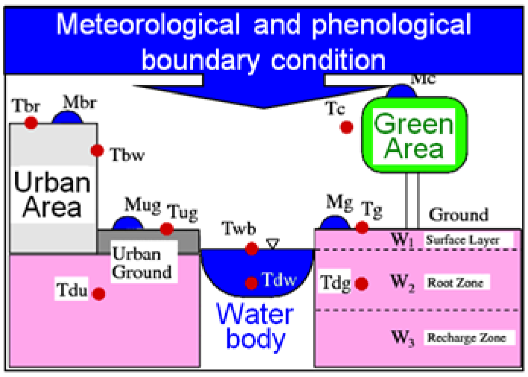

Fig. 2 Schematic image of SIBUC model

The fractions of these three land-use categories are fixed for each grid cell in SiBUC model. And surface fluxes are obtained by averaging the surface fluxes over each land-use weighted by its fractional area.

Data

Topographic data
The topographic data used in flow routing model 1K-FRM and land surface process model for two river basins in Kyushu area were the 30 arc-second (1-km) DEM and flow direction stored in HydroSHEDS (Lehner, 2006) for Asian regions. HydroSHEDS (Hydrological data and maps based on Shuttle Elevation Derivatives at multiple scales) provides hydrographic information for region and global-scale applications based on high-resolution elevation data obtained by NASA's Shuttle Radar Topography Mission.

GCM runoff generation data
GCM data used for flow routing model 1K-FRM is 3-hourly runoff generation data from super-high-resolution atmospheric general circulation model MRI-AGCM3.2S. It is the latest atmospheric GCMs based on a model jointly developed by the Japan Meteorological Agency (JMA) and the Meteorological Research Institute (MRI) (Mizuta et al., 2006). MRI-AGCM provides data for three climate experiments: present climate experiment (1979-2008), near future climate

experiment (2015-2044), and future climate experiment (2075-2104). The data used for future projection were based on the Special Report on Emissions Scenarios (SRES) A1B scenario.

Meteorological data

Meteorological data to force land surface process model SiBUC include seven components: precipitation, air temperature, specific humidity, surface pressure, wind speed, long wave radiation, and short wave radiation. In this study, the product of the Japanese 55-year reanalysis (JRA-55) project was utilized to use as inputs for SiBUC. However, JRA-55 precipitation and surface radiation data are forecast data, not reanalysis data. Therefore, other data sources were considered to use as substitution. For precipitation data, the Asian Precipitation - Highly-Resolved Observational Data Integration Towards Evaluation of Water Resources (APHRODITE's Water Resources) project was selected. And the Surface Radiation Budget (SRB) dataset was used to process long wave radiation and short wave radiation data.

The Japanese 55-year Reanalysis (JRA-55) is the second reanalysis project conducted by Japan Meteorological Agency (JMA) (Ebita et al., 2011). In this project, a sophisticated data assimilation system based on the operational system as of December 2009 and newly prepared dataset of past observations were used to produce a high-quality homogeneous climate dataset. The analysis period covers 50 years from 1958, when regular radiosonde observation began on a global basis. Table 1 and Table 2 summary information about JRA-55 meteorological data used for land surface process model SiBUC.

Table 1 Parameters of surface analysis fields

Field parameter	Unit	Level
Pressure	Pa	Ground or water surface
Temperature	K	2m
Specific humidity	kg kg-1	2m
u-component of wind	m s-1	10m
v-component of wind	m s-1	10m

Table 6.2 Parameters of two-dimensional average diagnostic fields

Field parameter	Unit	Level
Total precipitation	mm day-1	Ground or water surface
Downward solar radiation flux	W m-2	Ground or water surface
Downward long wave radiation flux	W m-2	Ground or water surface

The spatial resolution of JRA-55 data is 0.5625 degree. Parameters of surface analysis fields have 6-hour temporal resolution. And parameters of two-dimensional average diagnostic fields have 3-hour temporal resolution.

The Asian Precipitation - Highly-Resolved Observational Data Integration Towards Evaluation of Water Resources (APHRODITE's Water Resources) project was conducted by the Research Institute for Human and Nature (RIHN) and the Meteorological Research Institute of Japan Meteorological Agency (MRI/JMA) from 2006 to develop state-of-the-art daily precipitation datasets on high-resolution grids covering the whole of Asia (Yatagai et al., 2012). The datasets are created primarily with data obtained from a rain gauge observation network. The APHRODITE's Water Resources dataset is the only long-term continental-scale daily product that contains a dense network of daily rain-gauge data for Asia, especially Japan.

Precipitation data to force land surface process model for Kuyshu area was extracted from the APHRO_JP V1207 (Kamiguchi et al., 2010) dataset with spatial resolution of 0.05 degree. Temporal resolution of APHRO_JP precipitation data is daily.

Surface Radiation Budget (SRB) dataset is produced and archived by the NASA Langley Research Center Atmospheric Sciences Data Center (NASA/GEWEX). It is produced on a 1 degree x 1 degree global grid using satellite-derived cloud parameters and ozone fields, reanalysis meteorology, and a few other ancillary datasets. The SRB dataset contains 3-hourly long wave and short wave radiative fluxes.

Soil, vegetation, and land use data

Phenological boundary conditions related to soil type, vegetation type and land use data for Kyushu area in SiBUC model were collected from Ministry of Land, Infrastructure, Transport and Tourism (MLIT, Japan) field survey data and satellite databases such as ECOCLIMAP product and GLASS Leaf Area Index product.

Land use data for Kyushu area collected from MLIT consist of 16 categories including paddy, farmland, fruit farm, other farm, forest, waste land, building A, building B, road, other land, lake, river A, river B, beach, and unknown. Surface parameters related to land use for green area, urban area, and water body in SiBUC model was set based on this category. The spatial resolution of MLIT land use data is 100 m.

Parameters for vegetation type were derived from the GLASS Leaf Area Index (LAI) product, which generated by the Center for Global Change Data Processing and Analysis of Beijing Normal University (Xiao et al., 2013). The GLASS product is available from 1982 to 2012 with temporal resolution of 8 days and spatial resolution of 0.05 degree.

Soil parameters in SiBUC model such as root depth, soil depth, soil texture class, etc. were set baed on ECOCLIMAP product (Masson et al., 2003). ECOCLIMAP is a database of surface parameters at 1-km resolution which was implemented in the METEO-FRANCE operation models.

Resolution and simulation period of SiBUC model
The output data grid of SiBUC was set in the same coordinate, spatial resolution as MRI-AGCM3.2S runoff generation data. Input data with finer spatial resolution such as soil and vegetation were aggregated to create 20-km spatial resolution data. For coarser spatial resolution data, value of the nearest grid was selected in calculation.
SiBUC model was set to simulate runoff in Kyushu area for 1982-2010 period based on the availability of input data.

Bias correction of GCM runoff generation data

To correct biases in GCM runoff generation data, quantile-quantile mapping (QQM) bias correction method was selected. QQM was first introduced by Brier and Panofsky (1968) as empirical transformation. Methods based on quantile mapping are getting more popular and widely used to correct climate model outputs (e.g. Leimer et al., 2011; Vidal and Wade, 2008). Themeßl et al. (2011) and Teutschbein and Seibert (2012) compared various bias correction methods and showed that QQM performs better than others.
In QQM bias correction method, GCM output and observations are sorted for the same historical base period to construct cumulative distribution functions (CDFs). These CDFs is used to define the quantiles of simulated values and observations. Then, GCM simulated values is substituted with those of the identical quantile from the observational dataset. Fig. 3 shows the schematic representation of quantile-quantile mapping.

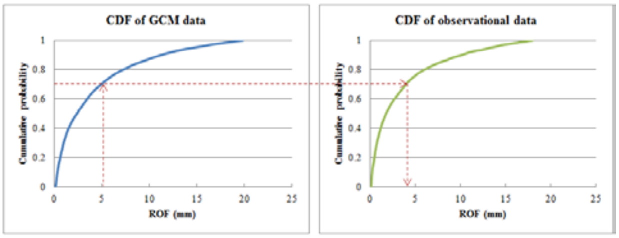

Fig. 3 Schematic representation of quantile-quantile mapping

In this study, runoff data simulated by SiBUC model were used as reference data to correct MRI-AGCM3.2S runoff generation data. Bias correction was applied to MRI-AGCM3.2S runoff generation data at each grid cell as follows:
Runoff generation data from MRI-AGCM3.2S dataset and SiBUC model at the same grid and in the same calendar month for the whole simulation period were sorted from smallest to largest to construct cumulative distribution functions.
Runoff generation data from MRI-AGCM3.2S dataset at each quantile was corrected by SiBUC runoff data at the equivalent quantile.
MRI-AGCM3.2S corrected runoff generation data were rearranged following the original time order.

Results and discussions

Reproduction of runoff generation data using SiBUC
Two simulations for Kyushu area were carried out using SiBUC model with different precipitation data sources, JRA-55 and APHRO_JP. Fig. 4 shows the annual mean runoff in Kyushu area simulated by SiBUC model. Simulation using APHRO_JP precipitation data shows a higher value of annual mean runoff compared to the one using JRA-55 precipitation data.

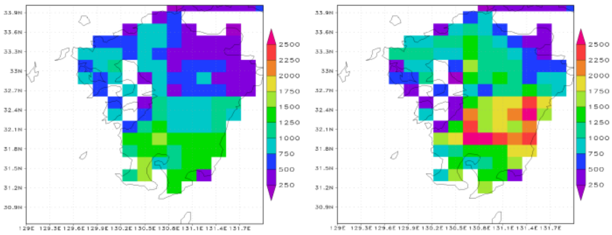

Fig. 4 Annual mean runoff in Kyushu area simulated using JRA-55 (left) and APHRO_JP precipitation data (right) from 1982-2008 (unit: mm/year)

To examine the reproduction of runoff generation data using land surface process model, river discharge in Kyushu area were simulated using runoff generation data given by SiBUC model. The runoff data simulated by SiBUC model using JRA-55 and APHRO_JP precipitation data hereinafter referred to as JRA-55 runoff data and APHRO_JP runoff data.
Flow duration curves for Oyodo River at Takaoka station and for Chikugo River at Senoshita station were constructed using the total-period method and the calendar-year method to compare simulated discharge with observations. Observational data at two stations mentioned above are available for 20 years period, from 1982 to 2001.
Fig. 5 and Fig. 6 show the total period and calendar-year flow duration curves for daily flow at Takaoka station, Oyodo River. Flow duration curves for Chikugo River at Senoshita are illustrated in Fig. 7 and Fig. 8 respectively.

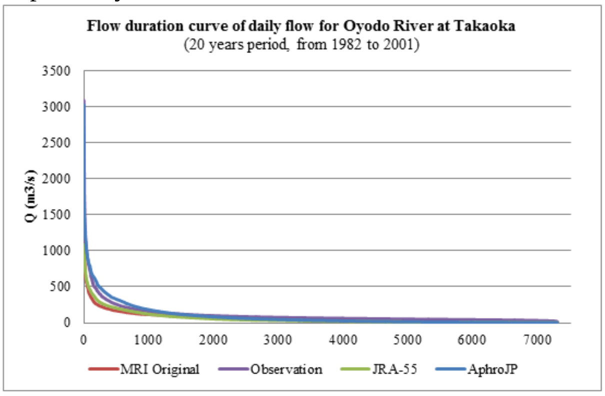

Fig. 5 Total period flow duration curve of daily flow for Oyodo Rirver at Takaoka

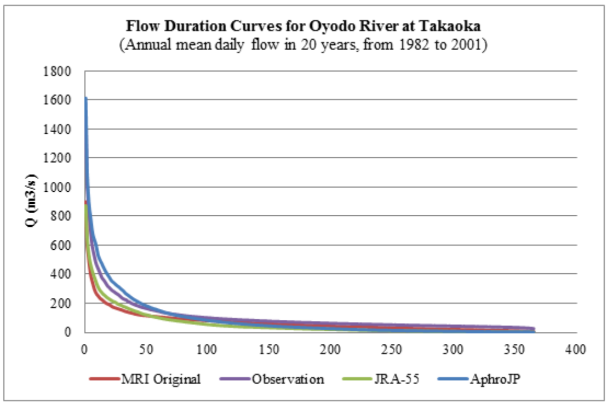

Fig. 6 Calendar-year flow duration curve of daily flow for Oyodo Rirver at Takaoka

As can be seen in Fig. 5, the flow duration curve from simulation using APHRO_JP runoff data was more close to observed data at Takaoka station, Oyodo River basin. River discharges simulated using original MRI runoff generation data and JRA-55 runoff data are lower than the observations. The calendar-year flow duration curves show the same pattern as the total-period flow duration curves (Fig. 6).

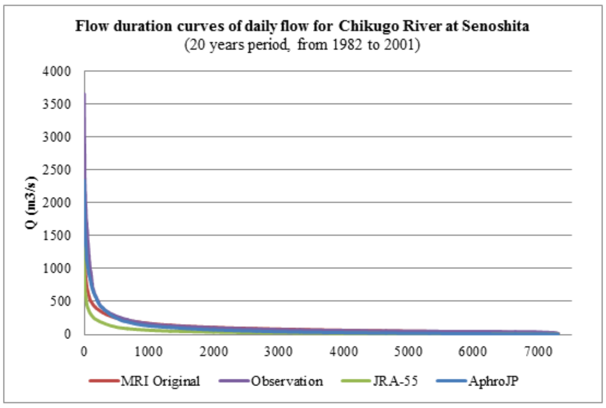

Fig 7 Total period flow duration curve of daily flow for Chikugo Rirver at Senoshita

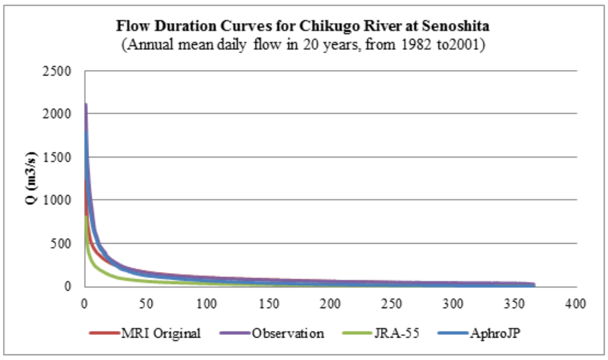

Fig. 8 Calendar-year flow duration curve of daily flow for Chikugo Rirver at Senoshita

At Senoshita station, Chikugo River basin, although all the simulation showed an underestimation of the simulated river discharges from the observation, the simulation using APHRO_JP runoff data still performs better than others (see Fig. 7 and Fig. 8). Therefore, in bias correction part, APHRO_JP runoff data were chosen as reference data to correct biases in MRI-AGCM3.2S runoff generation data.

Bias correction of runoff generation data

Biases in MRI-AGCM3.2S runoff generation data were corrected with APHRO_JP runoff data using quantile-quantile mapping method. Corrected MRI-AGCM3.2S runoff generation data were fed into flow routing model 1K-FRM to examine the effect of bias correction of runoff generation data on river discharge simulation.

Fig. 9 shows an example of the time series of MRI-AGCM3.2S runoff generation data, APHRO_JP runoff data, and corrected runoff generation data for 20 years period (1982-2001) at one grid upstream of Takaoka station, Oyodo River basin.

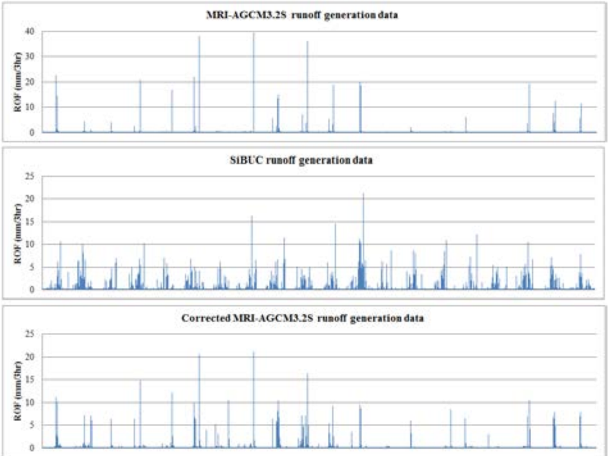

Fig. 9 An example of time series of runoff generation data for 20 years period (1982-2001)

It can be seen that, after bias correction, the temporal distribution pattern of corrected runoff generation data is similar to that of original MRI-AGCM3.2S data. However, comparing to reference data, the number of events with high runoff depth in the corrected runoff generation data is smaller but the density of high runoff depth in each event is higher. It may result in less flood events but higher peak discharge values.

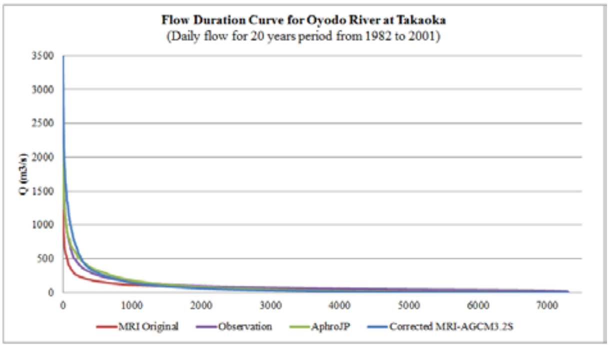

Fig. 10 Total period flow duration curve of daily flow for Oyodo Rirver at Takaoka

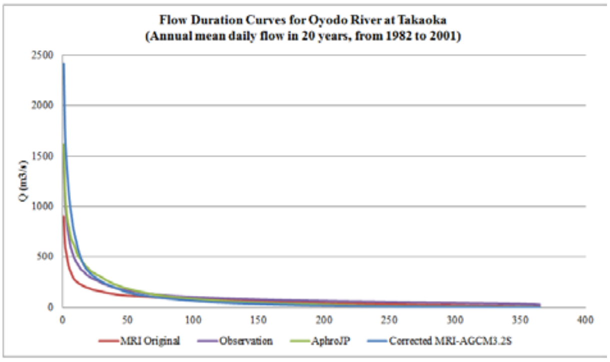

Fig. 11 Calendar-year flow duration curve of daily flow for Oyodo Rirver at Takaoka

Flow duration curves for river discharge simulated using corrected runoff generation data at Takaoka station, Oyodo River basin, are illustrated in Fig. 10 and Fig. 11. River discharge simulated using bias-corrected runoff generation data show an improvement comparing to original MRI-AGCM3.2S data. However, the peak discharge values are overestimated in comparison with simulation using reference runoff generation data. It may arise from the differences in temporal distribution pattern between corrected runoff generation data and reference data as mentioned above.

Conclusions

In this study, runoff generation data in the Kyushu area were simulated using a land surface process model SiBUC with reanalysis data. It was used as reference data to correct biases in MRI-AGCM3.2S runoff generation data.

SiBUC model showed a good performance in reproducing runoff generation data for Kyushu area. If high quality observed data are available, land surface process model will be a useful tool to reproduce runoff for a long-term period.

Bias correction of MRI-AGCM3.2S runoff generation data were also performed and showed an improvement in river discharge simulations. However, further works need to be done in bias correction of runoff generation data considering their temporal distribution pattern. The spatial correlation between neigbour grid-cells are also needed to be examined.

References

Brier, W., Panofsky, H. (1968) Some applications of statistics to meteorology. Mineral Industries Extension Services, School of Mineral Industries, Pennsylvania State College

Ebita, A., S. Kobayashi, Y. Ota, M. Moriya, R. Kumabe, K. Onogi, Y. Harada, S. Yasui, K. Miyaoka, K. Takahashi, H. Kamahori, C. Kobayashi, H. Endo, M. Soma, Y. Oikawa, and T. Ishimizu (2011) The Japanese 55-year Reanalysis "JRA-55": an interim report, SOLA, 7, 149-152.

Hagemann, S., Chen, C., Haerter, J. O., Heinke, J., Gerten, D., and Piani, C. (2011) Impact of a statistical bias correction on the projected hydrological changes obtained from three GCMs and two hydrology models, J. Hydrometeorol., 12, 556–578.

Hunukumbura, P. B. & Tachikawa, Y. (2012) River discharge projection under climate change in the Chao Phraya river basin, Thailand, using the MRI-GCM3.1S dataset. Journal of the Meteorological Society of Japan 90A, 137 – 150.

Kamiguchi, K., O. Arakawa, A. Kitoh, A. Yatagai, A. Hamada and N. Yasutomi (2010) Development of APHRO_JP, the first Japanese high-resolution daily precipitation product for more than 100 years. Hydrological Research Letters, 4: 60-64.

Lehner, B., Verdin, K., Jarvis, A. (2006): HydroSHEDS Technical Documentation. World Wildlife Fund US, Washington, DC. Available at http://hydrosheds.cr.usgs.gov.

Leimer, S., Pohlert, T., Pfahl, S., and Wilcke, W. (2011) Towards a new generation of high-resolution meteorological input data for small-scale hydrologic modeling. Journal of Hydrology, 402 (3-4): 317-332.

Tanaka, K. (2005) Development of the new land surface scheme SiBUC commonly applicable to basin water management and numerical weather prediction model. Doctoral thesis, Kyoto University.

Themeßl, M. J., A. Gobiet, and A. Leuprecht (2011) Empiricalstatistical downscaling and error correction of daily precipitation from regional climate models. Int. J. Climatol., 31, 1530–1544.

Teutschbein, C. and Seibert, J. (2012) Bias correction of regional climate model simulations for hydrological climate-change impact studies: Review and evaluation of different methods, Journal of Hydrology, vol. 456–457, pages 12-29.

Masson, V., Champeaux, J.L, Chauvin, F., Meriguet, C., and Lacaze, R. (2003) A Global Database of Land Surface Parameters at 1-km Resolution in Meteorological and Climate Models. J. Climate, 16, 1261–1282.

Vidal, J. P. and Wade, S. (2008) A framework for developing high-resolution multi-model climate projections: 21st century scenarios for the UK. International Journal of Climatology, 28 (7): 843-858.

Xiao Z., S. Liang, J. Wang, et al. (2013) Use of General Regression Neural Networks for Generating the GLASS Leaf Area Index Product from Time Series MODIS Surface Reflectance. IEEE Transactions on Geoscience and Remote Sensing.

Yatagai, A., K. Kamiguchi, O. Arakawa, A. Hamada, N. Yasutomi and A. Kitoh (2012) APHRODITE: Constructing a Long-term Daily Gridded Precipitation Dataset for Asia based on a Dense Network of Rain Gauge, Bulletin of American Meteorological Society.

River Discharge Assessment under a Changing Climate in the Chao Phraya River, Thailand by using MRI-AGCM3.2S

Supattana WICHAKUL[1, a *], Yasuto TACHIKAWA[1, b], Michiharu SHIIBA[1, c] and Kazuaki YOROZU [1,d]

Abstract In recent years, General Circulation Model (GCM) has been widely used in climate change impact studies. It is an effective tool for well understanding of a change in climate behavior in a long term. Nowadays, more than twenty GCMs have been developed in many research institutes around the world. We selected the latest version of GCM developed by Meteorological Research Institute (MRI), Japan Meteorology Agency, MRI-AGCM3.2S. The model has a horizontal resolution of triangular truncation 959 (TL959), and the transform grid uses 1920 x 960 grid cells, corresponding to approximately a 20-km grid interval with 64 vertical layers (top at 0.01 hPa).We used a regional distributed hydrologic model based on the concept of the variable infiltration capacity to generate runoff intensity and a kinematic wave model including effects of dam operation and inundation to simulate river discharge. The C.2 gauging station at Nakhon Sawan was selected to monitor changes in the river discharge. Input data of the distributed hydrological model, GCM precipitation and evapotranspiration, were corrected to remove biases using the quantile-quantile bias-correction method for precipitation and the different factor bias-correction method for evapotranspiration. The results of the experiment in projecting discharge of the Chao Phraya River under the near future climate (2015-2043) and the future climate (2075-2103) by using the bias-corrected GCM data set showed that 1) the mean annual discharge tends to increase in both near future and future projection periods, 2) During a dry season the tendency of low flow in the near future period tends to decrease. However, the flood frequency analysis using Generalized Extreme Value distribution (GEV) indicates that flood risk in the future will have more severities and damages to the country as the result of the analysis shows that, in the near future the magnitude of 80-year return period flood is greater than the devastating 2011 Thai flood. .

Keywords *Climate change, Discharge projection, Chao Phraya River, Distributed hydrological model*

S. Wichakul (supattana.w@gmail.com)
Research assistant at department of civil and earth resources engineering, Kyoto University, Japan

Y. TACHIKAWA
Professor
Department of civil and earth resources engineering, Kyoto University, Japan
tachikawa@hywr.kuciv.kyoto-u.ac.jp

M. SHIIBA
Professor
Department of civil and earth resources engineering, Kyoto University, Japan
shiiba@hywr.kuciv.kyoto-u.ac.jp

K. YOROZU
Assistant professor
Department of civil and earth resources engineering, Kyoto University, Japan
yorozu@hywr.kuciv.kyoto-u.ac.jp

Introduction

Prediction of the Chao Phraya River discharge has been conducted for water resources assessment of the basin by utilizing outputs of the MRI-AGCM3.2S (20 km resolution) without bias correction. The result showed that water availabilities in the CPRB increase all year round, both in the wet and dry seasons in the future climate experiment, and during dry season of the near future climate trends of projected discharge considerably reduced (Wichakul et al., 2014). However, direct usage of hydrological variables of the GCM does not provide reliable information on scales below about 200 km (Maraun et al., 2010). Therefore, for reliable and realistic prediction result of the river discharge situation of the Chao Phraya River, we introduced several bias correction methods to the MRI-AGCM3.2S outputs, precipitation and evapotranspiration. Bias in the GCM precipitation distribution was removed by the empirical distribution and quantile-quantile correction methods. For the GCM evapotranspiration, the multiplicative factor and different factor correction methods were applied.

The research aims to project discharge of the Chao Phraya River and to evaluate tendency of flood and drought risks under a changing climate by using the bias-corrected GCM precipitation for a reliable result.

Input data and study area

We used the MRI-AGCM3.2 variables from three (3) different climate experiments: are the present climate experiment (1979–2008), the near future climate experiment (2015–2044), and the future climate experiment (2075–2104). The GCM precipitation is rainfall reaching to soil layer (PRCSL) and the GCM evapotranspiration is a summation of evaporation from bare soil (EVPSL) and transpiration from root zone soil (TRNSL). The GCM variables covering the CPRB were extracted total 1,120 grids resolution 0.1875 (Cols=28 and Rows=40), which is defined as being between Latitude = 12.094 - 19.406 N and Longitude = 98.060 – 103.123 E.

To prepare the input data for the distributed hydrological model, the GCM variables were processed to remove biases by quantile-quantile bias-correction method for precipitation and the different factor bias-correction method for evapotranspiration. In the bias correction process, APHRODITE precipitation and the reference evapotranspiration (ETo) were used to simulate the reference as observed discharge. In our study, we obtained a reference crop evapotranspiration (ETc) calculated by the Royal Irrigation Department of Thailand (RID) using the FAO Penman-Monteith method (Allen et al., 1998) with recorded climatology data for the 30 years from 1981 to 2010 to be the truth reference data. Due to limitation of APHRODITE data which were available for 1979-2007, the bias correction was piloted for only a period of 29 years. Therefore our hydrological simulation was simulated for 1979-2007, 2015-2043, and 2075-2103 periods.

Study area is the Chao Phraya River basin, Thailand. The discharge monitoring is at C.2 located about 5 km downstream of the Ping River and Nan River confluence, beginning of the Chao Phraya River (15°40′N and 100°06′E). The location of the C.2 station can represent the overall situation of the Chao Phraya River.

Modeling approach

The regional distributed hydrological model composes of rainfall-runoff model and flow routing model including dam operation. The rainfall-runoff named the Simplified Xinanjiang model (SXAJ). It was established based on the concept of the variable infiltration capacity (Wichakul et al., 2013a). 1K-FRM is a 1 kilometer resolution flow routing using a kinematic wave equation. In part of flow routing, the 1K-FRM was additionally developed to include the inundation effect and reservoir operation model to improve predicted discharge for the Chao Phraya River Basin. (Wichakul et al., 2013b). **Fig. 1** shows the framework of model simulation.

The bias-corrected precipitation and evapotranspiration were input to the SXAJ model to generate runoff intensity represented 1120 (28 columns and 40 rows) grid cells covering the CPRB. Then, the runoff intensity was input to the 1K-FRM represented by 288,000 (480 columns and 600 rows) computational grid. The predicted discharge was extracted at the C.2 grid.

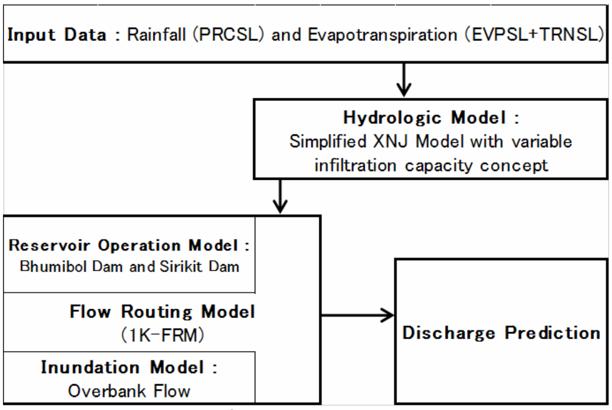

Fig. 1 Framework of the distributed hydrological model including inundation model by using the GCM output.

Result and discussion

River discharge assessment under a changing climate

By using the bias corrected precipitation and evapotranspiration as input to the regional distributed hydrological model, we generated series of daily discharge for twenty night (29) year in each climate experiment period. Mean monthly discharge at the monitoring station, C.2 station, has been calculated to detect trend of stream flow change under a changing climate as plotted in **Fig. 2**. It shows mean monthly discharge at for three climate experiments. For the future climate, comparison of the discharge of the present climate (1979-2007) and the future climate (2075-2103) shows significant increases about 10% to 41% of the mean monthly discharge in the present climate. For the near future, most of the months the mean monthly discharge shows a bit increase about 10% to 25% of the mean monthly discharge in the present climate. On the other hand, the discharge of the near future climate extremely rises up in October at the same rate of increase as the next three decades. Only in May, the mean discharge does not much change. According of the Thailand climatology, May is the end of summer season and beginning of rainy season. That is why effect of changes of temperature (or evapotranspiration) and rainfall intensity have less effect to the mean discharge in this month.
One of important tools to characterize the response of the river to a changing climate is flow duration curve. The

probability of exceedance (P) of mean annual flow magnitude of each climate experiment periods are illustrated in flow duration curves. **Fig. 3** presents mean annual flow duration curves with standard deviations for the three climate experiments. It clearly shows that the magnitudes of river flow considerably rise up for $P < 0.6$ in both the near future and future climate experiments. The magnitude of river discharge in the future period has a tendency to increase for all occurrence time.

For $P > 0.6$, there is no a significant signal of changes in mean annual flow for the near future and future period. According to the dam operation model embedded in the flow routing model for generating stream flow, discharge during low flow season was influenced by the dam model (Wichakul et al., 2011). It means that future inflow into dams dose not much change, so the dam operation model still operates and releases flow from storage water to downstream as operating in the current climate. However, to enlarge the low flow section, **Fig. 4** compares the flow duration curves constructed based on daily discharge of a period-of-record of each climate experiment at the low flow section. Therefore, it is clear that the low flow values tend to decrease in the near future experiment which might result in increased drought risk in the CPRB. Conversely, for the 21st century the low flow values tend to increase roughly 15 % of the flow in the present climate period. For the flood risk assessment, the frequency analysis of the extreme events is generally applied to evaluate to risk that we discuss in the next paragraph.

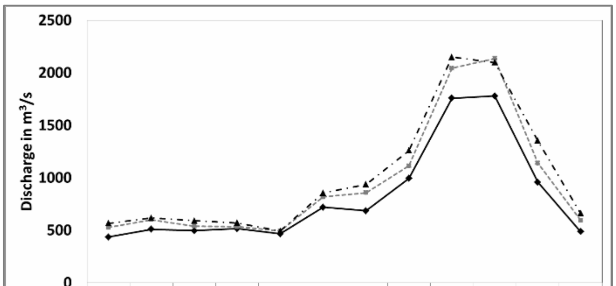

	Jan	Feb	Mar	Apr	May	Jun	Jul	Aug	Sep	Oct	Nov	Dec
SPA	435	509	497	515	466	720	686	993	1,757	1,778	957	487
SNA	526	601	540	533	491	818	856	1,112	2,043	2,136	1,140	594
SFA	566	617	591	570	493	855	936	1,259	2,149	2,099	1,353	661

Fig. 2 Mean monthly discharge at the C.2 station for the present (SPA), near future (SNA) and future climate experiments (SFA).

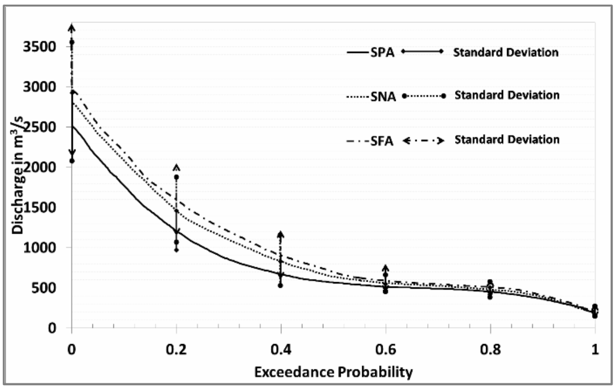

Fig. 3 Mean annual flow duration curves with standard deviation of the present climate (SPA), near future climate (SNA), and future climate (SFA) experiments.

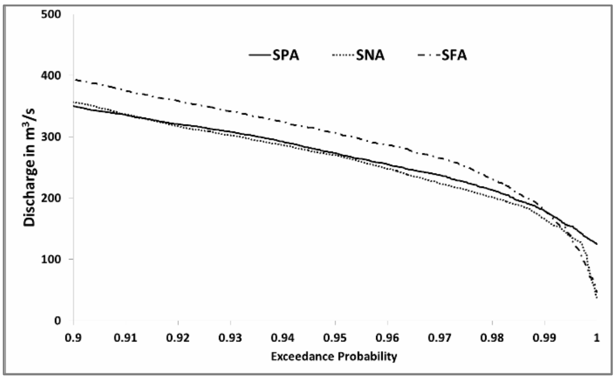

Fig. 4 Low flow section of the flow duration curves constructed based on daily discharge of a period-of-record of each climate experiment.

Frequency analysis of extreme events

Frequency of occurrence of the extreme events was analyzed by fitting the probability distribution function (PDF) of extreme values with three families of distribution functions, Square-root exponential type maximum distribution (SqrtET), Generalized extreme value distribution (GEV), and Gumbel distribution. The following are the cumulative distribution functions (CDFs) of each distribution.

The Square-root exponential type maximum distribution's CDF is as:

$$F(x;\ \beta,\ \lambda) = \begin{cases} \exp\{-\lambda(1+\sqrt{\beta x})\exp(-\sqrt{\beta x})\} & x \geq 0, \\ 0 & x < 0. \end{cases} \qquad (1)$$

In which β is the scale parameter, and λ is the frequency parameter (Etoh et al., 1987). The generalized extreme-value (GEV) distribution has a cumulative distribution function with a parameter k ≠0 as:

$$F(x; \xi, a) = exp\left[-\left(1-k\frac{x-\xi}{a}\right)^{1/k}\right] \qquad (2)$$

where x is an annual maximum daily discharge; a is a positive scale parameter; c is a location parameter and k is a negative shape parameter. In case of k = 0, the GEV distribution is equivalent to the Extreme Value Type I distribution or the Gumbel distribution. The cumulative distribution function of Gumbel distribution is shown as:

$$F(x; a, c) = exp\left[-exp\left(-\frac{x-c}{a}\right)\right] \quad (3)$$

For the Gumbel distribution, x is unbounded (-∞<x< ∞) (Takara, 2009).

The annual maximum series of river flow at the C.2 station was extracted from three periods of simulation, to fit with the distribution function as mention above. **Fig. 5, 6,** and **7** illustrate the CDFs of twenty night (29) values of annual maximum river flow fit with different functions for SPA SNA, and SFA, respectively.

Standard least-squares criterion (SLSC) is a criterion we used to evaluate goodness of fit of each distribution to the annual maximum daily discharge. It was proposed by Takara and Takasao (1998). Afterward, Tanaka and Takara (1999) proved that SLSC < 0.04 is acceptable to river discharge frequency analysis in Japan. However, the Chao Phraya River Basin topographic condition is very different to river basins in Japan. Therefore, we evaluated the acceptable SCSC by the smallest value among each probability distribution function. **Table 1** shows comparison of the goodness-of-fit for the annual maximum daily discharge at the C.2, Y.16, N.67 and P.17 stations for present climate (1979-2008) near future climate (2015-2043) and future climate (2075-2013).

The Y.16 is located at 16°45'N and 100°07'E on the Yom river upstream of the N.67 station (15°52'N and 100°15'E). Other monitoring location is at 15°56'N and 99°58'E on the Ping River named P.17 station. From the **Table 1**, it shows that among these probability distribution functions, GEV distribution function provides the best goodness-of-fit to the annual daily maximum discharge of the projection periods for all locations. Therefore, we selected the GEV for evaluating change in extreme floods and assessing flood risk.

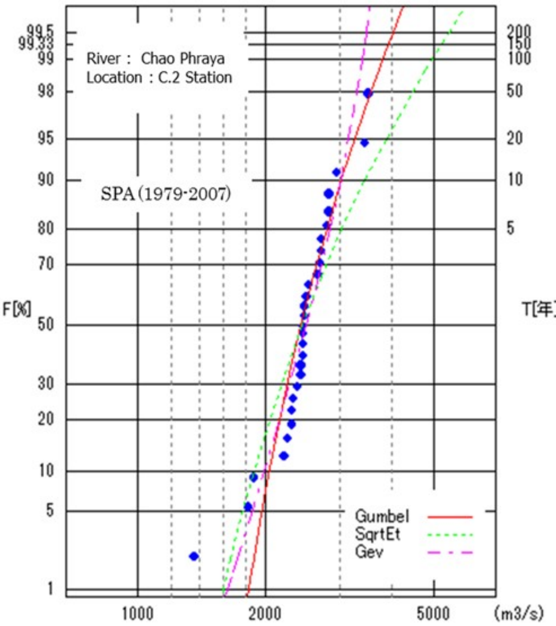

Fig. 5 Cumulative distribution functions of the annual maximum daily discharge at C.2 station for present climate.

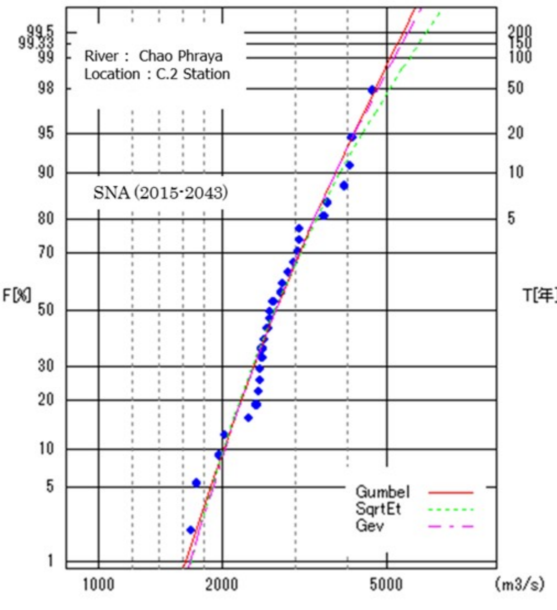

Fig. 6 Cumulative distribution functions of the annual maximum daily discharge at C.2 station for near future climate.

Table 1 Goodness-of-fit criteria for each probability distribution function. Standard Least Squares Criterion, SLSC

PDF	C.2			Y.16			N.67			P.17		
	SPA	SNA	SFA	SPA	SNA	SFA	SPA	SNA	SFA	SPA	SNA	SFA
Gumbel	0.071	0.036	0.043	0.035	0.056	0.058	0.047	0.031	0.054	0.036	0.087	0.120
SqrtEt	0.090	0.038	0.067	0.046	0.051	0.059	0.059	0.043	0.073	0.054	0.098	0.122
Gev	0.092	0.037	0.029	0.035	0.050	0.058	0.034	0.030	0.040	0.020	0.060	0.078

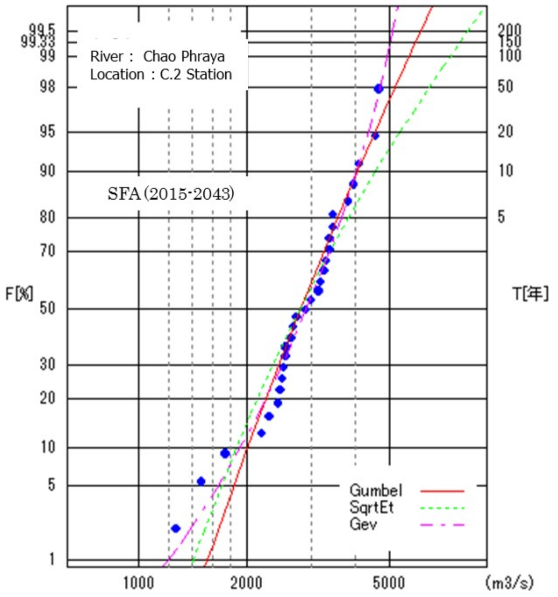

Fig. 7 Cumulative distribution functions of the annual maximum daily discharge at C.2 station for future climate.

Changes in return period of flood for different periods are illustrated in **Fig. 8** for four different locations; (a) for C.2 station, (b) for Y.16 station, (c) for N.67 station and (d) for P.17 station. The assessment has been conducted by comparing the return period of the 5-year, 10-year, 20-year, 30-year, 50-year, 80-year, 100-year, 150-year, and 200-year. The short return periods (shorter than 50-year return period) are relevant to flood related design structure according the impacts of climate change, such as irrigation structure, urban drainage and bridge. Refer to **Fig. 8a**, in 21st century the magnitude of extreme events at the C.2 station significantly increase for the return period shorter than 50-year and also it is larger than the magnitude of the flood events in the near future climate (2015-2143). For the long return periods (form 80-year return period), the magnitude of discharge is extremely high in the near future climate. That change in the C.2 station mostly corresponds to change in flood magnitude in the P.17 and N.67 stations for both near future and future periods, referring to **Fig. 8c** and **8d.**

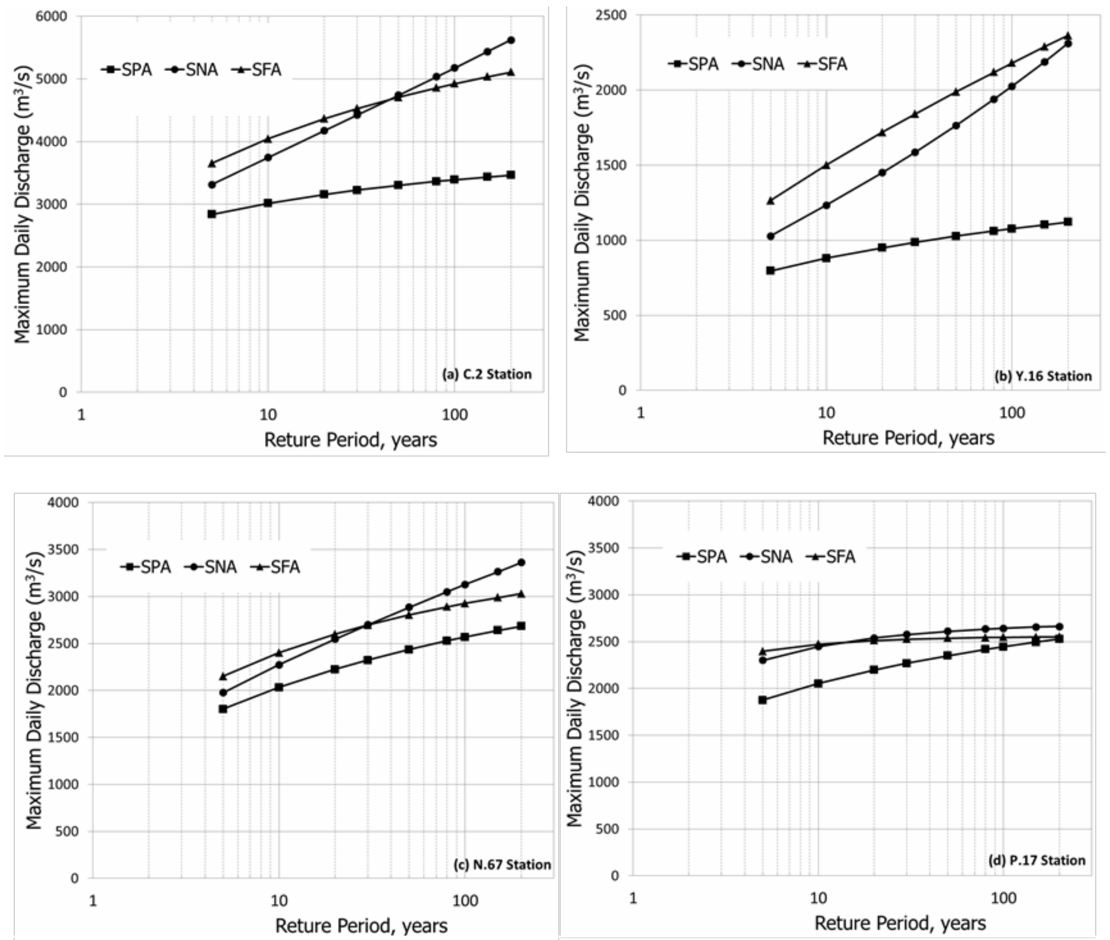

Fig. 8 Maximum daily discharge corresponding to different return periods for present climate (SPA), near future climate (SNA) and future climate (SFA) for each location.

Flood frequency analysis of the Y.16 station showed different pattern from other location as illustrated in **Fig. 8b** because location of the Y.16 station is far for the location of those another three stations. Flow from the Y.16 station merges with the Nan river at the confluence located upstream of the N.67 station.

The corresponding discharge of the C.2 station (5,034 m^3/s) at 80-year return period of the near future is larger than the peak discharge of Thai's flood 2011 (4,686 m^3/s). Consequently, overall trend shows the flood risk is increase in the future that will cause more damage to the CPRB.

Conclusion

Four sets of bias-corrected outputs of the MRI-AGCM3.2S, precipitation and evapotranspiration, were applied to the Chao Phraya River for projection river discharge in the present climate (1979–2007). The regional distributed hydrological model including the effect of dam operation and inundation simulated the river discharge. Simulated long term hydrographs from different sets of the input data were compared with the reference observed hydrograph. Result shows that the hydrograph simulated by using the bias-corrected precipitation by the quantile-quantile method with the bias-corrected evapotranspiration by the different factor achieved a well fit with the reference observed discharge at the C.2 station.

Consequently, the bias-corrected GCM data have been conducted for the near climate future and the future climate experiments. Changes in the projected river discharge at the C.2 station, Nakorn Sawan province can be concluded that 1) the mean annual discharge tends to increase in both near future and future projection periods, 2) during a dry season the tendency of low flow in the near future period leads to decrease. These findings of our study are also compatible with previous studies of Hunukumbura and Tachikawa (2012), and Kure and Tebakari (2012); but it is contradictory with the study result of Champthong et al., (2013). Furthermore, the GEV was applied for flood frequency analysis which indicates that flooding frequency has increased, leading high flood risk in the future. Flood in the basin will have more severity; especially in the near future (2015-2043) the magnitude of 80-year return period flood (5,034 m^3/s) is greater than the devastating 2013 Thai flood (4,686 m^3/s). Therefore, adaptation measures to protect damages of flood in the country are critical to accomplish.

References

Allen, R.G., Pereira, L.S., Raes, D., Smith, M., 1998. Crop evapotranspiration - Guidelines for computing crop water requirements. FAO Irrigation and drainage paper, 56, FAO, Rome. ISBN 92-5-104219-5.

Champathong, A., Komori, D., Kiguchi, M., Sukhapunnaphan, T., Oki, T., Nakaegawa, T. (2013). Future projection of mean river discharge climatology for the Chao Phraya River basin. Hydrological Research Letters. 7(2), 36–41, doi: 10.3178/HRL.7.36.

Etoh, T., Nurato, A., Nakanishi, M. (1987). SQRT-Exponential Type Distribution of Maximum, in: Singh, V. P. (Ed.), Hydrologic Frequency Modeling. Springer, Netherlands, pp. 253-264.

Hunukumbura, P. B., Tachikawa, Y. (2012). River Discharge Projection under Climate Change in the Chao Phraya River Basin, Journal of the Meteorological Society of Japan. 90(A), 137-150.

Kure, S., Tebakari, T. (2012). Hydrological impact of regional climate change in the Chao Phraya River Basin, Thailand. Hydrological Research Letters. 6, 53-58.

Maraun, D., Wetterhall, F., Ireson, A. M., Chandler, R. E., Kendon, E. J., Widmann, M., Brienen, S., Rust, H. W., Sauter, T., Themessl, M., Venema, V. K. C., Chun, K. P., Goodess,C. M., Jones, R. G., Onof, C., Vrac, M., and Thiele-Eich, I.: Precipitation downscaling under climate change: recent developments to bridge the gap between dynamical models and the end user, Rev. Geophys., 48, Rg3003, doi:10.1029/2009rg000314, 2010.

Takara, K. (2009). Frequency analysis of hydrological extreme events and how to consider climate change. Water Resources and Water-Related Disasters under Climate Change, -Prediction, Impact Assessment and Adaptation-, 19th UNESCO-IHP Training Course, Kyoto University.

Takara, K., Takasao, T. (1998). Criteria for evaluating probability distribution models in hydrologic frequency analysis. J. of Hydraulic Coast. Environ. Eng. 393II-9, 151–160.

Tanaka, S., Takara, K. (1999). Goodness-of-fit and stability assessment in flood frequency analysis. Annual J. Hydraulic Eng., JSCE. 43, 127-132. (in Japanese)

Wichakul, S., Tachikawa, Y., Shiiba, M., Yorozu, K. (2013a). Developing a regional distributed hydrological model for water resources assessment and it application to the Chao Phraya River Basin. J. Japan Society of Civil Eng. B1 (Hydraulic Eng.). 69(4), 43–48.

Wichakul, S., Tachikawa, Y., Shiiba, M., Yorozu, K. (2013b). Development of a flow routing model including inundation effect for the extreme flood in the Chao Phraya River Basin, Thailand 2011. J. Disaster Research. 8(3), 415–423.

Wichakul, S., Tachikawa, Y., Shiiba, M., Yorozu, K. (2014). Prediction of water resources in the Chao Phraya River Basin, Thailand. Proceeding from Hydrology in Hydrology in a Changing World: Environmental and Human Dimensions, 7th Global FRIEND-Water Conference (IAHS). Publ. 363. Montpellier, France. (151-157).

Designed Intensity-duration-frequency (IDF) curves under climate change condition in urban area

Ashish Shrestha [1, a *], Sutat Weesakul [1,b], Mukand Singh Babel [1,c] and Zoran Vojinovic [2,d]

Abstract Intensity-Duration-Frequency curves (IDF) are essential for design of storm drainage network especially in the urbanized area where surface runoff is high and localized flooding usually occurs. Climate change is expected to affect the rainfall pattern, prediction of future change in IDF is crucial and important for quantify this change of urban rainfall magnitude. This paper is based on a case study in a capital of Thailand, Bangkok. The objective of study is to develop IDF curves for future climate using stochastic weather generator LARS WG and rainfall disaggregation using HYETOS model which is based on Bartlett Lewis Rectangular Pulse process theory. Station data from Thai Meteorological Department (TMD) from 1980 to 2010 are used. Climate change impact study using Statistical Down Scaling Model (SDSM) and Long Ashton Research Station Weather Generator, (LARS WG) on future climate scenarios showed that LARS WG is more accurate in predicting extreme rainfalls and thus 15 GCMs results are analyzed under SRA1B and SRA2 scenarios for future time periods of 2011-2030 and 2046-2065. IDF curves for present and future cases are developed, using annual maximum series and Gumbel distribution, on sub-daily or hourly scale using observed, downscaled and disaggregated data. Statistical properties of maximum daily rainfall are preserved. IDF curves derived from disaggregated data showed underestimation especially in short rainfall durations less than 6 hours compared to IDF from observed station data. The graphical correction of IDF curves is derived from the existing IDF and the one computed from the present study. The correction equation is proposed using higher order equation which can be applied for variety of return period and all range of rainfall durations. This is improvement from the existing proposed linear correction from other study, which is limited applicable only for rainfall duration greater than 6 hours. The uncertainty band in intensities from different GCMs is found to be greater for higher return period. Further the results showed comparative increments in intensities while considering two particular GCMs of interest in SRA1B and SRA2 scenarios; and return periods of 2, 5 and 20 years. The same methods can be applied to other locations especially large cities to obtain designed IDFs under future climate scenarios.

Keywords *Urban Drainage, Intensity-Duration-Frequency Curves, Climate Change, future Climate. Climate*

Ashish Shrestha
Asian Institute of Technology (AIT)
Pathumthani, Thailand
ashish.shrs@gmail.com

Sutat Weesakul
Water Engineering and Management
Asian Institute of Technology (AIT)
Pathumthani, Thailand
sutat@ait.asia

Mukand Singh Babel
Water Engineering and Management
Asian Institute of Technology (AIT)
Pathumthani, Thailand
babel@ait.asia

Zoran Vojinovic
UNESCO-IHE Institute for Water Education, The Netherlands
z.vojinovic@unesco-ihe.org

Introduction

Several studies have concluded that future frequency, intensity, volume of the extreme precipitation will increase as the influence of global warming (Trenberth, 1999; Trenberth, 2011; Emori and Brown, 2005; Boo *et al.* 2006). There are several consequences of climate change on urban drainage including under capacity, surcharging and surface flooding. Therefore, it is essential to update IDF curves addressing future climatic condition (Mailhot and Duchesne, 2010; Guo, 2006). Intergovernmental Panel on Climate Change (IPCC) defined climate change as change in state of climate over time due to natural or human induced reasons and IPCC (2000), further categorized the scenarios of future climate based on carbon emission level. It can be summarized into four storyline A1, A2, B1 and B2 while A2 family is most extreme scenario in term of carbon emission. Downscaling using Global Circulation Models (GCMs) is most common in studying climate change implications. GCMs outputs are defined at 150-300 km which is coarser grid however, Regional Climate Model (RCM) resolution is up-to 12-50 km (Sunyer *et al.* 2012). There are basically two downscaling techniques: dynamic and statistical downscaling. Different downscaling techniques in practice are dynamical downscaling, statistical downscaling, regression based downscaling, weather typing procedure and stochastic weather generator (Wiley *et al.* 2002; Semenov and Barrow, 1997). The comparative study using Statistical Downscaling Model, SDSM (Wilby *et al.* 2002) and Long Ashton Research Station Weather Generator, LARS WG (Semenov and Stratonovitch, 2010) showed that LARS WG results showed better precipitation projection while SDSM results were better for temperature (Nyugen, 2005; Irwin *et al.* 2012). LARS WG incorporates predictions from 15 GCMs used in IPCC Assessment Report IV and climate predictions are available for the Special Report on Emissions Scenarios (SRES) - SRB1, SRA1B and SRA2 for most of the GCMs (Semenov and Stratonovitch, 2010). Liew S.C. *et al.* (2012), conducted the study for developing IDF curves for present and future, in the situation of data scarce condition by using dynamic downscaling using RCM, Weather Research and Forecasting (WRF) model. The linear adjustment of the IDF curve was studied to correct bias from the model results. The linear adjustments were possible when the duration was considered at higher scales for instance from 6 h to 24 h then curve will be of linear nature.

Intensity-Duration-Frequency (IDF) is the important design tool for urban drainage (Solaiman and Simonovic, 2011. However, most of the conventional IDF curves are postulated under stationary climate condition. One of the challenges in urban drainage modeling is requirement of IDF with very short duration owing to corresponding time of concentration of the catchment. The collection of continuous short duration climate variables information costs huge resources. Future projection of climate variables using climate downscaling techniques provide only output in daily scale. To generate IDF for future, such aggregate rainfall data requires disaggregation to fine scale. A methodology based on downscale-disaggregation-IDF generation is applied in the study as a possible approach for generating IDF for single site station in urban catchments under climate change condition.

Study area

Bangkok, the capital and commercial hub of Thailand, is one of the urbanized cities in Southeast Asia. Sukumvit Area, located at Eastern part of Bangkok is the case study area surrounded by major canals on eastern and northern part and Chao Phraya River on the Southern Part. The area is flat with average altitude of 1.5 m above mean sea level. The climate is tropical wet and dry with long hours of sunshine, fairly high temperatures year-round and high humidity. The rainy season are observed in mid-May with the arrival of the southwest monsoon. The average minimum temperature is approximately 20°C and high temperature is 35°C. Bangkok receives an average annual rainfall of 1500 mm and is influenced by the seasonal monsoon. The rainfall data of 3 h from 1981 to 2010 was used from Bangkok Metropolis rainfall station of Thai Meteorological Department for the study.

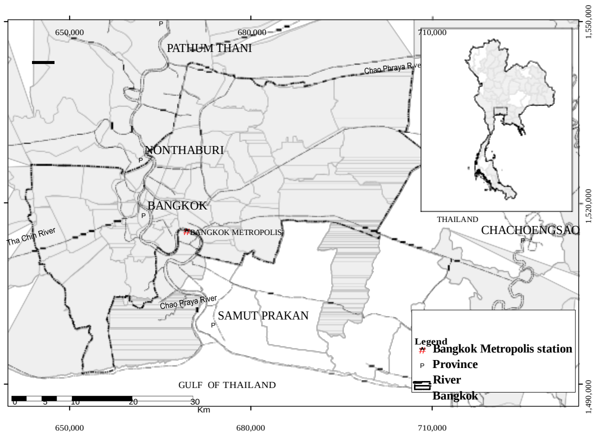

Fig. 1 Map showing study area in Bangkok, Thailand

Methodology

To develop the IDF curve for future, the study is subdivided into three processes which are spatial downscaling of precipitation from GCMs, disaggregation of daily rainfall series into hourly series and application of Gumbel distribution with annual maximum series to generate IDF curves for present and future.

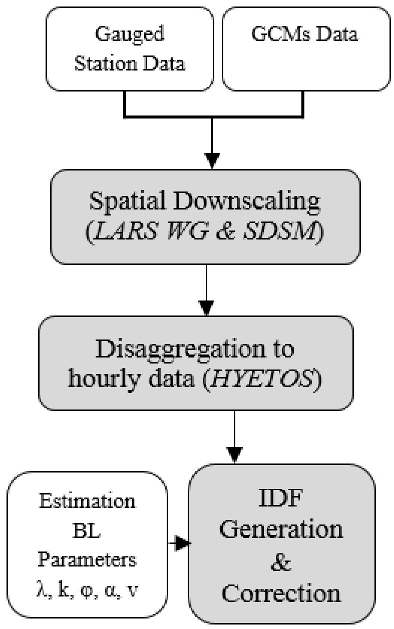

Fig. 2 Methodological Framework

Statistical downscaling using SDSM

Screening of variables was carried out using annual correlation, monthly correlation, partial correlation and P value. Three predictor variables are initially selected: 500 hpa vorticity, ncepp5_zas have the highest correlation (0.144) with predictand variable followed by Surface divergence, ncepp_zas (0.127) and Surface relative humidity, nceprhumas found to have good monthly correlation (0.038) in all the months. The observed data from 1961-1990 was used as predictand and predictor variables from NCEP GCM was used for calibration. While data from 1991-2001 and predictor variables from HADCM3 under A2 and B2 scenarios was used for verification.

Stochastic weather generator using LARS WG

LARS WG, follows two steps: first analysis of the observed weather parameters such as temperature, precipitation and solar radiation, followed by generation of synthetic daily weather data utilizing weather parameters. LARS-WG incorporates predictions from 15 GCMs which are namely BCM2, CGMR, CNCM3, CSMK3, FGOALS, GFCM21, GIAOM, HADCM3, HADGEM, INCM3, IPCM4, MIHR, MPEH5, NCCCSM and NCPCM; and climate predictions are available for emissions scenarios SRB1, SRA1B and SRA2 for most of the GCMs (Semenov and Stratonovitch 2010). Site analysis is done using only precipitation as the purpose was to develop IDF curves. The weather generation was done for 1981- 2000 and 2001-2010. The statistics chosen here are total monthly mean precipitation and maximum daily precipitation in each month.

Disaggregation to hourly data using HYETOS

Hyetos is single variate disaggregation model based on Bartlett Lewis Rectangular Pulse, BLRP, theory. The method follows the assumption of BLRP process that consist of five parameters λ, k, φ, α, v which mathematically elucidate the rainfall event (Koutsoyiannis, 2003; Koutsoyiannis and Onof, 1998). The method aims to preserve the statistical characteristics such as mean, variance, lag 1 autocovariance and proportion dry; of observed time series with the synthetically generated disaggregated time series. The details and equations for these statistics are explained in, Koutsoyiannis, (2003). Estimation of the BLRP parameters are done by calculating these statistics from the observed 3 h, 24 h and 48 h data from 1986 to 2000 for each month separately. The maximum peak daily rainfall occurred during 1986 to 2000. The parameters λ, k, φ, α, v, μX and σX are optimized using Excel solver to minimum relative error between synthetic and observed values. The synthetic rainfall shall simulate the rainfall with identical values that from observed data. Then, error is calculated giving weighted value of 10 for mean and 1 for variance, lag 1 auto covariance, proportion dry each for 0.125 days, 1 day and 2 days. The parameters of the respective months are used in disaggregation for present and future daily data. Due to brevity of the paper the results are not shown here.

IDFs generation and correction

Gumbel probability distribution and annual maximum series was used to generate IDF for observed 3 h data from 1981-2010 and disaggregated 1 h data for same period followed by graphical correction of the disaggregated IDF using higher order equation.

Results and discussion

Statistical downscaling using SDSM

The performance of SDSM model in projecting rainfall in summarized in table below. The mean precipitation are accurately projected with less error and high efficiency index. The maximum are poorly projected since the regression model couldn't project extreme values therefore the error is very high during calibration and verification stage and negative value for EI.

Table 1. RMSE and EI summary for calibration and verification process of SDSM

		RMSE	EI	RMSE	EI	RMSE	EI
		NCEP		HADCM3 A2		HADCM3 B2	
A	1	0.740	0.938	1.132	0.832	1.131	0.832
	2	110.633	0.398	109.912	0.406	110.024	0.405
B	1	2.412	0.600	3.705	0.131	3.341	0.293
	2	48.986	-0.938	53.844	-1.341	54.135	-1.366

*A-Calibration, B- Verification, 1- Mean, 2- Max

Stochastic weather generator using LARS WG

Comparison of mean precipitation totals and maximum between observed and simulated synthetic time series data between 1981-2000 and 2001-2010 are shown in Fig. 3 and 4.

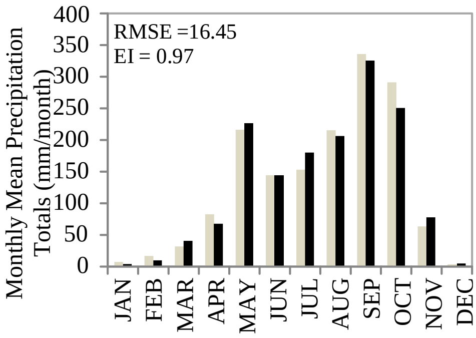

(a)

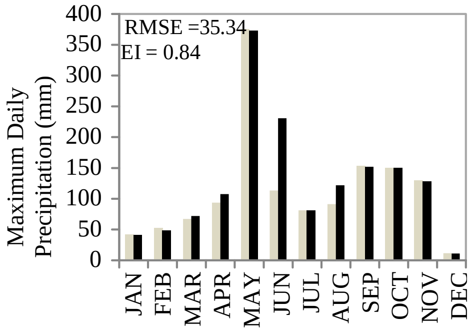

(b)

Fig. 3 Weather projection 1981-2000. Comparing monthly total mean and daily maximum for 12 months (Black Bar: Synthetic, Grey Bar: Observed)

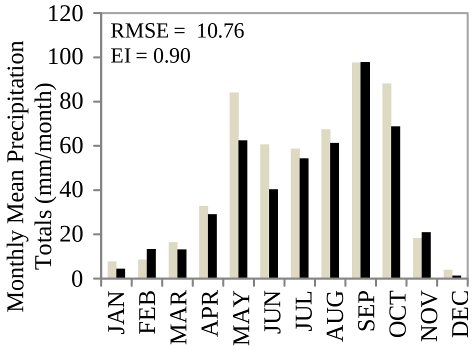

(a)

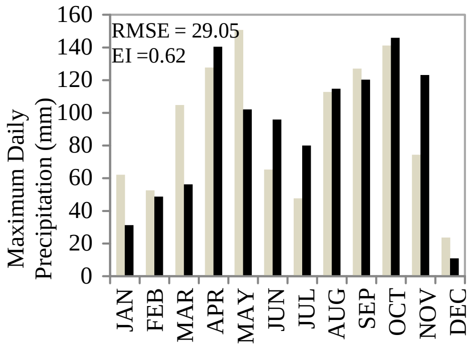

(b)

Fig. 4 Weather projection 2001-2010. Comparing monthly total mean and daily maximum for 12 months (Black Bar: Synthetic, Grey Bar: Observed)

In constrast to the SDSM results, LARS WG has better capability to project extreme range as well as monthly average more accurately. The RMSE and EI two weather projections are better for projecting extreme values. LARS WG was used for future projection of daily precipitation using 15 above mentioned GCMs in SRA1B and SRA2. These SRES scenarios cover range of minimum and maximum carbon emissions. During 2011-2030 the maximum daily value is projected as 420.3 mm which is 57.3 mm higher than observed maximum and minimum value projected is 309.3 mm which is 53.5 mm lower than the observed maximum. During 2046- 2065 the maximum daily value is projected as 438 mm which is 69.74 mm higher than observed maximum and minimum value projected is 301.4 mm which is 66.86 mm lower than the observed maximum.

Disaggregation and IDFs generation with correction

Optimized BLRP parameters for each months in HYETOS method disaggregated all the present and downscaled daily data into hourly data.

Using Gumbel probability distribution and annual maximum series to generate IDFs for observed 3 h data from 1981-2010 and disaggregated 1 h data for same period, generated IDFs which showed significant underestimation in rainfall intensity for shorter duration of 1 h and lesser towards higher durations. The correction factor was necessary to project the future IDFs accurately. The differences as well as ratios between observed and simulated was higher for shorter duration and less for higher durations. Within all duration the difference increased with the return period. Nevertheless, the ratio remains almost near to same value with only fractional difference within return periods

Table 2. Ratio and difference between observed and simulated rainfall intensities

Duration		**Return Periods**			
		2 Y	**5 Y**	**20 Y**	**100 Y**
3 h	R	1.39	1.39	1.39	1.39
	D	7.79	9.68	12.13	14.85
6 h	R	1.11	1.15	1.19	1.22
	D	1.56	2.77	4.35	6.09
12 h	R	1.02	1.033	1.04	1.04
	D	0.20	0.370	0.60	0.85
24 h	R	1.02	1.02	1.03	1.03
	D	0.10	0.18	0.28	0.39

*R-Ratio of observed/ modelled, D- Difference of modelled & observed

Therefore, the average ratio of observed to modelled data is fitted into a power equation with R^2= 0.889, and resulting equation is the function of duration, which is independent of return period.

The equation is given by,

$$y = 1.58\, x^{-0.14} \qquad (1)$$

where, correction factor y is dependent on duration. Using this equation downscaled-disaggregated IDFs from the 15 GCMs are corrected (Fig 5).

The 15 GCMs outputs under SRA1B and SRA2 scenarios are developed in IDFs. These will give the range of different values for intensities. All the results are not shown in this paper. Few GCMs are selected based on maximum 3 h rainfall depth. In the past events the catchment suffered surface flooding when 3h rainfall exceeds 100mm. In SRA1B scenario CGMR and IPCM4 GCMs were selected and for SRA2 scenario HADCM3 and GFCM21 GCMs were selected. The comparisons of present IDF curve and future IDF curves with consideration of emission scenario SRA1B are presented below.

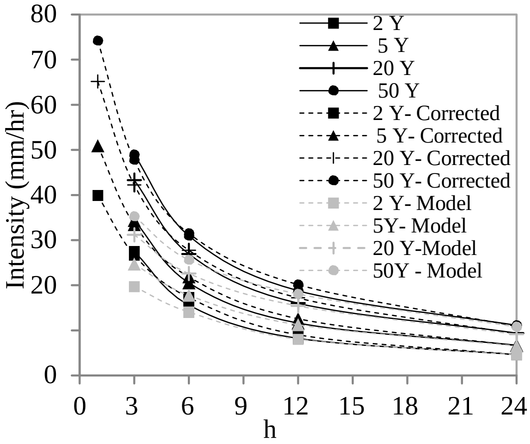

Fig. 5 Observed, modelled and corrected present IDFs for 1981-2010

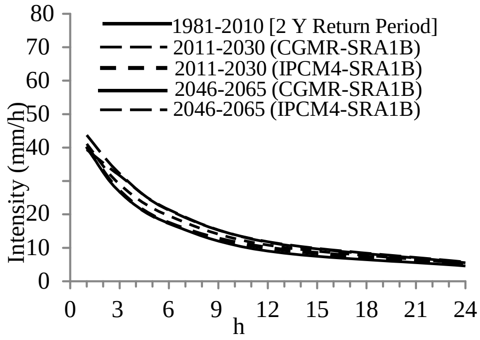

(a)

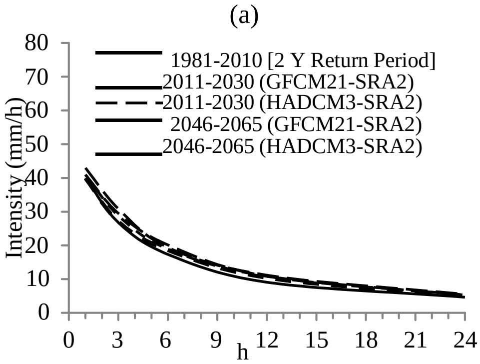

(b)

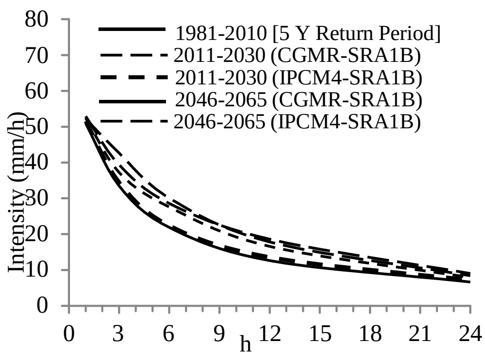

(c)

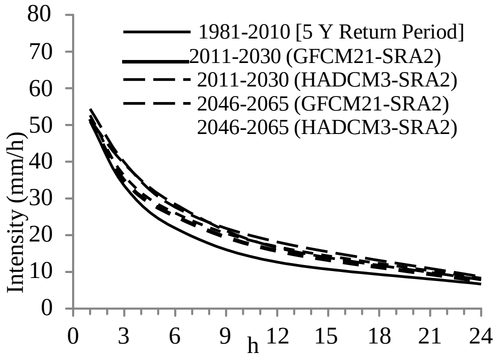

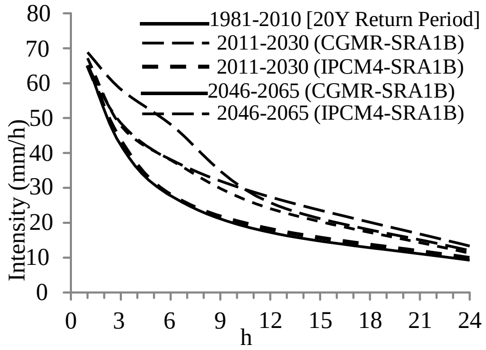

(e)

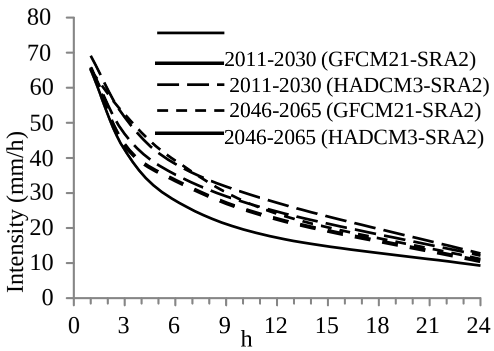

(f)

Fig. 6. Comparison of IDFs curves for 2, 5 and 20 years return period under SRA1B scenario (a, c, e) and under SRA2 (b, d, f) at different present and future time extents

Projected IDFs for 2011-2030 and 2046-2065 are shown in Fig. 6. The IDFs in all return periods shift to the higher intensities under climate change. In 2 year event, 3h depth will increase by 1.13 to 20.9 percent in SRA1B scenario and 0.9 to 12.3 percent in SRA2 during 2011-2030. During 2046-2065, there are +8.75 to 18.75 percent and +6.14 to 8.2 percent increment in SRA1B and SRA2 respectively. In 5 year event, 3h depth will increase by 3.4 to 18.1 percent in SRA1B scenario and 4.5 to 19.5 percent in SRA2 during 2011-2030. During 2046-2065, there are +12 to 28 percent and +8.45 to 18.3 percent increment in SRA1B and SRA2 respectively. In 20 year event, 3h depth will increase by 3.15 to 15.11 percent in SRA1B scenario and 3.5 to 22.15 percent in SRA2 during 2011-2030. During 2046-2065, there are +13.4 to 37.92

percent and +10.76 to 24.09 percent increment in SRA1B and SRA2 respectively. The drainage system in practice considers usually 2 and 5 years of return period. 20 year of return period is also considered here for the study purpose. In all the cases it is observed that the rainfall

Summary and conclusions

The study highlighted on one of the imperative challenge of obtaining high resolution spatial and temporal data for studying urban water system. The methodology of downscaling-disaggregation-IDF generation and correction can be applied to other places, while similar other downscaling and disaggregation methods shall be further explored. The downscaling from regression based SDSM showed significant bias in predicting extreme climate variable and while LARS WG showed satisfied results. IDF are basically generated from the maximum series values and most of the downscaling methods are less efficient to project extreme values. The downscaled-disaggregated IDFs showed underestimation in intensities especially in short durations, hence it was important to correct the IDFs. Graphical correction using higher order equation was developed to obtain correction factor. The 15 GCMs are analyzed and two GCMs are selected for SRA1B and SRA2 emission scenarios to develop future IDF curves. The overall result showed that there is increase in precipitation over the time period from 2020s to 2050s.

Acknowledgement

This study was conducted as the part of my master thesis of joint double degree program in Urban Water Engineering and Management between AIT and UNESCO IHE. Sincere thanks are extended to the advisors and faculties of both the institutions. Also, I would to extend my gratitude to Thai Meteorological Department (TMD) for providing data for the study.

References

Boo K.O., Kwon W.T., and Baek H.J. (2006). Change of extreme events of temperature and precipitation over Korea using regional projection of future climate change, Geophys. Res. Lett., 33, , L01701.

Emori S., and Brown S. J. (2005). Dynamic and thermodynamic changes in mean and extreme precipitation under changed climate, Geophys. Res. Lett., 32, , L17706.

Guo Y. P. (2006). Updating rainfall IDF relationships to maintain urban drainage design standards, Journal of Hydrologic Engineering, 11 (5), 506–509.

IPCC (Intergovernmental Panel on Climate Change) working group III (2000). IPCC Special Report Emissions Scenarios", IPCC.

Irwin S. E., Sarwar R., King L. M. and Siminovic S.P. (2012). Assessment of climatic vulnerability in the Upper Thames River Basin: Downscaling with LARS WG Water Resources Research Report, Department of Civil And Environmental Engineering, University of Western Ontario.

Koutsoyiannis D. (2003). Rainfall Disaggregation Methods: Theory and Applications. In Workshop on Statistical and Mathematical Methods for Hydrological Analysis, Rome, Italy.

Koutsoyiannis D., and Onof C. (2001). Rainfall disaggregation using adjusting procedures on a Poisson cluster model", Journal of Hydrology, 246(1-4), 109–122.

Liew S.C., Liong S-Y. and V. Raghavan S. (2012). A novel approach, using regional climate model, to derive resent and future IDF curves for data scare sites, Willis Research network.

Mailhot A., and Duchesne S. (2010). Design Criteria of Urban Drainage Infrastructures under Climate Change", Journal of Water Resources Planning and Management, American Society of civil Engineers, 201–208.

Nguyen V. T. (2005). Downscaling methods for evaluating the impacts of climate change and variability on hydrological regime at basin scale. Role of Water Sciences in Transboundary River Basin Management.

Semenov M.A. and Barrow E.M. (1997). Use of a stochastic weather generator in the development of climate change scenarios, Climatic Change, 35:397-414

Semenov M.A. and Stratonovitch P. (2010). The use of multi-model ensembles from global climate models for impact assessments of climate change, Climate Research, 41:1-14

Solaiman T. A., and Siminovic S.P. (2011). Development of Probability Based Intensity Duration-Frequency Curves under Climate Change, Water Resources Research Report. The University of Western Ontario, Canada.

Sunyer M. A., Madsen H., and Ang P. H. (2012). A comparison of different regional climate models and statistical downscaling methods for extreme rainfall estimation under climate change, Atmospheric Research, 103, 119–128.

Trenberth K. E. (1999). Conceptual framework for changes of extremes of the hydrological cycle with climate change, Climatic Change, 42, 327–339.

Trenberth K. E. (2011). Changes in precipitation with climate change", Climate Research, (2011), 47, 123–138.

Wilby R., Dawson C., and Barrow E. (2004). SDSM — a Decision Support Tool for the Assessment of Regional Climate Change Impacts", Environmental Modelling & Software 17(2), 145–157.

Wiley M. W., and Palmer R. N. (2008). Estimating the Impacts and Uncertainty of Climate Change on a Municipal Water Supply System", Journal Of Water Resources Planning And Management, American Society of Civil Engineers, 239–246.

*Evaluation of Precipitation over Northern Thailand in CMIP5 MRI-CGCM3 Simulations**

Parichat Wetchayont[1,3,a] and Srilert Chotpantarat[1,2,b*]

Abstract Northern Thailand is a major of water supply to Makong and Chaopraya rivers. We could avoid the damage from flooding and drought by concerning accuracy of precipitation estimation over northern area. Therefore, the objective of this study is to validate precipitation trends from a climate model, MRI-CGCM3, which participates in the Coupled Model Intercomparison Project Phase 5 (CMIP5). We used 29 rain gauges from Thai Meteorological Department (TMD) to compare with the MRI-CGM3 model output. The daily precipitation shows not clear in relationship between two data sets. However, monthly average precipitation exhibits overestimated trend. The analysis indicated that the overestimate is occurred during break monsoon period because the MRI-CGCM3 model unable to capture the break monsoon condition and reproduced artificial precipitation. In addition, Taylor diagram examined the consistency between the rain gauges and the MRI-CGCM3 model is so far.

Keywords *precipitation, rain gauge, Global Climate Models (GCMs), Northern Thailand, CMIP5*

Parichat Wetchayont, Srilert Chotpantarat
1: Department of Geology, Faculty of Science, Chulalongkorn University
Bangkok, Thailand
csrilert@gmail.com

Srilert Chotpantarat
2: Center of Excellence on Hazardous Substance Management (HSM), Chulalongkorn University, Bangkok 10330, Thailand
Bangkok, Thailand
csrilert@gmail.com

Parichat Wetchayont
3: Environmental Engineering and Disaster Management Program, Mahidol University, Kanchanaburi, Thailand
pwetchayont@gmail.com

Introduction

Severe flooding occurred in Thailand at the end of July 2011, which caused by a Tropical Storm, Nock-ten. The flooding extended from Northern Thailand through another area along Chao Phraya and Mekong river basins. The damaged area is in half of country. Therefore, accurate estimation of the spatiotemporal of precipitation in Northern Thailand is important for water resources management and also monitoring disaster such as flooding and drought.

Fundamentally, rain gauge measurements are assumed to be fact and its used to validate another precipitation data set for example, radar, satellite or model products. Global climate models (GCMs) are a well known as tool to show both historical and future projection of precipitation. The Intergovernmental Panel on Climate Change (IPCC) is the famous organization to achieve 29 modeling groups around the world together. They work based on Global warming theme. A new release version of the GCMs were used in the 5th phase of the Coupled Modeling Intercomparison Project (CMIP5) in which the results are contributed to 5th Assessment Report of IPCC (IPCC 2013).

Many efforts have been made on evaluation of precipitation from the CMIP5 model (Monerie et al. 2012, H.Chen et al. 2013, Yin et al. 2013, Su et al. 2013, H.Chen et al. 2014, E.Palazzi et al. 2014). They reported uncertainties from the CMIP5 model from global to local scale in various areas. However, there are small number of work had made in Northern Thailand (Chotamonsak et al. 2011). Here, we will show results of comparison between the CMIP5 data and rain gauge data over Northern Thailand during 1986 to 2005.

Data and study area

We analyzed the precipitation data over Northern Thailand, which obtained from the rain gauges from Thai Meteorology Department (TMD) as shown in Fig.1. Daily tipping rain gauges network consisting of 29 sites with 0.1-mm sensitivity was used in this study. The daily rainfall was observed from 1986 – 2005 (20 years). We used the rain gauge data to evaluate precipitation output from the CMIP5 model throughout this study.

MRI-CGCM3 model is a GCM that participated in the CMIP5 model and its output was chosen to use in the analysis because it has high spatial resolution. The MRI-CGCM3 model was developed by Meteorological Research Institute (MRI)/Japan Meteorological Agency (JMA) and conducted climate projection experiments under an idealized global warming scenario. Daily rainfall was performed by the MRI-CGCM3 based on historical scenario with a 1.125-degree grid resoution, 320 x 160 grid cells in horizontal and 8 levels coordinate in vertical (Yukimoto et al. 2011) will be examined in this study. We focused on historical simulations over continental area in northern Thailand during 1986-2005.

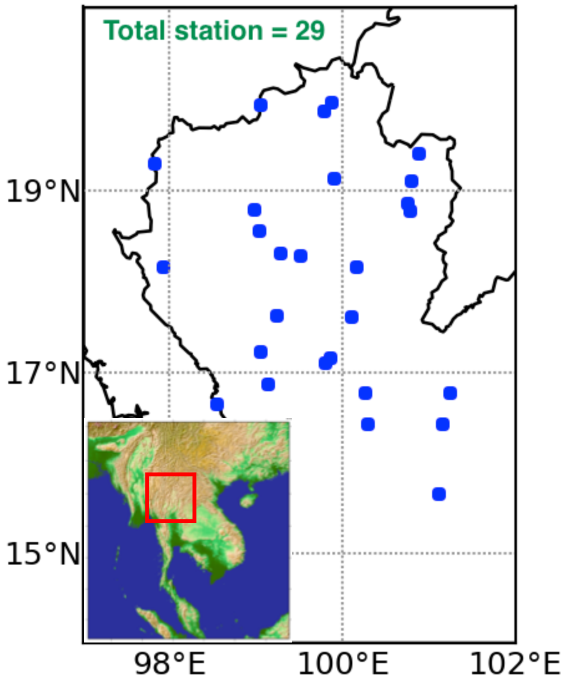

Fig. 1 The Study area and 29 rain gauge stations used in this study.

Methodology

To evaluate model performance according to observations, we used Taylor diagram (Taylor 2001). The Taylor diagram represented statistical relationship pattern in terms of root mean square (RMS), correlation coefficient (CC) and standard deviation (STD) as formulated as following:

1. Correlation coefficient (CC) as given in Eq. (1):

$$CC = \frac{\frac{1}{N}\sum_{n=1}^{N}\left(gauge_n - \overline{gauge}\right)\left(model_n - \overline{model}\right)}{\sigma_{gauge}\sigma_{model}} \quad (1)$$

Where n is number of data, gauge and model are precipitation, $\overline{gauge}$ and $\overline{model}$ are average precipitation, ρ_{gauge} and ρ_{model} are standard deviations of rain gauge and model, respectively.

2. Pattern root mean square difference (RMS) as formulated in Eq. (2):

$$E' = \left\{\frac{1}{N}\sum_{n=1}^{N}\left[\left(gauge_n - \overline{gauge}\right) - \left(model_n - \overline{model}\right)\right]^2\right\}^{1/2} \quad (2)$$

Results and discussion

Daily and monthly averaged precipitation

We matched up between the rain gauge data and the CMIP5 data, which located above the rain gauges in both daily and monthly scale. Fig.2 shows scatter plot of the matched pares. The rain gauge data set has maximum value of precipitation about 521.80 millimeters per day, which higher than that the MRI-CGCM3 model, 290.32 millimeters per day. The results suggested that the MRI-CGCM3 model couldn't estimate higher precipitation rate than 290.32 millimeters per day. The correlation coefficient value (R) was 0.07 that is very low, so we could not see any relationship trend from the scatter plot.

To examine the overall precipitation trend, we did the average process. Firstly, both of data sets will be averaged from daily to monthly scale, and then matched up and averaged data of each time step for each data set. Finally, we could get the time series of the monthly averaged precipitation in millimeters per day of the rain gauges and the MRI-CGCM3 as shown in Fig.3. The MRI-CGCM3 precipitation almost showed overestimation except in 2003. Moreover, while the rain gauge data clearly shows two peaks of precipitation regarding the monsoon onset, but the MRI-CGCM3 represented only one peak of precipitation.

The monthly precipitation climatology of 1985 to 2005 was presented in Fig.4. This is supported that the rain gauge can capture the two precipitation peaks during rainy season in northern Thailand associated with the intertropical convergence zone (ITCZ) movement. This result agrees with Chokngamwong (2007). The precipitation output from the MRI-CGCM3 trends overestimate and cannot distingue the break period of monsoon. This overestimation might be caused by the coarse spatial resolution or model calculation itself.

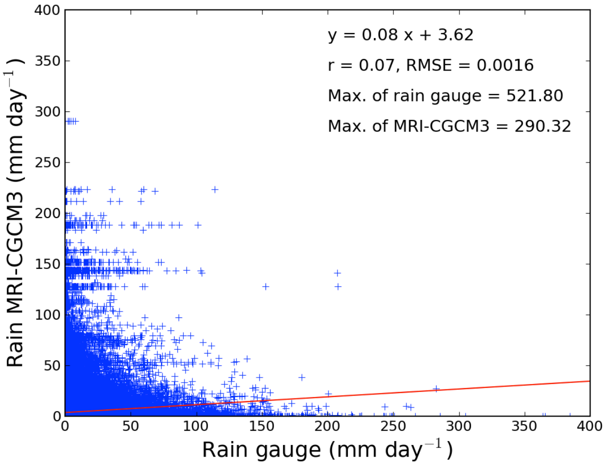

Fig.2 Scatter plot of daily precipitation between the rain gauges and the MRI-CGCM4 during 1986 to 2005.

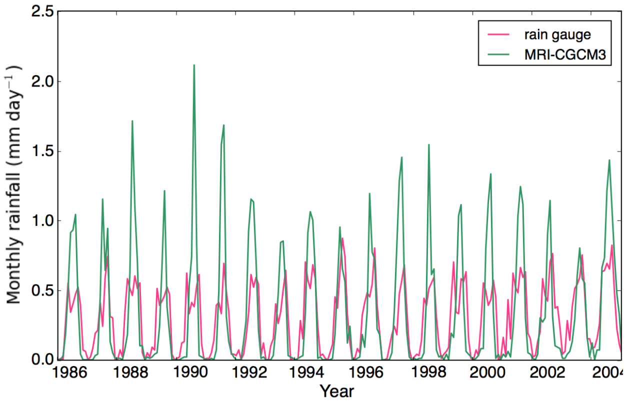

Fig. 3 The monthly averaged precipitation of the 29-rain gauge and the MRI-CGCM3 during 1986 to 2005.

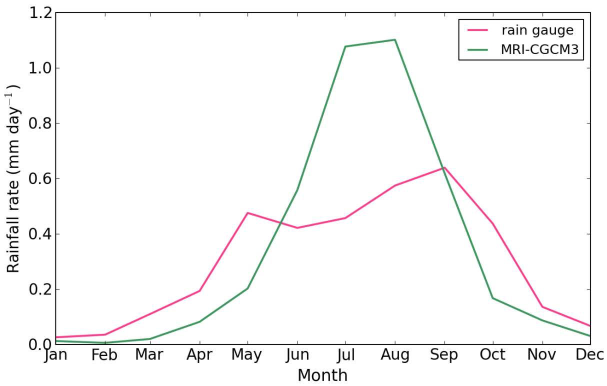

Fig.4 The monthly precipitation climatology of the 29-rain gauge and the MRI-CGCM3 during 1986 to 2005.

Statistic of precipitation event

The statistic of precipitation event in term of precipitation rate was examined by histogram plot of the rain gauge and the MRI-CGCM3 as shown in Fig.5 a) and b), respectively. The precipitation rate heavier than 1 millimeter per day will be used in this analysis. The daily precipitation rates binned at 5 millimeters per day interval. Histogram of precipitation rate from the rain gauges (Fig.5 a) presented continuous decreasing probability from low to high precipitation rate. While, histogram of precipitation rate from the MRI-CGCM3 showed that there is also continuous decreasing probability from value less than 80 millimeters per day. After that there is uncertainties in probability trend from value of 80 to its the maximum value of 290.32 millimeters per day. This result indicated that the MRI-CGCM3 model is reproduced precipitation in range of 100 to 300 millimeters per day more often than the truth. Moreover, we found that this precipitation rate range was produced during July to September (period of break monsoon). This results could explained that the MRI-CGCM3 model could not capture the period of break monsoon and reproduced artificial heavy precipitation during that time. This finding is consistent with Ajayamohan (2007) who found the FSUGSM model is could not capture the interannual variability of South-Asian monsoon and its teleconnection patterns.

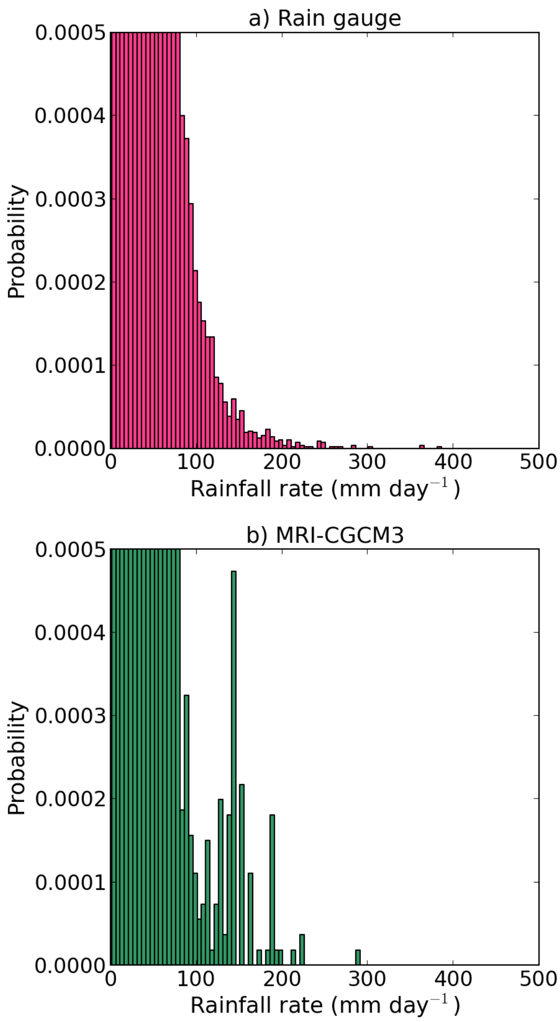

Fig.5 Statistic of precipitation event for the rain gauges and the MRI-CGCM3 in daily scale during 1986 to 2005.

Pattern of statistical summary

To evaluate consistency between the rain gauges and the MRI-CGCM3 model is performed by Taylor diagram, two points are plotted on a polar graph as shown in Fig.6. The diagram consists of STD of the rain gauges (11.49) is plotted along x-axis, the MRI-CGCM3 has STD of 12.16 is located by y-axis and correlation on curve line. The distance between two points is RMSE (16.20) as displayed summary in Table.1. The statistic results quantified that there are so far consistency between the rain gauges and the MRI-CGCM3.

Table 1. Statistical performance of the rain gauges and the MRI-CGCM3 model on daily precipitation

Data set	SD	CC	RMSE
Rain gauge	11.49		
MRI – CGCM3	12.16	0.07	16.20

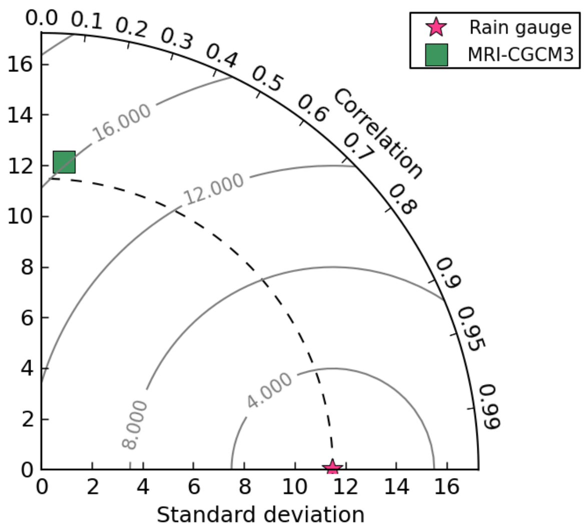

Fig.6 Statistic of precipitation event for the rain gauges and the MRI-CGCM3 in daily scale during 1986 to 2005.

Summary and conclusions

The CMIP5 MRI-CGCM3 precipitation product has large bias and it misses the observed heavy precipitation that occurred in September. Statistics analysis represented the CMIP5 MRI-CGCM3 product overestimates the event conditional rain rates when compared to the rain gauges. This uncertainties in model simulated precipitation in this study mainly caused by the MRI-CGCM3 model missing the break monsoon condition. The overestimation of monthly average precipitation was found from artificial precipitation event during the break monsoon. Taylor diagram reveals the consistency between the rain gauges and the MRI-CGCM3 model is so far. The results point to the need to further improve the CMIP5 MRI-CGCM3 precipitation and improve the estimation of heavy rainfall events in late of year over northern Thailand area.

Acknowledgement

We thank to Thai Meteorological Department (TMD) for providing rain gauge data. We acknowledge the World Climate Research Programme's (WCRP's) Coupled Model for their producing available model output. This work has been supported by the Office of the Higher Education Commission (OHEC).

References

Chakrit Chotamonsak, Eric P. Salathé, Jiemjai Kreasuwan, Sompron Chantara, Kingkeo Siriwitayakorn. (2011) Projected climate change over Southeast Asia simulated using a WRF regional climate model. Atmospheric Science Letters Online publication date: 1-Jan-2011.

Chen H. P. , J. Q. Sun, (2013) Projected change in East Asian summer monsoon precipitation under RCP scenario, Meteor. Atmos. Phys. , 121, 55-77.

Chen, H., Sun, J. and Chen, X. (2014) Projection and uncertainty analysis of global precipitation-related extremes using CMIP5 models. Int. J. Climatol., 34: 2730–2748. doi: 10.1002/joc.3871

E. Palazzi, J. von Hardenberg, A. Provenzale (2013) Precipitation in the Hindu-Kush Karakoram Himalaya: observations and future scenarios, J. Geophys. Res., 118, 85–100 http://dx.doi.org/10.1029/2012JD018697

H. J. Fowler, S. Blenkinsop and C. Tebaldi (2007) Review Linking climate change modelling to impacts studies: recent advances in downscaling techniques for hydrological modeling, Int. J. Climatol. 27, 1547–1578.

IPCC (2013) "Climate Change 2013: The Physical Science Basis" Working Group I Contribution to the IPCC Fifth Assessment Report of the Intergovernmental Panel on Climate Change, Stockholm, Sweden.

J. Chen, F. P. Brissette and R. Leconte (2013) Assessing regression-based statistical approaches for downscaling precipitation over North America, Hydrol. Process, DOI: 10.1002/hyp.9889.

Yin, L., R. Fu and E. Shevliakova (2013) How well can CMIP5 simulate precipitation and its controlling processes over tropical South America?, Clim Dyn, 41, 3127–3143 .

Monerie, P.-A., B. Fontaine, and P. Roucou (2012), Expected future changes in the African monsoon between 2030 and 2070 using some CMIP3 and CMIP5 models under a medium-low RCP scenario, J. Geophys. Res., 117, D16111, doi:10.1029/2012JD017510.

R. S. Ajayamohan. (2007). Simulation of South-Asian Summer Monsoon in a GCM. Pure and Applied Geophysics. doi:10.1007/s00024-007-0249-9

Su, F., Duan, X., Chen, D., Hao, Z. and Cuo, L. 2013. Evaluation of the Global Climate Models in the CMIP5 over the Tibetan Plateau. Journal of Climate 26: 3187-3208.

Taylor, K. E. (2001), Summarizing multiple aspects of model performance in a single diagram, J. Geophys. Res., 106(D7), 7183–7192, doi:10.1029/2000JD900719.

Climate change impact on groundwater recharge in Upper Central Plain and Plaichumpol Irrigation Project, Thailand

Chokchai suthidhummajit [1, a *], Sucharit Koontanakulvong[2,b]

Abstract. The Plaichumpol Irrigation Project is located in the Upper Central Plain of Thailand where farmers depended on both surface water and groundwater. Though there is the Sirikit Dams storing water to be used during dry period but water allocated is limited and still caused water shortage during dry season. Most of farmers turn to use groundwater to supplement irrigation water in the dry year. Groundwater resources are related to climate change through the direct interaction with surface water resources, and indirectly through the recharge process. The direct effect of climate change on groundwater resources depends upon the change in the volume and distribution of groundwater recharge both through river and land surface.

This study developed the recharge formula in terms of precipitation, evapotranspiration and temperature and soil type under monthly time series data and studied the impact of climate change on groundwater recharge and water table based on future climate condition using the bias-corrected MRI-GCM data. The groundwater flow model, MODFLOW, was used to determine groundwater flow movement and recharge parameter. The recharge mechanism in this study, considered only through land recharge, were analyzed in term of soil type data, rainfall and evapotranspiration data. The study found that future recharge, compared with the present period, will decrease in both near future and far future and groundwater level will decrease especially in the Plaichumpol Irrigation Project due to climate change by which proper adaptation measures should be considered to cope with the impacts.

Keywords: *Climate Change, Groundwater Recharge, MODFLOW, Upper Central Plain, Irrigation Project*

Chokchai Suthidhummajit
Department of Water Resources Engineering
Faculty of Engineering, Chulalongkorn University
Bangkok, Thailand
Email: chokchai.s@chula.ac.th

Sucharit Koontanakulvong
Department of Water Resources Engineering, Faculty of Engineering, Chulalongkorn University.
Bangkok, Thailand
Email: sucharit.k@chula.ac.th

Introduction

The climate change induced direct affects to irrigation area, e.g., Yom, Nan Basin or Chao Phraya Basin in the dry year when the storage amount is not adequate for summer rice and caused water deficit in many irrigation projects. Though in the central plain, two large reservoirs, i.e., Bhumiphol and Sirikit Dams store water to be used during dry period but most of agricultural area is in the rainfed area and water allocated is limited and caused water shortage during dry season and in the dry year. Most farmers turned to use groundwater to supplement irrigation water. This also caused groundwater drawdown and make farmers to dig deeper (shallow) wells which made more cost for agriculture (Chulalongkorn, 2010).

Agricultural area depends on both surface and groundwater sources (Chulalongkorn, 2005). Farmers in the irrigation project cultivate paddy all year round and need irrigation supply to crop requirement all time. Groundwater is an important water source for cultivation and becomes supplementary water source for farmers to ensure the cultivation. The yield capacity of the aquifer in irrigation area also can provide sufficient amount compared with other area which make the groundwater use in the area with high amount. The groundwater resources are limited and flow with complicated manner, hence the study of groundwater and its use was studied to find sustainable use and yield of the aquifer (Chulalongkorn, 2008). Furthermore, the climate change may affect the recharge and accelerate the groundwater use of the farmers in the area due to precipitation fluctuation and water deficit.

The focus of the present paper is to investigate the relationship of recharge rate with climate condition and to assess the impact on groundwater recharge in the Upper Central Plain and Plaichumpol Irrigation Project (as a sample of irrigation area) by applying MODFLOW and using the bias corrected MRI-GCM data.

Study area

Upper Central Plain is in the Northern part of Chao Phraya Plain covering the areas of Uttaradit, Sukhothai, Pitsanulok, Kampangphet, Pichit, and Nakornsawan Provinces. Total area is 47,986 square kilometers or 29,991,699 rais. Average height is approximately 40-60 meters above mean sea level. The areas consist of sediments which were changed from erosion and decay of rock, then accumulate and generate as plain, terrace, and swamp. Fig. 1 shows topography and boundary.

The climate of Upper Central Plain is under the influences of monsoon winds i.e. southwest and northeast monsoon. From the meteorological point of view the climate of Upper Central Plain can be divided into three seasons that are summer (mid-February to mid-May), rainy season (mid-May to October), and winter (November begin to mid-February). The study area is composed of 5 basins that are Lower Ping basin, Lower Yom basin, Lower Nan basin, Upper Sa-Grae-Grang basin, and Upper Chao Phraya basin, as shown in Fig. 1.

The main rivers in the study areas are the Yom and the Nan River which flow parallel from North to South and join at Ban Gei Chai, Amphor Chumsang, Nakornsawan Province. In addition, there is the Ping River which flows from west side and joins with the Yom and the Nan River at Amphor Paknampho, Nakornsawan Province. They become the Chao Phraya River, which continuously flow to the Central Plain.
From daily and monthly rainfall data of rainfall stations (68 stations) that collected during 1974 to 2003, the amount of rainfall in the Upper Central Plain is between 900 to 1,450 mm/year. From 52 station runoff data of Royal Irrigation Department that collected during 1994 to 2003, the total runoff 15,481.9 million cubic meters per year, divided into rainy season 13,625 million cubic meters, 88% of total runoff, and dry season 1,856.9 million cubic meters, 12% of total runoff.

Plaichumphol Irrigation Project, selected as a sample of irrigation area, has total project area of 273,000 rai and irrigation area of 211,476 rai. The irrigation area of 184,535 rai is located in Phompiram District, Muang District, Bangkatum District under Phitsanulok Province and another 26,941 rai is located in Muang District, Samgam District under Phichit Province (Plaichumphol Irrigation Project document, 2009) as shown in Fig. 2. The project is surrounded as followed.

North up to T. Nongham, T. Matong Phompiram District, Phitsanulok Province and next to Narasuan Diversion Project,

South down to T. Rangnok, Samguam District, Phichit Province and next to Dong Setthi Irrigation Project,

East next to main irrigation channel (PR C1) right hand side of Nan River Parallel with Nam River from the north end (T. Nongkam, Phompiram District, Phitsanulok Province) to the south end of main canal (PR km 80+000, T. Yarnyao, Muang District, Phichit Province)

West next to natural canal (started from the most north of the Project closed to Wangmakarm Canal, Mam Canal, Bangkao Canal to the south till T. Bangrakam, Bangrakam District, Phitsanulok Province then go along Yom River to the south boundary of the Project in T. Rangnok, Samgarm District, Phichit Province.

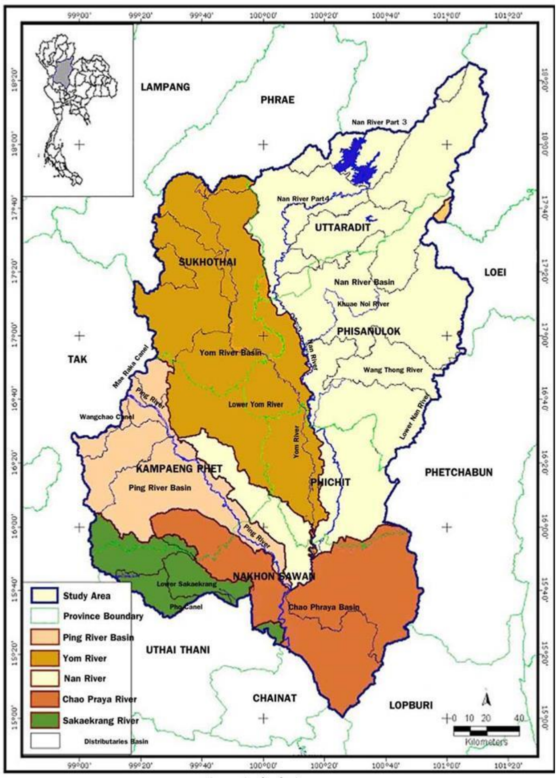

Fig.1 Upper Central Plain Basin

Methodology

There are two parts in this study, i.e., first part is to find the relationship of groundwater recharge rate from climate data, seven groups of soil data series and groundwater model (Koontanakulvong S., et. al, 2006) results, second part is to simulate the impact using the recharge relationship derived from the part 1 (river water level and water pumping assumed the same as in the past) and the projected bias corrected the MRI GCMs climate data (Koontanakulvong S., et.al., 2011) in two future time frames, i.e., near future (2015-2039) and far future (2075-2099) periods. A linear regression method was applied to develop relationship between recharge flux and value of monthly precipitation minus evapotranspiration via groundwater model recalibration. The improved groundwater model (MODFLOW) was applied to assess the impact of climate change on groundwater recharge and ground water table in the study area (upper central plain and Plaichumpol Irrigation Project area).

Groundwater model

Groundwater model using in this study is MODFLOW (the USGS's three-dimensional (3D) finite-difference groundwater model). MODFLOW is considered an international standard for simulating and predicting groundwater conditions and groundwater/surface-water interactions. Originally developed and released solely as a groundwater-flow simulation code when first published in 1984, MODFLOW's modular structure has provided a robust framework for integration of additional simulation capabilities that build on and enhance its original scope. The three-dimensional movement of ground water of constant density through porous earth material may be described by the partial-differential equation

$$\frac{\partial}{\partial x}\left[K_{xx}\frac{\partial h}{\partial x}\right]+\frac{\partial}{\partial y}\left[K_{yy}\frac{\partial h}{\partial y}\right]+\frac{\partial}{\partial z}\left[K_{zz}\frac{\partial h}{\partial z}\right]+W=S_s\frac{\partial h}{\partial t} \quad (1)$$

where

K_{xx}, K_{yy} and K_{zz} are the values of hydraulic conductivity along the x, y, and z coordinate axes (space function).
h is the potentiometric head (hydraulic head).
W is a volumetric flux per unit volume representing sources and/or sinks of water, where negative values are water extractions, and positive values are injections. It may be a function of space and time (i.e. W = W(x, y, z, t)).
S_s is the specific storage of the porous material (space function).
t is time.

Recharge equation
From the water budget analysis in the soil layer, the simple water budget is

$$P = ET+\Delta S+R_{off}+D \quad (3)$$

where
P is precipitation:
ET is evapotranspiration:
ΔS is change in water storage in soil column:
R_{off} is direct surface runoff: and
D is drainage out of the bottom soil which is equivalent to recharge(R)

From the above relation, The recharge can be approximated simpler by using following equation (Krüger, Ulbrich, & Speth, 2001):

$$R = P-ET-Q_0 \quad (4)$$

Equation (4) can be written again as follow:

$$R/P=a_i*(P-ET)/P +b_i \quad (5)$$

where
a_i and b_i are constant and can be found by using goodness fit test for each soil group.
P is precipitation, and ET is evapotranspiration and can be calculated by equation of temperature (T) (Singh, 1992):

$$ET = c*T+d \quad (6)$$

where c and d are constant and can be found by using goodness fit test for each month.

Results and discussion

Evapotranspriration

Evapotranspiration during the period 1979-2003 were collected from the report GCM Data Comparison and its application to water disaster adaptation measures in Thailand and the project on "The Impact of Climate Change on Irrigation Systems and Adaptation Measures" (Chulalongkorn, 2010). A comparison of evapotranspiration and mean temperature show that two variables have relationship as linear function as shown in Table 1

Table 1: Coefficients of linear function expressed relationship between evapotranspiration and mean temperature in each month.

Month	c	d	R^2
Jan	8.428	-107.57	0.43
Feb	8.428	-107.57	0.43
Mar	8.428	-107.57	0.43
Apr	2.9665	70.568	0.97
May	4.0509	27.342	0.99
June	2.9895	22.826	0.99
July	3.0688	23.886	0.99
Aug	2.9941	23.959	0.99
Sep	3.129	23.413	0.99
Oct	3.4886	23.991	0.86
Nov	5.0792	-20.275	0.99
Dec	3.9656	-0.8793	0.87

Groundwater model recalibration

Groundwater flow model (MODFLOW) was used to simulate groundwater flow conditions in the area during the period 1993-2003. This model was developed by Koontanakulvong S., et.al. 2006. Input data included river water level, observation groundwater level, and well abstraction used from the former project. In former model, recharge rates were defined by percent of rainfall in each soil group zone. In this study, soil zone was grouped in 7 zones by the similarity of soil series property as shown in Fig 2. In this study, the model was recalibrated compared with observation data using recharge equation derived. Results of recalibration model show that simulation values were closer with observation data compared with the former model calibration results as shown in Table 2.

Table 2: Comparison error of the former model and this study model.

Error(m)	Former model	This study	%Difference
Mean Error	2.85	2.11	26.16
Abs mean error	3.13	2.30	26.44
RMS error	4.59	3.90	15.00

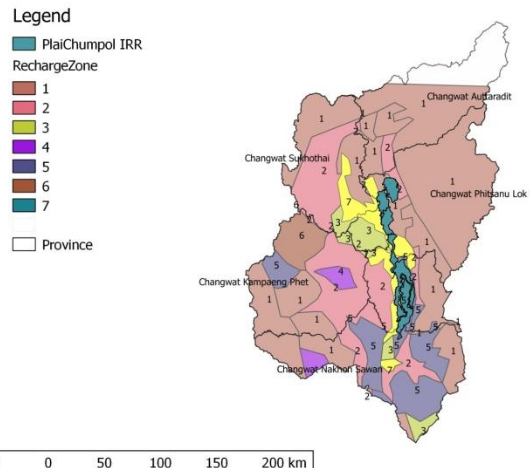

Fig 2. The soil group represent the recharge zone

Recharge function

The rates of groundwater recharge in each soil group zone from the step above were used to develop relationship between recharge and amount of monthly precipitation minus monthly evapotranspiration per precipitation (Equation 5). Results demonstrated good relationship between groundwater recharge fluxes with amount of monthly precipitation minus monthly evapotranspiration as shown in Table 3 and Fig 3.

Table 3: Coefficients of linear function expressed relation between (P-ET)/P and R/P.

Soil series group	a	b	R^2
1	0.0034	0.0009	0.93
2	0.0045	0.0012	0.93
3	0.0057	0.0015	0.94
4	0.0068	0.0018	0.94
5	0.008	0.0022	0.94
6	0.0091	0.0025	0.93
7	0.0113	0.0031	0.93

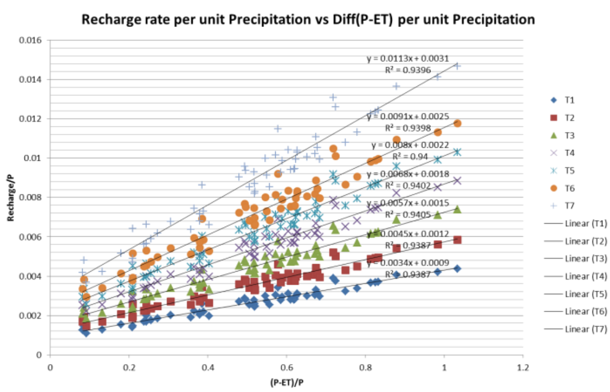

Fig. 3 The relation of recharge rate per precipitation for each soil series group

From the Permeability Class (O'Neal, 1952) and classification properties of each soil series (Suwanee Sridhavat Na Ayudhya 1995), Table 4 shows the classification of each soil series group of this study and Fig. 4 shows the relationship of the hydraulic conductivity/permeability and the coefficient of recharge per precipitation which shows good correlation and Fig. 4 could be used to estimate the coefficient of recharge for other soil series from hydraulic conductivity value.

Table 4 Classification of hydraulic conductivity of each soil series group of this study

Permeability Class(O'Neal 1952)	hydraulic conductivity(cm/hour)	Soil series Group(This Study)
Very Slow	<0.125	1
Slow	0.125-0.5	2
Moderately Slow	0.5-2.0	3
Moderate	2.0-6.25	4
Moderately Rapid	6.25-12.5	5
Rapid	12.5-25.0	6
Very Rapid	>25.0	7

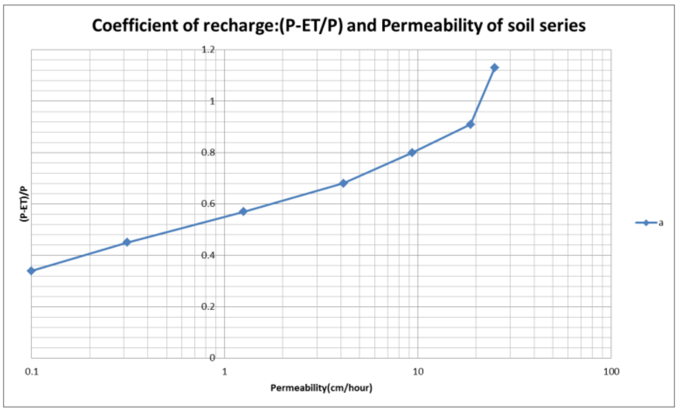

Fig 4 The relation of coefficient of recharge and permeability of soil

Impact of climate change

The impact of climate change is considered from the change of recharge and groundwater table compared with present period. The groundwater recharge rate from the above relationship for each soil series group, were calculated and input to groundwater model to simulate the impact of climate change with future climate data. Fig. 5 shows that recharge tend to decrease in the periods of both near future and far future and will be lower than in the past because of the increase of the evapotranspiration (temperature). The ratio of average recharge rate in near future and far future compare with present is 0.42, and 0.50 respectively. The heads of groundwater in the selected stations in the study area are shown in Fig. 6. It can be seen that climate change will induce lower water table in the north due to higher temperature (including Plaichumpol Irrigation Project area), i.e., water table will decrease approximately 0.23, 0.16 m/year in near future and far future periods respectively.

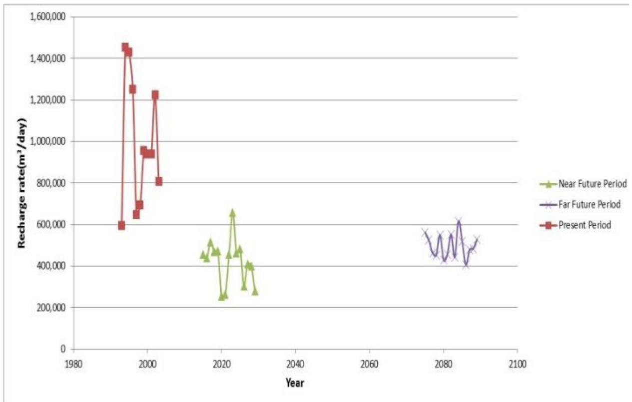

Fig.5 Average groundwater recharge rate from projected future climate data

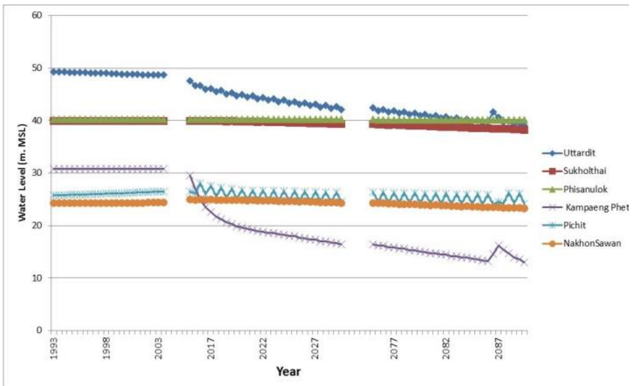

Fig.6 The groundwater levels at selected locations in each Province

From Fig. 7, the hot spot in lower water level will occur in some part of Uttraradit, Sukholthai, Phisanulok, Kampaengphet, Pichit and Nakhonsawan Provinces, especially in upper part of Plaichumpol Irrigation Project, the decrease of water level is up to 10 m

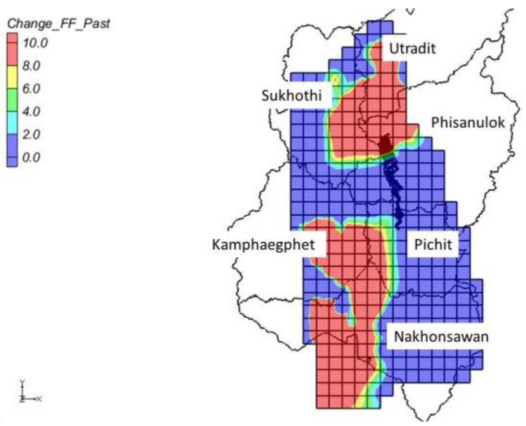

Fig 7 The change of water level (in meter) in the aquifer by the end of far future period

Conclusions

In this study, the relationship of recharge rate with climate data was developed in terms of precipitation, evaporation and temperature and soil type under monthly time series data and the study found that there were in good relationship and were used to study the impact of climate change on groundwater recharge and water table based on future climate data.

The future recharge , compared with the present, will decrease 58% in near future and 50% in the far future. Climate change will also induce impact on groundwater level, i.e., water table will decrease approximately 0.23 m/year in near future and 0.16 m/year in far future period, especially in upper part of Plaichumpol Irrigation Project, the decrease of the water level will be up to 10 m. Hence, in this area, proper adaptation measures should be prepared to reduce the effect of water table drawdown from the climate change.

Acknowledgement

The article could not be concluded without raw precipitation scenarios provided from various government agencies, e.g., Meteorological Research Institute (MRI, Japan We also grateful to staffs of Thai Royal Irrigation Department (RID) and Thai Meteorological Department (TMD) for observed historical rainfall data as well. This research has been partially support by Office of Thailand Research Fund (TRF). The research was also done under the Water Resources System Research Unit (CU_WRSRU) of Department of Water Resources Engineering, Faculty of Engineering, Chulalongkorn University.

References

Bejranonda W., Koontanakulvong S., Koch M. (2007) Groundwater modeling for conjunctive use patterns investigation in the upper Central Plain of Thailand, International Association of Hydrogeologists selected papers, Aquifer Systems Management: Darcy's Legacy in a World of Impending Water Shortage, Taylor & Francis Group, London, UK

Bejranonda W., Koontanakulvong S., Suthidhummajit C. (2008) Study of the Interaction between Streamflow and Groundwater toward the Conjunctive use Management: a Case Study in an Irrigation Project. 1st NPRU Academic Conference, Oct. Annals… p. 59-67

Bejranonda W., Koch M., Koontanakulvong S. (2011) Surface water and groundwater dynamic interaction models as guiding tools for optimal conjunctive water use policies in the central plain of Thailand. Environ Earth Sci, 8p

Chulalongkorn, Groundwater Use and Potential Study in the Lower Central Plain (2005) submitted to the Thailand Research Fund.

Chulalongkorn, Potential Groundwater Study of Phaichumphol Irrigation Project (2008), Technical Report.

Phaichumphol Irrigation Project, Phitsanulok (2009) (http://irrigation.rid.go.th/rid3/chumpol/ staff.html).

Chulalongkorn (2010) The Impact of Climate Change on Irrigation Systems and Adaptation Measures (Case Study: Plaichumphol Irrigation Project, Thailand), presented at JIID Seminar on Impact of Climate Change on Irrigation Systems, Bangkok, Jan 26.

Döll, P. (2009). Vulnerability to the impact of climate change on renewable groundwater resources: a global-scale assessment. *Environmental Research Letters, 4*(3), 035006.

Healy, R. W. (2010). *Estimating groundwater recharge*: Cambridge University Press.

Koontanakulvong S., et. al. (2006) The study of Conjunctive use of Groundwater and Surface Water in Northern Chao Phraya Basin, Final Report. Department of Groundwater Resources. Chulalongkorn University

Koontanakulvong S., Chaowiwat W. (2011) GCM Data Comparison and its application to water disaster adaptation measures in Thailand. Technical Report, Chulalongkorn University, March.

Koontanakulvong S., Chaowiwat W., Mizayato T. (2013) Climate change's impact on irrigation system and farmers' response: a case study of the Plaichumpol Irrigation Project, Phitsanulok Province, Thailand. Paddy and Water Environ. doi: 10.1007/s10333-013-0389-8

Koontanakulvong, S., & Suthidhummajit, C. (2000). Groundwater Recharge Study and Simulation—Kamphaeng Phet Case Study—*Groundwater Updates* (pp. 301-306): Springer.

Krüger, A., Ulbrich, U., & Speth, P. (2001) Groundwater recharge in Northrhine-Westfalia predicted by a statistical model for greenhouse gas scenarios. Physics and Chemistry of the Earth, Part B: Hydrology, Oceans and Atmosphere, 26(11), 853-861.

Land Development Department (2009a) Thailand Land Use Map of 2009. Thailand Government

Singh, V. P. (1992) *Elementary hydrology*: Pearson College Division.

Suwanee Sridhavat Na Ayudhya (1995) The analysis of the soil mechanic properties in each soil series of Thailand.

Vitor Vieira Vasconcelos, Sucharit Koontanakulvong, Chokchai Suthidhummajit, Paulo Pereira Martins Junior, Renato Moreira Hadad (2014) Analysis of Spatial-temporal Patterns of Water Table Change as a tool for Conjunctive Water Management in the Upper Central Plain of the Chao Phraya River Basin, Thailand, Appl Water Sci, DOI 10.1007/s13201-014-0240-4

Rainfall-Runoff-Inundation Simulation with Bias-corrected Satellite Based Rainfall: Case Study Yom River Basin

Teerawat Ram-Indra[1 *], Anurak Sriariyawat[2] and Piyatida Hoisungwan[3]

Abstract Yom River is an upstream branch of the Chao-Phraya River, located in the northern part of Thailand. The upper part of Yom catchment is mountainous area with limited numbers of rainfall stations. Satellite based rainfall is capable for providing information about intensity and spatial distribution of precipitation for the areas that do not have rain gauge stations. However, the satellite based rainfall still needs calibration and validation with existing rainfall stations due to the indirect measurements. Two bias correction methods, i.e. Distribution transformation and Geographical differential analysis, were used for calibrating satellite based rainfall data from Tropical Rainfall Measuring Mission (TRMM) with rain gauged network for temporal and spatial rainfall pattern in Yom river basin. The effectiveness of adjusted rainfall data were justified by streamflow data and inundation areas, which were the results of flood simulation using the rainfall-runoff-inundation (RRI) model. Comparison between the simulation results and observed stream flow data in terms of coefficient of determination (R^2) and normalized root mean square error (NRMSE) were used to validate for effectiveness, while the inundation area were compared with observed flood maps in terms of shape factor.

Keywords *Bias correction, RRI, Satellite based rainfall, TRMM, Yom basin*

Teerawat RAM-INDRA
Graduate student
Department of water resources engineering,
Chulalongkorn University, Thailand

Anurak SRIARIYAWAT
Lecturer, Department of Water Resources Engineering,
Chulalongkorn University, Thailand
Anurak.S@eng.chula.ac.th

Piyatida HOISUNGWAN
Lecturer, Department of Water Resources Engineering,
Chulalongkorn University, Thailandline
piyatida.h@chula.ac.th

Introduction

Floods always occur in Yom river basin and cause regular damage to the people in the areas. During the past, Yom river basin have suffered from the major flood events in years 1995, 1996, 1998, 1999, 2002, 2006 and especially in year 2011. Large areas of Yom river basin were inundated and caused a huge damage of crop production and human lives.

The flood prediction is one of essential non-structural measures to reduce and prevent the disaster damages. The rainfall data are important data for the flood simulation. The quality and quantity of both temporal and spatial coverage of rainfall stations are affected to accuracy of flood simulation. Unfortunately, most of rain gauge stations in Yom river basin are in the plain area, while no rain gauge station is established in the mountainous area. However, the satellite based rainfall is more widely used for flood forecasting but still requires the calibration with rain gauged data for adjusting and screening the bias by using the bias correction process (Pakoksung et.al., 2012). This study focuses on apply two bias correction methods, Distribution transformation and Geographical differential analysis (MRC, 2010), for flood simulation in the Yom river basin by using a Rainfall-Runoff-Inundation (RRI) model (Sayama et.al., 2010; 2012) to estimate streamflow and flood area in Yom river basin.

Study area

The study areas are located in the northern part of Thailand between latitude 19° 25' N to 15° 15' N and longitude 99° 16' E to 100° 40' E., with 23,616 km^2 catchment area that covers 11 provinces (RID, 2004) as shown in Figure 1. The length of the Yom River is about 736 km from upstream to outlet. The topography of the basin are varies from mountainous area in the northern part from Phayao province to Phrae province and floodplain area in the southern part at Sukhothai province to the downstream. The climate have influenced from the Southwest and Northeast monsoon, beside depressions and typhoons from the South China Sea that affect to rainy season in May to October. This causes the rainfall nearly 85% of the whole year. The averaged capacity of the channel along the river is varied about 220-2,000 m^3/s. Daily observed precipitation data for the period 1983 – 2012 are obtained from the Thai Royal Irrigation Department (RID) and Thailand Meteorological Department (TMD) for 25 stations comprising with the stations inside and surrounding Yom river basin as shown in Figure 2.

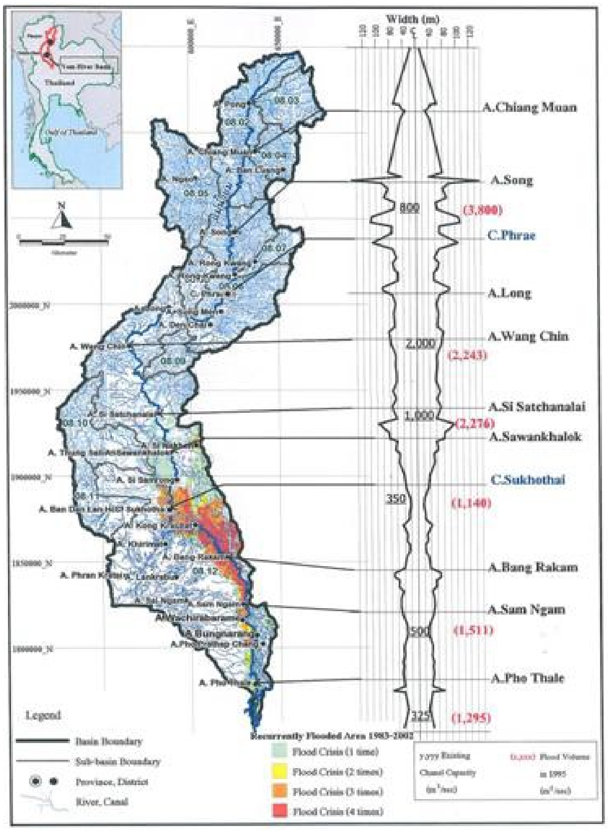

Fig. 1 Yom river basin cross section and capacity (Pakoksung et.al., 2012)

Characteristics of satellite based rainfall in the study

The Tropical Rainfall Measuring Mission (TRMM) was launched in November 1997 as a joint project by NASA and the Japanese Space Agency (JAXA). It was designed to monitor and study tropical rainfall and the associated release of energy that helps to power the global atmospheric circulation, shaping both weather and climate around the globe. The TRMM orbit is non-sun synchronous and initially was at an altitude of 350 km, until the satellite was boosted to 402 km on August 22, 2001. The primary rainfall instruments on TRMM are the TRMM Microwave Imager (TMI), the Precipitation Radar (PR) and the Visible and Infrared Scanner (VIRS). Additionally, the TRMM satellite carries two related EOS instruments: The Clouds and the Earth's Radiant Energy System (CERES) and the Lightning Imaging Sensor (LIS). (NASA, 2006)

This study used TRMM 3B42 V7, while 3B42 is a algorithm purpose to produce TRMM merged with high quality infrared precipitation and root-mean-square precipitation-error estimates. Characteristics of this product are 3-hour temporal resolution and 0.25 by 0.25 degree spatial resolution. The availability data from this TRMM product started from 01-01-1998 to present.

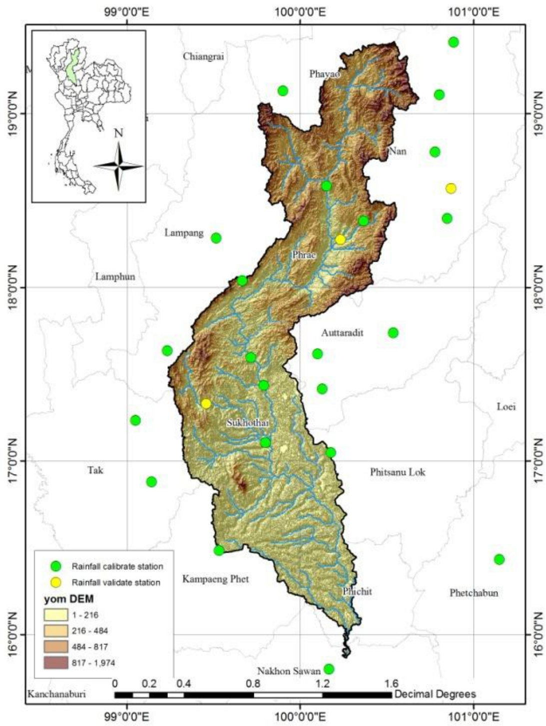

Fig. 2 The Study area and rain gauge stations used in this study

Methodology

Bias correction method

Two bias correction algorithms were applied for this study, i.e. Distribution transformation and Geographical differential analysis (MRC, 2010). Using data from 25 rainfall stations in Yom river basin and around Yom basin to corrected satellite based rainfall. 3 random stations are selected from all stations to validation process as shown in Figure 2. Distribution transformation method is used to determine the statistical distribution relationship between all rain gauged data and satellite based rainfall data at the same grid of rain gauged station on a particular day as the steps of distribution computation as following:

1. Determine mean ratio factor, μ_f, for each day by the corrected mean value of rainfall gauged data, μ_{obs}, divided by mean value of satellite rainfall data, μ_{sat} at each rain gauge station.

$$\mu_f = \frac{\mu_{obs}}{\mu_{sat}} \qquad (1)$$

2. Compute ratio of standard deviations, σ_f, for each day at the same position as done in the previous step by dividing rain gauge standard deviations, σ_{obs}, at particular day with satellite rainfall standard deviations, σ_{sat}.

$$\sigma_f = \frac{\sigma_{obs}}{\sigma_{sat}} \qquad (2)$$

3. After calculating the mean ratio factor and ratio of standard deviations, the corrected satellite rainfall, SAT_c, at all grids of satellite based rainfall data are computed by Eq. 3. If the value of reporting rainfall station are below than threshold that specified a default factor, μ_{fd}, is used for correct the satellite based rainfall data set as Eq. 4.

$$SAT_c = (SAT_o - \mu_{sat}) \cdot \sigma_f + \mu_{sat} \cdot \mu_f \qquad (3)$$

$$SAT_c = SAT_o \cdot \mu_{fd} \qquad (4)$$

Where SAT_o is original TRMM 3B42 rainfall data. This Eq. 3 and Eq. 4 can apply to all grid of satellite at the same day.

Another method for bias correction used in this study is Geographical differential analysis or Spatial bias correction. This method use the bias between rain gauge and satellite rainfall to create error map, which proposes to correct the missing pattern, when compare between rain gauge data and satellite grid data in particular day. The steps are:

1. Calculate the bias between rain gauge station and satellite based rainfall data sets at each station and TRMM grid.

$$\Delta R_{(x,y)} = R_{TRMM\,(x,y)} - R_{obs(x,y)} \qquad (5)$$

Where $\Delta R_{(x,y)}$ is bias value of each station between TRMM grid row X and column Y, $R_{obs(x,y)}$ is observed rain gauge data, and $R_{TRMM\,(x,y)}$, is TRMM 3B42 satellite based rainfall data at the same position as observed rainfall data grid.

2. After calculate the point error data from two data sets, interpolation point error data are computed by using inversed distance to create error map at same spatial resolution of TRMM data.

$$\Delta R_{(x,y)} \rightarrow \Delta R_{(x,y)ip} \qquad (6)$$

3. Subtract the error map, $\Delta R_{(x,y)ip}$, to the uncorrected TRMM data to obtain the spatial bias corrected rainfall, R_{cal}

$$R_{cal} = R_{TRMM\,(x,y)} - \Delta R_{(x,y)ip} \qquad (7)$$

Flood simulation model

The model that used for flood prediction in this study is a two dimension rainfall-runoff-inundation (RRI) model, which is developed by Dr. Takahiro Sayama (Sayama, et al., 2010; 2012; 2013). The model deals with slopes and river channels separately as shown in Fig 6. The river channel is located on the grid cell while the model assumes that both slope and river are positioned within the same grid cell. A channel is discretized as a single vector along its centerline of the overlying slope grid cell. The channel represents an extra flow path between grid cells lying over the actual river course. Lateral flows are simulated on slope cells on a two dimensional basis. Slope grid cells on the river channel have two water depths: one for the channel and the other for the slope (or floodplain). The inflow-outflow interaction between the slope and river is calculated based on different overflowing formulae depending on water-level and levee-height conditions.

Results

Bias correction method

Two bias correction methods are applied to TRMM 3b42 data to reduce the rainfall intensity bias. The correlation between the observed data and bias corrected TRMM 3B42 data for each station are shown in Table 1. The spatial pattern of rainfall from rain gauge data, original TRMM 3B42 data, and two methods of bias correction are presented in Figure 3.

Table 1. Performance evaluation of bias correction-method on monthly rainfall amount

Station		TRMM	Dis. Bias	Spa. Bias
1	R2	0.78	0.81	0.98
	NRMSE	0.2	0.16	0.1
2	R2	0.72	0.79	0.9
	NRMSE	0.2	0.19	0.12
3	R2	0.91	0.95	0.97
	NRMSE	0.11	0.09	0.08

Flood simulation

The result from simulations are compared with observed stream flow data at Y.14 station in terms of coefficient of determination (R^2) and normalized root mean square error (NRMSE) as shown in Table 2.

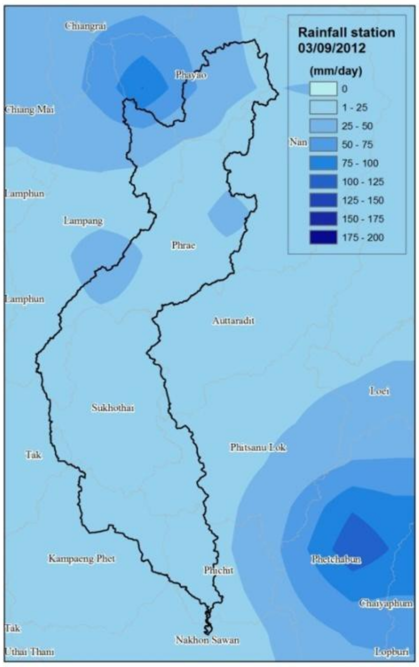

a.) Rain gauge data

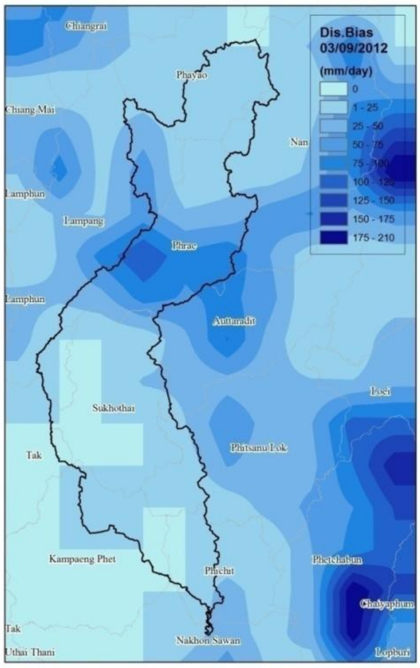

c.) Corrected TRMM 3B42 by Distribution transformation

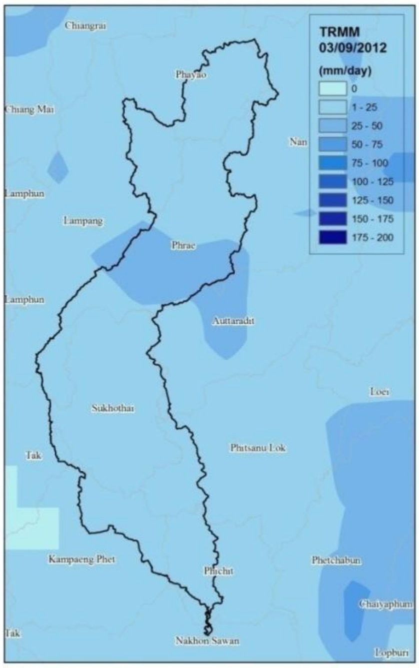

b.) TRMM 3B42

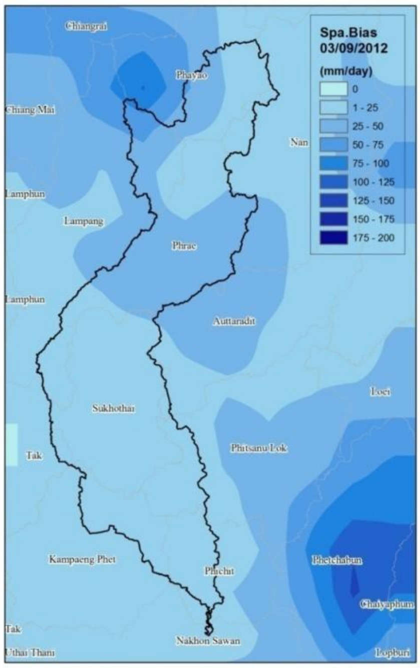

d.) Corrected TRMM 3B42 by Geographical differential analysis

Fig. 3 Comparing daily rainfall by spatial distribution

Table 2. Performance evaluation of bias correction-method by runoff

	IDW	TRMM	Dis. Bias	Spa.Bias
R2	0.70	0.41	0.56	0.69
NRMSE	0.11	0.17	0.13	0.12

The comparison between observed and simulated hydrographs from RRI model at Y.14 station, where is located at the middle of Yom river, are presented in cases of different sources of rainfall, i.e. rain gauge data, TRMM 3B42 data, Distribution transformation, and Geographical differential analysis, as show in Fig. 4, where the starting date is on 1st April 2011, and the end date of simulation is on 31st December 2011.

In this study, the performance of simulation result in terms of flood area is compared the simulation inundation area with satellite photos from Geo-Informatics and Space Technology Development Agency (GISTDA) at the days during crisis, 17th August, 11th September, and 9th October 2011 by computing the shape factor (f) as equation:

$$f = \frac{A_{sat} \cap A_{sim}}{A_{sat} \cup A_{sim}} \qquad (8)$$

where the shape factor (f) is defined as a ratio of the same inundation areas from both satellite image and simulation result (the intersection of A_{sat} and A_{sim}, $A_{sat} \cap A_{sim}$) by the overall inundation area from both sources (the union of A_{sat} and A_{sim}, $A_{sat} \cup A_{sim}$). A_{sat} is inundation area from satellite image data in km^2, and A_{sim} is the inundation area that is the result from simulation. Actually, the shape factor equal to 1 means the simulation is perfectly matched with the observed data (Sriariyawat et.al., 2013). Table 3 present the performance evaluation of bias correction methods by shape factor parameter on the crisis 17th August and 9th October 2011.

Table 3. Performance evaluation of bias correction-methods by shape factor

d/m/y	IDW	TRMM	Dis.Bias	Spa.Bias
170811	0.25	0.25	0.26	0.27
91011	0.35	0.33	0.3	0.36

Conclusions

Precipitation data are important to flood simulation in term of accuracy of intensity and spatial coverage. The rain gauge can provide accurate intensity but unable to collect rainfall in area that difficult to establish for example ocean, mountainous area. Satellite based rainfall can provide a good spatial coverage but the

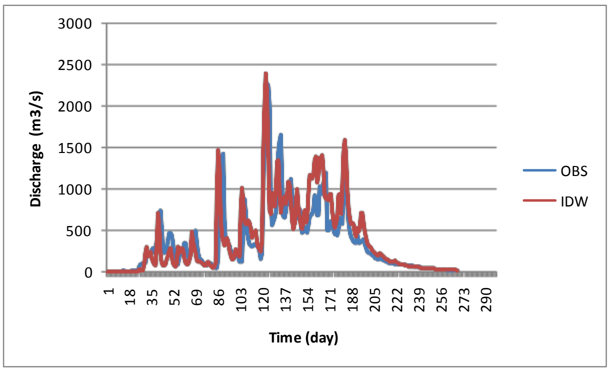

a.) Rain gauge data

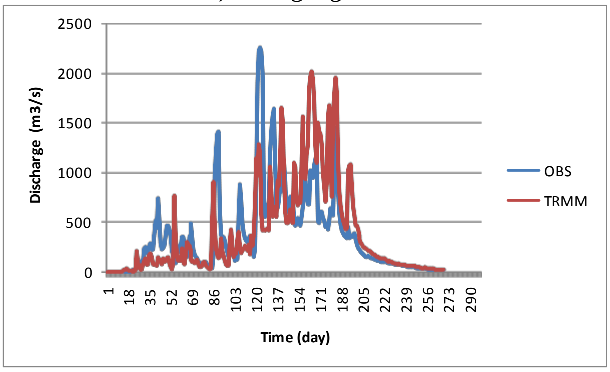

b.) TRMM 3B42

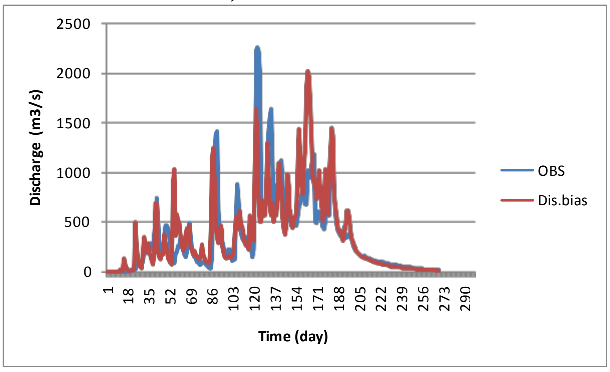

c.) Corrected TRMM 3B42 by Distribution transformation bias correction method

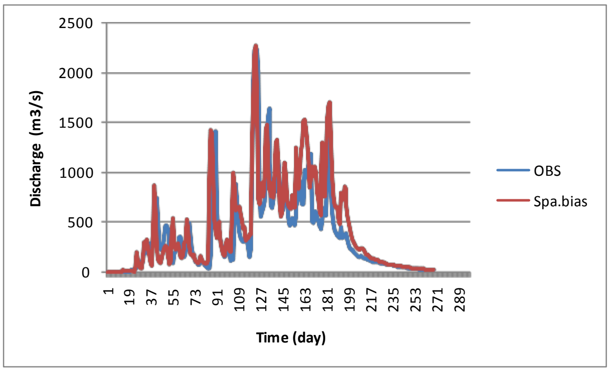

d.) Corrected TRMM 3B42 by Geographical differential analysis bias correction method

Fig. 4 Hydrograph from RRI at Y.14 station in year 2011 method to collect data is not measure rainfall directly thus satellite based rainfall data need to bias correction before use in the study. Distribution transformation bias only volume of rainfall, while Geographical differential analysis includes the spatial pattern of observed rainfall data to the bias correction process. This can be implied that the Distribution transformation has the magnitude of rainfall volume as observed data, but the rainfall pattern would be the same as TRMM, and the Geographical differential analysis gives the result of TRMM bias corrected data more or less the same as observed data in terms of rainfall volume and rainfall pattern.

From the discharge results show the simulation from rain gauge data has more accuracy than the other source of rainfall data. This can be implied that 25 rain gauge stations used in the study are sufficient to use for flood study in Yom river basin instead of using satellite based rainfall data to simulate flood. However, in case that the number of rain gauge station is lower than 25 stations, TRMM will be other choice to consider. When compare between two bias correction methods, Geographical differential analysis are more accurate than Distribution transformation method. It means that the spatial distribution of rainfall has more influence in flood simulation than the rainfall intensity.

Acknowledgement

The study cannot be concluded without satellite rainfall from Tropical Rainfall Measuring Mission (TRMM) staffs of Thai Royal Irrigation Department (RID) and Thai Meteorological Department (TMD) for observed historical rainfall data as well. The research also done under department of water resources engineering, faculty of engineering, Chulalongkorn University.

References

Mekong River Commission, 2010. Bias Correction for Satellite Precipitation Estimation used by the MRC Mekong Flood Forecasting System (Mission Report).

NASA, 2006 Earth Science Reference Handbook Mission TRMM.

Pakoksung, K., Koontanakulvong, S. and Sriaiyawat, A. (2012). Satellite data application for flood simulation.PAWEES 2012 International Conference.

Sayama, T., Fukami.K., Tanaka, S. and Kuniyoshim K, (2010) Rainfall–runoff–inundation analysis for flood risk assessment at the regional scale. Proceedings of the Fifth Conference of Asia Pacific Association of Hydrology and Water Resources (APHW), 568–576.

Sayama, T., Ozawa, G., Kawakami, T., Nabesaka, S. and Fukami, K. (2012). Rainfall-runoff-inundation analysis of the 2010 Pakistan flood in the Kabul River basin" Hydrological Sciences Journal, 57:2, 298-312

Sayama, T., Tatebe, Y. and Tanaka, S. (2013). "Large-scale Flood Simulation with Rainfall-Runoff-Inundation Model in the Chao Phraya River Basin" Journal of Geophysical Research

Sriariyawat, A., K. Pakoksung, T. Sayama, S. Tanaka, and Koontanakulvong, S. (2013). Approach to estimate the flood damage cost in SukhothaiProvince using flood simulation. J. of Disaster Research, 8:3, 406-414

Session B

Participatory Management for Water and Irrigation Project

Can Regional Climate Models provide proxies for sustainable water resources management over data sparse regions?

Shie-Yui Liong[1,2]*, Minh Tue Vu[1] , San Chuin Liew[1] and Srivatsan V Raghavan[1]

Abstract This paper presents applications of regional climate model data as good proxies over some data sparse Southeast (SE) Asia regions. Lack of good quality and/or long record rainfall data are common in SE Asia. This situation leads to challenges in, for examples, deriving reliable storm drainage design curves, assessing flow rate in transboundary catchment, anticipating flow rate for hydropower station and overall effective multiple water resources management. Two applications are discussed in this paper: (1) storm drainage design (Intensity-Duration-Frequency curves), and (2) transboundary catchment water resource management. The proposed proxy data come from dynamically downscaled reanalyses data for the domain of interest. In this study, a Regional Climate Model (RCM), Weather Research and Forecasting (WRF), was used for the entire SE Asia. The proxy data for the current climate were derived from WRF, for the SE Asia domain at a high spatial resolution of 30 × 30 km. For data sparse sites it is absolutely crucial to apply regional frequency analysis by using downscaled reanalyses data as proxies to derive IDF curves with longer records. The proposed approach has been successfully demonstrated and implemented on Singapore, Jakarta and Vietnam regions. Another issue is the trans-boundary problem where data sharing between two countries is often a challenge. This paper discusses scenarios over a transboundary catchment, Da River catchment, where upstream lies in the Chinese territory while the downstream lies in the Vietnamese territory. The Soil and Water Assessment Tool (SWAT) model was applied for hydrological simulations using the output derived from the WRF model. The findings suggest that precipitation data originated from downscaling are very useful proxies for the applications discussed herein.

Keywords *Dynamical downscaling, Proxy data, IDF, Trans-boundary*

1. S.-Y. Liong, M.T. Vu, S.C. Liew, S.V. Raghavan
Tropical Marine Science Institute
National University of Singapore
tmslsy@nus.edu.sg

2. S.-Y. Liong
Willis Research Network
Willies Re Inc.,
London, United Kingdom

Introduction

Rapid urbanization in Southeast (SE) Asia has given rise to many challenges to infrastructural designs and planning with respect to climate impacts. One of them is severe flooding. Jakarta (the capital of Indonesia), for example, was flooded in February 2007 up to 5m in some parts of the city and it was reported that 60% of the city was inundated for 2 weeks. The area of the city has nearly doubled in the last decade. Aside from less strict policy implementation, the city does not have a long rainfall record that is very critical for deriving storm drainage design curves, the Intensity-Duration-Frequency curves. Similarly, when data sharing in transboundary regions is an issue, the country in the downstream end is challenged with the assessment of flow rate originating from the upstream catchment lying in another country. Southeast Asia, being one of the regions strongly affected by climate change, faces the impacts of a changing climate in some of the hydrological challenges mentioned above. Developing IDF curves for SE Asia can be challenging especially for data sparse sites as well as regions that are experiencing rapid urbanization. Many of these poorly gauged regions are also among regions that are highly vulnerable to climate change. One of the anticipated changes is the increase in extreme rainfall intensities and their respective frequencies. The increase in extreme rainfall requires an update on the return periods and intensities of the IDF curves that in turn necessitates larger drainage dimension.

In this study, a Regional Climate Model (RCM), Weather Research and Forecasting (WRF), was used to study hydrological applications over some regions of SE Asia. The proxy data were derived from WRF (uses over places of data scarcity), driven by the European reanalyses data (ERA), for the SE Asia domain at a high spatial resolution of 30 × 30 km.

Model, data and methodology

Weather Research and Forecasting Model

Developed at the National Center for Atmospheric Research (NCAR) in the USA, the Weather Research and Forecasting (WRF) Model is suitable for a broad spectrum of applications across scales ranging from meters to thousands of kilometers. WRF allows researchers the ability to conduct simulations reflecting either real data or idealized configurations. The WRF software has a modular, hierarchical design that provides good portability and efficiency across a range of foreseeable parallel computer architectures. The model incorporates advanced numeric and data-assimilation techniques, a multiple nesting capability and numerous state-of-the-art physics options. Other than applications of weather forecasting, the model has found wide applications in climate research. Additional details can be obtained from http://www.wrf-model.org. Data obtained from this model are used as 'proxies' in this study.

Soil Water Assessment Tool (SWAT)

SWAT is a river basin scale model, developed by the United States Department of Agriculture (USDA) - Agriculture Research Service (ARS) in early 1990s. It is designated to work for a large river basin over a long period of time. Its purpose is to quantify the impact of land management practices on water, sediment and agriculture chemical yields with varying soil, land use and management conditions. Detailed information and several related publications are available at http://swatmodel.tamu.edu. SWAT version 2005 with an ArcGIS user interface is used in this paper.

ReAnalysis Data -- ERA40 and ERA-Interim

The ERA40 reanalyses (Uppala et al., 2005) provide information of climate variables every six hours, with a horizontal resolution of 2.5º × 2.5º and 23 vertical levels. The data cover more than 40 years (1957 to 2002). Most of the variables are available at a resolution of 2.5º × 2.5º on a regular latitude and longitude grid. The ERA40 reanalyses use a global spectral grid model and assimilate part of the observational data from a wide variety of observed sources. Details of the reanalyses project and this categorization scheme can be found in the aforementioned journal article. Additional details can be obtained from: www.ecmwf.int/research/era/. ERA-Interim reanalyses are a higher resolution reanalyses available from 1989-present, in preparation for the next-generation extended reanalyses to replace ERA40. ERA-Interim (Dee et al., 2011) was recently backdated to a decade, from 1979, and it continues to be updated forward in time. ERA-Interim products are also publicly available on the ECMWF Data Server, at a 1.5° resolution. Additional details can be obtained from: www.ecmwf.int/research/era/.

Climatic Research Unit Data

Developed at the Climatic Research Unit (CRU) at the University of East Anglia, UK), the CRU TS version 3.0 dataset is used in this study. It comprises monthly grids of observed climate, for the period 1901-2006 covering only the global land surface at 0.5° × 0.5° horizontal spatial resolution. Precipitation and Temperature variables from the simulations of the WRF are compared against this data over the period of 1961-1990 and 1980 - 2010. Further information on these datasets is available at http://www.cru.uea.ac.uk/cru/data.

Dynamical Downscaling Methodology

In this study, the dynamical downscaling is performed over the Southeast Asia region. The WRF was driven at a 30 × 30 km resolution by ERA40 Global Reanalyses from 1961 – 1990 and ERA-Interim for current climate 1980-2010. Dynamical downscaling was first performed to obtain high-resolution climate outputs. Firstly, the performance evaluation of WRF/ERA40 (WRF model driven by ERA40), for the study region (Figure 1) was done by comparing the simulation results with the CRU gridded observation data 1961 – 1990. As shown in Figure 1, the overall simulated mean daily precipitation of WRF/ERA40 compared reasonably well with CRU, though some sub-regional biases exist. Since the scope of the paper is not in evaluating the models, the figures have been presented for an idea of how good the simulation of the model is when compared to observations. Similar study has been done for the ERA-Interim period 1980-2010.

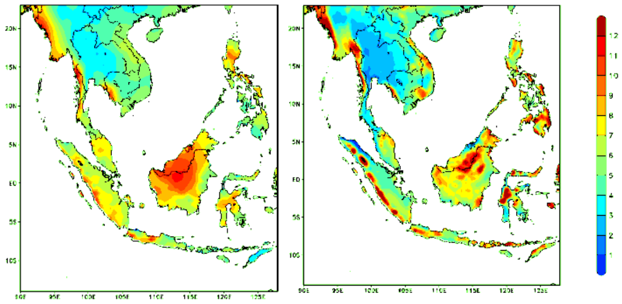

Fig. 1 Mean Annual Precipitation (mm/day): 1961 – 1990 (left) CRU (right) WRF/ERA40

Proxy rainfall data to derive IDF curves using regional frequency analysis

Analytical methods of hydrologic frequency analysis must be used to extrapolate beyond the range of data (e.g. 50 years of record) and estimate the 100-year return period peak flow. Even when analytical methods are used, the reality is that we are still estimating the size of 100-year event from 50 years of data. Most monitoring stations have a much shorter record. If we are uncomfortable with estimating the 100-year event based upon 50 years of data, how confident are we in estimating it from 15 years of data? (Tate, 1995). While estimates of flood return periods can be made with relatively short periods of records, the associated confidence level in the flood frequency statistics is much higher with a longer period of data (The Comet Program, 2010). For example, to estimate a 10–year flood with no more than a ±10 percent error, one would need 90 years of record. If a ±25 percent error is acceptable, then only 18 years of record is needed. Table 1 presented the length of data record needed to be within either ±10 percent or ±25 percent errors for the 10–, 25–, 50–, and 100–year floods. For data sparse sites it is absolutely crucial to apply regional frequency analysis by using downscaled reanalyses data as proxy to derive higher confidence level IDF curves with longer records. The proposed approach (Liong et al., 2014) has been successfully demonstrated and implemented on Singapore and Jakarta. This paper continues exploring its robustness on Vietnam regions.

Table 1. Guidelines for Length of Data Record vs. Expected Error Rate (USGS/The Comet Program, 2010)

Return Interval	± 10 % Error Level (years of record)	± 25 % Error Level (years of record)
10-year	90	18
25-year	105	31
50-year	110	39
100-year	115	48

With rapid urbanization in Southeast Asia, often, sufficiently long rainfall record to derive design curves (IDF) for storm drainage are not available. In this paper, the application of downscaled reanalyses ERA-Interim as proxy data to provide longer records for regional frequency analysis to facilitate the derivation of higher confidence level IDF curves is proposed.

Brief Description of Study Region, Red River Delta, Vietnam

Vietnam is located in Southeast Asia, bounded between the latitudes of 8°N to 23°N and longitudes of 102°E to 109°E. The total land area occupies 330,992 km^2. Vietnam has a 1400 km borderline to the North with China, 2067 km with Laos and Cambodia to the West. The coast line of 3260 km covers the East and the South. Apart from 2 offshore archipelagos, Hoang Sa (Da Nang province) and Truong Sa (Khanh Hoa Province), Vietnam also has a system of coast 3000 big and small islands with total area of more than 1600 km^2.

Red river delta (Figure 2) is the delta region with low topography over which lies Hanoi, the capital of Vietnam. During the winter or dry season, extending roughly from November to April, the northeast monsoon winds usually blow from the northeast along the China coast and across the Gulf of Tonkin. The Red River Delta area is 5,540 km^2. Annual rainfall strongly varies over the Red river area in a range 1200-2500 mm/year.

A 31 years daily record from 1980 – 2010 of the 7 Stations (Figure 3; Table 2) was selected for the analysis.

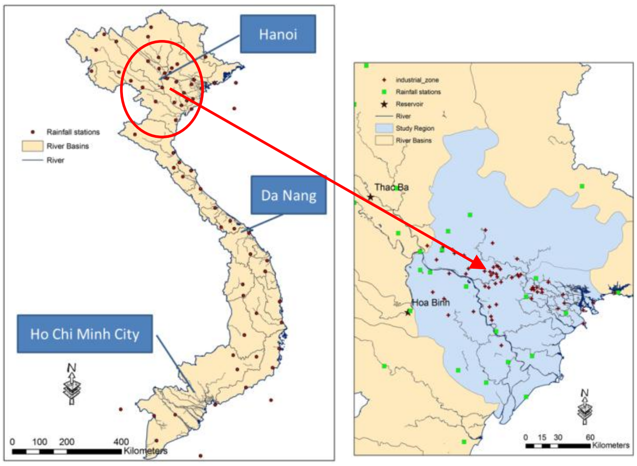

Fig. 2 Study Area, Red River Delta

Table 2. List of rainfall stations used in the analysis

Station	Longitude	Latitude	Elevation (m)
Thai Nguyen	105.83	21.60	36
Tam Dao**	105.65	21.47	897
Vinh Yen	105.60	21.32	10
Viet Tri	105.42	21.30	17
Ba Vi	105.42	21.15	20
Son Tay	105.50	21.13	16
Hanoi	105.80	21.02	5

*** The approach is sensitive to Topography, thus, Tam Dao Station is being taken out from the analysis.*

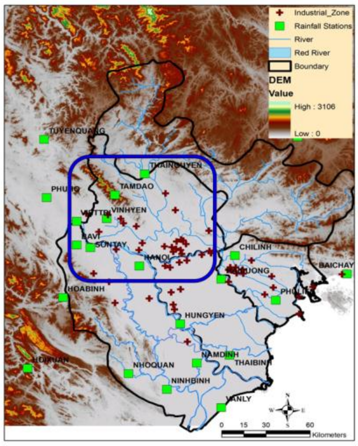

Fig. 3 Rainfall Stations (green square) at Red River Delta

As Red River Delta is a data sparse region and there are no IDF curves for the region, deriving IDF curves using longer data record is essential for drainage design, thus for flood analysis. In this study, Regional Frequency Analysis approach is used as proxy to derive higher confidence level IDF curves using downscaled Reanalyses datasets. The proposed approach has been successfully demonstrated and implemented on Jakarta and Singapore regions (Liong et al., 2014; Liu et al., 2014). Proof-of-Concept of the approach using

Singapore Stations is briefly discussed in the next section.

Proof-of-Concept of Proposed Approach using Four (4) Meteorological Stations in Singapore

The approach (Liong et al., 2014) was successfully applied on 4 Meteorological Stations (Tengah, Seletar, Paya Lebar and Changi Stations) in Singapore (Figure 4). The 4 stations have a complete length of 31 years (1980 – 2010) of datasets needed for this study which will be used to compare with the Depth-Duration-Frequency (DDF) derived from WRF driven by Reanalyses for same record length and period

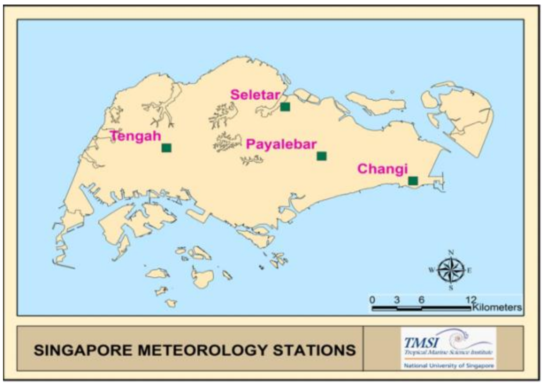

Fig. 4 Four Meteorological Stations in Singapore

Firstly, the observed data from 1980 – 1994 for the 4 Meteorological stations were used for regional frequency analysis to derive the regional Depth-Duration-Frequency (DDF 15) for 15 years. The same record length and period were extracted from downscaled reanalyses data to derive regional WRF/ERAI DDF15. Subsequently, the two DDFs were compared to obtain bias correction equations (Figure 5). The bias correction equation obtained is then used to bias correct WRF/ERAI DDF 31 (31 years; 1980 – 2010) derived from reanalyses data (The results of WRF/ERAI are not shown here due to brevity, but are comparable to WRF/ERA40, shown in Figure 1).

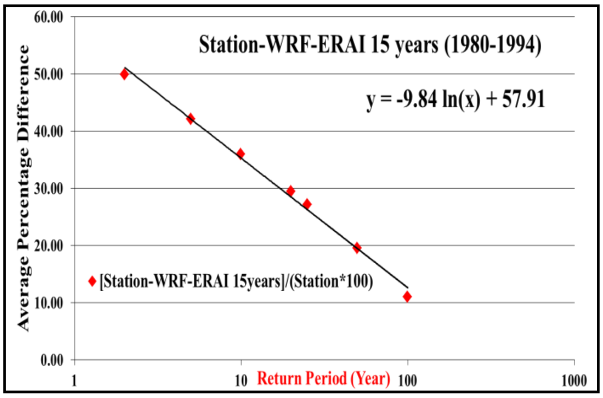

Fig. 5 Singapore Regional DDF (15) vs. Regional WRF/ERAI DDF (15): Percentage Difference Bias Correction Equation (1980 – 1994)

Lastly, the observed data from 1980 – 2010 for the 4 Meteorological stations were used to derive regional DDF31 for 31 years. The regional DDF31 was compared with the bias corrected regional WRF/ERAI DDF31 as shown in Table 3 and the percentage difference from the comparison were tabulated in Table 4. The comparison results from the proof-of-concept method are significant as they show the percentage difference of 10 – 15%, which is acceptable (see Table 1).

Table 3. Singapore Regional DDF (31) vs. Bias Corrected Regional WRF/ERAI (31): 1, 2 and 3-day Storm Duration (1980 – 2010)

	Difference (%)	Return Period (Year)						
		2	5	10	20	25	50	100
Station	1-day	116.6	158.7	190.2	223.5	234.8	271.6	311.7
WRF-ERAI	1-day	104.2	138.8	163.2	189.2	198.1	228.2	262.4
%		10.6	12.5	14.2	15.4	15.6	16.0	15.8
	Difference (%)	Return Period (Year)						
		2	5	10	20	25	50	100
Station	2-day	151.4	203.2	240.2	277.8	290.1	329.7	371.1
WRF-ERAI	2-day	139.8	177.4	206.5	239.7	251.6	292.8	342.1
%		7.7	12.7	14.0	13.7	13.3	11.2	7.8
	Difference (%)	Return Period (Year)						
		2	5	10	20	25	50	100
Station	3-day	173.7	231.9	272.0	311.6	324.4	364.6	405.7
WRF-ERAI	3-day	171.1	209.9	238.6	270.6	281.8	320.4	365.5
%		1.5	9.5	12.3	13.2	13.1	12.1	9.9

Applying Proposed Approach on Six (6) Stations in Red River Delta

The observed data from 1980 – 1994 for six (6) stations (Figure 3) were used for regional frequency analysis to derive the regional DDF (15) for 15 years. The same record length and period were extracted from downscaled Reanalyses data to derive regional WRF/ERAI DDF (15). Subsequently, the two DDF were compared to obtain the bias correction equation as shown in Figure 6. By assuming there is no data from 1980 - 2010, the bias correction equation obtained is then used to bias correct WRF/ERAI DDF (31) (31 years; 1980 – 2010) derived from Reanalysis data.

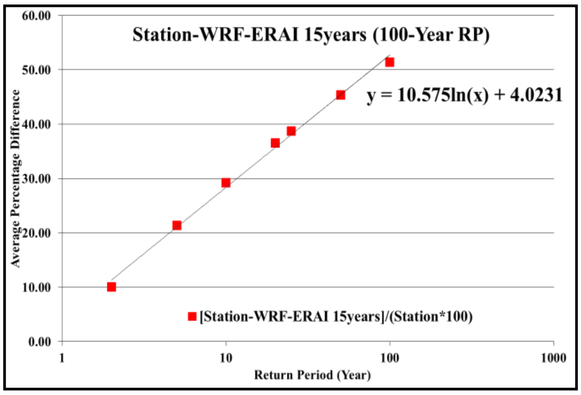

Fig. 6 Red River Delta (Region 1) Regional DDF (15) vs. Regional WRF/ERAI DDF (15): Percentage Difference Bias Correction Equation (1980 – 1994)

To proof that the proposed approach is robust, observed data from 1980 – 2010 for the six (6) stations were used to derive regional DDF (31) for 31 years. The regional DDF (31) was compared with the bias corrected regional WRF/ERAI DDF (31) as shown in Table 5 and the percentage difference from the comparison were tabulated in Table 6.

Table 5. Regional DDF (31) vs. Bias Corrected Regional WRF/ERAI (31): 1, 2 and 3-day Storm Duration (1980 – 2010)

	Difference (%)	Return Period (Year)						
		2	5	10	20	25	50	100
Station	1-day	120	170	213	262	280	341	414
WRF-ERAI	1-day	125	183	229	281	299	361	436
%		-4.5	-7.5	-7.6	-7.0	-6.7	-5.9	-5.4

	Difference (%)	Return Period (Year)						
		2	5	10	20	25	50	100
Station	2-day	157	226	284	349	372	452	545
WRF-ERAI	2-day	163	234	291	356	380	460	558
%		-4.0	-3.3	-2.6	-2.1	-2.0	-1.9	-2.4

	Difference (%)	Return Period (Year)						
		2	5	10	20	25	50	100
Station	3-day	177	253	316	388	414	503	607
WRF-ERAI	3-day	189	271	338	415	442	537	651
%		-7.3	-7.4	-7.1	-6.8	-6.7	-6.8	-7.3

Table 6. Regional DDF (31) vs. Bias Corrected Regional WRF/ERAI (31): Average Difference (%)

	1-Day	**2-Day**	**3-Day**
Average Difference (%)	- 6.4	- 2.6	- 7.1

The comparison results of the approach on six (6) stations in Red River Delta show a percentage difference of about 5% which is very good. The proposed approach demonstrates the usefulness of proxy data from regional climate model, WRF, in this case, to resolve the much needed rainfall data for storm drainage design curves for many regions in SE Asia and other part of the world. Shorter storm duration can be performed for catchment with shorter than 6-hour time of concentration. Nguyen et al. (2007) demonstrated an approach as to how to correlate sub-daily IDF information from daily IDF data.

Trans-boundary proxy rainfall data for river flow

Background of Da River Basin, Transboundary Catchment China-Vietnam

Another issue requiring proxy data in the place of observed data is the trans-boundary catchment where data sharing between two countries is a challenge. Here, again, downscaled reanalyses data are demonstrated to be excellent proxies for 'missing' rainfall' data. This paper shows a transboundary catchment, Da River catchment, where upstream is in the China's territory while downstream is in the Vietnam territory. A SWAT model is applied; upstream region's rainfall data are derived from the WRF model and applied, as proxies, to rainfall stations in China's catchment. Three downstream flow-gauging stations are used as performance measures in the model calibration, validation and verification.

Water resources management is very crucial in many countries and draws an added importance near the border regions between countries. Due to different governmental policies, conflicts arise in sharing of the water resources, more so when the advantage is more for the upstream user country of these water resources. Research by Lu and Siew (2006) showed that the series of dam constructions in China are affecting water discharge and sediment flux over Lower Mekong River over the last decades. For example, when availability of water resources needed to be assessed over northern Vietnam, the data from upstream region that lies in China's territory may not be available, as the water quantity over the downstream region over Vietnam depends on the flow from the upstream China part. This is a clear case of a trans-boundary problem, the issue cited earlier. Hence, this paper also describes an approach to resolve data requirement issues of a trans-boundary nature in managing water resources by employing a hydrological model, the Soil and Water Assessment Tool (SWAT) that uses data available from the internet with implications for climate change applications.
The study region over the Da River originates from the Yunnan Province in China and flows downstream through mountainous regions, crosses the border of China-Vietnam and joins as a tributary of the Red River in Vietnam. Due to its importance in the Vietnam hydropower system, Da River has been listed as the first in hydropower generation. The need for modeling comes with many challenges, such as (1) how to manage the water sources coming from China; (2) what will be the impact if there are dams constructed in China that may affect the quantity of water flowing into Vietnam. Location of the study region is shown in Figure 7.

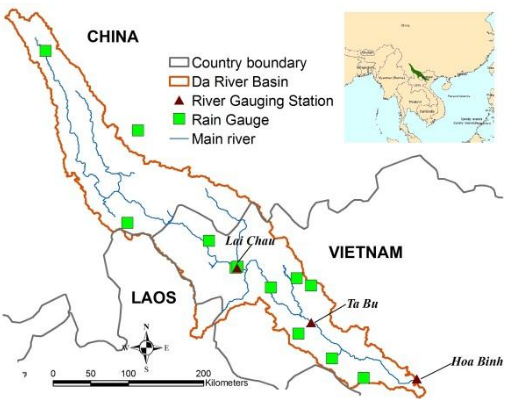

Fig. 7 Da river basin and the distribution of rainfall stations, river gauging stations

Methodology

In this study, with the availability of the meteorology variables at the downstream part of the basin in Vietnam, two scenarios, with respect to data availability over upstream China, are considered. Scenario 1: we use the limited data made available from upstream China. Scenario 2: we assume that China data in Scenario 1 is not available for the purpose of hydrological modeling; we then substitute the upstream region information with the proxy data stemming from regional climate model WRF driven by ERA40 (WRF/ERA40) reanalyses data. For the modelling part, we conduct calibration for these scenarios to showcase that the validation of the regional climate model in the latter case can be used as a proxy for the missing data in upstream catchment. This study is carried out for present day climate from 1961-1987.

The experimental study consists of four steps: (1) set up the SWAT model for the Da River basin; (2) calibrate and validate the SWAT model using observed rainfall data from both China and Vietnam for Hoa Binh station for the periods 1961-1980 and 1981-1987 respectively, the first year used as warm up period. Lai Chau and Ta Bu station (at upstream of Hoa Binh station) are the two different stations in Vietnam at which the verification of the SWAT simulated discharge are done to establish model performance; (3) substitute the China station rainfall with the proxy data (WRF/ERAI) from the regional climate model WRF and re-calibrate; (4) analyse the result from both scenarios.

Results

The Nash-Sutcliffe Efficiency (NSE) (Nash and Sutcliffe, 1970) and the Coefficient of Determination R^2 that is defined by squared value of the coefficient of correlation according to Bravais-Pearson, are used as the benchmarking indices for the simulation of runoff. The use of these correlation indices in hydrology has been discussed by Krause et al., (2005). The R^2 ranges from 0 to 1 with 1 as the best fit. The NSE shows the skill of the estimates relative to a reference and it varies from negative infinity to 1 (perfect match). The NSE is considered to be the most appropriate relative error or goodness-of-fit measures available owing to its straightforward physical interpretation (Legates and McCabe, 1999).
Considering the Scenario 1, the results for the daily time scale calibration at the Hoa Binh station for the 20 years period 1961-1980 show that the NSE and R^2 for the calibration part are quite promising with values of 0.87 and 0.89 respectively (Figure 8, Table 7). This is taken as an indicator for very good performance as such values have been obtained for modelling at daily time scale rainfall information (which are usually highly variable in space and time) compared to monthly time scales. The validation over a different period 1981-1987 also holds well with about the same values for NSE and R^2. The benchmarking indices at Ta Bu and Lai Chau show values of R^2 higher than 0.8 which again indicates good model performance. As Ta Bu is located between Lai Chau and Hoa Binh, it is understandable that the benchmarking index is reasonably higher than that at Lai Chau lying most upstream in Vietnam territory. The benchmarking indices, R^2 and NSE, show values greater than 0.8 and 0.6, respectively (Table 7), at Lai Chau gauging station also marks a good model performance.

Table 7. Benchmarking indices for daily discharge for 2 simulation scenarios:

Sta.	Scenario 1				Scenario 2			
	Calibration period		Validation period		Calibration period		Validation period	
	R^2	NSE	R^2	NSE	R^2	NSE	R^2	NSE
Hoa Binh	0.89	0.87	0.89	0.87	0.83	0.81	0.79	0.77
Ta Bu	0.88	0.85	0.88	0.85	0.81	0.80	0.77	0.74
Lai Chau	0.81	0.69	0.82	0.64	0.60	0.46	0.53	0.34

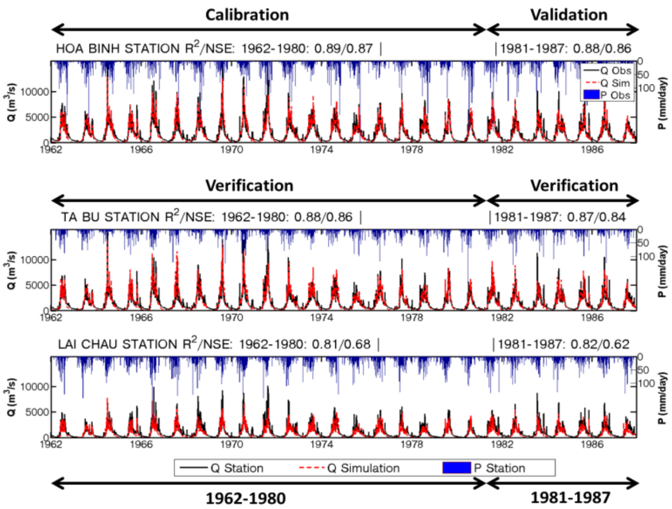

Fig. 8 Scenario 1 using observed rainfall from 3 China stations and observed rainfall from 9 Vietnam stations: - Used as input to SWAT model to simulate stream flow.

Considering the Scenario 2, that applied the WRF/ERA40 output, bilinearly interpolated to upstream China stations, as a proxy to replace its observed station data, the SWAT simulations indicate that the R2 and NSE values are less than their counterparts in Scenario 1, but yet showcasing good model performance with these calibration indices higher than 0.8 (See Figure 9 and Table 7). Ta Bu and Lai Chau locations also have slightly smaller values than Scenario 1, but with reasonable values of indices. This suggests that though the benchmarking indices might be lower than when using observed station data, the RCM derived output can be used as proxies, especially over regions where there are scanty/hardly any data.

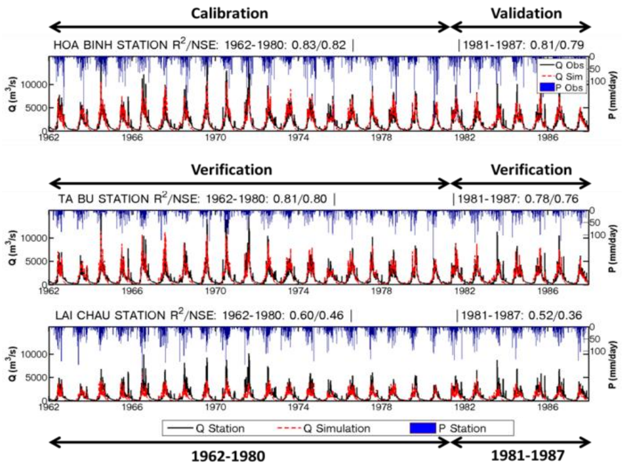

Fig. 9 Scenario 2 using WRF/ERA40 to replace rainfall from 3 China stations and remain observed rainfall from 9 Vietnam stations – Used as input to SWAT model to simulate stream flow.

The Flow Duration curve (FDC) is a cumulative frequency curve that shows the percent of time during which specified discharges were equaled or exceeded in a given period (Searcy, 1959). By using FDC, the hydrology model simulation is able to show the distribution of high and low flow as compared to observed station data. The FDC of 3 gauging station: Hoa Binh, Lai Chau and Ta Bu are displayed in Figure 10 for both scenario 1 (blue dotted curve) and scenario 2 (red dotted curve), for calibration and validation period. The SWAT model simulation for both scenarios shows similarity FDC. The low flow was resolved quite well at Hoa Binh and Ta Bu with the first 60% of time the discharge was equaled or exceeded. The high flow simulated by the hydrology model however was underestimated the station data. The hydrology model shows bias FDC at Lai Chau station which underestimated the observed data.

In order to see the effect of seasonal interannual flow, the discharge annual cycle at the 3 different station locations considered is shown in Figure 11 between observed, scenario 1 (blue) and scenario 2 (red). For scenario 1, the discharge at Hoa Binh and Ta Bu station are in close agreement against the station discharge data. Only at Lai Chau location, both scenarios show underestimation. So it implies that the SWAT derived runoff using the station rainfall data from Chinese upstream is not as good as the SWAT discharge over the downstream part in Vietnam. This could be due to considering only 3 rainfall stations over China (whatever was available for the study) whereas relatively more stations (9) were available from the Vietnam regions for this study. Similar result can be inferred for scenario 2, which uses the WRF/ERA data as proxy. The simulations are therefore consistent in both scenarios because Scenario 2 substitutes RCM data at the same 3 stations over China as considered in Scenario 1. What remains to be seen as usefulness is the application of the RCM data is as good as using the observations and hence the usage of RCM data as proxies stands justified.

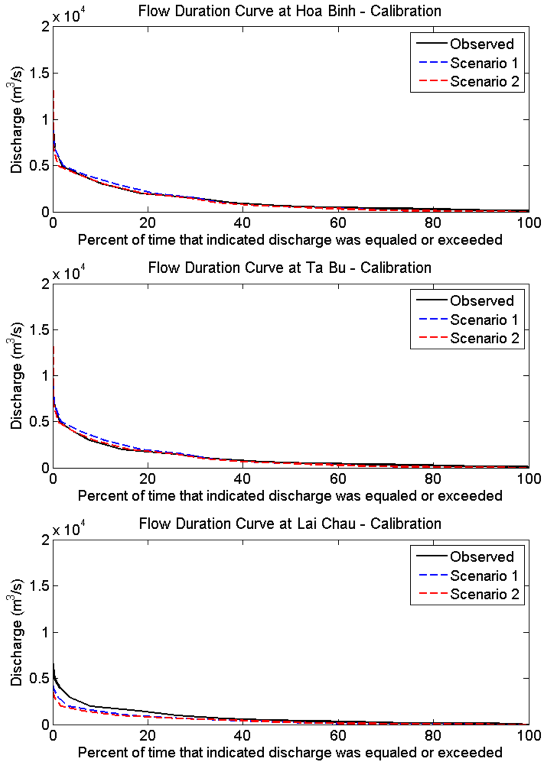

Fig. 10 Flow Duration Curve at 3 different locations (Calibration). From top to bottom: Hoa Binh, Ta Bu and Lai Chau.

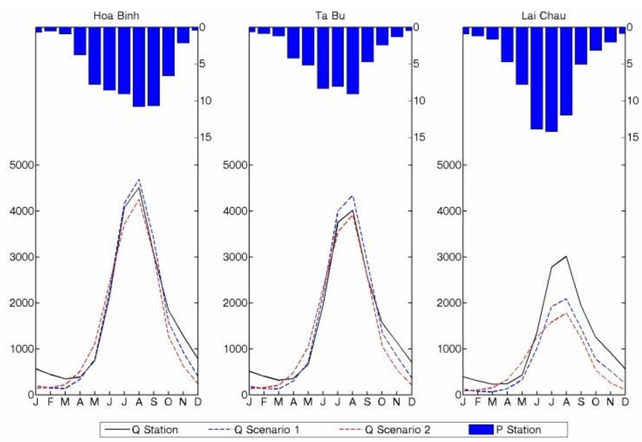

Fig. 11 Annual cycle of Stream flow at 3 different locations: from left to right: Hoa Binh, Ta Bu and Lai Chau, for the study period 1961-1987.

Discussion for Trans-boundary issue

The application of regional climate model data for hydrological studies has been practiced over the past few years owing to the 'added value' in high resolution climate simulations, compared to a coarse resolution coming from global climate models. Yet, the trans-boundary study that adequately uses this RCM information comes to an extra 'added value' as it solves the issue of data sharing between countries. Although the WRF model might not, in its entirety, be the best substitute for station data. Differences in the stream flow intensities are sort of model biases induced by the different rainfall outputs from the climate models that were used as inputs for driving the hydrological model. Since the overall present day signature of the stream flow simulations were satisfactorily derived using the SWAT model, it also places confidence that the RCM outputs can therefore be used to assess future stream flow using the changes in climate model derived future rainfall. Studies of Vu et al. (2012), Vu (2013), Raghavan et al. (2014), Liew (2013) and Liew et al. (2013) suggest the effectiveness of applying high resolution regional climate model outputs for impact studies at both regional and local scales, for impacts related to both basin scale water management and deriving IDF curves.

What these results showcase is that there are higher uncertainties in the regional climate model simulations at sub-regional scales. This also suggests that even higher resolutions (of about 5-10 km) might be necessary to improve the simulations over such smaller areas, but still remind us the need for dense observational networks against which the model performance can be further evaluated. Though further improvements might be necessary in the model simulations, the results suggest that the climate model outputs are reasonably good enough to be used for stream flow simulations. This provides a first-cut understanding of the use of these output and their usefulness for hydrological studies which have implications of assessment of changes in hydrological responses in a future climate. Given that many models will be used for climate projections, it stays with the modelling community to constrain uncertainties in models such as their physics and dynamics, incorporation of complex processes, atmospheric chemistry and simulations of extreme events, to make climate projections more reliable and useful for impact studies. While these improvements are underway, an 'ensemble' approach of using multiple GCM/RCM realizations for such studies will be more appropriate.

Conclusions

To this end, the applications of regional climate model results for two different climate applications, one for deriving IDF curves and the other, for a trans-boundary hydrological study, have been presented. It is evident that these high-resolution climate model data have good potential to be used as 'proxies' for observed data and find wide applications in engineering designs and hydrological applications, such as droughts, multiple reservoirs water transfer. The findings from the study also stress the need for more high resolution data derived from regional climate models.

References

Dee DP., Uppala SM., Simmons AJ., Berrisford P., Poli P., Kobayashi S., Andrae U., Balmaseda M.A., Balsamo G., Bauer P., Bechtold P., Beljaars ACM., van de Berg L., Bidlot J., Bormann N., Delsol C., Dragani R., Fuentes M., Geer AJ., Haimberger L., Healy S.B., Hersbach H., Hólm EV, Isaksen L., Kållberg P., Köhler M., Matricardi M., McNally AP., Monge-Sanz BM., Morcrette JJ., Park BK., Peubey C., de Rosnay P., Tavolato C., Thépaut JN. and Vitart F. (2011). The ERA-Interim reanalysis: configuration and performance of the data assimilation system. Quar. J. Royal. Met. Soc., 137, 553-597.

Krause P., Boyle DP. and Bäse F. (2005). Comparison of different efficiency criteria for hydrological model assessment. Adv. Geosci., 5, 89-97.

Legates DR. and McCabe GJ. (1999). Evaluating the use of "goodness-of-fit" Measures in hydrologic and hydroclimatic model validation. Water Resource Res., 35(1), 233-241.

Liew SC. (2013). A novel approach using regional climate model, to derive present and future intensity-duration-frequency curves, Phd Thesis, Dept. of Civil and Environmental Engineering, National University of Singapore.

Liew SC., Raghavan VS. and Liong SY. (2013). How to construct future IDF curves, under changing climate, for sites with scarce rainfall records?, Hydrol. Proc., 28(8):3276-3287.

Liong SY., Liew SC., Vu MT., Raghavan SV. (2014). Proxy Data from RCM Reanalyses: A Breakthrough for Drainage Design and Catchment Modelling, SATEC, China.

Liu J., Doan CD., Liong SY., Sanders R., Dao AT., Fewtrell T. (2013). Extreme Rainfall Events in Jakarta: Analyzing, Assessing by Regional Frequency Analysis with L-moments. Submitted. J. Natural Haz.

Lu XX. and Siew RY. (2006). Water discharge and sediment flux changes over the past decades in the Lower Mekong River: possible impacts of the Chinese dams. Hydrol. Earth Syst. Sci., 10(2), 181-195.

Nash JE. and Sutcliffe JV. (1970). River flow forecasting through conceptual models, Part 1 – A discussion of principles. J. Hydrol., 10(3), 282-290.

Nguyen VTV., Nguyen TD. and Cung A. (2007). A statistical approach to downscaling of sub-daily extreme rainfall processes for climate-related impact studies in urban areas, Water Sci. Tech.: Water Supp., 7(2), 183–192. IWA Publishing. doi:10.2166/ws.2007.05

Raghavan VS., Vu MT. and Liong SY. (2014). Impact of climate change on future stream flow in the Dakbla river basin. J. of Hydroinformatics, 16(1), 231-244.

Tate KW. (1995). Exactly what is a 100-year event? Rangeland Watershed Program, The Comet Program: Flood Frequency Analysis, University Corporation for Atmospheric U.C. Cooperative Extension and USDA Natural Resources Conservation Service.

The Comet Program. (2010). Flood Frequency Analysis, University Corporation for Atmospheric Research (UCAR).

Uppala SM., KÅllberg PW.,Simmons AJ., Andrae U., Bechtold V. Da Costa, Fiorino M., Gibson JK., Haseler J., Hernandez A., Kelly GA., Li X., Onogi K., Saarinen S., Sokka N., Allan RP., Andersson E., Arpe K., Balmaseda MA., Beljaars ACM., Berg L. Van De, Bidlot J., Bormann N., Caires S., Chevallier F., Dethof A., Dragosavac M., Fisher M., Fuentes M., Hagemann S., Hólm E., Hoskins B. J., Isaksen L., Janssen PAEM., Jenne R., McNally AP., Mahfouf JF. , Morcrette JJ., Rayner NA., Saunders RW., Simon P., Sterl A., Trenberth KE., Untch A., Vasiljevic D., Viterbo P., Woollen J. (2005). The ERA-40 reanalyses. Quarterly J. of the Royal Met. Soc., 131(612), 2961-3012.

Vu MT. (2013). Assessing regional hydro-climate impacts using high resolution climate modelling: A study over Vietnam, Phd Thesis, Dept. of Civil and Environmental Engineering, National University of Singapore.

Vu MT., Raghavan VS. and Liong SY. (2012). SWAT use of gridded observations for simulating runoff – A Vietnam river basin study. Hydrol. Earth Sys. Sci., 16, 2801-2811, doi: 10.5194/hess-16-2801-2012.

Climate Change Mitigation: Water and Energy Nexus in Urban Environments

TAMIM YOUNOS[1]

Abstract Energy demand for water infrastructure continues to increase globally due to growing population, increasing potable water demand and wastewater generation. In general, urban areas are characterized by high population density, high potable water demand and wastewater generation, and, therefore, energy consumption for water services in urban environments is significant and constitute a significant portion of total energy resources consumed around the world. At present, energy is mostly extracted from fossil fuels and it's recognized that fossil fuel-based energy production and consumption is a major contributor to global climate change. Worldwide, there is a significant need to develop adaptation and mitigation strategies to cope with climate change. The objective of this paper is to discuss mitigation strategies for reducing fossil fuel-based energy use in water infrastructure. Mitigation strategies discussed include energy use efficiency for water source development, water and wastewater treatment, and water distribution; approaches for water conservation by consumers; implementing decentralized water infrastructure such as rainwater harvesting systems and small-scale packaged water treatment systems; and using renewable energy (e.g., solar energy). Concepts and case studies related to climate change mitigation described in this paper can serve as a guide for providing safe water to global communities with reduced carbon footprint.
However, there is a need for developing structured strategies, financial incentives and regulations so that these systems become a norm in developing and implementing futuristic water infrastructure around the world.

Keywords water infrastructure, energy consumption, water conservation, decentralized water systems, renewable energy

1. Tamim Younos
The Cabell Brand Center for Global Poverty and Resource Sustainability Studies
Roanoke, Virginia USA
Email: tyounos@gmail.com

Introduction

Major challenges facing water scientists and urban water engineers/planners around the world include: 1) emerging contaminants in drinking water; 2) inadequate and/or deteriorating water infrastructure (water treatment/distribution systems and wastewater treatment/discharge systems); 3) increasing urban stormwater runoff from impervious areas; 4) declining groundwater tables; 5) increasing energy demand for water infrastructure; and 6) climate change and its potential impact on source water and water infrastructure.

In general, urban areas are characterized by high population density with high potable water demand and wastewater generation. In most cities, potable water for urban consumption is imported from outside urban boundaries by using pipelines and pumps which are energy dependent. In some locations, water is extracted from wells which are also energy dependent. Generated wastewater (treated and untreated) from urban areas is mostly transported and discharged to nearby surface waters (streams, lakes and rivers) inside or outside the city boundaries.

Water and Energy Nexus

Water infrastructures around the world use a significant portion of total energy resources (Table 1). For example, in the United States (U.S.), the energy use for potable water treatment and delivery is reported to be in the range of 0.25 – 3.5 kWh/1,000 gallons [note: 1,000 gallon = 3.785 m^3] (AWWARF 2007). It's estimated that about 4% of national energy consumption in the U.S. goes to water and wastewater services (56 billion kilowatt hours (kWh)) (CRS 2013). Plappally and Lienhard (2012) discuss energy use in water infrastructure. .

Future increase in potable water use will further increase energy, i.e., electricity demand in the water sector. It's predicted that energy use for water treatment will increase by approximately 30% over the next decades, partially due to the need for using alternative water sources such as saltwater and wastewater for potable purposes to meet increased demand (Stokes and Horvath 2005).

Table 1. Percent of total energy use for potable water and wastewater services in cities around the world (Lawson et al., 2014)

Geographic Location	Water Service Sector	Approximate percent of total energy use for water services (compiled from various sources)
Toronto, Canada	potable water and wastewater	2
India (various cities)	potable water and wastewater	<3-16
United States (overall)	potable water and wastewater	4
State of California (United States)	potable water and wastewater	19
State of Texas (United States)	potable water	0.5-0.7
China	potable water	0.5
Spain	potable water	5.8

Climate Change: Adaptation and Mitigation

The science of climate change and its potential impact on water resources are well established (for example, IPCC 2007; Younos and Grady 2013). Depending on geographic location, climate change may affect the water resources and water infrastructure in various ways: 1) occurrences of erratic weather patterns; 2) increase in heavy precipitation or less than normal total annual rainfall; 3) severe droughts; 4) decreased snowpack in the mountains, earlier snowmelt, and change in rivers' flow; 5) sea level rise and coastal flooding; 6) encroachment of salt water into freshwater aquifers due rising sea level; and 7) change in oceans' salinity and acidity.

Two approaches that promote climate change resilience and enable communities to cope with climate change are "Climate Change Adaptation" and "Climate Change Mitigation." Adaptation is defined as an adjustment in natural or human systems in response to actual or expected climatic stimuli (variability, extremes, and changes) for example measures to cope with sea level rise and crop production. Mitigation are actions taken to limit the degree of future climate change, such as practices that directly or indirectly reduce carbon dioxide and other greenhouse gas emissions to the atmosphere.

Climate change mitigation strategies include but are not limited to: energy conservation in industry, and infrastructure (building and transportation); and 2) reducing fossil fuel-based energy use in water infrastructure, and water conservation. These mitigation strategies can be reinforced by implementing policy options and financial incentives that encourages water and energy conservation in urban environments, and conducting educational and outreach programs to increase public awareness on water and energy conservation. As the title of this paper indicates, the content of this paper is limited to climate change mitigation, particularly item 2) - climate change mitigation via reducing or eliminating fossil fuel use in water infrastructure and water conservation in urban environments.

At present, world communities significantly depend on fossil fuels (coal, petroleum and natural gas) to generate electricity for water treatment and distribution. Table 2 shows the level of carbon dioxide (CO_2) emission, the major culprit in climate change, attributed to electricity generation from fossil fuels and volume of potable water delivered to consumers.

Table 2. Carbon dioxide emissions from electric power generation and water delivered (Kloss 2008)

Fuel Type	CO_2 Output Rate CO_2/kWh Electricity	CO_2 Output per MG Water Delivered (x 1.450 kWh)
Coal	2.117 lb	3,070 lb
Petroleum	1.915 lb	2,775 lb
Natural gas	1.314 lb	1,905 lb

Note: 1 MG (million gallon) = 3.785 x 10^9 cubic-meters 1 lb (pound) = 0.4536 kg

The following mitigation strategies are discussed in this paper: 1) energy use efficiency in water infrastructure; 2) water conservation; 3) decentralized water infrastructure; and 4) using renewable energy.

Mitigation Strategy: Energy Use Efficiency

From energy use perspective, three major units of municipal water infrastructure are: (a) water source development; (b) water and wastewater treatment systems, and (c) potable water distribution networks. These systems and networks are operated and maintained by public or private entities.

(a) Water source development

Pumps are used to lift up water from groundwater aquifer or transport water via pipelines from a surface water source to water treatment facility. In general, groundwater source development requires about 30% more energy than nearby surface water systems largely because of the required vertical lift to extract water from the underground aquifer (Mo et al., 2011). Energy efficiency for groundwater development is a factor of pump efficiency and groundwater depth. And therefore, pump selection is a critical criterion for groundwater development and energy use.

For surface water sources, energy efficiency is a factor of topography and water transport distance via pipeline. For example, in the U.S., New York City and Los Angeles represent extremes of the energy required for source water transportation. In the case of New York City, source water from upper New York State is transported by gravity flow to New York City. While for Los Angeles, source water is transported via the California Aqueduct, a system of canals, tunnels, pipelines and pumps that transports source water from the Sierra Nevada Mountains and valleys of Northern and Central California to Southern California, and uses 2.09 to 2.62 kWh of energy per cubic-meter of water transported (Lawson 2013).

(b) Water and wastewater treatment facilities

As was stated earlier, highly impure source (raw) water, such as wastewater, saltwater, and contaminated surface water or groundwater, require more energy for treatment compared to not significantly contaminated freshwater sources. For example, desalination of brackish and seawater for potable water consumes significant more energy than treating a freshwater source (Younos and Tulou 2005). Advanced water treatment technologies such as reverse osmosis (RO) are more energy intensive, compared for example to traditional sand filtration. Research and development of new membrane technologies and other innovative water treatment systems aim not only to remove a wide range of contaminants from water, but also to reduce the energy consumption for water treatment with less cost.

There is significant potential for reducing energy consumption at water and wastewater treatment plants by implementing sustainable management practices. The U.S. Environmental Protection Agency (USEPA) has introduced tools and guidance for energy efficiency at water and wastewater treatment plants. These tools and guidance are available on the USEPA website: http://water.epa.gov/infrastructure/sustain/energy_use.cfm.

(c) Water distribution and wastewater discharge networks

Wastewater discharge networks in urban areas are mostly designed to flow by gravity, as wastewater treatment plants are installed in lower elevations near water bodies where treated wastewater is discharged. Only occasionally pumps are used to collect or discharge wastewater. In comparison, potable water distribution networks are pressurized and some level of pressure is required at the faucet and other end point uses. Therefore, a significant amount of energy is used to transport pressurized potable water from water treatment systems to consumers. For a detailed discussion of water distribution systems, the reader is referred to Lee and Farooqi (2014).

As was noted, water distribution systems require significant amounts of energy and, therefore, energy use efficiency in distribution systems should be seriously considered as a critical element of energy saving and climate change mitigation strategies. Research shows that improvement in pump efficiency and system design can significantly reduce energy demand in water distribution systems. For example, Arzbaecher et al. (2009) estimated that in the U.S., improvements in pump and motor systems efficiency could save 2,600-7,800 million kWh of energy annually. Energy wastage due to leaking water distribution pipelines is another critical problem. It's estimated that about 25 to 30% of treated potable water is lost while water is transported from the treatment plant to consumers (Kirmeyer et al., 2001). For example, in the U.S., this water loss translates to about 1.7 trillion gallons/year (AWWA 2005), resulting in significant energy wastage. As a mitigation strategy, energy losses can be reduced by timely maintenance of water distribution pipes. Recent technologies allow monitoring of the under-the-ground water pipes for leak occurrence. Early leak detection prevents significant excessive water loss and energy wastage in water distribution systems. Another strategy "decentralized water infrastructure," that minimize the need for long distance water distribution, is discussed in a later part of this paper.

Mitigation Strategy: Water Conservation

Water consumers in urban areas include commercial facilities, public facilities such as governmental buildings and schools, and dwellers of apartment buildings and private residences. There are opportunities for water conservation that could result in energy saving and mitigating climate change (Younos and Parece (2012). Two possible in-building water conservation approaches are briefly described below.

Consumer education - not to waste resources - should be promoted. For example, Parece et al., (2013) discuss the concept of environmentally relevant behavior (ERB), its application and positive consequences to reduce carbon footprint of water consumption. A second approach for in-building water conservation is adapting water saving fixtures such as low volume showers and toilets, and water/energy efficient washing machines, dishwashers and water heating devices. The USEPA has developed guidelines for consumer water saving strategies, which are available on the USEPA's website: http://www.epa.gov/watersense/.

Mitigation Strategy: Decentralized Water Infrastructure

Obviously, conventional and centralized water infrastructures are not effective to sufficiently reduce energy consumption and there are limitations to water conservation as demand for potable water increases. Decentralized water infrastructures are small to medium scale infrastructures with potential to decrease the need for pumping and water transport, and can be installed and operated locally. Two types of decentralized systems described here are "small-scale packaged water treatment technologies" and "rainwater harvesting systems."

Small-scale packaged water treatment as a decentralized system

Incorporating small-scale advanced packaged water treatment technologies as a decentralized water treatment system will eliminate or minimize construction of energy intensive water distribution networks. Advances in small-scale and packaged water treatment technologies (for example, RO plus UV disinfection devices) allow installing small-scale decentralized water production systems as satellite systems in and around urban and sub-urban areas. A typical small-scale packaged water treatment system with a capacity of up to 50,000 liters/day can be a water treatment unit that is 1.2m long, 1.0m wide and 2.1m high and can easily fit in a small room and can be operated with minimum training. Proper design of integrated small-scale water treatment systems using local water sources such as captured rainwater, wastewater or saline water will alleviate scarcity of potable water at community level and minimize constructions of water distribution networks.

Bottled water production and distribution at the local level is an excellent case of using advanced packaged water treatment technologies to supply water and create jobs at the local level. Technically, bottled water can be categorized as a decentralized water supply system; it facilitates drinking water distribution via bottles or containers to consumers instead of constructing a high cost water distribution infrastructure. Normally, bottled water is energy intensive due to energy used to transport bottled water from production plant to the market (Younos 2014). However, local production and distribution of bottled water is less energy intensive. For example, packaged water treatment-bottling plants installed in several sub-urban Mexican communities use groundwater or other local water sources to produce safe drinking water for the local and nearby communities (Younos 2014).

Rainwater harvesting systems

Rainwater harvesting systems refers to collecting, storing and using captured rainwater from impervious sources for a variety of beneficial uses. Simple calculation shows that a 1,000 ft^2 rooftop can yield 620 gallons of water for a 1 inch of rainfall [note: 1,000 ft^2. = 93 m^2; 1 gallon = 3.785 liters; 1 inch = 2.54 cm). After losses (evaporation, splash, etc.) about 75-80% of captured rainwater can be used to substitute for public potable water. Small-scale rainwater harvesting has been performed around the world for many centuries. Large-scale rainwater harvesting from urban building rooftops is a recent phenomenon, where captured rooftop rainwater is used for flushing toilets, garden fountains, landscape irrigation, and community gardens. Table 3 illustrates an example of energy saving and climate change mitigation attributed to captured rainwater use and potable water saving.

Table 3. Potable water and energy savings attributed to rainwater harvesting in Virginia (Younos and Lawson 2011). [Note: 1,000 gallon = 3.785 m^3 1 pound (lb) = 0.4536 kg]

Building Location[1]	Type of Water Use	Harvested Rainwater[1] (Potable Water Saving) (Gallons/Year)	Estimated Energy Savings (KWh)[2]	Estimated CO_2 reduction (lb/Year)[2]
Oscar Smith Middle School, Chesapeake City, Virginia	Landscape Irrigation & Toilet Flushing	3,730,000	5,409	11,450
Western Virginia Regional Correction Facility, Roanoke County, Virginia	Laundry Facilities	4,600,000	6,670	14,080

1. Source: Rainwater Management Solutions, Inc. http://www.rainwatermanagement.com/
2. Calculated using values given in Table 1 (cited in Kloss 2008).

Less data is available on comparison of energy use by a centralized water supply system and a decentralized rainwater harvesting system. Ward et al. (2012) reported that the rainwater harvesting system is more energy efficient than using municipal water. Younos and Lawson (2011) illustrated a comparative example for a study site (Anacostia Senior High School, Washington D.C.). Based on average annual rainfall of 39.3 inch for Washington, D.C., the school building rooftops (approximately 83,000 square-ft.) with compensating for 30% loss will generate about 1.3 million gallons/year of water that can be used for non-potable uses, i.e., flushing toilets/urinals and landscape irrigation. The captured rainwater can substitute for an equivalent volume of potable water from public water supply system. Based on electricity use data, it was estimated that the school uses 3,145 kWh per year for using 1.3 million gallons/year. In comparison, the rainwater harvesting system requires 776 kWh per year for using the same volume of water resulting in 2,370 kWh per year of energy saving. In a recent study, Hammerstrom and Younos (2014) estimated the pumping requirement for distributing captured rainwater to a residential home as 1kWh/1,000 gallons of water. For further discussion on energy needs the reader is referred to Lawson (2013).

Mitigation Strategy – Renewable Energy Use

It's recognized that advantages of water and energy conservation are limited as the increasing trend in water demand will result in higher energy demand and increased CO_2 emissions. For climate change mitigation purposes (reduced CO_2 emission), reducing or eliminating dependency on fossil fuels is an essential goal. Incorporating renewable energy use for water treatment and distribution provides a significant opportunity to reach that goal.

At present, solar energy provides the best opportunity for integrating renewable energy use into water production systems. For example, Abou-Rayan (2104) discussed advances in using solar energy for desalination of salt water for potable purposes. Solar energy can also be used to power remote water pumping stations for a cost-savings over using diesel pumps (Al-Smairan 2012). Other potential renewable energy sources include small hydropower, bioenergy, wind and wave energy. Research development in the arena of cost-effective renewable energy use is an evolving field of science and technology, and integrating various renewable energy sources into water infrastructure system design is an upcoming area of research development and application. Figure 1 shows a futuristic vision of water and energy integrated decentralized water infrastructure.

Conclusion

This paper provides a summary of implications of climate change and possibilities for climate change mitigation from water consumption perspective. Concepts and case studies described in this paper can be used as a guide for providing safe and energy efficient water to global communities. However, there is a need for developing structured strategies, regulations and financial incentives so that these systems become a norm in developing futuristic water infrastructure around the world.

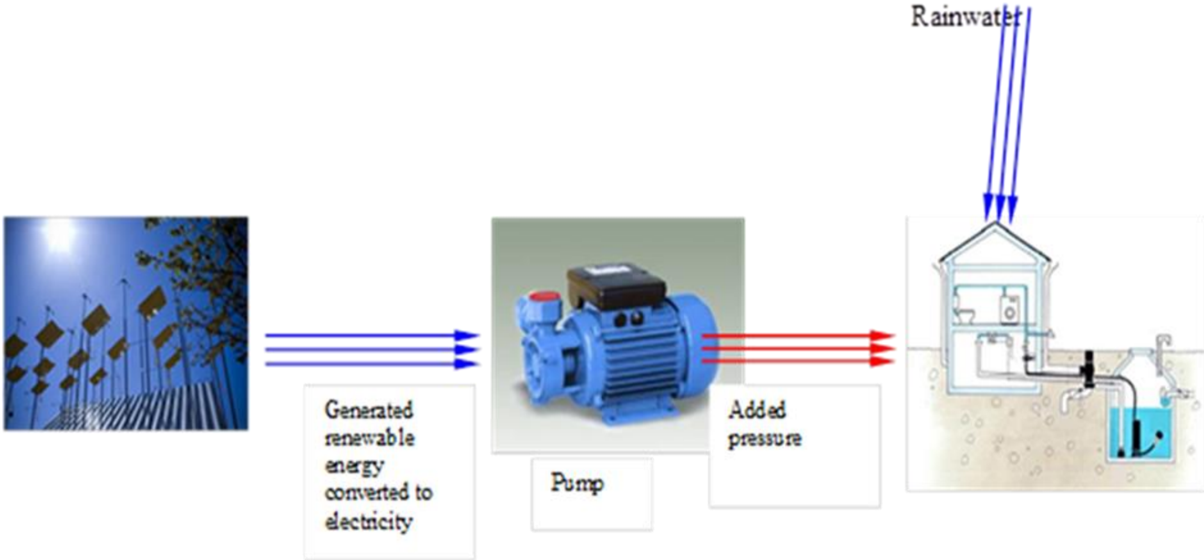

Figure 1. The vision for integrated water and energy use in decentralized green infrastructure (Younos et al. 2009)

References

Abou-Rayan, M. and Djebedjian, B. (2014) Advances in Desalination Technologies: Solar Desalination. In: Potable Water –Emerging Global Problems and Solutions (Eds. T. Younos and C.A. Grady), p. 181-211. The Handbook of Environmental Chemistry, Vol. 30, Springer, Heidelberg, Germany.

Al-Smairan, M. (2012) Application of photovoltaic array for pumping water as an alternative to diesel engines in Jordan Badia, Tall Hassan Station: Case study. Renewable Sustainable Energy Rev. 16: 4500–4507

Arzbaecher, C., Carns, K. et al. (2009) Program on Technology Innovation: Electric efficiency through Water Supply Technologies – A Roadmap. Electrical Power Research Institute (EPRI), Palo Alto, CA.

AWWA. (2005) Sizing Water Services Lines and Meters (M22). American Water Works Association, Denver, CO.

AWWARF. (2007) Energy Index Development for Benchmarking Water and Wastewater Utilities. American Water Works Association Research Foundation, Denver, CO.

CRS. (2013) Energy-Water Nexus: The Water Sector's Energy Use. Congressional Research Service (CRS) 7-5700. Washington, D.C.

Hammerstrom, J. and Younos, T. (2014) Single-Family Home Rainwater-Harvesting System Demonstration Project For Stormwater-Runoff Control and Utility-Water Saving. The Cabell Brand Center Special Report No. 100-2014. .

IPCC. (2007) Climate Change 2007: The Physical Science Basis. In: S. Solomon, D. Qin, M. Manning, Z. Chen, M. Marquis, K.B. Averyt, M. Tignor, H.L. Miller (Editors). Inetrgovernmental Panel on Climate Change (IPCC), Cambridge University Press, Cambridge, United Kingdom.

Kirmeyer, G., Friedman, M., Martel, K., Howie, D., LeChevallier, M., Abbaszadegan, M., Karim, M., Funk, J.and Harbour, J. (2001) Pathogen Intrusion into the Distribution System. American Water Works Association Research Foundation. Denver, CO.

Kloss, C. (2008) Managing Wet Weather with Green Infrastructure – Municipal Handbook – Rainwater Harvesting Policies. EPA-833- F-08-010.

Lawson, S. E., Zhang, Q., Joshi, M., and Tzu-Han Pai. (2014) The Effects of Water- Energy Nexus on Potable Water Supplies. In: Potable Water – Emerging Global Problems and Solutions (Eds. T. Younos and C.A. Grady), p. 125-151. The Handbook of Environmental Chemistry, Vol. 30, Springer, Heidelberg, Germany.

Lawson S. E. (2013) Mitigating Climate Change in Urban Environments: Management of Urban Water Supply. In: ClimateChange and Water Resources (Eds. T. Younos and C.A. Grady), p.145-168. The Handbook of Environmental Chemistry, Vol. 25, Springer, Heidelberg, Germany.

Lee, J. and Farooqi, O. (2104) Drinking Water Distribution: Emerging Issues in Minor Systems. In: Potable Water – Emerging Global Problems and Solutions (Eds. T. Younos and C.A. Grady), p. 95 - 123. The Handbook of Environmental Chemistry, Vol. 30, Springer, Heidelberg, Germany.

Mo W, Zhang, Q., Mihelcic, J.R. and Hokanson, D.R. (2011) Embodied energy comparison of surface water and groundwater supply options. Water Res 45:5577-5586.

Parece, T.E., Grossman, L., and Geller, E.S. (2013) Reducing Carbon Footprint of Water Consumption: A Case Study of Water Conservation at a University Campus. In: Climate Change and Water Resources (Eds. T. Younos and C.A. Grady), p. 199-218. The Handbook of Environmental Chemistry, Vol. 25, Springer, Heidelberg, Germany.

Plappally, A.K. and Lienhard, J.H. (2012) Energy requirements for water production, treatment, end use, reclamation, and disposal. Renewable Sustainable Energy Rev 16:4818-4848.

Stokes J, H. and Horvath, A. (2005) Life cycle energy assessment of alternative water supply systems. Int J Life Cycle Assess 11(5):335-343.

Ward, S., Butler, D., Memon, F.A. (2012) Benchmarking Energy Consumption and CO_2 Emissions from Rainwater Harvesting Systems: An Improved Method by Proxy. Water Environment Journal 26(2): 184-190.

Younos, T. and K. Tulou. (2005) Energy Needs, Consumption and Sources. In: Desalination – A Primer. Journal of Contemporary Research and Education. Issue No. 132, Universities Council on Water Resources, Southern Illinois University, Carbondale, IL, pp. 27-38.

Younos, T., Grady, C., Chen, T. and Parece, T. (2009) Conventional and Decentralized Water Infrastructure: Energy Consumption and Carbon Footprint. Extended Abstract In: Proc. of the American Water Resources Association – 2009 Spring Specialty Conference – Managing Water Resources and Development in a Changing Climate (Ed. H. Toniolo). May 4-6, Anchorage, Alaska.

Younos, T. and Lawson, S. (2011) Climate Change Mitigation at the Local Level: Decentralized Water Infrastructure – Opportunities and Challenges. Paper presented at the AWRA Spring Specialty Conference, April 18-21, 2011, Baltimore, MD (U.S.).

Younos, T. and Parece, T.E. (2012) Water Use and Conservation. In: 21st Century Geography: A Reference Handbook (Stoltman, J. Ed.), 40: 446-456, Sage, Los Angeles.

Younos, T. and Grady, C.A. (Editors). (2013) Climate Change and Water Resources. The Handbook of Environmental Chemistry, Vol. 25. Springer, Heidelberg, Germany.

Younos, T. (2014) Bottled Water: Global Impacts and Potential. In: Potable Water – Emerging Global Problems and Solutions (Eds. T. Younos and C.A. Grady), p. 213-227. The Handbook of Environmental Chemistry, Vol. 30, Springer, Heidelberg, Germany.

THA 2015 International Conference on
"Climate Change and Water & Environment Management in Monsoon Asia"
28-30January 2015, Bangkok, Thailand.

Participatory Approach on Management of Communal Irrigation Systems in Upland Areas: *Case Studies of Water Governance in Three Provinces of Northern Luzon*

Agnes M. Ramos[1,a,], Orlando F. Balderama[2,b,*]

Abstract. The study was conducted in three provinces in Northern Philippines to assess the impact of participatory approach for development and management system employed for Communal Irrigation System (CIS) which are owned and operated by Irrigators Association (IA).

In terms of net present value, internal rate of return and payback period, positive economic impact was due to increase in productivity and cropping intensity. Across all crops, average productivity per hectare was highest in vegetable producing areas.

The social impact, at the organization level, revealed the following benefits; 1) recognition of new leaders; 2) improved leadership and organizational skills; 3). increased participation of members in IA related activities; 4) enhanced cohesiveness among members and 5) better partnership and mutual existence between Local Government Unit (LGU) and the Irrigator's Association (IA). The LGU – IA partnership encouraged maximum utilization of the project as evidenced by increased cropping intensity and crop diversification.

The sustainability of the CIS are ensured through; (a) the internalized rules in the proper usage and maintenance of the systems ;(b) security of community livelihood against water scarcity and (c) improved leadership capabilities and high level of control in the IAs. Generated information and lessons learned are strategic information for proper governance of water resources in the upland areas.

Key words: communal irrigation system, irrigators' association, economic impact, social impact

[1]College of Business and Management, Isabela State University, Philippines
[2]Department of Agricultural Engineering, Isabela State University, Philippines

[a]isuagnesramos@yahoo.com;
[b]orly_isu@yahoo.com

I. INTRODUCTION

The environment is undeniably playing a critical role, especially in the economy of a developing country, like the Philippines. Economic activity has been the main source of pressure on the country's resource base. This is further compounded by the pressure due to the demand of the increasing population and the need to sustain food security.

In the Philippines, the uplands are among the most vulnerable ecosystem. This can be attributed, in part to the increasing migration of people to these areas in search for livelihood. This in turn has a tradeoff - environmental degradation that will eventually threaten the very existence of man.

This project through the partnership of the European Union and the Philippine government, is an integrated area development program aimed at promoting the agro-based local economy and sustainable development of the indigenous upland and highland communities in 19 municipalities of the three provinces in a mountain region namely: Benguet, Nueva Vizcaya and Nueva Ecija of northern Philippines (see **Figure 1**).

Figure 1. Project Site

The Communal Irrigation Systems(CIS) is a crucial component of the project and was implemented through the participatory approach. The beneficiaries were actively involved in the management and development of the CIS in their locality.

II. OBJECTIVE OF THE STUDY

The ultimate goal of the study is for the relevant stakeholders be informed on economic and social impact of the project under the framework of participatory irrigation management approach and to document information and experiences for the improvement and sustainability of the CIS projects.

III. METHODOLOGY

The methodology used in this study builds from earlier works done on participatory development for the past years. The methodology was based on the team approach on the assessment of the integration of participatory processes in community based projects. It intensively makes use of a combination of focus group discussion, triangulation supported by actual field visitation with the beneficiaries, interviews and actual physical assessment of fields served by the project. The data gathering and discussion however did not consider thoroughly issues with bearing on cultural sensitivity. Likewise, due to lack of logistics, not much data was collected to draw conclusions on the effect of the CIS in the environment.

The steps undertaken in the conduct of the study were as follows:

1. Actual Field Visitation, Survey and Focus Group Discussion

- Physical Data and Service Area of 16 representative CIS operating for at least six months were measured using the most appropriate equipment/method available;

- Socio-Economic, Management and Operations - Data on the management and operations of the Irrigator Association (IAs), social and economic impact of the project was gathered from sampled CIS units. It was done through interview with key informants and beneficiaries. The primary data were gathered with the use of questionnaire, and focus group discussion.

2. Determination of Sampling Size

Out of the 39 CIS completed and operational for at least one cropping, sixteen (16) CIS sample sites or 41% of the total CIS were selected for impact analysis. The criteria for selection were as follows: geographical location, type of system intervention, cropping system, type of irrigation, project cost, number of beneficiaries and declared service area.

4. Assessment and Analysis of Data

The indicator used in measuring economic impact of the various CIS was the increase in production per hectare as evidenced by: expansion in area served, increase in productivity (i.e. increase in production per hectare; and increase in cropping intensity.

The assessment for social impact was done in three levels; household (beneficiary level), Irrigator's Association and the community.

At the management level, the written reports on the participatory strategies employed in the implementation of the project were verified as to how these were implemented by the management and at the beneficiary level. At the beneficiary level, both focus group discussion and interview were used in the collection of data.

The levels of participation of the members of the IAs were rated using the following: 3-high, 2-medium and 1-low. Participation were measured in terms of level of the type of involvement namely; 1- if participation was for attendance to meetings only; 2- for attendance to meetings and participation to planning and decision making and; 3- for undertaking all of the items including contributing in labor, efforts and funds in the operation and maintenance of the IA and the CIS.

The context of sustainability is measured for the extent of participation, status of the physical structures (relative to vulnerability of the environment of the structure); records on activities undertaken (meetings, consultation, trainings); organizational control; commitment of leadership; availability of trained leaders and commitment of the leadership of both IA and LGU. These were scored by the evaluating team based from results of survey and field visits and later validated with the community. Each organization is scored based on the total value. These were correlated with other variables that will explain the sustainability of each IA.

Organizational control is scored by the beneficiaries based on the following items: 1) group cohesion; 2) attendance to meetings; 3) LGU complementation; 4) effectiveness of leader to enforce rules and discipline and influence members. This criterion was validated using problem identification with the beneficiaries through focus group discussion.

III. DISCUSSIONS

A. Project Profile

The irrigation systems in the CASCADE area are small, low-cost and located in vulnerable areas with slope greater than 20%. Water sources were either creek or Small River and spring water. The development intervention to CIS comes in three forms: a) capability building; b) communal irrigation systems physical structure (new construction, rehabilitation and improvement) and; c) other support services like microfinance and enterprise development. **Table 1** shows the type of infrastructure for the CIS's and the perceived impact on water supply. **Figure 2** shows the locationmap of the study sites and **Figure 3** presents some pictorials of CIS for rice and vegetable production in the area.

Table 1. Water acquisition facilities and their impact on water supply

Name of CIS	Infrastructure	Crop	Impact on water supply
Manamtam	River Intake	Rice	No impact
Dilan	Reservoir	Vegetable	new irrigation service area
Libawan	1 diversion weir	Rice+Vegetable	increased+more stable supply
Botilao	1 diversion weir	Rice+Vegetable	increased+more stable supply
Proper Pudi	1 diversion weir	Rice	increased+more stable supply
Lower Sisi	1 diversion weir	Rice	increased+more stable supply
Capintalan	1 diversion weir	Rice	increased+more stable supply
Yaway	River Intake	Rice + Vegetable	Stable water supply
Ammococan	1 diversion weir	Rice	increased+more stable supply
Decabacan	1 diversion weir	Rice	increased+more stable supply
Batu	River Intake	Rice-Rice-Onion	water supply is always enough – no impact
Dutac	River Intake	Rice + Vegetable	Stable water supply
Abogan	Spring Intake	Rice + Vegetable	Stable water supply
Balete-Bagtang	2 units Reservoir	Vegetable	new irrigation service area
Batawil-Sabdang	2 units Reservoir	Vegetable	increased+more stable supply
Dapong	3 small diversion weir	Vegetable	increased+more stable supply

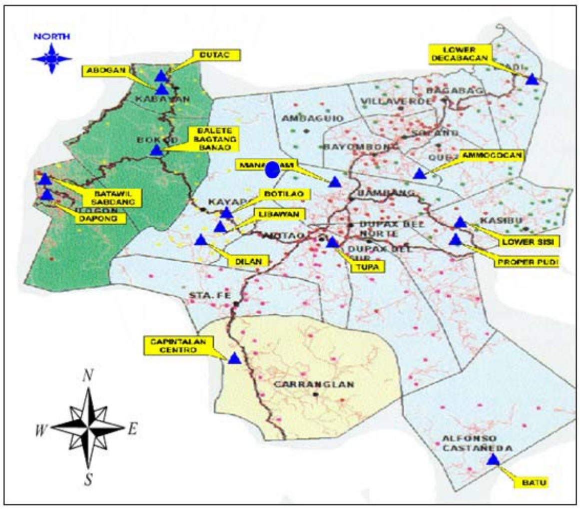

Figure 2. Map of the Project Area and Location of Sample CIS

Figure3. A typical view of rice and vegetable production in study area

The purpose of communal irrigation project is to increase production through increasing water supply, and protect the environment that supports the project with the community as the main actors of the development process. The project studied covers a total of 267 hectares planted into rice, a combination of rice and vegetables and vegetables only.

The Respondents

There were 128 respondents in the study, but only seven of which are women(see **Table 1**). Vast majority of the respondents were members of tribal communities called Ibalois and Kalanguyas - the indigenous people in the northern uplands of the country.

Table 1. Respondents Profile

Number of Respondents	128
Type of Respondents	
IA Officials	69
IA & LGU Officials	21
Members	38
Age bracket	45 – 74
Educational Attainment	At least elementary education
Average Household Size	5.4 heads
Average land area, mutiple cropped areas	.48 ha.
Average land area, single cropped (rice)	.96 ha.

In terms of the respective roles of the IA's in planning irrigation-related activities, it was observed that in general, there was no uniform practice across the system studied.

There was a poor collection of Irrigation Service Fee (ISF) except from the three project sites. All projects that were visited are believed to be functioning efficiently with minimal conveyance losses because of the use of pipes in the case of vegetable irrigation and lining of canals for rice irrigation.

B. Over-all Benefits derived from the Project

1. Economic Impact

Results show that most of the impact was due to increases in productivity and increases in cropping intensity. Only one CIS had an increase in area served. CIS average increased in productivity and cropping intensity is 23% and 22%, respectively.

In terms of the aggregate annual benefit per CIS and payback period, results revealed that most of the impact was due to increases in productivity and increases in cropping intensity. Only one CIS had an increase in area served. Across all crops, average productivity per hectare was highest in vegetable producing CIS. The average aggregate annual benefit per CIS was P215, 649. Considering the total construction cost as the initial investment of the various CIS and the increases in the value of benefits due to increases in productivity, cropping intensity, and area as the project benefits, the average payback period is 1.95 years. This payback period for investment projects is quite fast. This result implies that the investment cost in these CIS can be recouped very quickly. Also, this implies that the direct benefits from CIS are high.

Two common indicators of economic impact considering the time value of money were used in the analysis. These are the net present value (NPV) and the internal rate of return (IRR). Again, two levels of analysis were made, just like in the undiscounted measures discussed above, i.e. CIS level and farm level analysis. This is to capture the impact of the CIS on the aggregate and on the individual farm households. Assuming a discount factor of 12% (the social rate of return set by NEDA) and an annual operating and maintenance cost per CIS of 25% of the total project construction cost, the NPV and IRR were computed.

The annual net income per hectare was considered the benefit from the CIS, the computed CIS construction cost per hectare as the initial investment cost, and the 25% of the initial investment as the operating and maintenance cost. These annual benefits and costs were projected for a 10-year period (the economic life of the CIS). Based on the projected annual benefits and costs, the NPV and IRR per hectare was computed.Across all types of system intervention and across all cropping systems, the NPV and IRR results showed a positive NPV (P34,593) at 12% discount factor and an IRR of 35%. Both indicators show that benefits to the farmer beneficiaries more than offset the costs incurred. As to type of system intervention, lowest benefit is in new CIS. This is expected because constructing a new CIS is more expensive than in the case of rehabilitating or just improving an existing CIS.

2. Social Impact

The project created impact at three levels; community, organization (IA) and households' level. The positive impact at the community level included increased access to resources like the construction of water bridges out of collected service fees and external sources for micro-financing. At the IA level, impact indicators include effectiveness of operations, ability to establish partnership and in generation of funds. Under this category, mostly were rated medium to very high except Lower Sisi and Ammococan CIS. The IA's generally learned to cope up with maintenance problems especially when their livelihood security was threatened with inadequate irrigation water. These enhanced the cooperation among farmers and ness in others, leadership development, market integration among vegetable growers, and more cohesive relationship of the IAs and the LGUs.

On the community level, the impact of CIS were generally rated low. The probable reason for the assessment isthat because most of the indicators used have medium to long-term effect to the community such as improved environment, improved sanitation and nutrition and increased in off-farm income.

The overall impact of CIS at the household level is high. There was an immediate positive effect in terms of increasing access to information, education and market as well on empowerment.

C. Analysis on Strategies of Participatory Development among CIS

Participatory development in the communities was legally established through Republic Act 7160 signed in 1992. The law providesdecentralized decision making at the lowest local government unit – the barangay or village level. Projects were established based on needs of the community. Through the representation of their officials, the community decides on what type of projects will be established. Each barangay is granted Internal Revenue Allocation (IRA) from the national government based on their population, land area and revenue collections. The IRA is however utilized primarily for infrastructure projects like roads, bridges and buildings. With the assistance of the project, the covered communities were able to access other resources for development while making use of indigenous knowledge.

In the implementation of the Communal Irrigation Projects, the participatory development strategies employed are as follows;

1. Involvement of the local government officials from the provincial to the community in the planning, and operation of the projects. This strategy gave the local government a first hand look on the economic and environmental conditions in the project sites;

2. Facilitating the integration of various government services and programs into the community;

3. Formulation of "Rules-in-Use" by the members of the IAs;

4. "Counterparting Scheme" for various stakeholders (i.e. IAs contributing labor in the construction and operation and maintenance of the irrigation projects);

5. Trainings on capability building not only on maintenance and operation of the projects, but also negotiations, decision-making, resource generation and communications strategies.

D. Evidences of Participation

1. <u>Contribut ion to the Construction of the CIS</u>
   Participation is in itself shown primarily in the construction of the facilities. On the average, the beneficiaries contributed more than 22 % of the total project cost in the form of labor and food;

2. <u>Indicative Increase in Organizational Control</u>
   The level of organizational control increased in most of the CIS. Maintenance and operation has become easier to implement in IAs with high to medium level of organizational control.

3. <u>Development of New Leaders</u>

IV. SUMMARY AND CONCLUSION

Important results of the study show that most of the economic impact was due to increases in productivity and cropping intensity. Only one CIS had an increase in area served. Across all crops, average productivity per hectare was highest in vegetable producing CIS. Considering the total construction cost as the initial investment of the various CIS and the increases in the value of benefits due to increases in productivity, cropping intensity, and area as the project benefits, the payback period has an average of 1.95 years. This payback period for investment projects is quite fast. This result implies that the investment cost in these CIS can be recouped very quickly. Also, this implies that the direct benefits from CIS are high.

The project has also created social impact at three levels; community, organization (IA) and household's level. The positive impact at the community level included increased access to resources like the construction of water bridges out of collected service fees and external sources for micro-financing.

At the organizations' level, the IAs generally learned to cope up with maintenance problems especially when their livelihood security is being threatened due to inadequate irrigation water. These factors will enhance the cooperation and cohesiveness among farmers, promotes leadership development and mutual existence of the IAs and the LGUs.

V. REFERENCES

Balderama, O.F., Bareng L. and L. Alejo. 2014. Benchmarking for Performance Assessment of Small Irrigation Schemes in Cagayan River Basin. Isabela State University. Terminal Report

Balderama O. and B. Ausa. 2002. Terminal Report on Evaluation of Communal Irrigation Projects at the Sierra Madre Natural Park. Plan International, Isabela State University, Cabagan, Isabela, Philippines. Terminal Report

Cruz, R.D. 2002. Municipal Irrigation Master Plan for Diadi, Nueva Vizcaya. Volume 2 - Project Monitoring Tools. CASCADE, Bayombong Nueva Vizcaya, Philippines.

ERP-CASCADE/Economic self-Reliance Programme-Caraballo and Southern Cordillera Agricultural Development Programme-Philippines. January 1998. Global Work Plan for 1997-2004. Bayombong Nueva Vizcaya, Philippines

Ridder,D.,E. Mostert and H. Wolters (ed.) .2005. Learning Together to Manage Together-Improving Participation in Water Management. University of Osnabruck, Germany.

Assessment of Water Requirement of Chu'lsa Rice by using CROPWAT model

SIV VATANA, OEURNG CHANTHA, MEN NARETH

Department of Rural Engineering Institute of Technology of Cambodia, BP 86, Pochentong Blvd, Phnom Penh, Cambodia.

ABSTRACT

Field experiment with the dimension of 47.7m x 55.5m were performed at Cambodian Agricultural Research and Development Institute (CARDI), Cambodia, from February 01, 2014 to May 11, 2014. To calculate the reference and actual crop evapotranspiration of Chu'lsa rice (100 days), three main input data such as crop coefficient, meteorological and soil data were needed. The meteorological data was taken from Khmounh weather station, located about 10 km from the experimental filed; soil samples were collected from 5 zones in the field and analyzed in the laboratory and by SPAW Model; and the rice crop coefficient of CROPWAT Model were used in this study, which Kc (wet) were 1.05, 1.1, 1.2, 1.05 and Kc (dry) were 0.3, 0.5, 1.05, 0.7; in the initial, development, mid-season and late-season stages, respectively. The implementation of CROPWAT model was followed FAO Paper No 56 Penman-Monteith method.

In the field, the rice water requirement and average evapotranspiration rate are 518 mm and 5 mm/day, respectively. In the initial stage, ETc is around 3.65 mm/day with 20 days, but ETc much increases in mid-season, approximately 6 mm/day with 30 days, while ETc in the development is around 5 mm/days with 30 days, and 5.8 mm/day with 20 days at the late-season stage. This assessing is a very beneficial work for water irrigation management which helps stakeholder choosing the right method of water consumption to increase rice productivities, and to set a right schedule of irrigation.

KEYWORDS Crop water requirement, Rice, Crop coefficient, Evapotranspiration, CROPWAT model, Cambodia

1. INTRODUCTION

Cambodia, which located in the southern portion of Indochina Peninsula in Southeast Asia, has an area of 181.035 square kilometers and lies between latitudes 10^{o} and 15^{o}N, and longitude 102^{o} and 108^{o}E. Cambodia borders Thailand to the north and west, Laos to the northeast, and Vietnam to the east and southeast, as well as 443 kilometers of coastline along the Gulf of Thailand. The climate of Cambodia is dominated by monsoons, which is caused by annual alternating high pressure and low pressure over the Central Asian Landmass. In summer, the southwest monsoon, which is drawn from the Indian Ocean, brings the rainy season from mid-May to mid-September or early October. The flow is reversed during the winter, and the northeast monsoon brings back dry season from early November to April. Temperature range from 21^{o}C to 35°C, but in the dry season, it can rise to 40^{o}C, and drop to 22^{o}C in rainy season.

Rice is the dominant crop in Cambodian agriculture. It occupies more than 80 percent of cultivated land and is the most important agricultural export commodity. This should be complemented through an appropriate institutional framework to ensure that research centers focus on basic research and varietal development, while private companies focus on the multiplication and sale of certified seed. The improvements in the functioning of water user groups would go a long way to raise productivity and returns. To increase rice productivity in Cambodia, it is necessary to study on improving irrigation management.

The project team has formed and is collaborating well. Especially pleasing is the cooperation and camaraderie developing between Technical Services Centre (Ministry of Water Resources and Meteorology), CARDI (Min of Ag) and Institute of Technology Cambodia (Ministry of Education). This is a very important work of research such as assessing the water need of rice to improve the management of irrigation water and rice yield, saving water consumption, and setting the regular time of rice irrigation. This project is intended to improve the agricultural sector and Cambodian irrigation system to be more developed.

Experiments have been performed over three years to assess the evapotranspiration of rice crop. Yin Ratha (2012) performed experiments on water requirement of Chu'lsa rice in dry season, and the result of Cropwat model shows that the evapotranspiration required about 619 mm. Song Layheang (2013) used Cropwat Model to estimate the evapotranspiration of two types of rice crop. The results show that Chu'lsa rice (100 days) required the amount of water about 620 mm in dry season.

1.1. Rice Irrigation Water Requirement

The calculation of the irrigation requirements of wetland rice is different from other field crops. Extra irrigation water is required not only to cover evaporation losses but also to compensate for the percolation losses in the inundated fields. Furthermore, prior to transplanting, substantial irrigation water is required for the land preparation and the nursery. Input and calculation procedures will therefore differ from those of the crops for which a separate program is included in CROPWAT. Time of irrigation is usually governed by two major conditions namely, (1) water need of crops and (2) availability of irrigation water. Water need of crops is, however the prime consideration to decide the time of irrigation.

2. MATERIALS AND METHODS

2.1. CROPWAT model

CROPWAT 8.0 is an application software developed by several scientist (Doorenbos and Pruitt, 1976, 1977; Smith et al., 1991; Smith, 1992, 1993) for irrigation planning and management of the Water Resources Development and Management Service of FAO. CROPWAT is also a Windows based decision support system designed as a tool to help agro-meteorologists, agronomists, and irrigation engineers carry out standard calculations for evapotranspiration and crop water use studies, particularly the design and management of irrigation schemes.

The input data of CROPWAT model includes crop parameters, meteorology, and soil Table (1). The time step of the results can be any convenient one: daily, weekly, decadal or monthly.

Table 1 The input and output data of the CROPWAT model.

Data	Input	Output
Climatic	▪ Monthly/decade/daily minimum and maximum temperatures (^{o}C), or with average temperatures if minimum/maximum temperatures are not available. ▪ relative humidity (%) or actual vapour pressure (kPa) ▪ wind speed (km/day) or (m/s) ▪ sunshine (hours), percentage of daylight (%), or fraction of daylight (fraction)	▪ Reference evapotranspiration (ETo)
Rain	▪ Monthly/decade/daily rainfall (mm)	▪ Effective rainfall (Pe)
Crop	▪ Crop type ▪ Planting date ▪ Crop coefficient (Kc) ▪ Period of each stage (days) ▪ Rooting depth (m); Critical depletion (fraction); Yield response factor; Crop height (m)	▪ Actual crop evapotranspiration ▪ Crop water requirement (ETc) ▪ Irrigation requirement (Irriq)
Soil	▪ Total available soil moisture (FC-WP) (mm/meter) ▪ Maximum rain infiltration rate (mm/day) ▪ Maximum rooting depth (cm) ▪ Initial soil moisture depletion (%) ▪ Initial available soil moisture (mm/meter)	▪ Daily soil moisture deficit ▪ Estimated yield reduction due to crop stress
Irrigation	▪ Irrigation scheduling criteri a	▪ Irrigation scheduling

The CROWAT model operates in two modes by using: (1) the FAO Penman–Monteith equation to compute the actual evapotranspiration; (2) the evapotranspiration measurements values. Penman-Monteith method as recommended by the FAO Expert Consultation held in Rome in May 1990 to carry out the reference evapotranspiration calculation because it closely approximates grass ETo at the location evaluated, is physically based, and explicitly incorporates both physiological and aerodynamic parameters. Data are requested on the following:

- Basic information on the climate station: country name, station name, altitude, latitude and longitude.
- Monthly, decade, or daily climatic data on temperature, relative humidity, daily sunshine and wind speed.

The crop water requirements (CWR) is calculated as:

$$CWR = ETo * Crop\ Kc \qquad \text{Eq. (1)}$$

The average values of the crop coefficient (Kc) for each time step are estimated through linear interpolation between the Kc values for each crop development stage. In the case that the crop covers only 50% of the area, the ‘‘Crop Kc” values will be half of the Kc values in the crop coefficient data file. For this study, there were used a set of typical rice crop coefficient data files, as provided in the program of CROPWAT (FAO).

To estimate the amount of crop water requirement and to determine irrigation scheduling, it is necessary to have an equivalent daily or monthly value of rainfall data. The intake of rain into the soil is determined on a daily basis and rainfall losses due to deep percolation and surface runoff are estimated according to actual soil moisture content in the root zone. Total rainfall and not effective rainfall is therefore used for the water balance calculation; effective rainfall is calculated over the total growing season.

The effective rainfall will be calculated automatically in CROPWAT with rainfall data and choosing an appropriate method. Four different methodologies are given to determine the effective rainfall. The different options are: (1) fixed percentage of rainfall; (2) dependable rainfall; (3) empirical formula; (4) USDA Soil Conservation Service Method. The empirical formula was used in this study Eq. (1):

$$P_{eff} = 0.6\, P_{tot} + (-10) \quad \text{for} \quad P_{tot} < 75 \text{ mm}$$
$$P_{eff} = 0.8\, P_{tot} + (-25) \quad \text{for} \quad P_{tot} > 75 \text{ mm} \qquad \text{Eq. (2)}$$

Where P_{eff} denotes the effective rainfall; P_{tot} the measured (or generated) total daily rainfall.

The following is the daily climatic data of Khmounh Meteorological Station located about 10 km from CARDI was chosen for use in this study: minimum and maximum air temperature, relative humidity, wind speed, sunshine duration and rainfall (Figure 1). The temperature hovers around 15.3 °C and 37.5 °C respectively for the daily minimum and maximum daily temperature while the average relative humidity varies from 52.9% to 86.2%. In addition, the daily wind speed is about 1.4 m / s, and the sun is 0 to 5.4 hours per day. The rain occurs often from May to November as it is the rainy season. The total rainfall for this period is 1535 mm. Since CADRI meteorological station did not work, there will be some inaccurate data because of the long distance between the research field and weather station. The climatic data is taken from 1 June 2013 to 31 May 2014, are used to represent the data at CARDI. The crop is entirely assumed to be planted in two seasons (rainy and dry seas and to cover 100% of the experimental area.

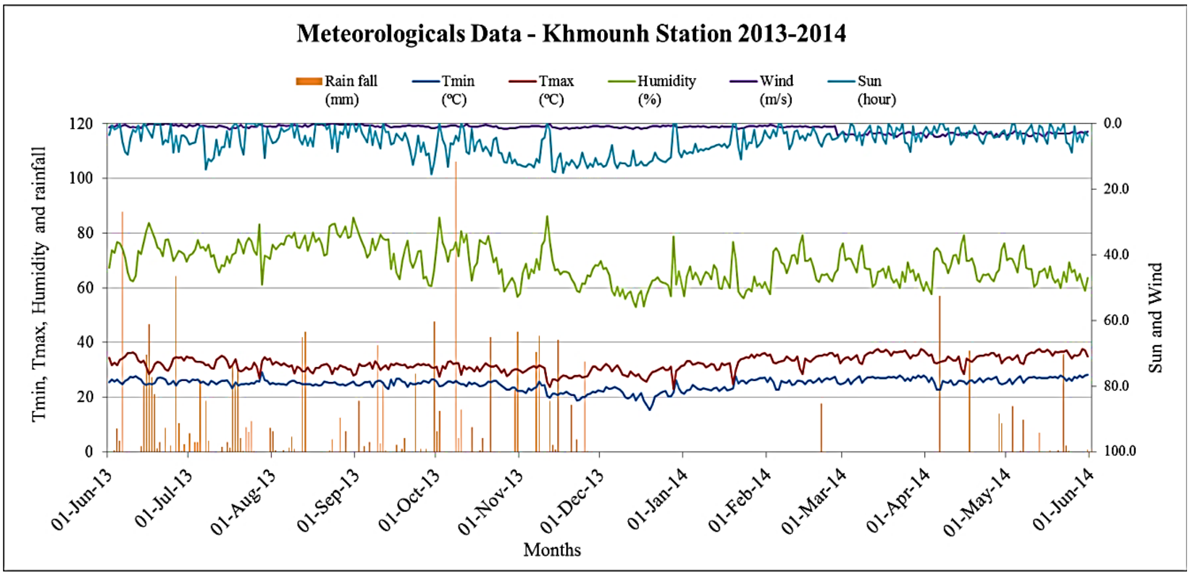

Figure 1 Meteorological Data of Khmounh Station

2.2. *Study area*

A small scale experimental field in CARDI was taken. The field is 10 m above the sea level with the dimension 55.5 m × 47.7m. Irrigation system of the field is operated by CARDI.

Soil is a very important component in irrigation system, and it is very necessary to know the characteristics of the soil in rice fields. Thus, soil texture determines the saturation, field capacity, the wilting point infiltration and percolation. These characteristics determine the retained water in the root zone. In this study, soil samples were collected at five locations in the depth of the root zone (20 - 40cm) to represent the soil on the ground. The gain size distribution of the soil grains are usually determined by the sieve analysis and hydrometer test. Determines the size of coarse particles larger than 0.075 mm (75 µ m) diameter, while the hydrometer test, using Stokes' law, smaller soil tests with a 0.075 mm diameter as that are sand, silt and clay. In the analysis of soil, among the five locations, there are four places with the same texture class (sandy loam), so that the soil in this area is supposed to be loamy sand that is in the class of light soil. After the soil characteristics (wilting point, conductivity field capacity, saturation, water availability, and water saturation) are obtained from the SPAW model (Table 2).

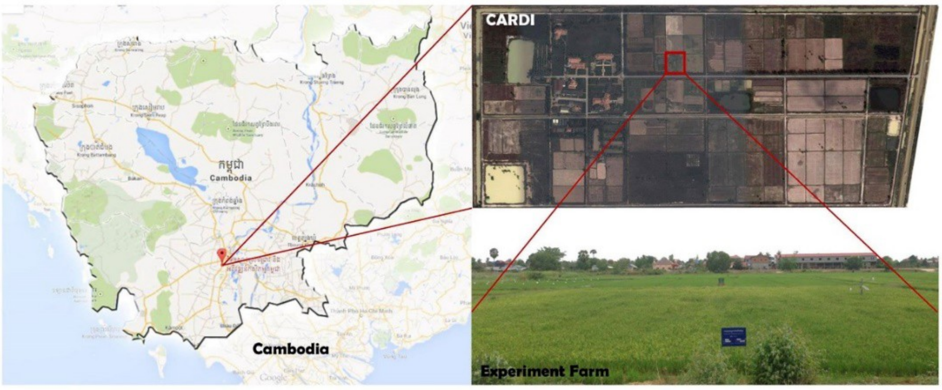

Figure 2 Cambodia Agricultural Research and Development Institute - CARDI (Google map)

**Cambodia Agriculture Research and Development Institute (CARDI), National Road N^{o}3, Prateah Lang Commune, Dangkor District, Phnom Penh, Cambodia.*

Table 2Soil parameter of CARDI's field

Soil Parameter of Filed at CARDI **Loamy sand**			
General soil data		**Additional soil data for rice calculations**	
Total available soil moisture (FC-WP) (mm/m)	70	Drainable porosity (SAT-FC) (%)	30
Maximum infiltration rate (mm/day)	24	Critical depletion for pudding cracking (mm WD)	0.4
Maximum rooting depth (cm)	900	Water available at planting (mm WD)	0
Initial soil moisture depletion (%)	0	Maximum water depth (mm)	200

2.3. Rice crop factor

In the study of water needs of crops, rice, Chu'lsar was sown directly with the growth period of 100 days from February 01 to May 11, 2014. Crop parameters are shown at below tables.

Table 3 each stages crop factor of Chu'lsa rice crop

Chu'lsa (100 days)										
Stage	Land Preparation	Initial		Development			Mid-season			Late season	
Period (day)	15	20		30			30			20	
Decade	-	10	10	10	10	10	10	10	10	10	10
Kc (wet)	1	1.1	1.1	1.12	1.16	1.2	1.2	1.2	1.2	1.05	1.05
Kc dry in CROPWAT	0.3	0.5		1.05						0.7	
Kc wet in CROPWAT	1.05	1.1		1.2						1.05	
Rooting depth (m)	-	0.1		0.6							
Puddling depth (m)	0.4	-		-			-			-	
Critical depletion	-	0.2		0.2						0.2	
Yield response factor	-	1		1.09			1.32			0.5	
Crop height (m)	-	-		-			1			1	

Source: Final report of Mr. YIN Ratha, 2012 and CROPWAT Rice crop session data

3. RESULTS AND DISCUSSION

The water needs of crops Chu'lsa from initial stages to the late season of the growing period of 100 days is 517.7 mm. During the initial phase, the water used of crop increases slowly from 35.6 mm to 37.1 mm per decade. At the first decade of the development stage, the crop evapotranspiration is 37 mm per decade and starts to increase to 59.4 mm per decade at the end of this phase. The water need of crop remains increase to 70.6 mm per decade at the first decade of mid-season, and decrease to 52.6 mm per decade at the end of the mid-season stage. It is also due to evaporation caused by meteorological factors. Finally, the water demand of rice crop begins decreased dramatically from 59.6 to 5.7 mm per decade at the second decade of late season. Moreover, at the last decade of late season is the harvest time, and the water in the field ought to be empty or drained. (Table 3)

Table 4 Crop and irrigation water requirement of Chu'lsa rice calculated by CROPWAT model

Crop water requirement of Chu'lsa rice in dry season							
ETo Station	Khmounh					Crop: Chu'lsa	
Rain Station	Khmounh					Planting Date: 1-Feb	
Month	Decade	Stage	Kc	ETc	ETc	Eff rain	Irr. Req.
			coeff	mm/day	mm/dec	mm/dec	mm/dec
Feb	1	Init	1.1	3.56	35.6	0	35.6
Feb	2	Init	1.1	3.71	37.1	0	37.1
Feb	3	Deve	1.11	4.62	37	7.2	29.8
Mar	1	Deve	1.14	5.33	53.3	0	53.3
Mar	2	Deve	1.16	5.94	59.4	0	59.4
Mar	3	Mid	1.18	6.42	70.6	0	70.6
Apr	1	Mid	1.18	5.63	56.3	37.3	19
Apr	2	Mid	1.18	5.26	52.6	21.3	31.3
Apr	3	Late	1.15	5.96	59.6	11.4	48.2
May	1	Late	1.07	5.05	50.5	14.4	36.1
May	2	Late	1.03	5.68	5.7	0.1	5.7
Total (mm)					**517.7**	**91.7**	**426.1**

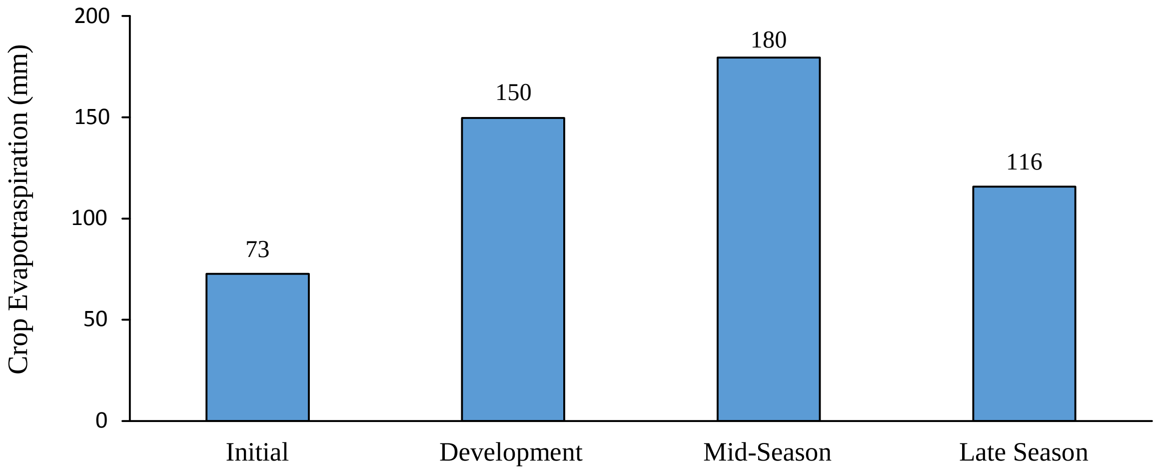

Figure 3 Crop Evapotranspiration in each stage of Chu'lsa rice in dry seaso

The crop water use of Chu'lsa rice in dry season in different stages. It shows that rice crop needs less water in the initial stage, around 73 mm, but it needs water the most with approximation of 180 mm in mid-season since during this stage is in the month of April, the hottest month of dry season. While the amount of crop water need in development is around 150 mm, and late season stage is around 116 mm. However, if compared in period of these two stages, the water used in development stage is greater than in the late season stage since the rainy season is starting at the month of May in late season.

The irrigation is applied to the field based on the irrigation time, and precipitation and a fixed depth of water of 100 mm, which corresponds to the intended depth to irrigate the field. This irrigation recharges at a fixed depth, 200 mm of water to compensate for the loss by evapotranspiration and percolation. These fixed levels can be defined in the model CROPWAT. The amount of water for irrigation is linked to crop water need, percolation and effective precipitation. Furthermore, the amount of water for irrigation will be reduced when there is rain. In this case, the water depth level of irrigation water will be less than 200mm.

Irrigation schedule of Chu'lsa in dry Season												
ETo Station	Khmounh		Crop: Chu'lsa						Planting Date : 1-Feb			
Rain Station	Khmounh		Soil: Loamy sand						Harvest Date : 11-May			
Date	Day	Stage	Rain	Ks	Eta	Puddl	Percol.	Depl.SM	Net Gift	Loss	Depl.SAT	
			mm	fract	%	state	mm	mm	mm	mm	mm	
17-Jan	-14	PrePu	0	1	100	Prep	0	1	121.5	0	120	
29-Jan	-2	Puddl	0	1	100	Prep	1	0	167.3	0	117.3	
4-Feb	4	Init	0	1	100	OK	2.9	0	99.8	0	-0.2	
19-Feb	19	Init	0	1	100	OK	2.9	0	97.7	0	-2.3	
6-Mar	34	Dev	0	1	100	OK	2.9	0	98.8	0	-1.2	
17-Mar	45	Dev	0	1	100	OK	2.9	0	95.6	0	-4.4	
28-Mar	56	Mid	0	1	100	OK	2.9	0	99.9	0	-0.1	
15-Apr	74	Mid	0	1	100	OK	2.9	0	96.2	0	-3.8	
6-May	95	End	0.	1	100	OK	2.9	0	98.9	0	-1.1	
11-May	End	End	0	1	0	OK	0	0				

Table 5 Irrigation schedule of Chu'lsa rice in dry season

4. CONCLUSION

In conclusion, the results from the CROPWAT computation are acceptable for the calculation of crop water requirement and irrigation water need. The rice water use of Chulsa rice in dry season, which is planted from February 01, 2014 to May 11, 2014, is around 518 mm in the period of 100 days. Hence, the rice water requirement is between 450 mm 700 mm for the total of growing period (FAO, 1986). CROPWAT can be used to compute the crop water requirement in all season and gives the acceptable results to the experimental field (CARDI) of different types of rice crop. Moreover, this model also has capabilities to calculate and estimate irrigation water requirement, irrigation scheduling as well as the scheme of irrigation.

After collaborating in this research, some recommendations to get the accuracy are made:

- The research should do on all kind of rice crop in order to determine the accurate crop water requirement.
- The meteorological station should be installed as more as possible.
- It is important to choose the right method to estimate effective rainfall, and scheduling since it is related to the amount of water irrigation as well as the productivity of crop yield.
- Before running CROPWAT, the user should check all needed data such as meteorological data, rainfall data, soil and crop data, especially, the error of the values, and also the unit of data.
- CLIMWAT data can be used to simulate in CROPWAT 8.0 as meteorological data did too.

Good management in irrigation is very crucial. Providing water to the crop in adequate amount, and timely irrigation enhances the crop yields and productivity. Moreover, the water will be saved or be not wasted. Since the water is well managed, irrigation system will be extended, and when an extension is implemented, more and more job opportunities simultaneously happen. This will lead to poverty reduction in Cambodia, which is a developing country mostly depending on agriculture sector. We believe that the improving of irrigation system will help our farmer to increase their crop productivities for internal consumption and as well as external exportation of our agricultural products to the world and bring our country into sustainable development.

Acknowledgement:

We would also like to acknowledge with much appreciation of "Australia supported by Center of International Agricultural Research" (ACIAR), and "Commonwealth Scientific and Industrial Research Organization" (CSIRO) from Australia for funding and technical supporting for this project study called "Improved Water Management to Increase Rice Productivity in Cambodia" N^{o} LWR/2009/046.

REFERENCE

Allen, R. G., Pereia, L. S., Raes, D. et Smith, M. 1998. Crop evapotranspiration-Guidelines for computing crop water requirement. FAO Irrig et Drain, 56.

Andreas, P. S. and Karen, F. 2002. Crop Water Requirement and Irrigation Scheduling-Irrigation Manual, Module 4. FAO Sub-Regional Office for East and Southern Africa.

Brouwer, C. and Heibloem, M. 1986. Irrigation Water Needs. *In*: FAO Irrigation Water Management, Training Manuals, paper-3.

Doorenbos, J. et Pruitt, W. O. 1976. Les Besoins en Eau des Cultures. Bull FAO Irrigation et Drainage, 24.

Doorenbos, J et Pruitt, W. O. 1975. Guidelines for predicting crop water requirements. FAO Irrigation and Drainage Paper 24.

Jean-Robert Tiercelin 1998. *Traité d'irrigation*, 159-230. Paris.

Allen, R. G., Jensen, M. E., Wright, J. L. and Burman, R. D. 1989. Operational estimates of reference evapotranspiration. Agron J 81 : 650-662.

Allen R. G. and Pruitt, W. O. 1991. FAO-24 reference evapotranspiration factors. J Irrig and Drain Engrg, ASCE 117 (5) : 758-773.

Dilip Kumar Majumdar, 2002. *Irrigation Water Management, Principles and Practice*, 151-153, 168-169, 261-267,. New Delhi.

Lagouard, J. P., Loustau, D., Courault, D. et Tournebize, R. 1996. Le bilan d'énergie d'un couvert végétal. *In : Actes de l'École- chercheurs INRA Bioclimatologie ; tome 1 : De la plante au consort végétal*, INRA Éditions :383-407.

M. H. Ali. 2010. *Fundamentals of Irrigation and On-farm Water Management*: Volume 1, 399-411. Bangladesh.

Mémoire de Mr. YIN Ratha. *Étude de besoin en eau du riz en utilisant le modèle CROPWAT*. 2011-2012. page 37 and 38.

Analysis of Hydrologic Variables Changes related to Large Scale Reservoir Operation by Using Mann-Kendall Statistical Tests in Thailand

D.Manee[1, a *], Y.Tachikawa[2,b] and K.Yorozu[3,c]

Abstract Recently, global warming has been significantly affected various hydrologic processes. The large scale multiple purposes reservoir is one of the countermeasures to manage and address both flood and drought problems. Therefore, an appropriate operation dam reservoir based on proper understanding of a change of hydrologic variable characteristics is important. This study applies the Mann-Kendall (MK) statistical trend test to analyze increasing, decreasing or trendless characteristics of precipitation, temperature, inflow to dam reservoirs, release from dam reservoirs, and storage volume in dam reservoir in Thailand from historical operation recorded data. The five large scale dam reservoirs located in the northern and central parts of Thailand are selected to analyze the trend of the Ping River basin (Bhumibol Dam), the Nan River basin (Sirikit Dam), the Pasak River basin (Pasak Jolasid Dam) and the Mae Klong River basin (Srinagarind and Vajiralongkorn dams). Those reservoir operation time series which consist of daily inflow, release, rainfall and temperature were analyzed and examined in association with various aspects of dam reservoir operations.

Keywords *Trend Analysis, Mann-Kendall trend test, Reservoir Operation, Thailand*

D.Manee
Department of Civil and Earth Resources Engineering
Kyoto University
Kyoto, Japan
Manee.donpapob.85v@st.kyoto-u.ac.jp

Y.Tachikawa
Department of Civil and Earth Resources Engineering
Kyoto University
Kyoto, Japan
tachikawa@ hywr.kuciv.kyoto-u.ac.jp

K.Yorozu
Department of Civil and Earth Resources Engineering
Kyoto University
Kyoto, Japan
yorozu@hywr.kuciv.kyoto-u.ac.jp

Introduction

Climate changes cause clear temperature increase for decades or even longer periods (IPCC, 2013)[1)], which significantly affects various hydrologic processes of time and space distribution pattern and quantity in such as precipitation and evapotranspiration. There are numerous earlier studies which focus on trend analysis of atmospheric and hydrologic variables in quantity and quality using historical data and GCM data. For example, Tao *et al*.[2)] analyzed the trends of streamflow in the Tarim River basin during the past 50 years using historical data, and Duong *et al*.[3)] examined the impact of river discharge changes by using a distributed river flow routing model and GCM datasets in the Indochina Peninsula region.

In the Southeast Asian countries such as Thailand, agriculture is the main source of the economy as well as ensures the well-being of the people. Thus, to sustain the water resource into the future is quite essential. Unless the water resources are utilized with a balance approach of supply and demand, its sustainability will become at risk. Therefore proper planning of water resource development as well as the utilization based on uncertainty in climate change impact is very necessary. The large scale multiple purposes dam reservoirs are one of countermeasures to manage and address water resources problems. Therefore, the appropriate operation of dam reservoir based on a proper understanding of a change of hydrologic variables is very important.

In this study, the trend of various hydrologic variables related to dam reservoir operations such as inflow to dam reservoirs, release from dam reservoirs, dam storage as well as precipitation and temperature using long historical record are examined with the Mann-Kendall test. The trend analysis is one of the methods to support and confirm the change of hydrologic variables to propose an adaptive dam release operation rules and constraint in advance combining with GCM data analysis for the future.

Materials and Methods

The study area is Thailand which is located in the Southeast Asia with an area 513,115 km2. Its climate is tropical climate with clear dry and wet seasons. The seasons are defined as follow: the dry season starts from November until April and the wet season starts from May until October in the central and northern part of Thailand. In the western river basins dry season starts from January until June and wet season begins July until December.

Study areas and data collection

The five large scale dam reservoir basins located in the northern, western and central parts of Thailand as shown in **Fig. 1** are selected to analyze the historical trend of precipitation, temperature, dam inflow, dam release, and storage. The five basins are the Ping River basin with the Bhumibol Dam (BB), the Nan River basin with the Sirikit Dam (SK), the Pasak River basin with the Pasak Jolasid Dam (PS), and the Mae Klong River basin with the Srinagarind dam (SR) and Vajiralongkorn dam (VRK).

Daily temperature and precipitation data were collected from 25 meteorological stations for the period 1980-2011 and time series of monthly inflow, release and storage data were obtained from the Electricity Generating Authority of Thailand (EGAT) and Thai Royal Irrigation Department (RID) for the period of starting reservoir operation. The reservoir characteristics of reservoir description are given in **Table 1.** The spatial distribution of the selected meteorological stations in Thailand is shown in **Fig. 1**.

Table 1 Characteristic features of selected reservoirs

Name	BB	SK	SR	VRK	PS
Location	17°14′33″N 98°58′20″E	17°45′50″N 100°33′48″E	14°24′31″N 99°07′42″E	14°47′58″N 98°35′49″E	14°51′41″N 101°03′58″E
CatchmentArea (km2)	26,386	13,130	10,880	3,720	12,292
Max.Storage (MCM)	13,462	9,510	17,745	8,860	785
Mean Inflow (MCM)	5,783	5,780	4,790	5,585	2,725
Opening Year	1964	1974	1980	1984	1999
Period (years)	50	40	34	30	15

Trend analysis methods

Detecting trends in hydrologic, climatic, water quality and other natural time series has been an active topic for more than three decades now. Statistical tests for the detection of significant trends in hydrologic and climatologic time series can be classified as parametric and non-parametric methods. The parametric trend tests require sample data to be independent and normally distributed, while the non-parametric tests need only that the data be independant[4].

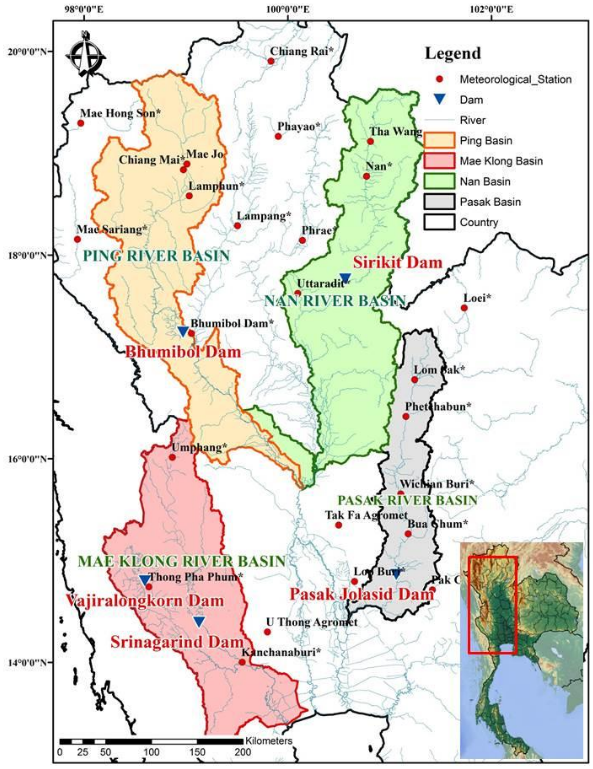

Fig. 1 Location map of large scale reservoirs and meteorological stations in Thailand

The Mann-Kendall trend test[4), 5)] is one of the widely used non-parametric tests to detect significant trends in time series. The Mann-Kendall trend test is based on the correlation between the ranks of a time series and their time order. For the statistics S is calculated as equation (1). This statistic represents the number of positive differences minus the number of negative differences for all the differences considered as

$$S=\sum_{i=1}^{n-1}\sum_{j=i+1}^{n}\operatorname{sgn}\left(x_j-x_i\right) \tag{1}$$

where n is the number of total data points, x_i and x_j are the data values in time series i and j ($j>i$), respectively, and sgn (x_j-x_i) is the sign function as:

$$\operatorname{sgn}\left(x_j-x_i\right)=\begin{cases}+1, & if\ \ x_j-x_i>0\\ 0 & if\ \ x_j-x_i=0\\ -1 & if\ \ x_j-x_i<0\end{cases} \tag{2}$$

The variance of Mann-Kendall statistic is calculated by equation (3) as

$$Var\,(S)=\frac{n(n-1)(2n+5)-\sum_{i=1}^{m}t_i(t_i-1)(2t_i+5)}{18} \tag{3}$$

where n is the number of total data points, m is the number of tied groups. The tied group mean a simple data having a same value. The t_i indicates the number of ties of extent i. In case of the sample size $n > 10$, the standard normal test statistic Z_S is estimated by equation (4) as

$$Z_S = \begin{cases} \dfrac{S-1}{\sqrt{Var(S)}}, if\ S > 0 \\ 0\ \ if\ S = 0 \\ \dfrac{S+1}{\sqrt{Var(S)}}, if\ S < 0 \end{cases} \tag{4}$$

The positive values of Z_S show increasing trends while negative Z_S values present decreasing trends. In this study 1% and 5 % significance level (α) were used. When $|Z_S| > Z_{1-\alpha/2}$, the null hypothesis is rejected and significant trend exists in the time series. $Z_{1-\alpha/2}$ is obtained from the standard normal distribution table. Therefore, the null hypothesis of no trend is rejected if $|Z_S|$ > 1.96 and $|Z_S|$ > 2.576 at the 5% and 1 % significance level respectively.

Data analysis

The observation data used in this study consists of a daily observation of precipitation, temperature, daily inflow, release and volume storage. The daily precipitation, dam inflow and dam release flow data were summed up for monthly, seasonally, and yearly and developed monthly, seasonally and annual time series data for the trend analysis. The daily temperature data were averaged monthly, seasonally, and yearly and developed for each time series data. Similarly the dam storage volume time series were averaged on each month. After compiling all-time series data on each parameter, the monthly time series in the designed month was selected to generate new time series for the Mann-Kendall trend analysis.

In addition, the seasonal analysis also calculate by dividing on dry season (November to April) and wet season (May to October) for the northern and central of study area. The climate for western of study area is delayed, so the calculation was chosen the dry season (January to June) and the wet season (July to December) based on each climate characteristics.

Results and discussion

Analysis of temperature and precipitation trend

Results of applying statistical tests for seasonal and annual temperature and precipitation trend over the period 1980-2011 are presented in **Table 2** and **Fig. 2**. In **Table 2**, the Z_S values in equation (4) are presented. The positive values represent the increasing trend and the bold values shows statistically significant at the 5% or 1% significant level.

All of the entire stations show the little significant increasing trends except some stations near to the BB dam stations while the other stations trends present increasing trend in term of temperature and rainfall. For the results of temperature trend, the Wichianburi and Maejo stations in the Pasak River basin and the Ping River basin showed dramatically insignificant increasing trends at the 1% significance level of temperature in all season. The other stations have slightly increasing and decreasing trends in dry and wet seasons. The temperature in the Pasak, Nan and Mae Klong River basins shows the increasing trends, which means the evapotranspiration trend in those river basins would increase because the temperature is a main factor of evapotranspiration components.

Table 2 Results of the statistical tests for seasonal and annual temperature and precipitation over the period 1980-2011

Station	Temperature			Precipitation		
	Dry Season	Wet Season	Annual	Dry Season	Wet Season	Annual
Bhumibol Dam	0.214	-0.714	-0.018	0.712	-0.188	-0.021
Chiang Mai	0.464	**-2.194***	-1.053	-0.335	-0.314	-0.649
Chiang Rai	**1.963***	0.839	1.731	0.251	-0.565	-0.523
Lampang	**2.569****	0.036	1.855	0.126	-0.628	-0.607
Lamphun	0.788	-1.632	-0.263	-0.068	1.564	1.19
Mae Hong Son	-0.244	-0.732	-0.619	0.555	0.795	0.795
Mae Jo	**2.963****	0.691	**2.904****	0.34	-1.216	-1.112
Phayao	-0.338	0.319	0.638	-0.187	**2.108***	1.836
Mae Sariang	0.143	-1.07	-0.749	1.13	0	0.251
Nan	1.035	0.125	0.517	0.272	0.188	0.293
Phrae	-0.393	-0.624	-0.232	1.193	0.649	0.733
Tha Wang Pha	-0.892	1.035	0.91	0.054	0.715	0.412
Uttaradit	1.427	-0.125	0.5	0	-1.047	-1.214
Phetchabun	1.285	0.178	1.285	**2.156***	0.9	1.465
Pak Chong	**2.623****	-0.963	1.267	0.921	**2.219***	**2.623****
Lom Sak	**2.177***	-0.125	1.409	0.076	0.195	0.433
Lop buri	0.178	0.071	0.107	0.23	-1.088	-0.481
Loei	1.249	-0.624	0.892	0.586	1.005	1.235
Bua Chum	0.393	0.225	0.161	-0.303	0.195	-0.206
Wichian Buri	**2.814****	**2.176***	**2.701****	1.741	0.108	0.966
Tak Fa	0.696	-0.731	0.232	0.954	1.047	1.17
Kanchanaburi	-0.892	1.873	0.232	-0.147	-0.586	-0.356
Thong Pha Phum	0.731	**2.301***	1.855	0.52	0.011	0.412
Uthong	-1.82	0.464	-0.892	**-3.181****	**2.972****	-0.544
Umphang	0.535	-1.356	-0.393	1.363	0.824	1.761

Bold Character represent trends identified with

*Statistically significant trends at 5% significance level (1.960)

**Statistically significant trends at 1% significance level (2.576)

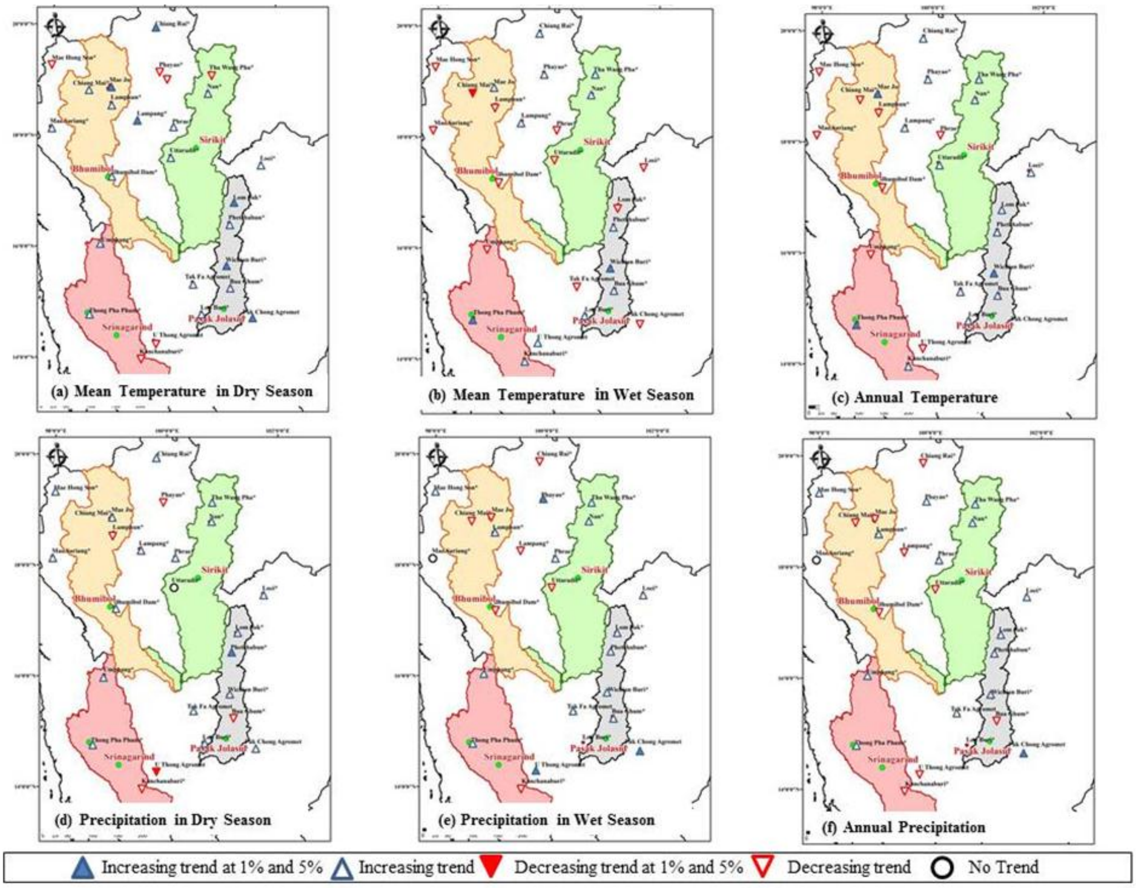

Fig.2 Spatial distribution of meteorological stations with increasing, decreasing and no trends for seasonal and annual data during the period 1980-2011.

According to the precipitation trend results, the precipitation trends of the Pasak, Nan and Mae Klong River basins also slightly increase as similar trends with the temperature.

Analysis of inflow trend

The output of the analyzed inflow series was summarized in **Table3**. The inflow series of the SK dam at the Nan River basin and the SR dam at the Mae Klong River basin were found significant increasing trends throughout the year, which are corresponding with the increasing precipitation trends. Both increasing and decreasing trends were detected at the BB, PS and VRK dams. The VRK and BB dam have a strong significant decreasing trend at 1% significance levels in early dry season. The Pasak reservoir was found only three months of slightly increasing trends comparing with other nine month significant decreasing trends, even though, the precipitation trends in the Pasak River basin have been detected increasing trends in all stations that cover the basin. This suggests the higher evapotranspiration rate occurred, which made the reducing the amount of water resources in the basin.

Table 3 Results of the statistical tests for monthly, seasonal and annual inflow over the period from the operation to 2013

Month/Season	Test statistic (Zs)				
	BB	SK	PS	SR	VRK
Jan	**-2.141***	1.27	0	0.415	**-2.12***
Feb	-1.824	**2.552***	-1.204	0.978	**-2.345***
Mar	-0.351	0.804	-0.985	1.038	-0.769
Apr	-0.97	0.781	0.109	0.326	**-2.157***
May	1.029	0.874	-0.495	0.83	0.732
Jun	0.151	0.408	-0.594	0.86	0.071
Jul	0.46	0.92	-1.188	**1.986***	**2.212***
Aug	-0.067	0.804	-0.891	**2.194***	1.249
Sep	-0.033	1.014	0.495	1.393	1.855
Oct	0.184	0.478	0.891	1.127	0.928
Nov	-1.422	0.384	-1.188	0.296	0.036
Dec	**-2.894****	**2.598****	**-2.078***	0.385	0
Dry Season	-1.939	1.766	-1.642	1.334	0.319
Rainy Season	0.151	0.851	0.396	1.186	**2.07***
Annual	-0.233	0.702	0.495	1.512	**1.97***

Bold Character represent trends identified with

*Statistically significant trends at 5% significance level (1.960)

**Statistically significant trends at 1% significance level (2.576)

Analysis of release flow trend

The monthly, seasonal and annual trends of release flow obtained by the Mann-Kendall test are given in **Table 4**. According to these results, the significant increasing trend at 1% significance level of release flow during dry season were found except the Pasak dam, however the release flow of the Pasak dam has a little significance increasing trends especially on December and January at the 1% significance level. The inflow trends of the BB and SK dams during early wet season (May to July) found increasing trends as shown in **Table 3**. Therefore, the release of the BB, SK and PS dams in wet season have significant decreasing trend to store the flood flows in the Ping, Nan and Pasak Rivers. In brief, the results found generally increasing significant trends in dry season of release flow in all reservoirs for high water demand, and decrease trends in the BB, SK, and PS dams to store water in the rainy season.

Table 4 Results of the statistical tests for monthly, seasonal and annual release flow over the period starting from the operation to 2013

Month/Season	Test statistic (Zs)				
	BB	SK	PS	SR	VRK
Jan	**3.543****	**4.928****	**3.266****	**3.579****	**2.72****
Feb	**4.215****	**3.944****	1.683	**4.092****	**4.858****
Mar	**2.595****	**2.179***	1.584	**3.765****	**3.395****
Apr	1.457	0.478	-0.792	**2.846****	**4.221****
May	-1.405	-0.711	0	**3.172****	**2.532***
Jun	-1.69	-0.151	0	2.046*	-0.469
Jul	**-2.476***	-1.456	-0.693	**2.075***	0.206
Aug	**-2.108***	-1.34	-0.693	1.66	1.069
Sep	**-3.279****	**-2.039***	-0.792	0.049	-0.019
Oct	-2.509*	-1.2	0.891	**3.143****	1.427
Nov	-0.569	-0.198	-0.891	**2.787***	**2.676****
Dec	1.941	**3.111****	**2.771****	**3.41****	**2.034***
Dry Season	**2.957****	**3.29****	0.766	**3****	**3.358****
Rainy Season	**-2.225***	-1.13	0.099	1.832	1.356
Annual	0.353	1.379	0.396	**3.13****	**2.72****

Bold Character represent trends identified with
*Statistically significant trends at 5% significance level (1.960)
**Statistically significant trends at 1% significance level (2.576)

Analysis of storage trend

Results of the Mann-Kendall test to the monthly storage volume at the end of each month are presented in Table 5. As shown, the majority of the monthly trends in the BB and PS dam have a significant decreasing trend due to reservoir operation based on existing rule curve while the SR dam shows increasing trend throughout the year. The SK and VRK dams remain the similar trends of increasing trends in wet season and of decreasing trends in dry season as a natural condition. Moreover, the significant decreasing trend at the 1% significance level from February to July of BB Dam and from January to April and August of PS dam were detected.

Insufficient and excess storage volume

Insufficient and excess storage volume below or exceeding the rule curves of all reservoirs were also evaluated from the beginning of each dam operation. The insufficient storage volume means the amount of volume below the lower rule curve while the excess volume represents the total of volume exceeding the upper rule curve. The explanation of insufficient and excess storage volume is illustrated as **Fig. 3.** The results of this analysis are summarized in Table 6. At the BB dam, increasing of insufficient storage volume trends was detected, which is corresponding on previous analysis of reduced inflow and increasing outflow trends results. The PS Dam also had a similar significant inflow and outflow trends results with the BB dam nevertheless the results of insufficient and excess storage volume results of the PS dam have indistinct. The SK, SR and VRK dams show gradually a rising trends of excess storage volume same an inflow trends of preceding section that represent the water resources in those areas would be increased.

Table 5 Results of the statistical tests for monthly, seasonal and annual storage over the period starting from the operation to 2013

Month	Test statistic (Zs)				
	BB	SK	PS	SR	VRK
Jan	-1.491	-0.012	**-1.971***	1.186	1.294
Feb	**-2.112***	-0.827	**-2.847****	1.127	0.807
Mar	**-2.629****	-1.456	**-2.956****	0.889	0.619
Apr	**-2.801****	-1.619	**-3.175****	0.741	-0.169
May	**-2.681****	-1.503	-1.534	0.415	-0.694
Jun	**-2.422***	-1.107	-1.782	0.682	-0.178
Jul	**-1.982***	-0.641	-1.881	0.652	0.107
Aug	-1.664	0.128	**-2.573****	1.275	1.534
Sep	-1.577	0.454	-1.089	1.571	1.249
Oct	-1.284	0.618	1.386	1.601	1.463
Nov	-0.957	0.757	1.089	1.423	1.427
Dec	-1.112	0.734	-0.693	1.156	1.463

Bold Character represent trends identified with
*Statistically significant trends at 5% significance level (1.960)
**Statistically significant trends at 1% significance level (2.576)

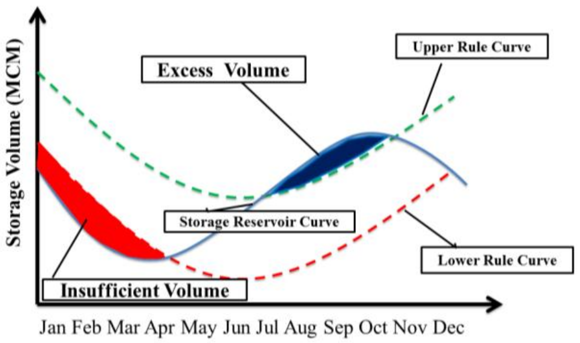

Fig. 3 Explanation of insufficient and excess storage volume

The number of insufficient events in the BB, SK and SR reservoir were found biennially on average. The PS dam has a small capacity comparing with other dams, so many insufficient and excess events detected within fifteen years. However, the VRK dam is also found the excess events with fourteen times to cope with flood. According to the dam characteristics in **Table.1**, the large scale reservoir such as the BB and SR dams have an advantage to address the flood for four and two events, respectively.

Table 6 Results of insufficient and excess storage volume.

Dam		Number of Event	Zs	
BB	Insufficient	24	1.15	Increasing
	Excess	4	-	-
SK	Insufficient	28	-0.01	Decreasing
	Excess	14	0.99	Increasing
PS	Insufficient	10	0.00	No Trend
	Excess	17	0.72	Increasing
SR	Insufficient	17	-0.03	Decreasing
	Excess	2	-	-
VRK	Insufficient	8	-1.86	Decreasing
	Excess	14	0.00	No Trend

Conclusions

The trends of precipitation, temperature, dam inflow, and dam release flow and volume storage were analyzed statistically based on long term historical data by using the Mann-Kendall trend test. Our findings are summarized as follows:

- Through the analysis, we found that the temperature and precipitation trends were increasing trends nevertheless Ping River basin temperature and precipitation trends were decreasing trends.
- The water resources availability in term of inflow to BB dam and PS Dam were decreasing trend during dry season. The inflow of all reservoirs in rainy season has increasing trends.
- For dam release from the reservoirs, generally increasing significant trends in dry season of release flow in all reservoirs. Only BB and SK dam has decreasing trends during rainy season.
- As a result, dam storage for BB dam found dramatically decreasing trends throughout the year while the SR dam detected decreasing trends.
- These insufficient and excess storage results indicate the increasing trends of water shortage in BB dam (Ping River basin) and PS dam (Pasak River basin) and also raising the trend of flood in SK dam (Nan River Basin) and both dams in Mae Klong River Basin.

We showed the climate change impacts have been already appeared in water resources in Thailand. The further study will be combined with the analysis of the historical data and GCM outputs. The analysis using a hydrologic model and GCM outputs are ongoing to predict future dam inflow under a changing climate to develop a new rule curve for adaptive dam reservoir operation.

Acknowledgement

This works is based on the data from Thai Meteorological Department for temperature and precipitation data, Thai Royal Irrigation Department and Electricity Generating Authority of Thailand for reservoir operation data. We gratefully acknowledge this support.

References

IPCC Working Group I (2013) Climate Change 2013: The Physical Science Basis. Contribution of Working Group I to the Fourth Assessment Report of the IPCC. Cambridge University Press, Cambridge, United Kingdom

Tao, H., Gemmer, M., Bai, Y., Su, B., Mao, W. (2011) Trends of streamflow in the Tarim River Basin during the past 50 years: human impact or climate change Journal of Hydrology: 400 (1-2), 1-9

Duong, D. T, Tachikawa, Y., Yorozu, K. (2014) Changes in river discharge in the Indochina Peninsula region projected using MRI-AGCM and MIROC5 datasets. Journal of Japan Society of Civil Engineers. Ser. B1 (Hydraulic Engineering): 70, 115-120

Milan, G. and Slavisa, T. (2013) Analysis of changes in meteorological variables using Mann-Kendall and Sen's slope estimator sttisticak tests in Serbia. Global and Planetary Change: 100, 172-182

Kendall, M.G., 1975 Rank Correlation Methods. Griffin, London, UK

Mann,H.B., 1945 Nonparametric tests againt trend. *Econometrica* 13, pp.245-259

Effect of AWDI Practices on Methane Gas Emission in a Small Scale Lysimeter Experiment

Abstract Rice is the most important cereal crop in the world. The demand of rice is rising with the increasing population. Rice paddy fields are thought to be a major GHG emitter. There are several studies to reduce the GHG emission from paddy field by applying AWDI (Alternate Wetting and Drying Irrigation). AWDI is a practice of water application in paddy field intermittently during the rice growing period. The study was conducted in small scale lysimeter (500X160) cm2 on the roof top of the University of Tokyo, Kashiwa campus. The study was conducted from May to December, 2013. The transplanted rice variety was *koshihikari*.The irrigation was done depending on rainfall event throughout the experiment. The lysimeter was left in natural condition without application of fertilizer. The main objective of the research is to clarify the mechanism of methane emission by observing the depth-wise soil chemical characteristics. Therefore, pH, Eh, temperature, and moisture of the soil were measured in different soil depths. At the same time, gas sampling was performed depending on the ponding condition of lysimeter and analyzed the gas by using gas chromatography. The experiment conducted in lysimeter showed that whenever soil ORP (oxygen level) is low in the soil layer, there is methane emission. When the ORP is higher (positive value), the methane emission is lower. In addition, plant height, tillers, leaves, spikelet and grain yield were counted. The 12 rice plants were randomly selected to measure the yield characteristics. The result of analysis showed that the four independent variables such as plant height, leaves, tillers and spikelet, number of grain yield have correlations with no of spikelet and tillers.

Keywords *Methane, Lysimeter, AWDI (Alternate wetting and Drying Irrigation), Soil Redox Potential, Ponding depth, Soil temperature*

1. Introduction

Rice is one of the most important cereals; especially having a long history of rice in the Asian countries. The demand of the rice is rising with the increasing population. The more the agriculture activity, the more it can affect to the environment direct and indirect way. Rice paddy fields are thought to be a major GHG (Green House Gaseous) emitter such as methane, nitrous oxide and carbon dioxide (Zhang, A. et al., 2013). According to IPCC report of 2007, agriculture contributes about 14% of GHG emission annually. There are few lysimeter experiments controlling the irrigation, fertilizer, soil Eh, and drainage valve to reduce the emission control. Soil Eh and pH depend on the organic matter and soil nutrients. Whenever the water from lysimeter is drained, there is percolate of soil organic and nutrients that make the decreased in CH4 gas emission (Yagi et al., 1998).

The continuous flooding of paddy field is considered to be the higher emitter of GHG. The irrigation management and intermittent irrigation are the effective in mitigating CH4 flux from rice fields. For the better rice yields and low greenhouse gas, SRI (System of Rice Intensification) has been introduced. It is the new farmer technique to improve the rice production with controlling water contents in the Paddy fields. It has been already proved that SRI with water controlling can produce higher yield of rice and save the water (30-40) % in comparison with conventional rice practices (Chapagain and Yamji, 2010). The New method of practicing water management is implied which is called (AWDI). AWDI (Alternate Wetting and Drying Irrigation) is a water management practice where rice fields are not kept in a ponding situation but are practised to dry intermittently during the rice growing time. The research shows that AWDI is effective to save water (29%) without reducing the production system of rice in compared to conventional practices (Chapagain et al., 2010)

The experiment conducted in the paddy field shows that emission rate of CH4 differed markedly with soil types and application of compost (Yagi,K.et al., 2012), water management like intermittent drainage can be an appropriate technology option to reduce the greenhouse gas from paddy field (Hadi, A.et al.,). The lysimeter experiment by (Kudo, K. et al. 2014) shows that GHG is reduced when intermittent irrigation was done. The present research will clarify the mechanism of methane emission from the paddy field. Moreover, it will help to understand the soil condition of paddy field and in which depth of soil is responsible for methane (GHG) emission.

2. Study area

2.1. Study site and experimental design

For the study of GHG impact practiced with AWDI, The experiment was conducted in a small Lysimeter of size (500X160) cm^2 in the roof top of the University of Tokyo, Kashiwa Campus. The study is conducted through the starting of May to end of December 2013. The transplanted rice nursery is *Koshihikari* (Japanese famous rice). Based on the size of Lysimeter, all together, 80 hills, per hill 3 rice nursery were transplanted. The study was conducted to understand the mechanism of methane emission so; there is no fertilizer application during the experiment conducted. The research was conducted until the end of December that aiming to know the methane emission after harvest and how is the condition change with rice roots (in fallow land).

2.2. Climatic features of the study area

In general, Japan has a rainy and highly humidity. The rainy season start mostly from early June to August. During this summer season rice farming is done. The experiment was conducted from May to end of December, 2013.The total rainfall during the rice farming season was June (171.0 mm) and maximum daily rainfall was 60.5 mm. The average maximum temperature was on August i.e. 27.2 degree Celsius and daily maximum was also recorded in same month. The maximum sunshine hours is recorded on August (May is longer sunshine but just rice planted started on 29th May.

2.3. Sample collection and instrument set up

To understand the methane gas emission from the paddy field, several parameters Soil ORP (Eh), Soil moisture sensors and water pressure are set up. The pH and ORP was measure by using PRN-41, produced by Fujiwara Company, Tokyo. Before using pH meter, the sensors were calibrated using standard solution of pH 6.86 and pH 4.01. pH and ORP of soil and ponding water depth was recorded once a day. The soil moisture and temperature were measured by ECH2O-5TE sensors made by DECAGON DEVICES. Before using in the actual field, the sensors were calibrated using the soil from the experimental field. The water pressure was recorded using data logger LR5000 series from HIOKI Company, Japan. The water pressure and soil moisture and temperature were continuous measuring throughout the experimental process. The data was recorded both moisture, temperature and water pressure in an every one hour interval.

Also, the height, tiller and leaf of the rice plant were also noted from time to time. The practices of intermittent were conducted and at the meantime, GHG gas was trapped depending on the ponding condition of Lysimeter. The Gas sample was taken on 7/23 (dry condition), 8/1 (wet condition), 8/10 (dry condition), 8/24 (wet condition) and after the rice harvest 10/11, 11/24, 12/26. When sampling the gas from the lysimeter, the plastic chambers (height 1 m) were used. The gas was collected from lysimeter making three replication and every 10 minute intervals. The collected gas was analysed using the gas chromatography made by shimadju japan-14a Gas chromatograph.

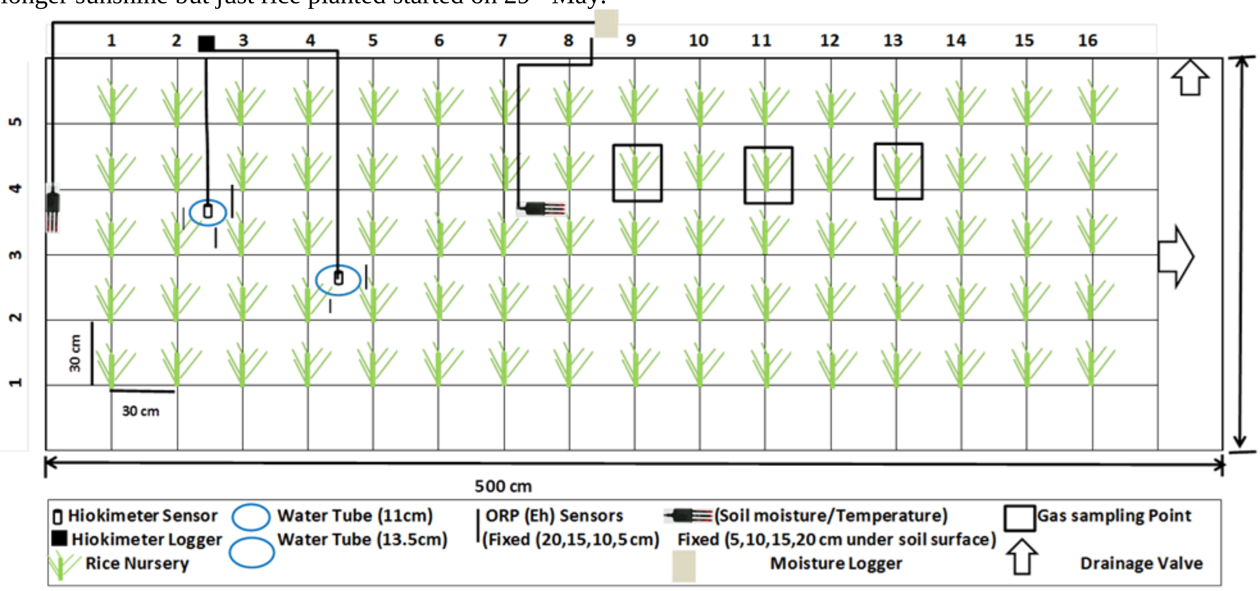

Fig. 1 Instrumental set up during experiment, 2013

3. Result and Discussion

3.1. Ponding depth and rainfall

In the lysimeter experiment, it was applied to observe the ponding condition by water tubes of 11cm and 13.5 cm diameters. In the initial phase of experiment, intermittent irrigation was done but after the mid of September, because of frequent rain, the lysimeter was ponding condition until the end of November. Irrigation was performed in accordance with rainfall and ponding condition of lysimeter.

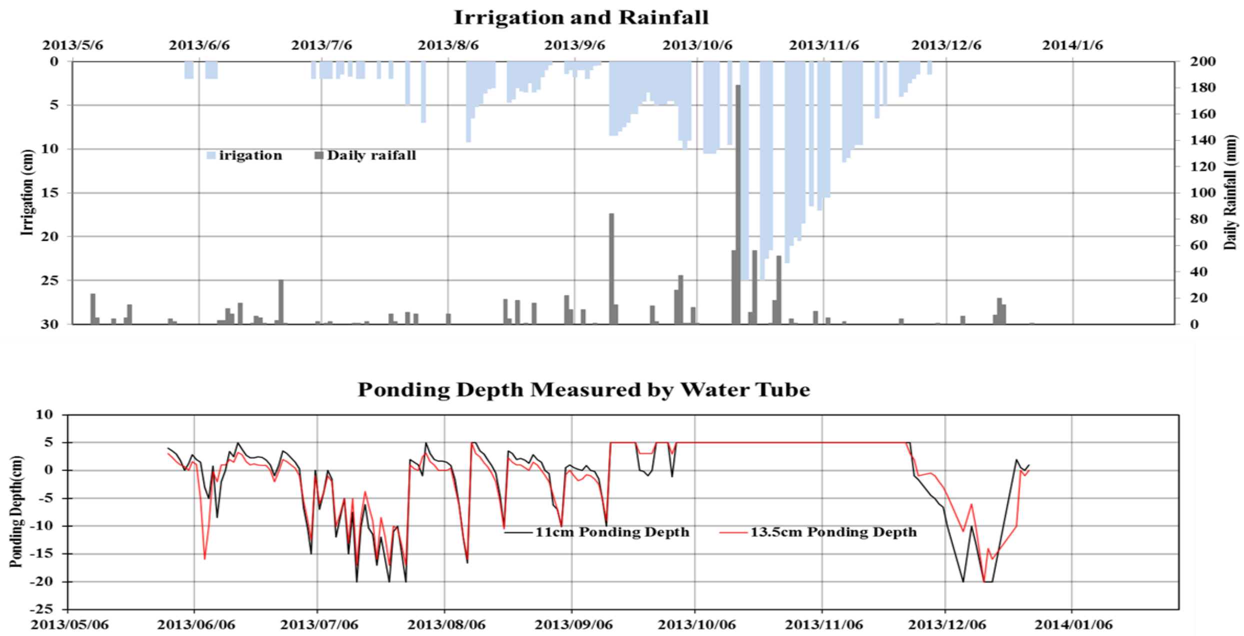

Fig. 2 Ponding Condition and Rainfall event during experiment, 2013

3.2. Redox potential (Eh) and pH of soil

In the initial phase, after the transplantation of rice on May 30, the pH value is constant until mid of July. After the mid of July, pH value shows slightly alkaline and increasing. Similarly the ORP value is highly fluctuating in initial phase because of soil solution mixed in plow layer and oxidation ability of rice roots. After the mid July, Eh drops gradually in every depth because of rainwater and irrigation, paddy was under ponding condition. When lysimeter is kept under the ponding condition, there will be lack of oxygen gas in plow layer.

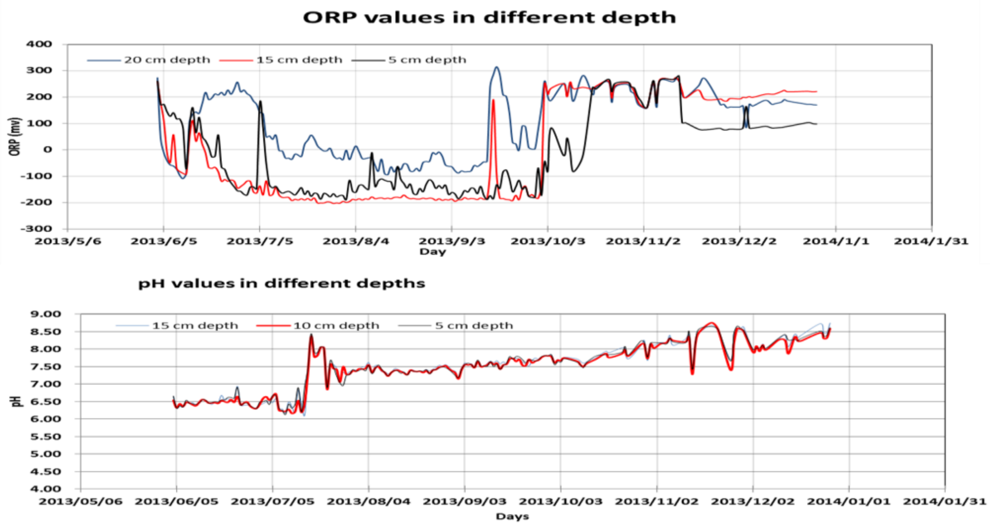

Fig. 3 ORP (Eh) and pH throughout the experiment, 2013

3.3. Soil moisture and temperature (depth wise)

In the case of soil moisture, it has shown the moisture content in 5cm and 10 cm is similarity, it means highly affected by irrigation management and temperature. But, in case of 15cm and 20 cm, moistures fluctuation is very slow. During the summer season, temperature in every depth is increasing but soil moisture is slightly fluctuating during the intermittent irrigation. After the rice harvest the moisture is constant as the ponding condition in lysimeter is positive as shown in **fig. 2.** (above the surface level) and temperature is decreasing rapidly.

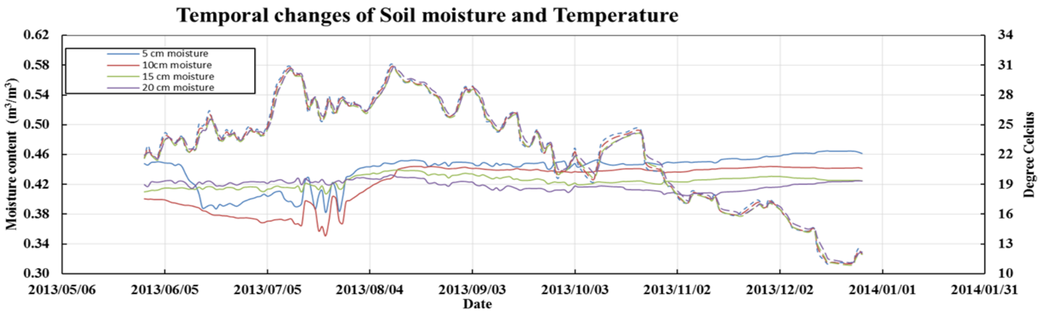

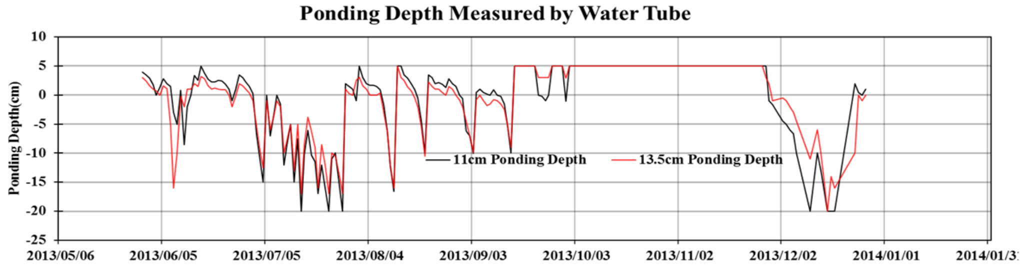

Fig. 4 Temporal changes of Soil moisture and Temperature, 2013

3.4. Methane emission

The first rice nursery was transplanted on May 29th of 2013. After that, lysimeter was kept under the flooding condition during two weeks until the rice plant gets strong. Then, intermittent irrigation was performed depending on the rainfall. The first gas sampling was done on July 23rd 2013, when the ponding water was dropped under -15 cm in a water tube. In that time, the methane flux is minus (no emission). The ORP (redox potential) values are minus in 5cm and 15 cm while in 20 cm is slightly positive as shown in **fig. 5**. In the day of August 4th and 10th, the methane is emitting. In comparison of august 4th, the methane emission is higher in August 10th. Although the water condition in lysimeter on Aug. 4th was dropping of ponding depth and Aug 10th is in a flooding condition. The ORP value is decreasing (minus) until the September 14th. After the September 14th, almost ORP value is showing positive (i.e. more oxygenated condition) until the end of December while there is no methane emission. The methane emission result shows that the methane flux is depend on the redox potential (ORP). If there is low oxygen inside plow layer, the methane emission will be higher and vice versa.

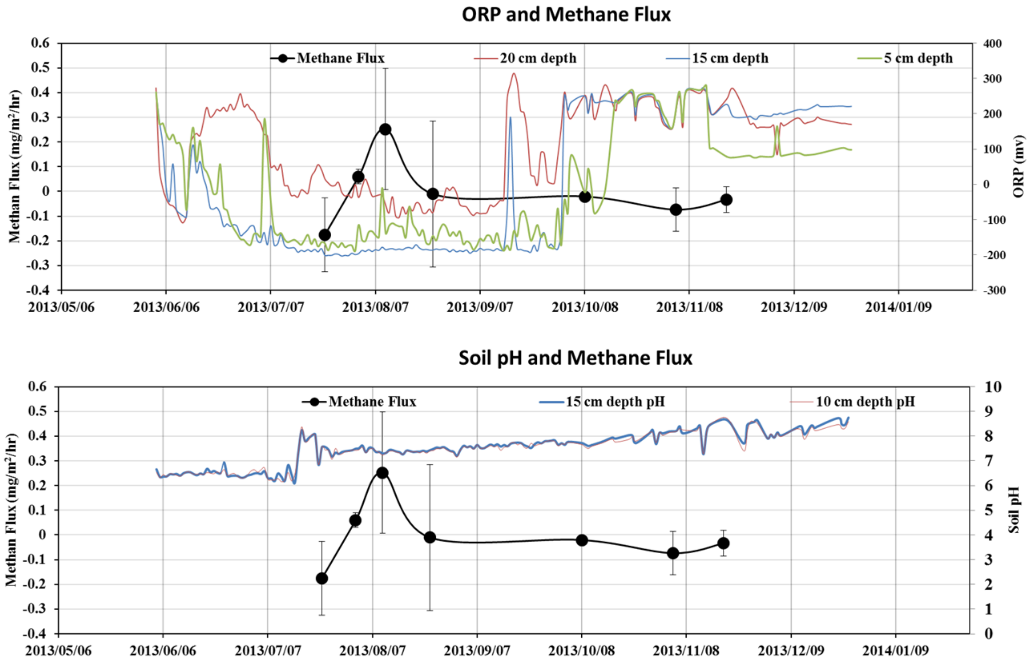

Fig. 5 The methane flux relation with ORP and ponding depth, 2013

3.4. Plant growth measurement and yield component

The height of rice plant and leaves are increasing steadily in the vegetative phase. In the reproductive phase (after the panicle initiation), lower leaves of rice stem decayed and decreased while the height of rice plant constant until the rice harvest.. The total average grain weight from per hill is found to be 19.66 gram. If it is converted to the production system in area hectare and ton, 1.57 ton rice with husk is produced from one hectare area.The different part of rice plant measurement was measured using correlation. The only correlated between no of tiller and no of leaves were found.

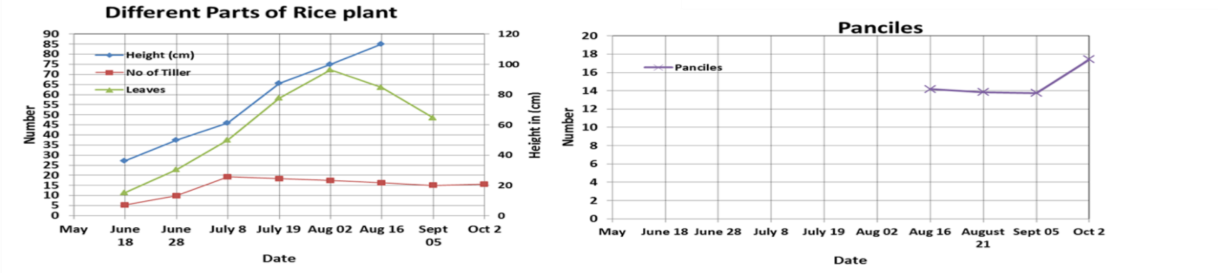

Fig. 6 Plant growth measurement and yield component, 2013

Conclusions

The mechanism of methane gas emission from paddy field is depending on the soil characters. Soil characters mean the soil pH, ORP (oxygen level) and moisture content. The experiment conducted in lysimeter showed that whenever soil ORP (oxygen level) is low in the soil layer, there is methane emission. When the ORP is higher (positive value), the methane emission is lower. It is also shown that from the temporal measurement of ORP in different depth (5cm, 15cm, and 20 cm) vary from each depth. To have a clear methane flux from soil surface, the ORP values should be lower (minus) in every depth of soil. Even after the rice harvest, it was supposed to be higher emission from the root decaying of rice plant but the results showed that there is no methane emission. Further research is needed to clarify whenever there is no methane emission, what will be the other gases like N2O and CO2 gas emission and effect of other factors like physical structure of drainage valve (surface drainage or drainage from the bottom of paddy field).

References

Zhang, A. et al, (2013). Effects of biochar amendment on soil quality, crop yield and greenhouse gas emission in a Chinese rice paddy: A field study of 2 consecutive rice growing cycles. Field Crops Research 127(27) pages 153-160

Irrigation Demand and the Flood Retention Potential by Changing of Cropping Calendar of the In-season Rice and Off-season Rice in Chao Phraya River Basin Area

Songsak Puttrawutichai[1, a *], Buncha Kwanyeun [2, b] and Thongplew Kongjun [3, c]

Abstract. The Chao Phraya river basin covers area of 157,926 sq.km., which is about 30 percent of Thailand area. The basin drains into the gulf of Thailand. Bangkok, the city of more than 8 million people, is located near the mouth of the Chao Phraya river.

The Chao Phraya river basin is Thailand's largest and most important geographical unit in terms of land and water resources development. Irrigation projects in the Chao Phraya river basin consist of 26 large projects, 14 medium projects, and 119 small projects, located in 15 provinces. Total project area is 70.4 percent of the Chao Phraya river basin. This area often suffers from water shortage and flooding. Therefore, water operation is essential for the prosperity of the area.

The headwaters of the Chao Phraya river originate in the mountainous terrain of the northern part of the country and consist of four large tributaries: the Ping, Wang, Yom and Nan rivers. There are three large reservoirs in the Upper Chao Phraya area including Bhumibol Dam, Sirikit Dam and Khwae Noi Bamrungdan Dam. In 2011 the Chao Phraya river basin had a large flood. It is considered to be the worst damage in the history of Thailand, extensive damage and losses which amounted to THB 1.43 trillion. The extreme flood harshly attacked the urbanized low-lying area, and caused heavy economic damage by disrupting production activities in industries for several months.

The changing of cropping pattern by adjusting the calendar of paddy transplanting from year round (3 crops/year) to 2 crops per year, which breaking period is in August – November. This approach reduces the flood damage, by diverting water into no cultivating paddy fields as retention area. Thus, it reduces flood peak in the Chao Phraya basin area.

The main motives of this research are irrigation demand and the flood retention potential. The changing of cropping calendar of the In-season rice and Off-season rice has the impacts directly on the irrigation demand. It is to calculate to what extent the capacity the flood retention potential in such areas is, where water diversion is planning to, in Chao Phraya river basin area.

Keywords: *Chao Phraya River Basin, Cropping Calendar, Irrigation Demand and Flood Retention Potential*

Songsak Puttrawutichai
Faculty of Engineering at Kamphaengsaen, Kasertsart University, Thailand.
songsak.tee@gmail.com
Buncha Kwanyeun
Faculty of Engineering at Kamphaengsaen, Kasertsart University, Thailand.
fengbak@ku.ac.th
Thongplew Kongjun
Office of Water Management and Hydrology, Royal Irrigation Department, Thailand.
tkongjun35@yahoo.com

Benchmarking for Performance Assessment of Irrigation Schemes: *Comparison of National Irrigation Systems(NIS) and Communal Irrigation System(CIS)in Cagayan River Basin, Philippines*

Eduardo Ramos [1,a], Orlando Balderama, [2,b]

Abstract. Degradation of irrigation schemes, low and variable land productivity, and inefficient use of production inputs are major concerns in the country today. That prompted this benchmarking analysis of three-small and one-large irrigation schemes located in the Cagayan River Basin. The objectives were to establish benchmarks for both productivity and performance of irrigation schemes along the valley, and to determine whether Communal systems function better than NIS or large schemes.

The performance evaluation study of the systems composed of three performance indicators, based on three (3) domains (a) System Operation Performance (b) Agricultural Productivity and Economics, and (c) Financial Performance. Each indicator was assessed based on the prescribed descriptors used by the International Water Management Institute (IWMI) and Food and Agriculture Organization (FAO).

Analysis showed an overall system performance efficiency of 59%, 55%, 47% and 36% for National Irrigation Administration-Magat River Integrated Irrigation System (NIA-MARIIS), Lucban, Garab, and Divisoria CIS's, respectively. In terms of annual productivity performance, Lucban CIS dominates the three other systems with 0.35 kg m^{-3}, which was classified moderately performing system while the rest were classified with low productivity index; financial sustainability of the systems were extremely poor with cost recovery ratio of 0.00, 0.33, 0.41 and 0.49 for Divisoria, Garab, Lucban and MARIIS, respectively, which were exceptionally below the standard value of at least one (1). Also, analysis of the indicators revealed that, on average, large schemes performed similarly to small-scale schemes, but small schemes were more variable, particularly in input-use efficiency.

Keywords:*national irrigation system, communal irrigation system, cagayan river basin, performance indicators*

[1]Magat River Irrigation System, National Irrigation Administration, Isabela Philippines
[2]Isabela State University, Philippines
[a]isuagnesramos@yahoo.com
[b]orly_isu@yahoo.com

INTRODUCTION

Benchmarking is already widely accepted and advocated by several organizations worldwide such as, IPTRID, IWMI, ICID, World Bank & FAO because it is aneffective management tool for analyzing and improving the performance of water resources projects. In the case of MARIIS, and CIS dilemma on the efficient water resource utilization has been an urgent issue to be addressed. Initial benchmarking on the current situation of the system using standard domains and indicators were considered to produce strategic information for effective short and long term measures and plan to manage water resources more efficiently, sustainably and productively which enables managers to compare the processes with the best practices and adopt suitable ones which would eventually improve the efficiency of the system and will result in savings in water usage thereby increasing the systems coverage.

For this study two irrigation domains were covered as follows: a) *Service delivery*: This domain includes two areas of service provision: (1) the adequacy with which the organization manages the operation of the irrigation delivery system to satisfy the water required; and (2) the efficiency with which the organization uses resources to provide this service (financial performance); b) *Productive efficiency*: Measures the efficiency with which irrigated agriculture uses water resources in the production of crops and fiber.

Case studies in the Philippines and other Asian countries reveals that full benefits from irrigation development are not fully realized for a variety of reasons resulting to sub-optimal performance of the irrigation system in terms of irrigated areas, cropping intensity, crop yield among others.

Lack of rainfall in the dry season and dry spells in the rainy season due to changing climate are, however, among the major constraints to rice production, and water productivity in paddy fields is perceived to be low. Improving the performance of irrigation scheme at MARIIS and CIS is an obvious issue for agricultural development. Irrigation efficiency, which is an indicator of effective water resources management, varies from area to area. A particular concern is water shortage within irrigation scheme command areas, particularly in the dry season or in dry spells during the rainy season. In many irrigation projects, there is no base-line information (physical, institutional and management) regarding levels of service to water users (farmers and fisherfolks) and the factors which affect those services. Establishing baseline information regarding levels of service, determining standards, and then determining how to meet them, could be crucial for improving the design, upgrading and management of irrigation and drainage projects.

Objectives of the Study

The study aimed to assess the performance of small and large reservoir irrigation schemes in Cagayan River Basin. Specifically, it aimed to determine and establish benchmarks for both productivity and performance using standard indicators: irrigation efficiency, adequacy of water supply, productivity of land and water resources and financial viability of the schemes.

Description of the Study Sites

The four systems (Small and Large Systems, namely Divisoria, Garab, Lucban CIS and NIA-MARIIS, respectively) were all situated within the Cagayan River Basin. The Cagayan River Basin (CRB) lies in the North-Eastern tip of the Philippines as shown in **Figure 1**. The Cagayan River flows through the four mainland provinces and is the largest river system in the country. The CRB is the largest river basin in the Philippines. It is located between $15^{0}52$'N-$18^{0}23$'N latitudes and $120^{0}51$'E-$122^{0}19$'E longitudes. Based on the NIA data, the potential irrigable area in the basin is about 472,640 hectares.

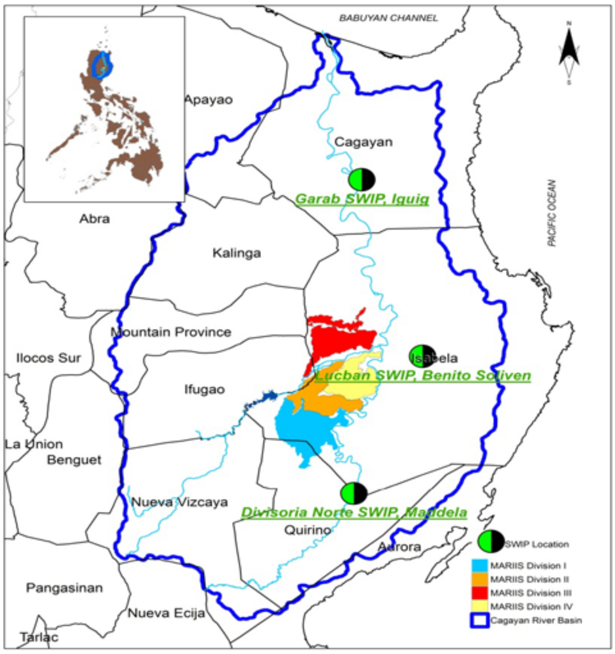

Figure 1. Cagayan river basin and study sites

The NIA-MARIIS has four distinct divisions I, II, III and IV. Study period considered in the benchmarking analysis is five years covering 2 cropping season from 2008 to 2012. The system was built in 1975 to provide dependable water supply for irrigation and for power generation. The project area has firmed-up service area of 84,795 hectares.

In the Philippines', rainwater harvesting project (i.e., with its institutional title Small Water Impounding Project or Communal Irrigation Systems) is a structure constructed across a narrow depression or valley to hold back water and develop a reservoir that will store rainfall and run-off during the rainy season for immediate or future use. As of December 2011, the Bureau of Soils and Water Management estimated that there are, there are 103 units of SWIP in the Cagayan Valley region with a total service area of 6,353 hectares and 4,929 farmer beneficiaries.

METHODOLOGY

Data Collection

General methods and activities were as follows: 1) review of documents and site validations; 2) key informant interviews, focus group discussions and household survey; 3) focus group discussions; 4) on-field measurements/inspections/ observations.

Review of documents and site validation

In the case of CIS, thorough study of previous reports, inventory, manuals and designs in Cagayan valley was conducted. Three (3) CIS pilot sites in Cagayan Valley were selected for detailed study. CIS Projects at Divisoria, Maddela, Quirino, Garab, Ilagan, Isabela and Iguig Cagayan were selected and subjected to validation visit. The selection was made based on the earlier studies and recommendations by the Regional Agricultural Engineering Group (RAEG) of the Department of Agriculture. Fielddata were collected related to water resources within the selected irrigation systems. Water discharges in various sections of main canals, cropped area for the two seasons and cropping intensity and paddy production.

Benchmarking Irrigation Systems Performance

The performance indicators used for this study was adopted from the internationally recognized standard indicators set by International Water Management Institute(IWMI), Food and Agriculture Organization(FAO), and International Commission on Irrigation and Drainage(ICID). Such irrigation domains covered in the study are as follows: a) *Service delivery*: This domain includes two areas of service provision: (1) the adequacy with which the organization manages the operation of the irrigation delivery system to satisfy the water required; and (2) the efficiency with which the organization uses resources to provide this service (financial performance); b) *Productive efficiency*: Measures the efficiency with which irrigated agriculture uses water resources in the production of crops and fibre.

The specific domains for benchmarking with their corresponding specific performance indicators selected are shown in **Table 1** below:

Table 1. Benchmarking performance indicators

Domain	Performance Indicator
Service/ System Operation Performance	System irrigation efficiency Annual irrigation water delivery per unit irrigated area (m^3/ha) Annual relative water supply
Productive Efficiency	Output per unit irrigated area (P/ha) Output per unit irrigation supply (P/m^3)
Financial Performance	Cost recovery ratio Revenue collection performance

RESULTS AND DISCUSSION

Systems Performance Indicators

The results of the irrigation performance indicators analysis based on three (3) domains (a) System Operation Performance (b) Agricultural Productivity and Economics, and (c) Financial Performance, respectively, were as follows:

a. System operation performance

The provision of water for irrigation and electric generation are the purposes of the NIA-MARIIS. However, the system's first priority is the provision of dependable irrigation water supply to farm lands. Though distribution of such water resource is influence by numerous factors, such as, physical, climatic, economic and other related factors which eventually affect the delivery performance of the system. Measurements on the system operation performance were based on specific indicators, such as, (a) delivery of the system, (b) annual relative water supply, and (c) annual relative water supply.

System irrigation efficiency (%)

The results of system delivery efficiency, annual irrigation supply, and relative water supply for MARIIS and the three CIS selected sites were presented in **Figure 2**.The system delivery efficiency was significantly differs for the whole MARIIS, Lucban, Garab, and Divisoria schemes. The MARIIS shows the highest efficiency value of 59 percent but Lucban CIS is statistically comparable with efficiency value of 55 percent, while the two other CIS's, namely, Garab and Divisoria were slightly lower than the previous systems with efficiency values of 47 and 36 percent, respectively. Although MARIIS and Lucban schemes are significantly higher compared to Garab and Divisoria CISs, these systems are quiet lower than irrigation efficiency of other irrigation schemes worldwide. Bandara, (2003) estimated the irrigation efficiency of major irrigation system in Sri Lanka to reach as high as 71 percent. Also, surface irrigation efficiency ranges between 50-60 percent in Israel, Japan and Taiwan as reflected in the work of Postal and Vickers (2001) as cited by Perry, C. 2009.

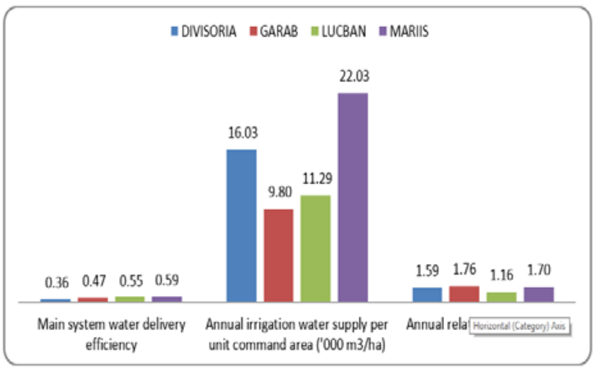

Figure 2 System-wise operation performance indicators

Annual irrigation water delivery per unit irrigated area (m^3/ha)

This indicator is measure on the total quantity of water supplied for irrigation throughout the year compared to the total area irrigated for the whole system selected. Although annual irrigation water supply per unit irrigated area depends on several factors, such as, water availability, cropping pattern climate, soil type, systems condition and management. The four systems average performance in terms of annual irrigation water delivery per unit irrigated area measured was significantly different as depicted in **Figure 2** with MARIIS registered the highest amount of 22,029.43 m^3/ha, tailed by Divisoria and Lucban CIS's with comparable amount of 16,026.37 and 11,289.10 m^3/ha, respectively, and Garab CIS registered the least amount of 9,795.96 m^3/ha.

Annual relative water supply

The relative water supply is a suitable indicator to show whether crop water requirements of an area were sufficiently provided.Annual relative water supply for all the systems considered was comparable (**Figure 2**). However, values are relatively lower as compared to the schemes of the world with only 1.70, 1.16, 1.76 and 1.59 for MARIIS, Lucban, Garab and Lucban CIS, respectively, while comparing that of the eighteen irrigation systems located in 11 countries vary between 0.8 and 4.0, with more a half of these systems have annual relative water supply of greater than 2 (Molden et al., 2009 and Karatas et al., 2009). These low values within the selected systems indicates that adequacy of supplied irrigation water is adversely affected by the low system delivery efficiencies.

b. Agricultural Productivity and Economics

Output per unit irrigation supply (kg/m3)

This water productivity indicator is a measure of the optimal utilization of water in relation to the total agricultural production served by the system. The comparison of data on output per unit irrigation supplied is shown in Figure 8. Although differences are not pronounced between Divisoria, Garab and MARIIS systems, however, Lucban CIS has significant output value of 0.35 kg m^{-3}. Adopting the water productivity categorization levels used by Cai et al., 2009 to rank the systems performance as low if less than 0.35 kgm^{-3}; moderate if 0.3 to 0.4 kg m^{-3} and high if greater than 0.4 kgm^{-3}. Accordingly, the productivity classification of Lucban CIS can be considered as moderate; while the rest, Divisoria, Garab and even MARIIS system are categorized under low productivity index. Subsequently, besides Lucban was considered to be the highest among the four irrigation systems under study, its grain productivity was still lower compared to global grain average ranging from 0.76 to 1.23 kgm^{-3} (Falkenmark et al., 2004).

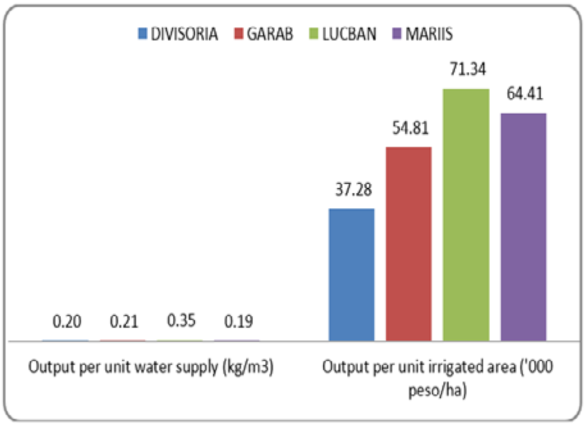

Figure 3 System-wise agricultural productivity performance indicators

Output per unit irrigated area (Peso/ha)

This indicator quantifies the performance of the system in terms of production output in a given unit irrigated area in Peso per Hectare basis. This indicator is very much important since water is the only factor on which the service provider has full control linked with the adoption of improved/ latest technology as the population grows while land holding per capita goes on reducing. For the four systems, land productivity performance is reflected in **Figure 3** where Lucban yielded the highest output with comparable output value of MARIIS with 71,336.22 and 64,412.15, respectively.Generally, results indicate a highly significant scope to increase land and water productivity for the four irrigation systems as indicated by the variable and low productivity performance.

c. Financial Performance

Revenue per cubic meter of irrigation water supply (Peso/m^3)

This is the ratio of the total revenue and gross volume of water supplied for irrigation during the irrigation year. This indicator is very important measure as every drop of water needs to be used efficiently and economically. In the case of Lucban, irrigation fee the collection performance is 100 percent; while 81 and 82 percent collection efficiency were attained atGarab and MARIIS, respectively, as shown in Figure 9. However, there was no collection effort made at Divisoria CIS.

Cost recovery ratio

This indicator is the ratio of recovery of water charges to the cost of providing the service. It is imperative to consider this indicator for the design of water rates and recovery mechanism for the sustainable operation of the system. On the basis of sustainability, the theoretical cost recovery ratio for any system should be at least equal to one. However, the four systems has poor cost recovery ratio of 0.00, 0.33, 0.41 and 0.49 for Divisoria, Garab, Lucban and MARIIS, respectively, as presented in **Figure 4**, where it is half-way below the theoretical value for system sustainability(IWMI 2009).

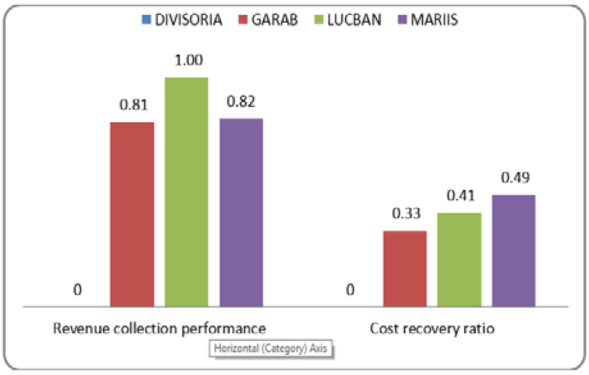

Figure 4 System-wise financial performance indicators

CONCLUSIONS AND RECOMMENDATION

This study was focused on assessment of the performance of small (Lucban, Garab and Divisoria CIS) and large (NIA-MARIIS) reservoir irrigation schemes. The results showed relatively low performance of the four systems being assessed as manifested by irrigation efficiency of 59, 55, 47 and 46 percent for MARIIS, Lucban, Garab, and Divisoria, respectively. Thereby improving the systems delivery and distribution efficiency could eventually support the targeted service area of each system as being indicated by the considerable amount annual relative water supply of 1.70, 1.16, 1.76 and 1.59 for MARIIS, Lucban, Garab and Lucban CIS, respectively, which is quite near the world's average relative irrigation water supply of 2.0.

In terms of water and land productivity of the four-scheme is 0.20, 0.21, 0.35, 0.19 kg $m^{-3}$and 37,276.01, 54,813.40, 71,336.22, 64,412.15 pesos ha^{-1}, respectively for Divisoria, Garab, Lucban and MARIIS schemes. Besides the low productivity of the systems, except for Lucban, classified as moderately performing but then quit low compared to global average productivity index ranging from 0.76 to 1.23 kg m^{-3}.

Financial sustainability of the systems were extremely poor as indicated by the low cost recovery ratio of 0.00, 0.33, 0.41 and 0.49 for Divisoria, Garab, Lucban and MARIIS schemes, respectively, which were exceptionally below the standard value of at least one (1). Thus to insure sustainable operation of the systems, wise mechanism recovery design should be implemented for each system being considered.

The study confirmed that small and large irrigation schemes within the Cagayan River Basin were on average performed similarly; however, both schemes performed quit below the world standard in terms of irrigation efficiency, land and water productivity levels and financial viability of the schemes. With the result of the analysis, it is therefore necessary to consider an over-all system improvement in terms of the three basic domains used, as such, (a) System Operation Performance –which includes but not limited to improvement on conveyance and distribution systems (b) Agricultural Productivity and Economics –which embraces superior production management practices, like adoption of high yielding varieties, appropriate fertilization technologies, water management scheme, etc. and (c) Financial Performance – which should considers wise mechanism recovery design and implementation.

REFERENCES

Bandara, K. M. P. S. (2003). Monitoring irrigation performance in Sri Lanka with high-frequency satellite measurements during the dry season. *Agricultural Water Management*, 58,159-170.

Burton, M. and Malano, H. 2001. Guidelines for Benchmarking Performance in the Irrigation and Drainage Sector. IPTRID, FAO. Rome, Italy

Falkenmark, M., &Rockström, J. (2004). *Balancing water for humans and nature: the new approach in ecohydrology*. London, UK.:Earthscan Publications Ltd.

IWMI, WorldFish, ILRI, NBI, 2009. The Nile Basin Focal Project, CPWF Project Number 59 Report.

Karatas, B. S., Akkuzu, E., Unal, H. B., Asik, S., &Avci, M. (2009). Using satellite remote sensing to assess irrigation performance in Water User Associations in the Lower Gediz Basin, Turkey.*Agricultural Water Management*, 96, 982-990.

Molden, D., Sakthivadivel, R., Perry, C. J., Fraiture, C. D., &Kloezen, W. H. (1998).*Indicators for comparing performance of irrigated agricultural systems*. Colombo: International Water Management Institute.

Molden, D. (2007). *Water for Food, Water for Life: A Comprehensive Assessment of WaterManagement in Agriculture*. Colombo, Sri Lanka: International Water ManagementInstitute.

Molden, D., Oweis, T., Steduto, P., Bindraban, P., Hanjra, M. A., &Kijne, J. (2009). Improving agricultural water productivity:Between optimism and caution. *Agricultural Water Management, doi:10.1016/j.agwat.2009.03.023.*

NIA-MARIIS. 2013. Internal Report and DataBase. Cauayan City, Isabela

Perry, C. (2005). Irrigation reliability and the productivity of water: A proposed methodology using evapotranspiration mapping. *Irrigation and Drainage Systems*, 19, 211-221.

Perry, C., Steduto, P., Allen, R. G., & Burt, C. M. (2009). Increasing productivity in irrigatedagriculture: Agronomic constraints

Seckler, D., Amarasinghe, U., Molden, D., de Silva, R., & Barker, R. (1998).*World water demand and supply, 1990 to 2025: Scenarios and issues*. Research Report 19:International Water Management Institute. Colombo, Sri Lanka.

Session C

Emerging Technologies in Water and Environment Management

Assessment of climate change impact on large scale flooding – a case study in the Chao Phraya River Basin via new modeling technology

Takahiro Sayama[1], Yusuke Yamazaki.[1], Yuya Tatebe[1, 2], Akira Hasegawa[1] and Yoichi Iwami[1]

Abstract Assessing the impact of climate change on large-scale flooding is one of the major concerns for water management. This paper presents a method to evaluate the impact of climate change by using GCM output and a Rainfall-Runoff-Inundation (RRI) model. The GCM used in this study is MRI-AGCM3.2S and 3.2H, the former one is the finest spatial resolution GCM in the world (20 km), while the latter one (60 km) is used to provide ensemble information with different cumulous schemes and sea surface temperature clusters to assess the uncertainty. In particular, this study focuses on flood inundation volumes in the Chao Phraya River basin in Thailand to evaluate how the frequency of devastating flooding like the one in 2011 will change in future under SRES-A1B scenario (2075-2099). The simulation results indicated the possible increase in average monsoon rainfall by approximately 1.1 times and the average flood inundation volume by 1.4 times, and accordingly shorten the return period of the large scale flooding in the future.

Keywords *Climate change, Rainfall-Runoff-Inundation (RRI) Model, Chao Phraya River, Thai flood, Sensitivity, AGCM*

Introduction

The impact of climate change on large-scale flooding is a great concern for water management. IPCC AR5 (2013) denoted that "*The contrast in precipitation between wet and dry regions and between wet and dry seasons will increase*". This calls for an attention to possible increases in frequency and intensity of flooding in current wet regions.

Under the monsoon climate condition, Thailand has been suffered from frequent flooding historically. In particular, the flooding in the Chao Phraya River basin in 2011 was extraordinary in terms of the extreme damage and the indirect impact on other regions and countries (The World Bank, 2012). Part of the reason for such a devastating economic damage was associated to the increase in the accumulation of assets by urbanization in flood prone areas. While the social vulnerability to flooding is often highlighted by media and other communities, there has been comparatively less attention paid to the severity of flood hazard itself in 2011.

The less focus may be due to the seemingly insignificant rainfall amount. The amount of six month rainfall, which has the direct impact on flood inundation volume, was approximately 1,400 mm in 2011. While the previous severe flood disasters including the ones in 1996 and 2005 were brought by about 1,200 mm rainfall, and the rainfall in normal years is approximately 1,000 mm in this region. Therefore the estimation of the impact of the additional 200 mm rainfall influences significantly on the interpretation of the 2011 flood hazard characteristics. To address the question, Sayama et al (2014) analyzed the sensitivity of flood runoff and inundation volumes to the rainfall amount. For the analysis, they used a RRI model (Sayama, et al. 2012) applied to the entire Chao Phraya River basin to estimate maximum flood inundation volume every year from 1960-2011 (52 years) and analyzed the relationship with rainfall amount. The result suggested the high sensitivity of additional 200 mm rainfall to the flood inundation volume, and therefore the small change in climate condition may affect significantly on the flooding in the basin.

Based on the finding, this study addresses how climate change projected by GCM impact on floods in the basin. Unlike many other climate change impact studies including the ones conducted in the Chao Phraya River basin (e.g. Hunukumbura and Tachikawa, 2012; Champathong et al., 2013; Kure and Tebakari, 2012; Meteo et al., 2014), the feature of this study is to assess basin-wide flood inundation volumes, which are more directly related to flood disasters in the basin. As for the GCM projection, we use the output by MRI-AGCM3.2S on A1B scenario. The AGCM has the finest spatial resolution among currently available GCMs. To quantify the uncertainty involved in the projection, we use also 3.2H (60 km resolution) with different cloud scheme and sea surface temperature patterns as additional 12 ensemble members for the future climate. For other GCMs, we did not conduct the detailed RRI simulation due to computational limitations; instead we investigate how the other 16 GCMs archived in CMIP5 project changes in precipitation in this region.

1. International Center for Water Hazard and Risk Management (ICHARM), Public Works Research Institute, Tsukuba, Japan
2. Currently at CTI Engineering, Co. Ltd., Tokyo Japan

Study site

The Chao Phraya River basin is located in the northern part of Thailand. The basin area is approximately 160,000 km^2, which include the basins of four main tributaries namely Ping, Wang, Yom and Nan. The four rivers meet at the central location called Nakhon Sawan. The upstream and downstream of Nakhon Sawan is a widespread lowland area, whose longitudinal gradient is approximately 1/12,000. In the basin, there are two major dams: Bhumibol dam (13.5 billion m^3, operated since 1964) in the Ping River and Sirikit dam (9.5 billion m^3, operated since 1974) in the Nan River. The dam reservoirs are primarily used for water resources and also power generation. During the floods in 2011, the Bhumibol and Sirikit dam reservoirs store flood water. The storages of the two dam reservoirs were about 57 % and 63 % in the beginning of July, and they became almost full by the beginning of October.

The 2011 floods caused levee breaches and overtopping mainly on the left side of the main Chao Phraya River (between Nakhon Sawan and Ayutthaya). The floodwaters submerged seven industrial parks near Ayutthaya and then the northern and western parts of Bangkok. The central business district of Bangkok City barely escaped from severe flooding after emergency embankment and drainage from the canals. As a result, 813 people were killed or missing and the economic damage and losses were 46.5 billion USD (The World Bank, 2012).

Method

Rainfall-Runoff-Inundation (RRI) model

The RRI model is a two-dimensional model capable of simulating rainfall-runoff and flood inundation simultaneously (Fig. 1) (Sayama et al., 2012). The model deals with land and river channels separately. In a grid cell where a river channel is located, the model assumes that both land and river are positioned within the same grid cell. The channel is discretized as a single line along its centerline of the overlying slope grid cell. The flow on the land grid cells is calculated with the 2D diffusive wave model, while the channel flow is calculated with the 1D diffusive wave model. For better representations of rainfall-runoff-inundation processes, the RRI model simulates also lateral subsurface flow, vertical infiltration flow and surface flow. The lateral subsurface flow, which is typically more important in mountainous regions, is treated in terms of the discharge-hydraulic gradient relationship, which takes into account both saturated subsurface and surface flows. On the other hand, the vertical infiltration flow is estimated by using the Green-Ampt model. The flow interaction between the river channel and slope is estimated based on different overflowing formulae, depending on water-level and levee-height conditions.

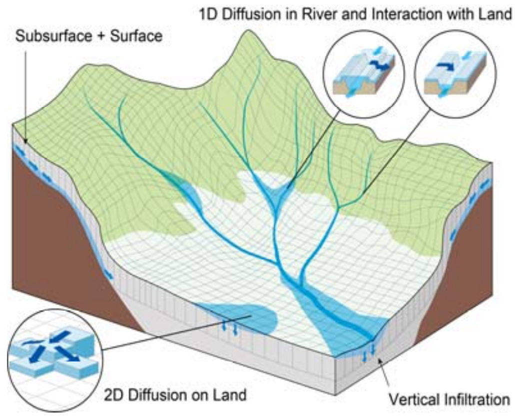

Fig. 1 Structure of RRI Model

Application of RRI model to the basin

The RRI model is applied to the entire Chao Phraya River basin. As the model was being set up, DEM, flow direction and flow accumulation were delineated from HydroSHEDS 30 sec and upscaled to 60 sec (approximately 2 km) resolution. Note that the RRI model uses flow direction and accumulation only to determine river channel locations but not for flood routing since the flow direction varies depending on local hydraulic gradients. River depths and widths were approximated by a non-liner equation with upstream contributing area as the explanatory variable. The parameters of the equation were estimated from regression analysis with cross 121 section data.

For the model calibration and validation as well as the following sensitivity analysis, we used a gauged rainfall observed by Royal Irrigation Department (RID) and Thai Meteorological Department (TMD) in Thailand. As for the potential evapotranspiration, we used Penman-Monthieth equation based on European Centre for Medium-Range Weather Forecasts (ECMWF) reanalysis. The Ecoclimap dataset, provided by Meteo France, was also used to identify seasonal and spatial variations of leaf area index. The periods of model calibration and validation are 1980-1999 and 2000-2011. We manually calibrated the parameter sets mainly focusing on the monthly discharge at Nakhon Sawan. In addition to the discharge, the model performance was also tested also in terms of flood inundation extents by comparing with remote sensing images. See Sayama et al. 2014 for more detailed model calibration and validation.

Sensitivity analysis of flood runoff and inundation

Based on the set-up RRI model, we run the model continuously for 52 years (1960-2011). Then we first analyzed the relationship between peak inundation volumes and rainfall amount in different periods (from 1 to 7 months). Figure 2 shows the estimated peak inundation volumes for each year on the x-axis and rainfall amount prior to the dates of the peak inundation volumes on y-axis. Note that the inundation volume (m3) was divided by the total basin area and convert the unit to (mm), so that we can compare directly to the amount of rainfall. According to the analysis, we found the six month rainfall has the highest correlation (R^2 = 0.85) to the peak inundation volumes.

In addition to the rainfall and peak inundation volumes, we also computed actual evapotranspiration, runoff and catchment storage based on the RRI model simulation for water balance and sensitivity analysis. Note that the runoff in this context is defined as all the water volume flowing out from the mouth of the Chao Phraya River basin as well as some flooded water flowing out directly from the basin into the sea. For the flood inundation volume, if surface water depths exceed 0.5 m due to accumulation of surface water, the volume of the water on land surface is considered as flood inundation.

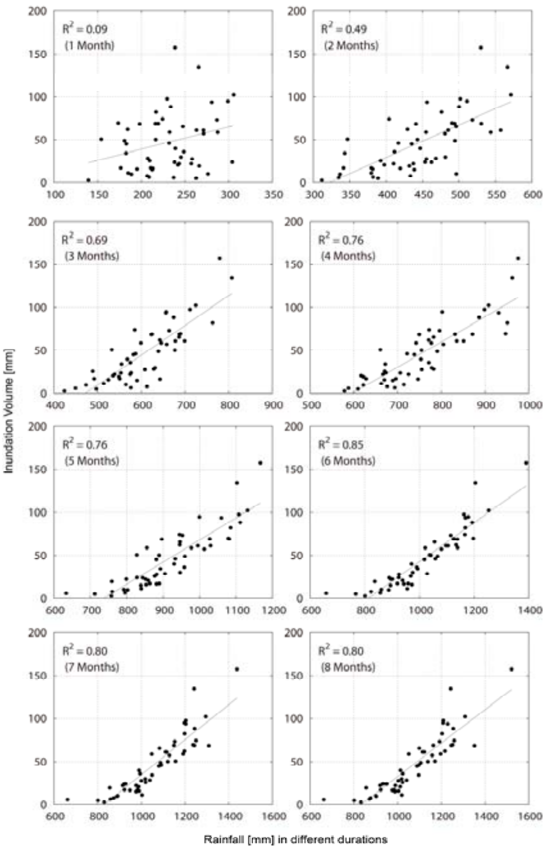

Fig. 2 Relationship between estimated flood inundation volume and rainfall in different durations

GCM data and bias correction

As described in the introduction, this study uses Atmospheric GCM (AGCM) output from Meteorological Research Institute (MRI) Japan. The product used in this study is named AGCM 3.2S and 3.2H based on SRES-A1B scenario. The model resolution of 3.2S product is 20 km, which is the finest GCM output as of today, while the resolution of 3.2H is 60 km. The period of the simulation is 1979-2003 (25 years) for present climate condition and 2075-2099 (25 years) for future climate condition. The benefit of using 3.2H product is to conduct ensemble simulations because it has total 12 different members with 3 cumulus convection schemes times 4 future SST anomalies. In total we used four cases for the present climate condition and 13 cases for the future climate condition. The GCM output was statistically downscaled and bias corrected with the local precipitation data.

Results and discussions

RRI Model calibration and validation

Figure 3 shows simulated and observed monthly discharge at Nakhon Sawan (C2). In this calibration, the effect of the dam reservoirs were removed from the observed C2 discharge by adding inflow and subtracting outflow from the two major dam reservoirs to the observed monthly discharge. The result shows that the model can reproduce the C2 monthly river discharge fairly well for both calibration (NSE = 0.89) and validation (NSE = 0.89) periods. For the other upstream locations also, we evaluated the simulated monthly river discharge for the two periods, the examples at N1 and P1 are shown in the figure.

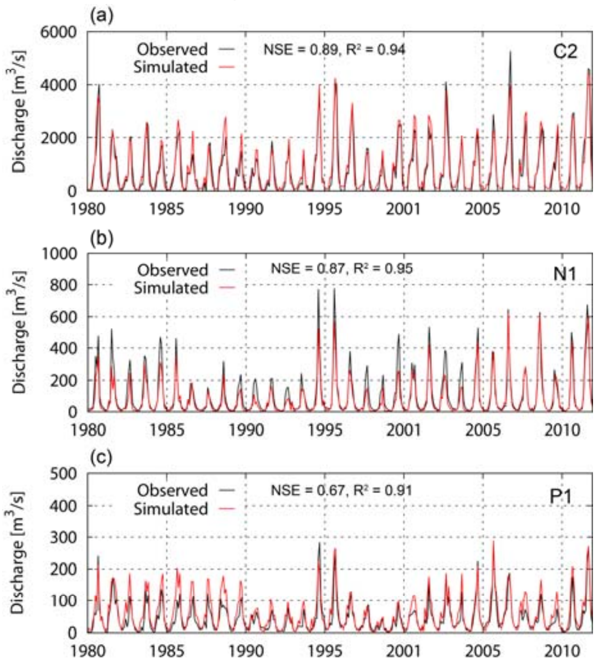

Fig. 3 Model calibration (1980-1999) and validation (2000-2011) with monthly discharges at C2, N1 and P1

Sensitivity analysis

After the model calibration and validation, we run the model again for 52 years continuously with gauged rainfall information. Then we calculated basin average daily rainfall, simulated ET, catchment storage, runoff and inundation for all the years. Figure 4 shows the results on the horizontal axis of the days of the year (DOY) from January 1 to December 31 and the variables in mm on the vertical axes. The solid red-line shows the result of 2011, while the other gray thin lines show the ones from the remaining 51 years. The average values are shown in the solid black-lines.

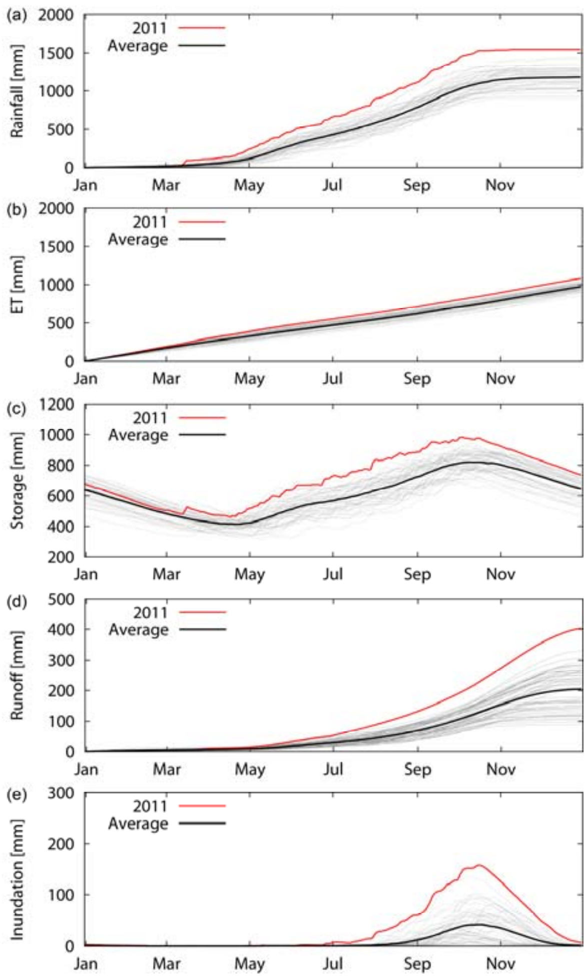

Fig. 4 Estimated water balance components for 2011 (red), the other 51 years (gray) and average (black): (a) cumulative rainfall, (b) evapotranspiration, (c) catchment storage volume, (d) runoff and (e) inundation

The figure shows the total volumes of rainfall, runoff and flood inundation in 2011 are generally much more than those in the other years. The trend of catchment water storage in 2011 was close to the average in January and February but it started to deviate from the average after the beginning of March. The estimated minimum and maximum catchment water storage in 2011 were about 500 mm and 1000 mm, respectively, while they were about 400 mm and 800 mm in the average year.

Figure 5 shows the relationship between six month rainfall P on the x-axis and the other terms including ET, ΔS, Q and ΔF on the y-axis for all the 52 years. The figure suggests that ET is almost constant irrespective of P, while the other terms tend to increase with the increase in P, except for ΔF in the range of P less than about 950 mm. The term ΔS also shows some correlation with P, although ΔS of 2011 suggests the possibility of plateauing with the increase of P.

The six-month rainfall in 2011 was about 1400 mm; that was about 1200 mm in past large-scale floods and about 1000 mm in normal years as shown in Fig. 7. In case of 2011, the estimated ΔF was 157 mm, which means that 11 % of the total rainfall turns out to contribute to inundation ($\Delta F/P$ = 0.11) if no dam reservoirs are taken into account. The figure also suggests that the slope of ΔF against P can be seen as nearly constant for the range of P greater than 950 mm. The estimated slope ($d\Delta F/dP$) by using a first order linear regression with top 35- year records (P > 950 mm) is 0.30. That means an additional 200 mm rainfall results in a 60 mm (= 200 mm x 0.30) increase in flood inundation volume. Hence the rainfall of 1400 mm in 2011 might have increased flood inundation volume by about 60 mm, compared with other previous large floods such as 1995 and 2006 under the naturalized condition.

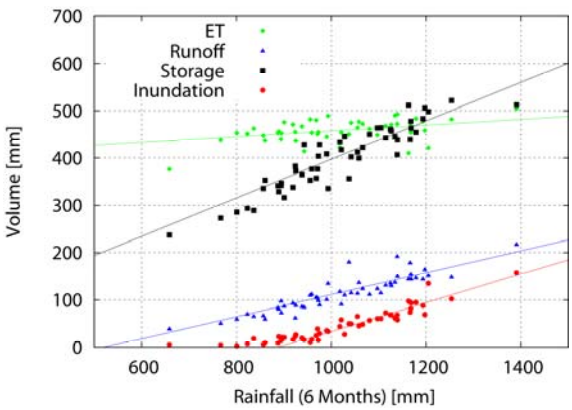

Fig. 5 Relationship between six month rainfall and other water balance components from the 52 years simulation

Climate change projection

The above analysis on historic precipitation records and the RRI model simulation helps us quantitative understanding about the relationship between rainfall and flood inundation volumes. Based on this understanding, now we investigate how the MRI-AGCM projects the future climate and its impact on flooding in this region.

Figure 6 shows six month rainfall under present and future climate conditions on Gumbel probability distributions. Note that there are four and 13 combinations of plots for present and future conditions, respectively, from 3.2S and 3.2H ensembles. In this study we consider each simulation result as equally important and their variations as uncertainty in the GCM projections. Average rainfall amounts in maximum six months are projected to increase from 994 mm in the present to 1078 in the future. In addition, analysis with

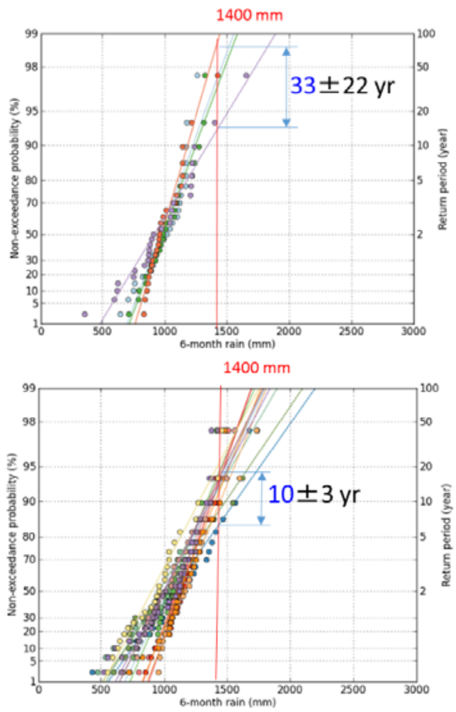

Fig. 6 Frequency analysis results on six month rainfall in present (up) and future (bottom) climate conditions

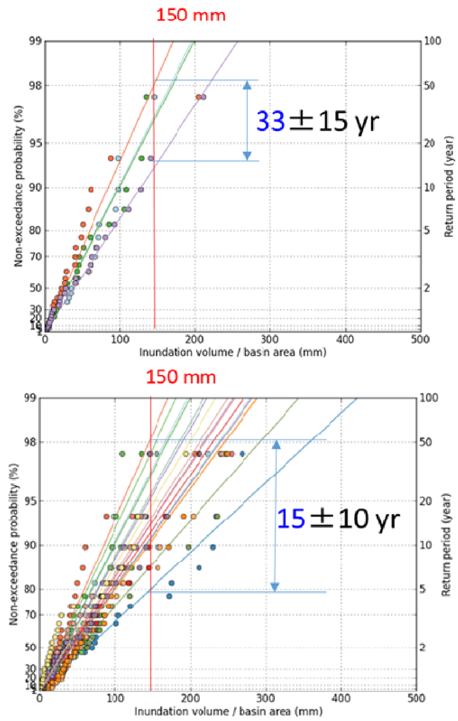

Fig. 7 Frequency analysis results on flood inundation in present (up) and future (bottom) climate conditions

Gumbel distribution suggest that the return period six month rainfall equals to 1,400 mm will become shorter from 33 ± 22 years in the present to 10 ± 3 years in the future.

Figure 7 shows the similar plots but with annual maximum flood inundation volumes estimated by the RRI model simulations with the AGCM outputs. The results suggest that average flood inundation volumes also increase from 42 mm in the present to 60 mm in the future. In addition, the frequency analysis inundation volume (i.e. 150 mm) will become also shorter from 33 ± 15 years in the present to 15 ± 10 years in the future.

Overall the simulation suggested that in both cases focusing on rainfall and flood inundation volume, the floods will become more severe and frequent in the future climate condition, although the ensemble members show rather wide variations among the results. In addition, it should be noted that the estimated return period of 2011 equivalent rainfall (i.e. maximum six month rainfall: 1400 mm rainfall) from MRI-AGCM is shorter than the estimated return period with observed records. According to our analysis with observed rainfall (based on annual maximum six month rainfall), the return period of 1400 mm rainfall was about 50 years. Hence the intrinsic uncertainty involved in the rainfall distributions in the original GCM as well as other uncertainty induced by all the simulation processes must be realized. Nevertheless, as discussed in the previous section, we have to be aware the natural characteristics of high sensitivity in flood inundation with rainfall.

Finally Figure 8 shows the spatial distributions of flood inundation frequency. We calculated annual maximum flood inundation depths for each year in the present and future climate conditions, and then counted how many times the annual peak inundation depths exceeded 0.5 m for each model grid-cell. Some areas close to the main river show very high frequency (e.g. more than 15 times among 25 years) even for the present condition, while some other areas such as south western part of the basin show relatively clear increase in the frequency. The visualization of the change in flood inundation frequency help for water management considering climate change impact.

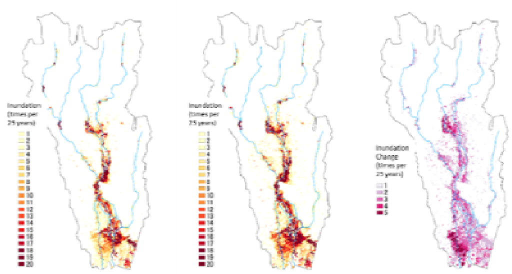

Fig. 8 Frequency of estimated flood inundation per 25 years in the present climate (left), the future climate (mid) and their difference (right)

GCM projections by other GCMs

As described above, this study primarily focused on the MRI-AGCM outputs. Meanwhile we investigated the general characteristics of other GCM projections stored in CMIP5 datasets. In this case, we could not conduct the detail RRI simulation due to the time limitation, and we focus only on the projected change in annual rainfall. 16 GCM outputs over the Chao Phraya River basin suggested that regardless the RCP scenarios (RCP4.5 and RCP8.5), almost all the GCMs indicated the increase of the annual rainfall in the basin. The average increase amount is 146 mm for RCP4.5 and 175 mm for RCP8.5. Based on the above sensitivity analysis, the increase of 200 mm rainfall in flood season has a significant impact on the flooding in this region. We must note that the increase of approximately 150 mm rainfall in average may have significant influence on the flood characteristics as discussed throughout this paper.

Conclusions

This study assessed the impact of climate change on large-scale flooding in the Chao Phraya River basin using a Rainfall-Runoff-Inundation (RRI) model. After the model calibration and validation, we conducted the 52-year long term simulation and analyzed the sensitivity of flood inundation volume to rainfall. Based upon the understanding of the general characteristics of flooding as well as the rainfall and flood inundation volume during the 2011 devastating Thai floods, we run the RRI model by forcing MRI-AGCMs outputs. The main findings are summarized as below:

1) According to the 52 years simulation, peak of flood inundation volumes at each year has the highest correlation (R^2 = 0.85) in the Chao Phraya river basin.2) In 2011, the basin received approximately 1,400 mm rainfall prior to the peak of flood inundation in the mid of October. As a result, the peak flood inundation volume was estimated to be 157 mm without dam reservoir effects.

3) The first order linear regression between six month rainfall and flood inundation volumes at every year showed that the slope of the regression line was about 0.30. This means for example additional 200 mm of rainfall may increase approximately 60 mm (= 9.8 billion m^3) of flood inundation volume, which is more than the total volume of the second largest dam, or Sirikit dam, in this basin.

4) MRI-AGCM3.2S and 3.2H projected that annual maximum six month rainfall in basin would increase by 84 mm. Similarly our estimates with the RRI model indicated that the average flood inundation volumes also increase by 18 mm.

5) Based on the frequency analysis, the return period of six month rainfall equivalent to 1,400 mm will become shorter from 33 ± 22 years in the present to 10 ± 3 years in the future. Similarly the flood inundation volume equivalent to the 2011 flooding (i.e. 150 mm) will become also shorter from 33 ± 15 years in the present to 15 ± 10 years in the future.

Although the use of 3.2S and 3.2H allows us to assess a certain degree of uncertainty induced by different settings in the GCM projections, obviously we could not assess all the potential uncertainty from different sources. Therefore we do not argue that the above quantitative estimates are the only solutions to be referred in the future. Instead, this study highlights the importance of understanding a sensitivity of a key variable directly related to disasters (in this case flood inundation volume associated to six month rainfall) and their projections by GCMs with s hydrologic model.

References

Champathong, A., Komori, D., Kiguchi, M., Sukhapunnaphan, T., Oki, T. and Nakaegawa T. (2013) Future Projection of Mean River Discharge Climatology for the Chao Phraya River Basin, Hydrological Research Letters, 7(2), 36-41.

Hunukumbura, P. B. and Tachikawa, Y. (2012), River Discharge Projection under Climate Change in the Chao Phraya River Basin, Thailand, Using the MRI-GCM3.1S Dataset, Journal of the Meteorological Society of Japan, 90A, 137-150.

IPCC AR5 (2013) Climate Change 2013, The Physics Science Basis, WG1, Fifth Assessment Report.

Kure, S. and Tebakari, T. (2012) Hydrological Impact of Regional of Regional Climate Change in the Chao Phraya River Basin, Thailand, Hydrological Research Letters, 6, 53-58.

Mateo, C. M., Hanasaki, N., Komori, D., Tanaka, K., Kiguchi, M., Champathong, A., Sukhapunnaphan, T., Yamazaki, D. and Oki, T. (2014) Assessing the Impacts of Reservoir Operation to Floodplain Inundation by Combining Hydrological, Reservoir Management, and Hydrodynamic Models, Water Resour. Res., 50, 7245–7266.

Sayama, T., Ozawa, G., Kawakami, T., Nabesaka, S. and Fukami, K. (2012) Rainfall-runoff-inundation analysis of the 2010 Pakistan flood in the Kabul River basin, Hydrological Science Journal, 57, 298-312.

Sayama, T., Tatebe, Y., Iwami, Y. and Tanaka, S. (2014), Hydrologic Sensitivity of Flood Runoff and Inundation: 2011 Thailand Floods in the Chao Phraya River Basin, Natural Hazard Earth System Science (under review).

The World Bank (2012) Thai Flood 2011, Rapid Assessment for Resilient Recovery and Reconstruction Planning, World Bank, Bangkok.

IWRM for Climate Change Adaptation in the Mekong River Basin

Kittiwet Kuntiyawichai[1,a], Stefan Uhlenbrook[2, b *], Wim Douven[2,b], Jaap Evers[2,b], Piet Lens[2,b], Assela Pathirana[2,b], Meine Pieter van Dijk[2,b], Joyeeta Gupta[2,b], Dimitri Solomatine[2,b], Erik de Ruyter van Steveninck[2,b], Charlotte de Fraiture[2,b], Shreedhar Maskey[2,b], Yong Jiang[2,b] and Mukand Babel[3,c]

Abstract It is widely accepted that Integrated Water Resources Management (IWRM) is the way forward to respond to efficient, equitable and sustainable development and management of water resources. Additionally, IWRM has also strong linkages with variability in climate conditions which causes various challenges for IWRM approaches. Besides the annual climatic trends and periodicities, the climate is still subject to change and its severe impacts, e.g. floods, droughts etc. are being recognized increasingly. It is therefore important to find out what actually drives the climate towards current and future changes. In response to climatic shifts, the programme called "Post-doctoral Research programme on Adaptation to Climate Change (PRoACC) in the Mekong River Basin" was initiated with its main objective to strengthen research output in the field of climate change adaptation and to better inform decision making. The project carried out by more than 20 researchers from all Mekong/Lancang countries led by UNESCO-IHE in collaboration with many regional and national partner institutes. Scientific and societal findings are expected as a minimum requirement from each individual post-doc research, which include journal articles, synergy papers, policy brief outlining the potential implementation of research outputs, and educational materials for curriculum and training. Collaborative platforms have been carried out to allow researchers and experts to share research and discuss their creative solutions related to climate change impacts on water resources. Moreover, developing model-based climate variation and change scenarios to determine potential vulnerabilities and adaptations were also executed to explore how mitigation/adaptation strategies can be made. To enable the synthesized research results to deliver their maximum impact, a continuing and facilitated dialogue for raising awareness with stakeholders on climatic extremes/risk is further required.

Keywords *Integrated Water Resources Management (IWRM), climate change adaptation, PRoACC*

Kittiwet Kuntiyawichai (Author)
Department of Civil Engineering, Faculty of Engineering
Khon Kaen University, Khon Kaen, Thailand
kkitti@kku.ac.th

Stefan Uhlenbrook
UNESCO-IHE Institute for Water Education
Delft, the Netherlands
s.uhlenbrook@unesco-ihe.org

Wim Douven
UNESCO-IHE Institute for Water Education
Delft, the Netherlands
w.douven@unesco-ihe.org

Jaap Evers
UNESCO-IHE Institute for Water Education
Delft, the Netherlands
j.evers@unesco-ihe.org

Piet Lens
UNESCO-IHE Institute for Water Education
Delft, the Netherlands
p.lens@unesco-ihe.org

Assela Pathirana
UNESCO-IHE Institute for Water Education
Delft, the Netherlands
a.pathirana@unesco-ihe.org

Meine Pieter van Dijk
UNESCO-IHE Institute for Water Education
Delft, the Netherlands
m.vandijk@unesco-ihe.org

Joyeeta Gupta
UNESCO-IHE Institute for Water Education
Delft, the Netherlands
j.gupta@unesco-ihe.org

Dimitri Solomatine
UNESCO-IHE Institute for Water Education
Delft, the Netherlands
d.solomatine@unesco-ihe.org

Erik de Ruyter van Steveninck
UNESCO-IHE Institute for Water Education
Delft, the Netherlands
e.deruytervansteveninck@unesco-ihe.org

Charlotte de Fraiture
UNESCO-IHE Institute for Water Education
Delft, the Netherlands
c.defraiture@unesco-ihe.org

Shreedhar Maskey
UNESCO-IHE Institute for Water Education
Delft, the Netherlands
s.maskey@unesco-ihe.org

Yong Jiang
UNESCO-IHE Institute for Water Education
Delft, the Netherlands
y.jiang@unesco-ihe.org

Mukand Babel
Asian Institute of Technology
Pathumthani, Thailand
msbabel@ait.asia

Introduction

The rising key challenges for water resources allocation and management is connected to the fact that too little is known on the understanding of the relationship between vulnerability and adaptation. It is foreseeable that various water-related management problems are expected to worsen with climate change. Unlikely events with a low probability of occurrence might cause tremendous consequences which may be considered unacceptable for human being. Many previous studies on the influences of hydrological changes on climate and outlining the observed and projected effects of climate change would close the gap in understanding (Masih et al., 2011; Hu et al., 2011; Di Baldassarre et al., 2011; Ranasinghe et al., 2013; Singh et al., 2014). Considering all relevant studies, they seem to correspond to the main purpose of the programme, the so-called "Post-doctoral Research programme on Adaptation to Climate Change (PRoACC) in the Mekong River Basin", which involves how water-related issues are connected to climate change and adaptation responses. The main motivation is to not wait until the extreme events happen, but rather to consider whether the consequences of climate change will exceed an unacceptable level or not. In brief, it is essential to not overlook the other aspects in order to accommodate non-climate change-related anthropogenic causes, e.g. urbanization, deforestation, pollution, etc. and improve the human's capability in handling the increased pressure on already stressed water resources in the Mekong River Basin.

Study area: The Mekong River Basin

The Mekong River Basin is a large international river basin with the total area of approximately 800,000 km^2 and is shared by six riparian countries: China (Yunnan Province, Lancang sub-basin), Myanmar, Lao PDR, Thailand, Cambodia, and Viet Nam. The river basin itself produces a total annual runoff of approximately 475,000 million m^3 during the rainy season (MRC 1997).

Approximately 70 million people live in the Mekong River Basin, which is mainly rural area with diverse ecosystem and they rely on a significant extent of agriculture. By 2050, the population is expected to increase by about 60 percent (Islam, 2010). The rapid population growth often causes conflicting demands on water and land resources, especially in the lower Mekong River Basin.

It is the fact that the Mekong is dominated strongly by monsoon rainfall pattern and the variability in the physiographic characteristics, i.e. topography, geology, soil, land use, etc., which affect the space and time variation of water resources availability. The average annual rainfall in the Mekong River Basin is 1,400 mm/year and varies between different regions (300-3,000 mm/year) (Räsänen, 2014), while the annual average discharge is approximately 14,900 m^3/s (Lu et al., 2006).

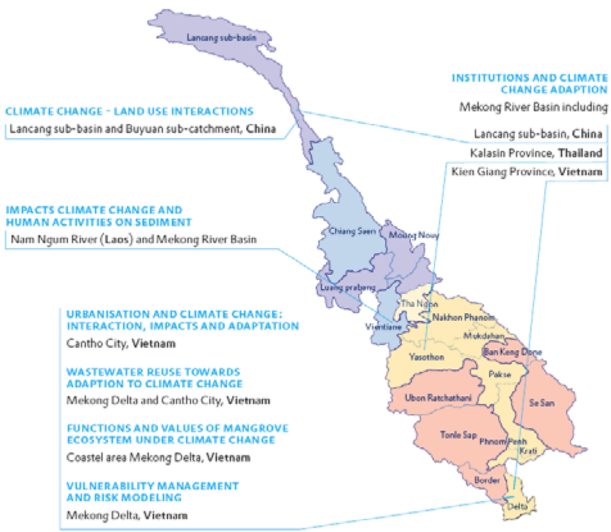

Fig. 1 The study area.

Issues of water resources and sustainability in the Mekong River Basin

Considering the Mekong River Basin as a whole, water resources are not highly developed and to some extent poorly understood (e.g. groundwater resources). Moreover, there are also several emerging issues related to the water usage perspective, which include (Hoanh et al., 2003, IPCC, 2007):

- further development of irrigation connected to more intensification of food production, i.e. change of cropping pattern/calendar, increased dry-season production, more harvests per year, increased fish production, etc.;

- catastrophic floods occurred in some areas and caused tremendous damage;
- reduction of low flows due to (mainly agricultural) water use upstream and consequently increased sea water intrusion in the delta region;
- hydropower development (proposed or under development) with unequal benefits across the riparian countries and sectors involved;
- land use changes (e.g. deforestation and maybe local reforestation efforts as adaptation measure; local urbanization) with impacts on local and regional water cycle dynamics;
- rapid population growths and economic development impacts water resources quality (surface water and groundwater); and
- over past decades, climate change is likely to cause further shifts in the monsoon weather patterns with increasing floods (more intense rainfalls) and droughts (longer and more severe dry spells), increased number of tropical cyclones, more severe heat waves in particular in larger urban areas, and possible more extensive ENSO phenomena with impacts on the regional climate. In addition, on top of that, sea levels will rise with significant impacts on coastal regions.

The abovementioned issues make the water resources management and development in the Mekong River Basin well-informed, which will essentially bring the scientifically sound adaptation measures into action.

Initiative idea towards interdisciplinary scientific research

The Mekong riparian countries recognized the need for a collaborative and integrative water resources management long time ago. Focusing on the lower part of the Mekong River Basin, the Mekong River Commission (MRC) revealed that the history of coordination and planning for water resources development has been taken into consideration for many years. Recent attempts and developments have been outlined in order to bring the upper part of the river basin closer to the other countries and their regional cooperative development approach.

The vulnerability to climate change makes the Mekong River Basin to be a suitable study area for a promising research study. The key contribution is to raise the understanding by increasing the knowledge base about the interplay of climate change and other changes (with various poorly understood positive and negative feedbacks) through well-targeted. To the end, the way towards interdisciplinary scientific research will be addressed as it is found to be essential for future sustainable planning and development of water resources.

About PRoACC

The post-doctoral fellowship programme on Climate Change Adaptation in the Mekong River Basin is part of the UNESCO-IHE Partnership Research Fund (UPaRF) that was established in April 2008 with the main direct sources of funding from: (i) the research facility under the DGIS (Dutch Development Cooperation) - UNESCO-IHE Programmatic Cooperation (DUPC), and (ii) the UNESCO-IHE Internal Research Fund (IRF), which is based on the general subsidy from the Dutch Ministry of Education, Culture and Science (OCW). The overarching objective of this programme is to strengthen research output in the field of Climate Change Adaptation of UNESCO-IHE in collaboration with its partner institutes.

In PRoACC Phase 1 (PRoACC-1), all post-doctoral fellows come from the region and are hosted by local/regional knowledge institutes. This will strengthen regional cooperation further and the objective is that the post-doctoral fellows will continue to work on related topics in the region after the programme is finished. The four main PRoACC-1 research themes are as follows:

1) Physical system and climate change adaptation;
2) Urban areas and climate change adaptation;
3) Delta system and climate change adaptation; and
4) Institutions and climate change adaptation.

Based on the results from PRoACC-1, a second phase of PRoACC (PRoACC-2) has continuously developed into four themes, which consist of 11 regional researchers implementing their research projects in close cooperation with UNESCO-IHE researchers. The research is to address the following PRoACC-2 thematic areas:

1) Enhancing the adaptive capacity and livelihoods of poor people to cope with climate change;
2) Managing sediments and nutrients across scales and climate change adaptation;
3) Urbanizing areas in the Mekong delta and climate change adaptation; and
4) Transboundary cooperation for sustainable water management and climate change adaptation.

Research outputs

In PRoACC research programme, eight individual post-doctoral research projects were implemented in PRoACC-1, while eleven specific research topics are being conducted in close collaboration with key stakeholder groups from the Mekong River Basin. In addition, by supporting researchers from the Mekong region, local capacities in research and education were supported. The scientific findings across several disciplines were translated for the development/implementation of better policies in the field of climate change adaptation in policy briefs. Additionally, the capacity building aspect of this post-doctoral programme was also realized to be significant and was prioritized as per the necessity.

To present the success of the PRoACC programme, the following scientific research and societal outputs are expected as a minimum from each individual PRoACC research theme:

- two peer reviewed international journal articles and papers in conference proceedings or chapters in books;
- one PRoACC Symposium Paper and contributions to 'synergy papers';
- one policy brief outlining the potential implementation of project outputs in the development/implementation of on-the-ground adaptation strategies in the partner country; and
- one digital case study to be used as educational product at partner institutes and UNESCO-IHE.

The expected societal outputs are:

- the contribution to river basin planning and management and answer to key questions related to climate change adaptation;
- the linkage between research and education by using knowledge and material in local university curricula and training; and
- the strengthening of local climate change and adaptation partnerships of government and academic partners.

Taken as a whole, the PRoACC-1 and 2 research findings showed their usefulness and validity by a list of relevant climate change peer-reviewed scientific journals relating to the qualitative research results as appeared in the reference list. It should be noted that the list of expected deliverables underline on some of the earlier findings from PRoACC-1. That is to say, the list is not intended to be definitive as the ongoing actions of current PRoACC-2 are still in progress.

PRoACC Phase 1 research outputs and description

The research conducted in PRoACC -1 has led to some further understanding of how climate change is affecting the Mekong River Basin. The main findings gained through PRoACC-1 was expected to enable researchers and involved stakeholders to address the knowledge on climate change adaptation based on both existing needs and future challenges. To meet the relevant challenges, a number of supervisors and researchers in PRoACC-1 incorporated and worked together in order to ensure effective research insights. As the possible impacts of climate change in the Mekong River Basin are manifold and cross-cutting, therefore, the growing climate threat is directly tied to multiple levels of time and space at all socio-economic and environmental sectors. Below, some of the PRoACC-1 relevant findings together with various adaptation issues are highlighted from the four identifiable collaboration themes.

Physical system and climate change adaptation

Based on the scientific evidence conducted under this research theme, it was revealed that the annual precipitation in the Lancang/Upper Mekong (China) surprisingly shows no significant trend although models expect an increase in the future. The variability, however, has increased in the form of longer dry spells and increased heavy rainfall events with increased frequencies of droughts and floods. It is found that this trend has grown stronger in the last few decades. Runoff has increased mainly due to likely land use changes, which result in changes in evapotranspiration caused by less wind and higher humidity. Because of the high uncertainty in predictions, improved monitoring and regional modelling will therefore be needed to support adaptation in the region and downstream. In addition, reservoir planning and operation also have to be conducted with a view to limit the potential impacts of increased variability.

To fulfill the research component, another research study carried out in the Nam Ou River Basin, Lao PDR reflected the impact of climate change on sediment discharge and the results could probably apply to many other sub-basins of the Mekong River Basin. Due to different rainfall and (though not studied in detail) land use, the river will contain a higher sediment load with the changing climate. However, because of the planned reservoirs in the basin, the load will decrease substantially. Depending on the number of reservoirs and their management, this might lead to a reduction of 80-95% which is far more than compensation by the expected increases. It will be necessary to study the potential impacts of the reservoirs at basin level. The impacts of sediment trapping will extend from behind the dams (filling up of reservoirs) to after the dams, e.g. increased river erosion, reduced nutrients to critical ecosystems (e.g. Tonle Sap), and into the coastal areas (less sediment: coastal erosion and negative impacts on mangrove forests). Integrated sediment management along the Mekong River will be needed to adapt to the changing climate and plan for the least negative impacts on impacts along the Mekong River. In the end, a significant part of the obtained research results was published in the peer reviewed journal in January 2013 (Shrestha et al., 2013).

Urban areas and climate change adaptation

It is crucial that urbanization and climate change would need to be underlined in this overarching theme as urbanization influences local climate, i.e. temperature is higher (urban heat island effect) and the intensity of heavy storms increases. Multiple causes could also result in urban flooding in the Mekong Delta, e.g. extreme rainfall, river floods, and floods from the sea (as strengthened by sea level rise and more severe surges). Relying on different measures, urban drainage in some areas needs improvement, including reservoirs and/or pumping stations, while flood protection (i.e. dikes, embankments) might be extended in other areas. Local rainfall storage, e.g. rooftop, gardens, underground, can contribute to diminishing flood depth due to heavy rainfall. Non-structural measures, i.e. city planning, early warning and flood-proofing strategies, are also important as they can prevent unsustainable situations and limit the impacts from flood drills through awareness raising, creating refuges etc. The Mekong Delta has an increasing demand for water in agriculture, along with changes in rainfall patterns, while traditional sources (i.e. rain, groundwater and surface water) are insufficient in the near future. The study in Can Tho city shows that urban wastewater is sufficient to cover about 16% of water demand in rice cultivation. Co-benefits are the nutrients, which can cover 12% (Phosphorus) to 20% (Nitrogen) of the agricultural demand, whereas re-use at the same time limits pollution and treatment costs of wastewater. In brief, the study in Can Tho can be an example for other cities in low land situations. The success of this research work is represented by the number of peer-reviewed journal publications (Huong et al., 2013; Trinh et al., 2013a; Trinh et al., 2013b).

Delta system and climate change adaptation

In this perspective, it is likely to state that climate change is leading to more runoff. In this regard, timely forecast and early warning are important adaptation options, apart from the structural and spatial planning measures. It is expected that the availability of water over the Bassac River and the Mekong River in the Vietnam Mekong Delta will change and as a result agriculture and aquaculture in the Ca Mau peninsula would be impacted. The coastal area at the East Sea side will heavily be impacted by sea level rise, which causes coastal erosion, flooding, and salt water intrusion. With respect to mangrove forests, it is obvious that they are a natural and effective protection against storms and wave attack. However, wave attenuation depends on mangrove characteristics (e.g. width and health), for instance, a width of 1.5 kilometers gives optimal decrease of wave height. The impacts of climate change on mangroves are uncertain, but decrease of sediment input, sea level rise and changes in river runoff all form severe threats. In short, local communities can play an important role in the management of the mangrove forests, but external support with knowledge, finances and regulations is necessary. Based on the insight findings described above, it seems to be valid for all mangrove areas along the Vietnamese coast. A more comprehensive picture of the overall research theme productivity/accomplishment is guaranteed as evidenced by peer-reviewed publications (Dinh et al., 2012; Van et al., 2012; Cuc et al., 2013).

Institutions and climate change adaptation

In the context of institutions, existing policies related to climate change adaptation have been studied in China, Thailand and Vietnam. Local farmers have been interviewed to find out how they are stimulated or counteracted in adapting to climatic conditions by local, provincial and national regulations. A mixed picture emerges where sometimes government supports local adaptation initiatives, but existing regulations sometimes hinder local stakeholders in their attempts to adapt. In all cases, stakeholders need support with knowledge (new and traditional) and finances (access to credit facilities) to be able to overcome prolonged periods of drought and to move towards more sustainable farming. This might require changes in local, provincial and national institutional arrangements including adapted regulations. Although differences appear between the three areas in the two studies, the main conclusions seem to be generally applicable. A scientific contribution derived from this research theme can be represented by several peer-reviewed journal publications (Li et al., 2012; Li et al., 2013; Bastakoti et al., 2014).

PRoACC Phase 2 initiation and linkages

A strong focus of the PRoACC-1 has been on developing climate scenarios, describing and projecting climate change impacts, and summarizing adaptation responses and future research needs for primary sectors in the Mekong River Basin. In PRoACC-2, an integrated assessment approach and model will be used to develop adaptation scenarios for future climate conditions using the climate scenarios and sector impact information generated during PRoACC-1, in combination with a range of stakeholder consultations and task team workshops. In this respect, PRoACC-1 provides a platform for undertaking detailed and high-level adaptation scenario development. While attention is drawn to the fact that a list of adaptation actions available at local and regional scales for the Mekong region is extensive, the key challenge is to organize these options so that stakeholders are not overwhelmed. Most importantly, a suite of possible adaptation alternatives proposed by this research is expected to be more informed and carefully considered with the interdisciplinary insight to enable the inhabitants to respond to the challenges climate change poses to the Mekong River Basin.

Details of research areas in PRoACC Phase 2

Under this PRoACC-2 collaborative research programme, there is a linkage between disciplines and a number of content-related research themes. Besides conducting the state of the art in each research area, the cooperation between various research themes is also highlighted via cross research theme in which each of them can share expertise, resources, data and results (as a synthesis), rather than individual-oriented. The sub-sections below go into more details for each specific research theme.

Enhancing the adaptive capacity and livelihoods of poor people to cope with climate change

In this theme, the main research objective is to contribute to poor farmer's livelihoods by improving their adaptive capacity to cope with climate change. The achievement will be obtained by making recommendations on how to improve adaptation programmes and policies implemented by governments and donors by bringing in farmer's perspectives.

In achievement of the overall theme objective, the following specific objectives are addressed:

- to assess farmer's perspectives on climate related risks;
- analyse farmer's risk management strategies, including mitigation, coping, and adapting strategies;
- compare farmer's responses to climate risks with government's (NGO's) programmes; and
- make policy recommendations to improve existing and future programmes.

Some conclusions:

Government and NGO programmes do not always correspond to the local needs of people to adapt to climate and socio-economic changes. In Cambodia, this resulted in spending millions US Dollars on agricultural projects while people prefer to sell their labor.

Managing sediments and nutrients across scales and climate change adaptation

The overall objective of this research theme is to provide improved understanding variability and change of sediment and nutrient flows, their impacts and adaptation in the Mekong River Basin under anticipated climate change or other human interventions

In addition, there are a set of underlying specific objectives, which are:

- assess basin-wide vulnerability of soil erosion and sediment yield under present and future climate conditions;
- assess the impact of climate change and reservoirs on sediment yield of the Chi River Basin;
- evaluate land management options for managing basin sediment yield in the Nam Ou and Chi River Basins;
- assess the impact of hydrological, sediment and nutrient changes on rice production in the Mekong Delta; and
- evaluate adaptation options for reducing impacts of hydrological, sediment and nutrient changes on rice production in the Mekong Delta.

Some conclusions:

Based on the present results, it may be helpful to contribute more details in understanding of sediment transport in the Delta floodplains. Any natural or artificial actions that change floodplain inundation, e.g. sea level rise, compartments/polder developments, and construction of dams affect sediment delivery to and spatial sediment deposition in the floodplains. Moreover, this also affects the production systems in the Mekong Delta.

Urbanizing areas in the Mekong delta and climate change adaptation

This research theme is driven by the key objectives, which are to understand urban development processes in Can Tho and similar cities, and to improve long-term livability and resilience by promoting flexible adaption options.

To fulfill the main aims of this research theme, a set of specific objectives is planned:

- to understand the nature of urbanization and the complexities, uncertainties, dynamics and interlinked factors driving development;
- to develop the modelling platform and future development scenarios of urban transformation and climate change that can be used for scenario analysis;
- to analyse achievability of future development planning scenarios based on governance, perception, and technology and financial aspects;
- to identify the pathways to flood resilience in the future urban development process; and
- to propose a feasible and flexible urban planning approaches adapting to future change.

Some conclusions:

1) urban people are already adapting to climate change;
2) improved intensive cooperation between science, policy makers, and other stakeholders in "joint learning alliances" can effectively contribute to realizing resilient cities.

Transboundary cooperation for sustainable water management and climate change adaptation.

The major research theme objective is to better understand how to move from conflict situations in transboundary water management to cooperation and sustainable water resource development.

In addition, this research theme also defines a set of specific objectives, namely:

- what are the characteristics of transboundary water development, and how can management measures and institutions be arranged by promoting cooperation towards sustainability and adaptation; and
- what are the hydrological impacts of dam development, climate change, socio-economic, and environmental implications across Vietnam and Cambodia?

Some conclusions:

- Dams in the upper Sesan River Basin have changed the downstream hydrological system;
- people's livelihoods in the lower Sesan River Basin are affected by the changes in the river system; and
- the MRC 1995 Agreement is insufficient to control dam developments, which raises concerns about water security issues in the international tributary of the Sesan River Basin.

Summary and conclusions

Despite the increasing recognition that water-related risks cannot be tackled in an isolated manner, therefore, Integrated Water Resources Management (IWRM) is the best option for sustainable and equitable water resources management. Through a holistic approach with a collaborative/well-coordinated and targeted adaptation measures, the way to handle water resources is still more complicated as climate change aggravates the already serious risk. That is why the PRoACC programme is remarkable as it zooms in and presents a more detailed view on the implications of climate change in relation to water related vulnerability.

Since the starting of the PRoACC programme in 2010, there was a platform for addressing and sharing knowledge on climate change driven research and adaptation for both current and future challenges and initiatives. Through networking from various individual PRoACC researchers, coordination and dissemination activities were fully integrated towards the underlying and unfolding of possible climate change impacts on water resources. To ensure the continuity and consistent information about the PRoACC research programme, a summary of some key messages emerging from PRoACC specific themes is highlighted briefly below:

- climate change impacts occur in the entire Mekong River Basin in which they interact with other influences from global/regional changes and cannot easily be isolated;

- with many reservoirs planned, integrated water-sediment management is necessary for the basin as a whole;

- droughts will occur more frequently in both upstream and downstream areas. More specifically, adaptation measures in agriculture are necessary. In urban areas, wastewater reuse for irrigation provides co-benefits on the reuse of nutrients and water;

- flood risks are increasing, especially from rivers and sea, as a result from human interference in the basin, climate change and sea level rise, but also due to increasing developments in flood prone areas (people and assets). Besides the hard engineering schemes, soft measures, such as early warning, are also important to be applied in the Mekong Delta, which is a hot spot for flood adaptation;

- mangrove forests are efficient in wave attenuation and coastal protection, however, they are threatened by many influences including climate change. Community based management is effective but needs government support, whereas government support sometimes counteracts the local adaptation initiatives;

- climate change adaptation requires action at multiple scales, i.e. basin, national and local levels. In this context, riparian countries of the Mekong River Basin can learn from each other's approaches. Enhanced and shared information supports cooperation in the area of climate change adaptation and related areas;

- there is a gap in the science-policy transfer, however, there is a good example presented, i.e. the case study of Can Tho city;

- a better cooperation with (local/regional/national) governments and NGOs is needed in order to realize further impacts from this research work; and

- there is a need for further basin wide multi/interdisciplinary studies in the Lancang-Mekong River Basins.

Finally, it is foreseeable that the PRoACC in-depth scientific findings are exemplary towards tackling the rising threat of climate change poses to the livelihoods and well-being of the Mekong and its people in the future. There is also a marked interest for extensively and thoroughly developing a thoughtful and responsible plan of action for successful and sustainable water management of the Mekong River Basin through further meaningful research.

Acknowledgements

The PRoACC research programme is financed by the DGIS (Dutch Development Cooperation) - UNESCO-IHE Programmatic Cooperation (DUPC), and the UNESCO-IHE Internal Research Fund (IRF), which is based on the general subsidy from the Dutch Ministry of Education, Culture and Science (OCW). The following institutions and organizations are to be specially thanked for the contributions from their staffs and associates, i.e. Centre for Water management and Climate Change, Vietnam National University, Vietnam, Asian Institute of Technology (AIT), Thailand, Cantho University, Vietnam, Water Resources University (WRU), Vietnam, Southern Institute of Water Resources Research (SIWRR), Vietnam, Chinese Academy of Sciences (CAS), China, Changjiang River Scientific Research Institute (CRSRI), China, Royal University of Phnom Penh, Cambodia, Khon Kaen University (KKU), Thailand, Ho Chi Minh City University of Technology, Vietnam, Institute for Environment and Resources, Vietnam National University, Vietnam, Water Resources University, Hanoi, Vietnam, and Institute of Meteorology, Hydrology and Environment (IMHEN), Vietnam.

References

Bastakoti, R.C., Gupta, J., Babel, M.S., van Dijk, M.P. (2014) Climate risks and adaptation strategies in the Lower Mekong River Basin. Regional Environmental Change. 14 (1), 207 – 219.

Cuc, N.T.K., Suzuki, T., de Ruyter van Steveninck, E.D., Hai, H. (2013) Modelling the impacts of mangrove vegetation structure on wave dissipation in Ben Tre Province, Vietnam, under different climate change scenarios. Journal of Coastal Research. pre-print online: [1-9].

Di Baldassarre, G., Elshamy, M., van Griensven, A., Soliman, E., Kigobe, M., Ndomba, P., Mutemi, J., Mutua, F., Moges, S., Xuan, Y., Solomatine, D., Uhlenbrook, S. (2011) Future hydrology and climate in the River Nile basin: A review. Hydrological Sciences Journal. 56(2), 199 – 211.

Dinh, Q., Balica, S., Popescu, I., Jonoski, A. (2012) Climate change impact on flood hazard, vulnerability and risk of the Long Xuyen Quadrangle in the Mekong Delta. International Journal of River Basin Management. 10(1), 103 – 120.

Hoanh, C.T., Guttman, H., Droogers, P., Aerts, J. (2003) Water, climate, food and environment in the Mekong Basin in Southeast Asia: Contribution to the project ADAPT, International Water Management Institute, Mekong River Commission Secretariat and Institute of Environmental Studies. Final Report, 57 p.

Hu, Y., Maskey, S., Uhlenbrook, S., Zhao, H. (2011) Streamflow trends and climate linkages in the source region of the Yellow River, China. Hydrological Processes. 25(22): 3399 – 3411.

Huong, H.T.L., Pathirana, A. (2013) Urbanization and climate change impacts on future urban flooding in Can Tho city, Vietnam. Hydrology and Earth System Sciences. 17, 379 – 394.

IPCC (2007) Climate Change 2007: Synthesis Report. Contribution of Working Groups I, II and III to the Fourth Assessment Report of the Intergovernmental Panel on Climate Change [Core Writing Team, Pachauri, R.K and Reisinger, A. (eds.)]. IPCC, Geneva, Switzerland, p.104.

Islam, N. (2010) The law of non-navigational uses of international watercourses: Options for regional regime-building in Asia. Kluwer Law International BV, The Netherlands.

Li, H., Gupta, J., van Dijk, M.P. (2013) China's drought strategies in rural areas along the Lancang River. Water Policy. 15(1), 1 – 18.

Li, H., van Dijk, M.P. (2012). Climate change and farmers response in rural China. International Journal of Water. 6 (3/4), 290 – 310.

Lu, X.X., Siew, R.Y. (2006) Water discharge and sediment flux changes over the past decades in the Lower Mekong River: Possible impact of the Chinese dams. Hydrology and Earth System Sciences. 10: 181 – 195.

Masih, I., Uhlenbrook, S., Maskey, S., Smakhtin, V. (2011) Streamflow trends and climate linkages in the Zagros mountains, Iran. Climatic Change. 104, 317 – 338.

MRC (1997) Mekong River Basin diagnostic study – Final report. Report No. MKG/R. 97010. Mekong River Commission, Bangkok, Thailand.

Ranasinghe, R., Duong, T.M., Uhlenbrook, S., Roelvink, D., Stive, M. (2013) Climate-change impact assessment for inlet-interrupted coastlines. Nature Climate Change. 3(1), 83 – 87.

Räsänen, T.A. (2014) Hydrological changes in the Mekong River Basin: The effects of climate variability and hydropower development. Ph.D. Thesis, Department of Civil and Environmental Engineering, Aalto University, Finland.

Shrestha, B., Babel, M.S., Maskey, S., van Griensven, A., Uhlenbrook, S., Green, A., Akkharath, I. (2013) Impact of climate change on sediment yield in the Mekong River basin: A case study of the Nam Ou basin, Lao PDR. Hydrology and Earth System Sciences. 17, 1 – 20.

Singh, R., van Werkhoven, K., Wagener, T. (2014) Hydrological impacts of climate change in gauged and ungauged watersheds of the Olifants basin: A trading-space-for-time approach. Hydrological Sciences Journal. 59 (1), 29 – 55.

Trinh, L.T., Duong, C.C., van Der Steen, P., Lens, P.N.L. (2013a) Exploring the potential for wastewater reuse in agriculture as a climate change adaptation measure for Can Tho City, Vietnam. Agricultural Water Management. 128: 43 – 54.

Trinh, L.T., Vu, G.N.H., van Der Steen, P., Lens, P.N.L. (2013b) Climate change adaptation indicators to assess wastewater management and reuse options in the Mekong Delta, Vietnam. Water Resources Management. 27(5), 1175 – 1191.

Van, P.D.T., Popescu, I., van Griensven, A., Solomatine, D.P., Trung, N.H., Green, A. (2012) A study of the climate change impacts on fluvial flood propagation in the Vietnamese Mekong Delta. Hydrology and Earth System Sciences. 16, 4637 – 4649.

Aerobic Rice Technology (ART) in the Philippines and Southeast Asia: *Improving Productivity and Enhancing Technology Adaption towards Rice Sufficiency and Climate Change Resiliency*

Orlando F. Balderama[1,a,*]

Abstract. ART is a new water-saving technology for rice production which involves growing drought and disease tolerant, high yielding and short-duration rice varieties in non-flooded and non-puddled soil in water-scarce areas such as rain fed lowland and upland and tail-end portions of gravity irrigation systems. The project aimed to improve eco-system based rice farming system through appropriate water-saving technologies to increase rice production and farmers' income through innovative research and extension modalities.

As a result, farmer-managed on-farm trials yielded 4-6 tons per hectare across climate types and variation of varieties, ecosystem, planting dates and planting methods. The water use efficiency obtained 2.2 grams per kg as compared with the traditional flooded rice production practice which has only about 0.4 g/kg. The financial viability of ART is also promising. For a low yield of 4.2 tons per hectare will yield the following: cost of production is P34,135.20; gross sales at prevailing rate is P84,000; net income of P49,864.8; with return of investment at 1.46.

Extension work activities such as training of trainers to agricultural extension workers & farmer leaders, farmer participatory trial & field day, and production & distribution of brochures & training manuals were conducted to enhance the information dissemination and adaption of technology. Upscaling of Aerobic Rice Technology was pursued through the conduct of National Aerobic Rice Conference and organization of ASEAN network.

Keywords: *aerobic rice, climate change, rice sufficiency, ASEAN*

Orlando F. Balderama
Isabela State University,Echague, Isabela Philippines.
orly_isu@yahoo.com

Autonomous Surface Vehicle for Bathymetric and Environmental Survey: Implementation and Results

Pasan Kulvanit[1*] and Pradya Prempraneerach[2]

Abstract This paper is focusing on the deployment of robotic vehicles in the role of surveyors for the tasks of bathymetric or environmental survey of water resources. The autonomous surface vehicles (ASV) developed in-house are either in the form of a modified electric kayak boat or an outboard motor boat with deft capability to maneuver the environment ranging from small canals, reservoirs, and the oceans. The robot can be controlled remotely via 2.4 GHz. radio frequency or can do self navigation via autonomous waypoints tracking algorithm. The on-board navigational sensors include global positioning system (GPS) and attitude/heading reference system (AHRS). The ASV’s autonomous waypoint tracking is custom designed to track a group of waypoints in any formation that are distributed around the targeting survey area. The robots are equipped with monitoring sensor such as an echo sounder to measure the water depth. The depth data and the GPS data are acquired at 1 Hz. The data set, in text format will be stored on board the robot’s computer before the user fetches it at the end of the survey run. The data will be analyzed using common GIS program such as ARCGIS to estimate upper-bound estimation of the volume of the water body. For the future work, the method can be integrated with a terrestrial or airborne LiDAR system to obtain the estimation of the water resource capacity. Three missions, related to water management or environmental survey, are demonstrated in the paper as examples of successful implementation of this method.

Keywords *Field mobile robot, Autonomous surface vehicle (ASV), Bathymetric survey, Hydrographic survey, Underwater photography*

[1*]Corresponding Author
Department of Science Service,
Ministry of Science and Technology
Bangkok, Thailand
Email: pasan@dss.go.th

[2]2nd Author
Rajamangala University of Technology Thanyaburi
Pathum Thani, Thailand
Email: ppradya@gmail.com

Introduction

It is common to see working robots in terms of robotic arms on the factory floor. The robotic arms are famous for their “manipulation” performance, which include pick & place and spot welding for instance. There are another group of robotic devices that are used in the outdoor environment. Since these robots can be controlled remotely or even can work autonomously, the unmanned nature of these robots fit the function of assisting human in various dangerous environments. They can also help relieving human from uncomfortable workplaces such as in the hot and humid forest, the vast space of large reservoir, or even the unforgiving underwater environment. These robots can take various forms such as unmanned aerial vehicle (UAV), remotely operated vehicle (ROV), autonomous underwater vehicle (AUV), or autonomous surface vehicle (ASV), which is the focus of this paper,

Environmental management is one of the ideal applications for the unmanned outdoor robots. Many robots have already found applications in the field. (Appelgren, 2013; Blackmore, 2007; Caccia et.al., 2008; Curcio et.al., 2005; Dunbabin et.al., 2012, Manley, et.al. 2008) With the advent of field mobile robots, there is hope that the robot will help speeding up the work process with high precision and accuracy while the covering work area is double or triple normal work rate done by the conventional method.

Fig. 1 The modified electric kayak

In this paper, we focus on the Robotics related works in the water and environment management applications that we have accomplished as a joint effort among the Department of Science Service (DSS), Rajamangala University of Technology Thanyaburi

(RMUTT), Walailak University, and Hydro and Agro Informatic Institute (HAII). Our main focus is to apply field mobile robotic to address problems in environment monitoring. We developed several versions of the ASV ranging from the 14-foot electric kayak boat (Fig 1), the 10-foot flat bottom hull, mechanical steering outboard motor robot boat, and, recently, the 10-foot V-shape hull hydraulic steering outboard motor robot boat (Fig.2). All robots have been tested in the real environment such as reservoirs, canals, rivers, and seas. The electric kayak robot, although, can work only 1.5 hour long per battery charge at the speed ranging from 4-7 km/hr offers environmentally friendly solution. It can operate quietly with zero emission. It is also easy to transfer from place to place. The ASV that is equipped with a 2-stroke petrol engine "outboard motor" offers much longer operation time/range than electric boat. The powerful 25 hp engine can deal with high speed current condition or a dense vegetation area. The top speed of this robot can reach 25 km/hr.

Fig. 2 Robot boat powered by an outboard motor and hydraulic steering mechanism

Both ASV can be instrumented with monitoring sensors such as echo sounders for measuring the depth of the water bottom or underwater cameras to take underwater photograph. A suit of on board navigational sensors gathers information from the terrain and informs the main controller to drive the robot using the autonomous waypoint tracking algorithm. The waypoints are pre-planned according to the user's needs. The method used in the application and the outcome from the robotic assisted tasks will be demonstrated by the three missions. The first two missions involved the use of the ASV to scan the reservoir to calculate the water volume and/or the capacity of the reservoir. The volume or capacity data will be useful to plan for water management for agricultural use or flood management during the disaster. The third mission is to use ASV in the task of shallow water photography. The image of the shallow water coral reef captured by the ASV will be used to help predicting the coral bleaching phenomena which many believe to be direct result from the climate change.

We conclude the paper by discussing what is needed to be improved to make the robotic surveying process more precise and reliable.

Methodology

The autonomous mode relies on waypoint tracking algorithm. This algorithm is used for the robot to track all waypoints pre-defined by a user before each mission. It needs two navigational sensors- a global positioning system (GPS) and an attitude and heading reference system (AHRS). The GPS helps the robot localizing its current location at all time. The GPS system can be used in standalone mode with horizontal positioning accuracy ~+/-2 meters or it can be used in RTK mode with horizontal positioning accuracy ~+/-1 centimeter. The AHRS gives the robot bearing information with respect to the next target waypoint. The two sensors work concurrently to feedback aforementioned information to the control computer to issue commanding throttling and steering information for the boat engine control and boat steering control. The controller used for this algorithm is composed of two PD control loops with one controls the speed and the other controls the heading of the robot boat. The control loop time depends on the update speed of the GPS; the LEICA GS-10 update rate is at 25 Hz. (Bibuli, et.al., 2008; Greytak, 2006; Prempraneerach, et.al. 2012)

The control hardware diagram is shown in Fig. 3. The control system can be switched between the manual mode and the auto mode. The manual mode relies on hand remote control. This mode is useful for positioning the robot where we desired.

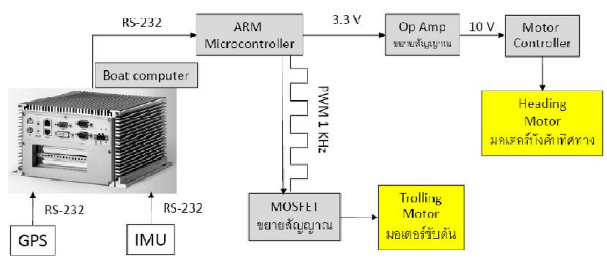

Fig. 3 The control system hardware in the autonomous waypoints tracking mode

The autonomous waypoint tracking algorithm works as follows:

- Recognize the target waypoint
- Steer and power the robot toward the waypoint
- Increase the current speed if the waypoint is still far away from the current position
- Decrease the current speed if the waypoint is close by
- Change target waypoint to the next in line when the target bound is reached (Note: The target bound is define as a ball of radius 2 meter circle around the target waypoint)

Gains tuning of the controller is crucial to the waypoint tracking performance of the robot. The tracking performance of the robot can be seen in Fig. 4. The robot is commanded to follow five waypoints to make a circuit run of four rounds. The trajectory is almost exact at each run. Some of the waypoints are reached by the robot exactly at the crosshair center. Slight deviation from the center target can be seen from the plot. Only the bound (2 meter radius) is hit to trigger the next target waypoint. This slight error may come from the navigational sensors drift errors. It can be corrected by improving gain tuning process.

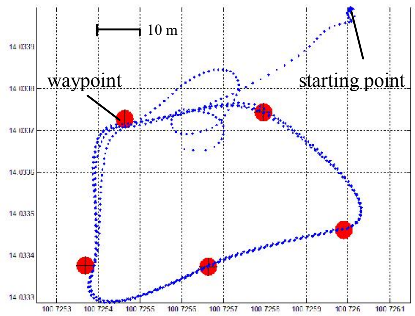

Fig. 4 Waypoints tracking performance of the robot repeating the circuit four times [Unit: Decimal degree]

The steps involved in robotic survey method are as follows:

- *Set up DGPS base station*
- *Set up RTK rover unit on robot*:
  New technology such as the inertial navigation system (INS) can work in tandem with the GPS to help improving the accuracy and precision of the position of the robot both in horizontal and vertical reference to the earth coordinate. The concept is to use Extended Kalman Filter (EKF) to fuse the information from two positioning sensors and output the most reliable position data in real time.
- *Draw boundary*:
  The boundary can be drawn electronically if the precise digital map of the target area is obtained. The other possible solution is to rely on real time mapping from aerial robot such as a UAV equipped with Photogrammetry technology. A boundary can be acquired by a manned control boat equipped with RTK GPS rover unit traversing around the target area boundary and all possible hazards that can be harmful to the robot boat.
- *Plan waypoints formation*:
  The waypoints are placed using the plotting software developed in-house. Plan and place the waypoints such that the target area is fully covered and no waypoints are put inside the possible hazardous area.
- *Launch the automated survey*
- *Obtain data for analysis*:
  The data is saved in the boat computer. If the user wants to observe the survey data in real time, this can be done by setting up remote sensing system via technology such as Coded Orthogonal Frequency Division Multiplexing (COFDM), WLAN, or ZIGBEE
- *Data analysis:* We use ARCGIS to plot the 3D points and integrate the data to get volumetric data, contour plot, and 3D render.

Results and discussion

Mission site 1: Rama IX reservoir

Rama IX reservoir (Fig.5) is a strategic flood detention area during the 2012 Thailand Great Flood. Its capacity is desired since the information will be useful for constructing flood protection plan or waterworks plan for Pathum Thani area. The main objective of this mission is to obtain the capacity of the reservoir. The reservoir is split into the reservoir_1 (south side) and reservoir_2 (north side). We deploy two electric robot kayaks equipped with echo sounder to scan the two reservoirs simultaneously to expedite the survey time. The choice of the boat system was purely decided by availability of the kayaks at the mission time. The mission should be completed quicker if the outboard motor robot is deployed due to its superior speed. It can also eliminate the hassle of battery changing.

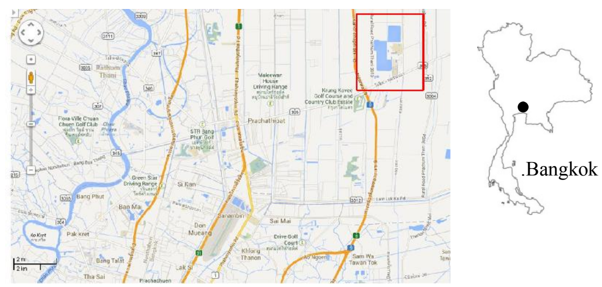

Fig. 5 RamaIX reservoir in the north eastern suburb of Bangkok, Thailand [UTM zone 47P, 685876.40 E, 1552863.31 N]

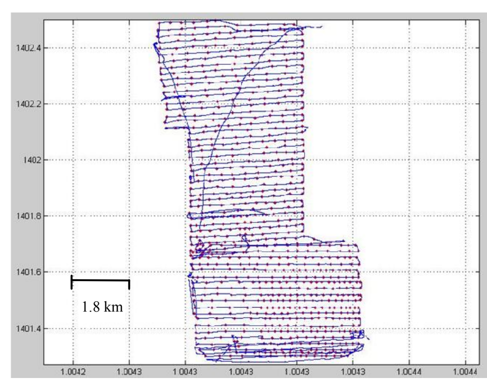

Fig. 6 Robot path tracking pre-plan waypoints of reservoir_1 [GPS unit]

The distance between grid lines is approximately 20 meter. The total operation time is approximately 2 days with two robot kayaks work simultaneously. The total surface area cover is approximately 2,205 rai or 3,528,000 m^2 or 882 acres. The capacity of the two reservoirs combined is approximately 37 million m^3. The robot can track 100% of the waypoints. Some cross trajectory that appears on the plot are the recorded trajectory during the manual mode control in order to bring the boat back to base station or move the boat to the desired positions. The tracking performance is as seen in Fig.6.

As seen clearly from the 3D render from Fig. 7, we discovered that the depth of the RamaIX reservoir is not uniform due to the digging run-over. The normal depth should average around 8 meters, however, the deepest part is around 25 meters. Note that the reservoir bank topological survey was done by the land survey team in order to combine the data with the bathymetric data to ultimately obtain the reservoir capacity.

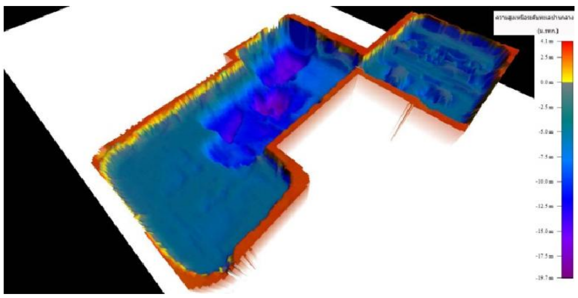

Fig. 7 3D rendition of the bathymetric data of the RAMA IX reservoir

Mission site 2: Maedeenoi reservoir

This mission involves the bathymetric survey of the Maedeenoi reservoir (Fig.8). The main purpose is to identify the amount of water in the reservoir at its current condition. The reservoir was established in 1983 by Royal Irrigation Department. The original capacity is 250,000 m^3. The volume of water calculated from the data obtained from the survey is estimated to be about 210,500 m^3. The reduction in water volume may be because of the sedimentation that has caused the reservoir to be shallower than original capacity.

The result from this mission will be used by the Royal Initiative Discovery Institution (RIDI) to plan for long term water storage and sourcing for the nearby agricultural land area in order to set the optimal utilization of water from the reservoir.

We select the kayak robot for this mission because the reservoir sets deep in the forest and High Mountain and it is not an easy access. Kayak system is small and light enough to be carried into the target site.

Fig. 8 Maedee noi reservoir project near Uthai Thani, Thailand [UTM zone 47P 530378.00 E, 1674410.00 N]

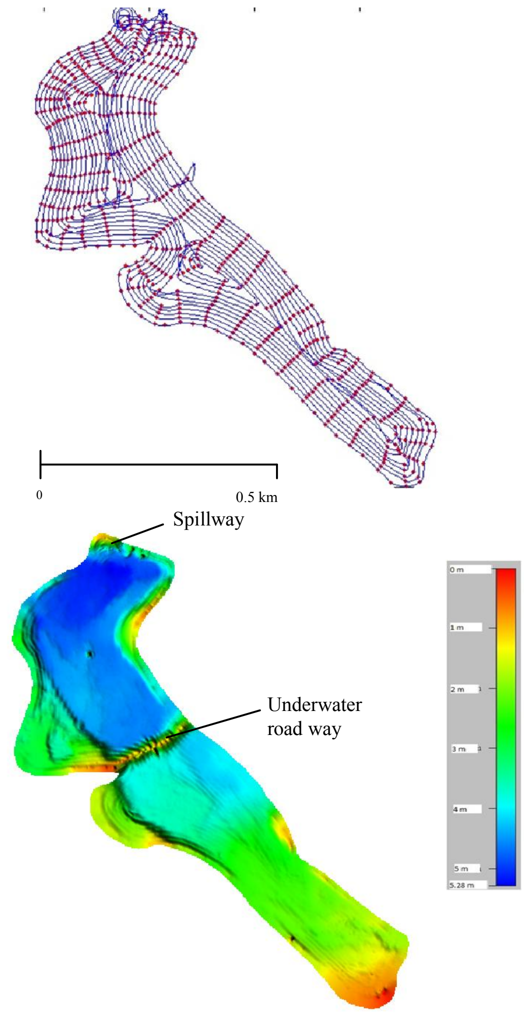

Fig. 9 Robot tracking performance (top) and the resulting underwater terrain map (bottom) of the Maedee noi reservoir

The distance between grid lines is approximately 5 meter. The total operation time is 2 hour 16 minute and 27 second. The total surface area covered is approximately 31.26 rai or 50,016 m^2 or 12.504 acres. The maximum depth of 5.28 meter is found at the area near the spillway (see Fig. 9)

Mission site 3: Racha Island

This mission at Racha Island near Phuket (Fig.10) is a joint effort with Center of Excellence for Ecoinformatics NECTEC/Walailuk University. The mission focuses on the environmental survey of the shallow water coral community around the island. The underwater camera system was mounted at the front of the robot boat to take high definition (HD 1080P) movie image while the robot is tracking the predefined waypoint. The echo sounder is also mounted near the camera to obtain depth information that can be tagged with the image frame. Moreover, the roll-pitch-yaw values from the IMU are also logged for later use in case we need to find the correction for camera rocking motion due to wave disturbance during survey.

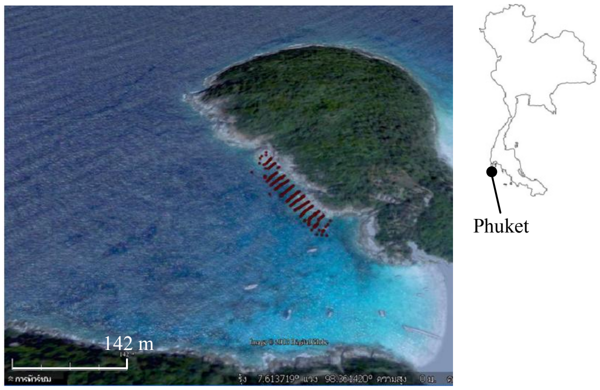

Fig. 10 Waypoints formation laid on the bay of Racha island near Phuket, Thailand [UTM zone 47N 429907.22 E, 841288.86 N]

The water depth ranges between 2-5 meters at the scanned area. In order to get the field of view of the camera to be in range, the gridlines distance was designed to be ranging from 1-3 meter. However since the horizontal resolution for the GPS in standalone mode is only about 2 meter then it only make sense to set the gridlines separation distance at 3 meters. Fig.11 shows the tracking performance of the robot boat. Note that the track between each waypoint is not as straight as when the system operates in the calm water of the reservoir. This is because the sea condition near the headland was quite rough on survey day and the track was also affected by disturbance wave from the speed boats that passed in and out the bay area. However, the control system of the robot can still bring the vehicle into the target points to within the target bound of 1 meter.

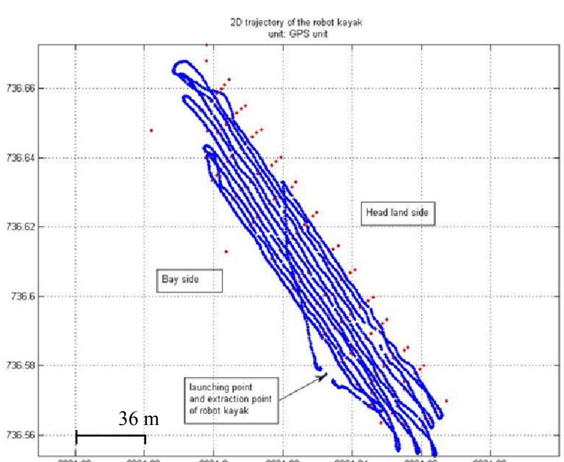

Fig. 11 Waypoints tracking characteristic of the robot boat

We chose the kayak system augmented with outrigger to deal with the ocean wave. The quietness of the DC propulsion motor also desired since one of the requirement was to capture the image of the sea life along the coral reefs. Although the outboard motor robot can negotiate the ocean condition better than the kayak and could be a better choice in terms of survey speed but the outboard motor is too noisy and will drive the fishes away.

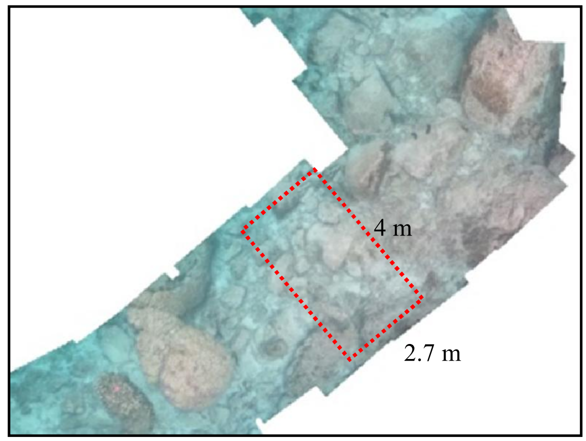

Fig. 12 Partial result of the stitched image of the underwater coral reef

The resulting image is obtained by the process of capturing multiple images and let the stitching software takes care of the overlapping and image reconstruction. The image in Fig.12 is only the partial sample of the bigger image. Note that the path of the image is actually the track that the robot passed while taking the pictures. The data that is logged from the robot is the video image, the time of operation in second, the 1 Hz depth data from the echo sounder, the 1 Hz roll-pitch-yaw orientation of the camera (boat) from the IMU sensor.

Summary and Conclusion

We have shown a glimpse of applications of the field mobile robot system in the field of water and environmental management. It can be seen that although the application changes, the robot boat still follows the same navigational methodology. What changes is only the choice of acquisition/monitoring sensors. The two forms of the robot can be chosen between a small modified kayak and an outboard motor boat depending on the environment and the requirement. Both robots use the same autonomous waypoint tracking algorithm which can be seamlessly adapted to the robot system to get the desired automated bathymetric survey results.

The tracking results can be improved further by upgrading the AHRS unit to a highly accurate one. We can also improve the navigation with data fusion from GPS, AHRS, and/or Inertial Navigation System (INS) system using algorithm such as Extended Kalman Filter (EKF). Gain tuning of navigation controller can also be improved to get better tracking result. We can also integrate a 3D terrestrial LiDAR system to help the robot avoid obstacle, localize itself, and build the map, simultaneously, i.e., SLAM (Leedekerken, 2014)

The aforementioned mission only gives us the information about the volume of the existing water at the time of the survey. If we need to know the total capacity of the reservoir, we need to have information regarding the bank of the reservoir. This information can be obtained by LiDAR system such as terrestrial LiDAR or Airborne LiDAR. Currently we are working on the terrestrial LiDAR that can be installed on board a boat. The information from the bathymetric survey coupled with the information from the reservoir's bank can yield a detail topological model of the reservoir. Fig.13 and 14 shows such system and its resulting scan.

Fig. 13 Motor boat equipped with INS-GNSS system and the LiDAR system can help scanning the terrain above water efficiently [Picture courtesy of GenSurv Co., Ltd.]

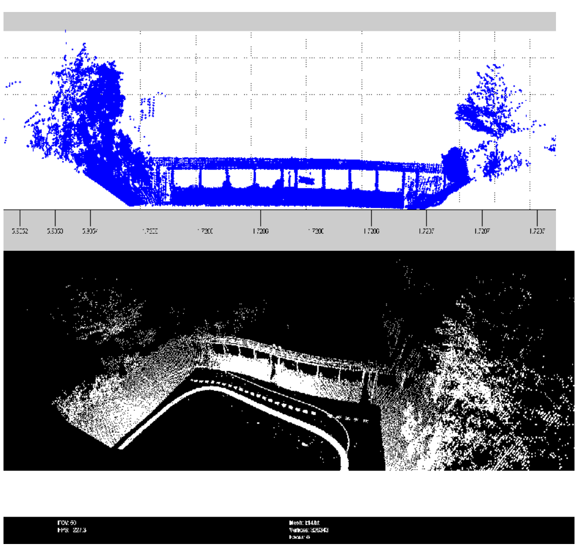

Fig. 14 3D point cloud rendering from data collected from the boat equipped with LiDAR/INS-GNSS system [Picture courtesy of GenSurv Co., Ltd.]

Acknowledgement

The author would like to thank Hydro and Agro Informatic Institute (HAII) for R&D research grant on the project "Development of automatic survey technology for depth and river bank measurement system" and HAII's great assistance in setting up DGPS ground stations and other land survey activities. The author also thanks the Royal Initiative Discovery Institute (RIDI) and Center of Excellence for Ecoinformatics NECTEC/Walailuk University for facilitating the robotic survey team during the bathymetric survey mission at the Maedee noi reservoir and the Racha Island, respectively.

References

Appelgren, J. (2013). Robotic Adventure Across the Pacific: 313 Days, 17,486 Nautical km, One Cyclone, Millions of Data Points. IEEE Robotics & Automation Magazine. Vol. 20, No.2, pp.24-30.

Bibuli, M., et al. (2008) Line following guidance control: Application to the Charlie unmanned surface vehicle. Proceedings of IEEE/RSJ International Conference on Intelligent Robots and Systems,

Blackmore, B. S. (2007). A systems view of agricultural robots. Precision Agriculture '07. ed. J. Stafford, V. Wageningen Academic Publishers. pp.23-31.

Caccia, M., et. al. (2008) Unmanned Marine Vehicles at CNR-ISSIA. Proceedings of the 17th World Congress, The International Federation of Automatic Control (IFAC).

Curcio, J., Leonard, J., and Patrikalakis, A. (2005) SCOUT- a Low Cost Autonomous Surface Platform for Research in Cooperative Autonomy. IEEE OCEANS.

Dunbabin, M. and Marques, L. (2012) Robotics for Environmental Monitoring: Significant Advancements and Applications. IEEE Robotics and Automation Magazine. Vol. 19. No.1. pp.24-39.

Greytak, M.B. (2006) High Performance Path Following for Marine Vecicles Using Azimuthing Podded Propulsion. M.S. Thesis, Massachusetts Institute of Technology.

Leedekerken, J.C., Fallon, M.F., and Leonard, J.J. (2014) Mapping Complex Marine Environments with Autonomous Surface Craft. The 12th International Symposium on Experimental Robotics. pp 525-539.

Manley, J.E. (2008) Unmanned Surface Vehicles, 15 Years of Development. Proceedings of MTS/IEEE OCEANS..

Prempraneerach, P., Thamchaitas, K., and Kulvanit, P. (2012) Autonomous waypoint tracking of kayak boat using state-variable feedback control. IEEE OCEANS.

Applying satellite communication for weather data to improve the efficiency of telemetry system in the upstream area.

Wasukree Sae-tia[1,a*], Thakolpat Khampuengson[2,b], Piyamarn Sisomphon[3,c], Surajate Boonya-aroonnet[4,d]

Abstract At present, data from weather station is transmitted over the cellular network. This is convenient because the network covers most areas of the country and the service is cheap. Problem is due to limitation of the cellular network the transmission of weather data in the remote area eg. river upstream is ineffective. The weather data especially from the upstream area is critical for water management and flood early warning but since the area is remotely located in the high mountain or within the forest area the transmission of weather data through the cellular network is very limited or not available. This paper presents the development of telemetering system applying the use of satellite communication at Khao Phanoen Thung in Phetchaburi Province, the upstream of Petchaburi river basin. The application of satellite communication is used to transmit the weather data via Inmarsat satellite which is a geostationary satellite type. Messaging a weather data via a satellite terminal making it possible to send and receive data at any time providing a real time data access with low power consumption. Therefore it reduces the limitation of data transmission over the cellular network and at the same time enhances the real time data transmission in the remote area. Satellite communication for weather data telemetering helps the assessment of real time monitoring providing an overview of a situation and a decision support for water management and early warning in a timely manner.

Keywords *Inmarsat satellite, Telemetry, Khao Phanoen Thung, Phetchaburi Province*

Wasukree Sae-tia[1,a*]
[1]Hydro and Agro Informatics Institute
HAII
Bangkok, Thailand
[a]wasukree@haii.or.th

Thakolpat Khampuengson[2,b]
[2]Hydro and Agro Informatics Institute
HAII
Bangkok, Thailand
[b]thakolpat@haii.or.th

Piyamarn Sisomphon[3,c]
[3]Hydro and Agro Informatics Institute
HAII
Bangkok, Thailand
[c]piyamarn@haii.or.th

Surajate Boonya-aroonnet[4,d]
[4]Hydro and Agro Informatics Institute
HAII
Bangkok, Thailand
[d]surajate@haii.or.th

1. Introduction

Telemetry is the highly automated communications process by which measurements are made and other data collected at remote or inaccessible points and transmitted to receiving equipment for monitoring. To date telemetering system has become an important device in water management, water quality and discharge monitoring. Having data available in near real time allows a quick assessment and effective decision to a situation in the field. At present there are a number of telemetering stations measuring weather data eg. rainfall, air temperature, relative humidity, water quantity and quality such as discharge, water level and salinity. This information is crucial in water management and its uses have been extended to many related water management applications such as air pollution control, water quality modeling and flood forecasting model, etc. However since the present system is most likely rely on a GPRS/3G technology. In some area where the signal is limited, the transmission of telemetering data is not effective. Especially in the mountainous upstream area where rainfall data is very crucial and required for flood management and early warning purposes, the data is not readily available. Therefore in this study it focuses on the applying of satellite communication technology to enhance the use of telemetering system in the remote area. Apart from reducing limitation of data transmission through a cellular network, the readily available of upstream rainfall data provides a better support on the flood management.

2. Development of mobile telemetering system

In 2003, the "Field Server" was introduced by National Agriculture and Food Research Organization (NARO),

Japan, in the Asia Pacific Advanced Network (APAN) conference. The participants from others countries were interested in this equipment because it was small, portable and easy to install, and had a low cost.
The National Electronics and Computer Technology Center (NECTEC), Thailand, had adapted this technology concept for appropriate utilization in Thailand. However at that time, Wi-Fi data communications had not yet been available everywhere for the whole country. Typical telemetry system in the market used wireless data communication packages - VHF or UHF which had limited frequency ranges. Therefore, NECTEC had selected the GPRS (General Packet Radio Service) as a communication method because it was uncomplicated and was a standard protocol for wireless data communication thru mobile network. After that, mobile service providers expanded their coverage to cover most areas of the country and did not pose restrictions in the connection. Nevertheless, some weaknesses of the mobile applications were that the data could not be transferred in off-network areas. Later Hydro and Agro Informatics Institute (HAII) has continued the development and extended its applications to a "mobile telemetry system" to supplement the SCADA telemetry system. This system has now become a standard platform of HAII telemetry system. With its simple work flow system, compact size, portability and low cost this system has been widely used for various applications in Thailand.

Figure 1 shows the telemetering with weather sensors to measure rainfall and other weather parameters

2.1 System components
Mobile telemetry system has simple workflow and focus on the use of standard interfaces that are easy to understand and be applied. A telemeter is divided into three parts according to how the device works.

1) Measurement sensors
It measures a physical quantity and provides signals in standard format of 0-5 V or 4-20 mA. Presently, manufacturers come up with a variety of sensor probes, depending on the applications. For telemetry system, all types of sensors with the above standard can be installed to the mobile telemeters. Examples include temperature, relative humidity, air pressure, solar radiation, and stream water level probes. The resolution and the accuracy depend on the specification by manufacturers. Rain sensor using tipping bucket mechanism was also developed for rainfall measurements. See Table 1 for the summary of devices for each system component.

Table 1 summarizes the list of devices for each system component

Electronics Sensor	Controller and Transmission	Power Supply
• Temperature Sensor • Humidity Sensor • Pressure Sensor • Light intensity Sensor • Rain Gauge • Water Level Sensor	• Data Logger • GPRS Modem	• Solar Cell (40 W.) • Battery (12 V. 35 Ah.)

2) Controllers and data loggers
It is a device controlling the operation and data transmission. This device is the heart of the operation, with the microcontroller to control all functions of the operation. It was developed and programmed in-house at HAII, so it can be customized and modified when needed. Timing for measurement recording and system operation can be set and data is transmitted in the standard format RS232 to the data transfer device via GPRS system. Data can also be recorded in the controller flash memory, allowing the user to extract data at a later time.

3) Power supply with anti-surge equipment
This system uses 12V and can utilize various electrical power sources such as the use of transformer to convert from 220V home electricity to 12V DC or the use of car battery. Present development includes the use of solar cell.

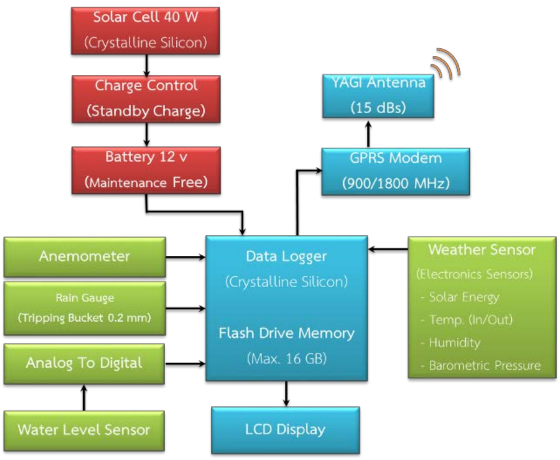

Figure 2 System diagram

2.2 Data transmission

Data transmission network is shown in Figure 3. Data logger is used to record data and transmit it using GPRS/3G modem to the main server. Data is archived for later assessment and warning messages are sent as short messaging service (SMS) via mobile phone.

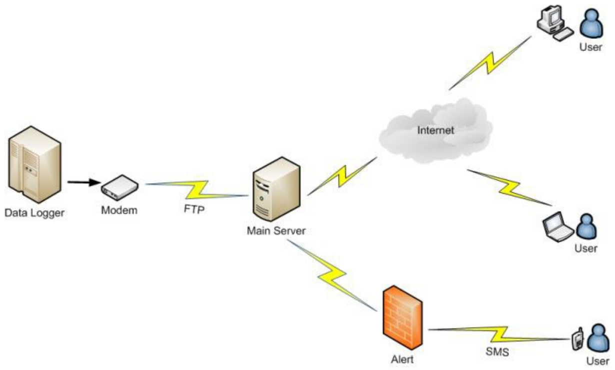

Figure 3 data transmission network

2.3 Data display

Data display (Figure 4) is available through web sites or a WAP browser for mobile phones. The user can choose to view data based on location or time period, in the format of numbers, graphs, or tables, as well as viewing operation status. Data can also be visualized in a geographic information system via internet. At present there are 853 telemetry stations with this mobile technology installed overall in Thailand in which 542 are weather stations, 308 water level stations and 3 water quality stations.

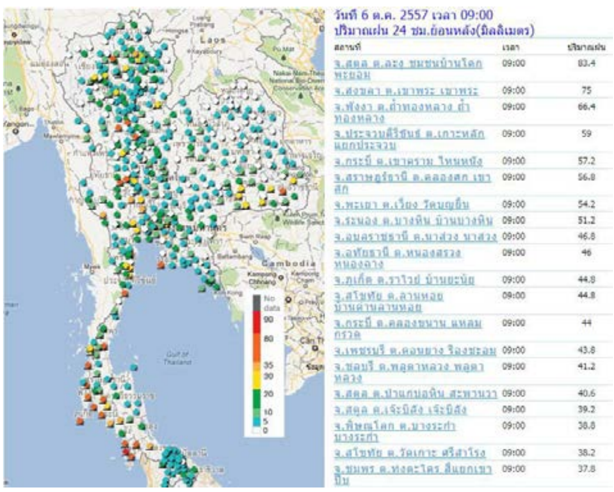

Figure4 Display of rainfall measurement from telemetry stations

3. Satellite communication system

Due to the limitation of the mobile applications, the data could not be transferred in off-network areas. This is not applicable since weather data in the remote area such as at the river upstream is very important to monitor as it can be used for flood early warning or for water management purposes. This area is normally located far from the city where the cellular network is denser; often it is located on the mountainous area or in the forest. Thus, in those areas, an alternative communication approach should be performed.

At present satellite communication technology has become widely available and applied in many survey and earth observation applications. Its main advantages are the spatial coverage and its signal availability. Messaging a weather data via a satellite communication making it possible to send and receive data at any time providing a real time data access with low power consumption. Therefore there is an attempt to apply satellite communication in the telemetering system to transmit the weather data via Inmarsat satellite which is a geostationary satellite type. The satellite messaging system is a two-ways communication service or a machine to machine communications. The satellite communication uses the Imarsat I-4 generation satellite network which consists of multiple beams with global coverage. Figure 5 shows the satellite messaging network starting from the application server to the satellite signal connection. The data is transmitted to the server to exchange with the gateway through the internet access. The gateway data center is then provides a web-based service interface to application servers and manage all the administration of the services. Messaging process occurs at the land-earth station providing a two-ways communication to the end terminal or mobile devices.

Figure 5 The Satellite messaging network.

The satellite messaging network system has been applied in the HAII mobile telemetering system to provide an almost real time rainfall measurement from a remote upstream area (Figure 6). The satellite terminal is installed at the telemeter for messaging the data to satellite and send back to the ground server.

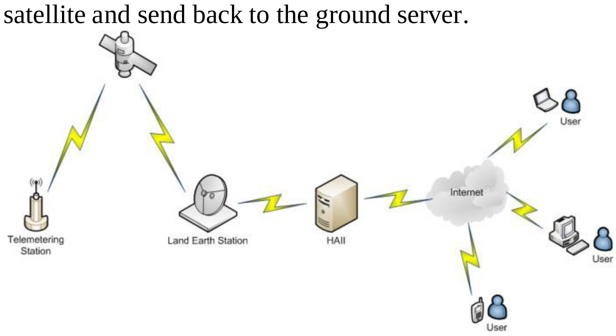

Figure 6 Telemetering data transmission using Satellite Modem

4. Pilot station

The upstream area of Khao Phanoen Thung in Phetchaburi Province, the upstream of Petchaburi river basin has been selected as a pilot site. The area is located in a high mountain (1,207 MSL) of the Kang Krajan national reservation park which is the largest national park of Thailand. It consists mainly of rain forests within the eastern slope of the Tenasserim Mountain Range. Two main rivers originate within the park area, the Pranburi River and the Phetchaburi River. The Phetchaburi is blocked by the Kaeng Krachan Dam at the eastern border of the park. The dam creates a lake covering an area of 46.5 km².

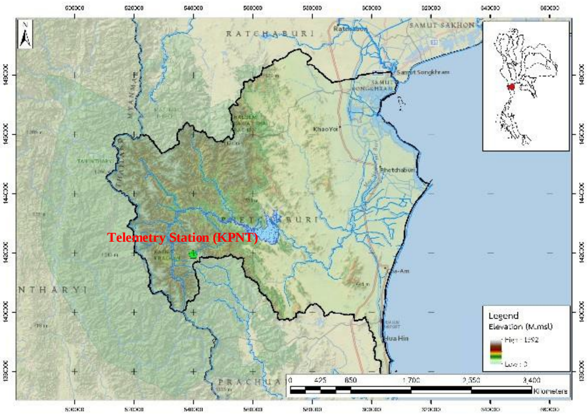

Figure 6 Phetchaburi river basin

The upstream of Phetchaburi River is located on Khao Phanoen Thung which is a high mountain area, and it is also located in a national park making its difficult to install and maintain the telemeters based on the GPRS network system. In the past the short messages based on SMS using 2G/3G Modem were used (Figure 7). This method is subjected to higher cost and needed to install the 2G/3G modem, due to limited or availability of the cellular network problems, the SMS system soon was terminated because of data transmission problem which significantly affected the data quality.

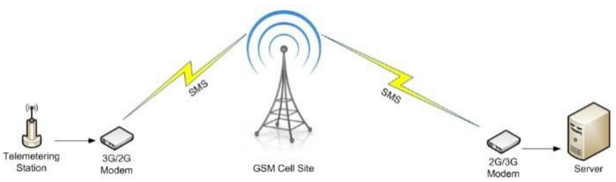

Figure 7 Data transmission using the SMS network

Because of the above mentioned problem, the satellite communication has been considered to replace the SMS system. With the advancement of space technology and its application, the cost is rather high but considered acceptable when compare to the long term maintenance and the quality of data. The choices of communication method depend on the location and the need of the monitoring information and of cause the available budget (see Table 2 for details of different communication methods).

Table 2 Comparison of the 3 communication methods used in the mobile telemetry

	3G/2G	SMS	Satellite
Location	Within cellular network		World wide coverage with no physical blockage
Cost	5000-10000 THB		>=30000 THB
Service cost	0.10 THB /Kb	3 THB /1 SMS	20 THB /Kb
Power consumption	8-30 V.		9-32 V.
Stability	Depends on cellular network		>90%
Programming	Java/Python/C		Lua
Operating Temp	-30 to +75 oC		-40 to +85 oC
Water resistant	No		Yes

With this case, the priority is the get the rainfall measurement from the upstream area therefore the satellite modem has been selected as a solution to the communication network. The satellite modem has been installed to the telemeter as the first pilot site at Phanoen Thung Camp of The Kaeng Krachan National Park (12.825330 N, 99.365549 E) (Figure 8).

Figure 8 weather station at Phanoen Thung Camp with satellite terminal installed

Its performance in term of percentage of data transmission is shown in Figure 9. The comparison of the percentage of data transmission between GPRS/3G system in 2013 and after the satellite communication has been replaced in 2014, compared at the same months. It can be seen that with the GPRS/3G system the data transmission is varied, depending on the network availability. Compared to the satellite communication, the data transmission is over 90%.

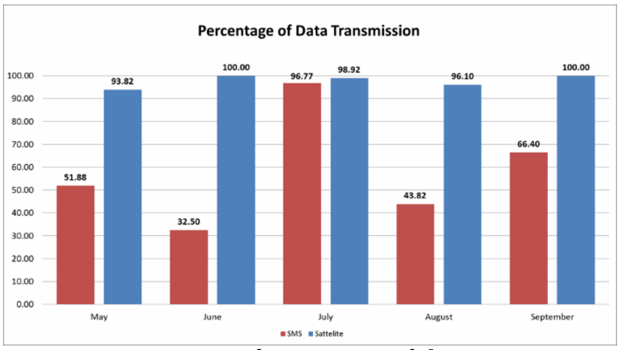

Figure 9 Comparison of percentage of data transmission at the same month (red-GPRS/3G system in 2013, blue-Skywave satellite communication system in 2014)

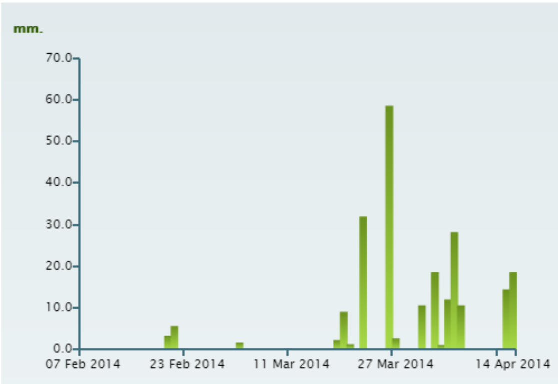

Figure 10 Daily rainfalls measured at Khao Phanoen Thung in Phetchaburi Province from February to March 2014

Conclusion

From the pilot experiment on applying the satellite communication technique for mobile telemetering system it was found that the data transmission can be significantly improved. The problems of data continuity are reduced. Another advantage is it can be installed at the remote mountainous area such as at the river upstream where the cellular network is not or rarely available. This is enhanced the water monitoring and management especially for flood early warning. The satellite communication application for mobile telemetry is still rather limited due to higher cost for hardware installation and service. Its application is recommended to important sites where the cellular network is not available. With the advancement of satellite technology when it becomes more widely use their cost is normally tend to be reduced. Compare to a better data control and having data at the remote area this application is very promising. The most benefit is the missing jigsaw of the water monitoring in the remote area that can be fulfilled.

References

Hydro and Agro Informatics Institute, "Mobile telemetry system", www.thaiwater.net, 2011.

Hydro and Agro Informatics Institute, "Development of data warehouse 25 river basins.", 2012.

Skywave Mobile Communications Inc., "IDP 600 SERIES Satellite Communication Terminals", www.skywave.com/en/our-technology/satellite-cellular-communication, 2014.

Development of a User-Friendly Web-based Rainfall Runoff Model

Khin Htay Kyi[1,a *], Minjiao Lu[2,3,b] and Xiao Li[4,c]

Abstract Parameter calibration is required for the implementation and operation of a hydrological model at the study basins. To support this process with user-friendly interfaces, an open access web-based conceptual Xinanjiang model was developed. This makes it possible to input model parameters and run the model repeatedly through a web page. After running model, automatically calculated Nash model efficiency and RMSE between predicted and observed discharge will be displayed together with the parameter set to show the model accuracy. One can run the model repeatedly by adjusting values of 15 parameters based on the user's experience and listed results of previous trials. With the help of "sorting" service which sorts the model efficiencies of previous trials in decreasing order, it is easy to pick up parameter sets providing good results. And rendering graph facility visualizes observed hydrograph and predicted hydrographs of selected trials, and helps the user to visually inspect the results and to find a parameter set which will probably improve the model accuracy. After getting satisfactory result, users can download the simulation result files through web browsers without any difficulties. In addition to the web-based model, a calibration support system is planned to further support the calibration process. At current point, a method proposed by Li and Lu (2014) is implemented to recommend suitable values for two data adjustment parameters by analyzing observed hydrological data.

Keywords: *Web-based Rainfall Runoff Model, Xinanjiang Model, Calibration, Aridity Index*

Htay Kyi Khin
Dept.of Civil and Environmental Engineering, Nagaoka University of Technology, Niigata, Japan.
ms.khinhtaykyi@gmail.com
Minjiao Lu
Dept. of Civil and Environmental Engineering, Nagaoka University of Technology,Niigata, Japan.
Chongqing Jiaotong University, Chongqing, China
lu@nagaokaut.ac.jp
Xiao Li
Dept. of Civil and Environmental Engineering, Nagaoka University of Technology, Niigata, Japan.
lixiaolsm@yahoo.com.cn

Strategy to Automatically Calibrate Parameters of a Hydrological Model: A Multi-step Optimization Scheme and its Application to Xinanjinag Model

Minjiao Lu[1, 2,a*] and Xiao Li[3,b]

Abstract Parameter calibration is fundamental for the implementation and operation of a hydrological model. Because hydrological models have been becoming more and more comprehensive and complicated, it is tedious and time consuming procedure even for an expert. The automatic calibration technique has been studied widely. However, even the most modern optimization schemes cannot always help us to obtain optimal parameter set due to high dimensionality of the parameter space and complex interactions between parameters. The main purpose of this study is test our strategy for automatic parameter calibration which includes two parts: lowing the dimensionality and narrowing the parameter space. The Xinanjiang model which is the most popular rainfall-runoff model in China and also widely used all over the world is selected as an example of hydrological model. Our modified Xinanjiang model include 15 parameters controlling data adjustment, runoff generation, runoff separation and runoff routing. A global sensitivity analysis technique proposed by Morris is used to get better understanding about the structure of the parameter space. It is found that the parameters have significantly different sensitivities at annual, monthly and daily scale. Also strong interactions between the parameters are detected at all three temporal scales. Based on these results, a multi-step optimization scheme is developed and tested. The 15 parameters are divided into three groups and optimized group by group at time scale they are sensitive by using SCEM-UA algorithm, a global optimization algorithm. It is shown that the newly developed multi-step optimization scheme is very efficient and robust.

Keywords: *Automatic calibration, Optimization, Global sensitivity analysis, Rainfall runoff model, Xinanjiang model*

Minjiao Lu
Chongqing Jiaotong University, Chongqing, China.
lu@nagaokaut.ac.jp
Xiao Li
Dept. of Civil and Environmental Engineering, Nagaoka University of Technology, Nagaoka, Niigata 940-2188 Japan.
lixiaolsm@yahoo.com.cn

Fluctuation and its change during rainfall events in water temperature at the upstream tropical forested watershed; study case: Kracak reservoir catchment - Indonesia

Luki Subehi[1&2], Kwansue Jung[2]

Abstract Tropical forested river watershed is one of the unique ecosystem which is functioning in both ecological and economic services. Water temperature is one of the important parameters in the aquatic systems. The objective of this study is to identify the characteristics of water temperature at Cianten River in Kracak reservoir catchment. Reservoir catchment (RC) and experimental catchment (EC) as two study sites were observed for representing of large and small watersheds, respectively. Air and water temperatures data were obtained from June 2011 to April 2013. In addition, the changes in water temperature during rainfall events were also analyzed. Next, root mean square (*Rms*) and harmonic methods for statistically analyzed were applied. From our analysis, the average values of *Tw* at RC and EC sites were 25.1 ± 0.9 and 21.2 ± 0.2, respectively. In addition, the average values of *Tw* fluctuation expressed by *Rms Tw*/*Rms Ta* were 0.81 ± 0.44 and 0.31 ± 0.08 for RC and EC sites, respectively. The higher value of *Rms Tw*/*Rms Ta* at RC site can be explained that the higher fluctuations in the water temperature with lower delay time at larger area (RC), indicating that water flow time influenced such fluctuations. Also, it was observed that the variations of *Qs* more significantly influenced water temperature through the change in flow paths compared with *Ta* during rainfall events. Moreover, the management of river tropical forested watershed influenced the flow paths differently through the changes of infiltration rate, surface runoff, subsurface flow and groundwater percentage.

Keywords: Water temperature – Tropical forested – Fluctuation - Root mean square – Harmonic method

Luki Subehi
[1]Research Centre for Limnology
Indonesian Institute of Sciences
Bogor, Indonesia
Luki@limnologi.lipi.go.id

Kwansue Jung
[2]International Water Resources Research Institute
Chungnam National University
Daejeon, South Korea
ksjung@cnu.ac.kr

Introduction

Water temperature influences physical, chemical, biological and changes in species composition on aquatic ecosystems (Caissie 2006; Tung et al. 2014). Therefore water temperature has a vital role in various processes that determine whether an aquatic environment is suitable for fish, organisms and human being. Water temperature links biologically to the metabolic rates, physiology, and life history of aquatic species (Caissie 2006) and influences rates of community processes such as nutrient cycling and productivity. Water temperature and its change are key factors for aquatic physical, chemical and biological processes (Caissie 2006) and it remains the subject of world-wide environmental research (Webb et al. 2008).

Characteristics of water temperature fluctuations at forested watersheds should be elucidated in order to manage downstream water quality (Subehi et al. 2010). As a hillslope hydrology characteristic, forested watersheds, which are one type of natural resources are an important subject of water resources and erosion-sedimentation processes. In addition, researchers found that the steep, forested hillside with thin soil layer condition was determining runoff processes (Tani 1997). Subehi (2013) pointed out the characteristics of fluctuation in water temperatures at River Cianten for one year period. Differently to previous paper at River Cianten, we analyzed two sites for comparing their characteristics. In addition, the water temperature was also analyzed during rainfall events.

Currently, regularly draining in the Kracak reservoir always is conducted four times in a year for flushing sedimentation and wastes. These activities require a high cost and time consuming (3 - 4 days). It disturbs the hydropower operation itself. Moreover, based on land use data 1996 - 2006, the largest changes part is forest, the reduction almost 50% become gardens, fields, shrubs, and settlements (Project report-PKPP 2011). In addition, it also influences ecosystem degradation.

The lack of consideration of the aspects of tropical region on forested watershed conditions which could play important roles in water temperature changes, has suggested the necessity of its investigation. The purpose of this study is to identify the characteristics of water temperature on Kracak reservoir catchment, especially at River Cianten as a tropical forested watershed type.

Methods

The studied river watersheds were located at Kracak reservoir catchment in West Java, Indonesia. We analyzed water temperature (*Tw*), air temperature (*Ta*), discharge (*Q*) and rainfall (*R*) in the upstream of river. In order to get the insight into tropical forested watershed condition on river water temperature characteristics, Reservoir Catchment (RC) near Kracak reservoir station in the downstream and Experimental Catchment (EC) in the upstream (about 9 km from RC) had been selected. We analyzed water temperature characteristics at RC and EC for representing of large and small watersheds, respectively (Fig. 1). The watershed area, elevation and slope gradient of RC were 12,490 ha, 337 m and 0.11, respectively. Those of EC were 4.9 ha, 787 m and 0.37, respectively.

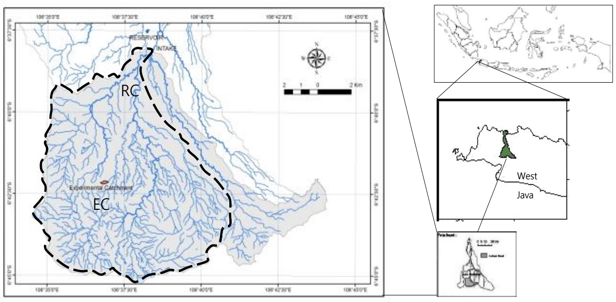

Fig. 1 Study area

We used microlite sensor HOBO for air and water temperatures data. They were taken at intervals of 30 minutes with completely sealed underwater temperature loggers with optical communication (MicroLite PRO 4-20mA USB Logger with 32k Memory and LCD Screen). The logger can measure temperatures from -40℃ to 80℃ with a precision of ± 0.3℃. Meanwhile water discharge was obtained based on water level data by HOBO U20 water level data logger – U20-001-01 with range 0 – 9 m and precision of 0.5 cm. Next, rainfall parameter was measured by the HOBO RG3 data logging rain gauge (range: up to 160 cm, resolution: 0.01 mm and accuracy: ± 1.0 %). Discharge and rainfall data were also taken at intervals of 30 minutes. Because of field conditions, all parameters were obtained from June 2011 to April 2013 and June – December 2011 for RC and EC sites, respectively.

In order to analyze the temperature fluctuations, we used not only the standard deviation (σ) but also the root mean square variation over 7 days (*Rms 7-days*). The equation can be described in the following manner:

$$Rms\ 7\text{-}days = \sqrt{(1/n)\sum_{i=1}^{n}(x_i - \overline{x}_i^{m})^2} \qquad (1)$$

where n represents the number of days analyzed (monthly: 28-31, yearly: 365),

x_i is the daily average temperature (℃), $\overline{x}_I^{m}$ is the m-day moving average of daily temperature. We used 7-days for *m*. The weekly average temperature is commonly used to quantify water temperature changes because the weekly (7-days) timescale gives a good correlation between air and water temperatures (Mohseni and Stefan 1999) and also eliminates most transient variations, including diurnal effects of solar radiation and air temperature.

The differences between standard deviation and *Rms 7-days* were not large for the river water temperature with R^2 = 0.890 and R^2 = 0.913 for at RC and EC, respectively (Fig. 2). Comparing them, *Rms 7-days* seems superior because this is less influenced by seasonal changes in air temperature and the seasonal variability could also be clarified.

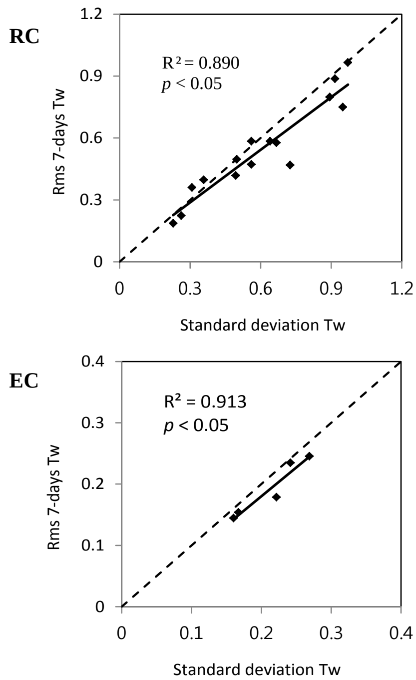

Fig. 2 Correlation between standard deviation and *Rms 7-days* of water temperature (*Tw*) at RC and EC

In addition, we used harmonic analysis, a branch of mathematics that studies the representation of functions or signals as the superposition of basic waves. The equation is defined as follows:

$$y_T = A \sin (c\ (t + \varphi)) \qquad (2)$$

where y_T represents the sine curve of temperature T; t is the time (day); A is the amplitude of temperature fluctuations; c equals $2\pi/L$ (L = time period = 365 days) and φ represents the phase shift or delay time (day).

Next, the changes in discharge, water and air temperatures were observed during rainfall events. Based on rainfall data (2003 – 2010) at Cianten watershed, the average of rainfall amount was 2,233.1 mm/year. In addition, the averages of rainfall amount (*R-a*) on wet (October – March) and dry (April –

September) periods were 1,287.3 mm and 945.8 mm, respectively. We selected the rainfall events on all periods in which the intensities were more than 10.0 mm/h with no rainfall at least 12 hours before and after those events. Based on those criteria, 10 sets of data on water temperature for 10 rainfall events were obtained at both sites.

Identifying different flow paths could be described by hysteretic loops observed in the relationship between water temperature (*Tw*) and specific discharge (*Qs*), defined as discharge divided by area. In addition, the relationship between air temperature (*Ta*) and *Tw* was also observed. The changes in water temperature (ΔTw), specific discharge (ΔQs) and air temperature (ΔTa) during those events (from 12 hours before the beginning of rainfall to the time when the discharge declined to near its initial value) were calculated by:

$$\Delta Tw = (Tw_{max} - Tw_{min})\,f$$
$$\Delta Qs = Qs_{max} - Qs_{min}$$
$$\Delta Ta = (Ta_{max} - Ta_{min})\,f \qquad (3)$$

f = -1, when maximum point came faster than minimum point (clockwise/*C*)
f = 1, when minimum point came faster than maximum point (counter-clockwise/*CC*)

in which, Tw_{max} and Tw_{min} are the maximum and minimum of water temperature, Qs_{max} and Qs_{min} are the maximum and minimum of specific discharge, Ta_{max} and Ta_{min} are the maximum and minimum of air temperature, respectively.

In addition, the *F-test* was used to evaluate the precision and equality of the variances of the two variables, with a value of $p < 0.05$ required for statistical significance.

Results and Discussion

Analysis of water temperature data

The annual difference of 7.0℃ between maximum and minimum daily water temperature at RC was larger than that of 1.2℃ at EC (Table 1). To compare with air and water temperatures at RC, the water temperature at EC showed less variability. On the other hand, the difference of 3.9℃ between average daily water and air temperatures at EC was larger than that of 0.1℃ at RC (Fig. 3). In addition, from our analysis, the average values of *Tw* at RC and EC sites were 25.1 ± 0.9 and 21.2 ± 0.2, respectively.

Table 1. The values of air and water temperatures at both sites (June – December 2011)

Values	*Ta* RC	*Tw* RC	*Ta* EC	*Tw* EC
Average	25.0	25.1	25.1	21.2
Max	28.3	29.8	27.0	21.6
Min	21.4	22.8	22.5	20.4
ΔT(˚C)	6.9	7.0	4.5	1.2

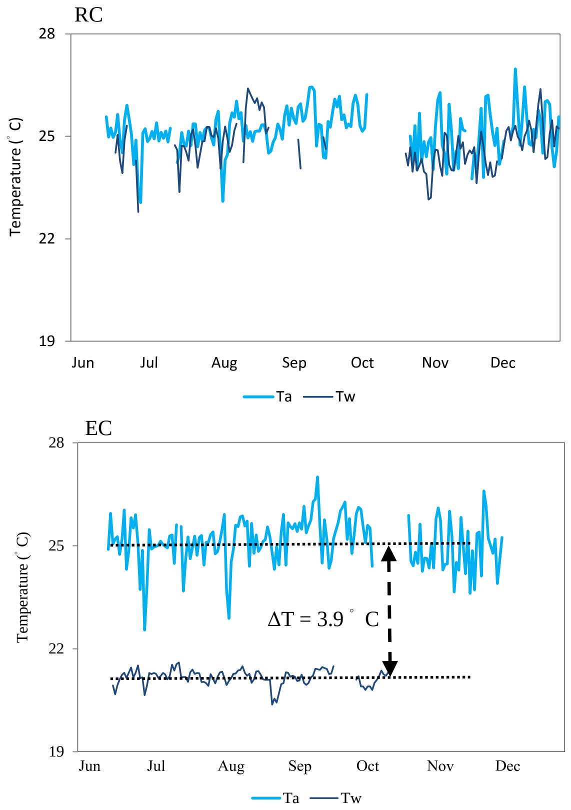

Fig. 3 Daily air and water temperatures (*Ta* & *Tw*) at both sites (June – December 2011)

Rms and harmonic analyses

Figure 4 shows monthly *Rms 7-days* of daily air and water temperatures. The average *r* values between *Rms 7-days* of *Ta* and *Tw* were fairly small (*r* values were 0.03 and 0.51 for RC and EC, respectively). These small values can be explained by noting that the seasonal variability of atmospheric conditions influenced fluctuations in *Ta* and *Tw* but not proportionally. Moreover, the average value of *Tw* fluctuation expressed by *Rms Tw*/*Rms Ta* at RC was larger than that at EC (0.81 ± 0.44 and 0.31 ± 0.08, respectively).

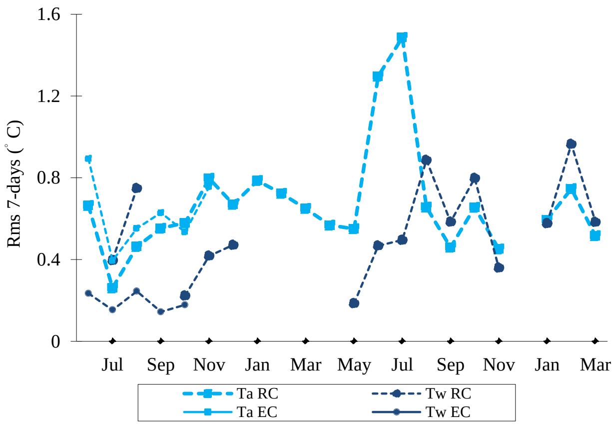

Fig. 4 Monthly changes in *Rms 7-days* of daily air and water temperatures at RC and EC sites

In the harmonic analysis (Fig. 5 & 6), based those two curves, the fluctuation with expressed by the value of *A-Tw*/*A-Ta* at RC also was larger than that at EC (0.92 and 0.40, respectively). To the contrary, the value of delay time (φ day) at RC was smaller than that at EC (0.6 and 4.4, respectively). The summarize of all results from fluctuation analysis were shown in Table 2.

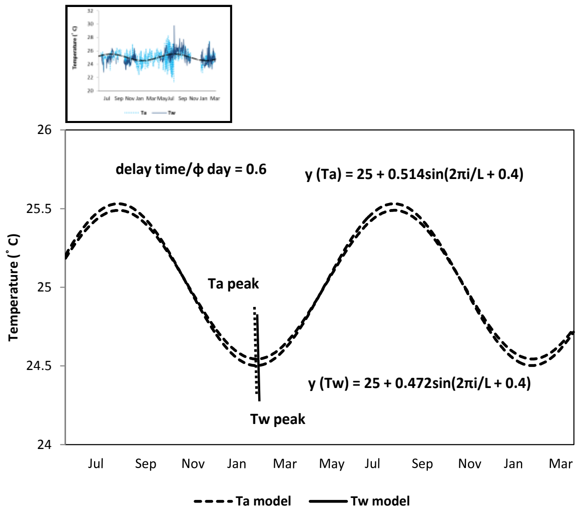

Fig. 5 Harmonic method of daily air and water temperatures at RC (model of *Ta* & *Tw*), with delay time/φ day = 0.6 (June 2011 – March 2013)

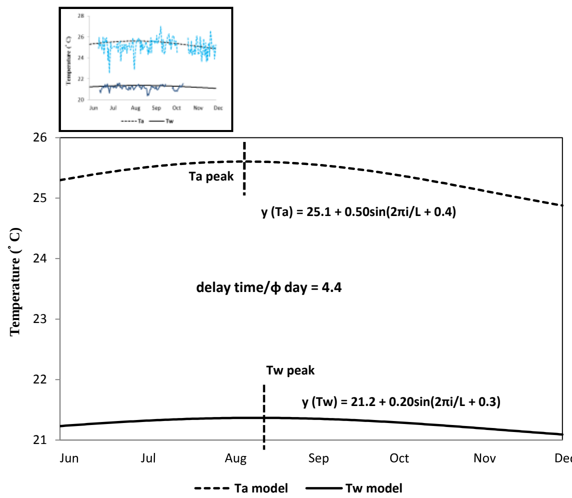

Fig. 6 Harmonic method of daily air and water temperatures at EC (model of *Ta* & *Tw*), with delay time/φ day = 4.4 (June – December 2011)

From Table 2, it shows that the higher fluctuations in the water temperature with lower delay time (φ), indicating water flow time influenced such fluctuations. From a hydrological aspect, the variability of groundwater inputs depends on aquifer heterogeneity; slope gradient and variability in land cover influence fluctuations in water temperature (Brown and Hannah 2008).

Table 2. Analysis results from both site locations

Parameters	RC	EC
Area (ha)	12,490	4.9
Elevation (m)	337	787
Slope gradient	0.11	0.37
Rms Tw /*Rms Ta*	0.81	0.31
A-Tw /*A-Ta*	0.92	0.40
Delay time/φ (day)	0.6	4.4

Analysis of water temperature during rainfall events

Based on Fig. 7, the values of *Tw* were larger and decreased slowly during recession period compared with *Ta*. In addition, the magnitude of *Qs* also influenced *Tw*. It was suggested that the Rainfall amount (*R-a*) influenced the flow speed recession.

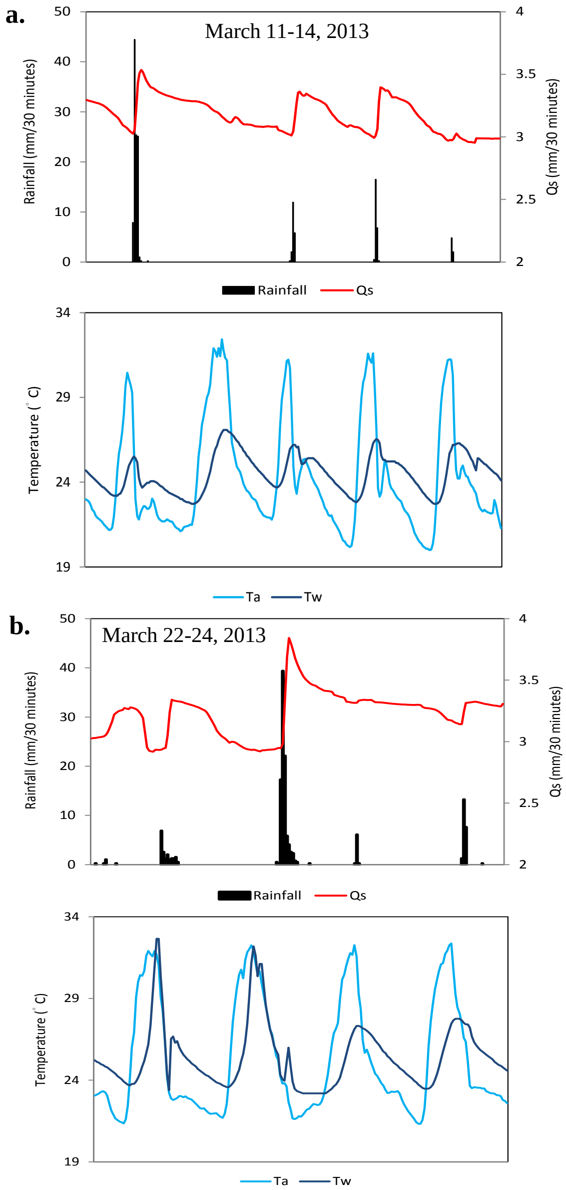

Fig. 7 The characteristics of *Tw*, *Ta* and *Qs* during rainfall events on March 2013 (a & b)

Based on selected events, 10 sets of data on water temperature for 10 rainfall events were obtained at both sites (Table 3). Rainfall amount (*R-a*) influenced the change in water temperature ($\varDelta Tw$) through the change in specific discharge ($\varDelta Qs$). The hysteretic loops were clockwise for all periods at both sites. In addition, the peaks of *Tw* were earlier than those of *Qs* for clockwise loops. In this case also suggested that the different period or season probably was not influenced the river flow temperature, resulting in a similar direction of the loop between *Qs* and *Tw*. It also seemed that run-off or surface flow dominantly at both sites.

Table 3. The values of *R-a*, $\varDelta Qs$, $\varDelta Tw$, $\varDelta Ta$ and *Qs* vs. *Tw* hysteretic loops at both sites

Rainfall Event	Site	*R-a*	ΔQs	|ΔTw|	|ΔTa|	*Qs* vs. *Tw* loops
Jun-11	EC	18.5	0.1	1.0	11.1	*C*
Jul-11	EC	23	0.2	1.0	9.0	*C*
Feb-13	RC	40.1	0.5	2.4	9.6	*C*
Feb-13	RC	56.6	0.7	3.2	9.6	*C*
Mar-13	RC	63.5	1.1	2.8	8.1	*C*
Mar-13	RC	104.4	1.3	2.2	8.7	*C*
Mar-13	RC	67.3	0.8	2.3	9.5	*C*
Mar-13	RC	95.8	2.4	7.9	8.3	*C*
Mar-13	RC	52.6	0.8	3.5	12.0	*C*
Apr-13	RC	27.4	0.3	3.1	9.4	*C*

R-a: Rainfall amount (mm), $\varDelta Qs$: changes of specific discharge (mm/hour), $\varDelta Tw$: changes in stream water temperature (℃), $\varDelta Ta$: changes in air temperature (℃), *C*: Clockwise.

In Fig. 8a & 8b, the initial rises of *Tw* occurred in all cases, and these rises were due probably to direct runoff or quick-flow accompanying thermal transfer (Ward and Robinson 2000). This is because the initial averages of *Ta* were warmer than those of *Tw* in all cases, which produced the initial rises of *Tw*.

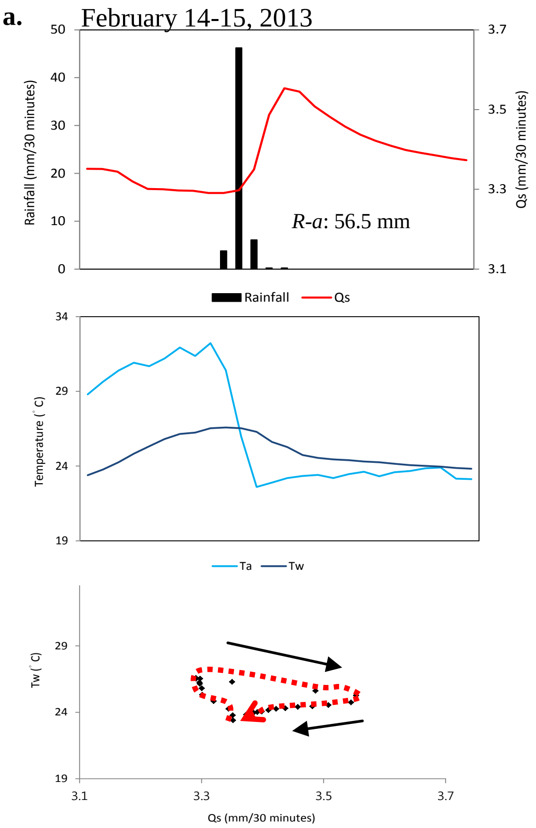

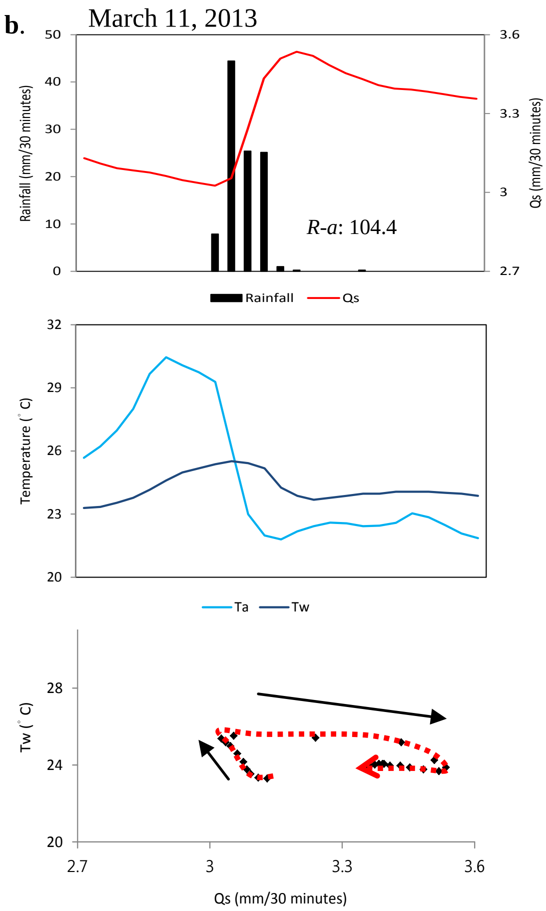

Fig. 8 Hysteretic loops during rainfall events on February 2013 (a) and March 2013 (b)

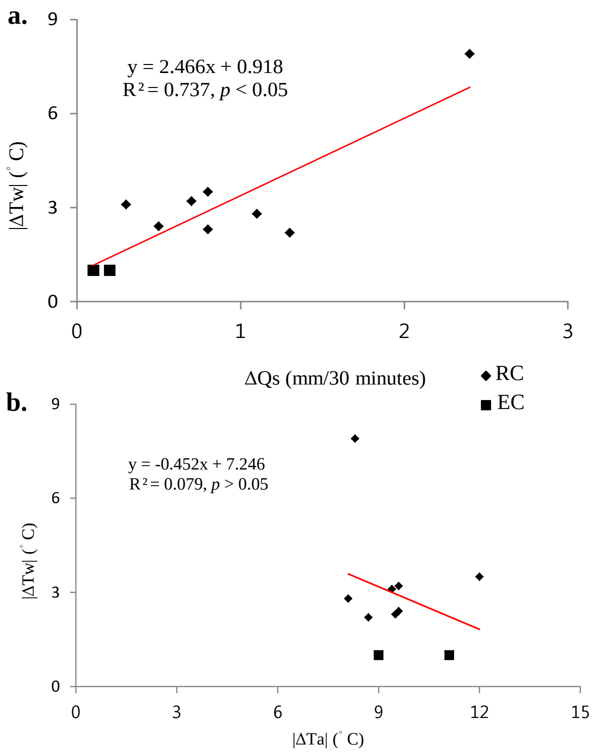

Fig. 9 Correlation between $\varDelta Qs$ vs. $|\varDelta Tw|$ (a) and $|\varDelta Ta|$ vs. $|\varDelta Tw|$ (b) during rainfall events

More specifically, Fig. 9 shows that the correlation between ΔQs and $|\Delta Tw|$ was more significant ($R^2 = 0.737$, $p < 0.05$) than that between $|\Delta Ta|$ and $|\Delta Tw|$ during rainfall events, suggesting that variations of *Qs* more significantly influenced water temperature through the change in flow paths compared with *Ta*.

Most likely, water temperature response to rainfall/storm events resulted from advective energy inputs, primarily from surface and subsurface hill slope pathways and by groundwater, rather than from a direct heat flux by falling precipitation (Brown et al. 2006). This is because the perennial channel system occupies only a small proportion (1% - 2%) of the area of the most catchments without lakes or swamps (Ward and Robinson 2000). Thus, the advective thermal energy flux from the upstream of the channel depends on the sources of runoff waters: surface/subsurface runoff and groundwater flow.

Shanley and Peters (1988) pointed out that there was no significant difference between rain and air temperatures observed at 1-minute intervals. In addition, *Ta* insignificantly influenced *Tw* ($R^2 = 0.079$, $p > 0.05$) during rainfall events. Then, it suggests that rainfall temperature also insignificantly influences *Tw*. The fluctuations of *Tw* in tropical forested watershed were influenced not only by *Ta*, but also *Qs* in all periods. Quick flow was dominantly, especially during rainfall events.

The magnitudes of ΔQs and ΔTw could be described as a large surface flow that it brings sediment from high erosion site potential. It also could be explained that water temperature changes could support on sedimentation model analysis, especially during rainfall events. In addition, the presence of Kracak reservoir as a hydroelectric power plant should be considered because it is associated with potential threats on sedimentation affecting reservoir age and the ability to store the water.

Summary and conclusions

The flow paths of water flow should be considered to investigate the hydrological dynamics. A relation on how rainfall and specific discharge would affect hydrological processes in various forested watersheds under different seasonal conditions was necessary to be investigated. Moreover, water temperature could be used to trace and evaluate the condition of forested watershed, including support on sedimentation model analysis.

Acknowledgement

This research was supported by a grant (11-TI-C06) from Advanced Water Management Research Program funded by Ministry of Land, Infrastructure and Transport of Korean government.

References

Brown LE, Hannah DM (2008) Spatial heterogeneity of water temperature across an alpine river basin. Hydrological Processes 22: 954 – 967

Brown LE, Hannah DM, Milner AM (2006) Hydroclimatological influences on water column and streambed thermal dynamics in an alpine river system. Journal of Hydrology 325: 1 - 20

Caissie D (2006) The thermal regime of rivers: a review. Freshwater Biology 51: 1389 – 1406

Mohseni O, Stefan HG (1999) Stream temperature/air temperature relationship: a physical interpretation. Journal of Hydrology 218: 128 – 141

Project report 2011, PKPP-Ristek. Impact of land use change on sedimentation and discharge flow; case study: the upstream cisadane watershed, National Incentive program for researcher and engineer

Shanley JB, Peters NE (1988) Preliminary observations of streamflow generation during storms in a forested Piedmont watershed using temperature as a tracer. Journal of Contaminant Hydrology 3: 349 – 365

Subehi L (2013) Characteristics of fluctuation in water temperatures as an indicator for sustainable water management at River Cianten, West Java. Proceeding of International Conference of Indonesian Inland Waters III (ISBN 978-602-8380-07-2), Palembang – Indonesia, November 2012, pp 209

Subehi L, Fukushima T, Onda Y, Mizugaki S, Gomi T, Kosugi K, Hiramatsu S, Kitahara H, Kuraji K, Terajima T (2010) Analysis of stream water temperature changes during rainfall events in forested watersheds. Limnology 11: 115 - 124

Tani M (1997) Runoff generation processes estimated from hydrological observations on a steep forested hillslope with a thin soil layer. Journal of Hydrology 200: 84 – 109

Tung CP, Lee TY, Huang JC, Perng PW, Kao SJ, Liao LY (2014) The development of stream temperature model in a mountainous river of Taiwan

Webb BW, Hannah DM, Moore RD, Brown LE and Nobilis F (2008) Recent advances in stream and river temperature research. Hydrological Processes 22: 902 – 918

Ward RC, Robinson M (2000) Principles of Hydrology. McGraw-Hill, UK, 450 pp

Detection of paddy fields in sub-state level by combined use of MODIS and Landsat imagery

Takanori NAGANO[1, a *], Yumiko ONO[1], Akihiko KOTERA[1] and Ranvir SINGH[2]

Abstract. Countries which keep monitoring land use/land cover change at plot/district level every year are limited. Although such information is vital for various strategies e.g. regional planning, validating subsidies and assessing flood/drought damages, monitoring is hampered by high cost of labor and information management.

For detection of paddy fields at state or country scales, MODIS images were often used in previous studies. While high temporal resolution and wide spatial coverage are advantages of MODIS, its coarse spatial resolution (250 m x 250 m) inhibited accurate detection of small paddy fields in Asian Monsoon regions. We developed a new method to detect paddy area by combined use of MODIS and Landsat. The methodology was designed for regions where ground truth data are poorly available for supervised classification. The study area was set to Haryana State in India where average farm plot size is small (4,000 m2) and cultivated areas are largely fluctuating from year to year due to water availability.

Firstly, paddy cultivated areas were detected by unsupervised classification of a set of multiple Landsat images available in a growing season of a specific year. Secondly two conditional parameters for time-series Enhanced Vegetation Indices and Land Surface Water Indices were optimized by Powell's method to best match the paddy area detected by MODIS to the area detected by Landsat. Thirdly calculated paddy areas were compared to municipal records. Until results showed reasonable agreements, paddy cultivated areas were reclassified in Landsat images and following procedures were repeated. Calculated area of cultivation from 2001 to 2013 were not in good agreement with the state's municipal record which had little change over the years. The fluctuation of calculated area was in fact well correlated to India's national production record. Our methodology of detection has more likely captured harvested paddy area than planted/cultivated area.

Keywords: *MODIS, Landsat, paddy, cultivated area*

Takanori Nagano, Yumiko Ono, Akihiko Kotera
Department of Agr. Engineering and socio-economics, Graduate School of Agric. Science, Kobe University Kobe, Japan
naganot@ruby.kobe-u.ac.jp
Ranvir SINGH
Institute of Natural Resources, Massey University, PB11222, Palmerston North 4442 New Zealand

Estimation of Evapotranspiration in Lam Ta Kong Basin using Surface Energy Balance Algorithm for Land (SEBAL) Model

Haruetai Maskong[1, a *], Preeyaporn Kosa[2,b] and Chatchai Jothityangkoon[3,c]

Abstract Evapotranspiration (ET) is a primary interest to many end-users of water management because it represents a loss of usable water from the hydrologic supply. Evapotranspiration is highly variable in both space and time similar to other hydrology data (precipitation, soil, vegetation). A remote image-processing model has been applied to estimate evapotranspiration in Lam Ta Kong Basin using Surface Energy Balance Algorithm for Land (SEBAL) model. For this SEBAL model, evapotranspiration is computed from Landsat 5 satellite images on May 7th 2010 and available climatic data from a limited number of ground weather station. SEBAL calculates evapotranspiration through a time series of input parameters including net surface radiation, soil heat flux and sensible heat flux to the air for energy balance equation. Estimated evapotranspiration over Lam Ta Kong basin can be presented with high temporal and spatial resolution. The SEBAL model is useful tool for estimating spatial pattern of evapotranspiration to fulfill the unavailable evapotranspiration data from weather station.

Keywords *Remote sensing, Penman–Monteith, Weather data, Spatial data*

Authors Name/s per 1st Affiliation (*Author*)
line 1 (of *Affiliation*): School of Civil Engineering
line 2- Institute of Engineering, Suranaree University of Technology
line 3- Nakhon Ratchasima 30000, Thailand
line 4- [a]haruetai.m@gmail.com

Authors Name/s per 2nd Affiliation (Author)
line 1 (of Affiliation): School of Civil Engineering
line 2- Institute of Engineering, Suranaree University of Technology
line 3- Nakhon Ratchasima 30000, Thailand
line 4-[b]kosa@sut.ac.th

Authors Name/s per 3rd Affiliation (Author)
line 1 (of Affiliation): School of Civil Engineering
line 2- Institute of Engineering, Suranaree University of Technology
line 3- Nakhon Ratchasima 30000, Thailand
line 4- [c]cjothit@sut.ac.th

Introduction

Evapotranspiration is the sum of evaporation and plant transpiration from the Earth's land and ocean surface to the atmosphere. Evaporation accounts for the movement of water to the air from sources such as the soil, canopy interception, and water bodies. Transpiration accounts for the movement of water within a plant and the subsequent loss of water as vapor through stomata in its leaves. Normally, evapotranspiration can be computed from weather data by Penman-Monteith (PM) equation. There are a few weather stations from the Thai meteorological department and sometime data are lost. In the study area, there are 3 weather data stations (431201, 431301 and 431401) around (Fig. 1). The evapotranspiration from Penman-Monteith equation is a point data which is not representative of the entire area. Therefore, the objectives of this study are to estimate the apace-time evapotranspiration using the Surface Energy Balance Algorithm for Land (SEBAL) Model.

Study area

Lam Ta Kong Basin is one of the eight sub-basins in greater Mun River Basin and consists of 220 km in length and 3,518 km^2 in a watershed area (Fig. 1). It covers about 4.67 % of the Mun River Basin. Mean annual rainfall is 1,373 mm and contributes to $510x10^6$ m^3 of the total average annual runoff. Headwater of the basin is in the Dong Phaya Yen Mountains at Pak Chong district, Nakhon Ratchasima province, Thailand. It flows through four communities including Pak Chong district, Sikhio district, Sungnoen district, and Nakhon Ratchasima city municipality. Channel slope of the upper basin between Pak Chong district to Lam Ta Kong dam is steep. While the central and lower basin area of Lam Ta Kong has low slope to the relatively flat.

Methodology

The Penman–Monteith (PM) equation is a generalization of the Penman equations that allows for a composited plant stomatal resistance to vapor transport that is specified through a bulk surface resistance (Penman, 1948; Monteith, 1965). The PM equation typically is written in terms of latent heat flux (the energy equivalent of actual evapotranspiration (ET_a)).

$$LE = \frac{\Delta(R_n - G) + \rho_a c_p (e_s - e_a)/r_a}{\Delta + \gamma(1 + r_s / r_a)} \qquad (1)$$

Where LE is the latent heat flux, R_n is the net radiation (MJ/m^{2}h), G is the soil heat flux (MJ/m^{2}h), Δ is slope of the saturation vapor-pressure curve (kPa/C); ρ_a is mean air density at constant pressure; c_p is specific heat of air; $e_s - e$ is the vapor-pressure deficit; e_s is saturation vapor-pressure of the air (kPa); e_a is actual vapor-pressure of the air(kPa); γ is the psychometric constant (kPa/C); r_s is bulk surface resistance; r_a is aerodynamic resistance.

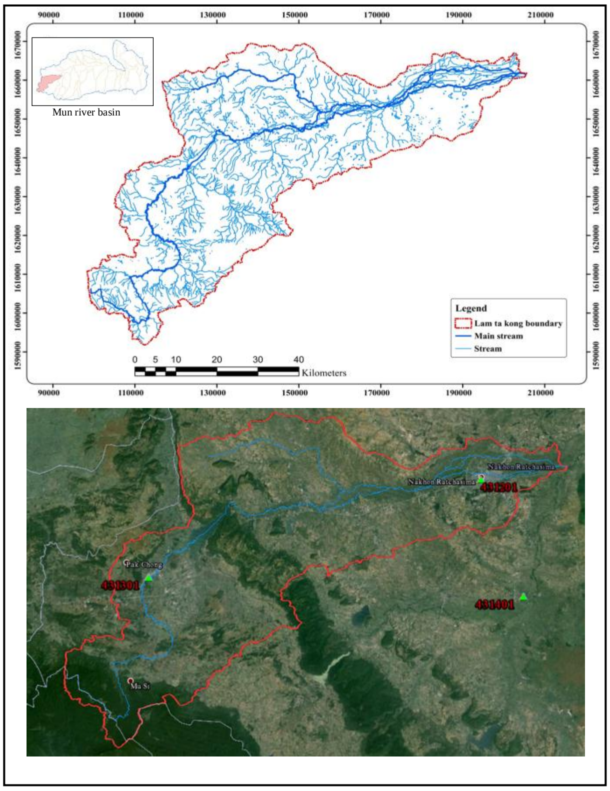

Fig. 1 The study area. Lam Ta Kong basin.

Reference crop evapotranspiration (ET_o) can be calculated on hourly basis using the Penman–Monteith equation (Allen et al, 2001). Application of reference conditions in Eq. (1) yields:

$$ET_o = \frac{0.048\Delta(R_n - G) + \gamma \dfrac{900}{T + 273.2} u_2 (e_s - e_a)}{\Delta + \gamma(1 + 0.43u_2)} \qquad (2)$$

where ET_o is reference crop evapotranspiration (mm/h), T is air temperature (C), u_2 is wind speed at 2 m (m/).

Eq.(2) is used to estimate evapotranspiration from a hypothetical short grass with a height of 0.12 m, a surface resistance of 70 s/m, and albedo of 0.23 (Allen et al., 1998: Allen et al, 2001). In this study, reference evapotranspiration was computed in spreadsheet using weather data and Penman–Monteith equation (Eq.2).

SEBAL is a method for evapotranspiration calculation using satellite image and weather data with the concept of energy balance. Principal components of the SEBAL which converts remotely measured spectrally emitted and reflected radiance's into the surface energy balance and land wetness indicators (Bastiaanssen et al., 1998a and Bastiaanssen et al., 1998b). SEBAL is used to compute the terms G (soil heat flux) and H (sensible heat flux) of the surface energy budget equation. The net radiation (R_n) is the net amount of radiant energy. SEBAL computes λET (latent heat flux) as a residual of net radiant energy after soil heat flux and sensible heat flux are subtracted:

$$\lambda ET = R_n - G - H \qquad (3)$$

The instantaneous evapotranspiration (ET_{inst}) of satellite image is estimated as follow equation.

$$ET_{inst} = 3600 \frac{\lambda ET}{\lambda} \qquad (4)$$

Where λ is latent heat of vaporize or the heat absorbed (J/kg). λ has different value in the different temperature. Which use for λ calculation is show in Eq.5.

$$\lambda = 2.501 - (2.361 \times 10^3)T \qquad (5)$$

Where T is surface temperature.

The reference evapotranspiration fraction ($ET_r F$) can be computed from following equation.

$$ET_r F = \frac{ET_{inst}}{ET_r} \qquad (6)$$

Where ET_r is reference evapotranspiration (mm/h). It is computed in spreadsheet from weather data in the same time of satellite image.

Twenty-four hour evapotranspiration (ET_{24}) can be calculated from following equation.

$$ET_{24} = ET_r F \times ET_{r\_24} \qquad (7)$$

Where ET_{r_24} is reference evapotranspiration (mm/day).

SEBAL quantifies the energy balance using satellite data as an input. Land surface characteristics such as surface albedo, leaf area index, vegetation index and surface temperature are derived from satellite imagery. Satellite image from Landsat 5 TM observed on May 7th 2010 is used in this study. (Fig.2) (GPR540431TM).

Idaho implementation (2002) explains a remote image processing model for predicting the evapotranspiration termed SEBAL. SEBAL was developed by ERDAS IMAGINE's Model Maker tool and experience with this software is a prerequisite. The concept of SEBAL method is shown by Fig.3. First is the computation of reference evapotranspiration in the spreadsheet using weather data and Penman-Monteith equation. Next is the calculation of surface albedo vegetation index, surface temperature, net radiation, soil heart flux, sensible heat at extreme evaporation point momentum flux and Sensible heat flux. Finally, the image processing model, create model to calculated actual evapotranspiration using ERDAS IMAGINE packet. All Equations in each step were shown in Idaho implementation (2002) and Kosa (2011).

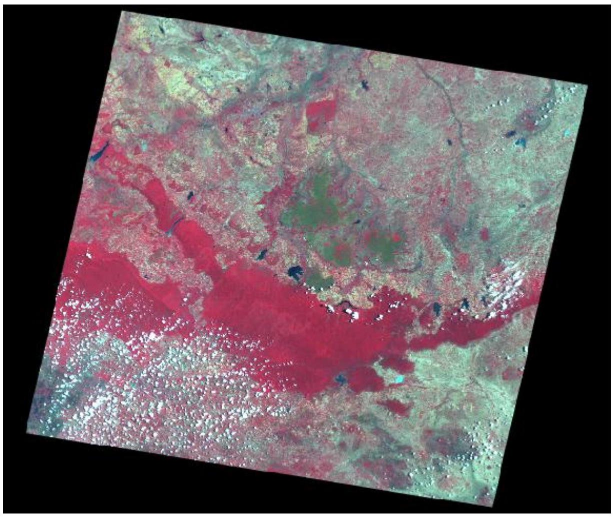

Fig. 2 satellite images (LANDSAT 5) for Lam Ta Kong Basin.

Results and discussion

There are many image results from SEBAL model. Only some images are shown in this part.

Albedo (α) is the relationship between reflected radiation and total incoming radiation. It is varies with the characteristic of the surface and angle of incidence or the slope of ground surface. Fig. 4 shows the Surface albedo, dark and light represent high values and low values, respectively. The maximum value is 0.34 and the minimum value is 0.021.

The Normalized Difference Vegetation Index (NDVI) is a numerical indicator that uses to represent the visible and near-infrared bands of the electromagnetic spectrum. It is adopted to analyze remote sensing measurements and assess whether the target being observed contains live green vegetation or not. Fig. 5 Shows the NDVI, dark and light represent high values and low values, respectively. The maximum value is 0.882 mm and the minimum value is 0.004 mm.

The net radiation (R_n) is the difference value between incoming and outgoing radiation of both short and long wave radiation. Fig. 6 shows the output of net radiation; dark and light represent high values and low values, respectively. The maximum value is 1012 W/m^2 and the minimum value is 440 W/m^2.

The soil heat flux (G) is energy that is used in heating soil. It is positive value in the condition of warming soil, and negative in the condition of cooling soil. Fig. 7 is an image G. The maximum and the minimum value are 155 and 30 W/m^2, respectively. Dark and light represent high values and low values.

The sensible heat flux (H) is the rate of heat loss to the air by convection and conduction, due to a temperature difference. Fig. 8 is an image of the sensible heat flux. The maximum and the minimum values are 211 and 10 mm, respectively. Dark and light represent high values and low values.

Latent Heat Flux (λET) is the rate of latent heat loss from the surface due to evapotranspiration. It is computed for each pixel using Eq.3. The 24 hour evapotranspiration (ET_{24}) is calculated from λET that show in Fig.9. The maximum and the minimum values are 4.11 and 1.13 mm/day, respectively.

The simulated results by SEBAL are compared with the calculated results by Penman–Monteith equation at the same point as shown in Fig. 10. It is found that homogenea value of SEBAL result can be predicted. The value of evapotranspiration from Penman Monteith equation and the simulated evapotranspiration are shown in Table 1.There are 3 weather stations around Lam Ta Kong basin but there are 2 stations into this satellite image scene (Fig.2). Therefore, there is no SEBAL result can be predicted at the 431301 station. However SEBAL can be used successfully to estimate evapotranspiration.

Table 1 comparison of point evapotranspiration results between by SEBAL and Penman–Monteith equation.

Weather station No.	Evapotraspiration (mm/day)		Different (mm/day)
	SEBAL	Penman–Monteith	
431201	3.20	4.92	1.72
431301	N/A	3.60	-
331401	3.15	4.84	1.69

Conclusion

Evapotranspiration from SEBAL can be presenting over spatial and temporal resolution. SEBAL is usefully algorithm which can be considered the estimation of evapotranspiration using satellite image and few available weather data from limited number of ground weather station. SEBAL stands in the concept of natural energy process so many climatic parameters are required.

This study focused on estimation of daily actual evapotranspiration using the SEBAL model applied to a remote sensing Landsat 5 TM sensor. All ground truth data for calibration of model was collected during the field campaign from weather station using Penman–Monteith equation on. Therefore, this study represent only one day a spatial evapotranspiration image. That is can present better than Penman–Monteith's point evapotranspiration. However, SEBAL should be carefully analyzed to do accurate evapotranspiration.

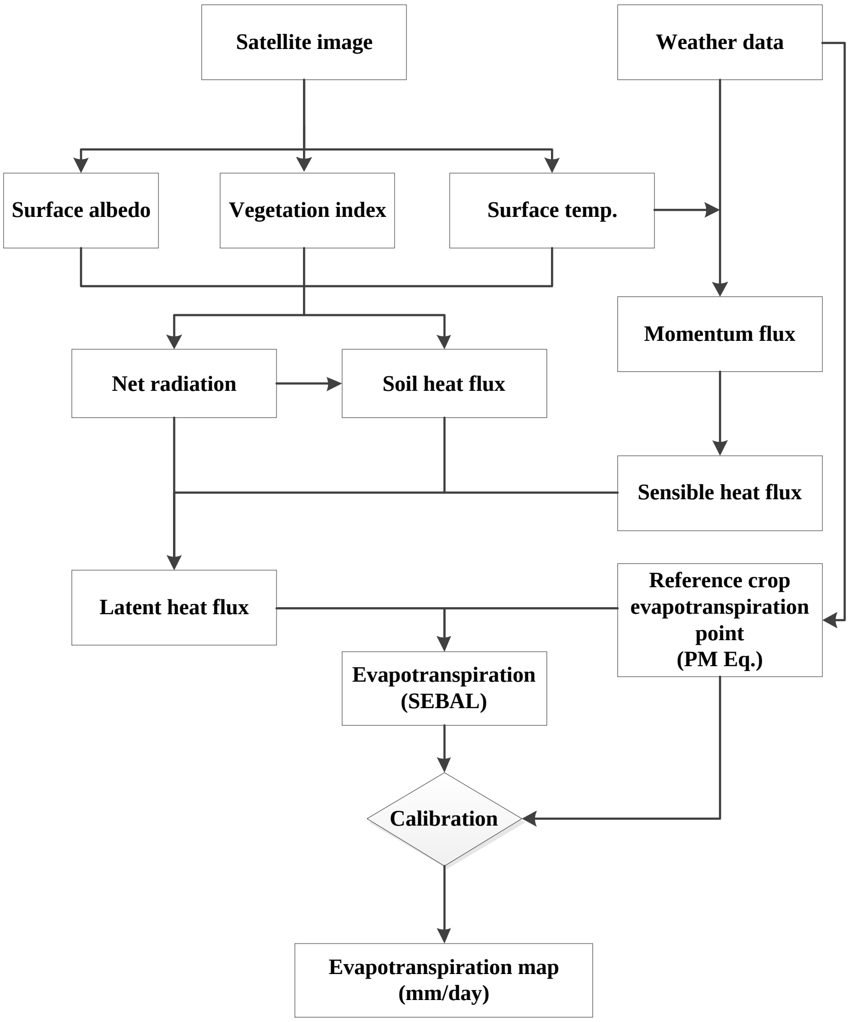

Fig.3 Flow chart representing algorithm of SEBAL model**.**

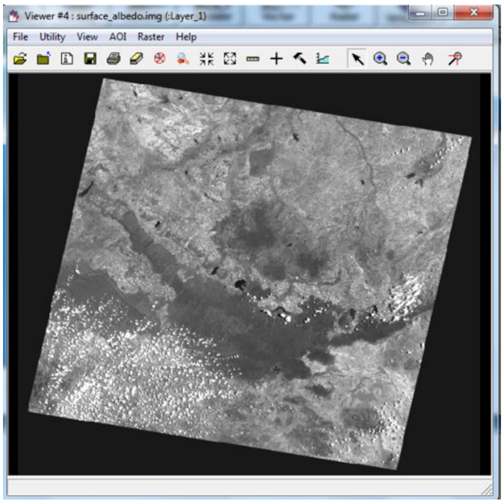

Fig. 4 Surface albedo image

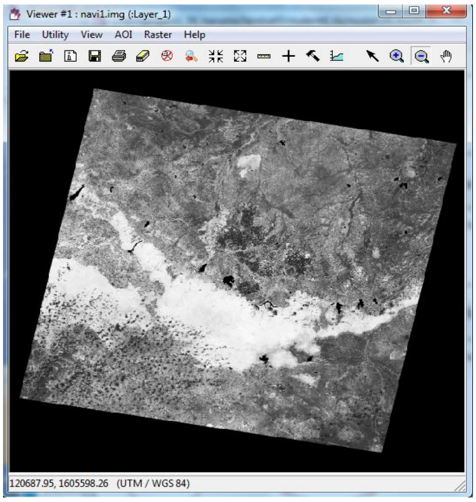

Fig. 5 NDVI image

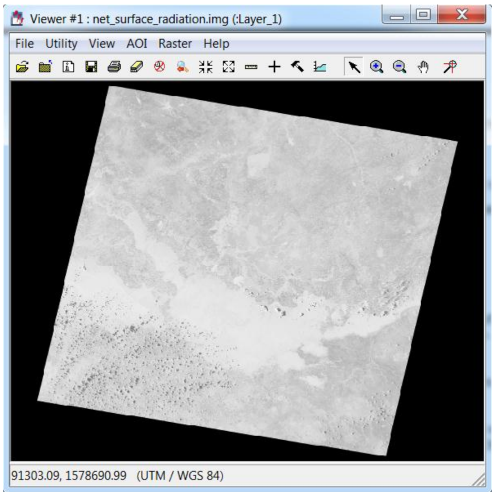

Fig.6 Net radiation (R_n) image

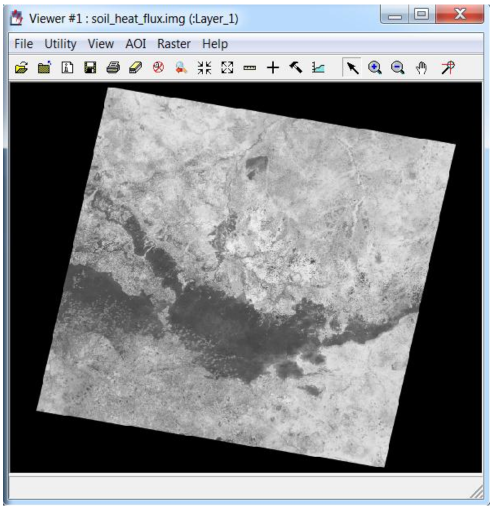

Fig.7 Soil heat flux (*G*) image

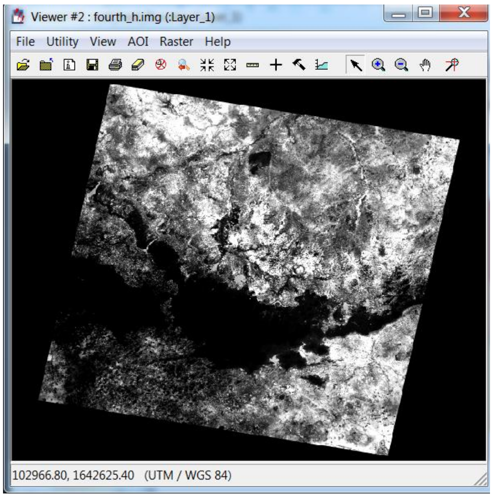

Fig.8 Sensible heat flux (*H*) image

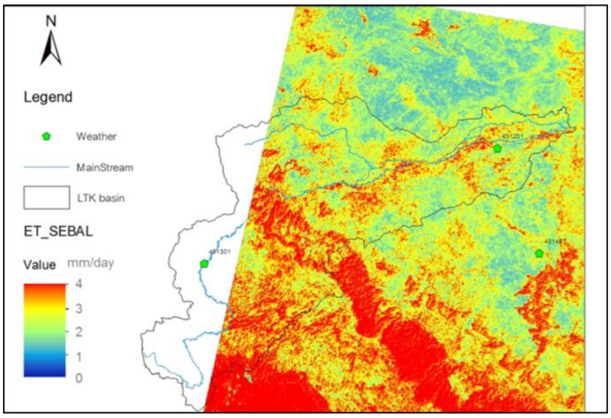

Fig.9 Twenty-four hour evapotranspiration (ET_{24}) image.

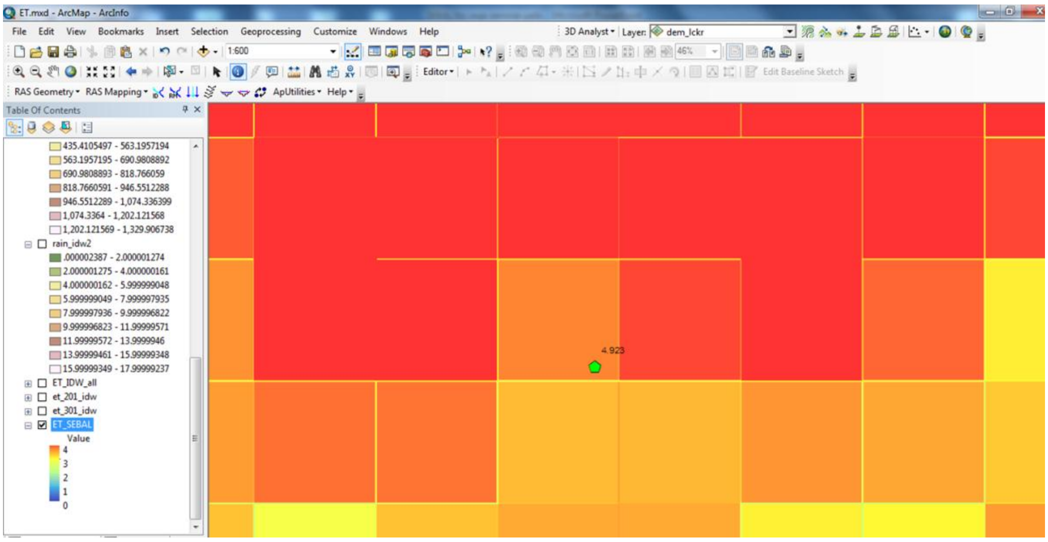

Fig. 10 comparison between simulated results by SEBAL and calculated result by Penman–Monteith equation.

References

Allen, R.G., Periera, L.S., Raes, D., Smith, M., 1998. Crop Evapotranspiration: Guidelines for Computing Crop Requirements, Irrigation and Drainage Paper No. 56. FAO, Rome, Italy, p. 300.

Allen, R. G., A. Morse, M. Tasumi, W. Bastiaanssen, W. Kramber and H. Anderson. (2001).Landsat Thematic Mapper for evapotranspiration via the SEBAL process for water rights management and hydrology water balances, SEBAL, Available Source:http://www.agu.org/meetings/sm01/sm01_pdf/sm01_B42C.pdf, August 8, 2003.

Bastiaanssen, W. G.M., M. Meneti, R. A. Feddes and A. A. M. Holtslag. (1998a). A remote sensing surface energy balance algorithm for land (SEBAL) 1 Formulation. Journal of Hydrology, Vol. 212-213, pp. 198-212.

Bastiaanssen, W. G.M., M. Meneti, R. A. Feddes and A. A. M. Holtslag. (1998b). A remote sensing surface energy balance algorithm for land (SEBAL) 1 Validation. Journal of Hydrology, Vol. 212-213, pp. 213-229.

Idaho Implementation. 2002. SEBAL Surface Energy Balance Algorithms for Land : Advanced Training and User's Manual. Funded by a NASA EOSDIS/Synergy grant from the Raytheon Company through The Idaho Department of Water Resources.

Kosa, P. 2011. The Effect of Temperature on Actual Evapotranspiration based on Landsat 5 TM Satellite Imagery. Evapotranspiration (Book) Janeza Trdine 9, 51000 Rijeka, Croatia, pp.209-228.

Monteith, J.L. 1965. Evaporation and environment, In: Proceedings of the 19th Symposium of the Society for Experimental Biology.Cambridge University Press, New York, NY pp. 205–233.

Penman, H.L. 1948. Natural evaporation from open water, bare soil, and grass. Proceedings of the Royal Society, London pp 120–146.

Deep Groundwater and Possible Signals for Human and Climatic Effects

Uma Seeboonruang

Abstract Groundwater data reflects hydrological processes, climate change and variability, as well as any anthropogenic influence. Hence, inversion of groundwater signals can provide significant information of the historic exposure to groundwater. This study aims to present a method of decomposing deep groundwater signals monitored at stations in the lower Chao Phraya basin in Thailand to reveal the effects of two major forces; anthropogenic and climatic effects. The anthropogenic effect and the impact from climate change are assumed to possess the long-term trend on the groundwater signal, while the impact of climate variability is assumed to be in the periodic pattern. The classical decomposition partitions a signal into three elemental components called trend, periodicity and random or irregular components. A detrending method is the first step applied to obtain the anthropogenic effects, e.g. those from a long-term groundwater development, and possibly climate change. Consequently, wavelet analysis is performed on the groundwater detrended residuals and the wavelet power spectrums are then related to some climatic variability indices, representing three important climate forces. This research focuses on the application of different mother wavelets on the detrended data. Morlet mother wavelet is proved to be best for this analysis. The outcome from the decomposition examination finds that the groundwater in the region is significantly under the influence of anthropogenic effect and the El Nino/Southern Oscillation and the Asian Summer Monsoons result in the periodic cycle of the groundwater signal. In addition, non-stationarity of the climate variability and groundwater oscillation are evident in the region. Therefore, future groundwater management should take into account of not only climate change but also climate variability as well for better sustainability and resilience.

Keywords *Groundwater, time series analysis, wavelet analysis, climate variability*

Assoc. Prof. Dr. Uma Seeboonruang
Department of Civil Engineering,
Faculty of Engineering, King Mongkut's Institute of Technology Ladkrabang
Ladkrabang, Bangkok, Thailand
Email: kseuma@kmitl.ac.th

Introduction

A groundwater system is naturally dynamic and changes with time in response to both human activities and climate stresses. Climate change has accelerated the already worsening state of groundwater resources and rendered the only available freshwater reserve less accessible (IPCC, 2007). The higher temperatures and precipitation fluctuations contribute to variations in soil moisture, runoff and eventually groundwater recharge. In addition to climate change, global water resources can be sensitive to climate variability, i.e. the reversible and periodic changes that occur over periods of a few years to decades (Hanson et al., 2004; Gurdak et al., 2007). Impacts of climate variability on groundwater are however little understood. Furthermore, the relationship between climate variability and groundwater is more complex than that between climate variability and precipitation or surface water.

In general, a regional climate may contain several modes of recurring fluctuations. The most widely known decadal-time scale climate variability, the El Nino/Southern Oscillation (ENSO) phenomenon is characterized by variations in the sea-surface temperature and in the barometric pressures. The interannual climate variability of ENSO includes periodicity ranging from 2 to 6 years, while the variations on slightly longer cycles of approximately 6 to 10 years may be due to monsoons. In addition, the Pacific Decadal Oscillation (PDO) could contribute to interdecadal variations of approximately 10 to 25 years (Mantua and Steven 2002) and 50 to 70 years (Minobe, 1997). Other influencing forces of climate periodicities include the North Atlantic Oscillation (NAO) with a periodicity of 7 to 8 years (Fye et al., 2006), and the Atlantic Multidecadal Oscillation (AMO) with a periodicity of 50 to 80 years (Kerr, 2000).

Thailand is situated right on the dividing line between the very different and equally powerful weather patterns of the Indian Ocean and the western Pacific Ocean. However, there have been only a handful of studies that analyzed a linkage between climate variability and rainfall variations in Thailand on longer time scales, i.e. the interannual and interdecadal scales (Limsakul et al., 2007; Limsakuland Goes, 2008). These studies reported that the rainfall and temperature variations in Thailand were associated with periodicities on multiple time scales ranging from seasonal to interannual to interdecadal. Asian summer monsoons, the Indian Ocean Dipole (IOD), and ENSO exert the most influence on climate variability in the region. The annual rainfall cycle was found to be in phase with the

Indian summer monsoon (IMI) and the western North Pacific summer monsoon (WNPMI) (Limsakul et al., 2007). IOD also influences the annual rainfall but its impact varies, depending on both the combined effect of IOD and ENSO and the strength of ENSO in the Pacific Ocean. The periodicity of IOD has been in a range of 1 - 4 years since 1990. ENSO has a 3-to-7-year cycle, with a four-year average to go from El Niño to La Niña.

Some of the key questions relating to these cyclical patterns are whether these aforementioned forces impose the stationarity and whether the signals can be detected in the groundwater resource. In addition, if these climatic forces do exert influence on groundwater, the management of groundwater for a sustainable future and the adaptation to climate change must take into account the stationarity, extents and periodicities of these variables.

Limited research studies have attempted to relate deep groundwater signals to climate change and climate variability (Green et al., 2011). Therefore, this current study aims to analyze the application of wavelet analysis to groundwater fluctuation in the Lower Chao Phraya Basin and of some climatic indices influencing the weather in the region. The analysis also focuses on the use of multiple mother wavelets in the wavelet and their validity on the groundwater signals.

Study area

Hydrogeologically, the Lower Chao Phraya Basin is located in the upper tertiary to quaternary strata of the Lower Central Plains of Thailand. The aquifers consist mainly of sands, gravels, and minor clay lenses of Pliocene-Pleistocene-Holocene geological age and can be zoned into eight principal confined aquifers separated by apparent thick confining clay layers. The depth of the aquifer system is approximately 500 meters. The main recharge to the aquifer system is from the Middle Chao Phraya Basin hydraulically connected to the north of this Lower Basin. Widespread exploitation of groundwater for urban water supply began in the 1950s, and the primary targets for water well construction were the 2nd, 3rd and 4th aquifers in a depth range of 100-250 meters below the ground surface.

Seeboonruang (2014) separated the anthropogenic effect of groundwater withdrawal from the groundwater time series by applying multiple detrending methods to six long-term monthly groundwater records collected at stations in Thailand's Lower Chao Phraya Basin. The 5^{th} order polynomial interpolation performed well as it yielded on average the best fitting of the trendlines linking to the human effect. The spectral analysis produced the periodograms of the detrended time series and the periodogram patterns were comprised of two bimodal distributions. The two means of the bimodal periodogram distributions, one with a periodicity of 3 - 5 years and the other with a periodicity of 10 - 13 years, indicated that the cyclical patterns of the deep groundwater in the Lower Chao Phraya Basin could be the result of climate variability phenomena, e.g. ENSO and IOD. However, the author did not perform any analysis to relate the groundwater oscillation to the climatic indices.

Introduction to wavelet theory

Previous studies on groundwater applied the time series analysis to analyzing groundwater records in response to stresses (Gurdak et al., 2007). Among the frequency-domain methods, the Fourier series analysis is widely used to decompose a single signal into constituent sinusoids of different frequencies. However, the spectral analysis methods can indicate periodicities that are stationary when amplitude and frequency do not change considerably in time. With wavelet analysis, a time series can be studied on time and multiple frequency scales concurrently (i.e. at low and high frequencies). The wavelet method of this current research follows that of Torrence and Compo (1998). The objective of the analysis is to decompose a signal, expressed as a function of the time variable, into various frequency components using building blocks. These building blocks are defined by wavelets. Once a wavelet is constructed, it can be used to filter or compress signals.

The continuous wavelet transform of a discrete time series x_n of N observations with a time increment of δt and the complex conjugate $\psi^*$of an analysis function $\psi(t)$ is given by

$$W_n(s) = \sum_{n'=0}^{N-1} x_{n'} \sqrt{\frac{\delta t}{s}}\, \psi^* \left[\frac{(n'-n)\delta t}{s}\right] \qquad (1)$$

where t is time, s is the wavelet scale, and n provides the time variation. The analysis function $\psi(t)$ is called a mother wavelet function, which must be localized in time and frequency space and should be admissible, and is assumed that $\psi(t)$ is normalized, i.e. $\int_{-\infty}^{\infty} \psi\psi^*\, d\eta = 1$. Varying *s* and *n* in the wavelet transform ensures the complete evaluation on frequency components and their corresponding time localization. There are many well-known mother wavelet functions. Three different mother wavelets in Torrence and Compo (1998) are the Morlet, Paul, and Derivative of Gaussian (DOG) wavelets. The choice of an appropriate wavelet depends on the nature of the signal and type of information to be extracted from the signal. Moortel et al. (2004) characterized the three wavelets as follows: The Morlet wavelet has a reasonably large number of oscillations, which will ensure a good frequency resolution. The Paul wavelet has far fewer oscillations but is much localized in time, and this may yield accuracy in time but a reduced frequency resolution. The DOG wavelet has relatively few oscillations in a much wider time domain.

Methodology

Available groundwater data

Data on long-term continuous groundwater levels are collected throughout parts of Thailand's Central Plains by the Department of Groundwater Resources. The data contain records of groundwater depths from the ground surface and some of the records date back to 1921. Most bores are located in the urban and built-up lands. The water level readings are taken roughly once a month. The deep groundwater time series of the CT7_2 site was selected for its reasonably long-term and constantly measured observations of water levels. This is to reduce uncertainty that could arise from interpolation due to unavailability of data during certain periods.

Initially, the time series was interpolated into monthly basis using a simple linear interpolation because the measurements of groundwater levels were taken at irregular intervals, ranging from monthly to bimonthly. Subsequently, detrending by the 5th order polynomial interpolation was performed on these selected time series. Seeboonruang (2014) proved that this detrending removed the anthropogenic effects on the groundwater signals in the Lower Chao Phraya Basin. The detrended residual function was obtained by subtracting the fitting trend from the interpolated data over the recording periods. The wavelet analysis was then performed on the detrended time series.

Climatic indices

Thailand's meteorological conditions are influenced by Asian summer monsoons, IOD and ENSO, so it is vital that the climatic indices in this research represent these forces. The Asian summer monsoons will be represented by the Indian summer monsoon (IMI) and the western North Pacific summer monsoon (WNPMI). IOD is defined as the SST anomaly difference between the western equatorial Indian Ocean (50E-70E, 10S-10N) and the southeastern equatorial Indian Ocean (90E-110E, 10S-0N), referred to as the Dipole Mode Index (DMI). Since ENSO refers to variations in the surface temperature of the tropical eastern Pacific Ocean and in air surface pressure in the tropical western Pacific Ocean, the indices that most reflect these variations are the Multivariate ENSO Index (MEI), the Japan Meteorological Agency Sea Surface Temperature Index (JMA SST), the Southern Oscillation Index (SOI), the Sea Surface Temperature (SST) and the Outgoing Long Wave Radiation (OLR).

Wavelet analysis

Groundwater and climatic time series were analyzed by using standard wavelet analysis and the program called Paleontological STatistics (PAST) (Hammer and Harper, 2006) was applied here. The algorithm is based on fast convolution of the signal with the wavelet at different scales using the Fast Fourier Transform (FFT). The wavelet result is presented in three configurations: the complete wavelet power spectrum contour plot, global wavelet power spectrum, and local wavelet power spectrum. The power spectrum or normalized power spectrum of the periodicity over time is used for classification and analysis of particular time series behavior and characteristics. Each periodicity is the length of a cycle of hydrologic or climatic variation event. One hydrologic or climatic event or time series is composed of an infinite number of sinusoids with particular periodicity and each sinusoidal wave has different magnitude or strength contributing to the time series.

The focus of this study is a straightforward assessment performed on a known sinusoidal time series in order to examine which mother wavelet performs best on the detrended groundwater and climatic time series. The shape of the mother wavelet is set to Morlet (wavelet number 6), Paul (4th order), 2nd and 6th Derivative of Gaussian (DOG). A sinusoid regression is given by $y(x) = a \times \cos\left(\frac{2\times\pi\times(x-x_0)}{T} - p\right)$, where a is the amplitude, T is the period and p is the phase. x_o is the first (smallest) x value. The detrended residual of the groundwater time series at CT7_1 is modeled with the sinusoidal regression analysis to find a suitable set of regression parameters. The algorithm is based on a least-squares criterion and singular decomposition (Press et al. 1992). R^2, the coefficient of determination, indicates how well an obtained sinusoidal model fits data. Wavelet analyses with the different mother wavelets are then performed on the obtained sinusoidal function. The mother wavelet that yields the best wavelet transform power spectrum is that with 4266-day stationary periodicity.

A global wavelet power spectrum is computed and defined as the average over all the local wavelet spectrums, which is given by Eqn. (2). Normalized power of a global wavelet spectrum is computed as $\widehat{W}^2(s)/\sigma^2$. A global wavelet spectrum can provide a useful measurement of the background spectrum against which peaks in the local wavelet spectrums should be tested and can provide an unbiased and consistent estimation of the true power spectrum of a time series.

$$\widehat{W}^2(s) = \frac{1}{N}\sum_{n=0}^{N-1}|W_n(s)|^2 \qquad (2)$$

Each wavelet power spectrum is also verified by significance test to identify the periods and the periodicities where areas of high wavelet spectrum are present. The background spectrum in this computation is assumed to be red noise. The lag-α in red-noise background spectrum is estimated from $(\alpha_1 + \sqrt{\alpha_2})/2$, where α_1 and α_2 are the lag-1 and lag-2 autocorrelations of the original time series. If a peak of the spectrum is well above the computed background spectrum, the periodicity of the peak then portraits the true major cycle of the time series. The significance level corresponding to $p=0.05$ is used to establish a null hypothesis for the significance of a peak in the wavelet power spectrum.

Finally, the Pearson Product Moment Correlation (PPMC) between sets of groundwater and climatic wavelet power spectrum is carried out to measure how well they are related. The Pearson correlation shows the linear relationship between any two sets of data.

Results and discussion

Assessment for a proper mother wavelet

To investigate the differences among various mother wavelets, the wavelet transform with four mother wavelets, i.e. the Morlet, Paul, m=2 DOG and m=4 DOG wavelets, is applied on a simple sinusoidal function. This function is obtained from the sinusoidal regression analysis on the detrended groundwater signal at CT7_2 with a least square error method. The obtained regression model for CT7_2 is expressed as the single sinusoidal equation (Eqn. (3)) and with R^2 = 0.61. This groundwater time series fits well with the 4266-day cycle signal (Fig. 1).

$$y(x) = 0.536 \times \cos\left(\frac{2\times\pi\times(x-x_0)}{4266} - 2.14\right) \qquad (3)$$

The wavelet power spectrums of the single sinusoidal CT7_2 function are shown in Fig. 2 for the Morlet, Paul, and m=4 DOG mother wavelets, respectively. Note that the Morlet wavelet yields the sharp transition and the wavelet spectrum with a narrow peak around the 4382-day periodicity from the start to the end time. The Morlet wavelet appears to yield the accurate spectrum both in the frequency and time components. On the other hand, the Paul and DOG power spectrums do not preserve the actual periodicity and localization of the trial sinusoidal function. The Paul power spectrum is more dispersed around its peak than that of the Morlet spectrum, and the peak of periodicity occurs at a shorter cycle than the actual periodicity. In particular, the spectrum wavelets from the DOG mother wavelets portray peaks of periodicity well shorter than the actual periodicity and are highly non-stationary as opposed to the stationarity of the actual periodicity. This may be because the Paul and DOG mother wavelets have relatively few oscillations compared with the Morlet wavelet, thus yielding less accurate wavelet in frequency (periodicity) resolution. In addition, the DOG mother wavelets have much wider time domain and thereby are less accurate in time.

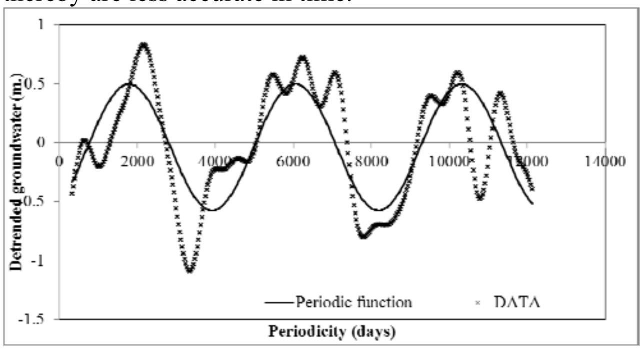

Fig 1. The detrended groundwater time series at CT7_12and the best fit sinusoidal function.

Next, the percentages of error between the cycles at the wavelet power spectrum peaks corresponding to particular mother wavelets and the actual cycle are computed and shown in Fig. 3. It is obvious from this trial case that the Morlet mother transform performs and yields the wavelet power spectrum with accuracy both in time and frequency (periodicity) resolution. The Paul wavelet transform is somewhat less accurate than that of the Morlet wavelet but still more accurate than both DOG transforms. The DOG wavelet transforms yield substantial localization of their resultant wavelet power spectrums, which can be seen from Figure 5. They also result in highly non-stationary periodicity and a small error percentage of the DOG transforms at some locations in time. Therefore, only the Morlet mother wavelet is adopted for analysis from this point onward.

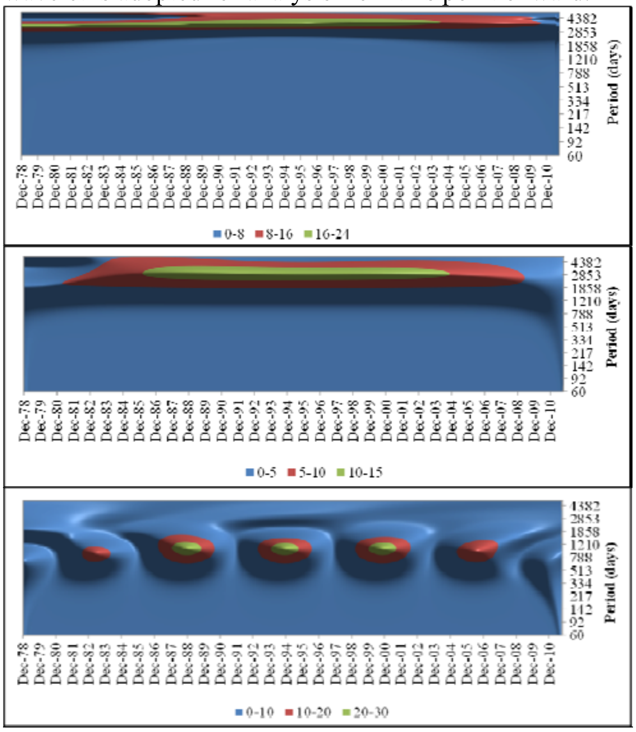

Fig 2. Power spectrum using the Morlet, Paul and DOG wavelets on the CT7_2 single sinusoidal function.

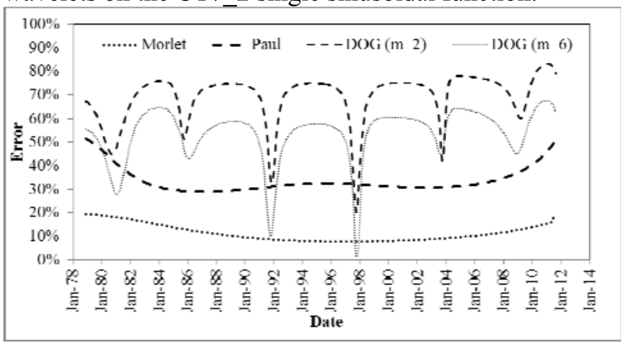

Fig 3. Percentage errors of the periodicities at the peak in comparison to the periodicity of the single sinusoidal function.

Wavelet transforms on detrended groundwater time series

The wavelet power spectrum at the observation well CT7_2 is shown in Fig. 4. The wavelet power spectrum reveals essentially the time-frequency distribution of waves with certain periods (or frequency) over time. The waves with dominant frequencies can describe the mean behavior of the subsurface system and the important recurring patterns of the series.

The wavelet power spectrum has the highest peak established around the 10-year periodicity between the 1980s and the 2000s. This can be assumed relatively stationary even though the peak range does not appear in the beginning and end of recording time period. The discontinuity of this periodic peak in time may stem from the analytical method itself, which is sometimes called the effect of the cone of influence. The cone of influence (COI) is the region of the wavelet spectrum in which the edge effects become significant. Hence, the edges (beginning and end) of the wavelet power spectrum are to be excluded from the analysis.

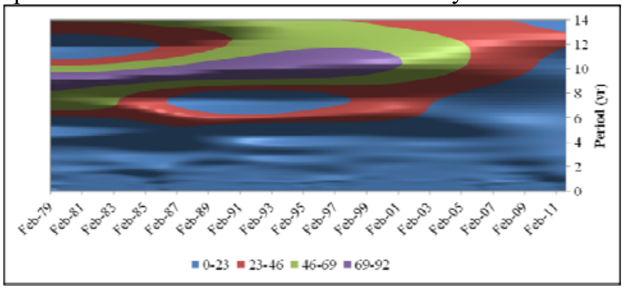

Fig 4. Power spectrum from the Morlet wavelet on the CT7_2 groundwater time series.

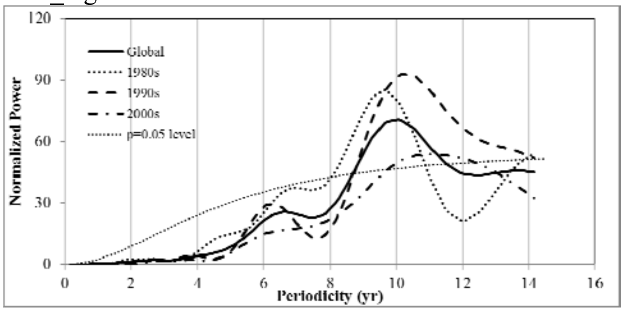

Fig 5. Global and local power wavelet spectrums of the CT7_2 groundwater time series.

Then, the decadal phase change of groundwater behavior is also assessed on the wavelet power spectrum. In order to compare different wavelet power spectrums, a normalized power spectrum is necessary and is defined by $|W_n(s)|^2/\sigma^2$. The normalization by $1/\sigma^2$ gives a measure of the power relative to white noise. The normalized power spectrums of four eras are computed and compared, and these wavelets are for the eras of global, the 1980s, 1990s, and 2000s. Fig. 5 compares the four localized wavelets with a p=0.05 wavelet spectrum line for the observation at CT7_2. The areas in the groundwater wavelet spectrum graphs that are higher than the p=0.05 background spectrum are identified as the true periods of the groundwater oscillations. In general, the groundwater is relatively time-invariant, which means that the groundwater fluctuation in each era or time span preserves the signals with the same frequency and amplitude. The highest peak of the power spectrum occurs at the long term periodicity and is higher than the p=0.05 significance level, indicating that the groundwater is under the strong influence of the low frequency or long period per cycle fluctuation. Note that a lower peak appears at the intermediate periodicity around 4 to 7 years of the power spectrum. This intermediate periodicity might also be a true feature of groundwater oscillation even though the height of this low peak is slightly lower than the p=0.05 significance level corresponding to the 95% confidence interval. This may be due to the width of the wavelet filter in Fourier space. At small wavelet scales (high frequency), the wavelet is very broad in frequency; therefore any peaks in the spectrum get smoothed out. Since the two peaks of spectrum ascend around and above the computed background spectrum, these long-term and intermediate periodicities can be portrayed as the true major cycles of the groundwater time series.

The intermediate periodic signal with a 4-to-9-year cycle has less influence on the groundwater in the 1990s than in the 1980s and the current groundwater. On the other hand, the pressure from the long term 9-to-13-year periodic variability governs the groundwater fluctuation, and the influence on the groundwater is slightly higher in the 1990s than in the 1980s and 2000s. The short-term fluctuation cannot be detected on the groundwater wavelet spectrum at any time period. However, as previously mentioned, the difference of the periodic wave compositions in time is not notably striking, showing relative stationarity of the groundwater regardless of the anthropogenic effects which are excluded by detrending the original time series. Long term monitoring and recording are very crucial for future proof of the variability trend in time.

Wavelet transforms on climate indices

The wavelet transform with the Morlet mother wavelet is performed on eight climatic indices that represent three well-known climate variability forces influencing the weather in the region. These climatic forces are Asian summer monsoons, IOD and ENSO. In general, SST-Nino4, an ENSO index, presents two major modes: intermediate and long-term variability. The intermediate variability is composed of periodic waves of approximately 4-6 years per cycle, and the long-term variability is composed of periodic waves of approximately 10-13 years per cycle. It is obvious that IOD has fluctuated only in a range of short to medium periodicity, i.e. in the range of 2 to 8 years. This fluctuation is however relatively variant with time. The influence of Asian summer monsoons is studied using two indices: IMI and WNPMI. The index reveals the multiple and non-stationary periodic modes.

Linkage between groundwater and climatic signals

The groundwater global wavelet spectrum is linked to the global wavelet power spectrums of the eight climatic indices using the simple Pearson Correlation Analysis. The result is presented in Table 1. The overall groundwater periodic behavior could be associated with several climatic indices, i.e. ENSO through ORL, NN4, and SOI, IOD through DMI, and the summer monsoons through IMI. The strength and periodicities of NN4 and SOI well match those of groundwater, and this high correlation suggests that the groundwater fluctuation generally corresponds to the NN4 and SOI climate variability, which represent the force from ENSO. In conclusion, the overall fluctuation of the deep groundwater in the Lower Chao Phraya Basin is conclusively associated with the climate variability, i.e. ENSO and Asian summer monsoons, but little can be said with regard to its association with IOD. However, ENSO shows a higher correlation to the groundwater behavior than the other two forces.

Table 1: Correlation between global wavelets of groundwater and climatic indices.

Indices	ORL	NN4	SOI	DMI	IMI
CT7_2	0.68	0.77	0.75	-0.55	0.71

Summary

The demand for and stress on groundwater have both been on the increase and will be amplified in the future due to the need to counterbalance the declines and uncertainty in surface water availability from sparing precipitation and climate change. Nevertheless, little is known about the direct impact of climate variability on the groundwater resource itself, particularly deep groundwater, which is believed to be the most resilient and dependable water resource.

The groundwater level measured at an observation well in the Lower Chao Phraya Basin is highly influenced by abstraction as shown in Seeboonruang (2014). Through the wavelet analysis on the detrended groundwater residuals, no short periodicity or high frequency of the deep groundwater was identified as anticipated probably because the frequency is likely to be dampened and filtered as the signals pass through soil, unsaturated and saturated zones of the aquifers. This yields the beneficially excellent buffer properties that provide resilience to water resources and associated ecosystems under short-term and high frequency climate extremes. However, larger-scale climate oscillations with long periodicity, such as ENSO, are likely to affect recharge and mechanisms in aquifers, and the response of groundwater to the long periodic climate oscillations can be detected as reported in this paper. Relatively stationary groundwater oscillations with the intermediate and long periodicities are established in the deep groundwater signals, and their periodic signals are significantly coherent with the climate variability, i.e. ENSO and Asian summer monsoons, in this region.

Acknowledgement

This research "Quantitative Analysis of Impacts of Climate Variability on Deep Groundwater Signals in an Intense Groundwater Pumpage Area" has been fully financially supported by 2015 TRF Research Career Development Grant. Special gratitude is paid to all research assistants and colleagues in the Department of Civil Engineering, KMITL.

References

Fye, F.K., Stahle, D.W., Cook, E.R., and Cleavel, M.K. 2006. NAO influence on sub-decadal moisture variability over central North America. Geophysical Research Letters, 33: L15707.

Green, T.R., Taniguchi, M., Kooi, H., Gurdak, J.J., Allen, D.M., Hiscock, K.M., Treidel, H. and Aureli, A. 2011. Beneath the surface of global change: Impacts of climate change on groundwater. Paper 851. USDA-ARS/UNL Faculty.

Gurdak, J.J., Randall, T.H., McMahon, P.B., Bruce, B.W., McCray, J.E., Thyne, G.D., Thyne, G.D. and Reedy, R.C. 2007. Climate variability controls on unsaturated water and chemical movement, High Plains Aquifers, USA. Vadose Zone Journal**,** 6: 533-547.

Hammer, O., Harper, D.A.T. and Ryan, P.D. 2001. PAST: Paleontological Statistics Software Package for Education and Data Analysis. Paleontologia Electronica, 4(1):1-9.

Hanson, R.T., Newhouse, M.W. and Dettinger, M.D. 2004. A methodology to assess relations between climatic variability and variations in hydrologic time series in the southwestern United States. Journal of Hydrology, 287: 252-269.

Intergovernmental Panel on Climate Change (IPCC). 2007. Climate Change 2007 – Impacts, adaptation and vulnerability working group II contribution to the Fourth Assessment Report of the IPCC.

Kerr R.A. 2000. A north Atlantic climate pacemaker for the centuries. Science, 288(5473): 1984-1986.

Limsakul, A., Limjirakan, S. and Suthamanuswong, B. 2007. Spatio-temporal changes in total annual rainfall and the annual number of rainy days in Thailand. Journal Environmental Research, 29 (2): 1-21.

Limsakul, A. and Goes, J. 2008. Empirical evidence for interannual and longer period variability in Thailand surface air temperature. Journal Atmospheric Research, 87: 89-102.

Mantua N.J., and Steven R.H. 2002. The Pacific Decadal Oscillation. Journal of Oceanography, 58: 35-44.

Minobe, S. 1997. A 50-70 year climatic oscillation over the North Pacific and North America. Geophysical Research Letters, 24: 683-686.

Moortel I., Munday S.A. and Hood A.W. 2004. Wavelet analysis: the effect of varying basic wavelet parameters. Solar Physics, 222(2): 203–228.

Seeboonruang U. 2014. An empirical decomposition of deep groundwater time series and possible link to climate variability. Global NEST Journal, 16(1): 87-103.

Torrence C. and Compo P.G. 1997. A practical guide to wavelet analysis. Bulletin of the American Meteorological Society, 79(1): 61-78.

THA 2015 International Conference on
"Climate Change and Water & Environmental Management in Monsoon Asia"
28-30 January 2015, Bangkok, Thailand.

Improvement of a Kinematic Wave-based Distributed Hydrologic Model to Predict Flow Regimes in Arid Areas

Tomohiro TANAKA[1*], Soe THIHA[2] , Yasuto TACHIKAWA[3] and Kazuaki YOROZU[4]

Abstract. To predict river discharge for Japanese river basins surrounded by the mountainous terrain, many studies have applied distributed hydrologic models based on a kinematic wave approximation with surface and subsurface flow components (DHM-KWSS). These models reproduce observed river discharge of catchments in Japan well; however, the applicability of DHM-KWSS to catchments with different geographical or climatic conditions has not been sufficiently examined.

This study applied 1K-DHM, which is one of distributed hydrologic models having the DHM-KWSS structure, to two rivers basins. One is characterized by relatively stable rainfall throughout the year, which is a similar climatic condition in Japanese river basins; another is located in an arid area climatically different from river basins in Japan. To examine the applicability of the DHM-KWSS model structure for basins with different climate and topography, model parameters were calibrated, and then the calibrated model was validated for other periods.

Our results showed that the model structure of the DHM-KWSS expresses flow regimes with wet conditions as well as main flood events in arid basins. On the other hand, this model structure cannot describe flow behavior in arid areas. One of the difficulties in the current model structure is a low predictability of flash floods at the beginning of rainy season. Therefore, we added one component to express the change in vertical infiltration due to dynamics of soil moisture into the model structure to improve reproducibility of flow regimes in arid areas. The performance of the improved model is demonstrated for two arid basins in Australia and Myanmar.

Keywords: *Distributed rainfall-runoff models, vertical infiltration, the Ayeyarwady river basin, arid basin, kinematic wave model*

Tomohiro Tanaka
Graduate School of Engineering, Kyoto University, Kyoto Japan.
tanaka@hywr.kuciv.kyoto-u.ac.jp
Soe Thiha
Graduate School of Engineering, Kyoto University, Kyoto Japan
thiha@hywr.kuciv.kyoto-u.ac.jp
Yasuto Tacikawa
Graduate School of Engineering, Kyoto University, Kyoto Japan
tachikawa@hywr.kuciv.kyoto-u.ac.jp
Kazuaki Yorozu
Graduate School of Engineering, Kyoto University, Kyoto Japan.
yorozu@hywr.kuciv.kyoto-u.ac.jp

SENSITIVITY OF SNOW COVERED AREA OF BRAHMAPUTRA RIVER BASIN TO TEMPERATURE

Abstract Due to climate change, glaciers in many parts of the Himalaya have undergone significant retreat which in turn leads to increase in discharge of the Himalayan Rivers. River Brahmaputra is originated from the Himalayas and many parts of the Brahmaputra River Basin is covered by snow and glaciers. In this paper, an attempt has been made to study how the snow cover area of the Brahmaputra River Basin changes with respect to the change in temperature. For this, MODIS image MOD09A1.5 (MODIS/Terra Surface Reflectance 8-Day L3 Global 500m SIN Grid) of 500m resolution consisting of seven bands has been taken to prepare the Normalized Difference Snow Index Maps of the study area. The NDSI map is then used to obtain the areal extent of snow in the Brahmaputra River Basin. The NDSI maps are prepared starting from 2002 to 2012 for three different months, i.e. January, April and October. For, temperature data, HadCM3 data of spatial resolution 2.5˚ × 3.75˚ (latitude by longitude) has been used. From the study, it is observed that, except for the month of January, for other two months, there is a decreasing trend of snow cover area with an increasing trend of temperature.

Key words: Snow cover area, remote sensing, GCM, Brahmaputra, NDSI.

Introduction

The River Brahmaputra is expected to be much vulnerable to climate change because of substantial contribution from snow and glaciers (Singh et al., 1997a; Singh and Jain, 2002). During winter, a large extent of mountainous area of Himalayan river basins is covered by snow which starts ablating in the spring due to rise in temperature. IPCC (2001a) has indicated that the average global surface air temperature has increased by 0.6 ±0.2°C since the late 19th century and it is projected to increase by 1.4–5.8° C over the period 1990–2100.
Mountain glaciers are used to detect and monitor local climate change in regions not typically monitored by instrumentation, as they are considered to be sensitive indicators of climate (Haeberli et al., 2007). Due to the large extent and difficult accessibility of high mountainous terrain, remote-sensing techniques provide an efficient way to collect data in such regions. Identification of snow cover using only the visible reflected light may be difficult because many things appear as white, such as clouds or even rocks. However, comparing the reflectance of other wavelength, such as infrared, it is possible to differentiate snow from clouds. Snow reflectance is high in the visible (0.5–0.7 μm) wavelengths and has low reflectance in the shortwave infrared (1–4 μm) wavelengths (Nolin and Liang, 2000) which enables to distinguish snow from clouds and other non- snow-covered conditions. Use of the ratio of a short-wave IR channel to a visible channel was determined by Kyle et al., (1978). This method is known as Normalize Difference Snow Index (NDSI) method. Moderate-Resolution Imaging Spectroradiometer (MODIS) imageries have successfully been applied in monitoring snow cover using the NDSI. Relative to similar sensors such as the Advanced Very High Resolution Radiometer (AVHRR), the MODIS sensor offers some significant advantages. For example, the MODIS provides observations at a nominal spatial resolution of 500-m versus the 1.1-km spatial resolution of the AVHRR. MODIS's data are available continuously (spatially and temporally) and has also several spectral band observations that span the visible and short-wave infrared wavelengths, useful for distinguishing the extent of snow cover (Salomonson and Appel, 2004).
The impact of climate change at regional scale can be studied effectively by the General Circulation Models (GCM), which describes the atmospheric process by mathematical equations. There is considerable confidence in global climate model simulations mainly because GCM principles are based on well established fundamental laws of physics such as conservation of mass, energy and momentum (Pitmans and Perkins, 2008). GCMs simulate temperature better than rainfall and therefore there is more confidence in predictions of temperature than rainfall (Masanganise et al., 2013). McMahon et al., (2014) in their study have found that the monthly pattern of temperature is generally well reproduced by the GCMs compared to the monthly pattern of precipitation. They also concluded that along with few other GCMs, HadCM3 is also a better performing GCM.
Most of the upper parts of the Brahmaputra catchment is covered by Himalayan snow. In this paper, the temperature factor has been taken into account to study its impact on the change in snow cover area of the Brahmaputra river basin.

Study Area

The Brahmaputra river basin that lies between the coordinates 23.9˚N to 31.5˚N latitude and 82.1˚E to 97.7˚E longitude is considered in this study. To determine the variation in temperature, the upper

Brahmaputra basin has been considered which is mainly responsible for the fluctuations in snow cover area. The drainage area of the Brahmaputra River is approximately 580,000 sq.km.

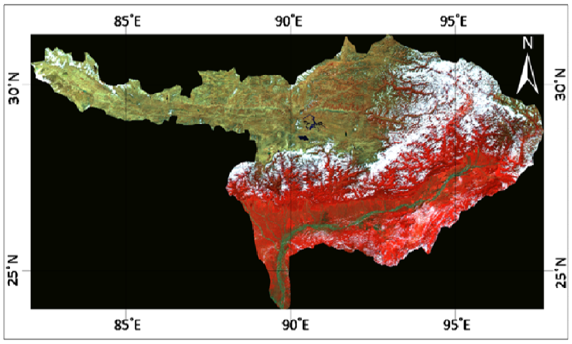

Fig.1 False Color Composite image of the Brahmaputra River Basin prepared from MODIS data.

Methodology

Data used

The variation of snow cover area in the Brahmaputra river basin has been studied using the MODIS image, MOD09A1.5 (MODIS/Terra Surface Reflectance 8-Day L3 Global 500m SIN Grid) of 500m resolution consisting of seven bands (band-1 to band-7). The climate change scenario data used in this study are based on simulations carried out using General Circulation Models (GCMs) for the Fourth Assessment Report (AR4) of the Intergovernmental Panel on Climate Change (IPCC, 2007). The gridded temperature data of HadCM3 (Hadley center Coupled Model version 3) model of A2 scenario having spatial resolution of 2.5˚ × 3.75˚ (latitude by longitude) were used to get the average temperature of the upper portion of the Brahmaputra River basin. A2 scenario considers the forcing effect of greenhouse gases and sulphate aerosol direct effect, which are based on IPCC SRES-A2 (Special Report of Emission Scenario A2). HadCM3 model was selected since it has the highest 'skill scores' for both precipitation and temperature of all the models used for the AR4 (Cai et al., 2009). Mavromatis and Jones (1999) evaluated precipitation and near surface air temperature in two successive versions of the Hadley Centre General Circulation Model (GCM) to consider to what extent GCMs are capable of simulating the mean and variability of local climates. Their conclusion was positive towards direct use of raw data of HadCM2. Taking the accuracy of GCMs' temperature data as the ground, in this paper, we have used directly the HadCM3 temperature data to study its impact on snowmelt of the Brahmaputra river basin. There were a total of fifteen HadCM3 points that fall in and around the upper catchment. Fig.2 shows the HadCM3 GCM points considered for temperature evaluation.

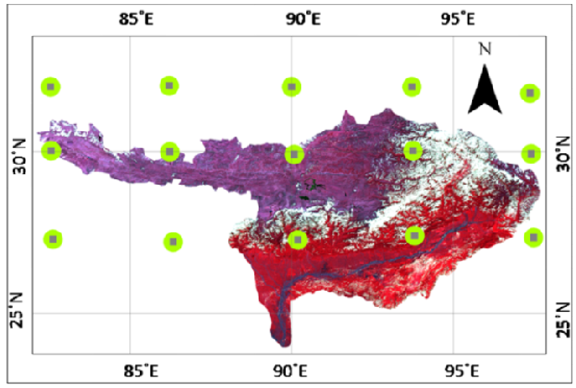

Fig.2 Map showing the HadCM3 points in and around the upper Brahmaputra basin taken to evaluate average temperature.

Normalized Difference Snow Index (NDSI)

NDSI method is generally used for snow cover mapping using satellite data (Hall et al., 1995, 2002, Kulkarni et al., 2002, 2006). NDSI uses the high and low reflectance of snow in visible (Green) and shortwave infrared (SWIR) region respectively. Additionally, the reflectance of clouds remains high in SWIR band, thus NDSI allows in discriminating snow and clouds. NDSI ranges from -1 to +1 and is defined by the following relation:

$$NDSI = \frac{Green - SWIR}{Green + SWIR}$$

Where, Green and SWIR are the reflectance of the green and shortwave infrared bands respectively. Snow has a high reflectance in band-4 (0.545-0.565µm, visible green) and a low reflectance in band-6 (1.628-1.652µm, shortwave near infrared) of the MODIS instrument. A threshold value of NDSI of 0.4 is defined for the pixels that are approximately 50% or greater covered by snow from imageries of different sensors (Xiao et al., 2001). However, identification of snow covered areas using NDSI is difficult if snow covered areas are mixed with vegetation (Hall et al., 1998). Distinguishing snow from other non-snow features such as water, or dense forests may be difficult because they have similar NDSI readings to snow. To overcome this difficulty it becomes necessary to examine other wavelengths. For this, reflectance in band-2 and band-4 are examined primarily to separate water bodies and forest respectively from snow. It is also important to examine the Normalized Difference Vegetation Index (NDVI) to see if a pixel is snow covered forest.

Preparation of snow map

The Erdas Imagine remote sensing software has been used to prepare the snow map of the study area. The various operations performed were: importing the original *.hdf* format of the image to *.img* format, mosaicing of all the tiles that cover the Brahmaputra river basin, re-projection of image to geographic latitude longitude and WGS84, sub-setting of the mosaiced image to get the shape of the Brahmaputra river basin and finally stacking operation was performed to get the image consisting of seven bands. NDSI method was applied to differentiate between snow and cloud cover of the satellite images. Pixels that are approximately 50% or greater covered by snow have NDSI values of 0.4 (Hall et al., 2002). Hence, a threshold value of 0.4 has been taken for snow (*i.e.* if NDSI > 0.4, then the pixel is snow, else not snow). Two functions were generated to make the numerator and denominator of the NDSI equation. For MODIS data, band-4 represents the green band while band-6 represents the short wave infrared band. If summation of band-4 and band-6 is equal to zero (the denominator), the NDSI was not performed as NDSI value will be infinity. Also, a data value of -28672 was ignored since -28672 is the value of pixels of no data. Again, another function in the model maker was created which considers the pixels having NDSI values of greater than or equal to 0.4 as snow. A total of 33 NDSI images were prepared from 2002 to 2012 for the months of January, April and October.

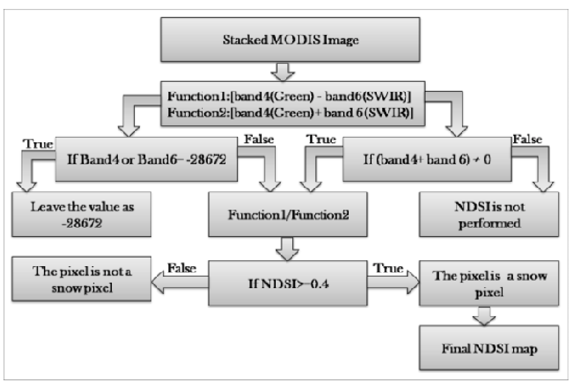

Fig.3 Flowchart for preparation of NDSI map in Erdas Imagine

Since water may also have an NDSI of 0.4, an additional test is necessary to separate snow and water. Snow and water may be discriminated because the reflectance of water is less than 11% in band 2. Hence, if the pixels with reflectance in band-2 (0.841- 0.876 µm) was found to be less than 11% even if the NDSI was greater than or equal to 0.4, was mapped as water. Similarly, for a pixel where the reflectance in band-4 (0.545-0.565 µm) was less than 10% was marked as dark forest (Dozier,1989). To identify the snow covered forests, the NDVI (Normalized Difference Vegetation Index) was examined. If a pixel NDSI value is less than 0.4 (not snow) but the NDVI is approximately 0.1, the pixel could be snow-covered forest (Hall et al., 2002, Klein et al., 1998). MODIS bands-2 (NIR) and band-1 (Red) are used to create NDVI which can be expressed as,

$$NDVI = \frac{MODIS\ band2 - MODIS\ band1}{MODIS\ band2 + MODIS\ band1}$$

In the NDVI model, the following function was added to create snow forest mask:

$$NDVI \geq 0.0\ and\ NDVI < 0.2$$

The created water, forest and NDVI masks were finally applied to the NDSI product to get the final snow map from which the snow cover area can be determined.

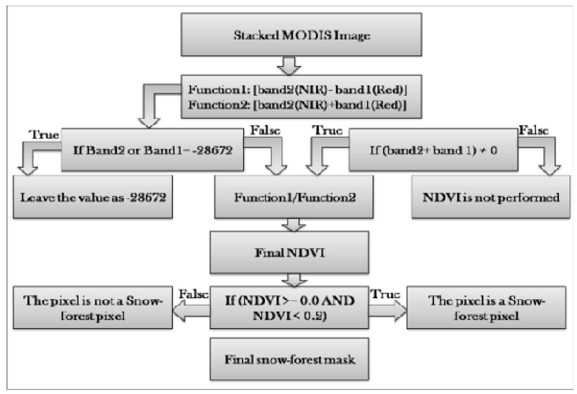

Fig.4 Flowchart for preparation of snow forest mask in Erdas Imagine

Comparison with Landsat data

Cloud free Landsat satellite data (Landsat 4-5 TM) of 30m resolution acquired on April 15, 2010 has been used to validate the snow map prepared from the MODIS image. Two small areas of the MODIS snow map have been compared with the high resolution Landsat data. It has been observed that the portions covered by snow for both the MODIS and Landsat images (shown in red rectangle in the figure) were same. Again, when the area covered by snow for both the MODIS and Landsat images of the selected portions were calculated, the results were almost equivalent. The NDSI map of the Landsat images were prepared by considering Band-2 (Green) and Band-5 (Short-wave Infrared). For the first portion [Fig.5(a)], the area covered by snow in the MODIS image (LHS) was found to be 6012.25 sq. km., while for the Landsat image (RHS) on the same date, it was 6245.65sq. km. Again, for the other segment [Fig.5(b)], the snow cover area in the MODIS image (LHS) was found to be 8393.25 sq.km., while for the Landsat snow map(RHS), it was 8562.25 sq.km.. As the snow cover area for both Landsat and MODIS images were found to be almost equal, the MODIS images can be used for studying the snow cover area variation in the present study.

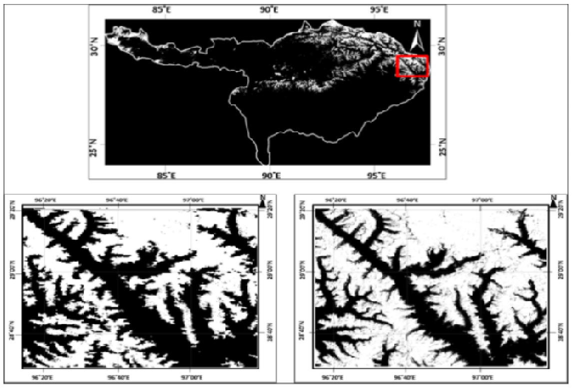

Fig.5(a) Snow cover map of MODIS (LHS) and Landsat (RHS) image for first portion.

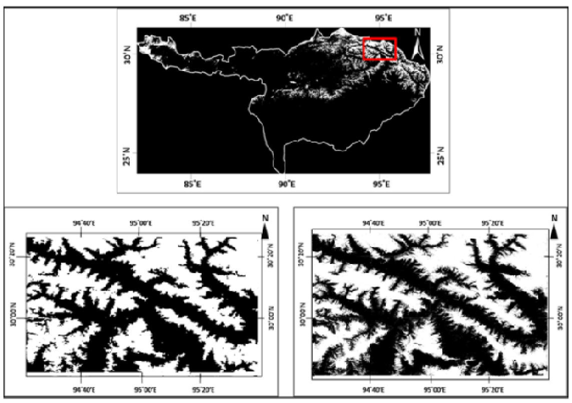

Fig.5(b) Snow cover map of MODIS (LHS) and Landsat (RHS) image for second portion.

Results and Discussion

The snow cover maps for January, April and October from 2002 to 2012 have been prepared in the Erdas Imagine software using the methodology discussed above. In Fig.6, the white pixels show the snow cover area while black pixels show the non-snow area.

The total area covered by snow for each image as well as the temperature data of HadCM3 for A2 scenario are given in the table 1.

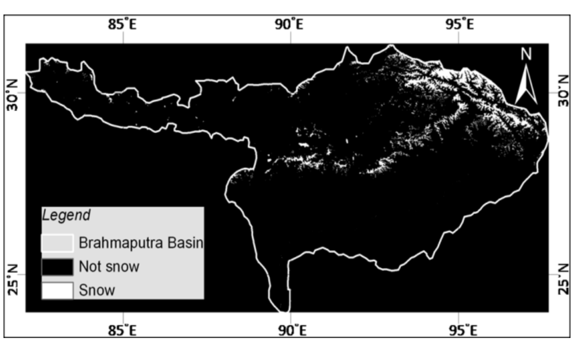

Fig.6 Final map showing Snow Cover Area of Brahmaputra River Basin.

The maximum snow cover area has been observed in 2012 for the month of January with a value of 138555 sq. km. and the minimum has been observed in 2007 for the month of October with a value of 12347 sq.km. The maximum temperature for the entire period from 2002 to 2012 has been observed in 2011 for the month of October (1.43˚C) and the minimum has been observed in 2009 for the month of January (-15.55˚C). Taking the maximum snow cover value as the base, when a percentage reduction graph was plotted from 2002 to 2012, the resulting trend showed an increasing order (Fig.7). It gives an idea about how the snowmelt is increasing year by year and that snowmelt water in turn gives rise to huge discharge at the downstream of the river.

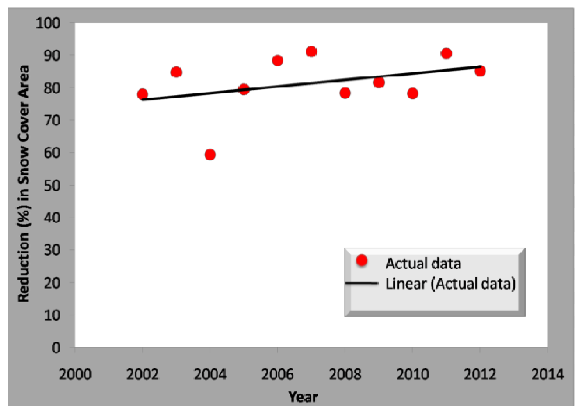

Fig.7 Percentage reduction in snow cover areas from 2002 to 2012.

The increasing and decreasing trend of snow cover area with respect to the change in temperature for all the three months from 2002 to 2012 are shown in Fig.8 (a, b and c). The results clearly display that the values of temperature taken from the GCM (HadCM3 A2 scenario) for the aforesaid months are increasing gradually from 2002 to 2012 which can be attributed to the fact of global warming. While building a relationship between the snow cover area and temperature data, it has been observed that for the month of January, the snow cover area is in an increasing trend with respect to the increasing trend of temperature. This can be attributed to the fact that a little increase in temperature at sub-freezing point may hardly effect the melting of snow. The minimum snow cover during this period was in the year 2008 with a value of 29822 square kilometer and the maximum was in the year 2012 with a value of 138555 square kilometer. While the minimum temperature was in the year 2009 (-15.55 ˚C) and maximum was in the year 2008 (-10.20 ˚C). For the entire study period from 2002 to 2012, the effect of temperature on snow melt was found to be the maximum in 2008.

Table 1: Snow Cover Area and temperature for different months

Year	January		April		October	
	Snow Cover Area (sq.km)	Temperature (˚C)	Snow Cover Area (sq.km)	Temperature (˚C)	Snow Cover Area (sq.km)	Temperature (˚C)
2002	30474	-14.92	114588	-2.70	84551	-0.67
2003	98414	-12.26	99972	-1.62	21069	-1.05
2004	64472	-14.22	56236	-1.09	63894	0.93
2005	74004	-11.66	83658	-0.92	28355	-0.28
2006	37285	-13.87	80162	-3.81	16157	-2.28
2007	49892	-14.43	87833	0.81	12347	1.12
2008	29822	-10.20	92263	0.16	32572	-2.00
2009	112736	-15.55	89539	-1.74	25427	1.38
2010	66618	-11.43	68848	-0.03	30162	-3.25
2011	62421	-12.88	74142	-1.69	13129	1.43
2012	138555	-11.65	89930	-0.82	20526	0.25

For the other two months *i.e.* April and October, the results plotted in graphs [Fig. 8(b) and (c)] show a positive correlation between increase in temperature and decrease in snow cover. Maximum changes have been observed in the month of October. For the month of April, minimum snow cover was observed in the year 2004 (56236 sq. km.) and maximum was observed in the year 2002 (114588sq. km.). For the month of October, the minimum was observed in the year 2007 (12347sq. km.) and the maximum was observed in the year 2002 (84551sq. km.). In case of temperature, the minimum in the month of April was observed in the year 2006(-3.81 ˚C) and maximum was observed in the year 2007 (0.81 ˚C). On the other hand, for the month of October, the minimum temperature was observed in the year 2002 (-0.67 ˚C) and maximum was observed in the year 2011 (1.43˚C). Apart from the role of temperature, other factors should also be taken into account to explain the reason behind the difference in snow melt trend of the other two months from that of January. For example, if the snow is older, its albedo will be lower and in such situation it absorbs more solar radiation. Again, if the temperature variation is not significant, snow melts faster in the windy condition than in the calm conditions.

Melting of snow with respect to the rise in temperature has a major impact on the hydrology of the rivers. Brahmaputra, the major river of the study area, is responsible for many natural calamities among which flood and erosion are the severe ones. Along with the heavy rainfall, the melting of snow at the origin of the river also has a major effect on change in its discharge. In mountain region particularly, global mean temperature has not been spatially homogeneous. A minor variation in temperature under low magnitude warming is more effective to changes in volume and area of glacier than high magnitude warming.

Conclusion

From this study, it has been seen that MODIS data can efficiently be used in mapping snow cover of large areas, because of its good spatial as well as temporal resolution relative to similar sensors such as AVHRR. Since snow reflects more energy in the visible part than in the mid-infrared, the NDSI ratio enhances the contrast between snow and bare ground. Additionally, the reflectance of clouds remains high in MODIS band-6. Thus, the NDSI can discriminate clouds and snow.

MODIS snow map prepared by the method of NDSI was found to be accurate while comparing with the high resolution LANDSAT data of same date. In both the images, the area covered by snow for the selected portions were found to be the same. In this study, an attempt has been made to correlate change in snow cover area with the change in temperature. It is found that except for the month of January, the snow cover area for other two months *i.e.* April and October show a decreasing trend with increase in temperature.

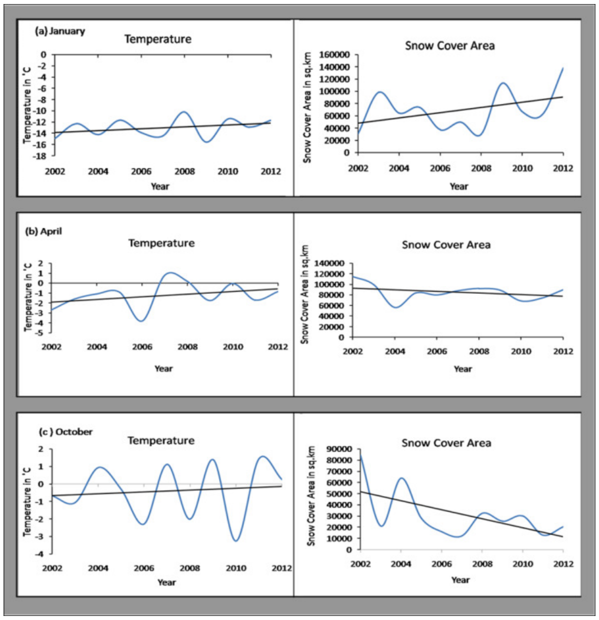

Fig.8 Trend showing variation of snow cover area w.r.t temperature for the month of (a) January, (b) April, and (c) October from 2002 to 2012.

References

Haeberli, W., Hoelzle, M., Paul, F., Zemp, M. (2007). Integrated monitoring of mountain glaciers as key indicators of global climate change: The European Alps. Annals of Glaciology: 46, 150-160.

Hall, D.K., Foster, J.L., Verbyla, D.L., Klein, A.G. and Benson, C.S. (1998). Assessment of snow-cover mapping accuracy in a variety of vegetation-cover densities in central Alaska. Remote Sens. Environ.: 66, 129–137.

Hall, D.K., Riggs, G. A. and Salomonson, V.V. (1995). Development of methods for mapping global snow cover using moderate resolution imaging spectroradiometer data. Remote Sens. Environ.: 54, 127–140.

Hall, D.K., Riggs, G.A., Salomonson, V. V., DiGirolamo,N. and Bayr, K. J.(2002). MODIS snow cover products. Remote Sens. Environ.,: 83,181–194.

Kulkarni, A.V., Singh,S. K., Mathur, P. and Mishra, V.D.(2006). Algorithm to monitor snow cover using AWiFS data of RESOURCESAT-1 for the Himalayan region." Int. J. Remote Sens.:27, 2449–2457.

Kulkarni, A.V., Srinivasulu, J., Manjul, S.S. and Mathur, P. 2(002b). Field based spectral reflectance to develop NDSI method for the snow cover. J. Indian Soc. Remote Sens.:.30, 73–80.

Kyle, H.L., Curran, R.J., Barnes, W.L. and Escoe, D. (1978). A cloud physics radiometer. Third Conference on Atmospheric Radiation, Davis, CA, 107-109.

Masanganise, J., Chipindu, B., Mhizha, T., Mashonjowa, E. and Basira, K. (2013). An evaluation of the performances of Global Climate Models (GCMs) for predicting temperature and rainfall in Zimbabwe. International Journal of Scientific and Research Publications: 3, 1-11.

Mavromatis, T. and Jones, P.D. (1999). Evaluation of HadCM2 and Direct Use of Daily GCM Data in Impact Assessment Studies. Climate Change:. 41, 583-614.

McMahon, T.A., Peel, M.C. and Karoly, D.J. (2004). Uncertainty in runoff based on Global Climate Model precipitation and temperature data- Part1: Assessment of Global Climate Models. Hydrol. Earth Syst. Sci. Discuss: 11, 4531-4578.

Nash, J.E. and Sutcliffe, J.V. (1970). River flow forecasting through conceptual models Part1- A discussion of principles. J. Hydrol.: 10, 282-290.

Pitman, A. J. and Perkins, S. E. (2008). Regional Projections of Future Seasonal and Annual Changes in Rainfall and Temperature over Australia Based on Skill-Selected AR4 Models. Earth Interact: 12, 1–50.

Singh, P., Jain, S.K.(2002). Snow and glacier contribution in the satluj river at Bhakra Dam in the Western Himalayan region. Hydrological Sciences Journal: 47, 93-106.

Singh, P., Jain, S.K., Kumar, N.(1997a). Snow and Glacier melt runoff contribution in the Chenab river at Akhnoor. Mountain Research Development:17,49-56.

Xiao, X., Shen, Z. and Qin, X.(2001). Assessing the potential of VEGETATION sensor data for mapping snow and ice cover: A normalized difference snow and ice index. Int. J. Remote Sens.: 22, 2479–2487.

Estimation of urban asset value for natural disaster risk assessment at the macro scale

Tiratas Suwathep[1, a *], Wee Ho Lim[1,b *], Yoshihiko Iseri[1,c] and Shinjiro Kanae[1,d]

Abstract. Natural disasters (e.g., flood, tropical cyclone, bushfire and earthquake) could cause damaging effect on the human society. To understand the magnitude of risk of a natural disaster at the macro scale (i.e., at the country level and beyond), basic socioeconomic parameters such as population or gross domestic product (GDP) are often used as proxy. Ideally, we would have enough information to evaluate the exposure and risk of a specific asset. However, such information is not always available. To that end, previous study (Hallegatte et al., 2013) demonstrated the prospects of relating the country GDP data to the produced capita (a term representing the urban asset class). That analysis used the market exchange rate (MER) instead of the purchasing power parity (PPP) to measure GDP, which is an important issue in examination of costs of policies in climate debate (Manne et al., 2005). This study aims to consider the PPP-based analysis of country GDP data to produced capita. We introduce a mathematical approach to quantify the statistically-justified range of uncertainty in our analysis. From that, we develop a more generalized method that incorporates the uncertainty range to quantify the produced capita. This is an improvement from previous studies (Hallegatte et al., 2013, Winsemius et al., 2013, Nicholls et al., 2008). The new approach might be useful for macro scale natural disaster risk assessment under climate change.

Keywords: *natural disaster, risk, socioeconomic, produced capita, GDP*

Tiratas Suwathep, Wee Ho Lim, Yoshihiko Iseri and Shinjiro Kanae
Tokyo Institute of Technology, 2-12-1-M1-6 O-okayama, Meguro-ku, Tokyo 152-8552, Japan
suwathep.t.aa@m.titech.ac.jp
lim.w.aa@m.titech.ac.jp
iseri.y.aa@m.titech.ac.jp
kanae@cv.titech.ac.jp

Water quality and hydraulic performance of the HMGDS Drainage Module.

Nor Amirah A.S[1]., Abustan, I[2]., Salwa M. Z. M[3]., Remy Rozainy M. A. Z[4] ., Mahyun A.W[5]

Abstract This paper discuss the new system of storm-water best management practice (BMPs) used extensively to reduce the peak flow of surface runoff and to remove runoff pollutant by infiltration as well as enhance the amenity value of water for both quality and quantity of groundwater discharge. Storm-water problem have become severe due to increase in urbanization. The increase in the amount of impermeable surface areas produces more storm-water runoff that is carried along to the receiving bodies of water which significantly will degrade the water quality in streams. The development of new urban storm-water drainage called Hexagonal Modular Green Drainage System (HMGDS) applied as drainage module when a series of hexagonal connect on a base grade system. A new drainage module is overlaid by a layer of porous media disclosed which capable of filtration whereas enhance the quantity and quality of the receiving water bodies. A laboratory experiment were conducted to test the infiltration rate and volume of surface runoff which HMGDS can captured through a series of rainfall events, furthermore for the water quality analysis the contaminated water seeping through module were investigated. As a result, the introduction of the new drainage module can handle excessive runoff and improved the filtration rate in higher flow condition. In laboratory testing, the prototype HMGDS was capable of achieving good infiltration rate efficiency over 80 % as well.

Keyword *Drainage module, storm-water management, rainfall-runoff, infiltration*

[1]PhD Candidates, School of Civil Engineering, Universiti Sains Malaysia (USM), Engineering Campus, 14300 Nibong Tebal, Pulau Pinang, Malaysia, naashamira@yahoo.com
[2]Professor , School of Civil Engineering, Universiti Sains Malaysia , Engineering Campus, 14300 Nibong Tebal, Pulau Pinang, Malaysia and Visiting Professor King Saud University, Kingdom of Saudi Arabia
[3,5]Lecturer, School of Environmental Engineering, Universiti Malaysia Perlis 02600 Arau, Perlis, Malaysia
[4]Lecturer, School of Civil Engineering, Universiti Sains Malaysia Engineering Campus, 14300 Nibong Tebal, Pulau Pinang, Malaysia

Introduction

In 2030 level of urbanization is expected to rise to 83% in Malaysia and storm water issues have gotten to be serious because of increment in urbanization. Walsh (2000) stated that urbanization will prompt storm water runoff bringing about expanded flooding whilst increase filtration and in addition increase metal sediment (Sansalone and Buchberger, 1997; Zanders, 2005). Urbanization influence the hydrology of a catchment, expanded storm water runoff volumes, anticipating infiltration and as well as reducing evapotranspiration, Expanded peak flood discharges owing to an increment in urban drainage contamination of catchment discharges, due to increment in erosive. Increase in impermeable surface area because of increase in storm water runoff that is conveyed along to the waterways which fundamentally will degrade the water quality in streams. Aisling et al., (2015) stated that a few methodologies have been used comprehensively to mitigate storm water. All the more as of late, there has been expanded focus on avoiding stormwater runoff such source control through green infrastructure. It was well known that Infiltration systems are one such structural stormwater management technique that is widely used, particularly throughout Europe (e.g. Barraud et al., 2002; Le Coustumer and Barraud, 2007) and Japan (e.g. Fujita, 1997). Argue and Pezzaniti (2005) concluded that infiltration based-systems are one such structural storm water best management practice that are widely used, particularly throughout to reduce storm runoff flow and volume, and to minimise pollution conveyance to receiving waters. Storm water infiltration systems are regularly designed to work for in over 20 years. Given the broad application of storm water invasion systems, the long-term pollutant-trapping performance of infiltration systems is an essential range of research area. Information regarding the spatial distribution of pollutants in infiltration systems will help to assess the risk of contamination of surrounding soil and groundwater, whilst knowledge regarding their temporal performance will inform the effectiveness of such systems in protecting receiving waters from the impacts of urban runoff. This paper presents the findings of a laboratory study that investigated the treatment performance of an infiltration system through the new approach drainage filtration module.

Hexagonal Modular Green Drainage System (HMGDS)

HMGDS is a new approach drainage module design acted as filtration-based system overlaid by a layer of porous media and a layer top of Hexagonal Modular (HM) as shown in Fig 1. Hexagonal Modular (HM) as shown in Fig 2 was arranged as interlocking with one and another from the view of top surface as though a kind of beehive structure. The details and specification of HMGDS component is describe in Table 1.

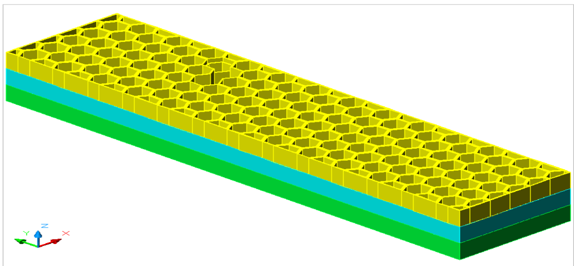

Fig 1: Layout of HMGDS overlaid top by HM and followed by porous media.

Fig 2: Hexagonal Modular Green Drainage (HMGDS)

Table 1: HMGDS Components and its specification

Components	Specifications	Details
HM	Shape	Hexagonal
	Dimensions	Height : 100 mm
		Diameter : 100 mm
		Wall Thickness : 5 mm
	Compressive strength	72 kN
	Material	Polyvinyl chloride (PVC)
Clean River Sand		Mean size between 0.5 to 2.0 mm
Gravel Aggregates		Mean size between 4mm to 20 mm

Methodology

Infiltration rate experiment

The physical model of the permeable drainage module layer was placed in a rectangular flume as shown in Fig. 3. In this new drainage layer module as mentioned before it has three different layers consists of Hexagonal Modular (HM) layer, gravel aggregates and clean sand river. The design of flume was constructed by 0.5 m x 0.5 m. The rainfall simulator with diameter of nozzle is 50 mm was set 1.0 meter over the highest point of drainage module layer to attain to terminal velocity state. A constant rate of rainfall was created with submerged pump however the flow meter can be adjusted by meter gauge. Different rainfall storms of uniform intensities were simulated to test the infiltration rate capacity and surface runoff captured in specified time. Flow rate and total storm water runoff retention was performed manually. The flow rates through the simulator were varied and were 5 L/min, 12.5 L/min, 25 L/min and 40 L/min. Experiment repeated three times for each flow rate to ensure the accurate measurement result taken.

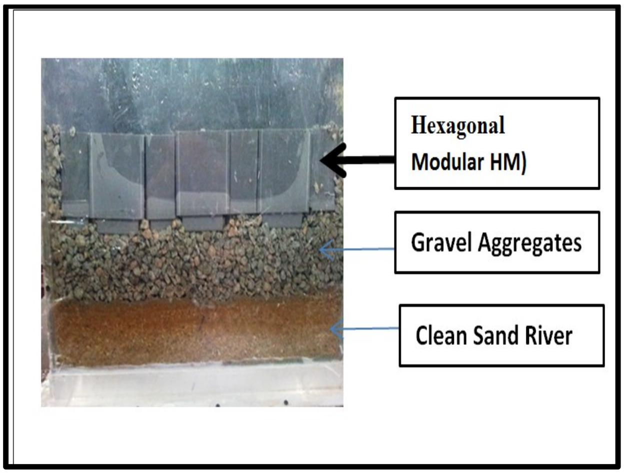

Fig 3: Physical Model of HMGDS

Green and Ampt Infiltration Model

Hillel (1972) explained that the Green and Ampt infiltration model can effectively estimate the infiltration rate and the volume of water infiltrated with time and additionally reported that the model parameters could be acquired by knowing the physical properties of the soil particle size distribution, bulk density and the initial moisture content. The Green and Ampt Infiltration model invasion amended by Mein and Larson (1973) is focused on initially unsaturated soil that accumulates water at the rainfall rate until the surface is fully saturated. Mein (1980) changed the Green and Ampt invasion demonstrate and displayed the expansion of the model and the relationship in the middle of time and the penetration rate as:

$$If\ I \leq Ks \qquad f = I; \quad F \ll Fs \tag{1}$$

$$If\ I > Ks \qquad Fs = \frac{M * Sav}{\frac{1}{Ks} - 1} \tag{2}$$

$$f = fp = Ks\left(1 + \frac{M*Sav}{F}\right) : F > Fs \tag{3}$$

$$Ks(t - ts) = F - (M * Sav)\log e - Fs + (M * Sav) - Fs + (M * Sav)\log e\ (Fs + M * Sav) \tag{4}$$

where

$f = infiltration\ rate\ (mm\ /\ (hr)$

$F = volume\ of\ infiltration\ at\ moment\ of\ surface\ saturation\ (mm)$

$Sav = average\ suction\ at\ wetting\ point$

$Ks = saturated\ hydraulic\ conductivity\ (mm|hr)$

$I = rainfall\ instensity\ ((mm|hr)$

$M = initial\ moisture\ deficit\ (vol|vol)$

$F = volume\ of\ infiltrated\ (mm3)$

$ts = time\ to\ saturation\ Fs = I\ (min)$

$t = time\ since\ start\ of\ the\ event\ ((t > ts)$

Initial Results and Discussion

In order to obtain the infiltration characteristics through the bedding layer and flow through the whole module for each rainfall events, the water flow through the bottom of module layer was collected at 200 sec intervals up to 2000 sec (20 minutes). Table 2 shows the relationship between inflow, outflow and percentage of inflow to outflow at 30 seconds time. Obtained from experiments conducted showed the lowest intensity of 5L/min has the highest level of infiltration of to 92.50%. Respectively for 12.5L / min, 25L / min and 40 L/ min respectively showed the percentage of infiltration within 30 seconds rate were 87.42%, 80.10%, and 77%. HMGDS bedding layer has higher permeability rate based on the results, the time taken to filtrate is very short compared to the conventional infiltration system.

Table 2: Relationship between inflow and outflow percentage

Inflow Rate (L/min)	Outflow rate at the equilibrium (L/min)	Inflow to Outflow at equilibrium (%)
5.0	4.63	92.50
12.5	10.93	87.42
25.0	16.02	80.10
40.0	30.8	77.00

The infiltrated water will first fill the voids in the Hexagonal Modular (HM) first before moving through the base of the system. The volume of water collected at each time interval showed an increments with time until the flow through the modular system is uniform and is in equilibrium. According to Green and Ampt infiltration when the rainfall intensity is lower than the saturated hydraulic conductivity, the infiltration rate (*f*) is equal to the rainfall intensity. For the remains of the rainfall events conducted, rainfall intensities were higher than pressure driven hydraulic conductivity. Fig 4 shows the initial infiltration rate differ with the rainfall intensity. Higher rainfall intensities the higher initial infiltration rate is. When the volume of water infiltrated is equivalent to the volume of water infiltrated at surface saturation, the infiltration rate is found to be independent to the rainfall intensity. The infiltration rate will decrease with the moisture content of the material. The time to saturate additionally fluctuated with the rainfall intensity. Once the bedding layer is fully saturated, the last infiltration rate (infiltration capacity) is just about equal to the saturated hydraulic conductivity and is independent of the rainfall intensity. The volume of infiltrated water increased with rainfall intensities particularly at lower rainfall intensities for 5L/min and 12.5 L/min. At the point when the precipitation intensities were higher than the hydraulic conductivity of the bedding material (Ks=0.145m/hr), the volume of water infiltrated is very nearly the same for all rainfall storms. This presumed that when the rainfall intensity is larger than saturated hydraulic conductivity of the material the volume of water infiltrated varies until the surface saturation. The total volume of water infiltrated is autonomous of the rainfall intensity after the surface is saturated whilst the higher rainfall intensity is expanding the time needed to channel the water. Fig 4 shows an enormous contrast of surface runoff between flow rate of 5L/min and 40L/min at the specific time. Surface water overflow could be said next no and practically nothing on the flow rate 5 L/min contrasted with 40L/min, which requires some time to filtrate the water.

While laboratory scale infiltration test was helpful in understanding the course of actions that occur within a modular layer. Chanel and Doeringv (2007) discovered they are not necessarily completely representative of a field infiltration system. Amount and quantity delivery of flows through the laboratory rig are different from those encountered in the field keeping a constant level, for instance, is not reflective of field conditions. However, these infiltrations help us to comprehend the processes responsible for hydraulic and water quantity behavior, in a way that is not possible to be done by using field monitoring (Abustan et al., 2012).

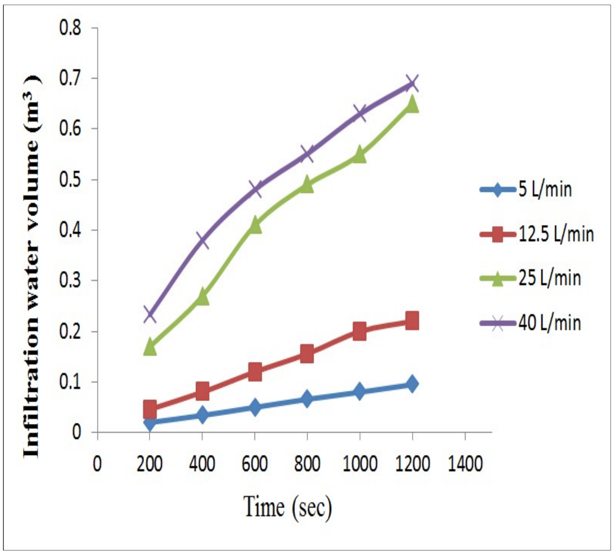

Fig 3: The relationship volume of infiltrated water and time for different storms

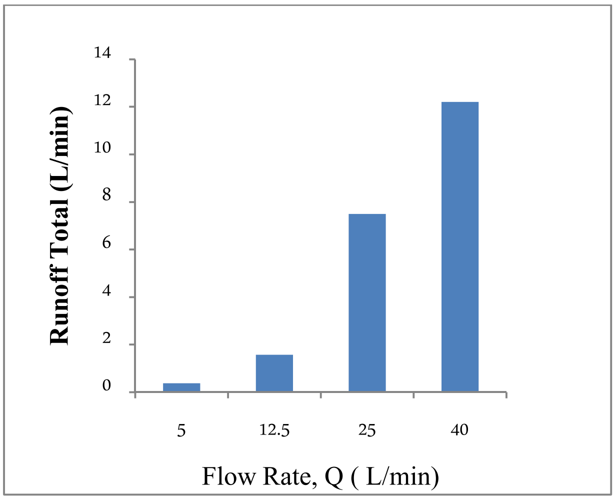

Fig 4: Storm water runoff retention capacity

Summary and Conclusions

Storm water management addresses issues such as controlling flood peaks, managing water quality and in general, managing the water cycle due to urbanization. Substantial research has been carried out to verify the capacity of HMGDS to reduce the amount of storm water quantity. Research had shown an improvement of water quantity runoff reductions by filtration through HMGDS. HMGDS module is another new urban storm water seepage applied as drainage filtration-based module. HMGDS bedding layer has a higher permeability rate based on the results, the time taken to filtrate is very short compared to the conventional infiltration system. The volume of infiltrated water increased with rainfall intensities especially at lower rainfall intensities of 5L/min and 12.5L/min. HMGDS has showed that it can lessen and reduce peak runoff or it could be said just about nothing runoff of the lower flow rate. The effective results acquired from the laboratory studies should be extended to a field based study to better comprehend issues related to scaling. Over the time the infiltration capacity could decrease due to the clogging of gravel filters are an effective treatment option for storm water runoff, where treatment of sediment and heavy metals is of principal concern the bedding material. The improvement to storm water quality should be monitored and modeled if harvested water is used for productive non-potable purposes .Further studies are being planned to investigate the performance of the HMGDS concerning of water quality which perhaps which work well in removing suspended solids and particularly heavy metals.

Acknowledgment

The analysis has been completed at the Hydraulic Laboratory School of Civil Engineering at the Universiti Sains Malaysia (USM) in Nibong Tebal, Pulau Pinang Malaysia. The author would like to acknowledge Universiti Malaysia Perlis (UniMAP) as her sponsors during studies as well as throughout this research.

References

Abustan I., Hamzah M.O., Rashid M.A., (2012b) A 3-dimensional numerical study of a flow within a permeable pavement. OIDA International Journal of Sustainable Development 04: 02(2012), 37-44.

Argue, J.R., and Pezzaniti, D. (2005) Infiltration systems. In: Wong, T.H.F (Ed), Australian Runoff Quality: A Guide to Water Sensitive Urban Design. Engineers Australia, Sydney.

Aisling, D.O., Daniel, W., Tyler, J.H. and Heidi, L.S (2015). Life cycle assessment modeling of stormwater treatment systems. Journal of Environmental Management (2015)149, 236-244.

Barraud, S., Gibert, J., Winiarski, T., Krajewski, J.L-B., (2007) Implementation of a monitoring system to measure impact of stormwater runoff infiltration. Water Sci. Technology. 45 (3), 203-210

Chanel, P.G., and Doering, J.C. (2007) An evaluation of computational fluid dynamics for spillway modelling. In Proceedings of the 16th Australasian Fluid Mechanics Conference (AFMC), Gold Coast, Queensland, Australia, 2007: 1201-1206.

Fujita, S. (1997) Measure to promote stormwater infiltration. Water Sci. Technology 36 (8-9), 289-293.

Hillel D. (1972) Soil and Water: Physical Principles and Process, 140-141.

Le Coustumer., and S., Barraud, S. (2007) Long-term hydraulic and pollution retention performance of infiltration systems. Water Sci. Technology. 55 (4), 235-243

Mein R.G. (1980) Recent developments in modeling of infiltration: Extension of the Green-Ampt Model. *Hydrology and Water Resources Symposium*.

Mein R.G. and Larson C.L. (1973) Modeling infiltration during a steady rain. *Water Resources Research*, Vol 9, No.2, 384-395.

Sansolene, J.J., and Buchberger, S.G. (1997). Partitioning and first flush of metals in urban roadway stormwater. J. Environ. Eng-Asce 123, 134-143.

Walsh, C.J. (2000) Urban impacts on the ecology of receiving waters: a frame-work for assessment, conservation and restoration. Hydrobiologia 431, 107-114.

Zanders, J.M. (2005) Road sediment: characterization and implications for the performance of vegetated strips for treating road run-off. Sci. Total Environ. 339, 41-47.

Zn removal from synthetic wastewater using modified zeolite

Salwa Mohd Zaini Makhtar[1,a*], Ismail Abustan[1,b], Nor Amirah Abu Seman[1,c], Mahyun Ab Wahab[1,d] and Abdulaziz Al-Bassam[2]

Abstract In this study, the technical feasibility of zeolite for Zn removal was investigated in batch studies using synthetic industrial wastewater. Zeolite is one of the minerals found in Indonesia. Natural zeolites contain organic and inorganic impurities covering the pore. Thus, these zeolites must be initially modified to increase absorption capacity. Surface modification of zeolite with oxidizing agents, such as sodium hydroxide (NaOH), was conducted to improve removal performance. Zeolite was activated by NaOH and heat treatment in a simple reflux apparatus at 100 °C for 3 h. The adsorption efficiency of the adsorbent was evaluated by measuring the extent of zinc adsorption in synthetic industrial wastewater. Operational parameters, such as agitation speed, dosage, and contact time, were also investigated. Results showed that zeolite chemically modified with NaOH evidently showed better Zn removal efficiency than natural zeolite. The Zn adsorption was 98% at an adsorbent dosage of 15g/L and agitation speed of 130 rpm from synthetic industrial wastewater solution with an initial concentration of 20 mg/L for 2 h.

Keywords *zeolite, NaOH, industrial wastewater, adsorption*

[a]Salwa Mohd Zaini Makhtar, PhD Student
[c]Nor Amirah Abu Seman, PhD Student
[d]Mahyun Ab Wahab, PhD Student

[1]School of Civil Engineering, Engineering Campus,
Universiti Sains Malaysia,
Nibong Tebal, Penang, Malaysia.
[a]salwa@unimap.edu.my
[c]naashamira@yahoo.com
[d]mahyun@unimap.edu.my

[b]Ismail Abustan, Professor
School of Civil Engineering,
Universiti Sains Malaysia
Nibong Tebal, Penang, Malaysia.
Visiting Professor
King Saud University, Riyadh, KSA
DPRI, Kyoto University, Japan
ceismail@usm.my

[2]Abdulaziz Al-Bassam, Professor
Faculty of Geology & Geophysics, King Saud
University, Kingdom of Saudi Arabia

Introduction

Rapid industrialization has led to increased disposal of heavy metals into the environment. The tremendous increase in the use of the heavy metals over the past few decades has inevitably resulted in an increased flux of metallic substances in the aquatic environment. Metals pose special problems because they persist in the environment. At least 20 metals are classified as toxic, and half of these are emitted into the environment in quantities that are hazardous to human health (Kortenkamp et al., 1996). The ability of a water body to support aquatic life as well as its suitability for other uses, however, depends on many trace elements.

Trace concentrations of zinc (Zn) are important for the physiological functions of living tissue and regulate many biochemical processes. However, similar to other heavy metals, when Zn is discharged into natural waters at increased concentrations in sewage, industrial wastewater, or from mining operations, it can cause severe toxicological effects on humans and aquatic ecosystems (Aremu et al., 2002).

Thus, removing Zn from industrial wastewater before transporting and cycling into the natural environment is necessary.

A number of technologies have been developed over the years to remove heavy metals from industrial wastewater. The most important technology includes coagulation/flocculation (Abdel-shafy et al., 1996; Amuda et al., 2006). Other conventional chemical methods include precipitation, ion-exchange, electrochemical processes, and membrane technology. All these chemical methods have proved to be much costlier and less efficient than the biosorption process (Preetha and Viruthagiri, 2005).

Heavy metal removal via ion exchange has existed for decades. Zeolite was one of the first materials or media used. Zeolite is a large family of minerals, including natural and synthetic species, which have a wide variety of uses in industry. Physical and chemical activation methods introduce the surface oxygen functional groups to the zeolite. Physical activation methods affect the reaction with hot oxidizing gas, such as steam, nitrogen, and CO_2, at temperatures more than 500 °C (Smisek and Cerney, 1970). Chemical activation methods affect the reaction between the surface and solutions of oxidizing agents, such as sulfuric acid, phosphoric acid, nitric acid, hydrogen peroxide, zinc chloride, potassium permanganate, ammonium persulfate, sodium hydroxide (NaOH), and potassium hydroxide.

In this study, zeolite was prepared by chemical activation and heat treatment in a simple reflux apparatus. The removal efficiency of adsorbent was investigated.

Materials

Synthetic industrial wastewater was employed for the adsorption studies. Reagents were prepared by dissolving Zn Atomic Absorption Standard Solution (Fisher Scientific) in deionized water.

An experimental solution containing Zn was prepared by diluting stock solution of the metal to the desired concentrations. The Zn concentration prepared from the stock solution was 20 mg/L.

The zeolite used in this study was obtained from Tit Enterprise in Sungai Petani, Kedah, Malaysia. The physical and chemical characteristics of zeolite are listed in Tables 1 and 2.

Table 1: Physical Properties of Zeolite from Tit Enterprise (2012)

Property	Results
Particle size (mm)	2.36–0.60
Cation exchange capacity (meq/100gr)	84.02
Color	Light green

Table 2: Chemical Analysis of Zeolite from Tit Enterprise (2012)

Parameter	Unit	Results
Iron Trioxide (Fe_2O_3)	%	2.23
Aluminium Trioxide (Al_2O_3)	%	12.17
Calcium Oxide (CaO)	%	2.24
Magnesium Oxide (MgO)	%	0.77
Manganese Dioxide (MnO_2)	%	0.07
Chromium Trioxide (Cr_2O_3)	%	Less than 0.01
Sodium Oxide (Na_2O)	%	1.09
Potassium Oxide (K_2O)	%	2.97
Silicon Dioxide (SiO_2)	%	70.95
Titanium Dioxide (TiO_2)	%	0.19
Loss On Ignition (LOI)	%	7.04

Methods

Chemical activation of zeolite

Oxidizing with NaOH

After being washed with deionized water and dried overnight in an oven, zeolite was oxidized with 1 N NaOH solution. A known volume of NaOH was heated in a simple reflux apparatus at 100 °C for 3 h. The adsorbent was then immersed into the solution (volume ratio of NaOH and zeolite = 5:1) and oxidized for 3 h. After cooling, the alkali solution was drained, and the oxidized adsorbent was washed with deionized water until the pH of the rinsing water remained constant. Finally, the samples were dried overnight in an oven at 105 °C, cooled at room temperature, and stored in an airtight container.

Batch adsorption experiments

Batch experiments were conducted at room temperature using the optimum conditions of all pertinent factors, such as dosage, agitation speed, and contact time, to maximize Zn removal by adsorbent (Chakravarty et al., 2002). Subsequent adsorption experiments were carried out with only optimized parameters.

Adsorption tests were conducted in the reaction mixture consisting of 200 mL of Zn solution with a concentration of 20 mg/L.

Zn analysis

The change in Zn concentration caused by adsorption was determined using an atomic absorption spectrophotometer (AAnalyst 800; Perkin Elmer).

The removal efficiency (E) of adsorbent on Zn was defined as follows:

$$E\ (\%) = [(C_0 - C_1) / C_0] \times 100 \qquad (1)$$

where C_0 and C_1 are the initial and equilibrium concentrations of Zn solution (mg/L), respectively.

Results and discussion

Effect of dosage

The effect of dosage was investigated by mixing 20 mg/L of Zn solution with different dosages of zeolite (1 g/L–50 g/L) for 3 h, while keeping other parameters constant.

Figure 1 shows that Zn removal efficiency increased with increasing dose of adsorbents. This result is expected because more binding sites for ions are available at higher dose of adsorbents. The highest Zn removal efficiency for NaOH-treated zeolite was 96% at 15 g/L dose of the adsorbent, and 35 g/L dose of natural zeolite exhibited 52% Zn removal.

At certain dose of adsorbent, adsorption peak is reached, and thus no adsorption of metal ion to the adsorbent is observed; moreover, the amount of free ions in the solution remains constant (Nomanbhay and Palanisamy, 2005). The difference in the surface modification of the adsorbents conferred on them different degrees of removal efficiency.

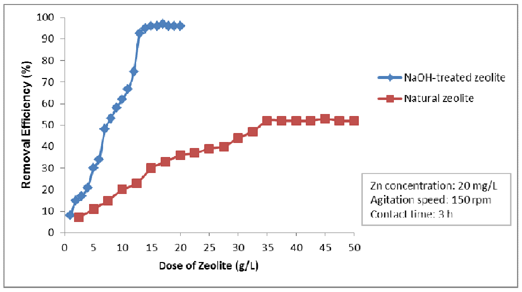

Figure 1: Effect of dose on the removal efficiencies of zeolite

Effect of agitation speed

The effect of agitation speed on Zn adsorption by zeolite was studied by varying the speed from 90 rpm to 190 rpm. Results are presented in Figure 2.

Figure 2 shows that equilibrium adsorptions were established at 130 and 150 rpm for NaOH-treated zeolite and natural zeolite, with Zn removal efficiencies of 96% and 63%, respectively. Given these results, NaOH-treated zeolite with highest binding sites for metal requires lower agitation speed to achieve high Zn removal efficiency.

The aforementioned result agrees well with that of Peniche-Covas et al. (1992) on the metal sorption by chitosan. They reported that increasing agitation speed significantly enhances the metal removal efficiency of the adsorbent.

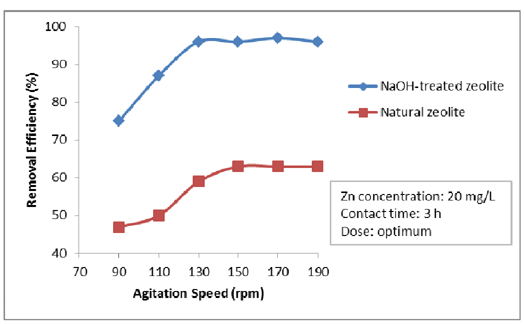

Figure 2: Effect of agitation speed on the removal efficiencies of zeolite

Effect of contact time

Equilibrium time is another important operational parameter for an economical wastewater treatment process.

The time-dependent behavior of Zn adsorption was measured by varying the equilibrium contact time in the range of 0.5h–6.5h. The Zn concentration was maintained at 20 mg/L, while the amounts of zeolite dosage added were 15 g/L for NaOH-treated zeolite and 35 g/L for natural zeolite. The adsorption efficiency of Zn is plotted in Figure 3.

The figure shows that Zn removal by natural zeolite increased from 8% to 75% with an increase in contact time until equilibrium was attained within 4 h and then became constant. The equilibrium time of NaOH-treated zeolite was achieved within 2 h with 98% removal. This finding can be attributed to the fact that the oxidative treatments of zeolite with oxidizing agents increased not only the negative charge of the surface functional group of zeolite but also the adsorption sites. Consequently, adsorption on the zeolite surface of NaOH-treated zeolite occurred significantly faster than natural zeolite.

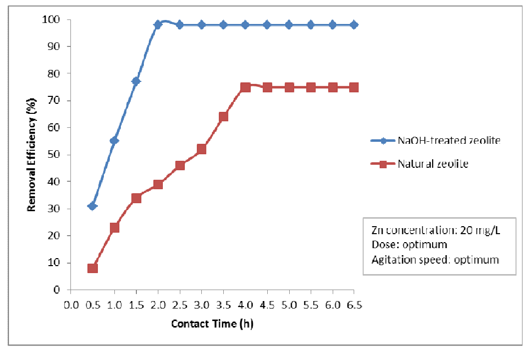

Figure 3: Effect of contact time on the removal efficiencies of zeolite

Conclusion

This study investigated the removal of Zn from synthetic solution using natural zeolite and NaOH-treated zeolite. The removal efficiency of Zn was greater than 95% at an adsorbent dosage of 15 g/L and agitation speed of 130 rpm for 2 h when using NaOH-treated zeolite. Zeolite can be effectively utilized for chemical activation and is a promising adsorbent for the removal of Zn from synthetic solutions.

References

Kortenkamp, A., Casadevall, M., Faux, S.P., Jenner, A.A., Shayer, R.O.J., Woodbrige, N., O'Brien, P., A role of molecular oxygen in the formation of DNA damage during the reduction of the carcinogen chromium (VI) by glutathione, Arch. Biochem. Biophys. 329 (2) (1996) 199–208.

Aremu, D.A., Olawuyi, J.F., Meshitsuka, S., Sridhar, M.K., Oluwande, P.A., Heavy metal analysis of ground water from warri, Nigeria, Int. J. Environ. Health Res. 12 (2002) 261–267.

Abdel-shafy, H., Hegemann, W., Guldner, C., Fate of heavy metals via chemical–biological upgrading of sewage sludge treatment plant, Environ. Manage. Health 713 (1996) 28–36.

Amuda, O.S., Amoo, I.A., Ajayi, O.O., Coagulation flocculation process in the treatment of beverage industrial wastewater, J. Hazard. Mater. B 129 (2006) 69–72.

Preetha, B., Viruthagiri, T., Biosorption of zinc (II) by Rhizopus arrhizus; equilibrium and kinetic modeling, African J. Biotechnol. 4 (2005) 506–508.

Nomanbhay, S.M., Palanisamy, K., Removal of heavy metal from industrial wastewater using chitosan coated oil palm shell charcoal, Electron. J. Biotechnol. 8 (1) (2005) 43–53.

Duren, T., Sarkisov, L., Yaghi, O.M., Snurr, R.Q., 2004. Design of new materials for methane storage. Langmuir 20, 2683–2689.

Biloe, S., Goetz, V., Marun, S., 2001. Dynamic discharge and performance of a new adsorbent for natural gas storage. AIChE J. 47, 2819–2830.

Parkyns, N.D., Quinn, D.F., 1995. Natural gas adsorbed on carbon. Porosity in Carbons. In: Patrick, J.W. (Ed.),. Edward Arnold, London, pp. 293–325.

Smisek, M., Cerney, S., 1970. Active carbon: manufacture, properties and applications. Elsevier, Amsterdam.

Chakravarty, S., Dureja, V., Bhattacharyya, G., Maity, S., Bhattacharjee, S., 2002. Removal of arsenic from groundwater using low cost ferruginous manganese ore. Water Res. 36, 625–632.

Peniche-Covas, C., Alvarez, L.W., Arguella-Monal, W., 1992. The adsorption of mercuric ions by chitosan. J. Appl. Poll. Sci. 46, 1147–1150.

Study on the Sustainable Sand Removal Capacity on Sand Mining Activities.

Abstract Sand is the most important and valued material in construction industry for almost thousand years. In Malaysia, the main source of sand is from river (in-stream mining). In-stream sand mining is currently a common practice in Malaysia because it is easily accessible and feasible, thus it becomes more cost efficient for abstracting of construction materials. Recently, the demand of sand is very high due to rapid development in Malaysia with estimated more than 6% annual growth. The increasing of demand in river sand can cause negative implication environmentally since it leads to illegal sand mining operation and improper management sand mining (such as over extraction). Excessive in-stream mining activities due to poor planning and management by mining operators could cause many major problems to the river itself such as over deposition at specific areas, scouring, unstable river band and loss of natural habitats. Furthermore, this over exploited mining activities could give impacts directly to hydraulics physical structures (bridges, piers, embankments, check dams etc.) along the river. Due to that, USM researchers have been adopted to a new approach as a guideline in on-stream activities including integration of hydraulics and geophysical measurements in order to estimate the sustainable amount of sand from the river. The new approach utilized sediment transport monitoring, estimation of flow by Acoustic Doppler Current Profilers (ADCP) and sub-surface 2D-Resistivity Survey. These new technology are able to simplify and assist the researcher in their field works. In addition, more accurate and reliable data could be obtained than the conventional way of sediment transport samplers' procedure. Finally, the new suggested approach is not only able to estimate the available sand locally, but it also can estimate the sustainable amount to be instream-mining. Moreover, the proposed practices could sustain the morphology of the rivers, and therefore, in the long run, it could reduce occurance of floods and improve flow capacity during flood event.

Keywords *Sand mining, ADCP, Resistivity method, sediment samplers.*

Introduction

Sand can be classified as one of natural resources (non-metallic mineral) that can be utilized as main construction materials. However, over exploited of sand mining can be temporary or permanent lowering of the productive capacity of land (Naveen, 2012). Based on statistical information, Malaysia produced 2.76 billion metric tons of natural aggregate which is worth about $14.4 billion in 2010 (Ashraf et al., 2011). NRE (2013) reported the production of sand and gravel in Malaysia is approximately 37,339,082 tonne and for silica sand is about 1,097,275 tonne in 2011.

In general practice locally, sand sediment is extracted directly from the in-stream river channel. However, if the in-stream sand mining is not being planned and managed properly, it can cause significant impacts to the morphology of river itself, its natural biota, and to the hydraulics structures (in its vicinity), as well as creating conflict with other users of the river (Ashraf et al., 2011).

In many developing countries especially, the sustainable method of in-stream sand and gravel mining is poorly managed. It is becoming more difficult to enforce an existing regulatory due to only little local information available (Harrison et. al, 2005). However, with proper local information, expertize and workable examples, the practices could be transfered to the sand mining operator and related government agencies so that the maximum volume of minable river sand with minimise the impacts on the stream physical morphology, water quality and ecological of river could be achived. In other words, the practices of on-stream sustainable sand removal capacity on sand mining activities.

Sand demand is on the increased since 1980's due to our rapid development (current account to GDP in Malaysia averaged 3.45 percent from 1980 until 2013). The demand of this natural river sand is becoming high for years due to the constant high demand by construction industries. To satisfy the high demand of sand as the main construction materials, there are many small scale companies (limited capital and lack of technologies and knowledge) operate in-stream sand mining that is normally based on limited period concesion permit by local land office. However, the local land office is normally governed by limited techical and enforcement units since their main duty is a local administrator. Therefore, the statement by Harrison et. al, (2005) is best suit to discribe the practices of sand mining activities *"the granting of permissions to remove or extract river sand is less formal or even non-existent, with illegal mining is commonplace"*. Due to these factors, the law enforcement in Malaysia is slightly unable to control the illegal in-stream sand mining.

Study area

The study area is located at Perak River, Bota Kanan, Perak, Malaysia at 4°22'41"N 100°54'6"E coordinate. Sungai (river) Perak is the second largest river in Peninsular Malaysia that drains from upstream Titiwangsa and Bintang mountain ranges with a catchment area of about 14,908 km^2. The Sungai Perak not only provides water sources for local people, but this river also used for recreational, fishery, mining, irrigation for paddy field, and many other human activities.

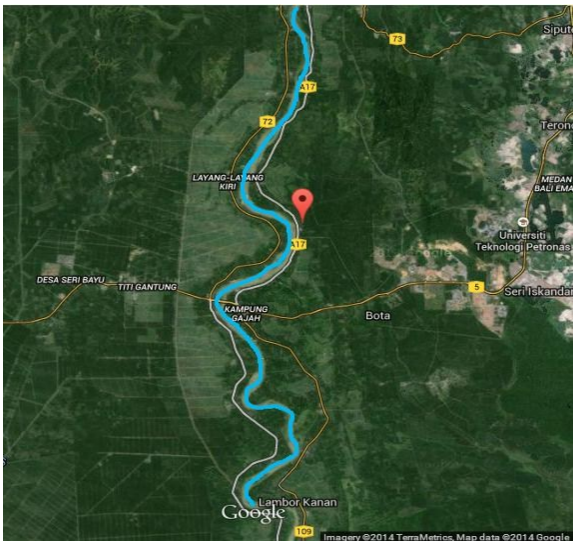

Fig. 1 Study area on Sungai Perak, Bota, Perak, Malaysia.

Methodology

The study focuses on preliminary assessment based on the geology or geotechnical characteristics of the surrounding area for sand potential. Then, an Acoustic Doppler Current Profiler (ADCP) is utilised to determine discharge capacity and the river profile. The sediment rates of transport have been sampled by the Helley Smith and Van Veen Graber samplers. These sediment samples will be analysed and calculated to determine sediment transport capacity. The utilization of equipment such as:

- 2D Resistivity Survey is used in determining the availability of potential suitable soil the study area and the equipment could measure subsurface profile up to 80 meters depth.
- Acoustic Doppler Current Profiler is utilized to make river profiler in term of velocity meshes and river bed depth. It also could measure the total discharge of a particular cross-section.
- Van Veen Grabber and Helley Smith sediment sampler are used to collect bed soil samples and determine sediment transport at the time of sampling. These two methods could estimate the suitability of available sand material and the flux of sediment transport locally.

In sum, the integrated field works will give a better indication on potential, suitability and sustainability of the site for sand mining.

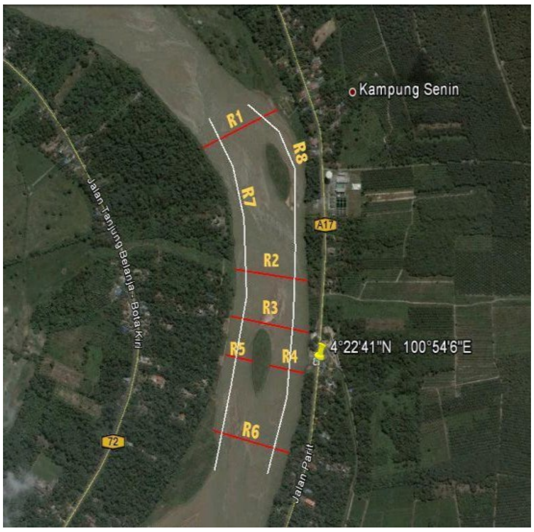

Fig. 2 Location of ADCP and 2-D Resistivity observation lines.

Results and discussion

For the results of the study it is consists of sand particle size distribution (PSD) analysis, river current profilers and subsurface profiler. All results were interpreted as to ensure the availability of sand and the sustainability of sand removal capacity at the proposed site along Sungai Perak.

Sieve Analysis

The sieve analysis determines the particle size distribution (PSD) curve by American Society for Testing and Materials (ASTM). Based on sieve analysis results, the bed materials of Sungai Perak were mostly consist of more than more than 90% of sand, 9% gravel and less than 0.5% silt as shown in Figure 3.

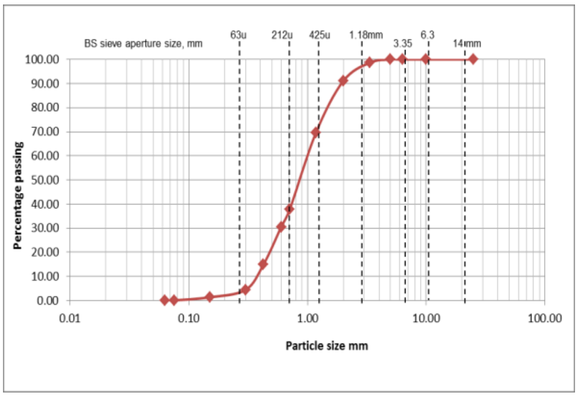

Fig. 3 A typical PSD of bed materials of Sungai Perak

ADCP

Figure 5 shows the observed data of flow profiler of each ADCP lines and it also determined the total discharge the specific river cross-section in a fast way (less than 15 minutes per cross-section). Based on result obtained, the maximum flow rate for this study area was $224.6m^3/s$ with a river width of 339.2m at line R3RB. It was noticed that the distribution of the river discharge was also uneven; one bank has a higher magnitude of velocity than another bank as shown in Figure 5. Ideally, a maximum discharge should be at the centre of the river cross section, however, in this case, the discharge was obstructed by temporary river sand islands, thus the maximum discharge of the river was flowed on either left or right side of river banks. This uneven discharge distribution leads to a local scouring or depositing. In this scenario, it is possible to exercise of sand mining at a specific area especially at the temporary sand island in order to improve the flow of the river.

Resistivity Survey

Four lines of resistivity survey were surveyed as shows in Figure 4. The objectives of this resistivity survey are to identify the material of subsurface and to determine thickness of sand deposited layer in the river. The survey was using 32 electrodes with 5m spacing between electrodes and it is successfully projected the subsurface layer up 25 to 30 meter depth as shows in Figure 6. The most distinct subsurface characteristics obtained from the electrical resistivity survey were the extensive zone of low resistivity at ground level for lines L1 and L2 and at 7 m sub-surface for lines L3 and L4. Based on 2D-resistivity survey, it indicated that the sand depositions in this area are highly saturated with water. It also indicated that substantial thickness of overburden sand in the resistivity image as a low resistivity zone which is between 100-250 ohm-m. It was observed that the thin layer of about 5-7 m with high resistivity value as shows in model L3 and L4 (red to orange colour indicated in the legend). This layer could probably consist of gravel and fill materials with less saturated condition in the range of resistivity values. This high resistivity value also probably indicates the high noise level of the data set especially in the upper part of the proposed lines. From this study it is proved that resistivity survey could provide additional essential subsurface information which is important for a feasible sand mining.

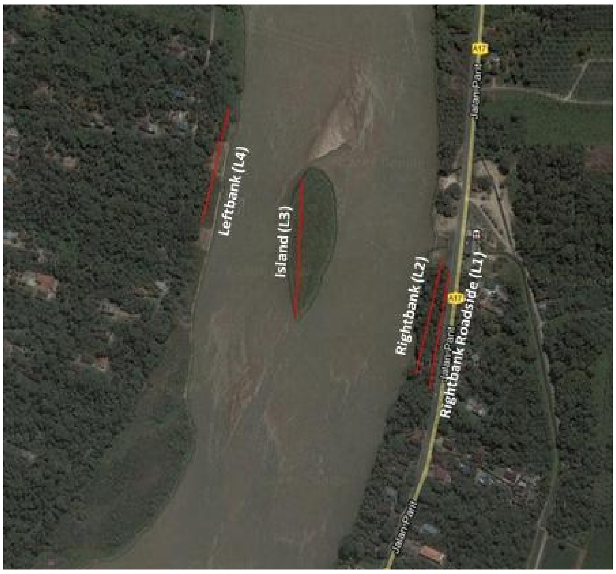

Fig. 4 The location of the Electrical 2D-Resistivity Survey Lines**.**

Sediment transport equation

The collected river bed load and transport materials using Van Veen Grabber and Helley Smith sediment sampler were analysed. PSD and these data are used to determine sediment transport at the time of sampling. It was found that the Engelund-Hansen equation shown the most suitable sediment transport equation. From the calculated values and the result in Table 1, it can be inferred that average amount of sand that can be in-stream mined was 2140 tonne per day. The average sediment recharge in this particular section was in the range of 0.12 $tonne/km^2/day$ to 0.49 $tonne/km^2/day$ and it is in a similar range of sediment transport capacity that was reported by Department of Irrigation and Drainage Malaysia (DID) in several observation stations along Sungai Perak (DID, 2010). This quantity is ample amount of sand quantity needed by a few small companies to sustain their operations. Further, the amount of available construction materials with a competitive price will not hamper the development of a nation.

Table 1. Summary of the Sediment Transport Calculation Using Engelund Hansen Equation.

Location	**Tj (Observed)**	**Tj (Calculated)**	**Disperancy Ratio (0.5-2.0)**	**Suitability**
R1	43.4457	24.686	0.568	Yes
R2	22.6617	6.169	0.272	No
R3	22.5810	34.956	1.548	Yes
R4	11.3419	14.538	1.282	Yes
R6	21.7458	20.89	0.961	Yes

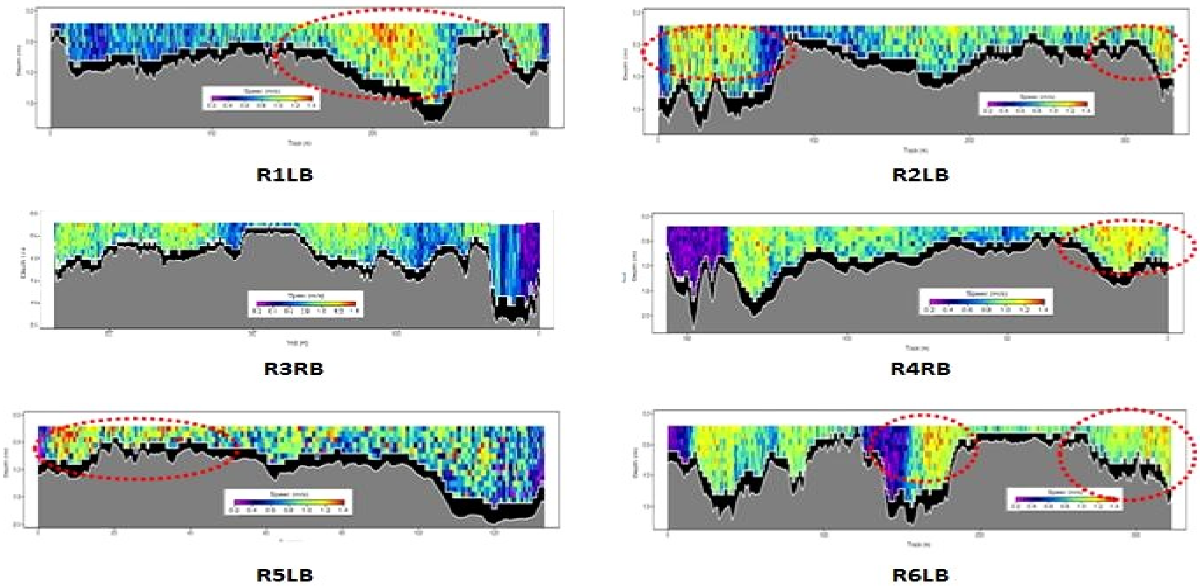

Fig. 5 Only R3RB has low flow and other profiles have some critical profiles which are mostly occurring on right or left bank.

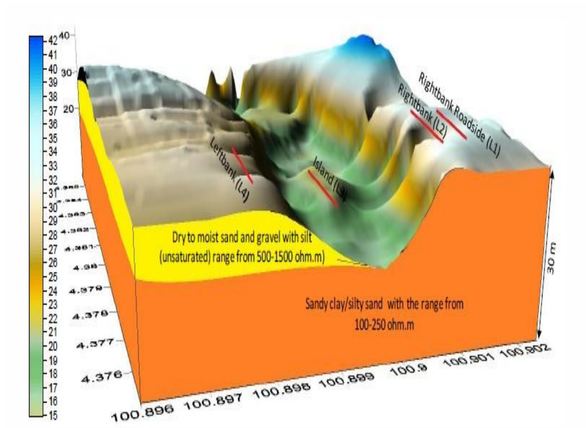

Fig. 6 Schematic figure of the Electrical 2-Resistivity results in 3-D

Application in Sungai Perak

According to British Geographer (2014), the purpose dredging of the river is to increase the cross section of river to reduce channel roughness and also increasing capacity and hydraulic performance. The other advantage of using dredging is that it maintains the natural aesthetics of the river channel. The existing of several river islands can cause local scouring due to deflected flow as indicates in Figure 7. Further, Ali et. al (2014) have listed the negative impacts of river islands or obstacles toward the uneven discharge distribution. These obstacles can cause reduce hydraulic performance of the river and change river cross sections that would reduce its capacity in coping with flood, and treating the banks stability at some locations due to deep eroding incisions in the river bed near these protections at the meanders.

From the results of this study, it proved that the existing of a river island acts as an obstacles for normal flow and for long term condition could lead to occurrence of local band erosion. The ADCP results shown that the river current profiler were uneven and had a tendency of concentrated high velocity in a particular area especially in the both sides of the temporary river island. Meanwhile, the 2D-Resistivity analysis shown that there are abundant of good sand on the island with more than 99% are sand and boulder. Further, the grab samples and the Engelund-Hansen model indicate that the sediment recovery capacity with minimum of 0.12 tonne/km^2/day could supply more than 2400 tonne/day that ample supply for local construction activities.

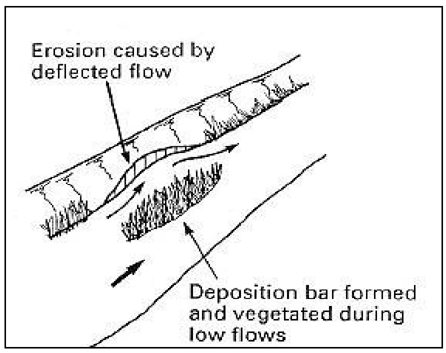

Fig. 7 Erosion due to deflected flow by river island (Hemphill et. al, 1989)

Summary and conclusions

Based on result, total potential volume of minable sand in Sungai Perak at Bota Kanan is 269,085 m^3 and the maximum replenishment period was 131 days if it is based on the allowable mining depth which is 1.5m. By extract sand on temporary river islands, it is possible to reduced local scouring at left or right bank of river. Based on the sieve analysis, the collected bed loads majority consist more than 90% of sand and more than 9% gravel. This type of materials is suitable for construction materials. Further, the findings also confirmed that the average recharge sediment transport in this river section is in range 0.12 tonne /km^2/day to 0.49 tonne/km^2/day. It fell in the range of sediment transport (0.04–1.4 tonne/km^2/day) in several Perak's rivers as reported by DID.

Fig. 8 Proposed sand mining sector along the study area

Table 2 shows the summary for all the volume of possible extracted sand based on 1.5m mineable depth. For the island, replenishment period is neglected because the existence of the island caused the occurrence of local scouring at the river bank.

Table 2. Volume of sand mining and replenishment rate

Area	Volume (m^3)	Mass per day (tonne)	Replenishment Period (day)
1	66,533.25	176,313.11	82.4
2	106,202.2	281,436.6	131.5
3	77,820.7	206,224.9	96.3
Island	18,527.9	49,099.0	-

Acknowledgement

The authors would like to acknowledge the Ministry of Education Malaysia for providing USM RUI Grant entitled Exploratory Study on the Sustainable Sand Removal Capacity on Sand Mining Activities (1001/PPKA/814218).

References

Ali, A., et al. (2014) Evaluation of Dredging Operations for Tigris River within Baghdad, Iraq. Journal of Water Resource and Protection, 6, 202-213

British Geographer, (2014), http://thebritishgeographer.weebly.com/floods-and-river-management.html

Department of Irrigation and Drainage (DID) Malaysia (2010), Review of the National Water Resources 2000-2050 and Formulation of Natural Water Resources Policy.

Conaway, J.S. (2005), Application of acoustic Doppler current profilers for measuring three-dimensional flow fields and as a surrogate measurement of bed load transport.

Harrison, D.J., Fidgett, S., Scott P.W., Macfarlane, M., Mitchell, P., Eyre, J.M. and Weeks, J.M., (2005), Sustainable river mining of aggregates in developing countries.

J. Merz, (2010), Discharge Measurements in Low Flow Conditions with ADCP Technology – First Experiences in Nepal

M. A. Ashraf, M. J. Maah, and I. Yusoff, (2011), Sand mining effects, causes and concerns: A case study from Bestari Jaya, Selangor, Peninsular Malaysia

M.H. Loke (2000), Electrical imaging surveys for environmental and engineering studies.

Ministry of Natural Resources and Environment (NRE), (2014), 4th National Report to the Convention on Biological Diversity the Fourth National Report.

M. Naveen Saviour and P. Stalin, (2012), Soil and Sand Mining: Causes, Consequences and Management

M. Muste; K. Yu; J. A. Gonzalez-Castro; M. Ansar; and R. Startzman, (2004), Methodology for Estimating ADCP Measurement Uncertainty in Open-Channel Flows

R. W. Hemphill; M. E. Bramley, (1989), Protection of River and Canal Bank

The Study of Relationship between Deciles and VCI in the Northern Part of Thailand

Aphantree Yuttaphan [1, 2, a *], Sombat Chuenchooklin [2,b] and Somchai Baimoung [3,c]

Abstract Drought is one of the most adverse weather related disasters that occur almost every year in the Northern part of Thailand. The main source of drought is the variation of rainfall amount. This study is based simply on the use of two databases: the first one was containing of Deciles database which was a meteorological drought index that calculated from monthly rainfall data over the period 1951-2012 at 25 meteorological stations. The other was containing of Vegetation Condition Index (VCI) database derived from The Moderate Resolution Imaging Spectro-radiometer so-called "MODIS" imageries over the period 2000-2012. To determine the effect of rainfall variation which is the main source of drought on the natural vegetation and agricultural crops therefore, the analysis of relationship between the average pixel values of monthly VCI with in 3 kilometers radius of surrounding station area and moving timescale of 1, 2 and 3 month deciles index during 2000-2012 using Pearson correlation techniques were used. Then, it was found that the preceding 2 and 3 month deciles were mostly correlated with the VCI products during January-April and December with R value ≥ 0.5. The Maximum R value was 0.893 on February at Chiangrai meteorological station. Therefore, it was concluded that these relationship techniques can be used for drought monitoring appropriately and furthermore also be applied for drought forecast using the numerical weather prediction products within 3-4 months ahead.

Keywords *Deciles, VCI, Drought*

[1] Thai Meteorological Department
Bangkok, Thailand
[a] Aphantreey@yahoo.com

[2] Naresuan University
Phitsanulok, Thailand
[b] sombatc@nu.ac.th

[3] National Research Council of Thailand
Bangkok, Thailand
[c] somchaib.mict@gmail.com

Introduction

Drought is widely recognized as a slow-onset natural hazard that occurs due to the natural climatic variability. In recent years, concern has grown world-wide that droughts may be increasing because of climate change (World Meteorological Organization and Global Water Partnership, 2010). Whether due to natural climate variability or climate change, consequently there is an urgent need to develop better drought monitoring and early warning systems.

However, drought means different things to different people and there are probably as many definitions as there are users of water (Tomar and Verma, 2008). In the point of view to meteorologist it is the absence of rain while to the agriculturist it is the deficiency of soil moisture in the crop root zone to support crop growth and productivity. To the hydrologist it is the lowering of water levels in lakes, reservoirs, etc., while for the city management it may mean the shortage of drinking water availability (SAARC Disaster Management Centre).

Intensity of drought refers to the degree of the precipitation shortfall and/or the severity of impacts associated with the shortfall. It is generally measured by the departure of some climatic parameter (e.g., precipitation), indicator (e.g., reservoir levels) or index from normal (Sivakumar et al, 2010). Over the years, many drought indices were developed and used by meteorologists and climatologists around the world (World Meteorological Organization, 2012). In general, the drought indices derived from meteorological parameters, may be used only the single or combine the meteorological parameters. The meteorological stations observe these parameters on a routine basis. Therefore, it is a very common way to approach drought situation by generating an index using meteorological data (Dunkel, 2009).

In Thailand, drought occurs on many parts of the country almost every year particularly in the Northern part of Thailand where the main area of agricultural plantation. The main source of drought is the variation of rainfall amount. The severity of drought has been impacting on various activities in Thailand such as agriculture, industry, and socioeconomic etc. Therefore, if we can look for some techniques for higher accuracy monitor drought or the prediction of drought can be done, it is advantage for planning to avoid or reduce any production loss from drought in the future.

This research study is focus on investigating of the relationship between the Deciles - meteorological drought index in several time scales and the effect of drought on the natural vegetation and agricultural crops in term of VCI.

Study area

The study area is the Northern part of Thailand which consist of 15 provinces namely Chiangrai, Chiangmai, Maehongson, Lamphun, Lampang, Phrae, Phayao, Nan, Uttaradit, Tak, Sukhothai, Phetchanulok, Phichit, phetchabun and Kamphangphet. The climate of the Northern part of Thailand is divided into three seasons such as rainy season (mid-May to mid-October), winter season (mid-October to mid-February) and summer season (mid-February to mid-May). The mean annual rainfall is 1230.9 mm, average minimum temperature is 21.2 °C and average maximum temperature is 32.9°C. The most areas are forests, paddy fields and crop fields. The study area and location of the meteorological stations in this study were shown on Figure 1.

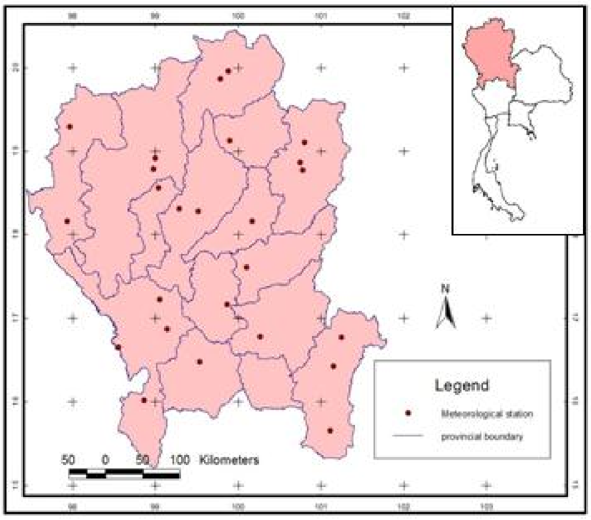

Fig.1 the study area and location of the meteorological stations

Methodology

Deciles Index

Deciles method was developed by Gibbs and Maher (1967). In this method, the amounts of precipitation distribution will be put in order from minimum to maximum in a long period and divided into 10 parts. Each of these parts is called a "Decile". The first decile is the precipitation amount not exceeded by the lowest 10% of the precipitation occurrences. The second decile is the precipitation amount not exceeded by the lowest 20%. These deciles are computed continuously until the precipitation amount as identified by the tenth decile which is the largest amount within long period record.

The deciles method is used in the Australian Drought Watch System and forms the basis for declaring drought and providing drought relief (White and O' Meagher, 1995). The classifications used in this system are shown in table 1.

Table 1. Classification system for the deciles method as used in Australia

Deciles	Climate Classification
1	Very much below average
2-3	Below average
4-7	Average
8-9	Above average
10	Very much above average

This study has been calculated deciles from total rainfall data in accumulation period or the time scale of 1, 2 and 3 months. The total rainfall (TP_n) for an n month accumulation period is defined as:

$$TP_n = P_0 + \sum_{i=1}^{n-1} P_{-i} \tag{1}$$

Where P_0 is the rainfall for the current month and P_{-i} is the rainfall for the previous i^{th} month. The moving timescale of 1, 2 and 3 month deciles index was calculated at 25 meteorological stations in the study area by using monthly rainfall data over the period 1951-2012.

Vegetation Condition Index (VCI)

Today several remotely sensed indices are used extensively for agronomic monitoring, especially vegetation stress and crop yield assessment. Though many vegetative indices exit, the most widely used index is Normalized Difference Vegetation Index (NDVI). NDVI was first suggested by Tucker (1979) as an index of vegetation health and density.

$$NDVI = (\lambda_{NIR} - \lambda_{red})/(\lambda_{NIR} + \lambda_{red}) \tag{2}$$

where λ_{NIR} and λ_{red} are the reflectance in the NIR and red bands, respectively. NDVI values range from -1 to +1, where vegetated area will typically have values greater than zero and negative values indicate non-vegetated surface features such as water, snow and cloud.

NDVI itself does not reflect drought or non-drought condition. But the severity of a drought may be defined if compare NDVI with long-term mean or record (Thenkabail *et al.*, 2004). VCI was suggested by Kogan (1995, 1997). It shows how close the NDVI of the current month is to the minimum NDVI calculated from the long-term record.

$$VCI_j = \frac{(NDVI_j - NDVI_{\min})}{(NDVI_{\max} - NDVI_{\min})} \times 100 \qquad (3)$$

Where $NDVI_{max}$ and $NDVI_{min}$ are calculated from the long-term record for that month (or week) and j is the index of the current month (or week). The condition of the ground vegetation presented by VCI is measured in percent. The VCI values around 50% reflect fair vegetation conditions. The VCI values between 50 and 100% indicate optimal or above normal conditions. At the VCI value of 100%, the NDVI value for this month (or week) is equal to $NDVI_{max}$. The different degrees of a drought severity are indicated by VCI values below 50%. Kogan (1995) illustrated that the VCI threshold of 35% may be used to identify extreme drought conditions and suggested that for the further research is necessary to categorize the VCI by its severity in the range between 0 and 35%. Low VCI values over several consecutive time intervals will point to drought development.

In this study, to derived VCI data, the surface reflectance (MOD09), geo-location (MOD03) and cloud mask (MOD35) products of the terra-MODIS over the period 2000-2012 were downloaded via access data from http://lpdaac.usgs.gov/. The daily NDVI has been calculated from the daily surface reflectance data of band 1 and 2 (red and NIR) with spatial resolution 250 meters. The process of cloud masking which all pixels containing cloud should be removed to no data was applied to daily NDVI data. Then monthly compositing of NDVI were done using the average compositing of daily NDVI values at the pixel of cloud-free observation. Afterward, the monthly composited NDVI data were use to calculated monthly VCI.

To investigate the relationship between deciles and VCI at the same location, then it was found that the VCI value at the meteorological station pixel was hardly to classify and collect particularly in rainy season due to the cloud coverage. Therefore, the average value of VCI within 3 kilometers radius of surrounding where would be the good representation and big enough area for the occurrence of drought event in Thailand were used. The Pearson correlation was performed to determine the statistical relationship between deciles for 1, 2 and 3 month time scales and average pixel values of VCI in surrounding area of 3 kilometers radius at each of the station.

Results and discussion

To calculate deciles for moving 1, 2 and 3 month time scales, the total rainfall data for each time scales and each period of time were ranked in order to relatively compare the total rainfall amount in that period for the interesting year with the total rainfall distribution of all recorded over the same period. Then the deciles for moving 1, 2 and 3 month time scales during 2000-2012 were derived to use in the next step.

The monthly composited NDVI images were produced from daily NDVI images during 2000-2012. The VCI images were produced using the maximum and minimum NDVI values of each month over 13 year periods. Therefore, the VCI would be normalized from NDVI according to its variability over 13 years and showed the situation of dry and wet years and the vegetation condition which was mainly related to the water availability in the soil during that time. The example of VCI image in March 2012 with overlaying by provincial boundaries was shown on Figure 2.

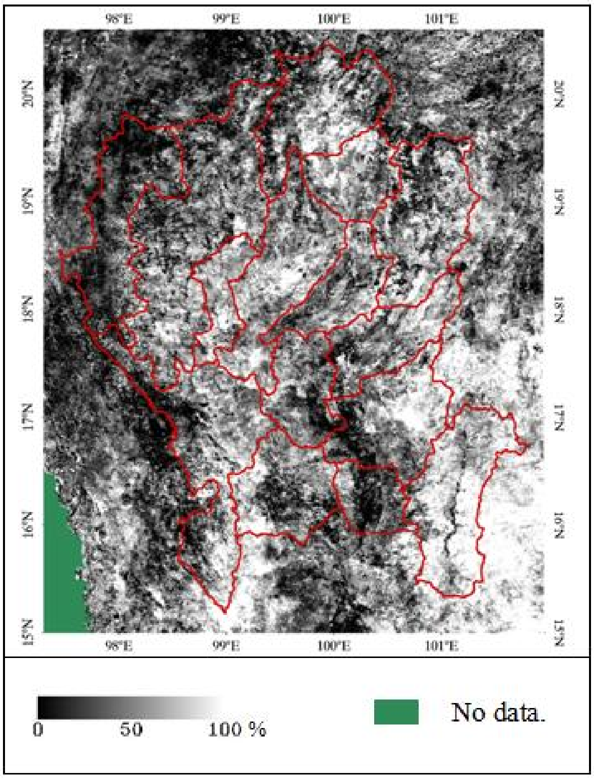

Fig. 2 the VCI image in March 2012

To determine the effect of rainfall variation which is the main source of drought on the natural vegetation and agricultural crops therefore, the analysis of relationship between deciles value for 1, 2 and 3 month time scales at each of the station and the average pixel values of VCI within 3 kilometers radius of surrounding station area during 2000-2012 were performed. The relationship between the deciles and VCI values was determined not only at the same month of deciles and VCI but also the moving time scale of 2 and 3 month deciles and VCI. Therefore, at the difference time scale of deciles and VCI then the relationship were determine only with the last month of the time scale (2 or 3 month) of deciles which was the same month of VCI. Lastly, the results would be the pair of relationship for 1 month deciles to VCI (deciles1-VCI), 2 month deciles to VCI (deciles2-VCI) and 3 month deciles to VCI (deciles3-VCI).

To investigate these relationships, the statistically significant at the 90% confidence level ($p \leq 0.1$) and the positive correlation coefficient (R) were used to consider altogether. It was found that the number of significant correlation with the R value ≥ 0.5 between deciles and VCI in the 1 month deciles time scale would be much smaller than in the 2 and 3 month deciles time scale. And also the most of significant correlation with the R value ≥ 0.5 would be during January-April and December which was the time in winter and summer season. The maximum R value between 3 month deciles and VCI was 0.893 on February at Chiangrai meteorological station. In May, the significant correlation with the R value ≥ 0.5 between 3 month deciles and VCI found in 13 stations where were more half of all stations in this study. But there was a little number of the significant correlation between 2 month deciles and VCI. For all pair of the relationship, it was found that there was a little number of the significant correlation during June-November. Table 2 show the examples of the correlation between deciles (1, 2 and 3 month time scales) and VCI in December for each station. In this month, the significant correlation with the R value ≥ 0.5 between all time scale of deciles and VCI was mostly found. Especially, the significant correlation between 2 month deciles and VCI was found almost all station.

Conclusions and recommendation

This study intended to investigate the duration of rainfall deficiency or meteorological drought that effected on the natural vegetation and agricultural crops. The deciles index in difference time scale such as 1, 2 and 3 months was selected to identify the duration and intensity of meteorological drought. The vegetation condition in term of VCI value from satellite images were used to represent the effect of the drought. The relationship between the deciles in difference time scale and VCI were investigated. It was found that the most of significant correlation with the R value ≥ 0.5 would be during January-April and December. And also the properly time scale of deciles for monitoring and warning meteorological drought impact would be 2 and 3 month period. Furthermore, these techniques can be applied for drought forecast using the numerical weather prediction products within 3-4 months ahead.

Acknowledgement

We have been much appreciated for the Thai Meteorological Department for supporting climatic data and all related facilities. Also, we would like to thank NASA for supporting all MODIS images via https://lpdaac.usgs.gov/.

Table 2. the correlation between deciles (1, 2 and 3 month time scales) and VCI in December

Station	deciles1-VCI	deciles2-VCI	deciles3-VCI
Maehongson	0.032	0.208	0.754**
Maesariang	0.192	0.533*	0.587**
Chiangrai	0.762**	0.629**	0.562**
Chaingrai agromet.	0.603**	0.705**	0.545*
Phayao	0.739**	0.769**	0.379
Maejo agromet.	0.724**	0.876**	0.798**
Chiangmai	0.608**	0.650**	0.670**
Lampang	0.760**	0.627**	0.656**
Lampang agromet.	0.617**	0.634**	0.777**
Lamphun	0.800**	0.699**	0.745**
Phrae	0.313	0.516*	0.422
Nan	0.539*	0.739**	0.642**
Nan agromet.	0.358	0.427	0.364
Thawangpha	0.516*	0.630**	0.648**
Uttaradit	0.654**	0.600**	0.354
Sisamrong agromet.	0.730**	0.626**	0.263
Tak	0.638**	0.768**	0.557**
Maesot	0.524*	0.771**	0.770**
Bhumibol dam	0.497	0.563**	0.643**
Umphang	0.441	0.526*	0.552
Phitsanulok	0.561**	0.678**	0.504*
Phetchabun	0.667**	0.716**	0.337
Lomsak	0.433	0.109	-0.059
Wichianburi	0.622**	0.764**	0.585**
Kamphaengphet	0.493	0.575**	0.513*

Note: Significant and positive correlations are indicate: *($R \geq 0.5$; $p \leq 0.1$), **($R \geq 0.5$; $p \leq 0.05$)

References

Dunkel, Z. 2009. Brief surveying and discussing of drought indices used in agricultural meteorology. Quarterly Journal of the Hungarian Meteorological Service. 113 (1–2). 23–37.

Gibbs, W.J. and J.V. Maher. 1967. Rainfall deciles as drought indicators. Bureau of Meteorology Bulletin No. 48, Commonwealth of Australia, Melbourne.

Kogan, F. N. 1995. Droughts of the late 1980s in the United States as derived from NOAA Polar-Orbiting Satellite data. Bull. Am. Meteorol. Soc. 76, 655–668.

Kogan, F. N. 1997. Global drought watch from space. Bull. Am. Meteorol. Soc. 78, 621–636.

SAARC Disaster Management Centre. Drought. Available from: http://saarc-sdmc.nic.in/pdf/drought.pdf [2014, November 8]

Sivakumar, M. V. K., Wilhite, D. A., Svoboda, M. D., Hayes, M. and Motha, R. 2010. Drought risk and meteorological droughts. Available from: http://www.preventionweb.net/english/hyogo/gar/2011/en/bgdocs/Sivakumar_et_al._2010.pdf [2014, November 8]

Thenkabail, P.S., Gamage, M. S. D. N. and Smakhtin, V. U. 2004. The use of remote sensing data for drought assessment and monitoring in southwest Asia. Research report 85. Colombo, International Water Management Institute

Tomar, A. and Verma, G. 2008. The devastating drought and strategies to combat it. Bhagirath: India Water Resources Quarterly. 15(1). 5-17.

Tucker, C. J. 1979. Red and photographic infrared linear combinations for monitoring vegetation. Remote Sensing Environ.8, 127–150.

White, D.H. and B. O'Meagher. 1995. Coping with exceptional droughts in Australia. Drought Network News 7(2):13–17.

World Meteorological Organization. 2012. Standardized precipitation index user guide. WMO-No. 1090. Geneva, Switzerland

World Meteorological Organization and Global Water Partnership. 2010. Consultation meeting on the proposed integrated drought management programme. 15-16 November 2010. Geneva, Switzerland

Effect of Particle Size Distribution to Remove Colour and Escherichia coli in a Shalow Groundwater

Nur Aziemah Abd Rashid[1,a*], Ismail Abustan[2,b], Mohd Nordin Adlan[3,c], Nur Atiqah Ahmad Awalluddin[4,d]

Abstract. Shallow groundwater in riverbanks along a permanent river could be utilized as water resources (water that presents in the shallow aquifer). These riverbanks normally contain various types of soil; sand, silt and clay. The particle distribution of these materials in soil could determine its permeability. In this article, the effect of particle size distribution (PSD) was studied in form of coefficient of uniformity (C_u). The soil ability to transmit water is influenced by soil PSD and it becomes one of the important criteria in riverbank filtration (RBF). In a study, a laboratory scale model was constructed in order to determine a horizontal hydraulic conductivity of local alluvial soil with different PSD. Further, the alluvium soils capability to improve water quality (colour and *Escherichia coli* (*E. coli*)) was studied for the different PSD as well. The results indicated that the local riverbank alluvial soil have a range of hydraulic conductivity from $6.87\text{x}10^{-4}$ to $8.96\text{x}10^{-4}$ m/s for the different C_u. It also found that the relationship between the hydraulic conductivity and C_u was almost linear. The study showed that the increasing of C_u can improve the removal capability of colour and *E. coli*. In this study, Sand A which was well graded PSD with the highest C_u value removed colour and *E. coli* up to 70% and 100%.

Keywords: *riverbank filtration, alluvium soil, hydraulic conductivity, particle size distribution (PSD), coefficient of uniformity (C_u).*

Nur Aziemah Abd Rashid
School of Civil Engineering, Universiti Sains Malaysia (USM), Penang, Malaysia.
nuraziemahabdrashid@gmail.com
Ismail Abustan
School of Civil Engineering, Universiti Sains Malaysia (USM), Penang, Malaysia
Visiting Professors, King Saud University, Riyadh KSA DPRI, Kyoto University, Kyoto Japan.
ceismail@usm.my
Mohd Nordin Adlan
School of Civil Engineering, Universiti Sains Malaysia (USM), Penang, Malaysia
cenordin@usm.my
Nur Atiqah Ahmad Awalluddin
School of Civil Engineering, Universiti Sains Malaysia (USM), Penang, Malaysia.
atiqah_pink@yahoo.com

Session D

Water Related Disaster Management

ANALYSES AND STRATEGIES FOR HANDLING OF CLIMATE CHANGE IMPACTS ON FLOODING

Ole Mark[1*], Birgit Paludan[2]

Abstract It is in the interest of society to provide protection for the population and to protect infrastructure against flooding and to protect the aquatic environments against polluted sewer overflows in a timely and cost efficient way. Climate changes (precipitation, increase in temperature and mean sea level) may have significant impacts on the urban water cycle. Hence, it is important to identify and quantify the impact on the main urban water systems, such as sewer systems, waste water treatment plants, storm water overflows and combined sewer overflows, to receiving waters, such as rivers, lakes, estuaries and the sea.

In the past, infrastructure, located facilities, buildings or new urban areas were designed based on the assumption that the future was like the past. Parameters were measured in nature, and they were used as design basis, for infrastructure, which should last for many years (100+) into the future. Today, we are in a situation where we know that it is insufficient to make decisions that have consequences far into the future - without taking into account the changes that we already know will happen in nature due to climate change. A climate adaptation strategy for urban water systems shall therefore be based on the protection of the society on the basis of the knowledge we already have, and optimize both existing and new infrastructure based on the knowledge we currently have about the movements of climate change. An adaptation strategy based on informed decisions for urban water systems will be presented.

Keywords *Adaptation, Climate Change, Informed Decisions, Modelling, Urban Flooding*

Ole Mark
Urban & Industry DHI,
Denmark
Ole.Mark@dhigroup.com

Birgit Paludan
M.Sc., Hydraulics,
Greve Solrød Water Utility
Denmark

Introduction

The aim of any climate adaptation strategy should be to adapt the society in such a way that:

1. The negative social consequences of climate change (including economic, technical, social and other effects) are minimized to a deliberately chosen level.

2. It creates confidence among the public that the consequences of climate change are identified and taken care of, and that the citizens' views are heard.

3. Climate change adaptation of the society becomes an integral part of the planning processes.

These three objectives must be achieved through conscious and informed choices about how we deal with the consequences of climate change. This requires that we have mapped both the possible effects of climate change and the associated uncertainty estimates. The conscious and informed choice on climate adaptation consists of the following equal elements:

• Assessments of the effects of climate change, and thus the usefulness of climate change adaptation measures are subject to uncertainties. In many situations, the uncertainties will not have a significant impact on the choice of adaptation measures. In this context it is important to acknowledge uncertainties and use that knowledge constructively, i.e. the uncertainties must not be used as an excuse for inaction. On the other hand, you cannot select solutions without considering the actions that are most robust against uncertainties. This is an important point that a deliberate and documented choice (which may also be doing nothing) must be taken – on the basis of acknowledged uncertainties.

• Climate changes may have serious impact on the living conditions for many urban citizens in connection with the urban water systems, e.g. in terms of increased urban flooding or a reduced supply safety for water. Hence, stakeholder involvement is essential - both in relation to the identification of problems, and when it comes to assessment of possible climate change adaptation measures. This provides the opportunity to involve all relevant information, and, not least, to achieve a high degree of common understanding of the problems and character. Many climate change adaptations require change in behavior of citizens and changing social environment, which in turn requires stakeholder involvement to anchor the decisions and behavior of citizens.

• Selection of climate change adaptation measures can have effects that are positive for one sector and negative for another, and perhaps unknown to a third sector. Cross-sectorial assessments are therefore essential to ensure socially sound and sustainable solutions. Cross-sectorial solutions often require priorities between different sectorial interests (stakeholders), which illustrate the need for stakeholder involvement.

• Handling of the extreme events due to climate change. Extreme events will always occur with strength, which exceed the design, even after design the standards have been updated based on the latest climate change projections. This is e.g. the case for urban flooding. The deliberate handling of extreme events consists of an analysis of the respective risk and damage from extreme weather events held up against the costs to manage them. The results of such analyzes provide valuable information for the long-term social planning, e.g. when drawing up plans for where new infrastructure can be built, and where existing infrastructure and buildings have to be moved from vulnerable areas. In addition to these primary economic analyzes there is also a need for outlining the general ethical and social consequences as the society can accept. Finally, the need comes for emergency plans for handling of extreme weather situations as they arise in the future and even today.

The core of the conscious and informed choice is that all relevant effects of climate change are identified (including uncertainties), and that there is a documented choice of what you choose to do. A conscious and informed choice of action can also be not to do anything today, but to wait for more knowledge in the field. Climate Change Adaptation (as described in points 1-4) must be integrated into the existing plan ¬ planning processes in the society. That is, climate adaptation of society becomes part of the continuous and rolling planning cycle within the authorities.

Predicted climate changes impacting on the urban setting

Future rain

In some places the annual rainfall may change so that the easily available water resources for the drinking water supply will be reduced. The rain seasons may shift a bit and more extreme rain events may occur, especially during summer. In the Northern hemisphere it is in many places expected that the precipitation will increase during winter; the accumulated precipitation will be reduced during the summer, but with an increase in extreme single extreme rainfall events. The question now is which changes will occur and how quickly will they come? Both issues are important to consider in planning the augmentations of urban drainage systems. In some cases there is a need for estimates of future precipitation in the rest of this century, while in other cases estimates of the future precipitation is only required for a shorter time scale. It depends entirely on the actual problem, not least on the potential to continuously adapt the system to increased load and to judge the consequences of an error estimate in the prediction. New local rainfall for design can today be estimated using statistical down scaling from GCM climate projections. At present, the local design storm found by means of this method indicated an increase in design rainfall in the order of 20-50% for urban drainage and storm water systems.

Future water levels in marine waters

In the future, the mean sea level along the coasts will increase due to climate-related sea level rise. In addition to this, new climate-related extreme wind fields will lead to backwater or increases in near shore sea level. Changing sea levels will affect the hydraulic conditions at the outlets in drainage systems which discharge by gravity to the sea (Domingo et al., 2010). More specifically, the mean sea level is expected to rise by 50 -150 cm during this century. Additionally, a wind contribution by storm surges of up to 50-100 cm in maximum sea water levels are expected around the world. The impact of the new extreme water levels for coastal municipalities should be calculated as: Sea level rise plus backwater from new climate-related extreme wind fields. Output from these oceanographic calculations will be extreme water levels for relevant return periods including a measure of duration (i.e. day maximum or similar). This information can be used to estimate the required pumping in a given urban drainage system and whether inflow from the sea through rivers may occur.

Future water levels in lakes and rivers

Rivers have large differences in water flow patterns. Some creeks have a relatively constant water flow with small differences between winter and summer flow. They can have a little sensitivity to extreme rainfall events, while other streams and rivers have large differences between winter and summer flow, and they can have a strong response to extreme rainfall events. This type of urban stream/river may have a tendency to dry out in summer. In the future it is expected that rivers will also be affected by climatic changes. Sea level rise will affect rivers and reduce the drainage capacity, and in situations of extreme water levels the impact is increased. Since the rivers often act as boundary condition to the urban drainage system, it is recommended to describe the river hydraulics together with the urban drainage network.

Future water levels / pressures in groundwater

Any changes in the groundwater conditions are interesting from an urban drainage point of view. If the groundwater table changes it might impact the infiltration to the urban drainage system, the secondary groundwater zone which has impact on the runoff on terrain to storm water and combined systems as well as the rivers. When heavier rainfall events occur the surface runoff from permeable areas to the urban drainage systems will increase. The expected increase in precipitation events with high intensity may have local impact on the groundwater conditions. Especially in areas with coarse, sandy sediments a rapid rise in groundwater table may occur under very intense rainfall with potential infiltration into sewers, basements and other underground structures. At the same time there may be disturbances in the dewatering plant pumping from the upper aquifers. The projected sea level rise in coastal areas would cause a rise in groundwater potentials. The risk of intrusion of saline water in coastal groundwater wells will increase and the drainage of coastal catchment areas will be disturbed or altered. In many cases the sea level rise will only have very local impact on groundwater conditions. However, it may have significant impact on runoff conditions in coastal rivers, where gradients are small, especially combined with the anticipated increased intensity of rainfall.

Changes in performance of the urban water systems
Urban flooding

Drainage systems are designed to be full flowing for a certain return period of rainfall, e.g. 5, 10, 25 years, depending on the location of the drainage system (e.g. rural, sub-urban, financial district) (Parkinson and Mark, 2005). Hence, if nothing is done to the urban drainage systems their performance will certainly drop in locations exposed to more frequent or extreme rain events. Consequently, city areas will be flooded with an increase in flood damages (Speight, 2006). Several studies suggest that the economic consequences by failing to change the city's design for the drainage systems is very large, the studies state that it pays off to extend the capacity of new pipes being built today, so they correspond to the lasts climate projections.

Overflows to receiving waters

Drainage systems are designed to relieve (send rainwater mixed with water) to recipients (e.g. lakes, rivers and estuaries) in case that the drainage system is overloaded. This design practice has changed over the years, and now it is more common to use objectives, which are determined on the basis of the vulnerability to water of the individual recipients. Increase in annual precipitation may increase sewer overflows, but no general statement can be made, and local analyses (e.g. by urban drainage modelling) are required to estimate an impact from the future rainfall on overflows.

Changes in inflow to waste water treatment plants

If the precipitation is increased during winter, biological wastewater treatments plants located in cold areas may have a readied efficiency as cold weather and water slow down the biological activity and reduce the efficiency of the wastewater treatment plant. Conversely, the generally higher temperatures in winter will reduce the need for preventing slippery roads by means of chemical and salt, and this will reduce the load of these substances on the wastewater treatment plant and the aquatic environment.

Adaptation of urban water systems

Climate change adaptation in urban areas is described in this section by applying risk assessments in practical solutions in order to achieve desired standards of services in preparation and layout of contingency plans (Djordjević et al, 2011).

Risk analysis - Damage assessment using a risk analysis
Assessing the risk of damages in an urban drainage catchment can be undertaken at different levels, from broad qualitative analysis to quantitative analysis. Other impacts may be taken into account in the analysis. Besides the influence of extreme rainfall there are also risks in the general operation of drainage systems.

A complete risk analysis of the system can be undertaken by systematically examining how the drainage system operates under different conditions during both extreme rain events and periods with disruptions in the service by weighting the various disruptions by their importance. A simpler risk analysis focused on extreme flooding is also possible. Analyses at both levels are very useful tools that can be used in prioritizing the maintenance, and operational actions should be continuously made to upgrade the drainage system.

Traditionally, damage caused by surcharged water on terrain is divided into three categories:

1. Direct damage - typically damage caused by standing or flowing water.
2. Indirect damages – e.g. traffic accidents due to aquaplaning, traffic disruptions, administrative costs, labor costs, loss of production, etc.
3. Social costs - negative long term effects of a more economical nature, such as reducing the value of property in areas subject to flooding and slower economic growth.

A big advantage of a risk analysis is that all causes of flooding are assessed and weighted. Hence optimizing the time and avoiding disproportionate spending of time on some measures, while others, perhaps more important, are overlooked. As an example a pump failure of a pumping station due to obstruction or power failure during a moderate rain event could result in flooding comparable to the flood caused by an extreme rainfall event. One method to find the cost related to flooding in urban areas is to collect information on documented flood incidents by the insurance companies, as e.g. made in Norway (König et al., 2002) or Brazil (Nascimento et al., 2005). An internationally recognized technique to quantify the damage is the use of "Flood Damage Curves", describing the extent of the damage as a function of land use and water level, refer (Nascimento et al., 2005). Currently, such "Flood Damage Curves" do not exist for any areas in Denmark. The following issues should be included in an assessment of damage related to flooding (Paludan et al. 2010):

1. To prevent that the population is brought into contact with a mixture of sewage and rainwater due to overloading of the drainage systems

2. That vital community functions, such as electricity supply, water supply, heat supply, communication points and access to hospitals are not out of operation due to flooding

3. That the number of affected basements and buildings are minimized

4. That the number of flooded electrical power cabinets and other equipment is minimized

5. The impact from flooding on traffic is minimized.

Risk analysis - Definition of risk concept

A plan for managing risk includes the following seven steps:

1. Identify the risks (e.g. what can go wrong?)
2. Assess the likelihood and consequences of these risks
3. Determine the risk mitigation options
4. Assess the economic, environmental, public relations and operational costs and benefits of the options
5. Prioritize the mitigation option
6. Identify the decision makers
7. Develop the implementation plan.

The steps in a risk analysis are illustrated in Figure . 1.

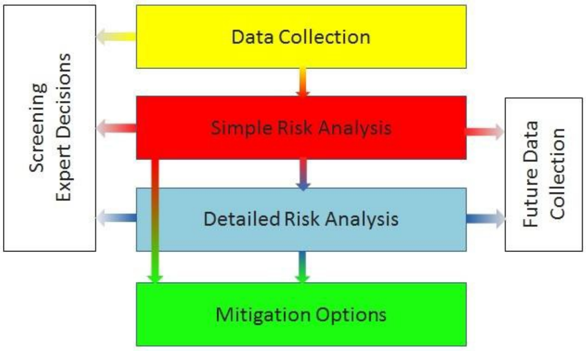

Figure . 1 – The process of risk analysis

The first step is data collection, where knowledge of the drainage system is obtained. This is followed by a coarse risk analysis during which a screening of infrastructure is undertaken by experts and special risk tools. After the coarse risk analysis, there are two options: Either to prepare a detailed risk analysis with focus on selected areas from the coarse risk analysis or to go directly on to identify mitigation measures. If it is decided to proceed with the detailed risk analysis, it is possible to quantify different priority risk mitigation measures. In order to prioritize the selected sites, it is necessary to establish three matrices:

1. A frequency matrix
2. A consequence matrix
3. A risk matrix

The frequency matrix consists of seven intervals named F1 to F7. F1 is an event that statistically occurs less frequently than once every 10,000 years. F7 is an event that statistically occurs 10-100 times a year. The frequency ranges are constructed according to a logarithmic scale. Because of the logarithmic scale it is not important to know the frequencies of adverse events accurately. It is important to know the magnitude of a given event to be used. The frequency matrix is shown in Figure 2.

Frequency Interval	Classification	Frequency per year
daily to monthly	F7	10 – 100
Monthly to year	F6	1 - 10
1 – 10 year	F5	0.1 – 1
10 – 100 year	F4	0.01 – 0.1
100 – 1000 year	F3	0.001 – 0.01
1000 – 10000 year	F2	0.0001 – 0.001
< 10000 year	F1	0.00001 – 0.0001

Figure 2 – The frequency matrix. Source: "Urban Climate Change", DANVA 2011

A logarithmic scale is used between the individual impact categories in the matrix to make it possible to compare the impact groups. "Negligible" for instance indicates an economic value of 10,000 to 100,000 DKK, while "Marginal" indicates a value between 100,000 and 1 million DKK. The economic scale used in the consequence matrix is not arbitrary. Each figure is estimated from available sources and practical guidance numbers. The consequence matrix can describe the different impact categories ranging from no/negligible impact to the disastrous impact described in both qualitative and quantitative terms. The accumulated risk matrix is shown in Figure 3.

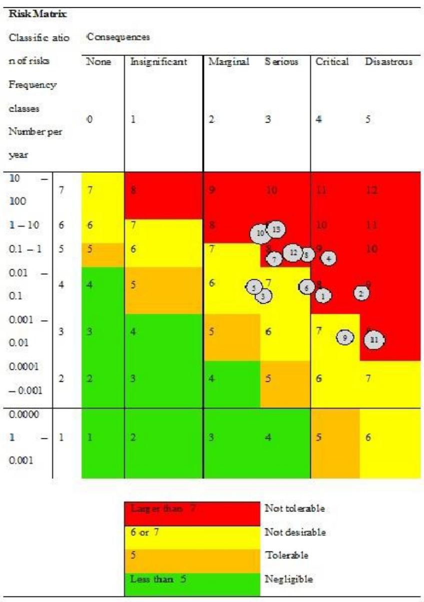

Figure 3 – Risk matrix. In the matrix are examples of selected sites in sewers placed in relation to the assessed frequencies and consequences. Source: "Urban Climate Change", DANVA 2011

Four colors are used in the risk matrix to indicate whether the calculated risk level for a given event is tolerable or not. A risk level above six or seven shall lead to implementation of defined actions to reduce risk levels. According to Figure .3 identified mitigation measures must be implemented for the two events classified in the non-tolerable region indicated by circle No. 4 and No. 13 in Figure 3.

All items located in the yellow area should be evaluated based on a cost-benefit-analysis that can determine what and how much is required to reduce the level of risk and whether an investment should be made here and now, or only when the impact occurs. An analysis provides the basis for assessing the risk level for the entire drainage system and to assess this level relative to the acceptance threshold defined in the risk matrix. For incidents above the acceptance threshold risk mitigation measures must be identified and implemented. For incidents which lie in the acceptance area, an identification of optional mitigation measures must be undertaken and assessed through a cost-benefit-analysis.

Risk of flooding from extreme rainfall

A risk analysis of flooding from extreme rainfall alone can be based on flood maps (Mark and Djordjević, 2006). The simulation results of rain with high return periods may be plotted using GIS themes or aerial photos in order to identify problematic areas. Each area must be assessed as to whether flooding is a problem and whether there may be damages. The assessment shall be based on the following considerations:

- If a park or football field is flooded for a given return period, is it acceptable? Is the inundation from a separate or combined system? How long does it take before the area can be used again and is clean-up required?
- What flood levels will affect basements, first floor, electrical cabinets or parked cars, etc.?
- How much does the number of different damages increase caused by climate change? Is there a risk of more damages related to urban development and what is the flood impact from planned upgrades of drainage system? Can damages caused by flooding be exported to other locations?
- What is the level of uncertainty in the model results? How well is the model calibrated, and has a safety factor been included? Is it reasonable to interpret the results directly, or should a safety factor be applied to the results?

Compilation of damages

The cost of flood damage varies depending on what is damaged, if the damaged items have been completely or partly written off, replacement cost, etc. Moreover, the cost depends on whether the flooding was caused by rain water and sewage, and where the flooding occurred. It is therefore very difficult to generalize the damage costs. A general list that accurately describes the cost of flooding of electrical cabinets, basements, houses etc. cannot be developed. It is therefore recommended to first determine the number of damages by type and then to cost the damage.

To quantify the loss by flooding it is desirable to have a geographical overview of what values might be flooded. Typically, municipalities have records of where the buildings are located, and housing registration contains information about location of basements. The basis for the comparison is established by combining the building theme and the house registration data. Public buildings will often have a higher value than a single dwelling, so it may be appropriate to categorize the public institutions in terms of use, i.e. as kindergarten or a nursing home.

Streets convey rainfall water into the drains. However, when the capacity of the drainage system is exceeded the water may surcharge to the roads. The roads are then used to convey the excess water during the rainfall event (Mark et al. 2004). In these situations it is important to know estimates of water depths, water velocities and where the water flows. Roads are usually designed to drain storm water quickly and efficiently. However, when there are significant amounts of water on roads, it might conflict with the original design of the road. If an analysis shows that a road under future climate conditions will be flooded more frequently, it should be discussed and resolved with the road authorities. The road construction may be adapted. In connection with damage assessments of roads it is pertinent to examine the criteria for the operation: How much water on the road is allowed by the authorities before the road must be closed? And to investigate the road quality, so it can be determined how much water it takes to destroy the foundation of the road and how long the road can be flooded before damage occurs.

Valuation

The following parameters can be used for valuation of flooding:

- Housing

- Kindergartens

- Nursing homes and sheltered housing

- Water distribution. Flooding of the building of the water treatment plant causing possible contamination of clean water

- Water wells, flooding may lead to contamination of the bore field

- Petrol stations where there may be a risk of water flowing into the tanks, so that the petrol runs out (Service Stations with newsstand sales, Auto Service, etc.)
- Areas of storage of oil and hazardous waste near recipients

- Companies with oil and petrol separators connected to the sewage system and storm water system. Oil/gasoline may either surcharge inside a building or outside (it will run approx. 50-100l from each separator)

- Especially for wastewater systems:
  - Avoid overflows from sewage pumping stations
  - Avoid swimming pools becoming contaminated with sewage.

It is important that people with the greatest knowledge of the area being examined are consulted to determine appropriate values for the various categories above. In some cases, the GIS staff has a good overview of the information available. The boundaries of what can be illustrated and calculated from GIS primarily depends on what information is available. Below are a few examples for inspiration.

Figure 4 shows a theme with houses inundated by various return periods. The GIS layer of simulated floods is linked to the GIS layer of houses taking into account the foundation level. In Figure 5 the electricity cabinets are illustrated with floods exceeding 40 cm, by which flooded electricity cabinets can be identified and counted. Figure 6 and Figure 7 show the specific buildings plotted together with extent of the flooding and flood depth. In this example schools, kindergartens and service stations are shown. This type of GIS illustration shows how and where health or environmental issues may arise.

Figure 4 – Example of GIS theme of the houses flooded at different return periods. Source: "Urban Climate Change", DANVA 2011

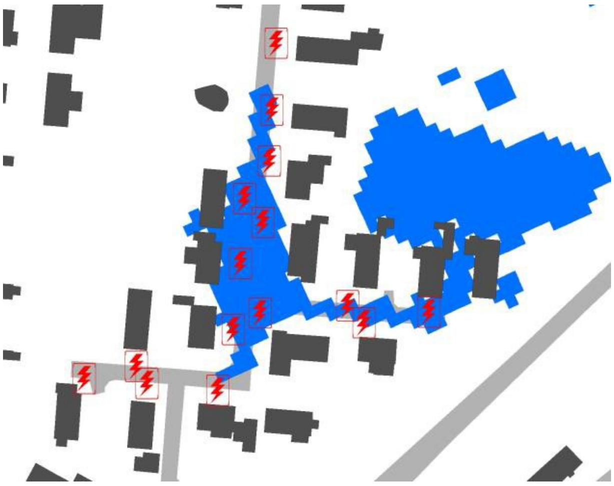

Figure 5 – Example of GIS theme of electrical cabinets damaged. Placement of electrical cabinets is pictured together with water levels above 40 cm. Source: "Urban Climate Change", DANVA 2011

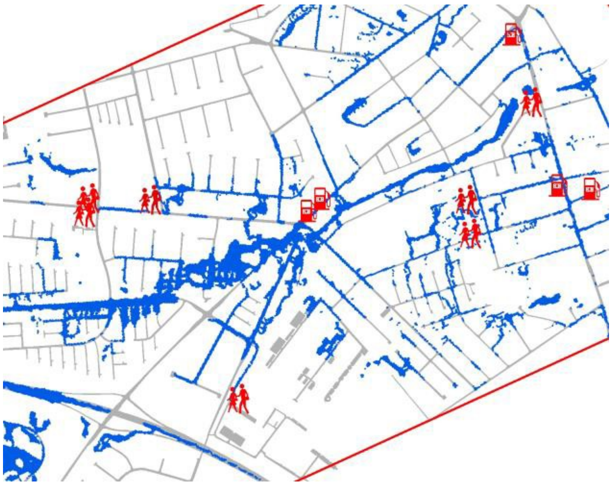

Figure 6 – Example of GIS theme showing specific buildings. Flood propagation is pictured together with the location of schools and kindergartens and gas stations. Source: "Urban Climate Change", DANVA 2011

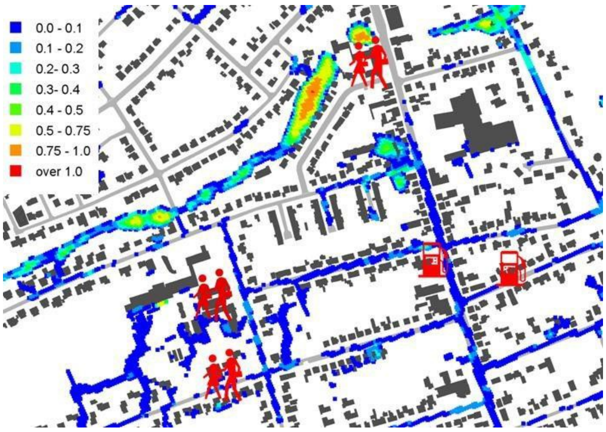

Figure 7 – Example of GIS theme showing specific buildings. Flood levels are pictured together with the location of schools, kindergartens and gas stations. Source: "Urban Climate Change", DANVA 2011

For valuation of a new road foundation the following should be noted:

- It varies according to thickness, etc.
- Most expensive is asphalt layered roads. In this situation it will be necessary to remove and deposit the asphalt before construction of new foundation, followed by a new asphalt pavement.
- In parts of the foundation there will be cables, and costs associated with coping and any repairs due to damage caused by replacement of the foundation are impossible to estimate. Worst case = much more expensive than road foundation and asphalt replacement.

Priority adapting to floods under a changing climate

As it appears the risk analysis can be used as a basis for prioritizing actions to prevent floods and to adapt to climate change, but in many cases it will not be necessary to implement the full risk analysis to get started. Analyses of climate adaptation can be achieved at many different levels. These methods can be used for different degrees of priority: Establishing a basis for getting started, where models shall be established, prioritizing measurement programs, prioritization of specific climate adaptation in the form of installations, priority for emergency action, etc. In relation to the specific climate adaptation it will be necessary to implement priorities of both the economy as technical measures, which are highly political decisions, but the political decisions must obviously be made on a sound technical basis. Priorities can be carried out based on assessments of risks of flooding, but can also be implemented based on economic assessments: Where do you get the greatest reduction in flood risk or most climate change adaptation for the money? Prioritization of climate change adaptation can be based on the climate-meter. Among others it will be possible to prioritize where to undertake registration of the pipe network if it is not available in a digital form. The digitization can be undertaken based on the relatively simple Depression Map Method combined with a simple hydraulic mode.

Flood emergency preparedness

Municipalities shall determine the desired standards of services which they will offer citizens. This has to be done under conditions that are more extreme than the defined desired standards of service which cannot prevent floods. However, it is possible to minimize damage and inconvenience by increasing emergency preparedness. The level of flood emergency preparedness needs to be balanced by the financial effort (see Section: Risk).

Preparedness involves a wide range of activities and assessments that can protect assets and people from damage caused by water. The contingency plans should of course contain important phone numbers and other important administrative information, but in this report only the hydraulic aspects of preparedness will be discussed.

Preparedness can be divided into before, during and after because the state of emergency must be investigated and planned before it occurs, actions may be required during the emergency situation and there will be an evaluation after the event where the experience will be evaluated and possibly incorporated into new updated contingency plans.

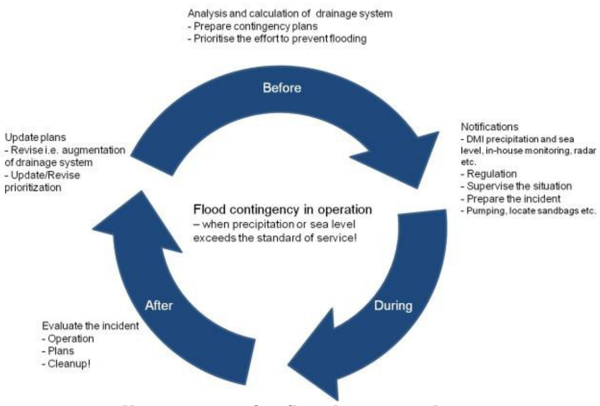

Figure 9 – Illustration of a flood preparedness

In the following sections the flood preparedness components are elaborated.

Before the rainfall event

Establishment of contingency plans if necessary for climate change adaptation.

All municipalities should, as a part of the overall civilian preparedness, have a contingency plan in place. There is currently no requirement for the municipalities to develop a specific plan for operation of urban drainage systems and wastewater treatment plants. Some municipalities have, however, made such plans which accommodate a number of issues that are critical to the operation of the urban drainage system, e.g. power failures, flood damages in exposed locations, staff/contractor preparedness for emergencies that could maintain a minimum service level.

Contingency plans are plans which are used by municipalities to respond to overloads to urban drainage system and water surcharges to terrain, and they include:

Actual physical measures to reduce the effects of an extreme rainfall situation and resulting floods such as earth embankments and walls designed to hold water back in pre-defined depressions.
Preparedness for emergency ad hoc efforts, i.e. placement of sandbags and use of mobile pumps
Information/alerts both internally within the municipality's operations and externally

Preparatory work must be undertaken where all details related to physical measures, acute ad hoc efforts, information and alerts are reviewed.

Priority for contingency plans

Contingency plans should be available to all urban and possibly rural areas where it is estimated that flooding may cause significant either human health related or costly damages. Once contingency plans have been established for a large area, e.g. a municipality or a region, priorities for all catchment areas in the region should be set. This must be done before a critical situation occurs, because there might not be sufficient personnel and equipment available to implement the effort in all catchments at once. A prioritized contingency plan would be a good decision support tool for incident management team. The hierarchy of plans can be implemented using the same principles as the prioritization of climate change adaptation.

Structural responses to flooding

In relation to obtaining a climate change service level for a catchment area, analysis and detailed projects will uncover the critical issues within the area. The solutions that exist could to some degree be expanded without significant additional costs. It may also be required to be able to protect vulnerable housing areas using banks of earth or terrain regulated through embankments or excavation so that water can be conveyed to less critical areas.

Examples of permanent measures include embankment at Godsparken in Greve, DK to prevent a river from flowing into an urban area, and a gutter near the Sports Park in Odense, which convey the water onto the running path to avoid damage to floors in buildings. The embankment at Godsparken is not expensive in construction and ensures not only against extreme long term rainfall, but also against extreme water levels in the ocean.

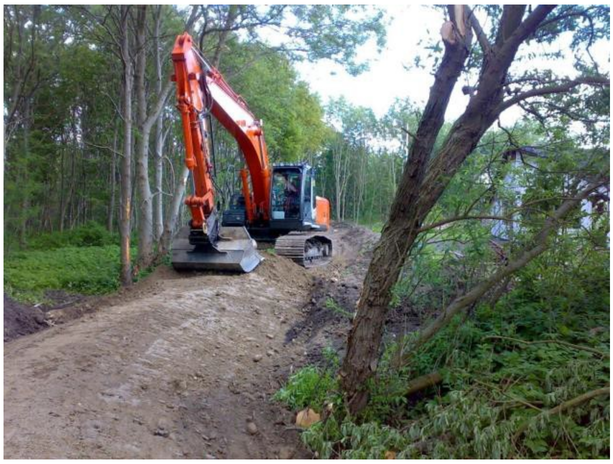
Figure 10 – Establishment of embankment at Godsparken in Greve. Source: "Urban Climate Change", DANVA 2011

Mobile preparedness actions

Besides the stationary emergency response there is a wide range of possibilities for mobile emergency measures, e.g. mobile pumps, sandbags and shutters. Partly through terrain analysis, calculations and experiences a strategy can be created in advance for how surface water is conveyed in an emergency situation and the necessary dimensions for pumps and mobile walls can be assessed. It is essential that the number and precise location of such sandbags is known and that everything is available in stock and ready before the situation arises.

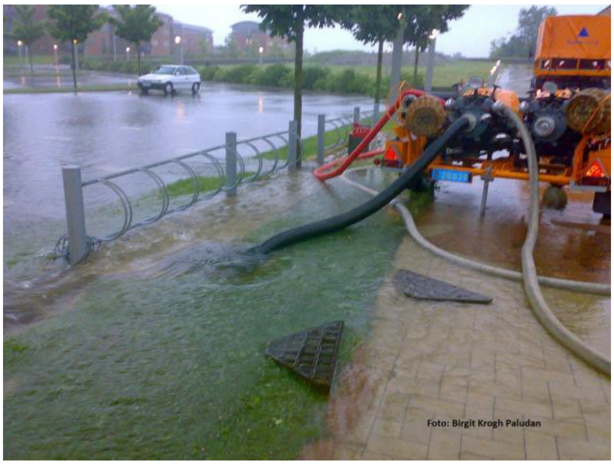

Figure 11 – Mobile pump used at Greve Gymnasium during extreme rainfall in Greve on 5th July 2010. Source: "Urban Climate Change", DANVA 2011

Warning

It is essential that the municipality and wastewater utility is warned about possible adverse events that should be acted upon. Meanwhile, it is also appropriate that citizens are warned that flooding is expected and advised to secure personal belongings.

A number of meteorological institutes forecast heavy rainfall events today, but the risk of subsequent floods in cities is often based on experience. This is inadequate because local conditions in the urban drainage systems determine if flooding occurs or not. Alerts are currently used in selected locations abroad to reduce costs associated with flooding. Can the urban drainage system for instance be partially emptied until rain arrives, or traffic radio can be used to warn people to stay away from urban areas at risk of flooding, cf. Chumchean et al. 2005.

Some floods are acceptable if people are informed in a timely and appropriate manner about how to behave. However, this requires that the municipality is in possession of an appropriate action and contingency plan that can be executed when an extreme rainfall is warned. If an analysis shows that there will be flooding in an area under future climate change conditions which are not acceptable, then it will take some time from the analysis is performed until new infrastructure is built. In this period a warning is useful.

When the warning comes into force, it is important that the wastewater utility has a communication channel set up through which information to the citizens about the measures affecting them can be communicated. Before the emergency situation occurs, citizens must be aware of how to seek information: Website, radio or similar.

It is appropriate to have a contingency plan based on a warning of heavy rainfall for viaducts or similar flood prone sites. Using the warning, such sites can be isolated before the flood is so high that people are at risk if attempting to walk or drive through the water. Whether the warning will be appropriate and economically viable must be assessed on a case-by-case basis.

Responses to the flooding may depend on:

- Existing storage basins, canals, streams, rivers and lakes that can be drained before the emergency situation arises, ensuring an optimum volume available in the systems.

- How soon operational staff can be warned so they are ready to implement contingency plans

- Existing grates, outlets, non-return valves, etc. are reviewed to ensure that they are fully operational before the rainfall occurs.

During the rainfall event

During the extreme rainfall and the time just after (depending on rainfall character) the urban drainage systems are monitored and the contingency plans are initiated when required.

Capture of evidence and experience

To ensure that the entire organization will be wiser from the experience gained during the incident, it is very important to conduct a detailed documentation of the incident. The documentation should include at least the log of adjustments and operation actions in urban drainage system (who has done what and when), and preferably include notes of why and on what basis the action was implemented. Observations in the field are very valuable (preferably with pictures) when experience should be used in further analysis and possible in updating the contingency plans.

After a flood event very detailed knowledge of what exactly happened during the incident is required.

After the rainfall event

After the floods a clean-up of both the urban drainage systems and the terrain is required. It must be ensured that facilities have not have damaged and that the function and capacity have not been reduced by trapped items.

Updating contingency plans

Thorough documentation and experience of the flooding incident may be used to evaluate whether the contingency plans need to be updated. This includes evaluation of the prioritization of the plans, whether the hydraulic model requires recalibration after the incident as well as finding solutions to the challenges or ensuring that service levels are met.

Operating experience

It is valuable to compare experiences with expectations and conclude if flooding is caused by operational problems or lack of capacity in the urban drainage systems.

Case Study

The method described above was used in Greve, Denmark to enable politicians to decide whether to adapt to climate change or not and to what extent. The method was applied to the most vulnerable area in the municipality and the cost was calculated. In Greve Municipality it is politically decided that the entire drainage system in the city shall be upgraded to a maximum flooding frequency of once every 10 year. Based on experiences from the flooding in 2002 and 2007 (see Figure 12) and a vulnerability map prepared using a GIS model the municipality is divided into 42 urban areas and the climate adaptation is prioritized over the next 12-15 years.

Figure 12 – Flooding, Greve 2002 – before adaptation to climate changes

Prioritization is carried out by the motto: those areas which have been hit the hardest will be adapted first. An approach which is politically accepted. The hydraulic models will be developed and improved through measurement campaigns and experiences. If these models show that there is reason to prioritize differently than is done here, reprioritization will be made and presented to the political system. Economic issues may similarly prove it necessary to reprioritize, e.g. if a relatively simple and

Inexpensive measures will have significant positive impact on climate adaptation. For the prioritization is used:

- Lessons from the floods in July 2007, which is reported directly from citizens or landowners.

- The digitization of storm water system.

- The digital terrain model for Greve Municipality which is used to calculate the depth of surface depressions.

GIS themes of buildings in the municipality and the theme of business and public buildings.

Figure 13 shows the prioritizing Greve. If only a few previous flooding experiences exist in a city, terrain models or/and hydraulic modelling can be used to prioritize which areas to work on first. In Greve a model of the total storm water system (including streams) has been developed. To simulate flow on the terrain the digital terrain model has been used to locate depressions in the city areas. This model, called "the strategic hydraulic model of Greve" has been used to quality assure the prioritization.

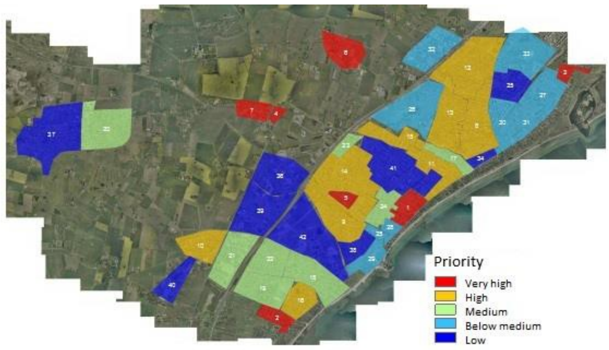

Figure 13 – The prioritized city area of Greve, Denmark

Detailed emergency plans are in the process of being prepared for all areas to minimize the material damage and health risk in case of extreme rainfall. An example is shown in Figure 14.

Figure 14 – Extreme rainfall. Left: Without activating an emergency plan. Right: Activating an emergency plan

Summary and conclusions

Increased frequency and intensity of flooding events, combined with trends in growing urban population in most countries have led to the need for increased and internationally coordinated efforts to enhance technologies and policies for dealing with floods. On the top of today's flood problems come the impacts from climate change, which in many places will aggravate the situation.

Estimates of impacts from climate changes are proposed to be carried out by use of flood modelling and based on the flood maps, transparent and informed decisions must be made – taking the uncertainty into account. After the flood impact assessment, the problems should be prioritized e.g. by use of risk assessment tools. Based on the findings the municipalities must develop a plan for timely management and mitigation of the impacts from climate changes. The plan should contain descriptions of how and when climate changes are analyzed and managed for:

1. Planning and design of new sewer systems.
2. Existing sewers where maintenance and reconstruction are already planned.
3. Existing sewers where no maintenance and reconstruction are scheduled today.

Case studies on the mitigation of the climate change impacts have been carried out in a number of places around The World, e.g. for catchment areas in Sweden and Denmark (Mark et al, 2008).

The development of flood mitigation strategies for sewer systems under the impact of climate changes has resulted in sets of guidelines for municipalities (DANVA, 2011). It is believed that such sets of guidelines will provide the municipalities with a timely and cost efficient strategy for coping with climate changes and their impacts on sewer system.

References

[1] Chumchean, S., Einfalt, T., Vibulsirikul, P., Mark, O. 2005. "To prevent floods in Bangkok: An operational radar and RTC application - Rainfall forecasting".10th International Conference on Urban Drainage, Copenhagen, Denmark, August 2005

[2] Nascimento, N., Baptista, M., Silva, A., Machado, M. L., 2005. "Flood-damage curves: Methodological development for the Brazilian context". 10th International Conference on Urban Drainage, Copenhagen, Denmark, August 2005

[3] Speight, L., 2006. "Analysis of the causes of flood risk in urban areas". The University of Newcastle upon Tyne.

[4] IPCC (2007) Rapports from FN's International Climate Panel. ipcc.ch/publications_and_data/ar4/syr/en/contents.html

[5] Domingo, N.D.F., Sunyer, M.A., Hansen, F., Madsen, H., Mark, O., Paludan, B., 2010. Modelling of sea level rise and subsequent urban flooding due to climate changes, SimHydro 2010: Hydraulic modeling and uncertainty, 2-4 June, 2010, Nice, France.

[6] Djordjević´. S., Butler, D., Gourbesville, P., Mark, O., Pasche, E. " New policies to deal with cli-mate change and other drivers impacting on resilience to flooding in urban areas: the CORFU ap-proach". Environmental science & policy 14 (2011) 864–873.

[7] Paludan, B., Brink-Kjær, A., Nielsen, N.H., Linde, J. J., Jensen, L.N., Mark, O. "Climate change management in drainage systems – A "Climate Cookbook" for adapting to climate changes. No-vatech, France 2010.

[8] Mark, O., Svensson, G., König, A., Linde, J. J., (2008). "Analyses and Adaptation of Climate Change Impacts on Urban Drainage Systems". 11th International Conference on Urban Drain-age, Edinburgh, Scotland, UK, 2008.

[9] Mark, O., Djordjević, S., (2006) "While waiting for the next flood in your city…". 7th Interna-tional Conference on Hydroinformatics – Nice, France.

[10] Parkinson, J., Mark, O. (2005). "Urban Stormwater Management in Developing Countries". A book - 225 pages published by "The International Water Association" (IWA). ISBN: 1843390574.

[11] Mark, O., Weesakul, S., Apirumanekul, C., Boonya Aroonnet, S., Djordjević. S. 2004. "Potential and limitations of 1-D modelling of urban flooding". Journal of Hydrology. 2004

[12] DANVA, 2011. "Urban Climate Change" (Orginal title: En kogebog for analyser af klimaændringers effekter på oversvømmelser i byer"). ISBN: 978-87-92651-04-4.

Mitigating Water Insecurity through Disaster Preparedness in Korea

CHOI Byungman

Abstract. Recently, the global environmental change including climate change, is the hot discussion topic in water resources and efficient water use, securement and management are emphasized for solution of urgent water insecurity problem. In Korea's water resources status, the annual average precipitation is 1,274mm and it is 1.6 times of the world average 807mm. The total amount of precipitation per capita is 2,660 m^3/yr and it is only 1/6 times comparing with 16,427 m^3/yr due to the high population density. Most of the rainfall is concentrated on Jun – Sep in Korea.

For water insecurity in Korea, according to the impacts of climate change, such as floods, drought and rising average temperature in parallel with the water management difficulties, a variety of efforts are need to solve mitigate these insecurity. As the concept of water activities, many water resources management techniques are integrated and applied such as national, regional and international levels of policy and structural/non-structural measures and related water management guidelines

To secure stable water and cope with climate change, the whole world including Korea has seek countermeasures for water-related disasters such as extreme floods and droughts, earthquakes, tsunamis, etc. In recent years, for conjunction with the concept of water insecurity, a variety of research, international activities and policy to response water insecurity are carried out and especially in terms of water quantity and quality. Detailed field activities led to major institutions around the water-related are as follows ① Mitigation of water-related disasters ② Water dispute ③ Water divide for a stable water supply ④ Balanced environment ⑤ Water reuse ⑥ reduce water pollution. Finally, the integration of a various measurement and policy is close to solve mitigation of water insecurity.

Keywords *Climate change, water disaster, insecurity, water security, enhancement*

CHOI Byungman
Executive Director of K-water Institute and Co-chair of the Regional Process Commission of the 7th World Water Forum
Daejeon, Korea
bmchoi@kwater.or.kr

Introduction

According to the Korea Meteorological Administration (KMA), the average annual wind speed, relative humidity and amount of cloud has expected no significant change in the level of both the RCP 4.5 and RCP 8.5 scenario in Korea, but temperature indices such as extreme heat wave days and tropical nights have been forecasted as rapid increase trends. Comparing with current climate pattern, the average annual rainfall shows the increment of early term 6.2%, middle term 10.5%, and late term 16.0% during the 21st century in the RCP 4.5 scenario and early term 3.3%, middle term 15.5%, and late term 17.6% during the 21st century in the RCP 8.5 scenario. About the Korea's future climate change, it is expected to remain in the observations of the past 30 years by 2100.

For the flood risk, the numbers of the localized heavy rain more than 100mm/day will increase more than 2.7 times as comparing the past. And the 100 year frequency flood will increase 20%, so embankment capacity to defense the present 100 or 200 year frequency flood will reduce half times. In addition, it is expected that the disaster such as debris flows and landslides increase.

For the drought risk, the drought period will increase at 3.4 times comparing the past because of the years of the less rain increase, therefore temperature rise will bring about the shortage of living, industrial, agricultural and river maintenance water. As rainy season move to July ~ September from June ~ August, the shortage of rainfall by June of expecting much agricultural yields will lead to the decrease of agriculture products.

For the water quality and river environment risk, because of the water temperature rise, hypoxia phenomena of river and reservoir will cause adverse impact of hydro-ecological system such as the fish mortality. The increase of rainfall intensity and long-term drought will cause turbidity and water quality deterioration

Such aspirations on the accurate prediction of water state is unattainable due to both complicated states of climate change and of the environment. However, water disaster, a difficult and unlcear problem, should also be addressed appropriately.

Insecurity of Climate Change in Korea

South Korea is more 65% mountainous area of the country, rainfall falls in intensive in June-August of the summer. Especially, it is hard to use water resource due to a big deviation of precipitation during a flood season in many water flowing into the sea, in fact it can be more severe serious circumstances.

In Korea's water resources status, the annual average precipitation is 1,274mm(1973~2011) 1.6 times of the world average 807mm. The total amount of precipitation per capita is 2,660 ㎥ and it is only 1/6 times comparing with 16,427 ㎥/yr due to the high population density.

However, the current important factor of climate change has been more added and became more difficult to manage water resource.

Fig.1 Topographical condition of Korea

Fig. 2 A variety of seasonal water-related disasters in Korea

Fig. 3 Variation of streamflow in Korea

Without a doubt, climate change due to global warming is one of the most urgent issues in today's world. Climate change is not a far-fetched threat in the distant future but a threat currently in progress. With the drastic rise in temperature and unpredictable precipitation changes and droughts, disasters never experienced before are happening more frequently. In the past 150 years, the Earth's average temperature increased by about 0.7℃ and sea level has risen about 15 ㎝. All around the world, drought, floods, human and material losses, as well as conflicts over water are increasingly intensifying because of unusual changes to the climate. According to data provided by the research institute of the Korea Meteorological Administration (KMA), yearly distribution of precipitation on the Korean Peninsula used to have two distinct heavy rain seasons in July and September with similar precipitation rates in the past. However, recent trends show that the distinction between the primary and the secondary heavy rain seasons is gradually disappearing and the secondary heavy rain season shows the concentration of heavy torrential rain.

The prospects of the climate changes projected by the KMA near the end of 21st century on the Korean Peninsula are approximately 4℃ increase in temperature and 17% increase in precipitation.

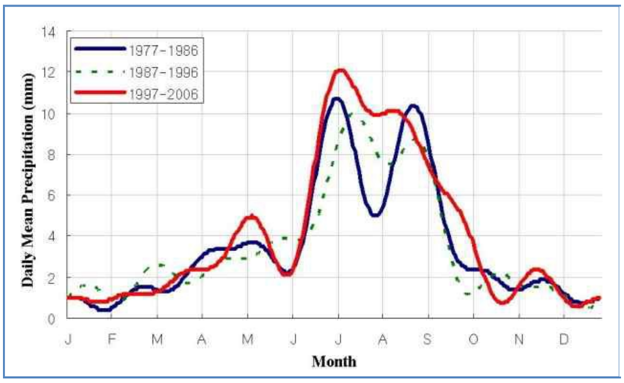

Fig. 4 Daily Mean Precipitation (Past vs. Present) Table

1. Flood Damages (2002 Rusa, 2003 Maemi, 2006 Ewinia)

	Nation	Han	Nakdong	Geum	Yeongsan	Others
Casualties	689	167	126	38	26	332
Damage Amount (Billion KRW)	15,112	2,936	3,943	899	716	6,618

* Total flood damage: $14 billion (2000-2010)

Table 2. Drought Damages

Year	Damages
1994~1995	86 Cities & Counties (173,269 ha)
2001~2002	86 Cities & Counties (304,815 people experienced water supply restriction)
2008~2009	77 Cities & Counties (1,227 Villages experienced water supply restriction)

* Severe drought cycle after 1990 : 7 year ('94→'01→'08)

Water Security

Recently, the global environmental change, including climate change, is the hot discussion topic in water resources and efficient water use, securement and management are emphasized for occurrence of urgent problem to be solved and solution of it. The concept of water security in the world, due to a stable securement of water and climate change the whole world including Korea to seek countermeasures for water-related disasters such as extreme floods and droughts, earthquakes, tsunamis, etc. is considered.

In recent years, for conjunction with the concept of 「water security」, all over the world a variety of research, international activities and policy to meet water security are carried out and especially in terms of water quantity and quality.
For water security in Korea, according to the impacts of climate change, such as floods, drought and rising average temperature in parallel with the water management difficulties, a variety of efforts are being performed.
As the concept of water activities, such as national, regional and international levels of policy and structural, non-structural measures, and corresponding guidelines that need to be managed organically integrated together to preemptively respond to climate change, sustainable water security efforts is required. In fact, these water crisis affects all aspect of national security.

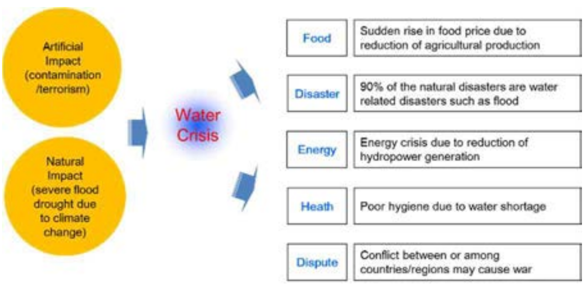

Fig. 5 Water crisis efffects

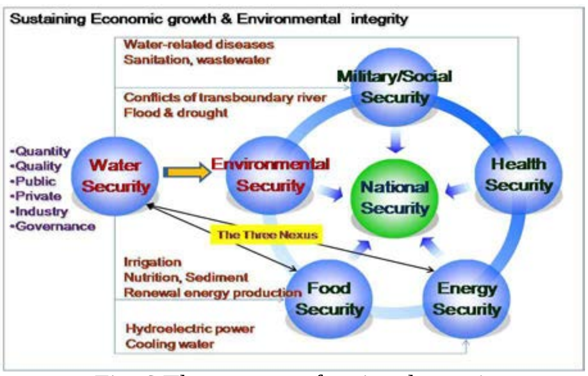

Fig. 6 Three nexus of national security

Enhancement of Flood Control Capacity

The trend of rainfall intensity during a flood season is increasing in the South Korea because of climate change affect. In 2002, the Rusa was the most powerful typhoon and the rainfall intensity was a record 870mm/day in Gangneung. The re-estimated PMP (Probable Maximum Precipitation) reflected recent flood indicates extremely overestimate at the Soyang River Dam (632 ㎜→810 ㎜, 132%, increase) and the Yeongcheon Dam (241→715 ㎜, 317%, increase) from baseline. According to increasing PMP used design criteria of Dam is extremely advancing adjustment.

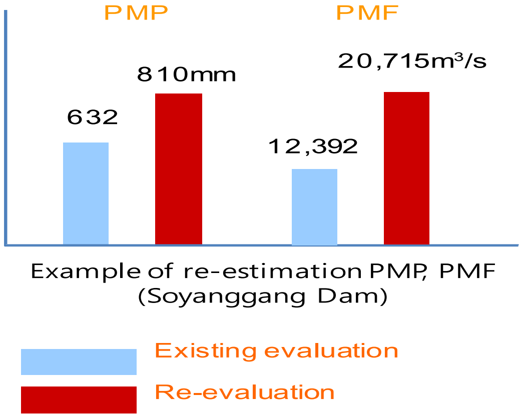

Fig. 7 Re-estimation of PMP, PMF (Soyanggang dam)

There are two methods to increase capacity of flood control and safety of Dam, one is preparing for installing dam at upstream to reduce inflow, the other is increase of overflow by installing water gates where among the current dam cannot response increased PMP or changes design under construction. The safety of dam is related to water resource management and it can be a key factor when the dam was destroyed by overflow during natural disaster. Therefore, this project is the one of the start a global business in earnest to prepare measures of dam safety for prevention dam overflow during flood season. The secure plan of safety increases an ability of flood control from existing dam facility depending on the structure measure or non-structured measure. The non-structured measures are a limited water level set up below a normal condition during flood season and establish a prior overflow plan. The structured measures are increasing dam scale, construction of upstream dam, installing auxiliary spillway and parapet wall, water gate and expanding existing spillway. Usually we apply structure measures to expand an ability of flood control.


Fig. 8 Enhancement of FCC (Soyanggang dam, Auxiliary spillway)

Fig. 9 Enhancement of FCC (Daechung dam, Auxiliary spillway)

Four Major Restoration Project

The Four Major Rivers Restoration Project (4MRRP) was started to respond to climate changes: it is a multi-purpose project that plans to obtain 920 million m^3 of flood control capacity and 1.3 billion m^3 volume of water to prepare for floods and droughts.

Fig. 10 Five Core Tasks of 4MRRP)

Some measures of the Project include the establishment of 570 million m^3 of river sediment dredging, construction of sixteen Weirs and three new Dams, etc. The challenges faced in securing such water resources are improvement in water quality, as well as improvements in the ecology and environment of the rivers. Despite the changes in the condition of flow pattern in the streams, the ratio of 2nd grade water quality will be augmented to 86% in 2012 from the current level of 76%. The Four Major Rivers Restoration Project (4MRRP) was announced in January 2009 as part of the "Green New Deal" policy. It aims to restore the Han River, Nakdong River, Geum River, and Yeongsan River in an eco-friendly manner to supply safe water, to prevent losses from floods, and to add vitality to the ecosystem. Since then, the Project has been included as part of the Five-Year State Plans with 22.2 trillion won state funding as of June 2009, and is currently being carried out. In preparation for future water shortage the 4MRRP aims to achieve the following objectives: securing abundant water resources, implementing comprehensive flood preventive measures, improving water quality, restoring the regional ecosystem, creating multi-purpose space for the local residents, and developing the region surrounding the rivers.

Flood Control	Dredging: 0.45 billion ton, Flood Control & Water Retention: 6 Reinforcing old Levees: 784 km	Decrease Flood Water Level (0.4 - 4m)
Water Security	Weir Construction: 16 Elevation of Reservoir Banks : 93	Increase 1.1 billion tons of water
Water Quality Improvement	Environmental Facilities: 1,281 Farmland Relocation : 156.8 sq. km	Water Quality Grade III → II
Ecological Restoration	Ecological Wetlands: 39 Preserving natural wildlife habitat Fish-way Restoration: 23 sites	Improve Natural Ecology & Promote Eco-tourism
Waterfront Development	Constructing bicycle roads: 1,757km Landscape Sequence Points: 36	Escalate people's quality of life
Green Energy	Small Sized Power Plant : 16 Gross Generation : 271 M kWH/yr	Savings equal to about 250,000 people/yr

Fig. 11 Detailed 4MRRP contents

By protecting such water bowls from the entry of pollutants and clearing farming fields and vinyl greenhouses to restore the rivers and wetlands, and by proliferating endangered fish, it is hoped that the environment and ecosystem of the rivers will come alive again. The Project intends to develop new water-friendly cultural complexes for the public to enjoy once the Rivers become richer and cleaner. In doing so, the Project will contribute toward regional development and increase the value of national territory.

Fig. 12 Disaster mitigation of flood

Fig. 13 Water securement by multi-purpose weir

Water Resources management with ICT

Recent climate change occurs an increase of drought and the frequency of extreme rainfall event, Ministry of Land, Transport and Maritime Affairs (Flood Control Office) and K-water manage advanced water system to make a scientific water resource management. Project of water resource information management is to build database based on a common catchment basin map. Each organization can do analysis for hydrological characteristic, prediction of water supply from each organization's water related data through shared system. We can build up policy and decision-making support system to manage reasonable flood control, water use and environment. We can expect to make integrated management system based on the total water related data from upstream to downstream.

Water resources information has been collected and analyzed by the each department of the Ministry of Land, Transport and Maritime Affairs, the Ministry of environment and Ministry of Agriculture and Forestry. At that time, it is difficult to share water resources information and inconvenient to search and utilize between organization. So we suggest a necessary of homogeneous system which represent a share program of water management information and information support department. And then, the further step is expanding area of water resources management. We firstly set up the network of water resource information as making a common catchment basin map based on the twenty-one basins and the one hundred-seventeen subbbasin to unite formation and unit from each organizations. The standard for water management information consist of 4 parts which are basin separation, work, code, operation system within a common catchment basin map is designated to retain a consistency and to promote cooperate work using integrated database.

Based on the database, 5 departments and 10 water related organizations such as the Ministry of Land, Transport and Maritime Affairs and Ministry of environment are shared by Water Management Information Networking System (WINS) including 65 parts such as a water related information which is hydrology, metrology, and spatial information and so on. Further aims are build up for international water related information circulation system to provide each organization such as the OECD and GEOSS.

Also, we provide a water resource information through Water Resources Management Information System (WAMIS) after scientific processing for collecting, formation, and analysis from each water related organization. WAMIS provides 10 categories which kinds of hydrological meteorology, basin, river, dam, groundwater, and water supply and around 300 a variety of basic database based on water resource unit map using GIS. In addition, it can search water related information depending on the options of the local government on the whole country (256 city public officials) / water resource subbasin (117 subbasins) / river (national/province).

Further propulsion system will compose the three sub system including basic data management system, analysis system, and policy support system to support comprehensive and systematic integrated management

Fig. 14 Water Resources Management Information System

Fig. 15 Technology for Monitoring, Evaluation and Prediction

Summary and Conclusions

For water insecurity in Korea, according to the impacts of climate change, such as floods, drought and rising average temperature in parallel with the water management difficulties, a variety of efforts are need to solve mitigate these insecurity. As the concept of water activities, many water resources management techniques are integrated and applied such as national, regional and international levels of policy and structural/non-structural measures and related water management guidelines

4MRRP is a multi-purpose project aimed at better adapting to the global climate change by responding to the uncertain effects of climate change in the future, as well as promoting the value of national territory by creating a space where the rivers and the people could co-exist.

And water security, enhancement of flood control capacity and management of ICT are essential to cope with uncertain climate change. Therefore, sustainable development and success of the water disaster management will require attention and focused investment in the post period, in various.

Impact assessment of climate change on water-related disasters for building up an adaptation strategy

Yasuto TACHIKAWA

Abstract To estimate probabilistic characteristics of extreme floods and to predict the magnitude of a largest-class flood under a changing climate are a key issue for building up an adaptation strategy. In this research, a physically-based method to estimate a probable largest-class flood and a flood damage assessment method considering probabilistic flood characteristics are introduced. Based on the future flood prediction techniques, an adaptation strategy to cope with flood disasters is discussed.

Keywords *river discharge prediction*, *climate change*, *a largest-class flood*, *flood risk curve*

Introduction

Flood predictions are classified into three categories: the flood magnitude prediction in terms of the flood frequency such as the annual maximum 100-year flood, the largest-class flood prediction such as a probable maximum flood (PMF), and the real-time flood prediction. To improve these flood prediction techniques is a key engineering issue to cope with flood disasters. In this study, a largest class flood prediction and a probabilistic assessment of flood damage occurrence are focused.

To estimate a largest-class flood, a physically-based flood prediction method using a multi-track ensemble numerical typhoon simulation (Ishikawa *et al*., 2012; Oku *et al*., 2014) is proposed. The method was applied to the historical large typhoon, the Ise-Bay Typhoon in 1959 under a present climate condition and a pseudo global warming condition (Takemi *et al*., 2013). The estimated precipitation data was given to a distributed rainfall-runoff simulation model (1K-DHM, Tachikawa and Tanaka) to predict river discharge. The estimated flood magnitude under a pseudo global warming condition is a central issue with respect to an adaptation measure to avoid catastrophic damage.

Yasuto TACHIKAWA
Department of Civil and Earth Resources Engineering, Kyoto University
Kyoto, Japan
tachikawa@hywr.kuciv.kyoto-u.ac.jp

Secondly, a method to develop a flood risk curve is presented to assess flood damage probabilistically. A flood risk curve is a relation between flood inundation damage and its exceedance probability. A procedure to develop a flood risk curve is below: 1) a probability distribution of annual maximum rainfall is obtained from historical record; 2) the relations between the *T*-year annual maximum rainfall and the maximum inundation water depth are obtained through rainfall-runoff and inundation simulations for different spatio-temporal rainfall patterns; 3) economic damage is estimated for each rainfall-runoff and inundation simulation; and finally 4) the relation between economic damage and its exceedance probability is obtained by integrating the exceedance probability of the annual maximum rainfall that causes the inundation damage for all spatio-temporal rainfall patterns. To cope with huge rainfall-runoff and inundation simulations, a nesting rainfall-runoff-inundation method is newly developed to reduce computational burden.

Largest-class flood prediction

Takemi *et al*. (2013) developed a heavy rainfall dataset based on an ensemble simulation of the historical extreme typhoon, the Ise-Bay Typhoon (1959) using a mesoscale meteorological model, the Weather Research Forecasting (WRF) model version 3.1.1. The ensemble simulation method realizes to generate different typhoon tracks perturbed from the original track of the typhoon by applying a potential vorticity inversion (PVI) method (Ishikawa *et al*., 2012; Oku *et al*., 2014). Fig. 1 shows the typhoon tracks simulated by the PVI method for the Ise-Bay Typhoon in 1959. The ensemble simulation approach was also applied to the typhoon under a pseudo global warming condition by setting a different sea surface temperature. The difference of the sea surface temperature was given based on the difference of the monthly mean SST in September between the end 21st century climate experiment (2075-2099) and the present climate experiment (1979-2003) simulated by MRI-AGCM3.2 (Mizuta *et al*., 2012).

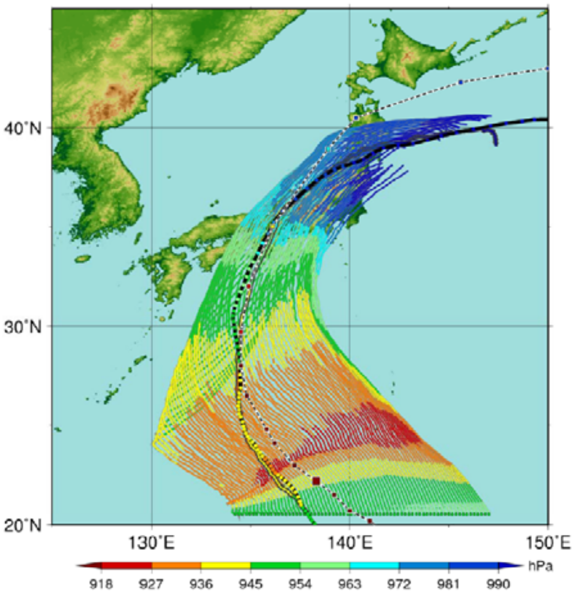

Fig. 1 Virtual shifting of typhoon's initial position for the Ise-Bay Typhoon in 1959 (Takemi *et al.*, 2013).

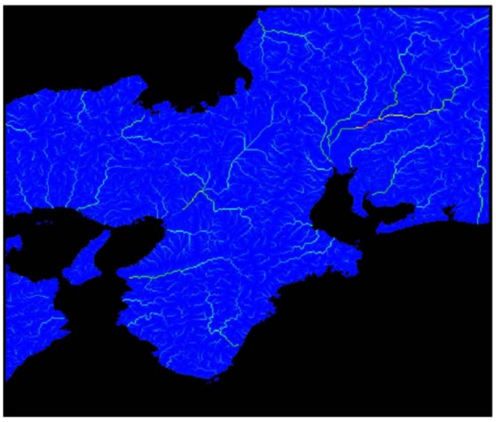

Fig. 2 Spatially distributed river flow for the Central and Kansai regions in Japan simulated by a distributed hydrologic model, 1K-DHM.

The simulated rainfall data was given to a distributed rainfall-runoff model (1K-DHM) developed for the Central and Kansai regions in Japan (Fig. 2). The simulated discharge for each typhoon track was stored with about 1km grid resolution. Fig. 3 shows the simulated hydrographs at the Hirakata station (7,281km^2) in the Yodo River basin for various typhoon tracks. For each grid cell in the study region, the typhoon track which causes the maximum discharge was analyzed. Fig. 4 shows a spatial distribution of the typhoon track number that caused the maximum discharge for each grid cell. The flood runoff simulation results for the present climate condition shown in Fig. 3 underestimate the observed data, however, the ones for the pseudo global warming condition clearly shows the increase of flood flow.

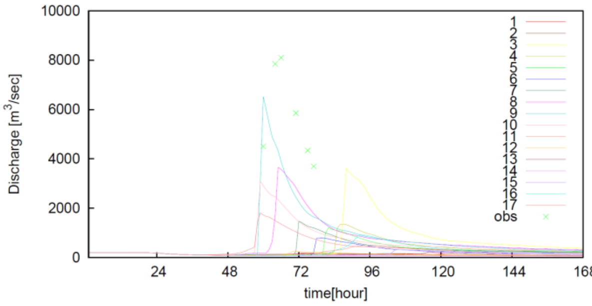

(a) Simulated flood hydrographs for the present climate condition.

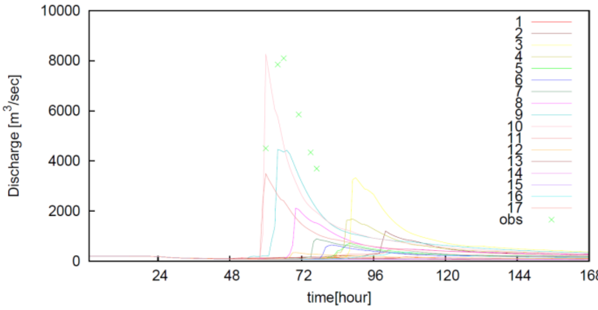

(b) Simulated flood hydrographs for the pseudo global warming condition.

Fig. 3 Simulated flood hydrographs at the Hirakata station (7,281km^2) for different conditions.

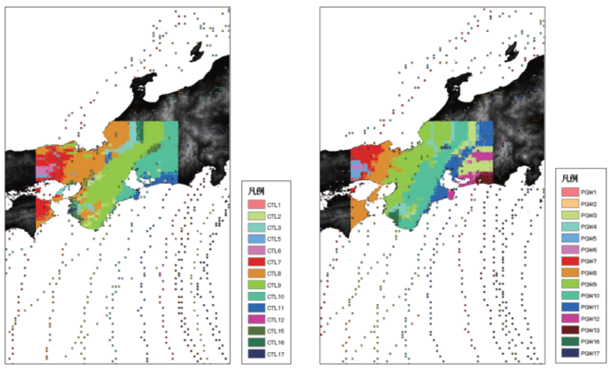

Fig. 4 Spatial distribution of the maximum discharge caused by different typhoon tracks.

New typhoon ensemble simulations using other boundary conditions and for other historical typhoons are ongoing. Improvement of the distributed hydrologic model including introduction of the dam reservoir operations and readjustment of model parameters are also underway. An inundation hydraulic simulation model will be combined with the hydrologic simulation. The method proposed here provides information on physically-based largest-class floods under a changing climate, which is basic information for building up an adaptation strategy.

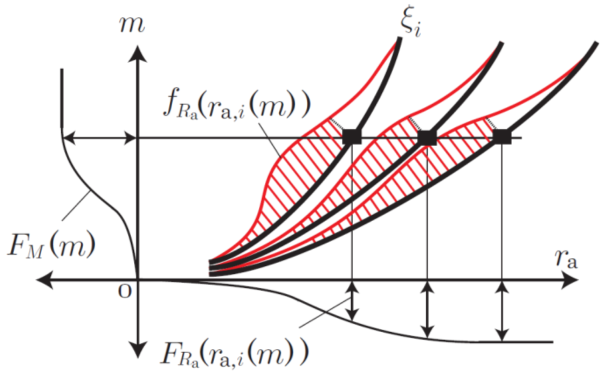

Fig. 5 Schematic explanation of the translation of a distribution function of the *D*-day annual maximum rainfall r_a to a distribution function of inundation damage *m* through various rainfall patterns (Tanaka *et al*., 2015).

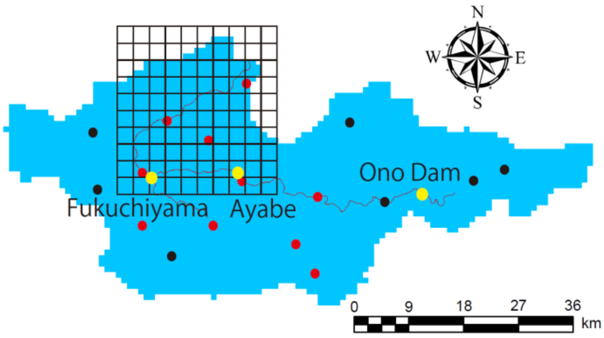

Fig. 6 Yura River basin (1,882 km^2) in Japan. A distributed hydrologic model 1K-DHM was applied to the entire basin and inundation simulations were applied to the gridded area. The black and red marks represent rainfall observation stations and the yellow marks represents river stage gauging stations.

Probabilistic assessment of flood damage using flood risk curve

To manage flood disasters flood risk control based on appropriate risk assessment is essential. To realize an integrated economic risk assessment by flood disasters, a flood risk curve plays an important role. A flood risk curve provides a relation between flood inundation damage and its exceedance probability. A method to obtain the flood risk curve considering the uncertainty of spatio-temporal rainfall distribution is newly proposed (Tanaka *et al*., 2015).

A flood risk curve is generated from a probability distribution function of the annual maximum rainfall distribution through the following processes (Fig. 5): 1) to prepare typical extreme rainfall patterns ξ_i; 2) to obtain a probability distribution of the annual maximum rainfall $F_R(r_a)$ from the historical data; 3) to obtain relations between *T*-year annual maximum rainfall and the maximum inundation water depth through a rainfall-runoff and inundation simulation; and 4) the economic damage m is estimated for each maximum inundation depth caused by the *T*-year annual maximum rainfall r_a. These procedures are conducted for each typical extreme rainfall pattern. Finally, the relation between economic damage m and its exceedance probability $F_M(m)$ is obtained by integrating the exceedance probability of each inundation damage. The schematic instruction of the development of the flood risk curve is shown in Fig. 5. This method requires many rainfall-runoff and inundation simulations, thus a nesting runoff-inundation simulation method to reduce computational costs was also developed.

The method was applied to the Yura River basin (1,882 km^2, Fig. 6) in Japan. Rainfall-runoff simulation was applied to the entire basin using a distributed hydrologic model 1K-DHM with about 1km spatial resolution. Then, inundation simulations were applied to the gridded area located at the lower part of the basin. The estimated spatial distributions of indention depth were used to calculate the indention damage amount using a guideline to estimate the economic damage (MLIT, 2005).

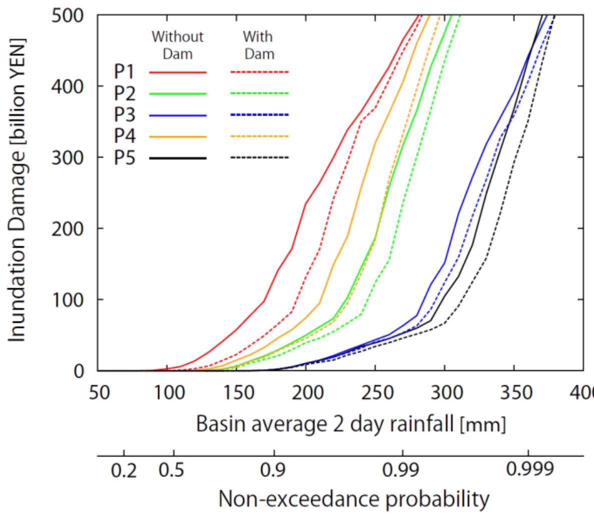

Fig. 7 Relation between the 2-day basin average rainfall and inundation damage estimated by rainfall-runoff and inundation simulations. The lines P1 to P5 show the relation for each rainfall pattern. Solid and dashed lines represent case studies with and without dam operation (Tanaka *et al*., 2015).

Fig. 7 shows the estimated relations between the 2-day basin average rainfall at the Yura River basin and inundation damage obtained by rainfall-runoff and inundation simulations. The lines indicated by P1 to P5 show the relation for each rainfall pattern. Solid and dashed lines represent case studies with the dam operation at the Ono dam and without the dam operation. Each risk curves reflect the magnitude of rainfall and a difference scenario of flood works.

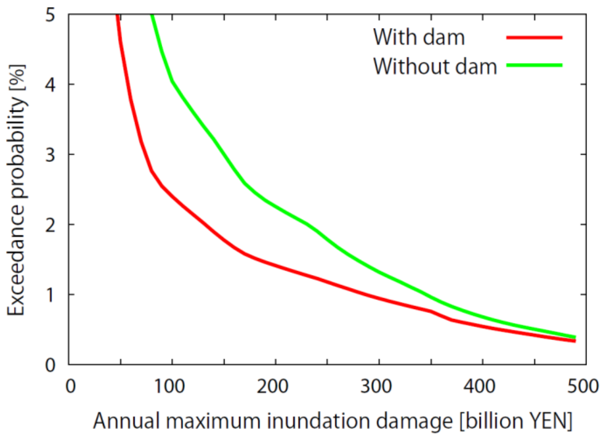

Fig. 8 Estimated flood risk curve at the Yura River basin (Tanaka *et al*., 2015).

Fig 8 show the integrated flood risk curve which was derived by integrating the relation shown in Fig. 7. The flood risk curve considers the spatio-temporal rainfall patterns and a distribution function of the magnitude of rainfall which cause inundation disasters at the Yura River basin. This information reflects the probabilistic occurrence of heavy rainfall and flood under various scenarios, which provides key information to cope with water-related disasters.

Summary and conclusions

In this study, predictions of a largest-class flood and a probabilistic assessment of flood damage occurrence are introduced. To provide a physically-based prediction of a largest-class flood, a rainfall-runoff simulation with the multi-track ensemble numerical typhoon simulation under a pseudo global warming condition was demonstrated. Then, a development of a flood risk curve was presented to assess flood damage probabilistically. The proposed methods provide essential information to develop an adaptation strategy to cope with water-related disasters

Acknowledgement

This research was conducted under the framework of the "Precise Impact Assessments on Climate Change" supported by the SOUSEI Program of the Ministry of Education, Culture, Sports, Science, and Technology. Prof. Takemi for providing the dataset of the multi-track ensemble numerical typhoon simulations was also acknowledged.

References

Ishikawa, H., Oku, Y., Kim, S., Takemi, T. and Yoshino, J. (2013) Estimation of a possible maximum flood event in the Tone River basin, Japan caused by a tropical cyclone, Hydrological Processes, 27(23), 3292–3300.

Ministry of Land, Infrastructure, Transport and Tourism of Japan, Water and Disaster Management Bureau (2005) A guideline of economic survey for flood control (in Japanese).

Mizuta, R., Yoshimura, H., Murakami, H., Matsueda, M., Endo, H., Ose, T., Kamiguchi, K., Hosaka, M., Sugi, M., Yukimoto, S., Kusunoki, S. and Kitoh, A. (2012) Climate simulations using MRI-AGCM3.2 with 20-km grid. J. Meteor. Soc. Japan, 90A, 233-258. doi:10.2151/jmsj.2012-A12.

Oku, Y., Yoshino, J., Takemi, T. and Ishikawa, H. (2014) Assessment of heavy rainfall-induced disaster potential based on an ensemble simulation of Typhoon Talas (2011) with controlled track and intensity. *Natural Hazards and Earth System Sciences*, 14, 2699-2709, doi:10.5194/nhess-14-2699-2014.

Tachikawa, Y., Ishii, D. and Yorozu, K. (2014) Probable maximum flood estimation by extreme typhoons under a changing climate, International Conference on Ecohydrology (ICE) in Conjunction with the 22nd Meeting of UNESCO IHP Regional Steering Committee (RSC) for South Asia and Pacific, Yogyakarta, Indonesia, 10-12, November 2014.

Tachikawa, Y. and Tanaka, T. (2014) 1K-FRM/DHM, A distributed river discharge simulation model based on kinematic wave theory using HydroSHED topography data, http://hywr.kuciv.kyoto-u.ac.jp/products/1K-DHM/1K-DHM.htm.

Takemi, T, Ishikawa, T., Oku, Y. and Okada, Y (2013) Ensemble experiment for the Ise-Bay Typhoon, SOUSEI Program for Risk Information on Climate Change, Research Report, Heisei 24, 16-18 (in Japanese).

Tanaka, T., Tachikawa, Y. and Yorozu, K. (2015) A flood risk curve development for inundation disaster considering spatio-temporal rainfall distribution, Journal of Japan Society of Civil Engineers, Ser. B1 (Hydraulic Engineering), 71(4), accepted (in Japanese).

Development of operational flood optimization within the flood forecasting system to determine the optimal release for Ubonrat reservoir for flood mitigation

Sathit Chantip [1, a *], Watin Thanathanphon [2, b], Piyamarn Sisomphon [3,c] and Surajate Boonya-aroonnet [4,d]

Abstract The development of flood forecasting and optimization system aim to determine the optimal reservoir release within the 7-days forecasting horizon. By taking into account the impact of the flood forecast together with the downstream flooding criteria, the optimal release can be computed to minimize the downstream flooding while still keeping the safety of the reservoir and its rule curve operation. The system has been developed on the platform of Chi-Mun Flood Forecasting System using DHI Solution Software. The Shuffled Complex Evolution (SCE) is used in the optimizing of reservoir release. The objective functions are reservoir safety, downstream flooding, rule curve and spills. The condition at discharge stations E.22B and E.8A are used as downstream flood control. The system works in parallel with the Chi-Mun flood forecasting system. Trickling by downstream flooding criteria, the system will run automatically when the forecast water level is above the control level. Based on the study results using the flood in 2006, the system performs satisfactory. It provides a better trade-off solution between reservoir safety and downstream adverse effects than considering only the rule curve operation.

Keywords *Optimization, Shuffled Complex Evolution, Flood mitigation*

Sathit Chantip
Hydro and Agro Informatics Institute
HAII
Bangkok , Thailand
sathit@haii.or.th

Watin Thanathanphon
Hydro and Agro Informatics Institute
HAII
Bangkok , Thailand
watin@haii.or.th

Piyamarn Sisomphon
Hydro and Agro Informatics Institute
HAII
Bangkok , Thailand
piyamarn@haii.or.th

Surajate Boonya-aroonnet
Hydro and Agro Informatics Institute
HAII
Bangkok , Thailand
surajate@haii.or.th

1. Introduction

Chi river basin is the biggest basin in the North Eastern part of Thailand. It covers 49,132 sq.km. or 29% of the total basin area in the region. With the constraint in the topography, having a flat flood plain area in the middle of rolling hills and mountains the area experiences flood and drought problems alternatively almost every year. In 2014 Hydro and Agro Informatics Institute (HAII) has developed the decision support system in which it contains both flood forecasting model and water resources management model embedded in the system. With the integration of rainfall forecast model (WRF) the two models utilize this information and run the operation forecast for flood and water balance for the next 7 days. This provides important information for the flood management and early warning. Due to a large volume of flood water river branches, the reservoir operation is considered as one of the important flood control in the Chi basin. Further development has considered the optimization to reduce the flood risk at downstream of Ubol Ratana dam. In this study this reservoir optimization has been developed within the flood operational platform. The 7-days flood forecast has been input to the optimization as one of the criteria to trickle the optimization run. The suggested optimal release with downstream flood risk has been minimized is obtained. This provides a recommendation to support the decision making process for a better flood management.

2. Study area

2.1. Chi river basin

Chi river basin covers an area of about 49,132 sq.km. with population of 6.6 million. The area is a semi-arid area with mainly sandstone plateau characterized by a high mountainous area on the West and the North with a rolling hill and a mild-to-flat slope area in the middle. The Chi River is 946 km long and considered as the longest river in Thailand. Started in the Dong Phayayen Mountains, the Chi River runs East through the provinces of Chaiyaphum, Khon Kaen and Maha Sarakham before turning South in Roi Et and Yasothon to meet the Mun river in Kanthararom District, Sisaket Province. The river runs further East for about 100 km to merge with Mekong River. Chi river basin is divided into 20 sub-basins. The annual averaged rainfall is 1,231 mm with highest averaged monthly rainfall in September (247 mm). The annual averaged runoff is 14,105 MCM which mainly distributed from May to September during the rainy season. The highest averaged monthly runoff occurred in September (2,812 MCM). Figure 1 shows the topography and sub-river basin of Chi river basin.

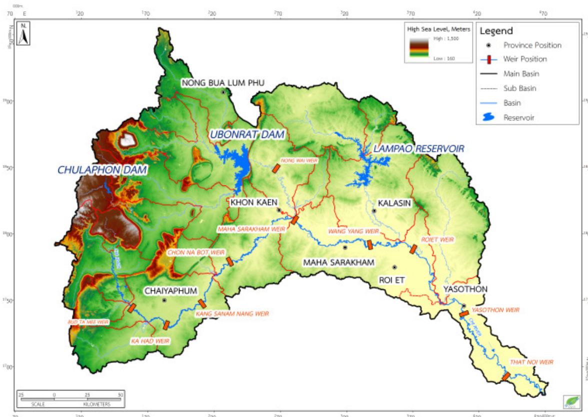

Fig. 1 Topography and sub-river basin of Chi river basin.

2.2. Hydro-meteor condition

Chi river basin is located in a tropical area under a monsoonal climatic condition (Figure 2). Therefore their climate is dominated by a monsoon winds that brings the seasonal changes from wet to dry with a so-called southwest monsoon (rainy) from mid-May to mid-October, and a northeast monsoon (dry or winter) from mid-February to mid-May where the a transition period in between is considered as a summer or pre-monsoon season. The averaged highest temperature is 32.1 °C occur in April and averaged lowest temperature is 21.2 °C occur in January. The hottest period ranges from March to May and the maximum temperature usually reach 40 °C.

2.3. Flooding condition

The study area is subject to frequent flooding. Due to its constraint in topography and high intensity of rainfall, a flood caused by a quick runoff from upstream is resulted in a flash flood downstream. In the middle part and along the flood plain area, the area is rather flat and the river has reduced in its capacity, the flood from upstream cannot propagate further causing inundate and stagnant floodwater. Floodwater usually accumulates in the vicinity of the Chi-Mun confluence. Table 1 summarizes the maximum discharge based on 2010 flood. The flood map is shown in Figure 3. It can be seen clearly that most of the flooding area is along the main river where the area is rather flat and receive a large volume of runoff.

Fig. 2 Climatic condition of Thailand.

Table 1. Maximum discharges and analysis of their return period based on 2010 flood.

Basin	Flooding area (Discharge station)	Max. Discharge (river capacity) (m^3/s)	Return period (years)
Chi	Muang Chaiyaphum, Chaiyaphum (E.23)	890 (456)	10
	Manjakiri, Khon Kaen (E.9)	1,220 (576)	10
	Kosumpisai, Maha Sarakham (E.91)	1,420.4 (940)	5
	Jang Han, Roi Et (E.66A)	1,129.4 (772)	4
	Thung Khao Luang, Roi Et (E.18)	881.8 (960)	2
	Maha Chana Chai, Yasothon (E.20A)	1,345 (1060)	3

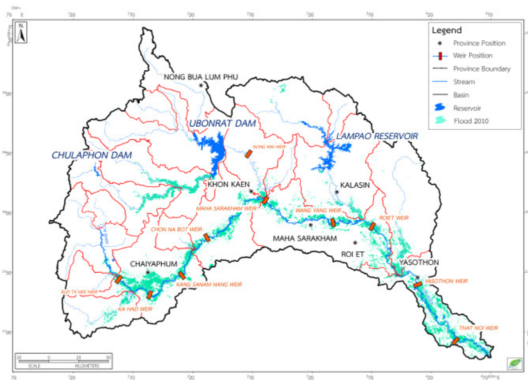

Fig. 3 Flood map of Chi river basin in 2010.

2.4. Ubol Ratana dam

Ubol Ratana dam is the biggest dam in Chi river basin. It was constructed with an earth core rockfill in 1964 and completed in 1966 to be used as multi-purpose functions: electricity generation, irrigation, flood control, transportation, fisheries and as tourist attraction. The dam is located in Ubonrat District, Khon Khane Province and store water from Pong River which is a sub branch of Chi River. The reservoir catchment area is 12,000 sq.km. or 24% of total Chi river basin (Figure 4). It has a storage of 2,431.3 MCM with effective capacity of 1,851 MCM. The averaged inflow is 2,470 MCM/year. The minimum water level is +175 msl, normal and highest water level are +182 and 186.6 msl consecutively. The maximum release through the spill way is 3,500 m^3/s.

Ubol Ratana dam is a multi-purpose dam operated by Electricity Generating Authority of Thailand (EGAT). The power plant has three turbines, each with an installed capacity of 8,400 KW (total 25.2 MW). The dam also provides water supply for domestic use within Khon Khane Province 30 MCM/year, to Nong-wai irrigation project (300,000 rai) 800-1,000 MCM/year and for ecological conservation 3 MCM/day. However due to fluctuation of reservoir inflow (figure 5) it is complicated to manage the reservoir both short and long term especially to control the release to meet all requirement while still keeping its control flood safety.

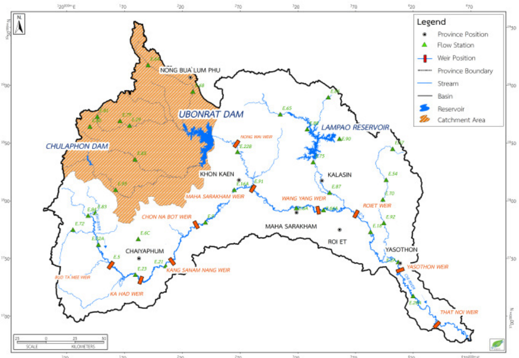

Fig. 4 Ubol ratana dam catchment area.

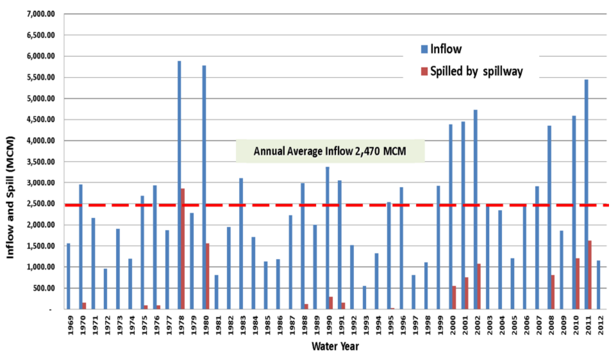

Fig. 5 Statistical Inflow and released by Spillway of Ubon Ratana dam 1969-2012**.**

3. Reservoir flood optimization

The goal of this optimization is to minimize short-term flood risk downstream of Ubol Ratana dam by taking account of the flood forecast within the DSS system. The Ubol Ratana dam is a multi-purpose reservoir including hydropower, irrigated agriculture and flood control. Flood control represents a short-term objective while water use for hydropower and irrigation are long-term goals. Hydropower and irrigated agriculture objectives are typically reflected in operation rule curves. The real-time discharge and water level data at downstream of the dam and forecast information will be used to optimize short-term operation with respect to downstream flooding while respecting long-term objectives (hydropower and irrigated agriculture).

3.1. Optimization approach

The hydrodynamic river model is a cut-out from a full Chi-Mun Mike 11 flood forecasting model (Figure 6). The model is actually just identical to that of the full Chi-Mun model, its introduction as a cut-out is just to reduce the computation time.

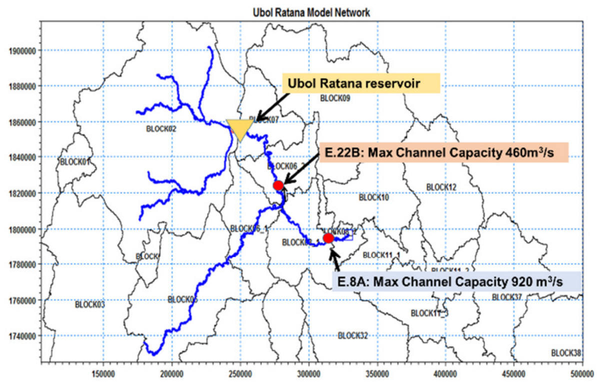

Fig. 6 River Network of Ubol Ratana MIKE 11 model**.**

The Shuffled Complex Evolution (SCE) algorithm is employed to optimize the flood risk. The SCE is a population based algorithm that minimizes a single function which is the weighted aggregate of several objective functions. Each population member is ranked according to its aggregated objective function value. A model run is required for each population member. The population is renewed during each iteration in the way that the procedure evolves towards a population with the smallest aggregated objective function values possible. The population size depends on specific parameters for the SCE. These parameters should be set to recommended values [DHI Manual, 2014, Duan et al., 1993, Madsen, 2000].

Figure 7 shows the simulation approach applying SCE algorithm to the real time flood simulation. The total release volume from the Ubol Ratana dam is chosen as decision variable. The WRF model forecasts rainfall for

7 days and consequently the optimization period equals 7 days. This information is input into the hydrodynamic model to estimate the discharge at downstream. This computed discharge will be compared to the downstream flood control criteria at E.22B and E.8A and together with other objective functions the optimization will start to optimize the optimal reservoir release to meet all the criteria. Specifically, the release volumes that are varied by the optimization tool are defined relative to the time of forecast (TOF): 6, 12, 24, 48, 96 and 120 hours after TOF. Table 2 shows the parameter used in the SCE algorithm

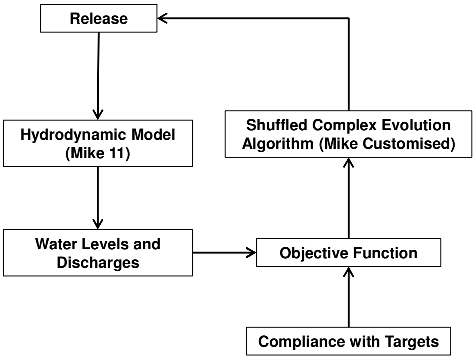

Fig. 7 Simulation-Optimization approach

Table 2. Parameter choice for SCE algorithm (n is the number of decision variables)**.**

SCE Parameter	Value	Recommended Value
Number of complexes	2	--
Number of points in a complex	13	2n+1
Number of evolution steps	13	2n+1
Number of points in each subcomplex	7	n+1

3.2. Objective function

The objective function is defined as follows:

$$\min \begin{cases} \max_t \{\omega_1 * \max\{0, H(t) - H_{\max}\}\} & (1) \\ +\omega_3 * \left(\sqrt{\frac{1}{N}\sum_{t=1}^{N}\left(Q_{E.8A,t} - Q_{E.8A,crit}\right)^2} + \sqrt{\frac{1}{N}\sum_{t=1}^{N}\left(Q_{E.22B,t} - Q_{E.22B,crit}\right)^2} \right) & (2) \\ +\max\{\omega_2 * \max\{0, H(TOF+7days) - H_{RC}(TOF+7days)\}\} & (3) \\ +\omega_4 * \sqrt{\frac{1}{N}\sum_{t=1}^{N} Q^2_{ubonrat,t}} & (4) \end{cases}$$

(Eq. 1) Do not exceed dam safety level

(Eq. 2) Mitigate downstream flooding

(Eq. 3) Comply with the rule curves at the end of the forecast horizon

(Eq. 4) Minimize spillage

H(t) represents the water level at the Ubol Ratana reservoir. H_{max} is the dam safety level which is set to 183 msl. The difference between the water level at Ubol Ratana and the highest rule curve level, H_{RC}, is taken at the end of the forecast horizon. The highest rule curve level comes either from the upper control rule curve (URC) or the flood control rule curve (FCRC). $Q_{E.22B}$ and $Q_{E.8A}$ represent the discharge at these two locations. The channel capacities are 460 m^3/s ($Q_{E.22B,crit}$) and 920 m^3/s ($Q_{E.8A,crit}$). Qubonrat stands for the release volume from the Ubol Ratana reservoir. The weights, ω_i (ω_1=1000000, ω_2=1000, ω_3=10000 และω_4=1), reflect unit differences in the objectives and user preferences.
Three convergence criteria can be chosen for the SCE algorithm (Table 3.): the number of model runs, the relative change of the aggregated objective function value over a number of iterations, and the aggregated objective function value as such. In many test optimization runs it was found that the SCE shows an acceptable degree of convergence after 720 model runs which corresponds to approximately 18 to 21 iterations. In this setup an optimization takes approximately 3 hours. Due to this computing time the first variable release volume was chosen to be 6 hours after TOF.

Table 3. SCE convergence criteria

Convergence Criteria	Value
Number of model runs	720
Number of iterations / Relative change aggregated objective function value	8 / 0.001
Aggregated objective function value	0

4. Off-line optimization

The event between 2006-10-01 to 2006-10-28 during the monsoon period in 2006 was selected as an off-line test case. The test has been performed as close as possible to a real time application. One optimisation run covered a period of 7 days (from TOF until TOF+7days) as it is implemented for the on-line application. TOF was set to 6:00:00 AM on each day during the optimisation period. Assuming that the optimised release volumes would be applied each day, the optimisation runs were executed sequentially taking a hotstart from the previous optimisation results. Figure 8 shows the convergence of all 6 decision variables. It can be seen that all 6 parameters have converged after 720 model runs. This indicates that the optimisation has successfully found a unique optimal solution which corresponds most probably to the global optimum of this optimisation setup. Figure 10 shows that as a consequence also the aggregated objective value converged to a unique solution during 720 model runs.

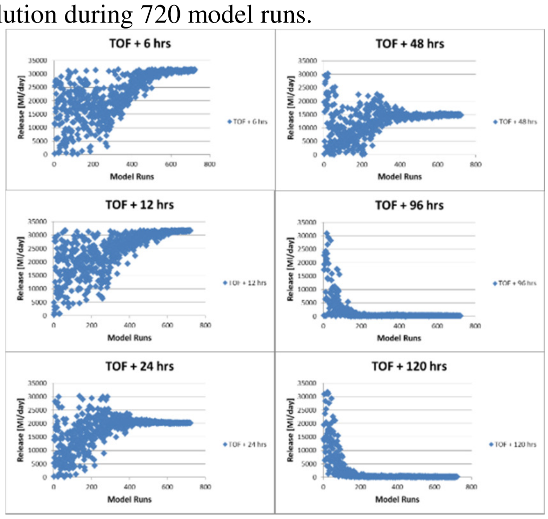

Fig. 8 Parameter convergence for the optimization run with TOF = 2006-10-01

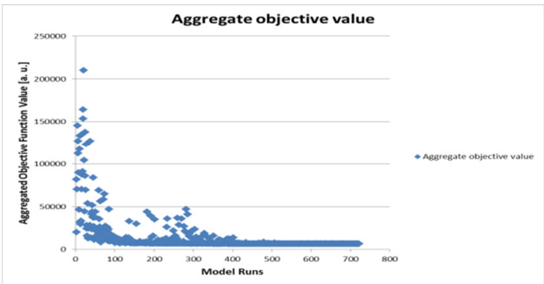

Fig. 9 Convergence of aggregated objective function value for the optimization run with TOF = 2006-10-01.

5. Off-line optimization results

The purpose of this sample off-line optimization was the comparison between rule curve based reservoir operation and optimized reservoir operation. Based on the off-line test case from 2006-10-01 to 2006-10-28 it was found that the rule curved based reservoir operation leads to flooding at the end of the forecast period while the optimized operation manages to mitigate flooding for the entire period. The reason is a different reservoir operation. The optimization sees the 'forecasted' runoff and reacts with pre-releases from the reservoir. The last three days of the forecast horizon represent the time in which the peaks of the inflow into the reservoir and the runoff further downstream start to coincide. In this period the optimization limits the release to the minimum release requirement. As a consequence of this operation strategy, the discharge volumes at the two downstream locations are pushed to the respective channel capacity (E.22B = 460 m^3/s; E.8A = 920 m^3/s) in the first 5 days of the optimization period while flooding is prevented at the end of the period. The rule curve based reservoir operation does not induce pre-releases and hence causes flooding at E.8A at the end of the forecast period.

Figure 10 compares optimization results with simulation results (rule curve based operation) for the reservoir release and discharges at E.22B and E.8A. It can be seen that the optimization manages to avoid flooding at E.22B (max channel capacity 460 m^3/s) for the entire monsoon period and reduces the flood peak at E.8A by approximately 250 m^3/s. Flooding is mitigated by prereleasing water in the initial phase of the monsoon period where the uncontrolled downstream runoff does not yet coincide with the increased inflow to the reservoir

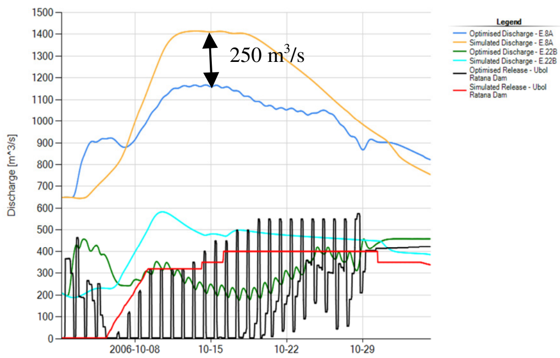

Fig. 10 Optimized release from Ubol Ratana (black line), Simulated release from Ubol Ratana (red line), Optimized discharge at E.22B (green line), Simulated discharge at E.22B (blue line), Optimized discharge at E.8A (dark blue line), Simulated discharge at E.8A (yellow line).

Figure 11 illustrates that the optimized water level exceeds the simulated water level by more than 0.5 m during the time of the peak inflow to the reservoir. However, the optimized water level does not exceed the dam safety level (183 m). Both optimized water level and simulated water level exceed significantly the rule curve water levels. The weights in the objective function were chosen to allow exceedance of the rule curve levels because the observed water level at the reservoir shows that rule curve levels are exceeded frequently during the monsoon period.

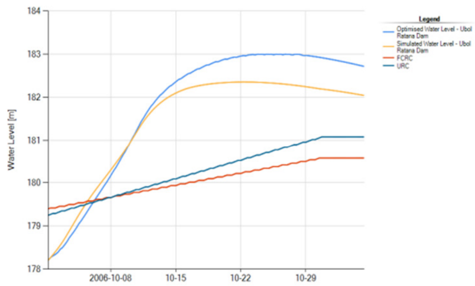

Fig. 11 Water level at Ubol Ratana reservoir during 2006 monsoon: Optimised Water Level (blue line),

Simulated Water Level (yellow line), Flood Control Rule Curve (red line), Upper Control Rule Curve (dark blue line).

6. Real time optimization

The real time optimization has been integrated in the "ESAN" operational flood forecasting system [Thanathanphon W., 2014, Chanthip S., 2014]. The ESAN model runs operationally at 7.45 hrs every day and use observed rainfall 4-days prior to TOF to calculate the initial condition before run for the 7-days forecast applying the rainfall forecast from WRF model. The data assimilation will take place if there is observation available. This model run will provide a hot start to the Ubol Ratana model in which will start to run at 8.45 hours, applying 3-days observed rainfall prior to TOF and run the forecast for 3 hours just to prepare a hot start for the optimization run. Figure 12 shows the scenario diagram of the ESAN and Ubol Ratana forecasting system. If the results of the Chi-Mun scenario indicate that the reservoir water level exceeds the highest rule curve level or that overflow occurs at E.22B or E.8A, then an optimization can be started (Figure 13).

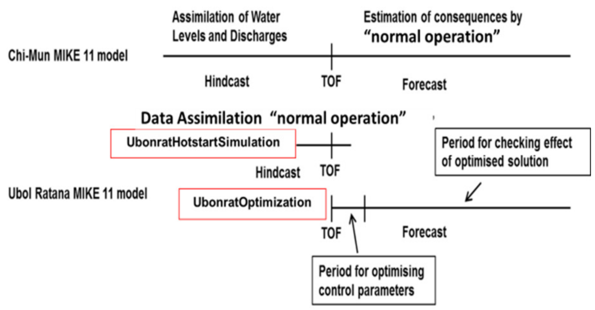

Fig. 12 Scenario runs in the real-time optimization.

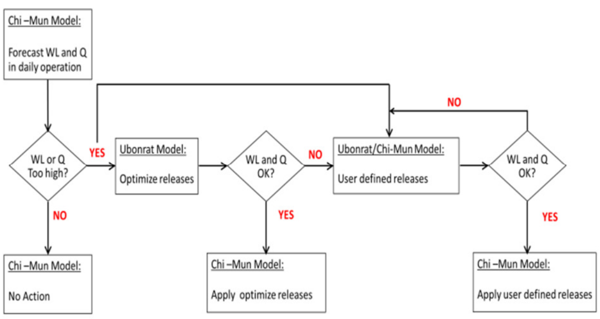

Fig. 13 Real-time optimize process.

In real-time, user defined releases should be specified for the releases during the first 6 hours after TOF in order to avoid release fluctuations due to different operation rules. Alternatively, the rule curves as such could be optimized to better reflect flood operation of the reservoir.

7. Conclusions

The results from an off-line optimization test case for Ubol Ratana dam downstream flood control show a promising flood risk minimization method. With the forecast information integrated in the system, flood minimization is achieved through effective pre-releases from the reservoir that free storage capacity for the period when controlled and uncontrolled runoff peaks coincide. It should be considered that the forecast uncertainty may lead to unexpected consequences when applying the optimized release results in real-time.
The test in an off-line application also provides a stepping stone in the development of optimization algorithm in the real-time model. This enhances the work of flood management since it gives alternative solution for the optimal reservoir release with respect to downstream flood risk minimization. Although this flood optimization approach shows a promising capability to reduce the flood risk at downstream, however there is limitation which is related to the uncertainty in the rainfall forecast and uncontrolled discharge volume which can affect the downstream condition.

References

Thanathanphon W., Chanthip S., Sisomphon P. (2014). Development of an operational real time monitoring system for flood risk assessment, forecasting and management of Mun and Chi river basins, Thailand. 19th IAHR-APD Congress 2014, Hanoi, Vietnam.

Chanthip S., Sisomphon P., and Boonya-aroonnet S. (2014). Development of a decision support and flood forecasting system for Chi and Mun river basins. 19th National Convention on Civil Engineering, 2014.

Thanathanphon W., Chanthip S., Sisomphon P. (2014). Development of a decision support system for flood management in Chi and Mun river basins 19th National Convention on Civil Engineering, 2014.IPCC Working Group III (2000) IPCC Special Report Emission Scenarios – Summary for Policymakers.

MIKE by DHI Manual, 2014. AUTOCAL User Guide, pp. 29-33.

Duan, Q. Y., Gupta, V. K. & Sorooshian, S., 1993. Shuffled Complex Evolution Approach for Effective and Efficient Global Minimization. Journal of Optimization Theory and Applications, 76(3), pp. 501-521.

Madsen, H., 2000. Automatic calibration of a conceptual rainfall-runoff model using multiple objectives. Journal of Hydrology, 235, pp. 276-288.

Hydrodynamics Simulation of An Overland Flow Over Low Lying Flat Land: A Case Study of The 2011 Severe Flood in Sam-Khok and Khlong Luang Districts

SAIFHON Tomkratoke[a*] and SIROD sirisup[b]

Abstract. The unprecedented flood event in the central Chao Phraya basin 2011 became one of the most catastrophic natural disasters affecting all Thai society and economic sectors in immense scales. In this event, the massive overland flow plays the major in damaging properties and environment systems. Besides, it is typical that natural drainage systems are rather ineffective in low lying flat land. Capability to effectively handle a flood problem under the mentioned condition is indeed a great challenge. To achieve the goal, the hydrological management schemes needed to be improved with an insightful knowledge of flood hydrodynamics as the key to provide essential foundations to derive those schemes. In this study, we aim to gain insight into the aforementioned issue by performing hydrodynamics simulation of overland flow in low lying flat land. The flood plain around Sam-Khok and Khong Luang districts is selected as the study area. The simulation has been performed with an unstructured-grid shallow water model together with a high-fidelity topographic data (LIDAR). The simulation results has been validated with the field observed data (water trace height). The major hydrodynamics mechanisms such as flow patterns, flow magnitudes will be characterized and the effective discharge quantity will be quantified.

Keywords: Overland flow, floods, low lying land, hydrodynamics simulation

SAIFHON Tomkratoke and SIROD sirisup
Large-Scale Simulation Research Laboratory, National Electronics and Computer Technology Center
112 Thailand Science Park, Phahonyothin Road, Khlong Nueng, Khlong Luang, Pathum Thani 12120 Thailand
saifhon.tomkratoke@nectec.or.th
sirod.sirisup@nectec.or.th

Assessment of river bank erosion and vulnerability of embankment to breaching:ARSand GIS based study in Subansiri river in Assam, India

Abstract Temporal Satellite Remote Sensing data of a river system of highly unstable bank can be analyzed in GIS environment for identification of river bank erosion as well as patches of embankment vulnerable to breaching. Acase study was carried out in the Subansiririver, a tributary of river Brahmaputra of Assam, to identify bank erosion location and patches of embankment vulnerable to breaching. Temporal dataset of cartosat1 imagery for the year 2007 and 2009 were used for mapping the flow channel of riverSubansiri. Embankments present in the river were mapped from the cartosat1 data with the help of embankment index map collected from Assam State Water Resource Department. Basedon the degree of convergence and narrowness between the flow channel and embankment, some patches of embankment identified as vulnerable to breaching and classified as very high, high and moderate vulnerable to breaching . Three patches of embankment were identified as very high vulnerable to breaching which came to be true in successive flood season of 2010. The method may be a good tool for predicting embankment vulnerability to breaching and can be implemented for planning of river bank protection work and preparedness for flood season for a flood prone state like Assam.

Keywords *RS and GIS, Bank erosion, Embankment,Vulnerability*

Introduction

Subansiri is one of the largest tributaries of river Brahmaputra [Rao(1979)]. It originates in the Himalaya, in China. Evidence indicate that the reach of Subansiri in the plain section represent one of the most dynamic and unstable alluvial rivers in the Brahmaputra valley [Gogoi and Goswami(2014)]. 1210.2 Sq. km area gets inundated every year due to flood in Subansiririver. To minimize these damages of this chronic flood, the river is confined by both side embankments since 1954 [Rao (1979)]. The silt which used to be deposited in the flood plain, now gets deposited inside the river channel leading to rising of river bed which again leads to increase the frequency of high flood. Floods of very high magnitude may be a contributing factor to channel widening and river bank erosion along with associated changes in the channel pattern [Schumm et. al (1963) and Schumm (1968)]. The most common associated channel changes due to high flood are formation of sand bars, bank erosion, meandering etc.

Embankments are the structures constructed parallel to the river utilizing mostly the materials in situ. Due to the meandering nature of the river, the geometry between the flow channel of the river and the embankment does not remain parallel to each other. More the angle between these two, higher the thrust of water flow on the embankment resulting high probability of embankment breaching. Remote sensing (RS) satellite data have the ability to provide comprehensive, synoptic view of fairly large area at regular interval. Integration of Remote Sensing and Geographic Information System (GIS), make it appropriate and ideal for studying and monitoring of river bank erosion, changes of channel configuration and the orientations between the river channel and its embankments. Various studies in this regards have been carried out for some major rivers [Surian N. (1999), Yang X.et.al (1999),Fuller I. C. et.al (2003), L. Q. Li. X. X. Luand et.al (2007)].Several investigators have been used RS data for mapping and ascertaining the channel changes of different rivers in the world. GogoiandGoswami (2014) studied on channel migration of theSubansiririver using RS data. Bardhan M. (1993) used RS and GIS technique and other data to identify relatively stable stretches of Barak river during the period 1910 to 1988. Space Application Centre (SAC) Ahmadabad in India and Brahmaputra Board Guwahati jointly studied to assess the extent of river erosion in Majuliisland in order to identify and delineate the areas of the island which have undergone changes along the bank line due to dynamic behavior of the river [SAC and Brahmaputra Board (1996)]. Naiket.al(1999) studied the erosion at Kaziranga National Park in Assam using RS data.

Study area

The present study describes to identify stretches of embankment of Subansiririver vulnerable to breaching due to bank erosion and changes in channel. Cartosat 1 data for the year 2007, 2009 and 2010 was acquired and analyzed to map the channel configuration in the respective years. Using these data as input to GIS, the changes in the channel configurations like sand deposition, bank erosion, shifting of bank line and distance of the river channel to the embankment and their geometry was mapped and identified the vulnerableembankments.
river

Subansiri is originated in China and flowing through Subansiri districts of Arunachal Pradesh and Lakhimpur district of Assam in India. Figure 1 showing the location map of the river system. This river causes flood in Lakhimpur district of Assam and concern authority constructed embankments for flood protection. Since embankment are present in Lakhimpurdistrict of the river, the study confine in this portion only. Lakmipur district is located in eastern Assam and to the north bank of river Brahmaputra.

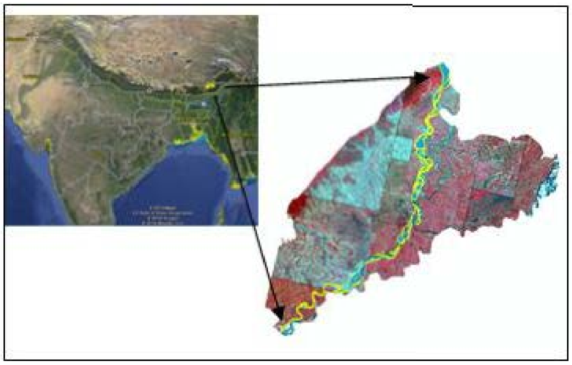

Fig. 1 Study area

The basic data used in this study are digital satellite images of Indian Remote Sensing (IRS) P5 (Cartosat 1) (Row/Path 614/271, 614/272,614/273) sensor, comprising of scenes for the year 2007, 2009 and 2010. The other co-later data used in present study is embankment index map of Lakimpur district prepared by state Water Resources department of Assam.

Methodology

Data analysis

ERDASImagine image processing software has been used for processing the satellite images and Arc Map is utilized for mapping thematic layers. The geo coded cartosat1 temporal dataset collected from NDC (NRSC Data Centre) were projected to UTM WGH 84 (zone 46) projection system and co-registered using ERDAS imagine software. The geo reference images of the same year have been mosaic together. Since Subansiri river covers by the images of same path of IRS P5 satellite, therefore the mosaic image is comprise of images of same data. The embankments are relatively permanent feature along the river. Since it is a linear feature associated with the water body (river) it appear uniquely in the panchromatic cartosat1 images of 2.5m resolution. The embankment index map for this district was referred while embankments were mapped from images. The channel configuration map was prepared using all the satellite image mosaic of 2007 and 2009. These two layers were combined in spatial analysis tools of Arc GIS to find out the changes areas. Places where the bank line has shifted outward the center line, it demarcated as erosion and the reverse is demarcated as deposition. The quantum of bank erosion was estimated in different locations of the channel. Looking at the quantum of bank erosion, angle between the embankment and channel flow

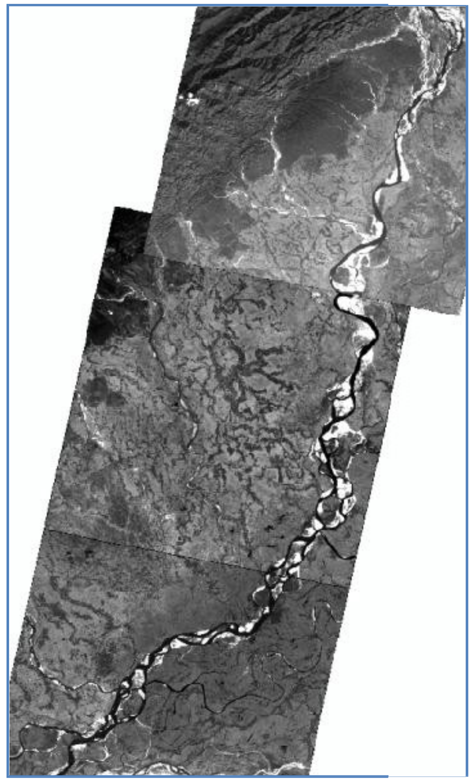

Fig.2 Cartosat1 data for the year 2007

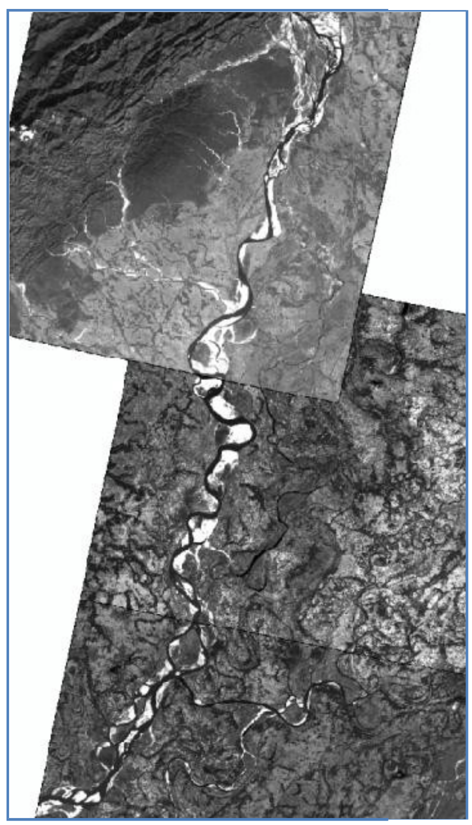

Fig 3: cartosat1 data for the year 2009

and distance between them the stretches of embankment vulnerable to breach were identified. The vulnerability to breaching for the identified stretches of the embankment was verified with ground formations during the flood season for successive year 2010 and simultaneously it was verified with post flood satellite data. The geo rectified and co-registered cartosat1 imageries are shown in figure2 and figure 3.

The embankments extracted from cartosat1 images are as shown in figure 4. The embankments are not continuous in the confluence points of sub tributaries of Subansiri. The right bank embankment is of 49.6 km length and the left bank embankment is 59 km.

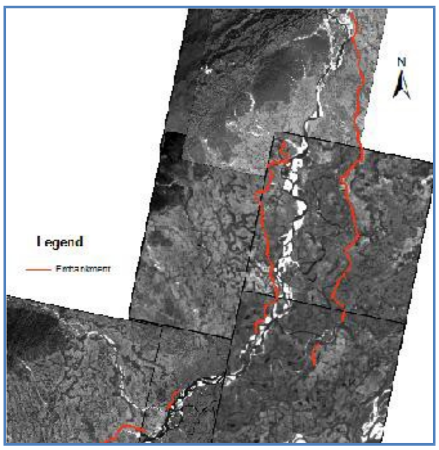

Fig. 4 Embankments present in Subansiri River

The channel configuration map of Subansiririver for the year 2007 and the year 2009 is given in the figure 5 and figure 6 respectively

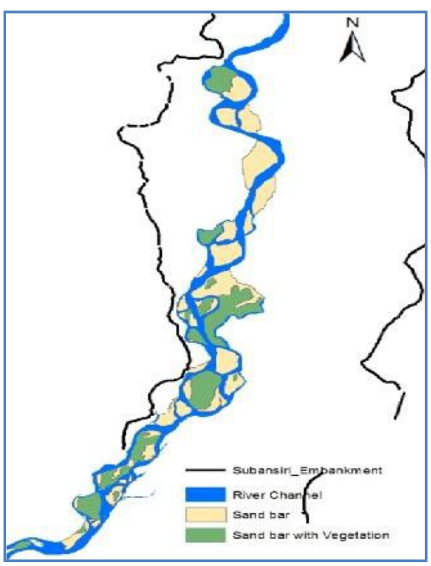

Fig. 5 Channel configuration of Subansiri river in the year 2007

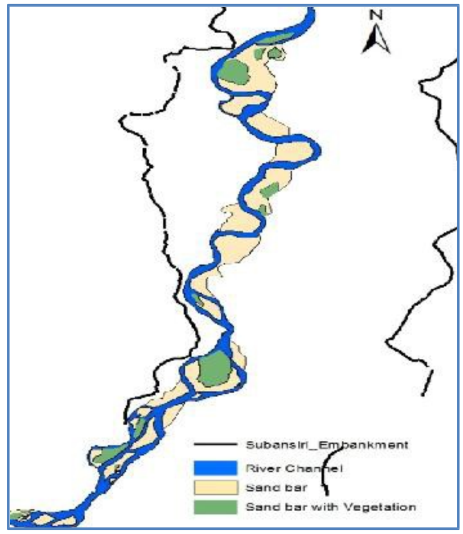

Fig 6**:** Channel configuration of Subansiririver in the year 2009

Results and discussion

The study shows that the river channel is quite dynamic. Lots of erosion and deposition occurs in the channel. As a hole the river bank shifted towards west during these two years 2007 to 2009. It has both braided and meandering nature. As a result of bank erosion and change in channel configuration, several stretches in the right bank embankment identified as vulnerable to breaching (figure 7).

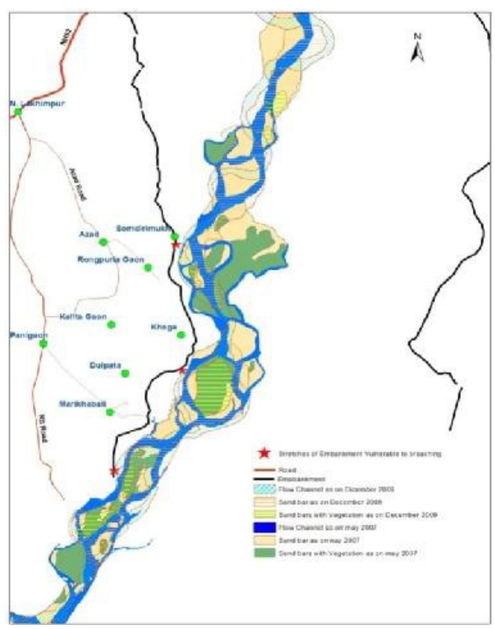

Fig.7 Changes in channel configuration of Subansiririver during the year 2007 to 2009

During the flood season of successive year 2010, the Water resources department had to take enormous river training work to prevent the embankment from breaching due to bank erosion. Cartosat1 satellite image was analyzed to verify the bank erosion in the identified locations and showed evidence of bank erosion (figure 8).

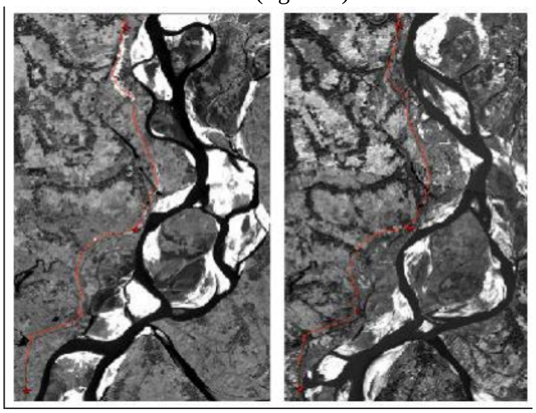

Fig. 8 Changes of channel configuration of Subansiririver during2007 to 2009 as viewed from cartosat1

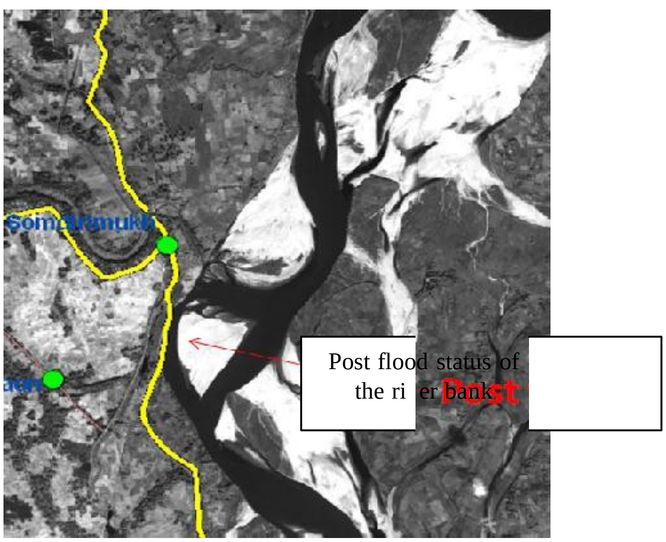

Fig. 9 Bank erosion of Subansiri river after the flood event in 2010 near Sumdirimukh as viewed fromcartosat1

Summary and Conclusions

A methodology has been developed which has successfully identified the changes in river configuration of the Subansiri river system of Assam, India. Erosion prone areas of the river stretch has been identified which are highly useful for planning of river bank protection work, river training work and preparedness for flood season of successive year for flood prone state like Assam.

References

Bardhan, M., 1993, Channel Stability of Barak River and its tributaries between Manipur - Assam and Assm - Bangladesh Borders as seen from satellite imagery, Proceeding National Symposium on Remote Sensing application for Resource Management with Special emphasis on N. E. Region, Guwahati, 25-27 November 1993.

Fuller I. C., Large A. R. G., and Milan D. J., 2003, Quantifying Channel development and Sediment Transfer Following Cute-Off in a wadering Gravel-Bed River, Geomorphology, 54(3-4), pp307-323.

Gogoi, C. andGoswami, D. C., 2014, A study on channel migration of the Subansiri river in Assam using Remote Sensing and GIS technology, Current Science,106(8).

L. Q. Li. X. X. Luand Z, Chen, 2007, River channel change during the last 50 years in the middle Yantze River: An Example of Zianli Reach, Geomorphology, 85(3) pp. 185-196.

Naik S. D., Chakravorty S. K., Bora T., and Hussain I., 1999, Errosion at Kaziranga National Park, Assam, A study based on Multi temporal satellite data, Project Report. Space Application Centre (ISRO) Ahmadabad and Brahmaputra Board , Guwahati p. 70

Rao, K.L., 1979, India's Water health, Orient Blackswan, pp 78 ISBN 978-81-250-704-3

Rinaldi M., (2003), "Recent Channel Adjustments in alluvial River of Tuscany, Central Italy", Earth Surface Prcesses and Landforms Vol. 28 No. 6 2003 pp, 587-608

SAC and Brahmaputra Board, 1996, Report on Bank Erosion on Majuli Island, Assam: A Study based on Multi temporal Satellite data, Space Application Centre, Ahmadabad and Brahmaputra Board, Guwahati.

Schumm, S. A., 1968, River adjustment to altered hydrologic regimen, Marrubidgee and placochannelsAutralia,U.S. Geol. Surv. Prof Pap., 1968 598,65.

Schumm, S. A., and Litchy, R. W., 1963, Channel widening and flood plain construction along Cimarron river in southwestern Kansas, U.S. Geol. Surv. Prof Pap., 1963 352 D71-88

Surian N., 1999, Channel Changes due to River Regulation: The Case of the Iave River, Italy, Earth Surface Processes and Landforms, 24(2), pp.1135-1151.

Yang X., Damen M.C. J., and Zuidam R. A. van., 1999, Satellite Remote Sensing and GIS for the analysis of Channel Migration Changes in the active yellow River Delta, China. International Journal of Applied Earth observation and Geoinformation, 1(2), pp 145-157.

Development of Technology for Monitoing, Evaluation and Predction of Global and Local Water-related disaster using Various Observation System

LEE Eulrae[1*] , CHAE Hyosok[2] , Hwang Euiho[3] , SHIN Hyungjin[4]

Abstract. It is important to develop infrastructure of earlier correspond to disaster based on real-time information of water-related disasters which are drought and flood using the big data analysis in Korean's Government 3.0. Recently, the report of the Korea Agency for Infrastructure Technology Advancement indicates accuracy of water-related disaster forecasts is around 71% which number means a middle state of comparing with advanced countries. Also, internationally the damage scales of rainfall intensity and economic development are increasing state depending on the climate change. So we need to develop an applicable technology of efficient monitoring, evaluation and prediction system for global and local water-related disasters. National water management system buildup is required to accept a vanity of database from Ministry of land, infrastructure and transport and Korea meteorological administration as well as integrate a satellite and rain radar data based on automatic weather station (AWS) from developed country to analyze integrated database. Within designed system should be utilized for national management sensor, observed data including in accuracy and reliability of analyzed data to improve integrated observed data. Expanding to obtain water related information from the current state from the South Korea to Southeast Asia and Africa contributes to efforts of climate change response involved in providing water-related disaster predication and acquires a key information to enter into a global water industry. In this study, we suggest a necessary technology of efficient monitoring, scientific evaluation and prediction with regard to water-related disasters which are drought, stream depletion, and flood based n integrated the current management monitoring data from obtaining global and local satellite imagery, rain radar, and automatic weather station.

Keywords *Monitoring, evaluation, prediction, satellite, AWS, X-Net*

LEE Eulrae (ph.D)
Water Resources Research Center
K-water Institute
Daejeon, Korea
erlee@kwater.or.kr

CHAE Hyosok (ph.D)
Water Resources Research Center
K-water Institute Daejeon,
Korea
hyosok.chae@kwater.or.kr

HWANG Euiho (ph.D)
Water Resources Research Center
K-water Institute
Daejeon, Korea
ehhwang@kwater.or.kr

SHIN Hyungjin (ph.D)
Water Resources Research Center
K-water Institute
Daejeon, Korea
shjin@kwater.or.kr

Introduction

Propulsion purpose

The objectives of designed system are to realize a happy homeland assured and power of water industry by developing a wide land observation sensor, building the regional water-related disaster information hub and technology of integrated management. Regional water related responses technology is developed to apply real-time monitoring, evaluation and prediction system surrounding the Korean peninsula based on SRA (Satellite, Radar, AWS) infra by considering X-net infra local observation of metrological/ hydrological information.

A Study on the Necessity

Entering upon the Government 3.0, it is to develop information-based technology for the public advantage and to support policies by analyzing and processing a wide range of information. In other words, future-oriented disaster foundation is required as prediction techniques and various real-time information analysis about water-related disasters such as drought, flood and river stream depletion directly connected to the human life, water, weather, space, IT, pure sciences, convergence and integration between core technologies in under developed nations water industry overseas expansion into new markets provide the necessary information to create various technical needs to be guided.

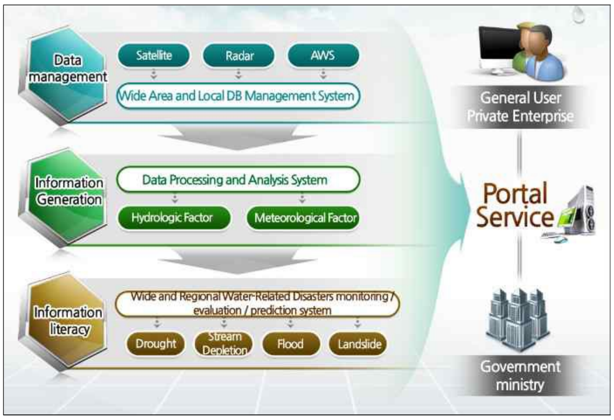

Study Background

Water deficit, Extreme weather phenomenon deepened

In addition, Extreme weather is now emerging as a "new normal". It is expected that Rainfall Characteristic would be changed because of increasing the influence of climate change with response to global warming from the IPCC AR5 Scenario. It is also forecasted that increment of severe rain storm, flooding and typhoon intensity would give rise to a serious natural disaster and drought. Recently, there are local weather characteristic changes due to climate change, and the incidence and magnitude of floods and drought, escalating the situation. Locality Rainfall occurs frequently. Rainfall intensity and the evapotranspiration increases. It is worried that the extreme drought would occur in strong rainy season. Because flood, typhoon and drought frequency has steadily increased globally, the water management is needed to ensure the accurate prediction, the extensive observation and the ability to respond immediately. Especially, the remote sensing data is very important because we have the complex topography and shorelines and we have little meteorological data about North Korea isolated like an island.

Recently, urban flood inundation occurs frequently in accordance with the rapid urbanization and it makes damages max when disaster happens. The overflow that causes people and property damage and induces social, environmental, economic and psychological harm may attack the foundation facilities such as electricity, gas and water in city. Thailand Flood 2011 shows that urbanization and industrialization can cause enormous national loss which are social, economic and security.
In particular, high-resolution real-time rainfall observations are needed precisely for Prediction and Warning flood inundation that can occur in the city.

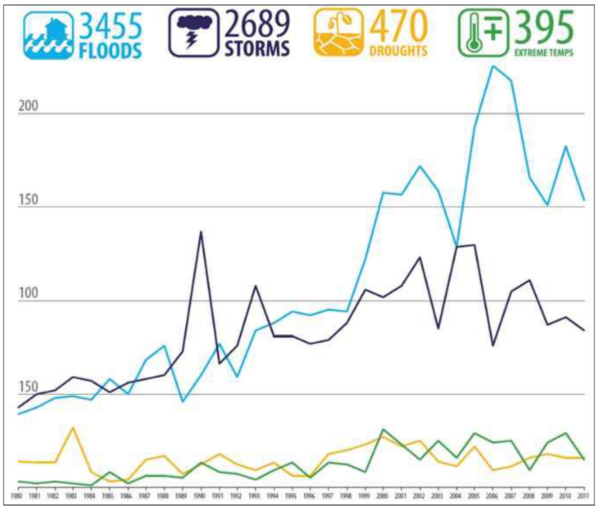

Inaccurate prediction about water resources is directly related to a large scale damage.

Flooding in the Watershed Level occurs frequently water-related disasters flood happen, depending on the difficulty in the management of dam floodgates. So, Flood Control Office. For the accurate flood forecasting, prediction and warning system through high-resolution observations of the precipitation, forecasting technology is required.
In Korea the National Weather Service under 25 when viewed by observatory '99 ~ '08 Severe rain storm a day more than 100mm incidence was increased 1.7 times compared to 221 times for 385 circuits '70 ~ '80 years.

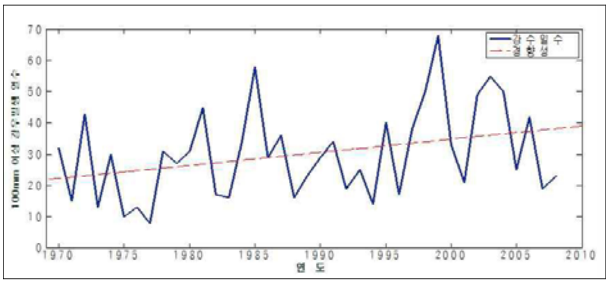

Spread of Satellite information·ICT·Big Data, etc. application

There are a number of countries to promote technology development and utilization of satellite-related policies, and incorporated into water resources management. USA, Europe, Japan holds specialized institutions for satellite utilization respectively USGS, ESRIN, RESTEC. The budget and policy are focused on the development of satellite-related hardware such as satellite and payload in Korea. So investment budget and policies for satellite utilization is vulnerable. In addition, satellite-related technology and utilization is rather low.
The ICT industry has shown average annual growth rate of 14% since 2005. Development of a full-fledged Big Data has been accelerating the convergence trend. ICT big data technology have enabled the rapid data acquisition and analysis of large amounts of data. Due to

this, made it possible to integrate analyze of the water resources information gathered from various observation equipment. Also made it possible in real time services. Real-time water resources information using satellite information demand is increasing due to the increased utilization of location-based information (location-based services). According to UN-affiliated organization ITU (International Telecommunications Union) published "Monitoring the Information Society report" in 2012, Korea have achieved the most advanced ICT economy in the world. The satellite information with this competitive advantage is expected to be effective. Water resources management service will be more diversify by convergence such as IT, BT, NT, GT, etc. In addition, it is possible to maximize the value of information. State-of-the-art technology-based water management technology can be provided to the public. This is expected to be available in the future to achieve high added value.

The investment of drought, flood prediction, related field have been strengthened, and recent overseas river management projects have been visible. Therefore, technical level difference is expected to be reduced.

(1) Technology of water resources information generation

Entry to developed countries to secure statistics data of water resources survey and information obtained by various observation system. And rapidly reducing the technology gap, the expected technology level of 90% of developed countries.

(2) Assessment and Prediction Technologies seeking Preparedness of Drought and Drying Streams

Developed countries are taking advantage of the climate change modeling and drought forecasting system using satellite data. To perform rapid complement of drought prediction and response techniques, the expected technology level of 95% of developed countries.

(3) Customized Flood Risk Assessment and Prediction

Effective management of river-related information on compatible paradigm shift in disaster management, and acquiring open and scalable technology of water resources information, the expected technology level of 95% of developed countries.

(4) Technology for Water Resource Information Service System Platform

Development of information technology using ICT, and establishment of portal system for real-time monitoring/assessment/prediction of water resources, the expected technology level of 95% of developed countries.

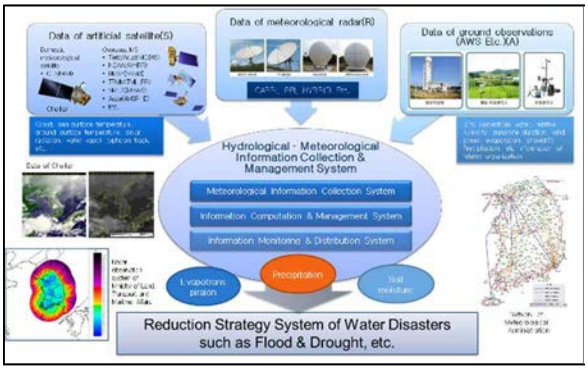

Research Status

Consisted of 4 subjects across the three areas such as; generic technology of information generation using convergence process of SRA based on observation data, application technologies for water disaster assessment and prediction, technology of providing information.

(Subject 1) Development of Technology for Hydrological Parameter and Information Generation Using Various Observation System

- Information generation of water disaster monitoring/assessment/prediction based on data using various observation system and X-Net demonstration test-bed

(Subject 2) Assessment and Prediction Technologies seeking Preparedness of Drought and Drying Streams for Water Security Reinforcement

- Monitoring water resources variable in (un)gauged watersheds using satellite images and hydrological radar information, effective assessment and prediction of drought and drying streams for water security reinforcement

(Subject 3) Development of Customized Flood Risk Assessment and Prediction Technology for Reduction Water Disasters

- Assessment and accurate prediction for broad and local flood using SRA and advanced monitoring system, dramatically reduce water disaster

(Subject 4) Development of Technology for Glocal (Global+Local) Water Resource Information Service System Platform Based on Big Data

- Portal system management information efficiently which based on SRA Glocal hydrological observation data, generation data and analysis information of water disaster, also provides a customized information

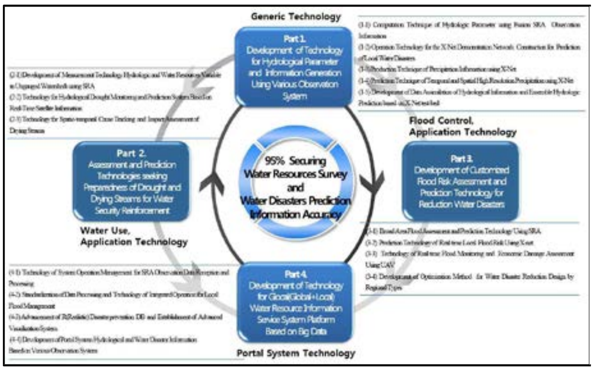

Research Vision and Strategy

Research Roadmap

Stage 1 (2014~2015)
By securing the basic data from a variety of land observation sensors, development and portal services platform of design of big data base of fusion foundation technology to promote, such as construction of the test bed.

Stage 2 (2015~2017)
Substantial operation of the test bed, land observation sensor based data generation and can be a development of fusion technology, to develop a disasters (drought / flood / Stream Depletion) application technology.

Stage 3 (2017~2018)
As a step for the commercialization of research and development results, performance verification of system, collaboration and modularity between the applied technology, water related disasters theme also advanced the creation and portal-based information service system.

Advancement of Technology

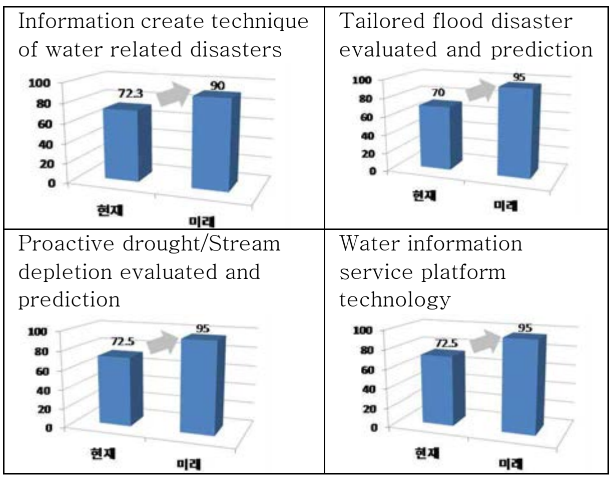

Core Expectation and Conclusion

□ (Social and economic) Contribution of an intelligent national water security system buildup through advanced water resource analytical technology using the extraction and utilization of specialized satellite data

○ Imrpovement for the quality of the people life and enhancement for global competitiveness of water industry with applying to control global and local region using advanced convergence technology

○ Business sharing between organizations for water related disasters and the public organization, support of rapid decision-making system, and service for the people.

□ (Technology) Securing core technology based on the current technology such as a wide area and urban areas including the Korean peninsula, water resources for water-related disaster management in the region, satellite, weather and IT

○ Contribution of water industry competiveness and the growth of the national income by providing the latest information to other country such as Southeast Asia using state-of-the art technology

○ Development of Korean type of water-related disaster measures technology and water-related modeling technology through X-Net infra set up and operation

Quasi-real-time satellite monitoring for assessing agronomic flood damage

Akihiko KOTERA [1 *], Yotaro UENO [2] and Takanori NAGANO [2]

Abstract This study aims to realize prompt, reliable, and safety survey for agronomic flood-damage assessment, performed by a quasi-real-time satellite image analysis. For damage detection, we focused on crop failure due to submergence of rice in the field before harvest. To detect the spatial distribution of crop failure, we examined the temporal relationship between the harvest time, estimated from the time-series enhanced-vegetation index (EVI), and the onset of inundation, estimated from the time-series land surface-water index (LSWI) and EVI. These time-series indices were derived from MODIS satellite data with an adequately downscaled 250-m resolution in 8-days interval. Quasi-real-time MODIS images are provided by U.S. Geological Survey (USGS) and they are then immediately processed. Validations compared with local flood damage reports in 9 districts in Thailand showed large underestimation in MODIS analysis, whereas validations with 7 states in Cambodia showed high consistency ($R^2 = 0.95$). Error in former result could be caused by a discrepancy in definitions of the flood damages. The new methodology and system using quasi-real-time imageries proposed in this study proved to be promising for agronomic flood-damage survey and assessment.

Keywords *inundation damage, MODIS, near real-time monitoring, submerged rice*

1. KOTERA, A.
Research Institute for Humanity and Nature
Kyoto, JAPAN
akotera@chikyu.ac.jp

2. UENO, Y. and NAGANO, T.
Graduate School of Agricultural Science
Kobe University
Kobe, JAPAN

Introduction

Flood damage on rice is a major issue affecting stability of production, income of farmer, and food security in the South East Asia region. Currently, most assessment of flood damage have depended on information from field surveys or reports from local organizations. However, implementation of field survey always involves difficulty and danger because of the bad field condition, particularly at the filed just after disaster.

Delay of the assessment also results a lot of negative effects on disaster response performed by policymaker. As time goes on from flood event, reliability of assessment implemented by filed observation, interview or the questionnaire investigation lose gradually, which may cause inequity in the context of damage rehabilitation and compensation issues. Another difficulty is that it must be required large cost, a lot of manpower and research technique to conduct reliable damage assessment in large scale. Therefore it is a pressing issue to develop a novel technique contributing prompt, reliable, low cost, and safety survey for agronomic flood damage assessment.

It is well known that the satellite-based remote-sensing technique is a promising tool for monitoring land surface conditions in large scale area promptly. Methods to analyze flood events using remote-sensing techniques have also been developed over the last decade (Brakenridge et al. 2003; Sanyal et al. 2004; Sakamoto et al. 2007) and have become operational (Dartmouth 2012; GISTDA 2012). The inundation area is generally detected by two different types of methodology either employing Synthetic Aperture Radar (SAR) images such as RADARSAT-1/2 and Phased Array type L-band Synthetic Aperture Rader (PALSAR) or optical sensor images such as Landsat Enhanced Thematic Mapper Plus and Moderate Resolution Imaging Spectroradiometer (MODIS).

However, these flood detection technologies did not show us the images in terms of an agronomic damaged area, just providing the images of inundated area. Damage may not always occur even though it was flooded in the paddy field. For example, the agronomic damage on rice never occur in the harvested paddy field. Although rice adapts well to being submerged in water, tolerance of rice varies depending on flood conditions such as duration of submergence and water temperature as well as growth conditions of the rice itself, such as growth stage, rice variety, and cultivation management

(Kotera et al. 2005). If a small part of a plant is present above water, rice can survive even during long-term submergence. However, submergence during the heading stage would seriously hinder pollination and the maturing process of rice. Thus, submergence during this maturing stage would damage grain production and quality (Kotera et al. 2005). This is referred to as agronomic damage.

This study aims to develop a prototype system to realize prompt, reliable, and safety survey for agronomic flood-damage assessment, performed by a quasi-real-time satellite image analysis using MODIS images. For damage detection, we focused on crop failure due to submergence of rice in the field before harvest. To detect the spatial distribution of crop failure, we examined the temporal relationship between the harvest time, estimated from the time-series enhanced-vegetation index (EVI), and the onset of inundation, estimated from the time-series land surface-water index (LSWI) and EVI. System tests and validations were performed at Mekong delta in Cambodia and Chao Phraya delta in Thailand as case study areas.

Methodology

Overview

Flood damage monitoring system is consist of four modules; image acquisition, preprocessing, flood and damage detection, and distribution, implemented in Interactive Data Language (IDL) 8.2 (Exelis VIS 2014) with PDP (Parallel Distributed Processing) (Fig. 1).

MODIS image acquisition

MODIS (Moderate Resolution Imaging Spectroradiometer) is a key instrument aboard the Terra (formally called EOS AM) and Aqua (EOS PM) satellites. The Terra crosses the equator at 10:30 AM local time (descending node), and the Aqua crosses at 1:30 PM local time (ascending node) thereby potentially providing two views of a given area each day.

In this study, two sets of Terra/MODIS surface-reflectance 8-day composite data (MOD09Q1 v005 (250-m resolution) and MOD09A1 v005 (500-m resolution)) were acquired from LP DAAC (Land Processes Distributed Active Archive Center, USGS) file server (http://e4ftl01.cr.usgs.gov) using downloader script on a regular basis a utomatically.

Preprocessing

To produce a 250-m resolution map, we resampled 500-m MOD09A1 data to 250-m resolution by applying ratio of red band (band 1) in MOD09Q1 to it in MOD09A1.

The enhanced-vegetation index (EVI) (Equation 1) (Huete et al. 2002), land surface-water index (LSWI) (Equation 2) (Xiao et al. 2005), and the difference between EVI and LSWI (DVEL) (Equation 3) (Xiao et al. 2005; Sakamoto et al. 2007) were used as indices for the analysis, and are defined in equations 1–3, respectively.

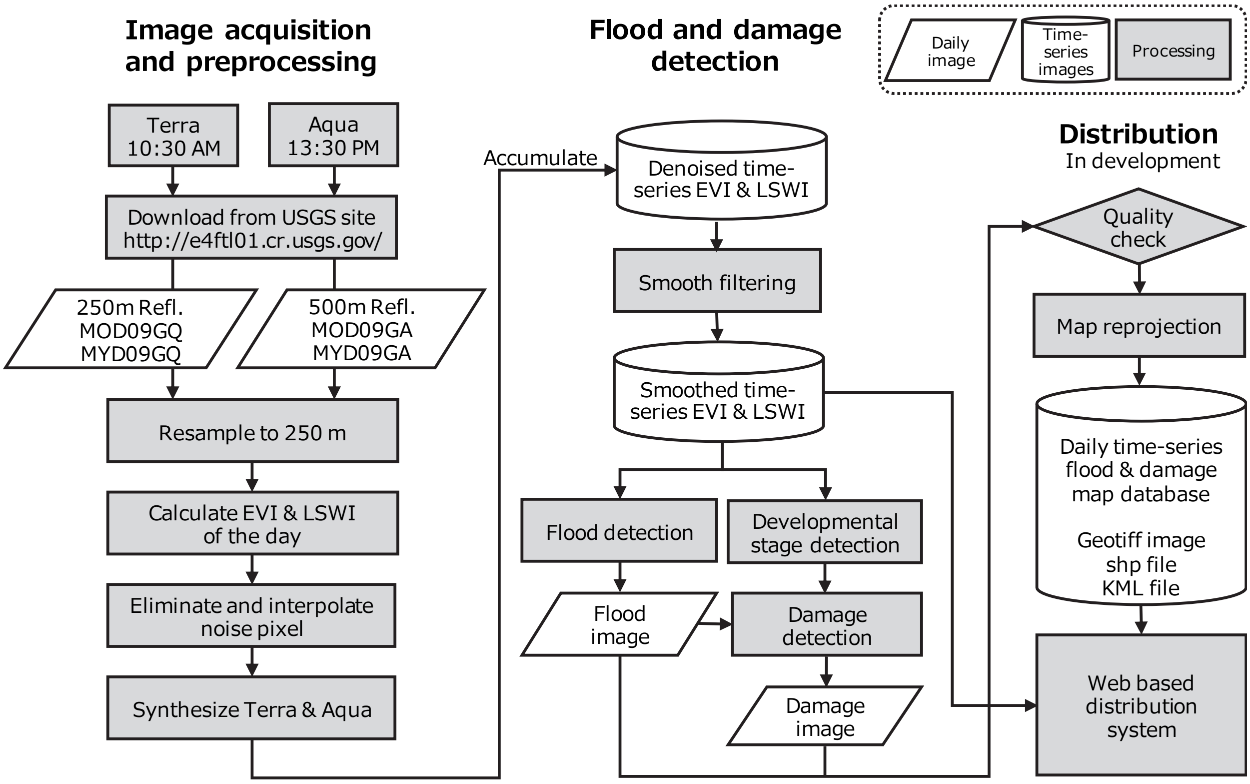

Fig. 1 Scheme of quasi-real-time satellite monitoring for assessing agronomic flood damage

$$\mathrm{EVI} = G \times \frac{NIR-RED}{NIR+C_1 \cdot RED-C_2 \cdot BLUE+L} \quad (1)$$

$$\mathrm{LSWI} = \frac{NIR-SWIR}{NIR+SWIR} \quad (2)$$

$$\mathrm{DVEL} = \mathrm{EVI} - \mathrm{LSWI} \quad (3)$$

Where NIR, RED, BLUE, and SWIR are surface reflectance in the near-infrared band (band 2), red band (band 1), blue band (band 3), and short-wave infrared band (band 6), respectively. G is the gain factor (G = 2.5). C1 and C2 are the coefficients of the aerosol-resistance term, which uses the blue band of MODIS to correct aerosol influences on the red band (C1 = 6.0 and C2 = 7.5). L is the canopy background adjustment (L = 1) (Huete et al. 2002).

MODIS 8-day composite-reflectance data consists of the best possible observation data available during the 8-day period selected on the basis of high observation coverage, low view angle, absence of clouds or cloud shadow, and aerosol loading (Vermote and Kotchenova 2008). However, the 8-days composite data observed in the study area still contained problematic pixels, such as those affected by monsoon clouds. To produce noise-free and smooth time-series, we applied following procedure to EVI, LSWI, and DVEL time-series data for the period of the recent 192 days (24 images);

1) Eliminate cloud and sensor noise pixels by referring the image quality information.
2) Reconstruct daily time-series data by referring the actual date of observation for each pixels.
3) Synthesize daily time-series Terra and Aqua.
4) Interpolate eliminated pixel value on time-series axis by liner interpolation method.
5) Apply the Savitzky–Golay (SG) filter (summarized in Gu et al. 2009; Chen et al. 2004) to time-series data to produce smoothed time-series data.

Detection of flood area

To detect the spatial distributions and temporal changes of inundation, we employ a methodology termed "Wavelet-based Filter for detecting spatio-temporal changes in Flood Inundation (WFFI)," developed by Sakamoto et al. (2007). We refer the reader to this original paper for a full description. Briefly, WFFI detects inundation by two different classes of pixels referred to as mixture and flood (Sakamoto et al. 2007), and has demonstrated a high degree of accuracy in predicting spatial and temporal trends in inundation following flooding of the Mekong River delta region in Vietnam (Sakamoto et al. 2007; Sakamoto et al. 2009) and Chao Phraya River delta region in Thailand (Kotera et al. 2012).

Detection of flood damage

Damage to rice due to submergence can be avoided significantly if the rice is harvested before inundation (Kotera et al. 2005, 2007). To do this, we detected the spatial distribution of the submerged rice, by examining the temporal relationship between the harvest time, estimated from time-series EVI and the evaluated onset of inundation. We categorized the flood damage to rice in the inundated field into three levels: no-loss, total-loss, and partial-loss.

A no-loss pixel represents an area where rice was harvested before the onset of inundation. The completion date of the harvest was estimated to be 40 days after the peak value of EVI, considering a ripening period of rice and heterogeneity of harvest time within the area of large-pixel size in the MODIS image. The peak value of EVI in the rice-cultivation field may indicate the time of the heading stage of rice (Sakamoto et al. 2005). The onset of inundation was obtained using WFFI, as described in the previous section.

A total-loss pixel represents an area where rice was completely submerged before harvesting. In this case, rice would be seriously damaged, and consequently, harvests would be lost. Even if it was harvested after the water had receded, the yield would be significantly reduced because of low grain quality. The total-loss pixel was observed in conditions when the flood pixel was identified within 40 days after the peak value of EVI.

A partial-loss pixel represents the area where the mixture pixel emerged within 40 days after the peak value of EVI. The mixture pixel derived from MODIS in this study may include a variety of submergence conditions, e.g., shallow submergence and mixture of full, shallow,

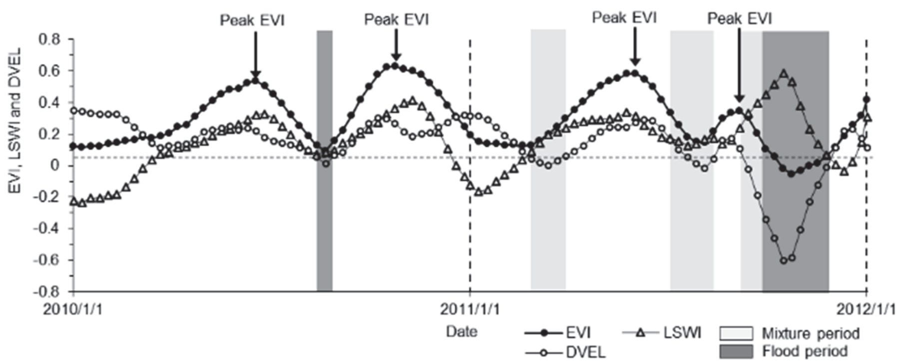

Fig. 2 Time-series of enhanced vegetation index (EVI) and the land surface-water index for a three-year period in the double-rice-cropping field (noise removed). Arrows indicate peaks of EVI and lightly and darkly shaded area show periods where inundation occurred (mixture and flood, respectively, as defined in the manuscript).

and no submergence in the pixel. Therefore, the degree of flood damage in the partial-loss pixel may cover a broad range between no-loss to total-loss.

As presented in Fig. 2, rice cropping in the 2011 monsoons (major rice crop season) may be recognized as total-loss due to complete submergence before harvesting from September 30, 2011. Conversely, flooding from August 8 to August 29, 2010 might have not damaged the rice because it was submerged for a relatively short period of time during sowing.

System test

In order to test the system, we chose the Mekong delta region in Cambodia in 2011 and the Chao Phraya delta region in Thailand in 2006 and 2011 as case study (Fig. 3). For the validation of the flood damage area derived from the MODIS image, the flood damage assessment reports (7 states in the Mekong delta issued by National Committee on Disaster Management, Cambodia on November 3, 2011 and 9 provinces in Chao Phraya delta issued by the Department of Agricultural Extension, Ministry of Agriculture and Cooperatives in Thailand on November 8, 2011) were compared. We also conducted field inspections on the both study site in 2012.

Results and discussions

Processing time

Total processing time measured from preprocessing to damage detection, except for image acquisition and distribution modules, were less than 30 minutes for each study areas. This delay time would be sufficient for practical use as quasi-real-time monitoring. However, there were delay of 10-14 days to be available for the latest 8-days composite MODIS image distributed by USGS. Although the composited image facilitated the image noise reduction, use of daily image could be examined for the next step to improve the total processing time.

Comparison between the flood-damaged areas derived from MODIS with provincial reports

The total estimated damage area across all 7 states in the Mekong delta, Cambodia in 2011 was 94,266 ha (Fig. 4). Validations compared with local flood damage reports in 7 states showed high consistency (R^2 = 0.95) (Fig. 5). In this comparison, the damaged area estimated from MODIS was calculated as the sum of total- and partial-loss areas. Spatial distribution of the damage extent (Fig. 4) also corresponded well with our field inspections and interviews with local farmers.

Whereas damaged area estimated 9 provinces in Thailand was much less than that stated in the provincial report (Fig. 7). Although the total estimated damage area across all 9 provinces in 2006 and 2011 were 56,302 ha and 79,189 ha, respectively, provincial report showed 149,348 ha (excluding the Saraburi province) and 143,700 ha, respectively. However, in individual provinces, the damaged area estimated by MODIS was sometimes greater than that stated in the provincial report (Fig. 7). For example, this was the case in the Nonthanburi province in 2006 and in the Ayutthaya, Pathum Thani, and Bangkok provinces, in 2011. From field inspections and interviews with local farmers in the Ayutthaya province in 2012, we confirmed that both the spatial extent of floodwater and the subsequent flood damage in 2011 were likely to have been much more severe than that in 2006, qualitatively supporting the MODIS estimation (Fig. 6). This difference might be a result of the definition of the damage area used in each case. Our method specifically detected agronomic damage due to inundation, while the provincial reports are likely to have included a wider classification of damage, such as destruction of equipment, and delay in sowing induced by delayed recession of floodwaters.

Conclusions

In this paper, we proposed the prototype quasi-real-time satellite monitoring system to realize prompt, reliable, and safety survey for agronomic flood damage assessment.

Once the system acquires MODIS surface reflectance image, the spatial extent of flood damages on rice was detected within 0.5 hour for each region by computing the temporal relationship between harvest time and the onset of inundation. The latency in current system is, therefore, limited by delay of MODIS data acquisition. This would be improved by incorporating with a new alternative data distribution such LANCE system (The Land and Atmospheres Near-Real Time Capability for EOS: http://lance-modis.eosdis.nasa.gov) that provides daily MODIS image within 0.5-3.5 hours after the shooting time. Using LANCE, we will able to produce the damage assessment at 2 PM to 4 PM in the day.

Reliability of the output from our system was positive in the case study in Cambodia, but still not clarified in Thailand case. Error in latter result could be caused by a discrepancy in definitions of the flood damages. We need to have more case validation study and need to consider "flood damage" from both of definitions, the agronomic definition and a local specific definition.

Although the system is still halfway to be put to practical use, the new methodology and system proposed in this study proved to be promising for agronomic flood-damage survey and assessment. We are also developing a distribution module to deliver flood and damage information with multi data format; image file, shp file, kmz file, and movie, through a convenient web interface.

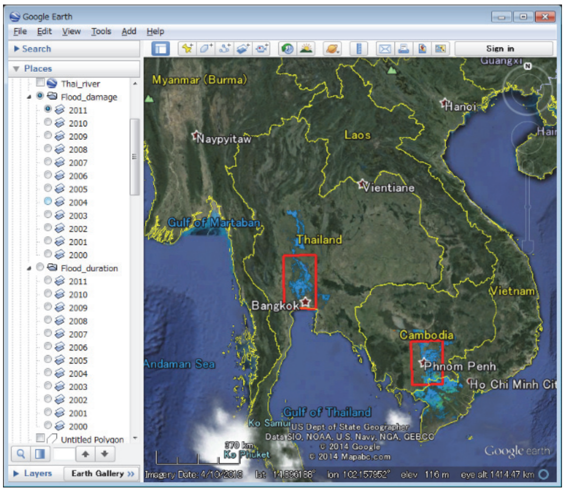

Fig. 3 Study areas (red squares)

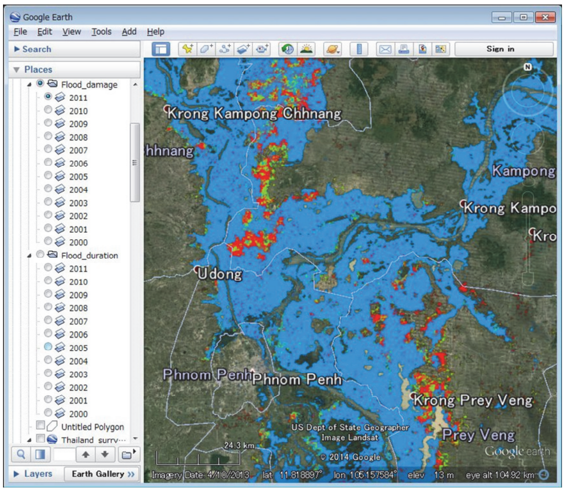

Fig. 4 Flood area (blue) and damaged area (red or green) in the Mekong delta, Cambodia in 2011.

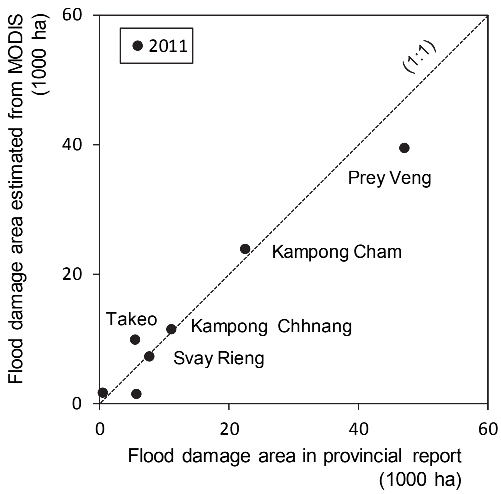

Fig. 5 Comparison between flood-damage area derived from MODIS and provincial reports in 2011.

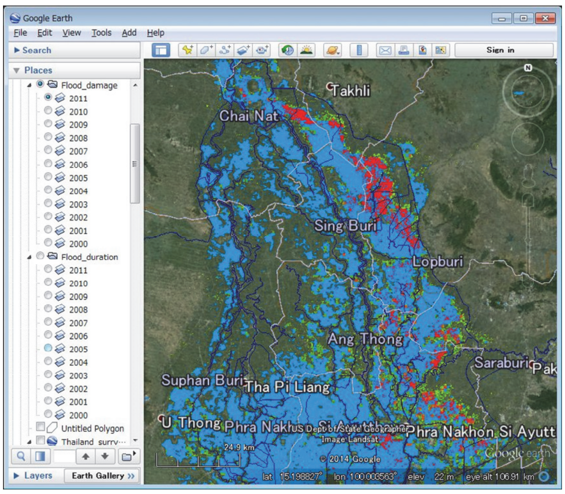

Fig. 6 Flood area (blue) and damaged area (red or green) in the Chao Phraya delta, Thailand in 2011.

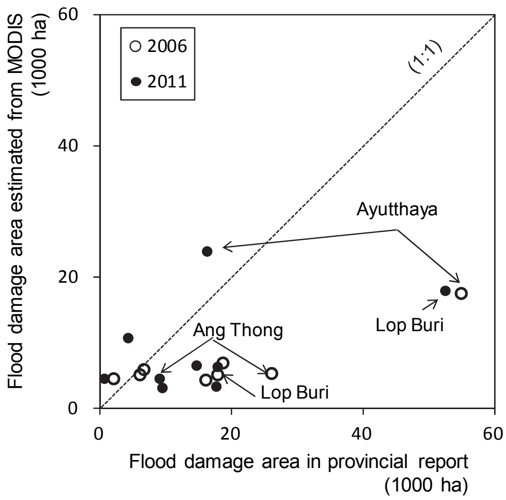

Fig. 7 Comparison between flood-damage area derived from MODIS and provincial reports in 2006 and 2011.

Acknowledgement

The authors would like to acknowledge the staff of the Thai Royal Irrigation Department (RID) and Ministry of Water Resources and Meteorology (MOWRAM). This research was partly supported by the research area "Innovative Technology and System for Sustainable Water Use" in the Core Research for Evolutional Science and Technology program of the Japan Science and Technology Agency (JST-CREST), the Japanese Institute of Irrigation and Drainage (JIID) and KAKENHI (26450365).

References

Brakenridge GR, Anderson E, Nghiem SV, Caquard S, Shabaneh TB (2003) Flood warnings, flood disaster assessments, and flood hazard reduction: the roles of orbital remote sensing. 30th International Symposium on Remote Sensing of Environment, Honolulu, HI, November 10–14, 2003.

Chen J, Jönsson P, Tamura M, Gu Z, Matsushita, B, Eklundh L (2004) A simple method for reconstructing a high-quality NDVI time-series data set based on the Savitzky–Golay filter. Remote Sens of Environ. 91:332–344.

Dartmouth Flood Observatory (2012) Space-based Measurement of Surface Water For Research, Educational, and Humanitarian Applications. Available at http://www.dartmouth.edu/~floods/index.html.

DOAE (2011) Department of Agricultural Extension, Ministry of Agriculture and Cooperatives, Thailand. Flood damage assessment reports issued on November 8.

EOSDIS (2012) NASA's Earth Observing System Data and Information System. Available at. http://earthdata.nasa.gov/

Exelis VIS (2014) IDL software, Boulder, CO, USA, http://www.exelisvis.com/ProductsServices/IDL.aspx (accessed 12 May, 2014).

GISTDA (2011) Geo-Informatics and Space Technology Development Agency. Thailand Flood Monitoring System. Available at. http://flood.gistda.or.th/

Gu J, Li X, Huang C, Okin GS (2009) A simplified data assimilation method for reconstructing time-series MODIS NDVI data. Advances in Space Research 44:501–509.

Hoque R, Nakayama D, Matsuyama H, Matsumoto J (2011) Flood monitoring, mapping and assessing capabilities using RADARSAT remote sensing, GIS and ground data for Bangladesh. Natural Hazards. 57:525–548.

Huete A, Didan K, Miura T, Rodriguez EP, Gao X, Ferreira LG (2002) Overview of the radiometric and biophysical performance of the MODIS vegetation indices. Remote Sens Environ. 83:195–213.

Kotera A, Hanittinan P, Sucharit K and Nagano T (2012) Assessing flood damages of rice in the Chao Phraya Delta, using MODIS satellite imageries. Full paper of PAWEES2012. International conference on "Challenges of Water & Environmental Management in Monsoon Asia", Thailand, 27-29 November.

Kotera A, Nawata E, Thao LV, Vuong NV, Sakuratani T (2005) Effect of Submergence on Rice Yield in the Red River Delta, Vietnam. Japanese Journal of Tropical Agriculture. 49:197–206.

Kotera A, Nawata E (2007) Role of plant height in the submergence tolerance of rice: a simulation analysis using an empirical model. Agricultural and Water Management. 89:48–58.

Sakamoto T, Nhan NV, Kotera A, Ohno H, Ishitsuka N, Yokozawa M (2007) Detecting temporal changes in the extent of annual flooding within the Cambodia and the Vietnamese Mekong Delta from MODIS time-series imagery. Remote Sensing of Environment. 109:295–313.

Sanyal J, Lu XX (2004) Application of remote sensing in flood management with special reference to monsoon Asia: a review. Natural Hazards. 33:283–301.

Vermote EF, Kotchenova SY (2008) MOD09 (SurfaceReflectance) User's Guide. Available at http://modissr.ltdri.org/products/MOD09_UserGuide_v1_2.pdf

Wilson BA, Rashid H (2005) Monitoring the 1997 flood in the Red River Valley using hydrologic regimes and RADARSAT imagery. Can Geogr. 49:100–109.

Xiao X, Boles S, Liu JY, Zhuang DF, Frolking S, Li CS (2005) Mapping paddy rice agriculture in southern China using multi-temporal MODIS images. Remote Sens. Environ. 95 (4): 480–492.

Technology Assisted Flood Management

Surajate Boonya-aroonnet[1,a], Peraya Tantianuparp[1,b], Sutat Weesakul[1,2,c*] and Royol Chitradon[1,d]

Abstract The great flood of Thailand in 2011 caused tremendous damage to the country. It is a long duration flood approximate 2 months in the central plain of Chao Phraya river basin with the flood depth varied from 0.5 to 2.5 m. Survey technologies were effectively applied to provide field information for operational flood management. Unnamed Aerial Vehicles (UAV) were deployed to investigate the inundation area, flood extent, flood conditions, obstruction in drainage system and to validate the field operation. There were totally 32 flights of UAV conducted in Bangkok and its vicinity. The recorded video were systematically stored and broadcasted for both official and private uses. Information was disseminated to public using social Medias. Other type of survey is the autonomous surveyed-vessel to survey the depth of drainage conveyance system in order to keep the effective flow of flooded water through Bangkok. Water depth could be quickly scanned during survey. Deposited sediment location could be identified and remedial can be conducted.

Keywords *Flood management, survey technology, Unmanned Aerial Vehicles (UAV)*

[1]**Hydro and Agro Informatics Institute (HAII)**,
108 Bangkok Thai Tower Fl.8,
Rangnam Rd., Phayathai, Ratchatewi,
Bangkok 10400,
Thailand

[2]**Asian Institute of Technology**,
PO Box 4,
Klong Lung,
Pathumthani 12120,
Thaiand

[a]surajate@haii.or.th,
[b]peraya@haii.or.th
[c]sutat@haii.or.th
[d]royol@haii.or.th

Introduction

At present, technology has been dramatically developed and effectively applied to different sectors. The remote survey technology using various sensors and optical system can be used in the first surveys of cadastral in rural area in Alaska as presented by Cunningham et al (2011). Unmanned Aerial Vehicle (UAV) is used in varieties of field work such as military service, traffic survey and supervision, fire prevention, etc. It can be used for investigation in hazard and disaster area. Hazard map can be generated for natural disaster assessment using UAV equipped with on-board digital camera transmitted real time to a spatial temporal GIS to share the information by Hirokawa et al (2007). Adams et al (2011) surveyed UAV usage for imagery collection in disaster research and management which showed a number of pioneer work in post-disaster assessment for a large scale events. Structural damaged by Hurricane Katrina was inspected for several multi-story commercial buildings by Pratt et al (2006). Bridges, seawalls and piers damaged by Hurricane Wilma and Ike were inspected by Steimle et al (2009). Devastated earthquake and subsequent Tsunami occurred in 2011. Fukushima Daiichi nuclear facility was significantly damaged and began to emit radiation. It was complicated to repair in a traditional effort and people were advised to leave that area. Remote operated UAV were deployed and perform imagery collection in orfer to cool the reactors as reported by Ackerman (2011). Lee at al (2013) stated that Korea Cadastral Survey Corp (KCSC) performed and survey to make flood maps caused by typhoon "SANBA" during September 14-17, 2012. A hexa-copter was used during investigation period for 36 days. The flood depth is 0.3 to 0.8 m for 59 hours. Photographs were taken at 300 m altitude with Ricoh GD D IV digital camera. Maximum takeoff weight for UAV is 7 kg. There were a pilot and a system man to operate UAV remotely and manually using flight controlled software. The ground survey has been conducted to verify and confirm the damage status of flooding area. The purpose of survey is preparation for compensation payment. Unmanned Aerial System (UAS) was successfully used in 120 years return period flood in Balkans in 2014.

UAS is equipped with sophisticated 3D data processing algorithm and used in support for damage assessment, area mapping and re-localizing the many explosive remnants of wars moved due to flooding and landslide as discussed by Cubber et al (2014). In addition, UAS was used to propose the optimal location to install high –pressure pumps. After pumping for few days, water levels did not decreased and UAS was used to inspect the undetected dike breaching. UAS assist in identifying where the flood waters from Sava River broke the dam. The flood waters flowed through these breaches and completely submerged the agricultural lands and all people needed to be evacuated. The relief team cannot approach the area due to high risk of shifted minefields during flood and landslides. UAS was used for aerial assessment and mapping of mine-suspected area and to find indicators of where the minefields.

The great flood of Thailand in 2011 caused tremendous damage to the country. It is a long duration flood approximate 2 months in the central plain of Chao Phraya river basin with the flood depth from 0.5 to 2.5 m. Proper flood management during crisis situation in 2011 is important and updated field data is necessary and required to support proper decisions. The flood extent covered a large area in the river basin and it propagated to Bangkok, a capital of Thailand. Technology can be used to assist in surveying works covering a large inundation area to get spatial data in the vicinity of Bangkok. The present objective is to demonstrate the technology assisted in flood management during the great flood in 2011 and to present the future preparation of Hydro and Agro Informatics Institute (HAII), Ministry of Science and Technology, for better technology to be used to improve flood management.

Aerial survey technology

HAII have 2 types of UAV with the followings information

Type I : Radius flight distance 12 km
: Flight time 1 hour
: Stabilized system for still photograph with Canon IXUS 230 HS, resolution 12 megapixels, and
: Real time video to ground station

Type II : Radius flight distance 40 km, covering 12 square kilometers
: Flight time 1 hour 30 minutes
: Stabilized system for still photograph with GeoPro Hero 3 resolution 12 megapixels
: Video system with resolution not less than 720 p, and
: Programmed for still image and video

Fig. 1 UAV Type I.

Fig. 2 UAV Type II.

Figure 1 shows UAV type I which is used for producing maps. Figure 2 shows UAV type II used for long range survey. During the 2011 flood, survey work using Unmanned Aerial Vehicle (UAV) with Siam UAV and Institute of FIeld roBOtics (FIBO), King Mongkut Institute of Technology, Thonburi. (KMITT) was conducted. The UAV equipped with Global Positioning System (GPS), digital aerial camera and real time video, Go Pro. It is the old model of UAV prior to be updated and classified into 2 types as described above. This model is similar to Type I UAV but there is no stabilized system and only video was taken during the field operation. It can be programmed to have automatic flight with planned routing to cover the target area with specified purposes. Videos were taken at altitude 200 m. The longest surveyed distance is 25 km. The purposes of UAV operation during flood 2014 are as follows:

- To investigate the condition of drainage facilities such as natural canals, drainage channel for any obstruction.
- To explore flood extent in flood plain as an overview of inundation area.
- To determine the flood and water quality condition at the target area such as industrial estates.
- To investigate and validate the operational flood management and relief operation.

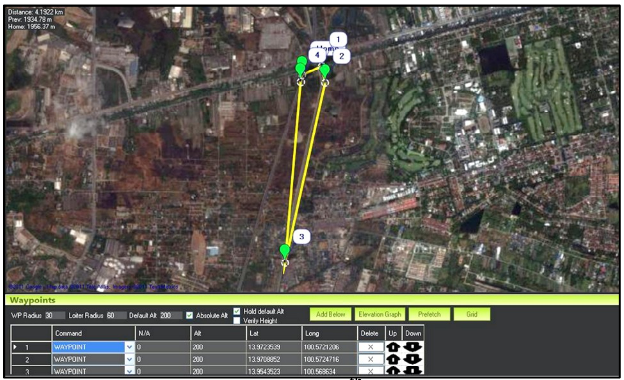

Fig. 3 Flight route of UAV on 4th November 2011.

There were 32 fights during 26 October to 29 November 2011. Recorded video are uploaded to www.youtube.com. The video recording from each flight was analyzed every day. Selected snapshots taken from video were input into a daily report so that the suggestion and output from each flight can be made. All detail and daily reports are provided at http://fibo.kmutt.ac.th/fiboweb/2013/index.php/th/menu-industrial-services-th/menu-industrial-publication-th/menu-industrial-flooding-survey-th/674-thai-categories/industrial-services-th/flooding-survey-th/901-uav. UAV may not be safe when it flies during rainfall. UAV was used to identify the flooded area and to monitor the work on ground for flood protection. Flight route of UAV on 4th November 2014 is shown in Fig. 3. Purpose is to investigate the flood condition in the vicinity of public raw water supply canal. Take off location is in the north of target. Flight distance is around 2 km with 200 m altitude. Snapshot were taken from recorded video as shown in Fig. 4. It showed the flooded water flow into raw water supply canal at the levee breaching location. In this case exact location can be identified and appropriate measure by mobile operation unit with policemen can be taken in a short time. The temporary levee using big bags was checked for damage and possible intruder from people outside levee on 8th November 2014. Flight route is shown in Fig. 5.

The take off point is close to Don Muang airport. UAV flew across it to the target in the east direction. Investigation and video were taken at position 2 to 3 in Fig.5. Results show that the temporary levees are in good condition. There is no damage based on visual inspection as shown in Fig. 6. Investigations of ground work using UAV were conducted in the west of Bangkok as well. Figure 7 depicts route of UAV on 15th November 2014. It showed canal dredging by an excavator close to a bridge in Klong Ratchamontri and dredged material were put at the side of canal in fig. 8. This is to confirm that work was been conducted as planned. The existing physical condition of Klong Ratchamontri was investigated as shown in Fig.9. The width is not uniform and some parts are narrowed so that it may not be a good conveyance corresponded to a pumping capacity at station as shown. Obstructions in Klong Lenpen is shown in Fig. 10. Recorded of video in UAV provided the information of floating weeds and rubbish in drainage canals which are locations, distanced that floating trash covered so that the proper planned can be made to get rid of them. UAVs were firstly used in Thailand for a huge flood in 2011. The flight time and distance are short at the beginning and it kept increasing up to 25 km flight distance in the ending of the surveys. Flood in 2014 covered wide area so that survey work can cover particular locations both west and east Bangkok. Dissemination of information can be conducted through social media to public to use during flood. There are totally 28,000 views. Information is useful for public to understand the conditions of flooding in many locations around Bangkok and it is used for decision making for further adaptation of their living.

Fig. 4 Flooded water flow to Raw water supply canal due to levee breaching.

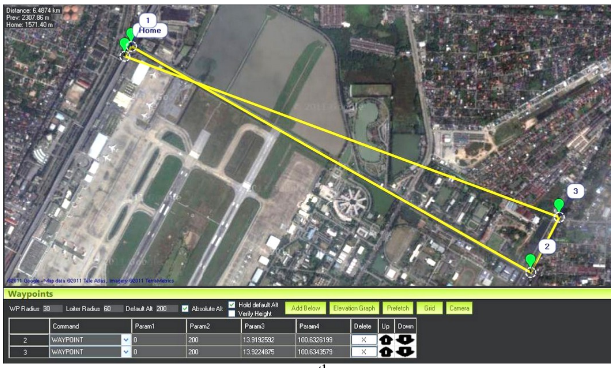

Fig. 5 UAV flight route on 8th November 2011.

Fig. 6 Temporary levee (Big Bag) condition in Don Muang district.

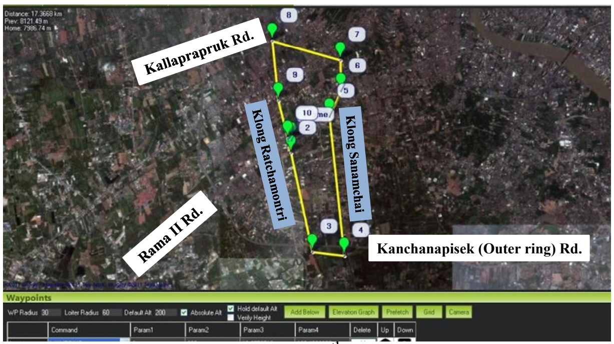

Fig. 7 UAV flight route on 15th November 2011.

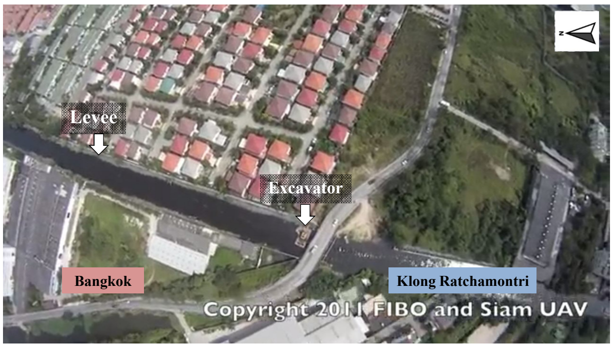

Fig. 8 Excavator is working to dredge deposited sediment in Klong Ratchamontri.

Fig. 9 Examine the width of Klong Ratchamontri at pumping station.

Survey technology by boat

In addition, there are surveyed boats developed with the collaboration between HAII, Department of Science Service (DSS) and Rajamangala University of Technology Thanyaburi. Installed equipment are shown in Fig. 10 and the list as follows:

- Inertial Measurement Unit (IMU) for directing the boat
- Main computing unit
- Wireless data link
- Differential Global Positioning System (DGPS)
- Pod propulsion, and
- Echo sounder

Fig. 10 Obstruction of flow in Klong Lenpen.

Automated control is used to navigate surveyed boat to the required route as planned. Surveys of depth of canals were carried out in 2011 but the automated boat cannot be used due to strong current in canals therefore all equipment were modified and mounted on a bigger boat as illustrated in Fig. 11. Output from survey is route of survey and measured water depth related to Mean Sea Level using DGPS. Surveys were conducted in Klong Lad Phrao, Klong San Saeb and Klong Mahanak. Those canals are important for conveyance flooded water intruded into Bangkok to be drained to a pumping station through tunnel and finally to Chao Phraya river. There are a number of shallow and deposited sediment locations especially at the junction of canals and expressways foundation. This survey can identify the exact locations to be dredged to improve capacity of discharge in canals. Figure 12 shows deposited sediment at foundation of expressway structures. Klong Lad Phrao has average depth from 2 to 2.5 m while depths at expressway structure are 1.6 to 1.8 m. Excavation work is then proposed at this point. Sediment accretion in front of pumping station is also found during survey work on 29th October 2014 as shown in Fig. 13. At junction of Klong Lad Phrao and San Saeb, there is a tunnel and a pumping station around 60 m^3/s. A pumping station may not be able to operate at high efficiency since Klong (or canals) as the conveyance system does not have good physical condition due to deposition. This pumping station is a strategic and important one because it works as flood bypass to convey flooded water in the north of Bangkok drain to Chao Phraya River. In the future, the exact cross section of canals in Bangkok can be obtained through only one survey route, improved technology with new concept idea for multi –scan is then proposed.

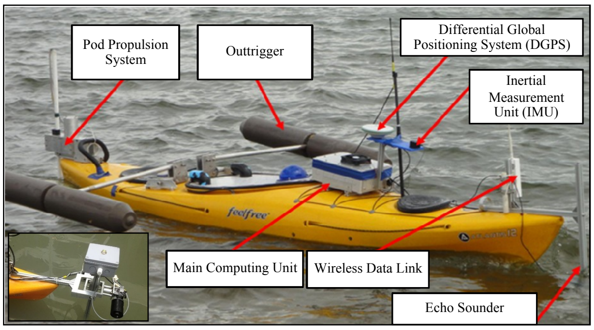

Fig. 11 Equipment and Accessories on board in surveyed boat.

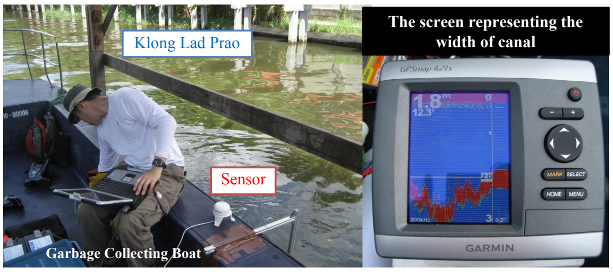

Fig. 12 Equipment on surveyed boat.

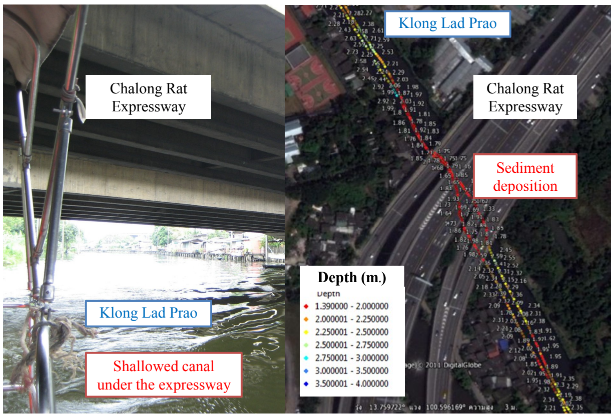

Fig. 13 Sediment deposition at foundation of expressway.

Land Survey Technology

There is another technology called Mobile Mapping System (MMS) that can be installed to any vehicle to survey the levee height and investigate the flood condition in the field. The MMS will be integrated with the Global Navigation Satellite System (GNSS) so that the positioning of vehicle can be identified correctly and survey can be conducted in a short time. IMU is installed on mobile as well. Optionally, the MMS can be integrated with laser scanner and ladybug 3D camera to survey surrounding data around the mobile vehicle such as levee height which vehicle cannot be on top over it. The temporary levees were constructed in many locations as for self-protection. Correct information of levee for location, height, type, material and time of construction is important for planning and modelling during crisis management. Fig. 14 shows equipment on mobile vehicle. At present, it is in the research phase and it will be used for operation further.

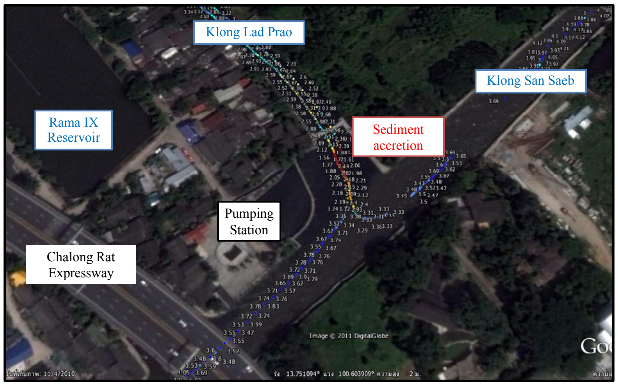

Fig. 14 Sediment accretion in front of San Saeb-Lad Phrao Tunnel pumping station.

Conclusions

Survey technology was intensively used during 2011 flood. Information from UAV survey covered wide range of application from monitoring the flood operation to update and identifies location of problem/obstruction in the near real time. Operational flood management can be conducted in a short with precise target from aerial survey results. Survey technology will be gradually improved using experiences during the actual flood crisis.

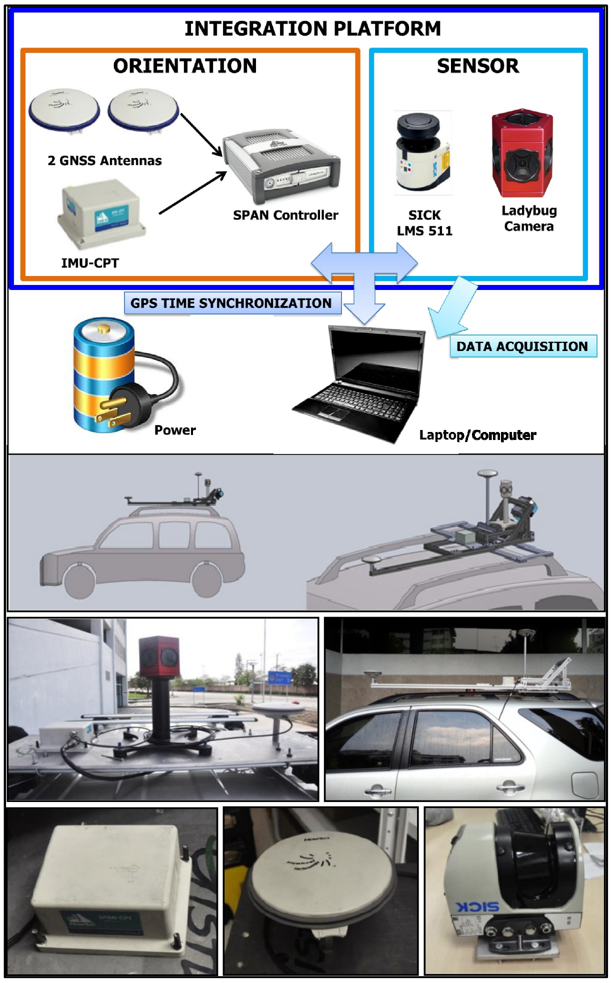

Fig. 15 Surveyed vehicle with MMS

References

Ackeman E (2011) Japan Earthquake: Global Hawk UAV may be able to peek inside Damaged Reactors, Spectrum, IEEE March.

Adams S. M., and Friedland C. J. (2011). A Survey of Unmanned Aerial Vehicle (UAV) usage for imagery collection in Disaster Research and Management, 9th International Workshop on Remote Sensing for Disaster Response, September.

Chitradon R., Boonya-Aroonnet S. and Weesakul S. (2014). Development of National Hydroinformatics and Climate Data Center for Operational Flood Forecasting, Proceeding of the 19th IAHR-APD Congress 2014, Hanoi, Vietnam

Cubber G.D., Balta H., Doroftei D and Baudoin Y., (2014) UAS Deployment and Data Processing during the Balkans Flooding, IEEE International Symposium on Safety Security and Rescue Robotics (SSRR). Toyako-cho, Hokkaido

Cunningham K., Walker G., Stahlke E. and Wilson R.,(2012) Cadastral Audit and Assessment Using Unmanned Aerial Systems, International Archives of the Photogrammetry , Remote Sensing and Spatial Information Sciences, Vol.XXXVII-1/C22 UAV-g, Conference on Unmanned Aerial Vehicle in Geoinformatics, Zurich, Switzerland

Hirokawa R., Kubo D., Suzuki S., Meguro J and Suzuki T.,(2007) A Small UAV for Immediate Hazard Map Generation, Aerospace Conference and Exhibition, May Rohnert Park, California, American, May.

Lee I., Kang J., and Seo G., (2013) Applicability Analysis of Ultra-Light UAV for flooding Site Survey in South Korea, International Achieves of the Photogrammetry Remote Sensing and Spatial Information Sciences, Vol. XL-1/W1, ISPRS Hannover Workshop, p.185-189, May.

Pratt K. and Murphy R.R., (2006) Requirements for Semi-Autonomous Flight in Miniature UAVs for Structural Inspection, AUAV's Unmanned Systems North America, Orlando Florida, Association for Unmanned Vehicle System International

Steimle, E.T., Murphy, R.R., Lindemuth, M., and Hall, M.L., (200(9) Unmanned marine vehicle use at Hurricanes Wilma and Ike, OCEANS 2009, MTS/IEEE Biloxi - Marine Technology for Our Future: Global and Local Challenges , vol., no., pp.1-6, October.

Derivation of Optimal Rule Curves for Flood Control Study of Ubolratana Reservoir, Thailand

Pich Hirun[1,a *] and Areeya Rittima[2,b]

Abstract The significant requirement of reservoir operation in Thailand is mainly focused on the effectiveness of water allocation for irrigation and other activities on the downstream side. However, the flood control purpose is highly emphasized and included for multi-purpose reservoir operations since some regions of Thailand encountered with the worst floods in 2011. In general, rule curves have been used as a major reservoir operation tool to achieve the expected outcome especially from large reservoirs. Owing to the effects of critical events, the optimal rule curves have been initiated using the embedded simulation-optimization techniques with various solving algorithms. This study proposed the optimal rules derived by GAs technique to manage the reservoir storage zone for flood control purpose and to satisfy the downstream water demand of the Ubolratana reservoir in Khonkean province. The daily hydrological data associated with the conventional mass balance principle since 2000 to 2014 was adopted to construct the reservoir operation model and the diverted water at Nong Wai weir was employed as the irrigation demand in the model. Three scenarios of operating policy to cope with incoming floods were created to derive the different types the optimal rule curves and compared the simulated results with the existing operation. The results indicated that these optimal rule curves could provide the progressive performances specifically flood reduction not to encroach the surcharge storage zone of Ubolratana reservoir. Moreover, they could satisfy the downstream water demand at reasonable level including the hydropower benefit.

Pich Hirun
Department of Civil and Environmental Engineering
Mahidol University, MU
Nakhonpathom, Thailand
hirunpich@gmail.com

Areeya Rittima
Department of Civil and Environmental Engineering
Mahidol University, MU
Nakhonpathom, Thailand
egart@mahidol.ac.th

Keywords *Reservoir Operation, Genetic Algorithm, Optimization Technique, Rule Curves, Ubolratana Reservoir*

Introduction

Usability of large reservoirs in Thailand has highly been expected to meet the multiple objectives such as domestic and industrial uses, irrigation, environmental flow, and hydropower generation. Meanwhile, the flood control purpose is also included and highly emphasized for multi-purpose reservoir operations since some regions of Thailand encountered with the worst floods in 2011. In general, the moderation of flood volume through storage reservoirs has been proposed and achieved by reservoir operation policies and flood control measures. Consequently, to minimize the downstream damages during critical floods and to ensure the dam safety, the optimal rule curves have been initiated and the optimization technique with various solving algorithm has been employed to carry out the preferable solution of optimal rule sets. Optimization models are normally used to evaluate predefined operating rules by considering various constraints of reservoir system in mathematical simulation (Oliveira and Loucks, 1997). Labadie (2004) proposed the state of art in optimization techniques including (1) Implicit Stochastic Optimization (ISO): Linear Programming (LP), Network Flow Optimization, Nonlinear Programming (NLP), Dynamic Programming (DP) (2) Explicit Stochastic Optimization (ESO): Stochastic Linear Programing (SLP), Stochastic Dynamic Programming (SDP), Real-Time Control with Forecasting and Heuristic Programming. Disadvantage and advantage of each optimization model were explicitly described to represent its advancement. Genetic Algorithms (GAs), heuristic programming model invented by John Holland, was strongly recommended to apply due to superior results. The great deal of GAs's performance is that it can be able to directly link with related historical data. Genetic algorithm is a searching technique that mimics the mechanism of natural selection in order to figure out the best solution (Holland, 1975). GAs technique have an efficient capability on handle with complex problem such as discontinuous, non-convex, non-linear and another complicated functions (Chang et al., 2005). For the fundamental procedure of GAs, the solution is randomly searching on the entire design space by applying genetic-based principle and probabilistic selection (Schreyer, 2006). Initially, many individual solutions are randomly generated to form the initial population. The fitness function which measures the quality of the represented solution is then evaluated to select the best solution. The population is generated from those selected solution in the next generation through the combination of GA operator; crossover and mutation. The process continuously proceeds until the best individual solution under designed conditions is met as shown in Fig.1.

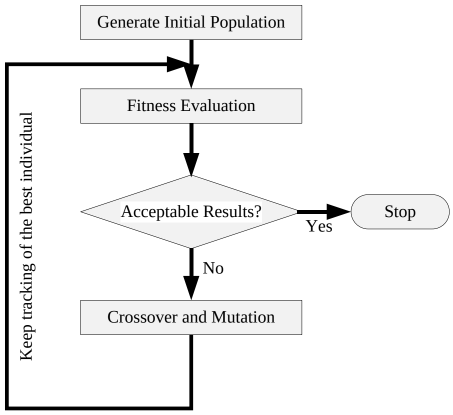

Fig. 1 The fundamental procedure of GAs

The application of GAs in reservoir operation field had the progressive development as compared to the traditional methods. The accomplished works usually proposed improvement of derived reservoir operation rules. For example, Olivera and Locks (1997) presented the developed operating rules for multireservoir systems by applying GAs in order to develop the satisfied policies especially for water supply and hydropower requirement. Chen (2003) developed a Real Coded Genetic Algorithm (RGA) to optimize operating rule curves for reservoir system in Taiwan. The results showed the performance improvement in term of shortage index performed by optimal rule curves. Mathur and Nikam (2009) developed optimal reservoir operating policies for an irrigation requirement by applying GAs method. The key parameters of GAs had been adjusted to search optimum setting point for the superior solutions. In Thailand, Hormwichian et al. (2009) proposed the Conditional Genetic Algorithms (CGAs) to derive the optimal rule curves to reduce water shortage and excess water of Lampao reservoir. Jothiprakash and Shanthi (2006) and Taesoon et al. (2008) mentioned that the GAs could generate the satisfactory outcome especially applied to a single reservoir. Rittima (2012) also applied GAs to develop optimal hedging policies for hydropower generation at Ubolratana reservoir. Therefore, GAs technique was applied in this study to derive the optimal rule curves specially emphasized on flood control management by minimizing flooded water together with water deficit.

Study area

The Phong basin is located in the upper northeast region of Thailand. The watershed is approximately 6,300 square kilometers covering the area of Chaiyaphum, Nong Bua Lumphu, Loei, Khon Kaen and Petchaboon provinces. The climate in Phong basin is dominated by the southwest monsoon. There is the main dam in the basin, Ubolratana dam which was constructed on the main stem of Phong river. Consequently Ubolratana reservoir was formed as the multi-purpose reservoir for the downstream water uses as well as power generation. The construction of reservoir was completed in 1966 with the total storage and the active storage of 2,263.60 and 1,761.30 mcm, respectively. The water released from Ubolratana reservoir is controlled at Nong Wai weir to serve for irrigation demand of Nong Wai Irrigation Project and downstream water uses. The associated hydro-meteorological data and reservoir description are shown in the Table 1. The schematic diagram of reservoir system is shown in Fig. 2.

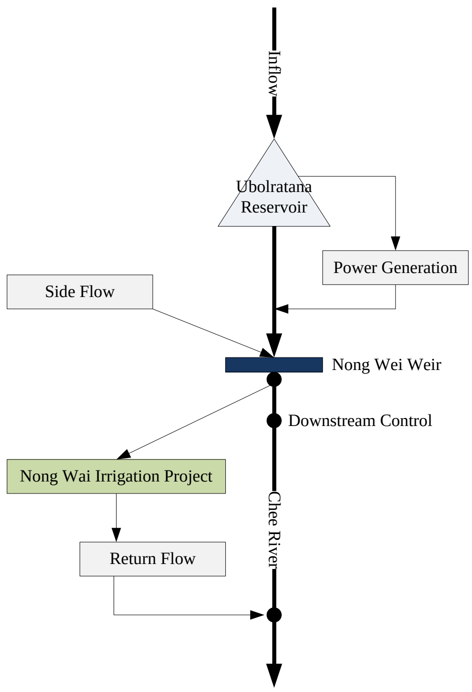

Fig. 2 The schematic diagram of Ubolratana reservoir system

Table 1. Hydro-meteorological data and description of Ubolratana reservoir

Hydro-meteorological data and reservoir description	
Drainage area (km^2)	12,104
Annual reservoir inflow ($mcm.yr^{-1}$)	2,393
Annual reservoir release ($mcm.yr^{-1}$)	1,943
Annual rainfall (mm/yr)	1,200
Average annual temperature (^oc)	26.7
Average annual evaporation ($mcm.yr^{-1}$)	542
Reservoir capacity (mcm)	2,264
Max.PL (m.msl.)	+ 186.6
NPL (m.msl.)	+ 182.0
MPL (m.msl.)	+ 175.5

mcm = million cubic meters, m.msl. = meters above mean sea level, Max.PL = maximum pool level, NPL = normal pool level, MPL = minimum pool level

Methodology

Data collection and water requirement estimation

The daily hydrological data of Ubolratana reservoir and associated data since 2000-2014 were collected from the Electricity Generating Authority of Thailand (EGAT), Royal Irrigation Department (RID), and Meteorology Department (MD) comprising rainfall data, inflow and evaporation data, energy production, and operating rule curves, etc. The collected data were primarily investigated by using time series plotting and filled up the missing and abnormal data by applying statistical analysis methods. In this study, the actual amount of water diverted to the canal distribution system at Nong Wai weir and minimum water release for environmental preservation were combined and considered as total water demand of the project.

Development of reservoir operation model

The conventional mass balance principle of reservoir was applied to check a correlation of associated data as well as to construct a reservoir operation model according to the schematic diagram of Ubolratana reservoir as described above. The optimization technique was employed and embedded in the reservoir operation model to generate the optimal rule curve on a monthly basis. In this study, three operating policies emphasized on the flood control management were proposed for determining water release from reservoir:

Policy 1:
In fulfilled situation when the water level in reservoir was rising up above the upper rule curve, the excess water would be released referring to the existing storage capacity ratio which was equivalent to the target water demand.

Policy 2:
During the filling stages of water in reservoir, the operating policy for flood control regulation was based on the concept of a cut-off reservoir level. Therefore, the surplus water above the upper rule curve would totally be released.

Policy 3:
Releasing excess water in fulfilled period was carried out following the concept of HEC-5 for flood control operation (US Army Corps of Engineer, 1998).

In addition, during the drawdown and normal periods, the operating rules resembling the standard operation policy (SOP) were employed for reservoir operation. In the other words, the amount of water release was specified equal to the downstream target demand in normal situation. However, the release might be reduced by some amount of water depending on the available water in the reservoir.

Derivation of optimal rule curves

(1) Objective function
The main objective of this study was to reduce flooded water and water deficit on the downstream side of Ubolratana reservoir. Therefore, the objective function was expressed as follows:

$$\text{Minimize } Z = \sum_{t=1}^{T}\left(R_t - R_{\max}\right)^2 + \sum_{t=1}^{T}\left(R_t - D_t\right)^2 \quad (1)$$

Where R_t is reservoir release (mcm), R_{max} is the maximum release according to the safe-carrying capacity of the downstream channel (mcm) and D_t is water demand

(2) Constraints
- Mass-balance equation

The relationship of reservoir water balance variables was given by the continuity equation:

$$S_{t+1} = S_t + I_t + P_t - E_t - R_t \quad (2)$$

- Reservoir storage constraint

$$S_{\min} \le S_t \le S_{\max} \quad (3)$$

- Limitation of hydropower generation

$$Gen_t \le G_{installed} \quad (4)$$

$$Gen_t = gQ_tH_tT_t\eta \quad (5)$$

- Reservoir release constraint

$$0 \le R_t \le R_{max} \quad (6)$$

- Water level control constraint

$$WL_{min} \le WL_t \le WL_{max} \quad (7)$$

Where S_{t+1} is reservoir storage in time period t+1, S_t is reservoir storage in time period t (mcm), I_t is reservoir inflow in time period t (mcm), P_t is rainfall data precipitated on the reservoir water surface in time period t (mcm), E_t is evaporation loss in time period t (mcm), R_t is reservoir release in time period t (mcm), S_{min} is storage capacity at MPL and S_{max} is the storage capacity at NPL, Gen_t is generated electricity in time period t (kWhr), $G_{installed}$ is the installed capacity of hydropower plant (kWhr), g is gravitation force (m/s^2), Q_t is the discharge through power plant in time period t (m^3/s), H_t is net head of water during time period t (m), T_t is number of operating hours (hr) and η is the overall efficiency of the power plant (%), R_{max} is maximum release according to the safe-carrying capacity of the downstream channel, WL_{min} is water level at MPL (m.msl.), WL is water level in the time period t (m.msl.) and WL_{max} is water level at NPL (m.msl.)

Results and discussion

The embedded simulation-optimization technique with GA algorithm was constructed by employing the daily reservoir data of Ubolratana reservoir. The significant parameters of GA such as population size and crossover probability were adjusted to increase the capability of optimization by referring to the recommendation proposed by Mathur and Nikam (2009) that population size and crossover probability were 250 and 0.75, respectively. The optimal rule curves for flood control management were derived based on three operating policies as proposed and the obtained results were shown in Fig.3. It was found that the ranges of upper and lower lines of the derived rule curves were wider than those of the existing rules. This could say that releasing adequate amount of water from reservoir especially in the normal period could keep the sufficient water storage for downstream water uses and could also provide enough space for flood control storage during refilled period. Therefore, the reliability of estimating the downstream demand played a vital role in determination of water release. The optimal rule curves obtained by policy 1 seemed to be similar to the existing rule curves both pattern and values. It reserved large vacant space to retain incoming flood at the beginning of wet season (May-Aug). The pattern of optimal rule curves taken by policy 2 and 3 tended to be similar both upper and lower lines. The upper rules were likely to be approach to the normal high water level. The reservation of flood control storage in reservoir started in May and ended in October. Additionally, it was not necessary to reserve some space for incoming flood at the end of wet season, therefore, the upper rules derived by policy 2 and 3 were at the normal high water level in November and December.

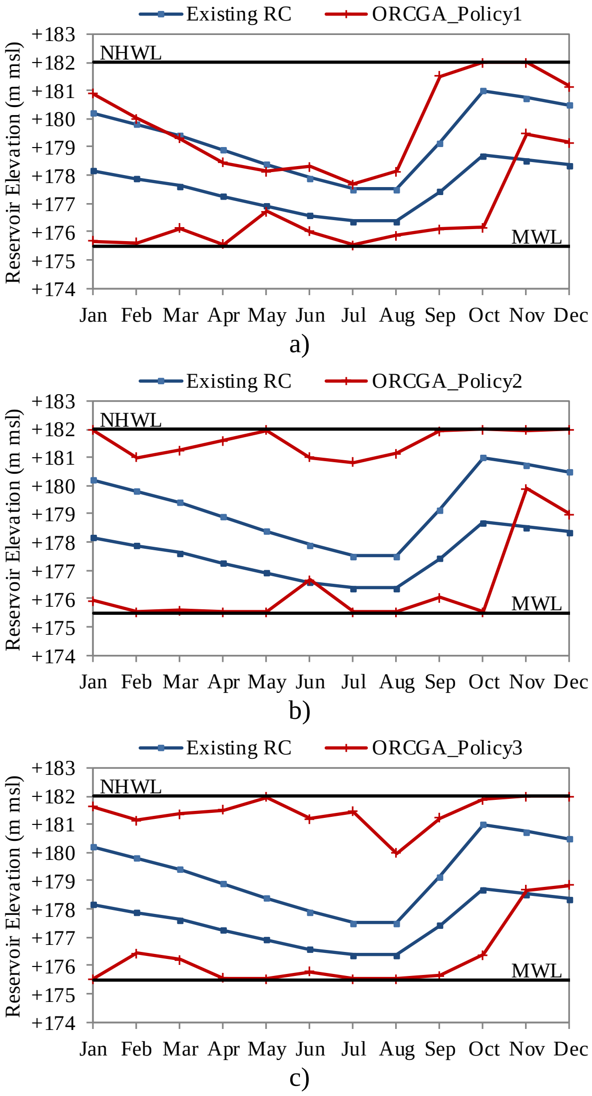

Fig. 3 Optimal rule curves for flood control study of Ubolratana reservoir

Fig.4 showed the volume of spilled water through the spillway structure using the optimal rue curves and compared the operational results with the actual discharge as recorded since 2000-2013. It was found that using optimal rule curves taken by policy 1 and 2 for reservoir operation could reduce the volume of spilled water especially in 2008, 2010, and 2011 compared to those performed by the existing rule. However, applying the optimal rule curve due to policy 3 to manage huge flood in 2011 was not good enough because it gave the higher volume of spillage compared to the actual surplus water.

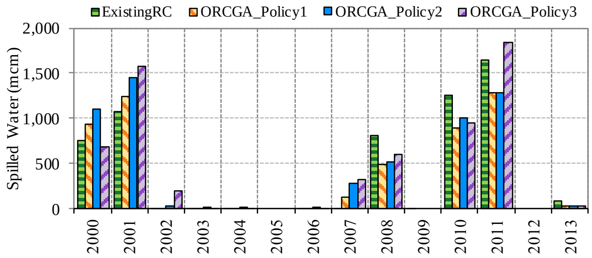

Fig.4 Annual spilled water through spillway structure performed by the existing rule and 3 optimal rules.

In addition, the simulated reservoir operation results in Table 2 indicated that using optimal rule curves derived by policy 1, 2, and 3 could rise up the average water level in the long run. The water level in the reservoir is considered as a part of water head calculation by finding the difference in height between the headwater level in the reservoir and tail water level. In the other words, the amount of potential energy generated is proportional to the water head.

Consequently, it was appeared that releasing water by these three optimal rules could slightly provide the better energy outcomes which were 72,774.62, 72,560.72 and 77,174.89 MWhr per year, respectively compared to those obtained from the actual operation. The results also showed that the capability to provide firm energy (minimum energy production) would potentially be improved if there three optimal rules were performed which ranged from 0.47%-0.96% for policy1 and policy 2, and 12.80% for policy 3. However, the ending reservoir storage done by policy 1 and 2 was slightly lower than the actual one.

In this study, the key performance indicator of reservoir operation; reliability index, were examined in two aspects; water shortage and water spillage. The condition of shortage failure was referred to the incapability to allocate sufficient water to downstream water demand. For the condition of spillage failure, it was specified when surplus water was controlled passing through spillway with unsafe carrying capacity of the channel.

Table 2. Simulated reservoir operation results

Results	Reservoir operation policy			
	Actual operation	ORCGA Policy1	ORCGA Policy2	ORCGA Policy3
▪ Simulated results				
1. Total release (mcm/yr)				
- Minimum annual release	379.01	376.80	376.80	376.80
- Maximum annual release	4,752.25	4,924.51	4,761.72	4,897.27
- Average annual release	2,381.57	2,458.91	2,460.18	2,422.53
2. Reservoir water level (m.msl)				
- Minimum water level	175.08	175.28	175.38	178.39
- Maximum water level	183.24	182.24	182.35	183.41
- Average water level	178.59	178.60	178.92	180.50
3. Reservoir storage (mcm)				
- Minimum reservoir storage	518.52	541.99	554.11	1,109.41
- Maximum reservoir storage	2,821.19	2,394.33	2,445.67	2,925.49
- Average reservoir storage	1,255.54	1,245.74	1,328.53	1,779.32
- Active storage/Ending storage (%)	54.61	46.27	45.28	64.56
4. Annual energy production (MWhr/yr)				
- Minimum annual energy production	13,626.30	13,757.06	13,690.36	15,371.10
- Maximum annual energy production	117,869.90	130,269.98	125,155.64	133,554.53
- Average annual energy production	72,495.97	72,774.62	72,560.72	77,174.89
▪ Reservoir performance indices				
1. Reliability indices* (%)				
- Shortage mode	49	86	89	87
- Spillage mode	92	94	94	95
2. Volume of spilled water (mcm/day)	1.08	0.96	1.10	1.19

mcm = million cubic meters; m.msl = meters above mean sea level; MWhr = megawatt hour.

* Reliability index = $REL = (1.0 - \frac{FAIL}{N}) \times 100$; FAIL = number of failures, N = total number of events.

It was found that the operational results performed by three optimal rules gave the satisfactory outcomes in handling with water shortage problems in a long run even the lower rule lines were closer to minimum water level. The reliability of shortage mode increased up to 86%-89% as presented in the table. This meant that employing optimal rules required more frequent needs to control water following normal operation scheme to satisfy the target demand on the downstream side. However, the reliability index received from these optimal rules and existing rule curve for the spillage mode seemed to be closer to each other. This could be explained that the frequency of failure among these rules was not intensively different, however, employing optimal rules specially policy 1 and 2 could reduce the volume of spilled water as described above.

Conclusions

The main purpose of this study was to derive the optimal operating rule curves for flood control study of Ubolratana reservoir by minimizing the volumes of flood water together with water deficit. The simulation-optimization technique with GAs solving method was embedded together to construct reservoir operation model. The simulated results showed the satisfactory performance in terms of flood reduction, increase in energy production, deduction of water deficit which represented the usability of the multipurpose reservoir system.

References

Chang, F.J., Chen, L. and Chang, L.C. (2005). Optimizing the reservoir operating rule curves by genetic algorithms. Hydrological Processes. 19(11): 2277-89.

Chen, L. (2003). Real coded genetic algorithm optimization of long term reservoir operation. Journal of the American Water Resources Association. 39(5): 1157-65.

Holland, J.H. (1975). Adaptation in Natural and Artificial Systems. University of Michigan Press.

Hormwichian, R., Kangrang, A. and Lamom, A. (2009). A conditional genetic algorithm model for searching optimal reservoir rule curves. J. Applied Sci. 9(19): 3575-80.

Jothiprakash, V., Shanthi, G. (2006). Single reservoir operating policies using genetic algorithm. Water Resour Manage. 20(6): 917-29.

Labadie, J. (2004). Optimal operation of multireservoir systems: state-of-the-art review. Journal of Water Resources Planning and Management. 130(2): 93-111.

Mathur, Y.P. and Nikam, S.J. (2009). Optimal reservoir operation policies using genetic algorithm. International Journal of Engineering and Technology. 1(2):1793-8236.

Oliveira, R., Loucks, D.P. (1997). Operating rules for multireservoir systems. Water Resources Research. 33(4): 839-52.

Rittima, A. (2012). Optimal hedging policies for hydropower generation at Ubolratana reservoir. Kasetsart J(Nat Sci). 46(5): 812-25.

Schreyer, A. (2006). GA Optimization for Excel Version 1.2, Quick Start Manual.

Taesoon K.J-HH., Bae, D.H. and Kim, J.H. (2008). Single-reservoir operating rules for a year using multiobjective genetic algorithm. Journal of Hydroinformatics. 10(2): 179-xx.

US Army Corps of Engineers. (1998). HEC-5 Simulation of Flood Control and Conservation Systems Hydrologic Engineering Center.

THA 2015 International Conference on
"Climate Change and Water & Environment Management in Monsoon Asia"
28-30 January 2015, Bangkok, Thailand.

The basin-wide disaster impact assessments under extreme climate scenario-a case study in Kao-Ping River Basin

Hsin-Chi Li [1], Hsiao-Ping Wei [2], Tingyeh Wu [3] , Hung-Ju Shih[4], Yuan-Fong Su [5] and Yung-Ming Chen [6]

Abstract This study selected the Kao-Ping River Basin, Taiwan, one of the most serve disaster area during typhoon Morakot, as a demonstration area and adopted dynamical downscaling data to simulate the most extreme typhoon precipitation events in the future (from 2075 to 2099) under climate change condition. The SOBEK flood model was used to build a model of the Kao-Ping River basin, and data regarding the river channel cross-sections, hydraulic constructions, precipitation in future climates, land use, and water levels were used to simulate potential flooding caused by extreme typhoon events in the future. The Taiwan Typhoon Loss Assessment System (TLAS) established by the National Science and Technology Center of Disaster Reduction (NCDR) was used to evaluate the potential losses associated with the extreme events. The calculation of property loss includes 27 types of land use modules, such as agriculture, forestry, fishery, and animal husbandry loss; industrial and commercial service loss; public building loss; and traffic and hydraulic facilities loss. Finally, the results indicate that the most severe loss of Kao-Ping River Basin in the end of century is the land-usage of commerce, which even worse than typhoon Morakot, followed by industry and household.

Keywords *Extreme climate, Loss assessment, SOBEK, TLAS, Kao-Ping basin*

[1]Hsin-Chi Li
National Science and Technology Center for Disaster Reduction (NCDR)
Taipei, Taiwan, R.O.C.
hsinchi@ncdr.nat.gov.tw

[2]Hsiao-Ping Wei
National Science and Technology Center for Disaster Reduction (NCDR)
Taipei, Taiwan, R.O.C.
weiph@ncdr.nat.gov.tw

[3]Tingyeh Wu
National Science and Technology Center for Disaster Reduction (NCDR)
Taipei, Taiwan, R.O.C.
Tingyehwu1060@ncdr.nat.gov.tw

[4]Hung-Ju Shih
National Science and Technology Center for Disaster Reduction (NCDR)
Taipei, Taiwan, R.O.C.
shihruby713@ncdr.nat.gov.tw

[5]Yuan-Fong Su
National Science and Technology Center for Disaster Reduction (NCDR)
Taipei, Taiwan, R.O.C.
yuanfongsu@ncdr.nat.gov.tw

[6]Yung-Ming Chen
National Science and Technology Center for Disaster Reduction (NCDR)
Taipei, Taiwan, R.O.C.
ymchen@ncdr.nat.gov.tw

Climate data

This study used the climate projection simulated by the high-resolution (~20km horizontal resolution) atmospheric general circulation model (AGCM) developed by the Meteorological Research Institute (MRI) under the Japan Meteorological Agency (Mizuta et al. 2012) as the initial and boundary conditions to drive a regional model for conducting dynamical downscaling. The vertical resolution of the dynamical downscaling was 36 levels and the number of horizontal grid points was 380 × 400. The simulation area is shown in Figure 1. Climate simulations for three periods (1979-2003, 2015-2039, and 2075-2099; 25 years per period) were conducted in dynamical downscaling. To prevent significant climate drift during downscaling, causing discrepancies between large-scale circulation features and the global model, this study adopted the spectral nudging method to reduce it. To preserve the added value of using high-resolution topography and land surface data, spectral nudging only applied to the wind, geopotential height, and temperature fields above the boundary layer.

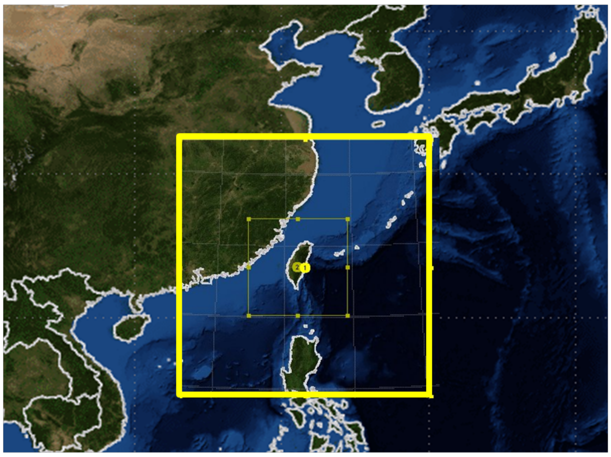

Fig. 1 The range in Taiwan simulated by the 5-km resolution dynamical downscaling is framed in the yellow box. A total of 380 × 400 grid points exist, covering an area of 1900 × 2000 km^2.

Flood simulation model

Common flood models currently used in Taiwan include FLO-2D, HEC-RAS, SOBEK, Storm Water Management Model (SWMM), and cell model.(Hsu, 1996 ; Yen et al. ,1997 ; Shih, 2006 ; Tang et al., 2006 ; Ko et al., 2006) . Because of SOBEK was adopting by Water Resource Agency (WRA), becoming the official flood model. Therefore, this research used SOBEK to simulate the flood impact. The SOBEK model, developed by Deltares(formerly WL Delft Hydraulics), the Netherlands, integrates the commercial hydrologic and hydrodynamic programs of urban drainage systems along with river and regional drainages. SOBEK comprises three model sets, that is, SOBEK Rural, SOBEK Urban, and SOBEK River. These models include rainfall runoff, channel flow, sewer flow water quality, sediment transport, real-time control, overland flow, and groundwater modules. Currently, the SOBEK model is commonly employed for regional flood simulations and hydrodynamics of rivers and urban sewer systems. The simulation results can serve as reference for flood prevention and the management, decision-making, and analysis related to water resources.

Loss assessment model

Based on welfare economics, Li et al. (2008) and Li (2010) divided residential loss into human resource loss and property loss (e.g., housing structure loss, furniture and household appliance loss, transportation vehicle loss, and other losses), collected data of various types of losses using questionnaire surveys, and established a residential disaster loss model. The variables of flood depth, house possession, household member, flood duration, apartment mansion, residential years, and incomes were included in the model. Because the flood loss model including hazard, exposure and vulnerability characteristic variables for a user can further describe risk and generate more policy. Furthermore, Li et al. (2013) utilized all kinds of loss researches and empirical survey data in Taiwan, mainly including land loss, household loss, agricultural loss, industry and commerce loss, transportation and hydraulic use (show as Table 1), and combine the technology of geographic information system., to built Taiwan Typhoon Loss Assessment System (TLAS), the loss function show as table1. This automatically evaluating system estimates not only disaster loss immediately after disaster occurrence, but also probable loss under scenario of mitigation measures and meteorological data by numerical scheme.

Table. 1 Loss function of Taiwan Typhoon Loss Assessment System (TLAS)

Model	Function
Influence Population	$INP = \sum_{i=1}^{N} PD_i \times IA_i$ *INP : Influence Population(people)* *PD_i: Population Dansity (People/m^2)* *LA_i : Influence Area (m^2)*
Land Loss	$LL = \sum_{i=1}^{N} LV_i \times LLA_i$ *LL : Land Loss(NT dollar)* *LV :Land Value(NT dollar/m^2)* *LLA : Land Value Area (m^2)*
Household Loss	$Ln(Flood\ \ loss) =$ $-0.421 + 1.875Ln(Flood\ \ Depth)$ $-1.06(House\ \ Possession)$ $+0.736Ln(Household\ \ Member)$ $+0.637Ln(Flood\ \ Duration)$ $-0.834(Apartment/mansion)$ $-0.028(Residential\ \ Years)$ $+1.159Ln(Income)$
Agricultural Loss	$CL = \sum_{i}^{N} \alpha_i[CPA_i \times CLA_i]$ *CL : Cropper Loss per Aare(NT dollar/m^2)* *CPA_i: Cropper Price (NT dollar /m^2)* *CLA_i : Cropper Loss Area (hectare)* *α_i :Modify Function* *i: Different Crop*
Industry and commerce loss	$ICL = \sum_{i}^{N} \alpha_i[ICP_i \times ICLA_i]$ *ICL : Industry and Commerce Loss(NT dollar)* *ICP_i: Industry and Commerce Price (NT dollar / m^2)* *$ICLA_i$: Industry and Commerce Loss Area (m^2)* *α_i :Modify Function* *i: Different place(county)*

Public Building Loss	$BL = \sum_{i=1}^{N} \sum_{j=1}^{M} \alpha_i [BC_{ij} \times BLA_{ij}]$ *BL : Building Loss(NT dollar)* BC_{ij}: *Building Cost (NT dollar / m^2)* BLA_{ij} *:Building Loss Area(m^2)* α_i *:Modify Function* *i: Different Place(county)* *j:Different Building*
Transportation and Hydraulic use	$THL = \sum_{i=1}^{N} \alpha_i [SUC_i \times SLN_i]$ *THL : Traffic and Hydraulic Loss (NT dollar)* *SUC :Structure Unit Cost (NT dollar/m or NT dollar/m^2)* *SLN : Structure Loss Number(m or m^2)* α_i *:Modify Function* *i: Different Structure*

Flood impact simulation result

Flood simulation

The typhoon precipitation data for future climate projection used in this study were the aforementioned dynamical downscaling data with 5 km horizontal resolution provided by Ministry of Science and Technology, Taiwan. Due to high-resolution models of MRI-AGCM and CLWRF, typhoons can be explicitly simulated. The top 1 most extreme typhoon precipitation event between 2075 and 2099 was selected based on the total accumulated precipitation over the Kao-Ping River basin. For flood simulation, the mean precipitation selected from four grid points near the precipitation station of the Water Resources Agency (WRA) was the input data of SOBEK to analyze the flow of the basin hydrological model. The precipitation stations and the locations of the grid points are shown in Figure 2. No tide stations are located at the estuary of the Kao-Ping River basin, the astronomical tide model FVCOM (Chen, C. et. al., 2006) was used to estimate estuary tide levels along with the flood-tide water levels caused by typhoons. These data were employed as estuary and downstream boundary water level data for conducting hydrodynamic algorithms.

Relevant data such as the catchment area, length, and river gradient of the basin were obtained using the geomorphologic instantaneous unit hydrograph of a 2005 management project (i.e., The Development of Geomorphic and Hydrologic Information Inquiry System for Integrated Basin Management of Major Rivers in Taiwan). Data of the river cross-sections were sourced from large cross-section measurements conducted recently for relevant hydraulic management projects and by various river management offices of the WRA.

Finally, the result of Top1 flood event was show as Figure 3. According to the result, we found that flooding area was larger than typhoon Morakot event, which cause the most sever damage in Taiwan typhoon historical records. The main reason caused flood was the water overflow from the Kao-Ping River and inside inundation. Therefore, the flooded areas mostly distributed along the riverside and gathered in the low-relief areas.

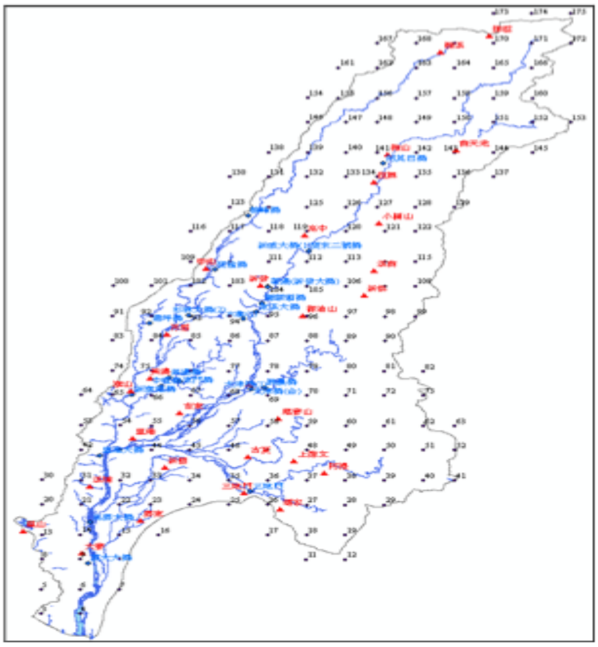

Fig. 2 Kao-Ping river basin area

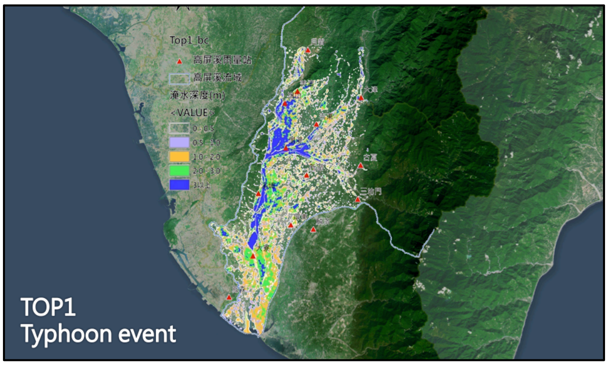

Fig. 3 Kao-Ping river basin simulated flood depth (m)

Food loss assessment

After completed flood simulation, we can directly assesse the flood loss by Taiwan Typhoon Loss Assessment System (TLAS), the interface of this system show as Figure 4. TLAS includes land loss, household loss, agricultural loss, industry and commerce loss, transportation and hydraulic use models. It can automatically evaluate loss according the categories of land use type. Therefore, the users just need to input the disaster magnitude information, including flood area and depth, the calculation process show as Figure 5.

Fig.4 TLAS platform interface

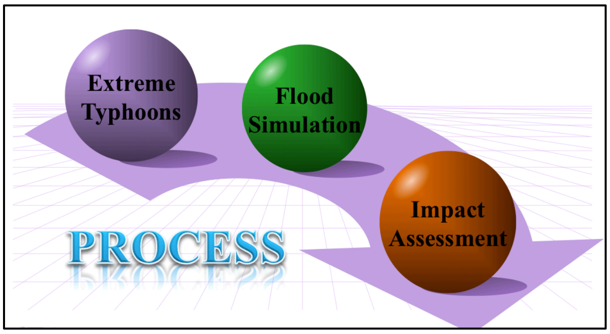

Fig. 5 Loss assessment process

Based on the TLAS result, the TOP1 event caused 377 towns flooded in Kao-Ping river basin. The total flood area was 1,932 km^2, and 26,886 households were flooded. Among all the flooded towns, totally 5 towns over 1500 households are all urban area (Figure 6). Furthermore, according to the loss assessment result, total loss was 689 billions NTD, over three times of typhoon Morakot loss. It showed that Taiwan would face more worse typhoon event by the influence of climate change in the end of this century. Referring to loss analysis, the most severe land use type was commerce during 27 kinds of flooded land use types, occupied 51 % of total loss. Second highest land use type was industry, occupied 23 % of total loss, then third one was housing, occupied 18 % of total loss. Two of the most severe towns were selected for further discussion here, which are Gi-Ray and Niao-Hsong.

In figure 7, Gi-Ray Town was located on the north part of this basin, which was near Kao-Ping River. The main reason of the flood in this town was the water overflow from Kao-Ping River. In the graphic of Gi-Ray town, we found that the most flooded area was agriculture, and housing was the second one. But through the analysis of monetizing process, commerce became the highest loss land use type. This result shows the difference between the approach of area and loss to assess flood impact. The same result shows as Niao-Hsong town. The most flooded areas for these three land use types were leisure-facility, crop and housing, but the highest three loss land use types were commerce, housing and leisure-facility.

Comparing Gi-Ray town with Niao-Hsong town, we could find that the traditional way to analyze loss, using flood area factor to assess impact situation, could not exactly explain the real impact. Because of the flood area factor could not reply the influence of socio-economic condition. On the contrary, the monetizing approach of loss assessment could show the true value of property. This results let decision makers could choose correct policy more easily.

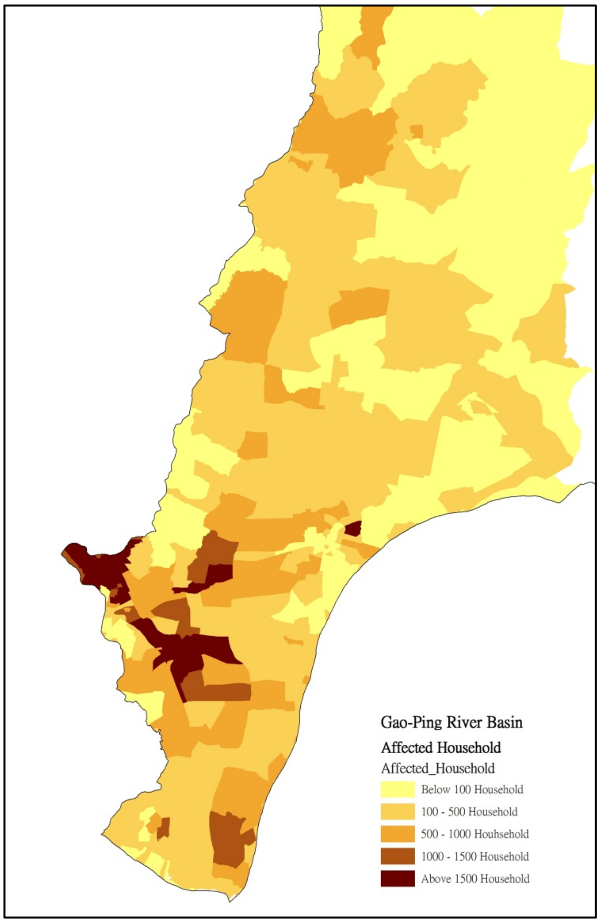

Fig. 6 Influence households

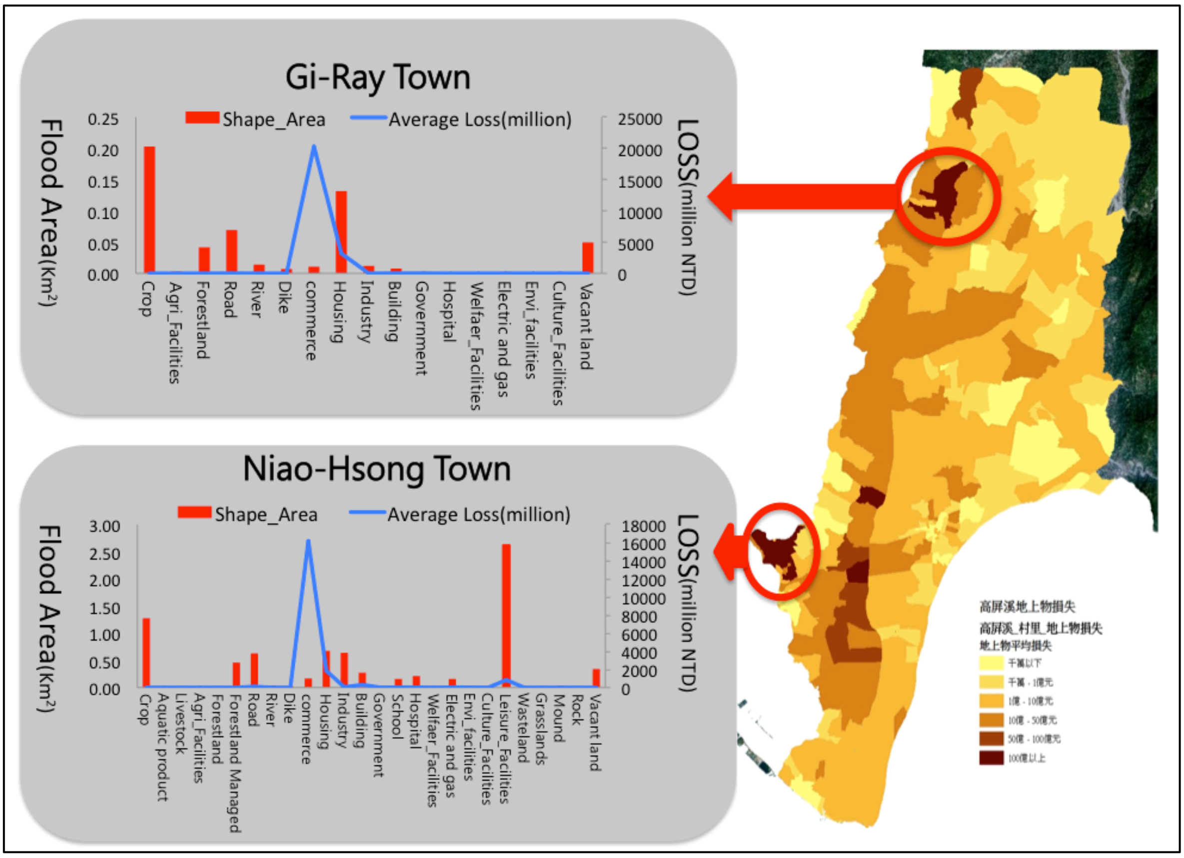

Fig. 7 Two of the most sever towns (Flood loss)

Summary and conclusions

According to the combination of the SOBEK simulation and TLAS evaluation results, the Top 1 event caused the greatest damage with an affected 26,886 households (nearly 100,000 people) and a loss of NT$ 689 billion. The relevant data also shows a large amount of population will be flooded by this extreme typhoon event. So, short-term strategies to strengthen hydraulic protections in the urban area become first prioritized issue. The second issue is about the land use redistribution. The land use analysis results have clarified the commerce was the most damaged land use types, and the industry is the second most. These two types accounted for 74 percent of total loss. Therefore, if we went to reduce the future flood impact in Kao-Ping River basin, land use redistributions would be the other important issue. The suitable trading policy for land use type exchange could be a probable strategy for government to reduce the three-forth of disaster loss under extreme typhoon event. Finally, this paper showed the different analysis methods, the monetizing approach, to evaluate flood impact assessment, which could help decision makers to get more detail and reliable disaster information.

Acknowledgement

The authors show their deep appreciation to Dr. Akio Kitoh of Japan Meteorological Research Institute for the provision of MRI data, and another anonymous reviewer for their helpful comments. This project was funded by the Taiwan National Science Council (MOST 103-2621-M-865-001).

References

Mizuta, R., H. Yoshimura, H. Murakami, M. Matsueda, H. Endo, T. Ose, K. Kamiguchi, M. Hosaka, M. Sugi, S. Yukimoto, S. Kusunoki, and A. Kitohj. (2012) Climate simulations using the improved MRI-AGCM with 20-km grid. J. Meteor. Soc. Japan, 90A, 235-260.

Hsu, M. H. (1996) North Embankment Flooding and a Flood Forecast Model for the Ba-Zhang River Basin (2). Research Program Report, National Science Council.

Yen, C. L., Tsai, Y. P., Chen, L. C., Hsu, M. S., Lin, M. L., and Lo, C. H. (1997) National Disaster Prevention Technology Program—Plan Report.

Shih, M. W. (2006) Simulation Study on Applying 2D Inundation Model for Three Drainage Systems in Chang-Hua County. Unpublished Master's Thesis, Department of Soil and Water Conservation, National Chung Hsing University.

Tang, C. Y., Hsieh, P. C., and Lin, L. L. (2006) The Application of FLO-2D and HEC-GeoRAS for Simulating the Flooding in Na-Hu Creek Caused by Typhoon Mindulle. Journal of Soil and Water Conservation, Vol. 40 (4), 455-467.

Ko, T. F., Yeh, C. T., Wu, C. H., and Wang, Y. M. (2006) Identifying Potential Floods in Low-Lying Urban Areas and Operating Flood Detention Ponds. Journal of University of Science and Technology Beijing, Vol. 28(S2), 148-151.

WL| Delft Hydraulics. (2006) SOBEK Software User's Manual. Delft, the Netherlands.

Li, H.C., Y.L. Kuo, D. Shaw, and T.H. Huang (2008) The Household Benefits Assessment of the Flood Reduction Plan in a Flood-prone Area: A Case Study of Sinwen, Chiayi, Taiwan, Agricultural and Resources Economics , Vol.5 (2), 41-58.

Li Hsin-Chi (2010) A Household Loss Model for Debris Flow, Journal of Social and Regional Development，Vol.2(2), 29-52.

Hsin-Chi Li, Yi-Chen Chen, Mei-Jun Guo (2013) The Development and Application of Taiwan Typhoon Loss Assessment System (TLAS), Journal of Taiwan Agricultural Engineering, Vol. 59 (4), 42-55. (In Chinese)

Ko-Fei Liu, Hsin-Chi Li, and Yu-Charn Hsu (2009) Debris flow hazard assessment with numerical simulation, " Natural Hazards, Vol. 49(1), 137-161.

Chen, C., R.C. Beardsley, and G. Cowles (2006) An unstructured grid, finite-volume coastal ocean model (FVCOM) system. Oceanography, Vol.19(1), 78-89.

Impact of Climate Change on Urban Flood Management: A Case Study in Mae Sot Municipality in Tak Province, Thailand

CHUENCHOOKLIN Sombat[1, a *] and PUROTAGANON Man[2, b]

Abstract The impacts of climate change on the urban water management particular flood data preparation in the ungauged catchments containing with small municipality such as Mae Sot City in Tak Province of Thailand was presented. The increasing of capability building and strengthening participation for some community leaders in the city and related agencies to conduct in the process of water system management in this urban area particular for database management and simply analyze were carried out. As well as some modernized techniques related to the ahead short period rainfall forecasting system, such as using the global forecast system via the integrated data viewer program combined to hydrological models was introduced which can be further applied for flood forecasting and mapping systems in their urban areas.

Keywords *Climate change, urban flood management, hydrologic model, rainfall prediction model.*

Introduction

Thailand is located in the South East Asia region which is mostly a developing country particular in remote countryside. It is vulnerable to climate change and its variability includes shift of weather pattern and more frequent occurrence of floods and droughts. The changes of mean temperature and others result to the change of amount of precipitation and runoff too. These kinds of changes will affect poor water management in basin-wise scale particular in upstream watersheds in remote area (IPCC, 2007). Consequently, water demand for each activity in the downstream also faces considerable uncertainties in the future and availability of water supply, particularly in the irrigation system. Furthermore, flood management in wet season has to be adjusted. From the current issue of impacts of climate change, it is impacting on the urban water management in the small basins containing with many large community areas. Because of most of small basins are ungauged catchments which usually they are lacking of some useful hydrological data of both stream gagging recorded and basin information. Therefore, more frequent flood events with more intensity, higher flow velocity, stronger flood peak, and losses from severe floods were increased.

Since, many flood package models including river analysis system need the input flood discharge from historic or simulated runoff using observed rainfall data through the hydrologic model system. The example is the HEC-RAS model (USACE, 2010) to be simulated water level in a small river which needs simulated discharge from HEC-HMS (USACE, 2009) based on rainfall over ungauged basins (Chuenchooklin, 2014; 2013; 2012; Chuenchooklin et.al, 2014). Since recently, some numerical weather prediction models were developed which can be used for generating short range of rainfall data such a forthcoming week. The Integrated Data Viewer (IDV) was freeware developed at the Unidata Program Center, part of the University Corporation Atmospheric Research (UCAR). The IDV is a Java-based software framework for analyzing 2-3 dimensional visualizing geoscience data. It can preview all scientific data including geo-referenced, net-CDF data, Vis5D data, McIDAS/ADDE (satellite, radar, surface and upper air), Archive Level II radar, GrADS, ASCII/TEXT, and social data including geographic information system (GIS)'s shape files both vector and raster data (Unidata, 2010; Abrahart, et.al, 2002). It is also further capable applied for flash flood forecasting via public domain system model using numerical weather prediction: NWP model with every 3 hours for 3 days or a week (Tonjan, 2010; PhromsakhanaSakhon-nakhon et.al, 2011).

The focus of the present paper is a part of overall target to increase capability and strengthening participation of those community leaders and related local agencies that conducted in the process of system water management in this urban area in order to increase efficiency of urban water management of the Mae Sot Municipality. Learning process of data collection with simply analyze for further flood management were aimed of this study. Moreover, some modernized technique related to the ahead short period rainfall forecasting system, such as using the global forecast system via IDV program was also introduced. It can be further applied for flood forecasting combine to HEC-HMS, HEC-RAS and risk mapping in their urban areas.

[1] Director of Water Resources Research Centre, Faculty of Engineering, Naresuan University, Phitsanulok, Thailand
sombatc@nu.ac.th
[2] Secretary for Thai Water Partnerships, Bangkok, Thailand
purotaganon@gmail.com

Study area

The Salween River Basin, or Thanlyin in Myanmar, is the international river as boundary between Thailand and Myanmar (Fig.1). Most topography covers mainly in the province of Mae Hong Son and some of Tak with total catchment area in Thailand of 19103.5 square kilometers (km^2). Its mean annual rainfall is 1305 mm and produces annual streamflow runoff of $9400x10^6$ m^3 which can feed overall agricultural land of 19.2% of the watershed. Apart from this land it is only 6% or 1.2% of the watershed suitability for growing cash crops. It is only 4.1% of total agricultural area or 0.8% of the watershed for potential irrigation development.

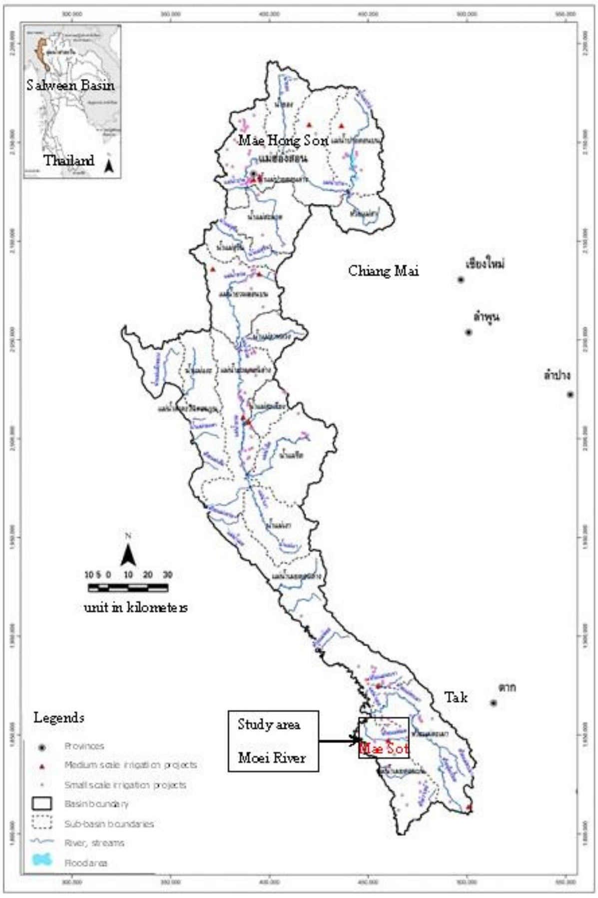

Fig.1 Map of Salween Basin and study area (HAII)

The Huai Mae Sot is one catchment of the Moei River in the Salween Basin which flows from east to west direction through the Mae Sot Municipality**.** It stretches from latitude 16.6994 N to 16.7912 N and from longitude 98.5146 E to 98.7233 E, with a catchment area of 199 km^2 (Fig.2). It includes 9 tributary streams in the Mae Sot which are namely Huai Mae Sot, Huai Laeng, Huai Luek, Huai Seio, Huai Mae Ku, Huai Haeng, Huai Pong, Hui Tu Pa and Huai Mae Pa, respectively. Mae Sot has a tropical savanna climate. Winters are dry and very warm. Temperatures rise until April, which is very hot with the average daily maximum at 36.8 °C. The monsoon season runs from May to October, with heavy rain and somewhat cooler temperatures during the day, although nights remain warm (Tak Chamber, 2014). The mean annual rainfall is 1468.3 mm with average rainy day of 145 days, and means humidity of 76.1% (TMD, 2011).

Mae Sot City is a small town with only 27.2 km^2 in Tak Province and about 493 km northwestern of Bangkok in Thailand. It is situated on the Huai Mae Sot stream one tributary streams to the Moei River, across from Myaewady, Karen State, Burma (Arnold, 2004; Tak Chamber, 2014). It is the main gateway between Thailand and Myanmar. It comprises of 20 local communities as for city administration management. Since Thai’s economic has been rapidly growth according to the Thai National Economic and Social Development Board (NESDB) under east-west economic corridor development plan. Therefore, many migrant workers from Myanmar have been employing to work in Mae Sot’s industrial areas which seem to be larger Thai workers. However, they also utilize local natural resource and environment including electricity, water supply, and others (Maneepong, 2006). Flash flooding is typically caused by heavy rainfall in the upper watershed because of lack of a large water reservoir in the upper basin. As well as inadequate drainage shallow and more obstruction structures across the streams i.e. poor city planning and transportation systems was reported by HAII (2010). Lack of information about useful hydrological data related to contribute to flood management was reported. Moreover, no one uses climatological data and basin characteristic to contribute to flood management in this area yet. The events of the flood include overflow from the streams and flood ponded in agricultural lands and lowland urban area in the Mae Sot Municipality after heavy rain occurs. Moreover, the side slopes of drainage channels easily collapse during a flood flow pass. The evidence in 2013 with most severely flood events and losses in this area already occurred.

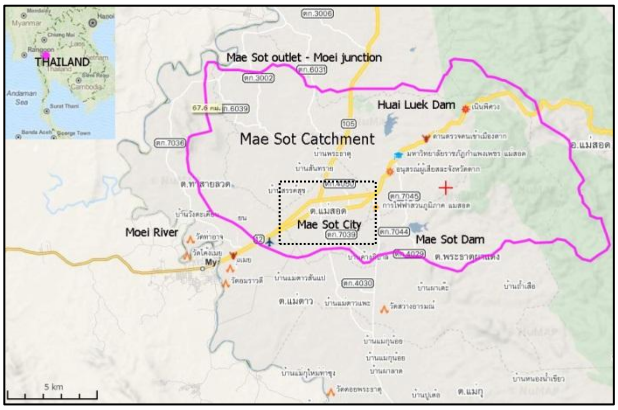

Fig.2 Map of Mae Sot catchment and Mae Sot City in the middle Moei river sub-basin of Salween

Methodology

First of all the increasing of capability building and strengthening participation for those community leaders in the city and related agencies to conduct in the process of water system management in this urban area particular for database management was trained with data collection. Those contained of the construction of rainwater collector with used can containers and river water level measurements with simple rulers and installation in the field. The simple method using tape meter as for stream cross-sectional profiles were taught to survey too. Moreover, the World Wide Web availability of free weather, rainfall, and dam outflow data archived relevant this area were also introduced to the local community leaders. In addition simply flood mapping from previous most severely flood event in 2013 was taught.

The second part was more complex and done by the authors e.g. the application of prediction of flood hydrograph and river water depths in the Mae Sot City using available rainfall data and basin characteristic through HEC-HMS and RAS (USACE, 2009; 2010) with can be applied by using time step less than 1 day and length step larger than 500 m according to available surveyed data (Chuenchooklin, 2014; 2013; 2012; Chuenchooklin et.al, 2014).

The last part was introducing the short range of rainfall forecasting using Unidata’s IDV program with the aim for further applying with HEC-HMS and RAS.

Results and discussion

The location of all 20 communities in Mae Sot municipality was shown in Fig.3. The construction of a simply rainwater collector using a can container was installed at the community no.19 located at the upper part of the city area as shown in Fig.4. In addition the 5 simply river water level gauges were installed at upstream and midstream of Huai Mae Sot stream, and at midstream of Huai Luek stream as shown in Fig.4. The surveying work for cross-sectional profiles with 4 to 12 m wide and 3 to 6 m depth was an example shown in Fig. 4 and Fig.5. The community’s handwrite of their own flood maps based on previous severely flood event in 2013 and interpretation to a flood risk map of the city was shown in Fig.6 and Fig.7, respectively. The rehearsal of flood disaster preventive and preparedness of Mae Sot City from 20 communities was shown in Fig.8.

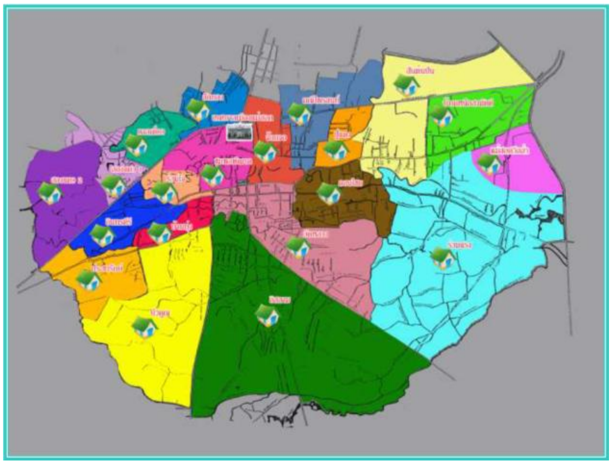

Fig.3 Map of Mae Sot City and 20 communities.

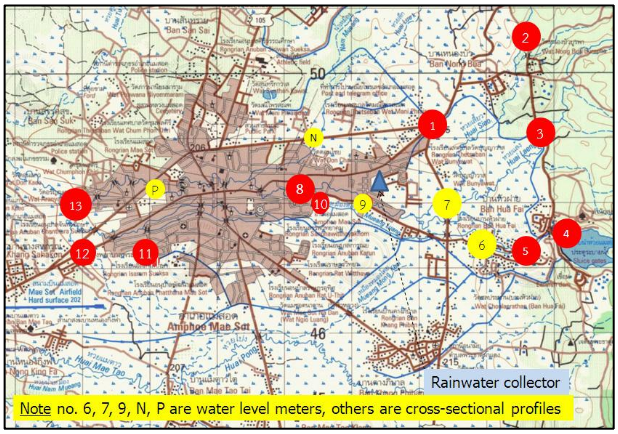

Fig.4 Map show location of measurement installations and cross-sectional profiles points

Fig.5 Picture of Huai Mae Sot and Huai Luek’s survey of some cross-sectional profiles

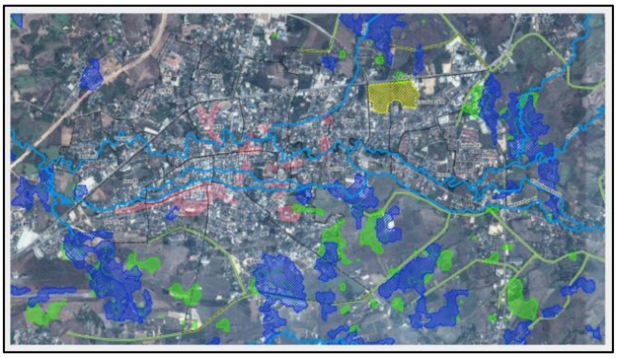

Fig.6 Severely flood mapping in Mae Sot city in 2013

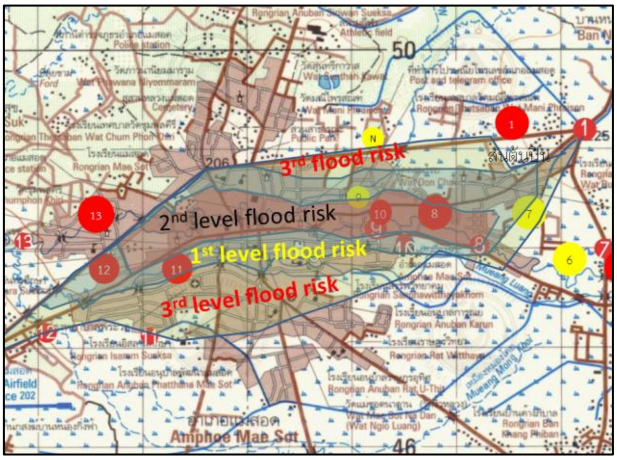

Fig.7 Flood risk mapping from 3 levels in Mae Sot city

Fig.8 The rehearsal of flood disaster preventive and preparedness of Mae Sot City from 20 communities

The second part was more complicate and done by the authors e.g. the application of prediction of flood hydrograph and river water depths in the Mae Sot City using available rainfall data and basin characteristic through HEC-HMS and RAS (USACE, 2009; 2010) mentioned above (Chuenchooklin, 2014; 2013; 2012; Chuenchooklin et.al, 2014) as shown in Fig.9 and Fig.10, respectively.

The last part was introducing the short range of rainfall forecasting using Unidata's IDV program with the aim for further applying with HEC-HMS and RAS as shown in Fig.11.

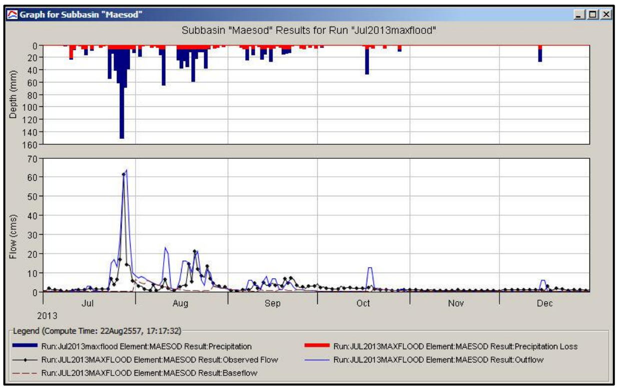

Fig.9 Calibration of flood hydrograph in HEC-HMS based on rainfall data during severely flood in 2013

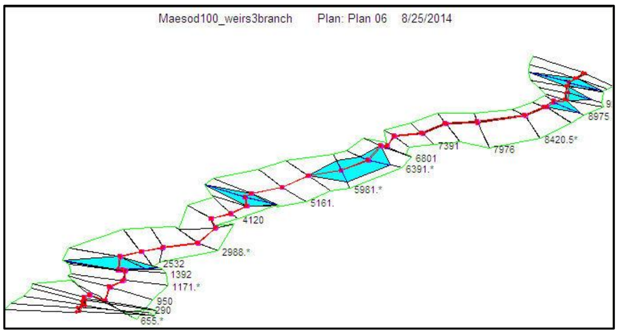

Fig.10 Flood water level produced from HEC-RAS during severely flood on 29-30/07/2013

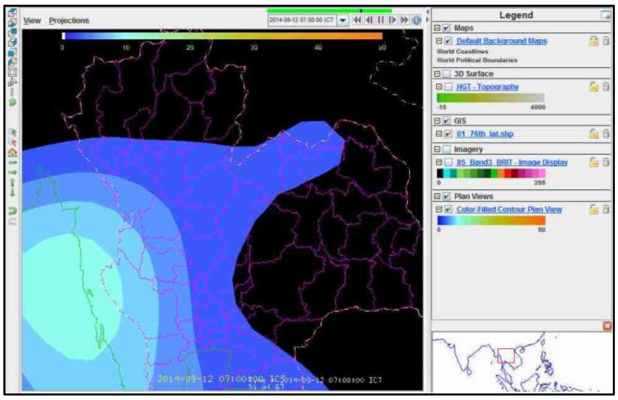

Fig.11 IDV's rainfall forecasting map with every 3-hour as example on 12/09/2014 07.00-10.00 AM

Summary and conclusions

The Mae Sot Municipality was attached by severely flood in 2013 and result good experience to those local community leaders to prepare their own database formulation with further efficient water management. If they can apply modernized techniques for rainfall forecasting combined to hydrological models in near future, it will be full efficient flood management systems. Both rainfall forecasting model using IDV and hydrologic models include HEC-HMS and RAS need more consultancies should be applied and trained to the municipality engineer or the one whom response for flood disaster planner in near future as well.

Acknowledgment

The Mae Sot Municipality The study cannot be concluded without raw precipitation scenarios provided from various government agencies, e.g. The Royal Irrigation Department (RID) and Thai Meteorological Department (TMD) for observed historical rainfall data and outflow discharge released by Mae Sod dam as well. This research has been partially support by the Community Network for Disaster Management (CNDM) and the Local Development Institute (LDI). The research also has done a part of the Water Resources Research Centre (NU-WRRC) of Faculty of Engineering, Naresuan University. The authors really thank to the Mae Sot Municipality and 20 community leaders whom made very worm, well consultancy, and work hard with us.

References

Abrahart, JR. and See, L. (2002) Multi-model data fusion for river flow forecasting: an evaluation of six alternative methods based on two contrasting catchments, Hydrology and Earth System Sciences, vol. 6(4), pp.655-670

Arnold, D. (2004) The Situation of Burmese Migrant Workers in Mae Sot, Thailand. Southeast Asia Research Centre (SEARC) Working Papers Series, No. 71

Chuenchooklin, S. (2012) Streamflow Modeling for a Small Watershed using Limited Hydrological Data, WASET J. Vol.6 No.10, article:160

Chuenchooklin, S. (2013) Community's Water Resource Management in Upstream Catchments of Large River Basin: a Case Study in Pua Watershed, J. of Society for Social Management Systems: SSMS's Abs. Book p4, #SMS13-3349

Chuenchooklin, S. (2014) River Analysis System Model for Proposed Weirs at Downstream of Large Dam, Thailand, WASET J. Vol.8 No.9, article:152

Chuenhooklin, S. and Chidchob, P. (2014) Application of the River Analysis system model for the Planning the cascade weirs in the Ping river in Tak province, Proc. 9th THAICID National Symposium on Irrigation & Drainage

Hydro and Agro Informatics Institute: HAII (2011) Information of 25-river basins in Thailand (in Thai). Available from http://www.haii.or.th

IPCC Working Group I (2007) Climate Change 2007: The Physical Science Basis. Contribution of Working Group I to the Fourth Assessment Report of the IPCC. Cambridge University Press, Cambridge, United Kingdom

Maneepong, C. (2006) Regional policy thinking and industrial development in Thai border town. Labour and Management in Development Journal, Volume 6, Number 4, Asia Pacific Press

PhromsakhanaSakhonnakhon, K., Tonjan, S., and Yamada, T. (2011) Numerical simulation of heavy rainfall in the south of Thailand with cumulus parameterization schemes and runoff RUNOFF forecasting. Proc. of the 1st EIT conference on water resources engineering, pp.163-176

Tak Chamber (2014) Information of Tak Province and Mae Sot District (in Thai) retrieved from http://www.takchamber.com

Thai Meteorological Department: TMD (2011) Climate data for Mae Sot in 1981–2010

Tonjan, S. (2010) An Investigation of The Precipitation Prediction Results of The Public Domain System Model (WRF), Journal of Research in Engineering & Technology, Kasetsart University, vol.7#3, pp.27-34

Unidata (2010) Integrated Data Viewer IDV program and user guide. Unidata Program Center University Corporation for Atmospheric Research. Available from http://www.unidata.ucar.edu/

USACE: Army Corps of Engineers (2009) HEC-HMS Hydrologic Modeling System. User's Manual. Retrieved from http://www.hec.usace.army.mil. Public distribution unlimited

USACE: Army Corps of Engineers (2010) HEC-RAS River analysis system. User's Manual. Retrieved from http://www.hec.usace.army.mil. Public distribution unlimited

Drought Monitoring using the Normalized Difference Infrared Index (NDII) for the Upper Ping River Basin

Nutchanart Sriwongsitanon[a*], Thanongsak Suksiri[b], Ekkarin Maekan[c], and Sansarith Thianpopirug[d]

Abstract

Remotely sensed data were used to monitor the drought conditions of the Upper Ping River Basin (UPRB) in northern Thailand. The 8-day-period satellite data sensed by the Terra's Moderate Resolution Imaging Spectroradiometer covering the study area from 2001 to 2013 were used to evaluate the Normalized Difference Infrared Index (NDII). It was shown that NDII values decreased sharply at the end of the wet season and reached their lowest values in February and May. Their values increased abruptly between late April and June. NDII values varied in an insignificant manner from the middle to the late rainy season. Temporal and spatial distribution of drought conditions in the UPRB was detected by NDII. It was observed that the UPRB experienced drought during the dry season in 2004-2005, 2003-2004, and 2009-2010, and that 3 sub-basins comprising Nam Mae Haad, Nam Mae Li, as well as Ping River Section 2 experienced drought more than other sub-basins. Using the drought indicator provided by NDII values, water management and mitigation measures can be applied in the right place and at the right time to effectively reduce the effects and damages caused by drought. The 24-day average NDII values were found to correspond to the 56-day accumulated rainfall depth for all of the 14 sub-basins and the 13 years of paired data, providing an average coefficient of determination (r^2) of about 0.762. The results prove that NDII reflects the vegetation water content which is affected by soil moisture condition and is directly related to accumulated rainfall amount.

Keywords: *Remote Sensing; Drought Monitoring; NDII; Rainfall Depth; Upper Ping River Basin.*

Department of Water Resources Engineering
Faculty of Engineering, Kasetsart University
Bangkok, Thailand

[a]fengnns@ku.ac.th

[b]thanongsaksuk@gmail.com

[c]son_petroleum@hotmail.com

[d]sansarith@hotmail.com

*corresponding author

Introduction

Droughts are recognized as climatic events leading to water shortages, economic losses, and adverse social consequences (Thenkabail *et al.*, 2004). Droughts can occur in almost all climatic zones and are characterized by lower than expected or normal precipitation (Mishra and Singh, 2010). Assessment of droughts is crucial for water resources planning and management to mitigate their impacts and damages. Drought can be normally monitored using drought indices such as Palmer Moisture Anomaly Index (Z-index), Palmer Drought Severity Index (PDSI; Palmer, 1965), Standardized Index (SPI; McKee et al., 1993), and Crop Moisture Index (CMI; Palmer, 1968). Meteorological data from weather stations are necessary for calculating these indices; they give the drought indicator only at available observed stations. Spatial interpolation techniques are necessary for averaging these indicators at observed stations in the area of interest. High uncertainties may exist during interpolation processes; they are caused by the structural nature of the technique, especially by limited sampling gauges. Remote sensing is therefore another promising alternative to drought monitoring and has even gained more attention than conventional meteorological drought indices because it can be used to extract meteorological and biophysical characteristics of terrestrial surfaces. The Normalized Difference Vegetation Index (NDVI) introduced by Rouse et al. (1974) has been widely used for drought monitoring. NDVI can be derived from spectral reflectance data (ρ) of discrete red (R) and near-infrared (NIR) channels such as (ρNIR−ρRED)/(ρNIR+ρRED) (Rhee *et al.*, 2010). The contrast between intense chlorophyll pigment absorption in the red channel and high reflectance of leaf mesophyll in the near infrared channel is the main characteristic used for operating NDVI. It can be used to indicate vegetation stress, particularly due to water shortage which is the main factor affecting vegetation processes and controls leaf pigment content and integrity (Maselli, 2004). Spectral reflectance within the red channel increases as aerosol optical depth increases because of dominant aerosol and molecular scattering effects (Gao, 1996). These atmospheric effects caused a reduction of NDVI values during the wet season over the area of the Upper Ping River Basin in Northern Thailand (Suksiri and Sriwongsitanon, 2014). Normalized Difference Infrared

Index (NDII) was later developed by Hunt and Rock (1989) using ratios of different values of near infrared reflectance and short wave infrared reflectance, and their sum described as (ρNIR−ρSWIR)/(ρNIR+ρSWIR). NDII can be effectively used to detect plant water stress according to the property of shortwave infrared reflectance which is negatively related to leaf water content due to the large absorption by the leaf. Yilmaz et al. (2008) found a significant relationship (R^2 = 0.85) between equivalent water thickness (EWT) and NDII. They also discovered a significant indirect relationship between NDII and vegetation water content (VWC) which is the most successful parameter for retrieval of soil moisture content from microwave data, based on the allometric relationships between canopy EWT and VWC, and the linear relationship between canopy EWT and NDII. NDII was selected for drought monitoring of the Upper Ping River Basin in northern Thailand because of its potential in detecting equivalent water thickness within the leaves affected by soil moisture content. The relationships between average NDII and accumulated rainfall depth were evaluated at the 14 sub-basins to be used as an indicator to prove the effectiveness of NDII before it can be recommended for drought monitoring in other basins in Thailand.

Study site and data collection

Study site

The Upper Ping River Basin (UPRB), the study site, is situated from latitude 17°14′30″ to 19°47′52″ N, and longitude 98°4′30″to 99°22′30″ E in northern Thailand and can be separated into 14 sub-basins (Fig. 1) (Mapiam, et al., 2014). It has an area of approximately 25,370 km^2 in the provinces of Chiang Mai and Lam Phun. The basin landform ranges from an undulating to a rolling terrain with steep hills of elevations of 1,500 to 2,000 m, and valleys of depressions of 330 to 500 m (Mapiam and Sriwongsitanon, 2009; Sriwongsitanon, 2010). The Ping River originates in Chiang Dao district, north of Chiang Mai and flows downstream to the south to become the inflow for the Bhumiphol dam - a large dam with an active storage capacity of about 9.7 billion m^3 (Sriwongsitanon, 2010). The climate of the region is controlled by tropical monsoons. The rainy season is influenced by the southwest monsoon and brings about mild to heavy rainfall between May and October. Annual average rainfall and runoff of the UPRB are approximately 1,170 and 270 mm, respectively. Land cover was dominated by forest of about 86.1% in 1988 but reduced to approximately 75.5% in 2005, while agricultural area increased from 9.5% in 1988 to 18.3% in 2005 (Sriwongsitanon and Taesombat, 2011).

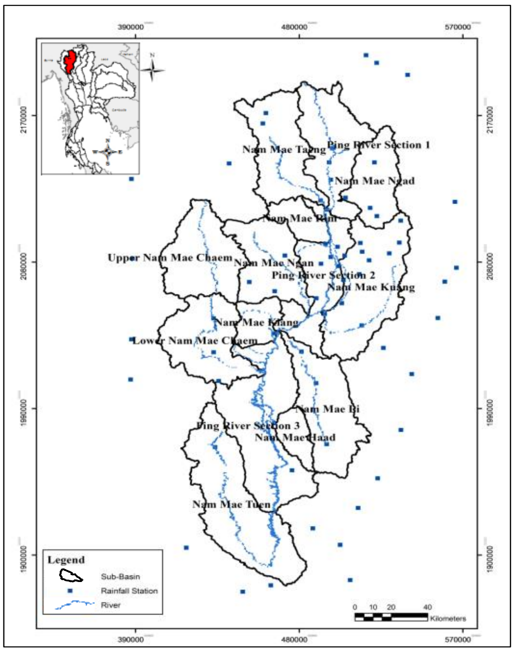

Fig. 1 The Upper Ping River Basin and the locations of the rain-gauge stations

Remote sensing data

The 8-day surface reflectance with 500 m resolution (MOD09A1, collection v005) sensor by The Terra MODIS (Moderate Resolution Imaging Spectroradiometer) covering the UPRB were downloaded from ftp://e4ftl01.cr.usgs.gov/MOLT. The 13 year period of 2001-2013 was used. HDF-EOS Conversion Tool was applied to extract the desired bands (bands 2 and 6) and re-project into Universal Transverse Mercator (Zone 47N, WGS84).

Rainfall data

A total of 65 non-automatic rain-gauge stations were selected from 2001 to 2013. Forty-two stations were located within the UPRB while 23 stations were situated in its surroundings. These rain-gauges are owned and operated by the Thai Meteorological Department (TMD) and the Royal Irrigation Department (RID). Quality control of these rainfall data was performed by comparing them to adjacent rainfall data. Unusual rainfall data were excluded from the analysis.

Methodology

NDII drought index

The normalized difference infrared index (NDII) from 2001 to 2013 covering the UPRB was computed using the 8-day surface reflectance data of near infrared (band 2: wavelength between 780-900 nm) and short wave infrared (band 6: wavelength between 1550-1750 nm) as described by the Eq. (1).

$$NDII = \frac{NIR-RED}{NIR+RED} \quad (1)$$

The 8-day NDII values during the study period were averaged out for each sub-basin to be used for identifying the order of basin moisture content. The 8-day average NDII values for each sub-basin were also averaged out for the time windows of 8, 16, 24, 32, 40, 48, 56, 64, 72, 80, 88, and 96 days to be further related to the accumulated rainfall depth of each sub-basin.

Accumulated areal rainfall depth

Daily areal rainfall depths for the 14 sub-basins were calculated using Inverse Distance Square (IDS) (Eqs. (2) and (3)) together with rainfall depth observed at the 65 daily rain-gauge stations within the UPRB and its surroundings. Accumulated areal rainfall depth over the time windows of 8, 16, 24, 32, 40, 48, 56, 64, 72, 80, 88, and 96 days were calculated from April to October since rainfall normally starts in the middle of April until the end of October.

$$W_i = \frac{\frac{1}{d_i^2}}{\sum_{i=1}^{n}\frac{1}{d_i^2}} \quad (2)$$

$$P = \sum_{i=1}^{n} p_i W_i \quad (3)$$

where W_i= weighting factor for rainfall depth at station i
d_i = distance between rain-gauge station i and the centroid of sub-basin
p_i = rainfall depth at rain-gauge station i
P = rainfall depth at the centroid of each sub-basin
n = number of rain-gauge stations

Relationships between the average NDII values and accumulated areal rainfall depth

Regression analyses were carried out to examine the relationships between average NDII values and accumulated areal rainfall depth of each sub-basin for the time windows of 8, 16, 24, 32, 40, 48, 56, 64, 72, 80, 88, and 96 days. The optimal time window for averaging NDII values and accumulated areal rainfall depth at each of the 14 sub-basins to provide the highest coefficient of determination (r^2) was investigated. The relationships were analyzed separately from 2001 to 2013 according to the different NDII values at the beginning of the rainy season, which are the results of different paired coordinates between average NDII values and accumulated areal rainfall depth.

Results and discussion

NDII values for the 14 sub-basins of the UPRB

The 8-day NDII values with 500 m resolution for the UPRB from 2001 to 2013 were calculated. Fig. 2 shows examples of average NDII values in March and September for the UPRB in 2004, which is the year with the lowest annual average NDII value among the 13 years of the results. NDII values in Fig. 2 was presented using 4 different colors which are green (NDII between 0.15 and 0.30), yellow (NDII between 0 and 0.15), orange (NDII between -0.15 and 0) and red (NDII<-0.15) to indicate relatively high-, medium-, low-, and very low- basin moisture content. The figure shows that NDII values correspond to the basin moisture content which are higher during the wet season (May to October) and lower during the dry season (November and April). Less amount of rainfall between November and April brought about continuous reduction of NDII values. On the other hand, higher amount of rainfall between May and October resulted in increasing NDII values. However, NDII values seem to be insignificantly altered between July and October. This could have been caused by saturated moisture content within the leaves during the wet period.

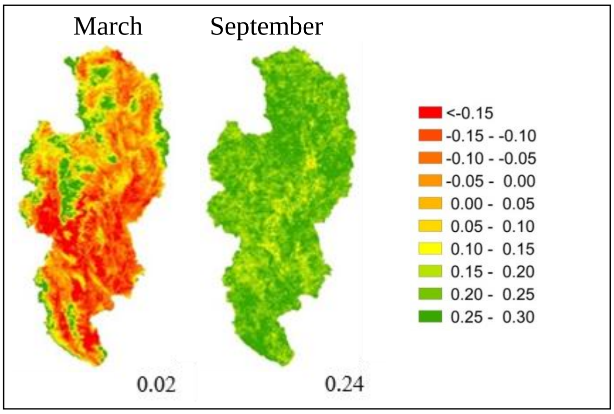

Fig. 2: Average NDII values in March and September for the UPRB in 2004

The 8-day NDII values were averaged out for the whole catchment area for each year from 2001 to 2013. The average NDII values during the wet season, the dry season, and the whole year within the 13 years are presented in Table 1. The table also shows the order of basin moisture content ranking from the highest (number 1) to the lowest (number 13) NDII values. It can be seen that annual average NDII value for the whole basin is approximately 0.165 while the values during the wet and the dry season are about 0.211 and 0.118, respectively. The highest moisture content (NDII = 0.177) for the whole year was reported in 2002-2003 while the lowest (NDII = 0.149) was in 2004-2005. The highest (NDII = 0.149) and lowest (NDII = 0.088) moisture content during the dry season were reported in 2002-2003 and 2004-2005, respectively. On the other hand, the highest moisture content (NDII = 0.224) and the lowest (NDII = 0.197) during the wet season were observed in 2006-2007 and 2010-2011, respectively. It can be concluded that a dry year with relatively low moisture content and a wet year with high moisture content as specified by NDII values do not normally occur in the same year.

Table 1: Average NDII values during the wet season, the dry season, and the whole year from 2001 to 2013, and their order of basin moisture content

Year	Wet season (May - Oct)	Dry season (Nov - Apr)	Annual
2001-2002	0.223 (2)	0.119 (7)	0.171 (4)
2002-2003	0.205 (9)	0.149 (1)	0.177 (1)
2003-2004	0.218 (5)	0.091 (12)	0.155 (12)
2004-2005	0.210 (8)	0.088 (13)	0.149 (13)
2005-2006	0.200 (11)	0.128 (3)	0.164 (7)
2006-2007	0.224 (1)	0.111 (10)	0.168 (5)
2007-2008	0.222 (3)	0.13 (2)	0.176 (2)
2008-2009	0.221 (4)	0.123 (5)	0.172 (3)
2009-2010	0.213 (7)	0.101 (11)	0.157 (11)
2010-2011	0.197 (13)	0.128 (4)	0.163 (8)
2011-2012	0.216 (6)	0.116 (9)	0.166 (6)
2012-2013	0.201 (10)	0.118 (8)	0.159 (10)
2013-2014	0.199 (12)	0.123 (6)	0.161 (9)
Average	0.211	0.118	0.165
Maximum	0.224	0.149	0.177
Minimum	0.197	0.088	0.149

The 8-day NDII values were also averaged out for each of the 14 sub-basins within the UPRB from 2001 to 2013. These NDII values were later used for identifying the order of basin moisture content from the highest (number 1) to the lowest (number 14) NDII values. The results show that Nam Mae Taeng, Nam Mae Rim, and Upper Mae Chaem, and are 3 sub-basins which have higher moisture content than other sub-basins; their annual average NDII values during the 13 years are about 0.206, 0.198, and 0.197, respectively. On the other hand, Nam Mae Haad, Nam Mae Li, and Ping River Section 2 are 3 sub-basins with lower moisture content than other sub-basins; their annual average NDII values are about 0.123, 0.124, and 0.127, respectively. Monthly average NDII values for these 6 sub-basins are presented in Fig. 3. It can be seen that during the dry season, NDII values of the 3 sub-basins with the lowest values are a lot lower than those of the 3 sub-basins with the highest NDII values. However, NDII values for these 2 groups are not significantly different during the wet season compared to the dry season.

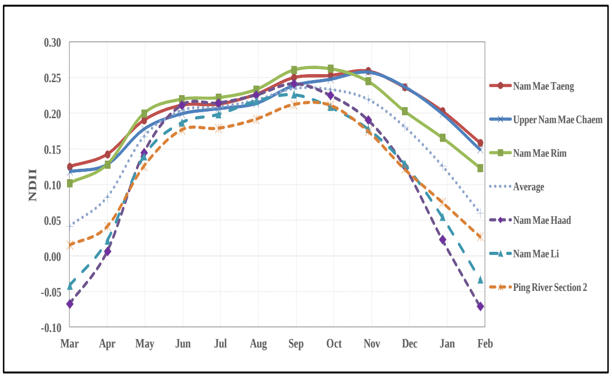

Fig. 3: Monthly average NDII values for the 6 sub-basins with higher and lower NDII values compared to other sub-basins in the UPRB

Fig. 4 shows monthly maximum and minimum NDII values within the 13 years, and the NDII values in 2004-2005 which is the lowest annual NDII value. The figure shows that NDII values in the dry season of 2004 are equal the minimum NDII values. However, NDII values within the wet season of 2004 are between the maximum and the minimum. The figure also reveals that NDII values tend to continuously increase from relatively low values in March to higher values in June. The values slightly fluctuate during the wet season before sharply falling once again when the rainy season ends, and reach their minimum values in February.

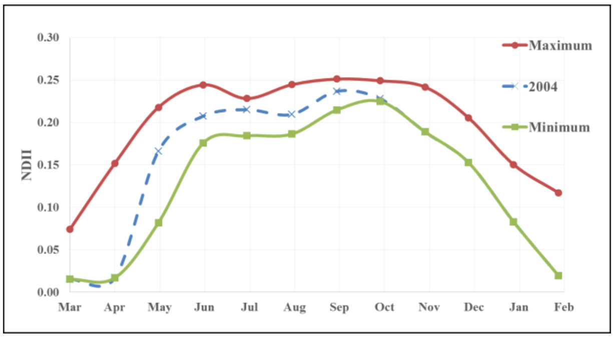

Fig. 4 Monthly maximum and minimum NDII values of the UPRB and monthly NDII in 2004

Relationships between the average NDII and accumulated areal rainfall

Exponential equation was the most suitable form used to produce the best fit between average NDII values and accumulated areal rainfall depth of each sub-basin for the time windows of 8, 16, 24, 32, 40, 48, 56, 64, 72, 80, 88, and 96 days. However, the time windows for the average NDII values and for accumulated rainfall depth providing the highest coefficient of determination (r^2) at each sub-basin are different. Table 2 shows the highest r^2 of the exponential relationships between average NDII and accumulated rainfall depth for the 14 sub-basins with different time windows. The average r^2 values for the 14 sub-basins are between 0.608 and 0.862; the average of these values is about 0.782 which is very high. The table also shows the values of r^2 for exponential relationships between the same time window of 24-day average NDII values and 56-day accumulated rainfall depth at each station. The average r^2 values of the 14 sub-basins reduced to between 0.574 and 0.862; the average of these values is about 0.762 which is still very high. An example of the relationship between the 24-day average NDII and the 56-day accumulated rainfall depth at Nam Mae Taeng in 2004 is shown in Fig. 5. It should be noted that the best exponential relationships were obtained using the data values from April till the end of August. When the data values of September and October were used for the analyses, the values of r^2 were reduced. This is because the average NDII values are not significantly changed between September and October, while the accumulated rainfall depths increase continuously. The

NDII values are slightly altered (insignificantly) during the period by the saturated moisture content within the leaves. It therefore can be concluded that NDII effectively reflects the vegetation water content during the dry season and early wet season, supported by the high values of coefficient of determination found in all sub-basins and in all the 13 years of data collection between April and August. During the late rainy season, the leaves of the plants are not under water stress and this caused NDII to vary insignificantly. However, once soil moisture reduces at any time of the wet season, NDII would reduce once again reflecting the lower values of vegetation water content.

Table 2 Coefficient of determination of exponential relationships between average NDII and accumulated rainfall depth for the 14 sub-basins of the UPRB

Sub-basins	Time windows (days) providing highest r^2			r^2 (24-day average NDII and 56-day accumulated rainfall depth)
	Average NDII	Accumulated rainfall depth	r^2	
Ping River Section 1	24	56	0.854	0.854
Nam Mae Ngad	40	56	0.758	0.752
Nam Mae Taeng	40	56	0.722	0.668
Ping River Section 2	24	56	0.862	0.862
Nam Mae Rim	40	56	0.727	0.685
Nam Mae Kuang	16	48	0.862	0.831
Nam Mae Ngan	40	56	0.750	0.722
Nam Mae Li	24	56	0.858	0.858
Nam Mae Klang	40	56	0.608	0.574
Ping River Section 3	24	56	0.814	0.814
Upper Nam Mae Chaem	40	56	0.692	0.664
Lower Nam Mae Chaem	24	56	0.822	0.822
Nam Mae Haad	24	56	0.848	0.848
Nam Mae Tuen	32	56	0.771	0.709
Average			0.782	0.762
Maximum			0.862	0.862
Minimum			0.608	0.574

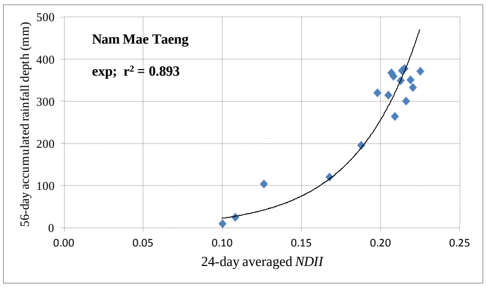

Fig. 5: Exponential relationship between 24-day average NDII and 56-day accumulated rainfall depth at Nam Mae Taeng in 2004

Conclusions

Normalized Difference Infrared Index (NDII) was used to investigate drought for the UPRB from 2001 to 2013. Monthly average NDII values are shown to be spatially distributed over the UPRB relating to the seasons and area based characteristics. NDII values seem to be lower during the dry season and higher during the wet season as a result of increasing basin moisture content influenced by the high amount of rainfall in the wet season. NDII has shown its ability to be used for investigating the temporal and spatial distribution of drought situations of the UPRB. For temporal distribution, it was found that the UPRB experienced drought during the dry season in 2004-2005, 2003-2004, and 2009-2010; the average NDII values for these years are lower than the average value of the 13 years. For spatial distribution, it was also found that Nam Mae Haad, Nam Mae Li, and Ping River Section 2 are among the 3 sub-basins which have been experiencing drought more than other sub-basins. Water management and mitigation measures therefore need to be applied in the right place and at the right time to be able to effectively reduce the effects and damages cause by drought.

To prove the effectiveness of NDII for drought monitoring, the relationships between average NDII values and accumulated rainfall depth at each sub-basin from 2001 to 2013 were evaluated using the time windows of 8, 16, 24, 32, 40, 48, 56, 64, 72, 80, 88, and 96 days. To obtain the best fit at each sub-basin of each year, the time windows of the average NDII value should lie between 16 and 40 days while those of the accumulated rainfall depth should be between 48 and 56 days. The average coefficient of determination (r^2) for all 14 sub-basins and 13 years of data set are found to be approximately 0.782, which is a very high value. Since the most suitable time windows for averaging the NDII values and accumulating the rainfall depth were shown to be 24 days and 56 days respectively in 6 out of the 14 sub-basins, these time windows were then applied to all of the 14 sub-basins. The r^2 values then reduced to about 0.762 which is still a very high value that indicate very well paired and corresponding values between average NDII and accumulated rainfall depth at each sub-basin. Undoubtedly, NDII is one of the most suitable drought indices that has been effectively used for monitoring drought situations in the river basin. The results of our study correspond to many studies (Hunt and Rock, 1989; Gao, 1996; Ceccato et al., 2002; Fensholt and Sandholt, 2003), especially the study carried out by Yilmaz et al. (2008) who found that NDII has a significant relationship with equivalent water thickness (EWT) as well as vegetation water content (VWC). However, only the paired data from April to August gave the best fit between average NDII and accumulated rainfall depth. When the paired data set from September to October were used, the relationships were reduced. From this phenomenon, we can conclude that NDII can effectively be used for drought monitoring within the dry season and the early wet season. During that period, the plants are exposed to water shortage and leaf-water saturation deficit increase steadily. Once leaf-water is close to or stays within its saturated zone occurring mostly in the late rainy season, leaf characteristics would not vary significantly. Reflectivity data of bands 2 and 6 detected by remote sensing and used for calculating NDII will also not be significantly altered causing NDII values to remain virtually unchanged. However, when soil moisture is saturated for a longer time during the flood period, the leaves of a plant will once again be under stress because flood waters can cause the air filled pores in the soil to become filled with water and this greatly limits the amount of oxygen roots can obtain. Under these conditions, NDII would reduce again. More thorough researches need to be undertaken to prove the ability of NDII to detect leaf characteristics under flooding period. An understanding of the effect of soil water on leaf characteristics which can be evaluated by NDII – drought index investigated by remotely sensed data – gives insight into the relationships between soil moisture and leaf characteristics that can be detected by remote sensing data reflected from the earth to the atmosphere.

Acknowledgement

We gratefully acknowledge Kasetsart University Research and Development Institute for financially supporting this research. We also appreciate RID and TMD for providing the rainfall data. Finally, we sincerely thank the MODIS Land Discipline Group for creating and sharing the MODIS LAND data used in this study.

References

Ceccato, P., Flasse, S., and Gregoire, J.M. (2002) Designing a spectral index to estimate vegetation water content from remote sensing data: Part 2, Validations and applications. Remote Sensing of Environment, 82, 198−207.

Cheng, Y.B., Zarco-Tejada,P.J., Riaño, D., Rueda, C.A., and Ustin, S.L. (2006), Estimating vegetation water content with hyperspectral data for different canopy scenarios: Relationships between AVIRIS and MODIS indexes. Remote Sensing of Environment, 105, 354-366.

Fensholt, R., and Sandholt, I. (2003) Derivation of a shortwave infrared stress index from MODIS near- and shortwave infrared data in a semiarid environment. Remote Sensing of Environment, 87,111−121.

Gao, B. (1996) NDWI - A normalized difference water index for remote sensing of vegetation liquid water from space. Remote Sensing of Environment 58, 257-266.

Hunt, E.R., Jr. and Rock, B.N. (1989) Detection of changes in leaf water content using near- and middle-infrared reflectances. Remote Sensing of Environment, 30, 43-54.

Mapiam, P.P. and Sriwongsitanon, N. (2009). Estimation of the URBS model parameters for flood estimation of ungauged catchments in the upper Ping river basin, Thailand. ScienceAsia, 35, 49-56.

Mapiam, P.P., Sharma, A., and Sriwongsitanon, N. (2014) Defining the Z~R relationship using gauge rainfall with coarse temporal resolution: Implications for flood forecast. Journal of Hydrologic Engineering (ASCE), 19 (8).

Maselli, F. (2004) Monitoring forest conditions in a protected Mediterranean coastal area by the analysis of multiyear NDVI data. Remote Sensing of Environment, 89, 423-433.

McKee, T.B., Doesken, N.J., and Kleist, J. (1993) The relationship of drought frequency and duration to time scales, 8th Conference on Applied Climatology. American Meteorological Society, Anaheim, CA.

Mishra, A.K.and Singh, V.P. (2010) A review of drought concepts. Journal of Hydrology, 391, 202-216.

Niel, T.G.V. and McVicar, T.R. (2003) Calculating environmental moisture for per-field discrimination of rice crops. International Journal of Remote Sensing, 24(4), 885-890.

Numata, Izaya, et al. "Characterization of pasture biophysical properties and the impact of grazing intensity using remotely sensed data [J] ", Remote Sensing of Environment, 2007,109 (3): 314-327.

Palmer, W.C. (1965) Meteorological drought. Research Paper No. 45, U.S. Department of Commerce Weather Bureau, Washington, D.C.

Palmer, W.C. (1968) Keeping track of crop moisture conditions, nationwide: the new crop moisture index. Weatherwise 21, 156–161.

Rhee, J., Imb, J. and Carbone, G.J. (2010) Monitoring agricultural drought for arid and humid regions using multi-sensor remote sensing data. Journal of Hydrology, 114, 2875-2887.

Rouse, J. W., Hass, R. H., Schell, J. A., and Deering, D. W. (1974) Monitoring vegetation systems in the Great Plains with ERTS. Proceedings of the 3rd Earth Resources Technology Satellite-1 symposium. 309−317, Greenbelt, MD: NASA SP-351.

Sriwongsitanon, N. (2010). Flood forecasting system development for the Upper Ping River Basin. Kasetsart Journal (Natural Science), 44 (4).

Sriwongsitanon, N. and Taesombat, W. (2011) Effects of land cover on runoff coefficient. Journal of Hydrology, 410 (3-4), 226-238.

Suksiri, T. and Sriwongsitanon, N. (2014) Cloud effects on the accuracy of an evaluation of NDVI; case study: Upper Ping River Basin. 19th National Convention on Civil Engineering,14-16 May 2014, Khon Kaen, Thailand.

Thenkabail, P. S., Gamage, M. S. D. N. and Smakhtin, V. U. (2004) The use of remote sensing data for drought assessment and monitoring in Southwest Asia. Research Report 85, International Water Management Institute, 26pp.

Mainstreaming Disaster Risk Management in the Governance of Cagayan River Basin: *Institutional Design and Stakeholder Participation towards Development of Integrated River Basin Masterplan*

Orlando Balderama, [1,a*] Eugenio Diaz [2,b,]

Abstract. The Cagayan River basin is the largest in the Philippines with an estimated drainage area of about 27,300 square kilometers and length of 520 kilometers (km). Quite recently, there are more frequent and intensive as well as extensive flooding during the monsoon season from May to October and droughty during the years with dry months such as the effect of El Nino. The inundation and drying of of Cagayan River and its tributaries have caused great loss of lives and property and substantial losses to the local and national economies.In the preparation of development and management plans, an integrated river basin management approach is applied to Cagayan River basin. It is intended to address several concerns related to watershed conservation and rehabilitation, climate change adaptation and disaster risk reduction due to flood and water related hazards. The study involves collection and analysis of secondary data as well as conduct of key informants interview, focus group discussions and workshop series with stakeholders, for benchmarking and analysis of perceived problems. This paper presents situationer and analysis of problems on the water resources, social, institutional and organizational conditions of the basin and framework in the implementation of watershed and water resources management in the river basin scale.

Keywords: *integrated river basin management, disaster risk reduction, climate change adaptation, cagayan river basin*

[1]Department of Agricultural Engineering
Isabela State University,
Isabela, Philippines
[a]orly_isu@yahoo.com

[2]River Basin Control Office,
Department of Environment and Natural Resources,
Quezon City Philippines
[b]eugene2066@yahoo.com

I. Introduction

The Cagayan River basin is one of the 18 major river basins in the Philippines as originally identified in the 1970's and updated to 20 major river basins in the 1990's. These basins are considered the lifeblood and driver of the Philippine economy thus need to be managed sustainably. An integrated river basin management approach need be applied in the preparation of the management plan for Cagayan River basin. It is intended to address several concerns related to watershed conservation and rehabilitation; flood mitigation; secure source of clean water as well as livelihood and economic opportunities in the area. It is the largest in the Philippines with an estimated drainage area of about 27,300 square kilometers and length of 520 kilometers (km). It is located in the Cagayan Valley region in northeastern part of Luzon Island and traverses the provinces of Cagayan, Nueva Vizcaya, Quirino, Isabela, parts of Mt. Province, Ifugao, Kalinga, Apayao and Aurora. These provinces have an approximate population of two million people, mostly farmers and indigenous tribesmen.

From an inter-agency committee report, major problems were presented in the Cagayan River summarized as follows: (1) decreasing water discharge, (2) diminishing bio-diversity, (3) river siltation, and (4) river pollution. The two main causes and effects are: inundations at the tributaries and flood plains with great loss of lives and properties as well as inadequacies in irrigation and domestic water supply affecting both the local and national economies. In addition, observations on the lack of collaborative participation among institutions and stakeholders in the integrated approach to river basin planning and management were also noted.

Integrated Water Resources Management is widely used but its understanding and the capacity to implement IWRM-based Basin Development Strategies and plans is still lacking. IWRM capacity needs to be built to capture the informed opinions of all stakeholders on what would be an acceptable level of basin development. The IWRM-based Basin Development Strategy is based on: i) balancing social/economic/

environmental issues; ii) treating the basin as an interconnected whole; and iii) balancing the benefits.
Cognizant on the urgency to implement sustainable governance of the river basin, this study aimed at assessing the various concerns and needs and providing management input in the creation of institutional framework and physical structure for the management of the river basin.

Objectives

The objectives of this study are as follows:

1. Conduct an overview study on the current physical, social, institutional and organizational conditions in the cagayan river basin;

2. Undertake stakeholders' and institutional analysis of the cagayan river basin;

3. Develop institutional framework on the creation of river basin organization to manage the cagayan river basin through stakeholders participation;

4. Integrate disaster management and climate change adaptation in planning.

Methods and Approaches

Documentation, Desk Review and Field survey

Description of current natural and socio-economic condition and trends within the river basins, water governance approaches and highlighting current problems in the water sector of the river basin; It involves stocking of knowledge of known institutional arrangement, good practices and data in integrated river basin management from a number of sources. A field survey on existing water infrastructure was also undertaken at the start of the study.

Conduct of workshop for multi-stakeholder engagement and involvement

Four workshops in the various sections of the basin and key informants interview conducted were aimed: (i) to identify the stakeholders who are now or in the future may be directly or indirectly involved in and affected by the development and management of the water sector in the basin; (ii) to ascertain the directions to take and arrive at the development; (iii) to determine the interests, perceived problems, extent of resources and mandate of the concerned institutions; and (iv) to describe the nature of the perceived problems indicating the causes and implications.

Identification of Management Thematic Areas in the River Basin

To adequately address complex concerns, integrated approach to water resources management in a river basin context was adapted to include various thematic areas as follows:

1) Watershed Management (protection of the remaining forest land and rehabilitation, which include implementation of soil conservation strategies in cultivated areas and agroforestry) Management (starting from ridge-water divide but affecting up to the reef-coastal fringe, including community based forest management;

2) Water Resources Management (following a total approach from rain drops falling at the remotest part of the watershed routed to the main river channel and joining the waters from the tributaries until they exit through its mouth);

3) Disaster Risk Reduction and Climate Change Adaptation;

4) Coastal Resources Management where the aquatic fish and marine life may be affected by pollutants brought down from the watershed and confluence of the tributaries into the main river;

Each strategic theme is supported by several objectives and enabling policies and strategies leading to several key actions supports each objective. These key actions are major steps or initiatives required to accomplish the objectives.

Discussion of Results

A. Geographical Setting of the Cagayan River Basin

The Cagayan River Basin as shown in **Figure 1** is the largest basin in the Philippines with an estimated drainage area of 27,753 sq km and length of about 520 km. It is located in the Cagayan Valley region in the northeastern part of Luzon, Philippines. It traverses the provinces of Cagayan, Nueva Vizcaya, Quirino, and Isabela comprising 69% of the basin area. Parts of Mt. Province, Ifugao, Kalinga, Apayao and Benguet of the Cordillera Administrative Region (CAR) consist of 29.5 %. Portions of Aurora and Nueva Ecija in Region 3 are 1.5 % of the said basin area.

Figure 1. Map of the Cagayan River basin

B. Socio-Economic Conditions

The population in the Cagayan River Basin is estimated at 3.5 million, while the growth rate is 2.61 % per annum. The urban population is estimated at 21% of total population or 751,478 with Tuguegarao City having the biggest population of 129,539. The basin is still under-developed or categorized as a depressed area. The identified major cause of underdevelopment is flood inundation resulting to low regional economic development and the most frequently affected are the lower Cagayan River municipalities and drought due to frequent occurrence of El Nino phenomenon. Deforestation, which is mostly man-made, is a serious cause of under-development. River pollution is now becoming a serious cause of under-development in the municipalities in the lower Cagayan River. The most serious problem encountered in the regional development is low investment and financial constraints.

C. Politics and Local Government

Politics is practiced democratically along the party line system in the four levels of local governments like provinces, cities, municipalities and barangays. These are dominated mostly by traditional politicians-technocrats. Local governments in the basin consists of the provinces of Cagayan, Isabela, Nueva Viscaya and Quirino (Region 2), the provinces of Ifugao, Mt. Province, Kalinga and Apayao (CAR) and a minimal portion of Aurora and Nueva Ecija (Region 3).

D. Institutional and Organizational Situationer

Analysis of the Existing Management of Cagayan River Basin

In the series of workshops conducted for stakeholder profiling and analysis of perceived problems, the presence of the following problems were found:

<u>LackofInstitutionalCollaboration</u>

The lack of coordination for program planning and implementation between and among the key government institutional stakeholders of the CRB have been validated;

<u>Poorimplementationofprojects</u>

While there are existing plans to refer to, very little implementation of projects in the master plan was confirmed mainly due to budgetary constraints and absence of a single agency empowered to implement a basin-wide program initiatives**.**

<u>WeakImplementationofExistingLawsandPolicies</u>

Major impact of this concern has aggravated further degradation of the natural environment as evidenced by: Uncontrolled, and unplanned cutting of trees; contamination of aquifers and water bodies due to direct discharge of untreated domestic effluents and solid waste into water bodies; Increased extraction of surface and underground water for domestic and agricultural uses; Flooding due to continued denudation of forest cover over extensive areas opened for both upland and lowland agriculture; Severe siltation of water bodies due to erosion resulting from forest denudation, upland agriculture, and opening of timberland/public lands to human settlements.

Identification of Stakeholders

Stakeholders in the Cagayan River Basin were categorized into three groups, namely:

<u>PrimaryStakeholders</u>
Primary stakeholders refers to the direct beneficiaries like people’s organization, farmers cooperatives, irrigation associations, fisher folks, mining & power companies, water districts, and individuals or groups who derive their livelihood directly from the forest, land, and water resources of the basin. Primary stakeholders have major risks or stakes and are directly implementing and/or directly affected by the project

<u>SecondaryStakeholders</u>

Development facilitators and providers like government agencies, government-owned & controlled corporations, local government units, foreign aid organizations and institutions. Secondary stakeholders have interests in the implementation and will be consulted by the stakeholders

TertiaryStakeholders

Advocates like the church, civil society, academe, and business enterprises. Tertiary stakeholders also refer to those who are affecting the projects

Workshop Output on general issues and problems identified

The methodology used to analyze the results of the focus group discussion (FGD) is quite similar to a frequency distribution method. In this study, all the issues, concerns and problems from all thematic groups and workshops were tabulated. Since most of the issues were recurring in all workshops and somewhat similar to other issues, these were counted as one and clustered into one general subject/ issue. For this study, there were 14 classified general subjects/ issues that are enumerated below.

- Agriculture
- Data, Research and Development
- Different Land Use
- Environmental Degradation
- Erosion, Siltation and Sedimentation
- Flooding
- Funding
- Health
- Infrastructure, Equipments, Facilities and Manpower
- Institutional
- Socio-economic
- Uncontrolled Problems
- Unregulated Resource Extraction
- Water Supply

E. Institutional Framework in Establishing River Basin Organization

At present there are five types of existing River Basin Organizations in the Philippines as listed below. From the list, a closer study should be done to determine which model would be most appropriate for the Cagayan River Basin.

1. Authority (such as the Laguna Lake Development Authority);
2. Commission (such as the Pasig River Rehabilitation Commission);
3. Council (such as the Cagayan de Oro River Basin, and Lake Lanao Watershed Protection and Development Councils);
4. Project Management Office (PMO) (such as the Bicol River Basin PMO, the Cotabato-Agusan River Basin Development PMO and the Cagayan River PMO;
5. Inter-agency Committee such as the Manila Bay River Basin Coordinating Committee and the Mindanao River Basin Task Force.

It was recommended that Cagayan River Basin Development Authority be established to implement the plans and programs in the basin

F. Mainstreaming on Climate Change Adaptation and Water Related Disaster Management

In addressing water related disasters, The Philippine government is putting serious efforts in institutionalizing actions in local context in accordance to the Hyogo Framework for Action (HFA) adopted in January 2005 during the World Conference on Disaster Reduction. The HFA calls for the effective implementation of Disaster Risk Reduction (DRR) efforts to substantially reduce disaster losses by 2015 and beyond in terms of lives and in the social, economic, and environmental assets of communities and countries, as an essential condition for sustainable development. The HFA specifically called on governments to mainstream risk reduction within development and land use planning, ensure that scientific inputs influence risk assessment processes and that risk factors are addressed through sound environmental and natural resource management and social and economic development practices, among others *(NEDA, 2008).*

The Department of Interior and Local Government (DILG) prepared a climate change adaptation and disaster risk reduction management (CCA-DRRM) intervention framework that aims to share knowledge, promote tools and methodologies in mainstreaming to Comprehensive Land Use Plan (CLUP), and develop capabilities of LGUs and communities to be safe and resilient. The DILG has refocused its targets from the 27 vulnerable provinces to the contiguous local government units (LGUs) in the periphery of the 18 major river basins in the country consisting of 47 Provinces.

The preparation of the integrated masterplan also identified CCA-DRRM as a major thematic area.

Scientific Basis/ Framework

Research and development will also be pursued actively following the framework presented in **Figure 2**.

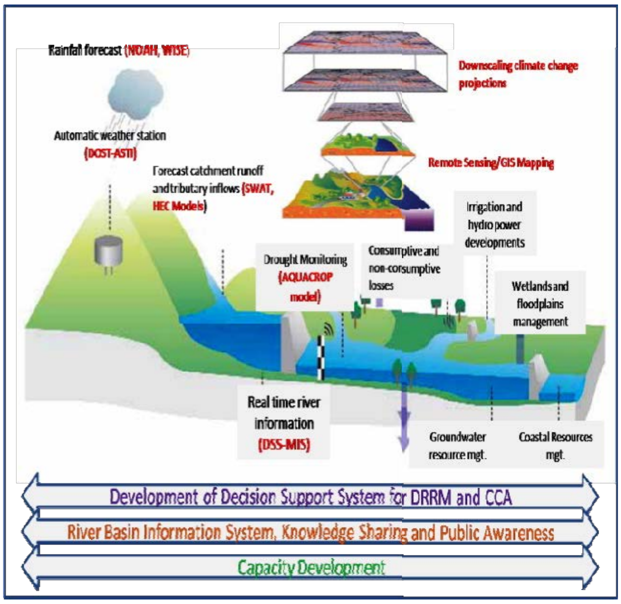

Figure 2 .Research and Development Framework

The components and activities in the river basin are described/explained as follows:

UtilizationofExistingModels,DataandFacilities

The research program will utilize research products of existing DOST sponsored projects such as NOAH, WISE, LIDAR MAPPING and other agencies as primary data input in the development of decision support system for the river basins. Furthermore, available computer models such as HEC, SWAT, AQUACROP will be calibrated and validated for simulating hydro meteorological events and development of early warning forecast of hazards including future climate scenarios

Thematicareasinintegratedriverbasinmanagement River basin management will be categorized in four thematic components:

a) flood control, drought and other hazard;

b) water resources management;

c) watershed and environmental management;

d) coastal resources management

Cross-cutting SupportServices

a. River basin Management Information System

River basin organizations need to create a basin information system that will meet their ownparticular needs, both for managing the data they collect and for delivering information to different groups of users in formats they can understand and make use of. Sound governance of water in the basin depends on effective information systems. The MIS platform should be capable of managing all types of information: geographic, alphanumeric, text and multimedia. The main components of the RBMIS are:

- a database and geographic information system (GIS): these are vital tools for managing data and translating them into, for example maps, graphs, indicators;
- tools to manage a catalogue of data sources on line;
- decision-support and modelling tools; and
- a web portal for sharing and disseminating information

b. Capacity Development

Conduct of trainings, educational tours, development of training manuals and IEC for advocacy and public awareness campaigns

Conclusion and Recommendation

The results of the four zonal workshops show that the main and most frequent issue identified by the stakeholders of the Cagayan river basin is regarding socio-economic conditions as a result of frequent hydrometeorological hazard such as floods, drought, and landslides.

In addressing water related disasters, The Philippine government is putting serious efforts in institutionalizing actions in local context in accordance to the Hyogo Framework for Action (HFA) adopted in January 2005 during the World Conference on Disaster Reduction. The HFA calls for the effective implementation of Disaster Risk Reduction (DRR) efforts to substantially reduce disaster losses by 2015 and beyond in terms of lives and in the social, economic, and environmental assets of communities and countries, as an essential condition for sustainable development.

Another important issue underscored, is on institutional concerns. Majority of the institutional issues raised concerns the overlapping, conflicting, fragmented and weak enforcement of policies and functions of relevant institutions. Therefore, it is highly recommended that a single body, organization, or institution be established that will govern the Cagayan river basin.

To ensure the success of the river basin organization and the sustainable development within the Basin in a long-term perspective, the organization should strive to work for an authority status to ensure the continuity of the institution and the implementation of its plans and programs.

References

Asian Development Bank. 2008. Philippines: Master Plan for the Agusan River Basin. Manila, Philippines.

Cleaver F and Franks T (2005) How Institutions Elude Design: River Basin Management and Sustainable Livelihoods. BCID research paper 12.

Murray-Darling Basin Ministerial Council. 3-10-2005, Basin Sustainability Plan. Murray-Darling Basin Commission.

Global Water Partnership. 2003, Effective Water Governance: Learning from the Dialogues. Report from "3rd World Water Forum" Kyoto, Japan .

Global Water Partnership. 2000. Integrated Water Resources Management. TAC Background Papers No.4,

Japan International Cooperation Agency. 2002. The Feasibility Study of the Flood Control Project for the Lower Cagayan River Final Report. Volume II. Manila, Philippines.

Mainstreaming Disaster Risk Reduction in Subnational Development and Land Use/Physical Planning in the Philippines.2008. NEDA

RDC-NEDA. 2005. Cagayan Riverine Zone Development Framework Plan 2005-2030. Tuguegarao City, Philippines.

Tuddao V. Jr. 2009. Center for River Basin, Organization and Management. Solo, Central Java, Indonesia. www.crbom.org

Reviewers

Full name	Organization	Country
Dr.Anurak Sriariyawat	Chulalongkorn University	Thailand
Prof. Dr.Ke-Sheng Cheng	National Taiwan University	Taiwan
Prof.Shie-Yui Liong	National University of Singapore	Singapore
Prof.Yutaka Matsuno	Kinki University	Japan
Assoc.Prof. Dr.sucharit koontanakulvong	Chulalongkorn University	Thailand
Dr.Takahiro Sayama	Public Works Research Institute	Japan
Dr.Yutthana Talaluxmana	Kasetsart University	Thailand
Prof. Dr.Yasuto Tachikawa	Kyoto University	Japan
Dr.Somchai chonwattana	Asian Institute of Technology	Thailand
Dr.Ole Mark	Danish Hydraulic Institute (DHI)	Denmark
Dr.Sutat Weesakul	Asian Institute of Technology/Hydro and Agro Informatics Institute (HAII)	Thailand
Asst.Prof. Dr.Aksara Putthividhya	Chulalongkorn University	Thailand
Asst.Prof.Sangam Shrestha	Asian Institute of Technology	Thailand
Dr.Piyatida Ruangrassamee	Chulalongkorn University	Thailand
Dr.Jiaguo Qi	Zhejiang University	China
Dr.Pongsak SUTTINON	Chulalongkorn University	Thailand
Assoc.Prof. Dr.Bancha Kwanyuen	Kasetsart University	Thailand
Prof. Dr.Kwansue Jung	Chungnam National University	Korea, Republic of
Assoc.Prof. Dr.Amnat Chidthaisong	King Mongkut Institute Technology Thonburi	Thailand
Dr.Thammarat Koottatep	Asian Institute of Technology	Thailand
Asst.Prof. Dr.Jerasorn Santisirisoomboon	Ramkhamhaeng University	Thailand

Supported by

Sponsors: